

**FORMULATION DEVELOPMENT, OPTIMIZATION  
AND EVALUATION OF *ALPINIA GALANGA* EXTRACT  
LOADED NANOEMULSION**

A

Thesis

Submitted For the Award of the Degree of

**DOCTOR OF PHILOSOPHY**

in

**PHARMACEUTICS**

By

**Arya K R**

**(Reg. No. 11815948)**

**Supervised By**

**Dr. Sheetu**

**Co-Supervised by**

**Dr. Sachin Kumar Singh**



**LOVELY PROFESSIONAL UNIVERSITY**

**PUNJAB**

**2022**

## **DECLARATION**

I hereby declare that the present dissertation entitled “**Formulation development, optimization and evaluation of *Alpinia galanga* extract loaded nanoemulsion**” embodies the original research work carried out by me. It is further stated that no part of this dissertation has been submitted either in part or full for the award of any other degree of Lovely Professional University or any other University/Institution.

**Arya K R**

Dept. of Pharmaceutical Sciences

Lovely Professional University

Jalandhar-Delhi G.T. Road

Phagwara, Punjab 144411

## CERTIFICATE

This is to certify that the present dissertation entitled “**Formulation development, optimization and evaluation of *Alpinia galanga* extract loaded nanoemulsion**” embodies the original research work carried out by Arya K R under my supervision and guidance. It is further stated that no part of this dissertation has been submitted either fully or in part for any other degree of this or any other university.

### **Supervisor**

**Dr. Sheetu**

Associate Professor

Dept.of Pharmaceutical Sciences

Lovely Professional University

Jalandhar-Delhi G.T. Road

Phagwara, Punjab, 144411

### **Co-Supervisor**

**Dr. Sachin Kumar Singh**

Professor

Dept.of Pharmaceutical Sciences

Lovely Professional University

Jalandhar-Delhi G.T. Road

Phagwara, Punjab, 144411

## ACKNOWLEDGEMENT

*Behind every successful journey, it is always said that there is an invisible force, who direct us in the right path to reach the destination. I bow myself towards that divine power “ALMIGHTY GOD”, for bestowing me with wisdom, good health, strength, enthusiasm, anything and everything, to accomplish our dream “Research work” towards success.*

*With the deep sense of gratitude, I would like to extend my sincere thanks to my supervisor Dr. Sheetu, Associate Professor, School of Pharmaceutical Sciences, Lovely Professional University, Phagwara for the timely and fruitful guidance, persistent encouragement, motivation, support, constructive criticism and wholehearted help. I would like to thank Mam for helping me to endeavor with perfection.*

*I consider it my distinct privilege and honor to express my deepest sense of indebtedness and gratitude to my co-supervisor, Professor, Dr. Sachin Kumar Singh. His keen interest, scientific input, invaluable guidance, generosity, constant inspiration and painstaking efforts for me throughout the stint of my doctoral project, starting right from the initial stage of this work till its final compilation and completion are much appreciable. He has always been there for motivating and cheering me during my down. Apart from the academic contributions, he taught me the subtle art of having a positive attitude towards life. Sir, the respect for you from day one as a guide gradually transformed into some “inexpressible reverence” that I hold for you as a person who can be idolized and someone who shall always be in the same frame as my parents.*

*I extend my sincere thanks to Dr. Monica Gulati, Professor and Sr. Dean, School of Pharmaceutical Sciences, Lovely Professional University, Phagwara, who allowed me to avail the departmental facilities whenever needed. Her motivation, enthusiasm and immense knowledge have been the source of inspiration for me. She has been a strong and supportive advisor to me throughout my PhD research and always motivated me to perform the “best”. Thanks a lot Madam for helping and guiding me.*

*I express my gratitude and thankfulness to Harpreet Singh, Assistant Professor, Lovely Faculty of Applied Medical Sciences, Lovely Professional University, Phagwara for all the support and guidance provided to me for learning the staining and microtome tissue cutting techniques. He is a well experienced personality as well as an optimistic person, I ever met. It gives me immense pleasure to express my gratitude and thankfulness to you sir. Thank you, sir.*

*Thanks and gratitude to all my teachers especially Dr. Bimlesh Kumar, Dr. Bhupinder Kapoor, Dr. Vijay Mishra, Dr. Pradeep Sharma, Dr. Rajan Kumar for their support and guidance. Thank you all.*

*I extend my thanks to Dr. Abraham Mathew, Assistant Professor, Department of Botany, St. Peter’s College, Kolenchery, Kerala for carrying out authentication of plant and receiving my herbarium. It was my beginning stage of research study and the detailed information given to me regarding plant was useful throughout my research journey.*

*My sincere and special thanks to staffs of Central Instrumentation Facility, Lovely Professional University for carrying out droplet size analysis, zeta potential and gas chromatography-mass spectroscopy analysis. Thanks to Anju Kumari, Baljit Bangar, and Amarinder, you all were very supportive and co-operative while carrying out the analysis.*

*I also express my indepth gratitude to Dr. Gowthamarajan Kuppusamy, Professor, JSS Ooty, for supporting me to continue my research activities during the pandemic situation. I also thank Mr. Aaravid, Ph.D Scholar from JSS Ooty for extending his hands to carry out the analysis in their laboratory without hesitation.*

*I express my thankfulness to the staffs of Central Instrumentation Facility (CIF), Panjab University, for providing the necessary facilities for performing High resolution Transmission electron microscopy, rheometer, and confocal laser scanning microscopy which was core characterization techniques that were required for further carrying out my research work.*

*Thanks to Dr Kusum Joshi, Senior pathologist from Medicos Lab. Chandigarh, for her valuable discussion and examination of histopathology samples. I learned a significant part of my research work from you Mam. You also taught me age is just a number. Learning and building carrer can be done at any stage of life if we have the desire. Thanks to Mam and whole Medicos Labmates specially to Mrs Akhilesh.*

*I also wish to acknowledge the technical support and co-operation extended to me particularly by Head of Laboratory Dr. Dileep Singh Baghel. I am also thankful to Manawar and Vinod Kumar for their kind help at the right time for carry out the laboratory works.*

*It was a beautiful experience and lively ambience working with all my lab mates, Mr. Ankit Awasthi, Ms. Jaskiran, Ms. Shak Rahana Parveen, Mr. Leander Corri, Mr. Hardeep, Mr. Sukriti Vishwas, and Ms. Gagandeep. Special thanks to Dr. Rubiya Khursheed for her effortless support and relevant scientific support throughout the journey.*

*Thanks to my dear friends Mrs. Hafila Manaf, Mrs. Archana Ramesh, and Mr Kuldip Kumar as they have been the source of moral support to me and have extended their helping hands without any fail in my entire thick and thin.*

*I must take this opportunity to express my deep sense of gratitude and gratefulness towards my family and in-laws. I owe a lot to my parents, who encouraged and helped me at every stage of my personal and academic life, and longed to see this achievement come true. I am deeply indebted to my Father, Mother and in-laws for their love, prayers, care and sacrifices for educating and preparing me for my future. They have just showered me with unconditional love and care during my toughest time.*

*I must thank my son "Master Aaravh" for his effortless support that he has done to me regardless of his age. He was the one and only one, who stood in front me always saying me "Mama you can do it". He was the real motivator. Being at his age, he realized what really hard work, sacrifice, and patience means. It's not only me who took the effort, but he is the one who took the responsibility of mother in taking care of our sweet princess "Aahana" and managed her throughout the journey. He supported me mentally as well as physically in achieving our dream. I'm the luckiest mother to be blessed with such a wonderful son like you. Thank you so much my dear dearest.*

*Without my best half, how can I begin this journey? I take this opportunity to express my heartfelt thanks to my best friend and husband Jithu, for the unconditional love, support, encouragement and care that he have showered on me. At this moment I remember the quotes*

*of Donovan Bailey that he has shared to me when we begin our journey “Follow your passion, be prepared to work hard and sacrifice, and above all, and don’t let anyone limit your dreams”. It’s not only me who did the hard work and sacrifice but a countless part was from your end. Words are not enough to express the gratitude that you deserve for all that you have done to me for successful completion of this dream journey.*

*The list is never-ending and I am thankful to one and all who played their part successfully for the accomplishment of this task. This thesis would not have been possible without the blessings, guidance, sacrifice, love and moral support of many people.*

**Arya K R**

## LIST OF ABBREVIATIONS

Abbreviations/symbols	Full form
%	Percentage
↑	Increase
↓	Decrease
μg	Microgram
μL	Microliter
2D	Two-dimensional
3D	Three-dimensional
5-FU	5-Fluorouracil
ABTS	2,2'-azino-bis(3-ethylbenzothiazoline-6-sulfonate)
ACA	1'-acetoxychavicol acetate
ADP	Adenosine diphosphate
AEAC	Ascorbic acid equivalent antioxidant activity
AG	<i>Alpinia galanga</i>
AGE	<i>Alpinia galanga</i> extract
AGE NANE <sub>H</sub>	High dose of <i>Alpinia galanga</i> extract loaded non-aqueous nanoemulsion
AGE NANE <sub>L</sub>	Low dose of <i>Alpinia galanga</i> extract loaded non-aqueous nanoemulsion
AMPK	Adenosine monophosphate activated protein kinase
ANOVA	Analysis of Variance
ASO	<i>Annona squamosa</i> seed oil
BBD	Box- Behnken Design
°C	Degree celcius
CAT	Catalase
CC	Column chromatography
CCD	Central Composite Design
CD-40	Cluster of differentiation -40
CLSM	Confocal laser scanning microscopy
CMA <sub>s</sub>	Critical material attributes
COX	Cyclooxygenase
CPI	Catastrophic phase inversion

---

CPPs	Critical process parameters
CQAs	Critical quality attributes
CSF-1	Colony stimulating factor-1
CV	Coefficient of variance
CXCL	Chemokine motif ligand 1
DCs	Dendritic cells
DLA	Dalton's lymphocyte ascites
DM	Dispersion medium
DMF	N, N'-dimethyl formamide
DMSO	Dimethyl sulphoxide
DNA	Deoxyribonucleic acid
DoE	Design of Experiment
DP	Dispersed phase
DPPH	1,1-diphenyl-2-picrylhydrazyl
DTNB	5,5'-dithio-bis (2-nitrobenzoic acid)
ED <sub>50</sub>	Effective dose 50
EE	Entrapment efficiency
FD	Factorial design
FDA	Food and Drug Administration
FFD	Fractional Factorial Design
FIC	Ferrous ion chelating
g	Gram
GC	Gas chromatography
GRAS	Generally recognized as safe
GSH	Reduced glutathione
GWAS	Genome wide association studies
h	Hours
HCl	Hydrochloric acid
HET-CAM	Hen's egg test- chorioallantoic membrane
HETP	Height equivalent to theoretical plate
HLA	Human leukocyte antigens
HLB	Hydrophilic-lipophilic balance
HPTLC	High performance thin layer chromatography

---



---

HQC	Higher quality control
HR-TEM	High resolution transmission electron microscopy
Hz	Hertz
i.p	Intra-peritoneal
IAEC	Institutional Animal Ethical Committee
IC <sub>50</sub>	Half-maximal inhibitory concentration
ICH	International Conference on Harmonisation of Technical Requirements for Pharmaceutical for Human Use
IFN	Interferon
IFPA	International Federation of Psoriasis Association
IgE	Immunoglobulin E
IKK	I kappa B kinase
IL	Interleukin
IMQ	Imiquimod
iNOS	Inducible nitric oxide synthase
IR	Infrared spectroscopy
JAK	Janus kinase
KGF	Keratinocyte growth factor
kHz	Kilohertz
KMO	Kojic monooleate
LFA-3/CD-2	Lymphocyte function associated antigen-3/cluster of differentiation-2
LOD	Limit of detection
LOQ	Limit of quantification
LPS	Lipopolysaccharide
LQC	Lower quality control
MAPK	Mitogen activated protein kinase pathway
MBC	Minimum bactericidal concentration
MCAO	Middle cerebral artery occlusion
MCT	Medium chain triglyceride
MDA	Malondialdehyde
mg	Milligram
MHC	Major histocompatibility complex

---

---

MIC	Minimum inhibitory concentration
min	Minute
mL	Milliliter
mM	Millimolar
MMP	Matrix metalloproteinase
mol	Mole
MPa	Megapascal
MQC	Middle quality control
MS	Mass spectroscopy
MTT	3-(4,5-dimethyl thiazol-2-yl)-2,5-diphenyl tetrazolium bromide
mV	Millivolt
NANE	Non-aqueous nanoemulsion
NANE-B	Blank non-aqueous nanoemulsion
NaOH	Sodium hydroxide
NFAT	Nuclear factor of activated T-cell
NF- $\kappa$ B	Nuclear factor kappa B
NLC	Nanostructured lipid carrier
nm	Nanometer
NMR	Nuclear magnetic spectroscopy
NPC	Non-polymeric phenolic content
Nrf2	Nuclear factor-erythroid 2 related factor 2
OA	Oxalic acid
OECD	Organization of Economic Co-operation and Development
ORAC	Oxygen radical absorbance capacity
PAMAM	Polyamidoamine
PASI	Psoriasis area severity index
PBD	Plackett Burman Design
PB-PEO	Polybutadiene-b-poly(ethylene oxide)
PBS	Phosphate buffered saline
PDI	Polydispersity index
PE	Pickering emulsion
PEG	Polyethylene glycol

---

---

PIC	Phase inversion by composition
PIT	Phase inversion by temperature
PPG	Polypropylene glycol
PT	Polymeric tannin
PtBuS-PEO	Poly(ter-butylstyrene)-poly(ethylene oxide)
p-TPD	Pseudo-ternary phase diagram
PUVA	Psoralen plus ultraviolet A
QbD	Quality by Design
QTPP	Quality target product profile
$r^2$	Correlation coefficient
$R^2$	Coefficient of regression
RAD	Rhodamine aqueous dispersion
RH	Relative humidity
R-NANE	Rhodamine loaded non-aqueous nanoemulsion
RP-HPLC	Reverse phase -High Performance Liquid Chromatography
rpm	Rotations per minute
RSD	Relative standard deviation
RT	Retention time
S.D.	Standard deviation
SCZ	Suconazole
SMD	Sauter mean diameter
$S_{mix}$	Surfactant-cosurfactant mixture
SOD	Superoxide dismutase
SPC	Soy phosphatidyl choline
STAT	Signal transducer and activator of transcription
TAA	Total antioxidant assay
TBARS	Thiobarbituric acid reactive substance
TD	Taguchi design
Th	T-helper
TLC	Thin layer chromatography
TNFAIP 3	Tumor necrosis factor-alpha induced protein 3
TNF- $\alpha$	Tumor necrosis factor-alpha
TPC	Total phenolic content

---

---

TTO	Tea tree oil
U/mL	Units per milliliter
UPLC-QTOF MS	Ultra high performance liquid chromatography coupled with quadrupole/time of flight mass spectroscopy
UV	Ultraviolet
UV-Vis	Ultraviolet-visible spectroscopy
v/v	volume/ volume
VEGF	Vascular endothelial growth factor
w/w	weight/weight
$\alpha$	Alpha
$\beta$	Beta
$\gamma$	Gamma
$\psi$	Psi

---

## TABLE OF CONTENTS

<b>CHAPTER 1</b> .....	<b>1-9</b>
<b>Introduction</b> .....	<b>1</b>
1.1. Psoriasis.....	1
1.2. Prevalence rate of psoriasis .....	1
1.3. Types of psoriasis.....	1
1.4. Current treatment options for psoriasis .....	3
1.4.1. Topical therapy .....	3
1.4.2. Phototherapy .....	4
1.4.3. Systemic therapy.....	4
<b>1.4.3.1. Oral dosage forms</b> .....	<b>4</b>
<b>1.4.3.2. Injectables/ Biologics</b> .....	<b>4</b>
1.5. Herbal formulations - An alternative option for psoriasis treatment .....	5
1.6. AG for psoriasis .....	6
<b>CHAPTER 2</b> .....	<b>10-78</b>
<b>Review of Literature</b> .....	<b>10</b>
2.1. Psoriasis and its pathogenesis .....	10
2.1.1. Role of genes and transcription factors .....	10
2.1.2. Role of immune system and inflammatory pathway .....	12
<b>2.1.2.1. Events in innate immunity</b> .....	<b>12</b>
<b>2.1.2.2. Events in acquired immunity</b> .....	<b>12</b>
2.2. Mode of inheritance of psoriasis .....	12
2.2.1. Genetic.....	12
2.2.2. Epigenetic .....	13
2.2.3. Environmental triggers .....	13
2.3. Disease severity and selection of route for treatment .....	13
2.4. Topical therapy.....	14
2.4.1. Synthetic drugs .....	14
<b>2.4.1.1. Tar preparation (Coal tar)</b> .....	<b>14</b>
<b>2.4.1.2. Emollients and moisturizers</b> .....	<b>14</b>
<b>2.4.1.3. Anthralin (Dithranol)</b> .....	<b>14</b>
<b>2.4.1.4. Non-steroidal anti-inflammatory drugs</b> .....	<b>14</b>
<b>2.4.1.5. Calcineurin inhibitors</b> .....	<b>14</b>
<b>2.4.1.6. Retinoids</b> .....	<b>15</b>
<b>2.4.1.7. Corticosteroids</b> .....	<b>15</b>
<b>2.4.1.8. Vitamin D analogues</b> .....	<b>16</b>
<b>2.4.1.9. Pyrimidine antagonist</b> .....	<b>16</b>
2.4.2. Herbals.....	17
2.4.2.1. Herbs for psoriasis .....	17
<b>2.4.2.1.1. Nigella sativa</b> .....	<b>17</b>

2.4.2.1.2. <i>Rubia cordifolia</i> .....	17
2.4.2.1.3. <i>Smilax china</i> .....	17
2.4.2.1.4. <i>Thespesia populne</i> .....	18
2.4.2.1.5. <i>Cassia tora</i> .....	18
2.4.2.1.6. <i>Kigelia africana</i> .....	18
2.4.2.1.7. <i>Solanum xanthocarpum</i> .....	18
2.4.2.1.8. <i>Annona squamosa</i> .....	18
2.4.2.1.9. <i>Pongamia pinnata</i> .....	19
2.4.2.2. Oils.....	20
2.4.2.2.1. <i>Tea tree oil (TTO)</i> .....	21
2.4.2.2.2. <i>Rose geranium oil</i> .....	21
2.4.2.2.3. <i>Lavender oil</i> .....	21
2.4.2.2.4. <i>Kalonji oil (black seed oil)</i> .....	21
2.4.2.2.5 <i>Matricaria recutita (chamomilla) oil</i> .....	21
2.4.2.2.6. <i>Medium chain triglycerides (MCT)</i> .....	22
2.5. Herb of choice - AG.....	23
2.5.1. Taxonomy of the plant.....	24
2.5.2. Phytochemistry and bioactive components.....	24
2.5.3. Pharmacological activities of AGE.....	27
2.5.3.1. <i>Antioxidant</i> .....	27
2.5.3.2. <i>Anticancer activity</i> .....	29
2.5.3.3. <i>Anti-inflammatory activity</i> .....	30
2.5.3.4. <i>Antipsoriasis activity</i> .....	31
2.5.3.5. <i>Gastroprotective effect</i> .....	32
2.5.3.6. <i>Neuroprotective effect</i> .....	33
2.5.3.7. <i>Antimicrobial activity</i> .....	34
2.5.3.8. <i>Antiallergic/antiasthmatic activities</i> .....	35
2.5.4. Selection of marker.....	37
2.5.5. ACA profile.....	37
2.6. Novel carrier systems explored for topical delivery.....	39
2.7. Nanoemulsions.....	49
2.7.1. Preparation of NANEs.....	50
2.7.1.1. <i>Oil/oleaginous phase</i> .....	51
2.7.1.1.1. <i>Vegetable oils</i> .....	52
2.7.1.1.2. <i>Paraffins</i> .....	52
2.7.1.1.3. <i>Synthetic oils</i> .....	53
2.7.1.2. <i>Non-aqueous polar phase</i> .....	54
2.7.1.3. <i>Surfactants</i> .....	55
2.7.1.4. <i>Polymeric materials</i> .....	55
2.7.1.5. <i>Silica</i> .....	56
2.7.1.6. <i>Phospholipids</i> .....	56
2.7.2. Methods of preparation.....	57
2.7.2.1. <b>High energy method/ Mechanical process</b> .....	57
2.7.2.1.1. <b>Rotor-stator stirring method</b> .....	57

2.7.2.1.2. High-pressure homogenization method .....	57
2.7.2.1.3. Ultrasonic emulsification .....	58
2.7.2.1.4. Microfluidization .....	59
2.7.2.2. Low-pressure homogenization .....	59
2.7.2.2.1. Phase inversion emulsification method .....	60
2.7.2.2.1.1. Phase inversion by composition (PIC) .....	60
2.7.2.2.1.2. Phase inversion by temperature (PIT).....	60
2.7.2.2.2. Membrane emulsification .....	60
2.7.2.2.3. Microchannel emulsification method .....	61
2.7.2.2.4. Spontaneous emulsification .....	61
2.7.2.2.5. Solvent evaporation method .....	61
2.7.3. Mechanism of drug encapsulation in NANEs .....	62
2.7.4. NANE explored for preservation of drug stability .....	63
2.7.5. Patented non-aqueous emulsions.....	66
2.7.6. Stabilization of nanoemulsions.....	67
2.7.6.1. Factors involved .....	67
2.7.6.2. Associated stability problems.....	67
2.8. Quality by design approach for optimization.....	70
2.8.1. Steps involved in QbD implementation.....	71
2.9. DoE.....	71
2.9.1 Application of DoE.....	73
<b>CHAPTER 3 .....</b>	<b>79-82</b>
<b>Rationale of the study .....</b>	<b>79</b>
3.1. Hypothesis.....	79
3.2. Aim.....	82
3.3. Objective .....	82
<b>CHAPTER 4.....</b>	<b>83-121</b>
<b>Experimental work .....</b>	<b>83</b>
4.1. Materials and Instruments .....	83
4.1.1. Materials .....	83
4.1.2. Instruments and equipment.....	86
4.2. Methods.....	88
4.2.1. Collection of AG plant and its rhizomes .....	88
4.2.2. Physicochemical standardization of powdered rhizomes .....	88
4.2.2.1. Loss on drying .....	88
4.2.2.2. Total ash value.....	88
4.2.2.3. Acid-insoluble ash value .....	88
4.2.2.4. Water soluble ash value.....	89
4.2.2.5. Sulphated ash value .....	89
4.2.2.6. Extractive value.....	89

<b>4.2.2.6.1. Alcohol soluble extractive value</b> .....	89
<b>4.2.2.6.2. Water-soluble extractive value</b> .....	89
4.2.3. Preparation of the extract .....	90
4.2.4. Phytochemical screening of the extract.....	90
4.2.5. GC-MS of AGE.....	91
4.2.6. Analytical method development and validation of ACA by reverse phase high performance liquid chromatography (RP-HPLC) .....	92
4.2.6.1. Preparation of standard ACA solution.....	92
<b>4.2.6.1.1. Preparation of standard stock solution</b> .....	92
<b>4.2.6.1.2. Preparation of working standards for calibration curve</b> .....	92
4.2.6.2. Analytical method validation.....	93
<b>4.2.6.2.1. Linearity and range</b> .....	93
<b>4.2.6.2.2. Accuracy</b> .....	93
<b>4.2.6.2.3. Precision</b> .....	93
<b>4.2.6.2.4. Limit of detection (LOD) and limit of quantification (LOQ)</b> .....	94
<b>4.2.6.2.5. Robustness</b> .....	94
<b>4.2.6.2.5.1. Change in flow rate</b> .....	94
<b>4.2.6.2.5.2. Change in composition of mobile phase</b> .....	94
<b>4.2.6.2.5.3. Change in wavelength</b> .....	95
<b>4.2.6.2.6. Specificity</b> .....	95
4.2.7. Preliminary screening of parameters - Factorial experiment .....	95
4.2.7.1. Selection of solvent for extraction of ACA from AG rhizomes.....	95
4.2.7.2. Effect of temperature on extraction process .....	95
4.2.7.3. Effect of mean particle size on extraction .....	96
4.2.7.4. Effect of solid to solvent ratio on extraction .....	96
4.2.7.5. Effect of time on extraction .....	96
4.2.7.6. Effect of extraction steps .....	96
4.2.8. Optimization of the extraction process.....	97
4.2.9. Preformulation studies.....	98
4.2.9.1. Screening of components for NANE.....	98
<b>4.2.9.1.1. Excipient screening</b> .....	98
<b>4.2.9.1.2. Solvent selection</b> .....	98
4.2.9.2 Selection of oil phase and non-aqueous polar phase .....	99
4.2.10. Formulation of AGE loaded NANE.....	99
4.2.11. Preliminary screening of formulations based on emulsification .....	99
4.2.12. Phase behavior study using pseudo-ternary phase diagram (p-TPD) .....	100
4.2.13. Experimental design for optimization of NANEs .....	103
4.2.14. Characterization of developed AGE NANEs.....	106
4.2.14.1. Droplet size analysis and PDI.....	106
4.2.14.2. Zeta potential .....	106
4.2.14.3. Drug loading .....	106
4.2.14.4. Thermodynamic stability testing of the selected AGE NANEs .....	106
4.2.14.5 Optical microscopy of AGE NANE .....	107
4.2.14.6. High resolution transmission electron microscopy (HR-TEM) .....	107



4.2.14.7. Refractive index, pH and viscosity .....	107
4.2.14.8. Spreadability .....	108
4.2.14.9. In vitro diffusion studies and release kinetics .....	108
<b>4.2.14.9.1. In vitro diffusion studies</b> .....	108
<b>4.2.14.9.2. Release kinetic</b> .....	109
4.2.14.10. Ex vivo skin permeation and retention studies .....	110
<b>4.2.14.10.1. Collection and preparation of skin specimen</b> .....	110
<b>4.2.14.10.2. Ex vivo permeation studies</b> .....	110
<b>4.2.14.10.3. Drug retention studies</b> .....	111
4.2.14.11. Depth of Penetration - Confocal laser scanning microscopy (CLSM) .....	111
4.2.14.12. Stability studies .....	112
4.2.15. Pharmacodynamic studies .....	112
4.2.15.1 HET-CAM test for anti-angiogenic activity .....	112
4.2.15.2. Acute dermal toxicity study .....	113
4.2.15.3. Antipsoriatic activity in IMQ induced mouse model .....	115
<b>4.2.15.3.1. Induction of psoriasis lesion</b> .....	116
<b>4.2.15.3.2. Evaluation parameters for antipsoriatic activity</b> .....	118
<b>4.2.15.3.2.1. PASI</b> .....	118
<b>4.2.15.3.2.2. Ear thickness</b> .....	119
<b>4.2.15.3.2.3. Spleen to body weight index</b> .....	119
<b>4.2.15.3.2.4. Histopathology</b> .....	119
<b>4.2.15.3.3. Biochemical estimation of the antioxidant activity in the dorsal skin tissue</b> .....	120
<b>4.2.15.3.3.1. Estimation of SOD</b> .....	120
<b>4.2.15.3.3.2. Measurement of CAT activity</b> .....	120
<b>4.2.15.3.3.3. Estimation of GSH</b> .....	120
<b>4.2.15.3.3.4. Estimation of TBARS</b> .....	121
<b>4.2.15.4. Statistical analysis</b> .....	121
<b>CHAPTER 5 .....</b>	<b>122-246</b>
<b>Results and Discussion.....</b>	<b>122</b>
5.1. Collection of AG plant and its rhizomes .....	122
5.2. Authentication of the collected plant .....	122
5.3. Physicochemical evaluation of powdered rhizomes .....	124
5.4. Preparation of the extract .....	124
5.5. Phytochemical screening of the extract .....	124
5.6. GC-MS .....	127
5.7 Analytical method development .....	131
5.8. Analytical Validation .....	133
5.8.1. Linearity and range .....	133
5.8.2. Accuracy .....	134
5.8.3. Precision .....	134
5.8.4. LOD and LOQ .....	134

5.8.5. Robustness .....	135
5.8.6. Specificity .....	135
5.9. Preliminary screening of parameter for extraction process .....	140
5.9.1. Selection of solvent for extraction of ACA from AG rhizomes .....	140
5.9.2. Effect of temperature on extraction process .....	140
5.9.3. Effect of mean particle size on extraction .....	141
5.9.4. Effect of solid to solvent ratio on extraction .....	141
5.9.5. Effect of time on extraction .....	142
5.9.6. Effect of extraction steps .....	142
5.10. Optimization of the extraction process .....	143
5.11. Preformulation studies .....	148
5.11.1. Screening of components for nanoemulsion .....	148
<b>5.11.1.1. Excipient solubility</b> .....	148
<b>5.11.1.2. Solvent system</b> .....	151
5.11.2. Selection of oil phase and non-aqueous polar phase .....	153
5.11.3. Formulation of AGE loaded NANE .....	153
5.11.4. Screening of emulsification efficiency .....	154
5.11.5. Construction of p-TPD .....	161
5.11.6. Optimization of AGE loaded NANE .....	163
<b>5.11.6.1 DoE</b> .....	163
5.11.7. Characterization of AGE loaded NANE .....	205
<b>5.11.7.1. Droplet size analysis and PDI</b> .....	205
<b>5.11.7.2. Zeta potential</b> .....	206
<b>5.11.7.3. Drug loading</b> .....	207
<b>5.11.7.4. Thermodynamic stability testing of the selected NANE</b> .....	207
<b>5.11.7.5. Optical microscopy of AGE NANE</b> .....	207
<b>5.11.7.6 HR-TEM</b> .....	208
<b>5.11.7.7. Refractive index, pH and viscosity</b> .....	209
<b>5.11.7.8. Spreadability</b> .....	210
<b>5.11.7.9. In vitro drug diffusion studies</b> .....	210
<b>5.11.7.10. Ex vivo skin permeation studies</b> .....	214
<b>5.11.7.11. Drug retention studies</b> .....	215
<b>5.11.7.12. CLSM</b> .....	215
<b>5.11.7.13. Stability studies</b> .....	217
5.12. Pharmacodynamic studies .....	218
5.12.1. HET-CAM test for anti-angiogenic activity .....	218
5.12.2. Acute dermal toxicity study .....	224
5.12.3. Antipsoriatic activity in IMQ induced animal model .....	225
5.12.3.1. Evaluation parameters for antipsoriatic activity .....	227
<b>5.12.3.1.1. PASI</b> .....	227
<b>5.12.3.1.2. Ear thickness</b> .....	232
<b>5.12.3.1.3. Spleen to body weight index</b> .....	234
<b>5.12.3.1.4. Histopathology</b> .....	236

5.12.3.1.5. <i>Biochemical estimation of the antioxidant activity in the dorsal skin tissue</i> .....	241
5.12.3.1.5.1. Estimation of SOD.....	241
5.12.3.1.5.2. Measurement of CAT activity.....	242
5.12.3.1.5.3. Estimation of GSH .....	243
5.12.3.1.5.4. Estimation of TBARS .....	244
<b>CHAPTER 6</b> .....	<b>247-248</b>
<b>Conclusion and future perspective</b> .....	<b>247</b>
<b>CHAPTER 7</b> .....	<b>249-287</b>
<b>Bibliography</b> .....	<b>249</b>

## List of Tables

Table 1. Types of psoriasis with its symptoms and causes.....	2
Table 2. Marketed dosage forms for psoriasis treatment.....	5
Table 3. Classification of corticosteroid based on the potency .....	15
Table 4. Isolated phytoconstituents with its mode of action.....	20
Table 5. Taxonomical classification .....	24
Table 6. ACA profile .....	38
Table 7. Colloidal novel drug delivery systems for psoriasis.....	40
Table 8. Enlist few synthetic oils utilized in the fabrication of nanoemulsions .....	53
Table 9. NANE explored so far for delivery of drugs .....	64
Table 10. Patents on non-aqueous emulsions .....	66
Table 11. Design explored for extraction optimization by ultrasound-assisted technique .....	74
Table 12. Design explored for optimization of nanoemulsion .....	76
Table 13. Various materials employed in the research work.....	83
Table 14. List of instruments and equipment used in various stages of work.....	86
Table 15. Composition of formulation by varying the ratio of oil, $S_{mix}$ and non-aqueous polar phase .....	102
Table 16. Experimental levels of independent variables .....	103
Table 17. Composition of NANEs containing oil phase, $S_{mix}$ and non-aqueous polar phase .....	105
Table 18. Dosing pattern in HET-CAM test.....	113
Table 19. Details of dosing in acute dermal toxicity studies .....	115
Table 20. Draize scoring system.....	115
Table 21. Experimental details for animal study .....	117
Table 22. Physicochemical evaluation of the powdered rhizomes.....	124
Table 23. Phytochemical screening of the ethanolic AGE .....	126
Table 24. Accuracy results based on the percentage recovery of ACA.....	137
Table 25. Precision results .....	138
Table 26. Robustness .....	139
Table 27. Selection of solvent based on the amount of ACA in the extract.....	140
Table 28. Effect of temperature on the amount of ACA in the extract.....	140
Table 29. Effect of mean particle size on the amount of ACA.....	141
Table 30. Effect of solid to solvent ratio on amount of ACA.....	141
Table 31. Effect of time on the amount of ACA.....	142
Table 32. Number of extraction steps on amount of ACA extraction .....	142
Table 33. CCD with process variables and experimentally observed responses of the extracts .....	145
Table 34. Fit summary for the amount of ACA (Y) .....	146
Table 35. ANOVA for quadratic model .....	147
Table 36. Summary of the preliminary screening studies for emulsification efficiency.....	161
Table 37. Optimization of NANE based on the selected factors (X1- X4) for specific responses (Y1- Y5) using BBD .....	164
Table 38. Results of regression analysis for the selected responses .....	166

Table 39. Kinetic release model and correlation coefficient ( $r^2$ ) for optimized AGE NANE .....	212
Table 40. Stability studies for AGE NANE and results of various parameters .....	218
Table 41. Results of anti-angiogenic activity in HET-CAM .....	220
Table 42. Skin irritation study .....	224

## List of Figures

Figure 1. Mechanistic action of AGE inside physiological system .....	7
Figure 2. Events involved in immunopathogenesis of psoriasis.....	10
Figure 3. Schematic representation of components and structure of NANE.....	51
Figure 4. Schematic representation of drug encapsulation A) NANEs B) Pickering NANEs	63
Figure 5. Phases of instability issues in nanoemulsions .....	69
Figure 6. Hypothesis of the research.....	81
Figure 7. Diagrammatic representation of study design .....	118
Figure 8. Various parts of AG (A) Flower, (B) Specimen for herbarium, (C) Plant collected for authentication, (D) Fresh rhizomes of the collected plant, (E) Dried rhizomes for research work.....	122
Figure 9. Herbarium of AG.....	123
Figure 10. Observation of phytochemical screening study for (1) Phenolic compounds (2) Protein (3) Acidic compounds (4) Carbohydrates (5) Glycosides (6) Alkaloids (7) Tannins (8) Steroids (9) Terpenoids (10) Flavonoids (11) Saponins .....	125
Figure 11. GC of AGE.....	128
Figure 12. (A) Mass spectrum of eluted ACA from AGE (B) Mass spectra of ACA obtained from MS library .....	130
Figure 13. Chromatogram of ACA in (A) Acetonitrile: water (40:60, v/v) (B) 0.1% v/v Orthophosphoric acid in water: acetonitrile (50:50, v/v) (C) 0.1% v/v Orthophosphoric acid : methanol (30:70, v/v) (D) Methanol: water (70:30, v/v) (E) Methanol: water (60:40, v/v) (F) Acetonitrile: 0.1% v/v formic acid (60:40, v/v).....	132
Figure 14. Chromatogram of standard ACA.....	133
Figure 15. Calibration curve of standard ACA.....	134
Figure 16. Comparison of retention time of standard ACA and isolated ACA from AGE...	136
Figure 17. Peak purity index of isolated ACA from ethanolic extract .....	136
Figure 18. (A) Perturbation plot represents influence of variable $X_1$ and $X_2$ on the yield of ACA (B) 3D-response surface plot represents the effect of sieve number and solvent volume on the yield of ACA.....	147
Figure 19. Overlay plot represents the optimized parameters for the effective extraction of ACA.....	148
Figure 20. Solubility profile of AGE (ACA) in various oils .....	149
Figure 21. Solubility of AGE (ACA) in various surfactant and co-surfactant .....	150
Figure 22. Solubility profile of AGE (ACA) in various solvent systems .....	152
Figure 23. Preliminary screening designated as "F". $F_1 - F_{27}$ formulations containing $S_{mix}$ as Tween 80 and Transcutol P, Capryol 90 as oil phase and glycerin as non-aqueous polar phase. ....	155
Figure 24. Preliminary screening designated as "N". $N_1 - N_{27}$ formulations with Capryol 90 as oil phase, Cremophor RH 40 as surfactant and glycerin as non-aqueous polar phase .....	156
Figure 25. Preliminary screening designated as "E". $E_1 - E_{81}$ with Capryol 90 as oil phase, glycerin as non-aqueous polar phase, Cremophor RH 40 and Transcutol P as $S_{mix}$ . ....	158

Figure 26. Preliminary screening designated as “M”. M <sub>1</sub> - M <sub>81</sub> formulations having MCT oil as oil phase, glycerin as non-aqueous polar phase, Cremophor RH 40 and Transcutol P as S <sub>mix</sub> .....	160
Figure 27. Selected NANE designated as M <sub>70</sub> , M <sub>71</sub> , M <sub>79</sub> and M <sub>80</sub> .....	160
Figure 28. p-TPD for (A) S <sub>mix</sub> 1:1 (B) S <sub>mix</sub> 1:2 (C) S <sub>mix</sub> 2:1 .....	162
Figure 29. Formulation prototype designated as “FM” and 29 formulations (FM1 to FM29) obtained as per BBD design .....	163
Figure 30. Perturbation plot (A) Droplet size (B) Zeta potential (C) % Drug loading (D) % Cumulative drug permeated (E) % Drug retained in skin. ....	170
Figure 31. Contour plots for the effect of (A) MCT oil and Cremophor RH 40 (B) MCT oil and Transcutol P (C) MCT oil and Glycerin (D) Cremophor RH 40 and Transcutol P (E) Cremophor RH 40 and Glycerin (F) Transcutol P and Glycerin on droplet size .....	175
Figure 32. 3D response surface plot for the effect of (A) MCT oil and Cremophor RH 40 (B) MCT oil and Transcutol P (C) MCT oil and Glycerin (D) Cremophor RH 40 and Transcutol P (E) Cremophor RH 40 and Glycerin (F) Transcutol P and Glycerin on droplet size.....	178
Figure 33. Contour plots for the effect of (A) MCT oil and Cremophor RH 40 (B) MCT oil and Transcutol P (C) MCT oil and Glycerin (D) Cremophor RH 40 and Transcutol P (E) Cremophor RH 40 and Glycerin (F) Transcutol P and Glycerin on zeta potential .....	181
Figure 34. 3D response surface plot for the effect of (A) MCT oil and Cremophor RH 40 (B) MCT oil and Transcutol P (C) MCT oil and Glycerin (D) Cremophor RH 40 and Transcutol P (E) Cremophor RH 40 and Glycerin (F) Transcutol P and Glycerin on zeta potential .....	184
Figure 35. Contour plots for the effect of (A) MCT oil and Cremophor RH 40 (B) MCT oil and Transcutol P (C) MCT oil and Glycerin (D) Cremophor RH 40 and Transcutol P (E) Cremophor RH 40 and Glycerin (F) Transcutol P and Glycerin on drug loading .....	187
Figure 36. 3D response surface plot for the effect of (A) MCT oil and Cremophor RH 40 (B) MCT oil and Transcutol P (C) MCT oil and Glycerin (D) Cremophor RH 40 and Transcutol P (E) Cremophor RH 40 and Glycerin (F) Transcutol P and Glycerin on drug loading .....	190
Figure 37. Contour plots for the effect of (A) MCT oil and Cremophor RH 40 (B) MCT oil and Transcutol P (C) MCT oil and Glycerin (D) Cremophor RH 40 and Transcutol P (E) Cremophor RH 40 and Glycerin (F) Transcutol P and Glycerin on % cumulative drug permeated.....	193
Figure 38. 3D response surface plot for the effect of (A) MCT oil and Cremophor RH 40 (B) MCT oil and Transcutol P (C) MCT oil and Glycerin (D) Cremophor RH 40 and Transcutol P (E) Cremophor RH 40 and Glycerin (F) Transcutol P and Glycerin on % cumulative drug permeated .....	196
Figure 39. Contour plots for the effect of (A) MCT oil and Cremophor RH 40 (B) MCT oil and Transcutol P (C) MCT oil and Glycerin (D) Cremophor RH 40 and Transcutol P (E) Cremophor RH 40 and Glycerin (F) Transcutol P and Glycerin on % drug retained in the skin.....	199
Figure 40. 3D response surface plot for the effect of (A) MCT oil and Cremophor RH 40 (B) MCT oil and Transcutol P (C) MCT oil and Glycerin (D) Cremophor RH 40 and	

Transcutol P (E) Cremophor RH 40 and Glycerin (F) Transcutol P and Glycerin on % drug retained in the skin. ....	202
Figure 41. Overlay plot represents the optimized parameters for obtaining nanoemulsion ..	204
Figure 42. Optimized AGE NANE .....	205
Figure 43. Globule size analysis and PDI of optimized AGE NANE .....	206
Figure 44. Zeta potential of optimized AGE NANE .....	207
Figure 45. Optical microscopy of methylene blue loaded AGE NANE.....	208
Figure 46. HR-TEM image of the optimized AGE NANE .....	208
Figure 47. Relationship between viscosity and shear rate .....	209
Figure 48. Comparison of % cumulative drug diffused from AGE <i>per se</i> and AGE NANE with respect to time.....	211
Figure 49. Prediction of kinetic release model for optimized AGE NANE (A) Zero-order kinetics-Percentage cumulative drug released versus time (B) First-order kinetics- In cumulative drug remaining versus time (C) Higuchi model-Percentage cumulative drug released versus square root of time (D) Korsmeyer- Peppas model- Log percentage cumulative drug released versus log time (E) Hixson-Crowell- Cube root of cumulative amount of drug remaining versus time .....	213
Figure 50. Comparison of cumulative amount of AGE (ACA) permeated through porcine ear skin with respect to time.....	215
Figure 51. CLSM in porcine skin (a) RAD (b) R-NANE.....	217
Figure 52. A comparison of blood vessel formation (before treatment) and inhibition (after treatment) in the HET-CAM model (A) Normal control (B) Positive control (C) Negative control (D) AGE <i>per se</i> (E) Blank NANE (F) AGE NANE .....	223
Figure 53. Phenotypic variations observed in all the groups (I-VII) before induction (1st day), after induction (7th day) and after treatment (14th day) .....	226
Figure 54. PASI scoring in IMQ induced psoriasis mice model during the study (A) Erythema (B) Scaling (C) Skin thickness (D) Cumulative PASI scoring.....	231
Figure 55. Morphological changes observed on mice right ear in all groups after treatment i.e on 14th day .....	233
Figure 56. Graphical representation of variation in ear thickness during study period .....	234
Figure 57. Effect of IMQ and various treatments applied on spleen length .....	235
Figure 58. IMQ induced splenomegaly and effect of treatment on spleen to body weight index .....	235
Figure 59. Photomicrograph showing histopathology of dorsal skin of groups (I-VII) .....	238
Figure 60. Photomicrograph showing histopathology of dorsal ear skin of groups (I-VII) ..	240
Figure 61. Effect of treatment on SOD level .....	242
Figure 62. Effect of treatment on catalase activity .....	243
Figure 63. Effect of treatment on reduced GSH level .....	244
Figure 64. Effect of treatment on TBARS .....	245



## **LIST OF ANNEXURES**

Annexure 1: Letter of Candidacy for Ph.D

Annexure 2: Plant Identification Certificate

Annexure 3: Approval by Institutional Animal Ethics Committee

Annexure 4: List of publications, patents, presentations and workshops attended

## Abstract

The aim of the present study was to develop a topical formulation containing *Alpinia galanga* extract (AGE) for treatment of psoriasis. Ethanolic extract obtained from rhizomes of *Alpinia galanga* (AG) was reported with numerous phytoconstituents, however, major component reported was 1'-acetoxychavicol acetate (ACA) which is involved in down regulation of nuclear factor kappa B (NF- $\kappa$ B) signaling pathway and increased expression of tumor necrosis factor-alpha induced protein 3 (TNFAIP 3), hence exerted antipsoriasis activity. But major limitation of ACA is its volatility and tendency to undergo hydrolytic degradation (aqueous instability). Hence, to preserve the stability of ACA, an aqueous free nano-formulation system was proposed i.e non-aqueous nanoemulsion (NANE).

AGE loaded NANEs were prepared using Palmester 3595 (MCT oil) as oil phase, Cremophor RH 40-Transcutol P® as surfactant-cosurfactant ( $S_{mix}$ ), and glycerin as non-aqueous polar continuous phase. The composition was optimized by applying three-level, four factor Box-Behnken design (BBD). The mean droplet size and zeta potential of the optimized AGE NANE was found to be  $60.81 \pm 18.88$  nm and  $-7.99 \pm 4.14$  mV, respectively. High resolution transmission electron microscopy (HR-TEM) of AGE NANE represented spherical shape droplets and measured average size of the droplets to  $65.40 \pm 23.07$  nm that complies with the results of droplet size analysis. The HR-TEM images clearly exhibited nanosize ( $< 100$  nm) spherical globules with no agglomeration. The *ex vivo* permeation studies of AGE NANE and AGE *per se* on porcine skin reported flux of  $125.58 \pm 8.36$   $\mu\text{g}/\text{cm}^2 \text{h}^{-1}$  and  $12.02 \pm 1.64$   $\mu\text{g}/\text{cm}^2 \text{h}^{-1}$ , respectively. Therefore, the enhancement ratio has shown 10-folds increase in the flux for AGE NANE when compared to AGE *per se*. Later, confocal laser scanning microscopy (CLSM) confirmed that AGE NANE was able to penetrate into skin's stratum by trans-follicular transport mechanism. The optimized AGE NANE was reported to show no phase separation after centrifugation, freeze-thaw cycles and heating/cooling cycles, confirming their thermodynamically stability. Accelerated stability studies of optimized AGE NANE also reported its stability at  $40 \pm 2^\circ\text{C} / 75 \pm 5$  % RH.

The efficacy of AGE NANE was evaluated *in vivo* on imiquimod (IMQ) induced mouse model. The mice treated with low and high doses of AGE NANE (groups VI and VII) showed significant ( $p < 0.05$ ) amelioration of psoriasis. Results of histopathology indicated reduction in psoriasis area severity index (PASI) in AGE NANE treated mice (group VI and group VII), thus confirmed the therapeutic efficacy of the developed optimized AGE NANE.

# Chapter 1



---

## Introduction

---

## **Chapter 1**

### **Introduction**

#### **1.1. Psoriasis**

Psoriasis is an autoimmune inflammatory skin disease where the epidermal cells show marked hyperproliferation and abnormal differentiation (Liang et al., 2017). This condition is characterized by red/silvery white crusty scales/plaques that cause itchiness and pain (Dev et al., 2017). This condition can affect all parts of the body, however, most typical body sites involved are extensor surface of elbows, knees, natal cleft, umbilicus, scalp and nails (Meier and Sheth, 2009). This skin condition is associated with multiple comorbidities and disabilities which substantially diminishes the quality of patient's life as it causes psychological stress among the patients. The sudden outbreak and its notable scars make the patient stigmatized in attending public events that hinder the mental well-being of the person and their quality of life. Some of the comorbidities associated with psoriasis are metabolic diseases, cardiovascular diseases, obesity, vascular diseases, Type 2 diabetes, gastrointestinal diseases such as inflammatory bowel disease (Crohn's disease), infections, mood disorders such as depression, anxiety, and stigmatization, etc. (Takeshita et al., 2017). Psoriasis and its related comorbidities are observed in genetically predisposed patients as well as those who are susceptible to environmental, dietary as well as emotional changes (Furue et al., 2018). The exact cause of the disease is not known, but alteration in the skin cells occur due to various reasons such as stress, smoking, skin infection, climatic condition, and certain medication etc. (Pandey, 2020). The occurrence of psoriasis is usually found in teen (or) early adult age (i.e. between 15-30 years), however, it may also occur in late 50's (Li and Armstrong, 2012).

#### **1.2. Prevalence rate of psoriasis**







In 2021, **International Federation of Psoriasis Association (IFPA)** has recognized more than 125 million psoriatic people across the world ((IFPA), 2021). IFPA recognized that the psoriatic patients are at higher risk of developing diabetes and psoriatic arthritis. These multiple morbidities have shown great impact on patient life and affecting them physically, emotionally, economically and socially (IFPA, 2021).

#### **1.3. Types of psoriasis**

Clinical presentation of psoriasis ranges from the mild condition with the presence of isolated patches on the skin to severe condition with confluent plaques formation on multiple areas of

the body (Li and Armstrong, 2012). Various types of psoriasis with their symptoms are described briefly in **Table 1** as follows (Ramanunny et al., 2018; Schleicher, 2016):

**Table 1.** Types of psoriasis with its symptoms and causes

Types	Prevalence	Symptoms	Causes	Image
Plaque psoriasis (Psoriasis vulgaris)	Mainly 80-85% on elbows, knees, scalp and lower back	<ul style="list-style-type: none"> <li>• A spherical lesion which grows into patches</li> <li>• Red colored lesions which are silvery, loose and shining</li> </ul>	<ul style="list-style-type: none"> <li>• General infections</li> <li>• Sunlight</li> <li>• Skin abrasion</li> <li>• Stress</li> <li>• Medications</li> <li>• Smoking</li> <li>• Drinking</li> </ul>	
Guttate psoriasis	Around 10% on the trunk, arms, legs, and scalp	<ul style="list-style-type: none"> <li>• Lesions are minute raindrop size</li> <li>• The eruption of lesion results with upper respiratory infection</li> </ul>	<ul style="list-style-type: none"> <li>• Contagious viral/bacterial infection</li> <li>• Skin wounds, burns</li> <li>• Insect bites</li> <li>• Sunlight</li> <li>• Medications</li> </ul>	
Psoriatic arthritis	Generally, occur in 6% to 40% of the population having a skin disorder and inflammatory condition of joints in hand and feet	<ul style="list-style-type: none"> <li>• Inflated, sore, thick and painful joints</li> </ul>	<ul style="list-style-type: none"> <li>• Shock or wounds</li> <li>• Medication</li> <li>• Agents that cause skin irritation</li> <li>• Smoking</li> <li>• Drinking</li> </ul>	
Pustular Psoriasis	Occur in less than 5% of population affecting feet, hands or finger-tips	<ul style="list-style-type: none"> <li>• Fluid-filled lesion on the soles and palms</li> <li>• Very scaly skin</li> <li>• Alteration in nails</li> <li>• The eruption of the lesion after discontinuation of creams and some medications.</li> </ul>	<ul style="list-style-type: none"> <li>• Systemic steroids</li> <li>• Mental and emotional stress</li> <li>• Over exposure to UV light</li> <li>• Sudden withdrawal of certain medication</li> </ul>	
Erythroderma (Exfoliative psoriasis)	Very uncommon type but lethal	<ul style="list-style-type: none"> <li>• Whole body with inflation and soreness</li> <li>• The skin may slough off which is tender and generally itchy</li> </ul>	<ul style="list-style-type: none"> <li>• Steroid</li> <li>• Extreme Sun burn</li> <li>• Drinking alcohol</li> <li>• Contagious disease</li> <li>• Sensitivity</li> </ul>	
Nail psoriasis	Uncommon type	<ul style="list-style-type: none"> <li>• Yellow or brownish spots</li> <li>• Deposition of cells under the nails which are impenetrable</li> </ul>	Unknown, but generally consider genetic factors	

#### **1.4. Current treatment options for psoriasis**

A wide variety of treatment options are available for this multifactorial condition. The pathogenesis of psoriasis involves both protein transcription factor and immune system activation, hence a large number of chemical mediators and corresponding immune cells are involved in the disease's progression (Ramanunny et al., 2020). However, no satisfactory treatment approach has been available till date.

The choice of treatment is based on the degree of disease's severity. The Medical Advisory Board of the National Psoriasis Foundation has grouped disease severity into three types (i.e., mild, moderate and severe) by accessing the percentage of body surface area affected and its impact on their quality of life (Dogra and Yadav, 2010) . Mostly the mild condition is treated with topical administration of drug or combination of phototherapy either with oral formulations or topical formulations. However, in moderate or severe cases the oral administration of drugs alone is preferred. The advance research in this area includes the use of biologics that are developed with recombinant DNA technology and are preferred to use when the disease become severe (Gisoni et al., 2017).

##### **1.4.1. Topical therapy**

The anti-inflammatory, anti-proliferative and immunosuppressive action of drugs plays a significant role in psoriasis treatment. Corticosteroids were considered as the “gold standard” for the treatment of psoriasis until the development of other non-steroidal drugs such as methotrexate. These steroidal drugs include betamethasone, clobetasol, hydrocortisone, mometasone, triamcinolone etc. These formulations are available in different dosage forms such as ointments, gels, lotions, sprays, and creams in varying strength of 0.01% w/w, 0.05% w/w, 0.1% w/w, and 2.5% w/w (Uva et al., 2012).

Mostly the practitioners prescribe these formulations based on severity of the psoriatic condition. For instance, hydrocortisone is prescribed in the varying strength of 0.5% w/w to 2.5% w/w in case of having mild severity whereas clobetasol 0.05% w/w is prescribed to psoriatic patients having moderate severity.

Other classes of drugs for topical therapy include emollients, anthralin (dithranol), tar preparation (coal tar), keratolytic agents (salicylic acid), calcineurin inhibitors (tacrolimus, pimecrolimus), retinoids (tazarotene), vitamin D analogue (calcipotriene, calcitriol) and pyrimidine antagonist (5-Fluorouracil) (Ramanunny et al., 2020). Although, the topical formulations of aforementioned drugs are in routine practice, there exist some limitations related to their use (Lebwohl et al., 2021; Svendsen et al., 2020). These include:-

- Poor patient compliance (Lack of adherence and withdrawal)
- Skin irritation and skin thinning (Long term use of medications)
- Recurrence / relapse (Upon withdrawal)

#### **1.4.2. Phototherapy**

Phototherapy is found to be effective when the patient is suffering from mild to moderate severity. For psoriasis treatment, phototherapy is categorized into three types such as narrowband ultraviolet B phototherapy, balneophototherapy, psoralen plus ultraviolet A (PUVA) therapy. In phototherapy, the affected skin surface is exposed to ultraviolet light that causes a reduction in skin cell proliferation as well as inflammation which are the characteristic features in psoriasis (Lebwohl and Ali, 2001). However, the long term use leads to patient incompliance and repeated use of UV-light causes skin cancer, which are the major limitations with this therapy.

#### **1.4.3. Systemic therapy**

The systemic administration of drugs is carefully chosen for patients with moderate to severe psoriasis. These are administered either orally or as injectables.

##### ***1.4.3.1. Oral dosage forms***

Mostly prescribed oral drugs are folic acid antagonist (methotrexate), calcineurin inhibitors (cyclosporine), retinoids (acitretin), phosphodiesterase-4 inhibitors (apremilast), Janus kinase (JAK) inhibitors (tofacitinib), fumaric acid esters (dimethyl fumarate). However, the reported organ toxicity such as nephrotoxicity, hepatotoxicity, etc., reduces its application for long-term use and moreover, on administration of these drugs, constant monitoring of the patient's pharmacokinetic profile is necessary (Ramanunny et al., 2021c) .

##### ***1.4.3.2. Injectables/ Biologics***

Biologics are a newly developed human monoclonal antibody derived medication. Some of the biologics developed are lymphocyte function-associated antigen-3/cluster of differentiation-2 (LFA-3/CD-2) antagonist (alefacept), interleukin (IL)-12/IL-23 antagonist (ustekinumab), tumor necrosis factor-alpha (TNF- $\alpha$ ) (etanercept, infliximab, adalimumab) (Farhangian and Feldman, 2015). These medications are administered intravenously or subcutaneously to act specifically on the immune or genetic mediators involved in psoriasis pathogenesis. The ability of these medications to act on specific target makes them effective and safe. Hence, it is administered to patients who are intolerant or unresponsive towards standard systemic therapy as reported in section 1.3.3.1. But the cost of the biologics is too

high making it unaffordable for the patient to undergo treatment. Apart from this economic issue, some of the side effects associated with the administration of these medications include injection site reaction (Berg and Carrasco, 2017), chances of infections (Kalb et al., 2015) and risk of developing non-melanoma skin cancer (Sârbu et al., 2017).

Some of the marketed dosage forms for the treatment of psoriasis according to the route of administration are mentioned in **Table 2**.

**Table 2.** Marketed dosage forms for psoriasis treatment

Drug	Brand name	Strength	Manufacturer
<b>Topical</b>			
<b>Clobetasol propionate</b>	Tenovate™	0.05% w/w	Glaxo SmithKline Pharmaceuticals Ltd.
<b>Betamethasone propionate</b>	Diprolene	0.05% w/w	Lupin Ltd.
<b>Betamethasone valerate</b>	Betanovate	0.1% w/w	Glaxo SmithKline Pharmaceuticals Ltd.
<b>Betamethasone propionate and calcipotriene</b>	Taclonex	0.064% w/w and 0.005% w/w	LEO Pharma Inc.
<b>Calcipotriene</b>	Diavonex	0.005% w/w	LEO Pharma Inc.
<b>Coal tar</b>	Psoriasisin	2% w/w	Alva-Amco Pharmacal Companies, LLC
<b>Anthralin</b>	Psorisode	0.5% w/w	Lifecare Innovations
<b>Tazarotene</b>	Tazret Forte	0.1% w/w	Glenmark Pharmaceuticals
<b>Oral</b>			
<b>Methotrexate</b>	Imutrex	2.5 mg, 7.5 mg, 10 mg	Cipla Ltd.
<b>Cyclosporine</b>	Imusporin	25 mg, 50 mg, 100 mg	Cipla Ltd.
<b>Acitretin</b>	Acetec	10 mg, 2.5 mg	Dr. Reddy Laboratories Ltd.
<b>Injectables</b>			
<b>Etanercept</b>	Enbrel	50 mg/mL	Pfizer
<b>Infliximab</b>	Remicade	5 mg/kg	Janssen Biotech, Inc.
<b>Adalimumab</b>	Humira	10 mg/0.1 mL	AbbVie
<b>Ustekinumab</b>	Stelara	90 mg/mL	Janssen Biotech, Inc.

### 1.5. Herbal formulations - An alternative option for psoriasis treatment

To overcome the pitfall in the above-mentioned therapies, herbals with medicinal values are utilized for anti-psoriasis effect. Herbals are rich sources of phytomedicines that offer their best outcomes in crude extract form or pure isolated form. The ability to act upon multiple mechanisms at a time and to exert synergistic effect provides a new insight for the exploration of herbals. Along with these benefits, minimum side effects reported with herbals are utilized in chronic external and internal diseases.

Some herbal extracts have shown its potential anti-psoriasis activity during *in vitro* cell line studies. Saelee *et al.* demonstrated the anti-psoriasis activity of *Curcuma longa*, *Annona squamosa* and AGE using HaCaT cell lines (Saelee et al., 2011). This *in vitro* study has highlighted the capability of each herbal extract to act against psoriasis by controlling the NF-



$\kappa$ B activity. Some other herbal extracts which are subjected to pre-clinical studies are *Nigella sativa* seed extract (Dwarampudi et al., 2012), *Smilax china* rhizome extract (Vijayalakshmi et al., 2012a), *Rubia cordifolia* root extract (Lin et al., 2010), and *Thespesia populnea* bark extract (Shrivastav et al., 2009).

It is an essential requisite to evaluate the therapeutic outcomes of these herbals in the dosage form for its future application in psoriasis. However, the research to transform these into a dosage form, its characterization and *in vitro* - *in vivo* evaluation are limited.

### 1.6. AG for psoriasis

AG is a widely explored plant species of Zingiberaceae family. The rhizomes of the plant are well known for its nutritive as well as therapeutic actions. Solvents of different polarity have been used in preparing various extracts of AG and they have demonstrated a variety of activities such as antifungal (Janssen and Scheffer, 1985), anti-ulcer (Al-Yahya et al., 1990), antimicrobial, antioxidant, (Wong et al., 2009), antipsoriasis (Saelee et al., 2011) antitumor (Samarghandian et al., 2014a), antidiabetic (Verma et al., 2015) and anti-inflammatory (Subash et al., 2016), etc.

The crude concentrated ethanolic extract of AG was analyzed by gas chromatography-mass spectroscopy (GC-MS) and found that the major portion of the extract contained 1'-S-1'-acetoxychavicol acetate (ACA) (76.49%). Other compounds identified are p-coumaryl diacetate (7.96%), palmitic acid (3.19%), acetoxyeugenol acetate (3.06%), 9-octadecanoic acid (2.28%) and traces of eugenol,  $\beta$ -bisabolene,  $\beta$ -farnesene and sesquiphellandrene (Oonmetta-aree et al., 2006). Among these phytoconstituents, ACA was found to possess antiallergic (Matsuda et al., 2003a), antimicrobial (Phongpaichit et al., 2006), antioxidant (Mahae and Chaiseri, 2009), antiobesity (Narukawa et al., 2010), antimentia (Kojima-Yuasa et al., 2016) and antitumor activities (Baradwaj et al., 2017). Most of these reported activities are due to the presence of basic phenylpropanoid structure containing para or ortho substitution of acetoxy and 1-acetoxy propenyl groups at the benzene ring respectively (Matsuda et al., 2005). Structural activity relationship of ACA is associated with many activation and inhibition mechanisms such as inhibition of xanthine oxidase activity, inhibition of nitric oxide synthase expression, inhibition of translocation of NF- $\kappa$ B, activation of adenosine monophosphate-activated protein kinase (AMPK) signaling pathway and induction of apoptosis via mitochondrial/Fas- mediated mechanism and production of reactive oxygen species (In et al., 2012; Kojima-Yuasa and Matsui-Yuasa, 2020). These

multiple mechanisms of action of AGE have shown its potential role in the prevention of various life threatening diseases (Kojima-Yuasa and Matsui-Yuasa, 2020; Ramanunny et al., 2021a).

Other phenyl propanoid phytoconstituents present in AG include p-coumaryl diacetate, which is reported with anti-inflammatory and antioxidant activities (Yu et al., 2009) where as 1'-acetoxyeugenol acetate have antimycobacterial (Roy et al., 2012), and anticancer (Aun et al., 2011; Hasima et al., 2010) activities as well as neuro-protective effect (Chellammal et al., 2019).

Some of the flavonoids reported in AG rhizomes are chrysin (Lakshmi et al., 2019) and galangin (Zha et al., 2013). They have shown anti-inflammatory, antioxidant (Divakaran et al., 2013) and antipsoriasis activity (Li et al., 2020a; Sangaraju et al., 2021).

The overall mechanism of action exerted by AGE inside the physiological system is represented in **Figure 1**.

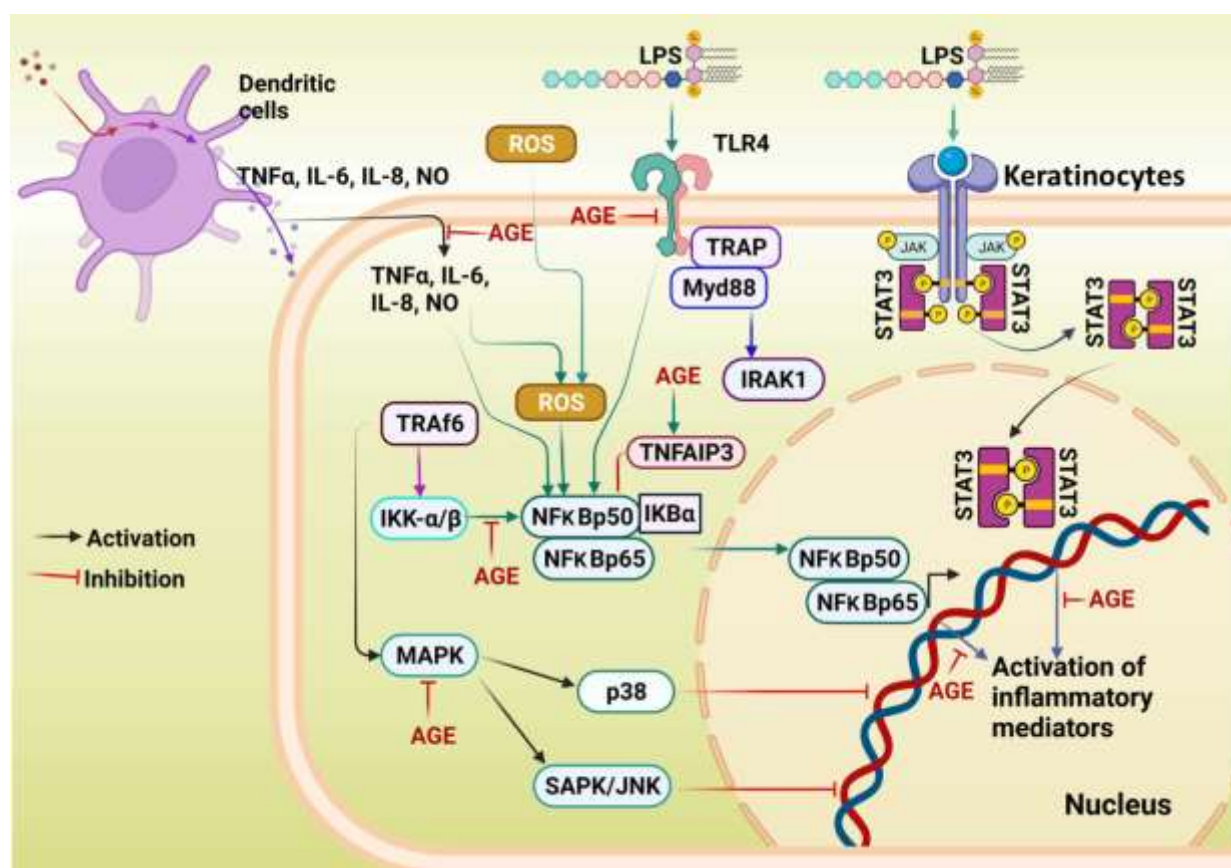


**Figure 1.** Mechanistic action of AGE inside physiological system

Owing to the pharmacological benefits of the potential phytoconstituents present in the AGE, it was thought to develop its topical formulation. However, delivering an extract through a conventional topical formulation has certain limitations such as low bioavailability, poor

penetration and inadequate drug retention. Hence, developing a nanocarrier using nanotechnology can overcome the aforementioned challenges. Structural and physiological changes occur in psoriasis and the skin stratum appears with outer thick scaly patches. Therefore, for the treatment of this disease, the selection of a nanocarrier system that penetrates through the thick scaly lesions is crucial.

Nano-sized carriers help in enhanced permeation across the skin strata, higher drug loading capacity increases drug flux into the skin, also the feasibility to incorporate both hydrophilic and lipophilic drugs (Goyal et al., 2016). Also nanodroplets provide higher interfacial area and ensure increased permeation of the drugs into the skin with an improved drug release profile as well as protection of the drugs from hydrolysis and oxidation (Solans et al., 2005; Thakur et al., 2012).

In the present research work more importance is given to ACA, which being the major component in the ethanolic extract and reported to have multiple therapeutic benefits. However, ACA possesses aqueous degradation which would be a major challenge while developing an aqueous nanoemulsion or nanosuspension. In addition, the advantages of formulating nanoemulsion includes utilization of simple techniques that can be available at any laboratory circumstances, possibility of scaling up, improved physical stability, small-sized droplets having greater surface area providing greater spreadability at the disease site upon topical application, and better solubilization of lipophilic drug in the isotropic mixture of oil, surfactant and co-surfactant (Jaiswal et al., 2015). Indeed, dispersing the lipophilic drug in an oily solution could offer solubility to drug to certain extent, however, use of isotropic mixture of oil, surfactant and co-surfactant as components of nanoemulsion offers better solubility, entrapment as well as stability to the formulation as that of oily solution (Jaiswal et al., 2015; Kadukkattil Ramanunny et al., 2022). The nanosuspensions are usually prepared using top down or, bottom-up technique. Both the techniques have some limitations. Media milling and high-pressure homogenization are the two widely used techniques for formulation of nanosuspension. In both the cases, considerable heat is generated which may cause degradation of heat sensitive active pharmaceutical ingredients (APIs) (Mahesh et al., 2014). In previous studies, mechanical activation at drug particle surfaces has been observed during milling process. Crystal defects due to disordering of the crystal surface and generation of localized amorphous regions have been implicated in increased surface energetics (Heng et al., 2006). Reordering of crystal defects and re-crystallization of amorphous regions has resulted in both physical and chemical instability of processed

materials on storage. Alternatively, the bottom-up process can adversely influence nanosuspension formulations as well by the generation of various unstable polymorphs, hydrates and solvates during processing. These approaches involve the use of solvents which are usually difficult to completely remove (Patravale et al., 2004). Any residual solvent can cause physical and chemical instability of the formulation. Moreover, bottom-up approaches usually result in needle shaped particles due to rapid growth in one direction which influences the physical stability of the nanosuspensions (Rabinow, 2004; Singh et al., 2011b; Verma et al., 2009). Such challenges are not associated with nanoemulsions.

These challenges can be overcome by developing a NANE. NANE could provide protection to ACA as well as other components in AG formulation. In addition to this, it also ensured stability while transporting across /into the skin membrane by entrapping the drug in the emulsion droplets.

In a nutshell, the aim of the study is to develop a NANE loaded with ethanolic extract of AG for the effective treatment of psoriasis in IMQ induced mouse model. In the present study, ACA has also been used as the marker compound for carrying out quantification of extract during characterization and evaluation of nanoemulsion. In addition to this, using ACA as marker will also ensure the efficiency of NANE to protect ACA in the formulation.

# Chapter 2



---

## Review of Literature

---

## Chapter 2

## Review of Literature

## 2.1. Psoriasis and its pathogenesis

Psoriasis is a chronic relapsing skin disease characterized by the clinical and histological skin cell alterations (Sabat et al., 2007). Even though the exact cause is not known, the condition happens to be multifactorial. The pathogenesis of psoriasis involves innate and acquired immune system, activation of the inflammatory pathway, and over-expression of alleles in the genes (Di Meglio and Nestle, 2017). Various mediators involved in the disease progression are shown in **Figure 2** (Ramanunny et al., 2020).

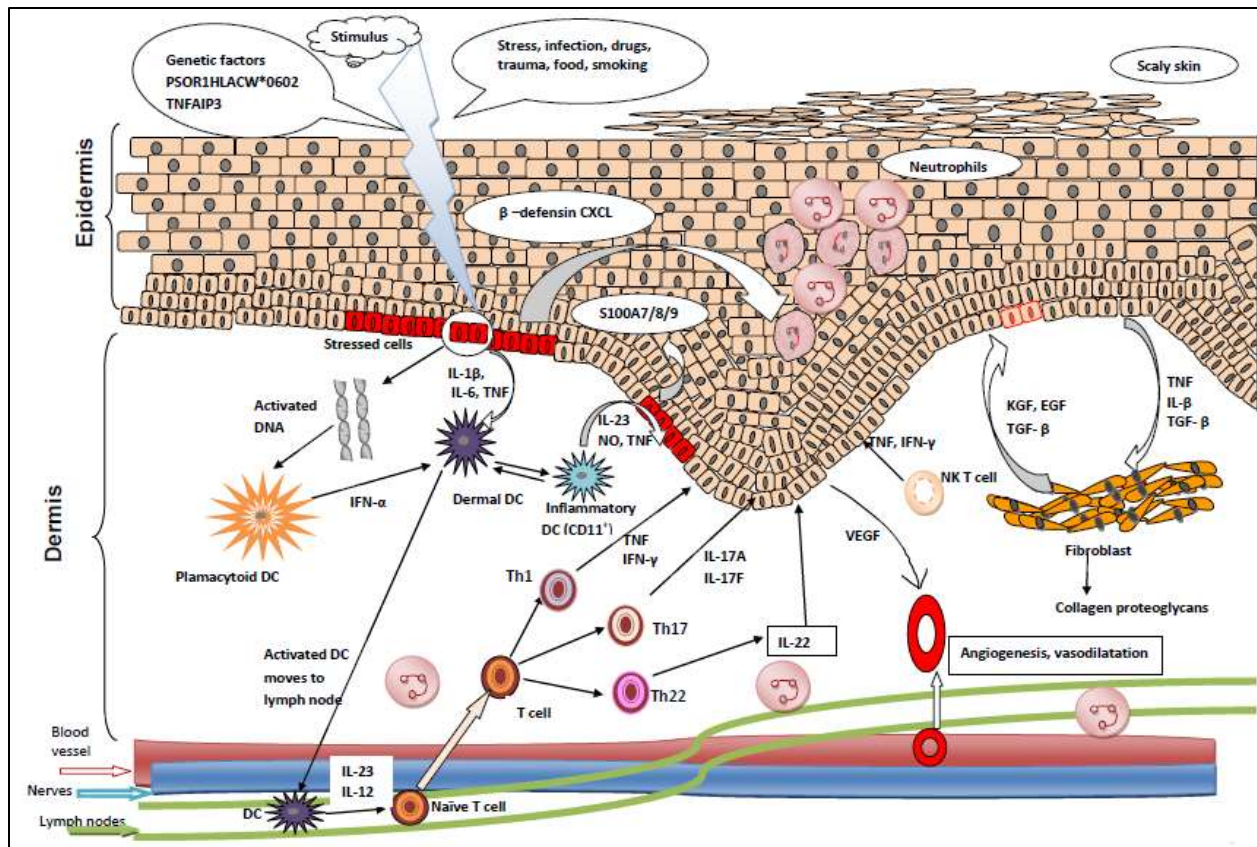


**Figure 2.** Events involved in immunopathogenesis of psoriasis

## 2.1.1. Role of genes and transcription factors

Genetic factors play a crucial role in the pathogenesis of psoriasis which has been well studied by the genome-wide association studies (GWAS). The genome and immune responses are strongly associated with disease development (Boutet et al., 2018). More than 1300 genes are expressed in psoriatic lesions which are regulated by transcription factors that belong to the

signal transducer and activator of transcription (STAT) family, of which STAT-1, STAT-3, and NF- $\kappa$ B transcription factors are more prominent. The activity of STAT1 is regulated by TNF, IL-1, IFNs, IL-20, IL-22, and NF- $\kappa$ B. The activated transcription factors amplify inflammatory cells which further synthesize inflammatory T cells, activate pattern recognition receptors (Toll-like receptors, C-type lectin receptors), heat shock proteins, keratinocytes derived cytokines (platelet-derived growth factor, vascular endothelial growth factor (VEGF), keratinocytes growth factor (KGF) which are the key mediators regulated in hyperproliferation of the cells. The increased level of VEGF contributes towards angiogenesis, dilatation, and high endothelial venule formation in the psoriatic lesion (Dogra and Yadav, 2010; Mahajan and Handa, 2013). The genetic contribution to psoriasis is complex and is influenced by environmental and immune factors. More than 10 susceptible loci are identified of which the common gene is PSOR1 with human leukocyte antigen (HLA)-Cw\*0602 allele (Ramanunny et al., 2020).

Based on the presence or absence of this allele, psoriasis is classified into 2 types (Gudjonsson et al., 2006).

a) HLA-Cw\*0602 positive (Type I): It is early-onset psoriasis that occurs before 40 years of age. It is inherited from the parents and the condition is very aggressive. It accounts for approximately 75% of patients.

b) HLA-Cw\*0602 negative (Type II): It is late-onset psoriasis acquired mostly between 55-60 years of age. Most of them presented stable psoriasis with nail involvement and it is not inherited.

Apart from these, any external stimulus can trigger polymorphism in the alleles of the cytokines which may alter the release of corresponding cytokines. The single nucleotide polymorphism is expressed for cytokines such as TNF- $\alpha$  (rs 1800629 and rs 361525), IL-23 (rs11209026), and IL-12B (rs3212227). Polymorphism in the TNF- $\alpha$  gene (rs 1800629 and rs 361525) may alter the release of its cytokine in healthy subjects. The pro-inflammatory cytokines are overexpressed in the psoriatic lesions (Prieto-Pérez et al., 2013).

## **2.1.2. Role of immune system and inflammatory pathway**

### ***2.1.2.1. Events in innate immunity***

When an external stimulus such as trauma, stress, or infection occurs on the skin barrier i.e. stratum corneum, the effector cells such as neutrophils, plasmacytoid dendritic cells (DCs), and myeloid dendritic cells (CD 11c<sup>+</sup> DCs) present in the keratinocytes are activated. The activated keratinocytes release several cytokines and chemokines especially IL-8, chemokine (C-X-C), motif ligand 1 (CXCL), and some proteins such as S100A7/A8/A9 which create an environment for the neutrophil migration into the epidermal lesional site. On activation, plasmacytoid DCs release interferon (IFN)- $\alpha$  and myeloid dendritic cells release IL-23, IL-20, TNF- $\alpha$ , and inducible nitric oxide synthase (iNOS). These chemical mediators initiate cell hyperproliferation and aberrant keratinocytes differentiation resulting in silvery scaly skin, the characteristic feature of psoriasis (Lowe et al., 2007).

### ***2.1.2.2. Events in acquired immunity***

T-lymphocytes, mainly T-helper (Th) cells are involved in the hyperproliferation of the cells which are mediated by various cytokines such as IFN- $\gamma$  and TNF- $\alpha$  from Th1 cells, IL-17A and IL-17F from Th-17 cells, and IL-22 from Th-22 cells. The peripheral blood monocyte cells are more abundant in the suprabasal keratinocytes. The characteristic feature of this cell is the presence of CCR6, a chemokine receptor with CCL20 ligand. In normal physiological conditions, the level of CCL20 expressed in epidermal keratinocytes and dermal endothelial cells seems to be low but its level is raised in the psoriatic condition by stimulation of the pro-inflammatory cytokines such as TNF- $\alpha$ , IL-1 $\alpha$ , IL-17, and IFN- $\gamma$ . The CCL 20 expressed in the epidermis may recruit more of the CCR6 cell into the inflamed epidermis which enhances the release of IL-17. Hence, the level of CCR6 is elevated both in the skin and blood of the psoriatic patients (Lee and Hwang, 2012).

## **2.2. Mode of inheritance of psoriasis**

The mode of inheritance of psoriasis can be due to genetic, epigenetic, or environmental triggers

**2.2.1. Genetic:** Familial background, an epidemiological investigation among the population, and involvement of HLA and major histocompatibility complex (MHC) account for the genetic background. The pattern of inheritance can be autosomal dominant and autosomal recessive. Further investigation of the psoriatic susceptibility loci can be performed with the help of gene



mapping methods includes linkage analysis and allele sharing method. The linkage method helped in mapping psoriasis susceptibility loci which include PSORS1 on 6p21.3, PSORS2 on 17q, PSORS3 on 4q, PSORS4 on 1cenq21, PSORS5 on 3q21, PSORS6 on 19p, PSOR7 on 1p, and PSORS9 on 4q31. The allele sharing method helped in analyzing the HLA alleles which are responsible for the pathogenesis of psoriasis. The presence of HLA-Cw\* 0602 on chromosome 6p is associated with a more severe and early onset of psoriasis (AlShobaili et al., 2010).

**2.2.2. Epigenetic:** In addition to genetic factors, epigenetic modifications such as DNA methylation play major role in the pathogenesis of psoriasis. The aberrant DNA methylation occurs in the PSOR region due to overexpression of DNA methyltransferase 1 in the skin tissues and peripheral blood mononuclear cells which thereby significantly affect the expression of pathogenic genes. This is the major reason for the histopathological changes in the keratinocytes. (Chandra et al., 2018).

**2.2.3. Environmental triggers:** Apart from the genetic and epigenetic factors, some of the environmental risk factors such as UV exposure, diet, medication, intake of alcohol, smoking has a negative impact on the psoriasis condition. These factors can cause genetic polymorphism or epigenetic changes triggering the release of cytokines such as TNF and IL which activate the immune system and exacerbate the psoriatic condition (Zeng et al., 2017a).

### **2.3. Disease severity and selection of route for treatment**

The early diagnosis and treatment route selection plays a noticeable role in disease progression. The diagnosis of disease severity is based upon the percent surface area covered with psoriatic lesions. The degree of disease severity has been classified into three types as follows (Dogra and Mahajan, 2016)

2.3.1. Mild psoriasis: In this case less than 5% of the body surface area is affected and disease does not alter the patient's quality of life and treatment selected shows minimal risk.

2.3.2. Moderate psoriasis: Mostly 2-20% of the body surface area is involved and disease alters patient's quality of life. However, selected treatment shows no serious risk.

2.3.3. Severe psoriasis: More than 10% of the body surface area is affected and reported with comorbidities that influences the patient's quality of life. However, the selected therapies have not shown satisfactory response.

## **2.4. Topical therapy**

The treatment of skin diseases prefers the usage of topical dosage forms such as ointment, cream, gel, lotion, emulsion, spray etc. (Jindal et al., 2020). Most of the synthetic as well herbal drugs are administered in their conventional dosage forms for the treatment of psoriasis lesions. This can provide intimate contact with the affected area, which ensures more effectiveness and bypasses systemic adverse effects.

### **2.4.1. Synthetic drugs**

Some of the commonly used synthetic drugs in the treatment of psoriasis are as follows (Ramanunny et al., 2020):

**2.4.1.1. Tar preparation (Coal tar):** It was routinely used as dressing regimen along with UVB therapy. The combination of coal tar preparation along with juniper tar was reported to form an adduct with DNA through covalent bonding. This was found to be carcinogenic and its use is diminishing these days (Schoket et al., 1990; Slutsky et al., 2010).

**2.4.1.2. Emollients and moisturizers:** Petroleum jelly, liquid paraffin which can provide protective action, prevent microbial invasion, and reduces transepidermal water loss (Gelmetti, 2009; Nola et al., 2003).

**2.4.1.3. Anthralin (Dithranol):** This is very effective in case of localized plaque psoriasis and scalp psoriasis. But its use is less preferred due to its staining property and occurrence of skin irritation due to its high dose. Mostly it is applied at night time to the site at a concentration of more than 1% w/w and this is considered as short contact anthralin therapy (Runne and Kunze, 1982).

**2.4.1.4. Non-steroidal anti-inflammatory drugs:** Under this category mostly used drug is salicylic acid which has keratolytic and anti-inflammatory action. It is applied topically at a concentration of 2-10% w/w. An intercellular binding of salicylic acid with corneocytes occurs that results in desquamation, swelling, hydration and softening of stratum corneum. This helps in the removal of excessive stratum corneum layer (Fluhr et al., 2008).

**2.4.1.5. Calcineurin inhibitors:** Tacrolimus, sirolimus, and pimecrolimus exerts an inhibitory action on calcineurin phosphatase-nuclear factor of activated-T cell (NFAT), thereby cytokine release is inhibited. The high molecular weight of these drugs makes them unable to penetrate the psoriatic scales. The penetration can be improved by the combination therapy with

keratolytic agents (Reynolds and Al-Daraji, 2002). The most common side effects are the local burning sensation and itching but doesn't account to the withdrawal of therapy.

**2.4.1.6. Retinoids:** Tazarotene, the first synthetically developed vitamin A derivative. It is a prodrug, converted to tazarotenic acid on esterase hydrolysis. The active form will bind to the retinoic acid receptor- $\beta/\gamma$ , which is involved in gene expression modification. This will down-regulate the inflammatory markers, normalize the abnormal keratinocyte proliferation and differentiation (Duvic et al., 1997). It is used in maintenance therapy of stable plaque psoriasis. Localized skin irritation is the only reported side effect which can be neglected by using a combination of topical corticosteroids (Weinstein et al., 2003).

**2.4.1.7. Corticosteroids:** Topical corticosteroids were considered as the gold standard for psoriasis treatment until the introduction of newer drugs such as methotrexate. When applied topically, corticosteroid binds to the glucocorticoid receptors in the cytoplasm. Upon activation, this complex moves into the nucleus and binds to DNA which results in transcriptional changes in mRNA and stimulates synthesis of lipocortin. The formation of lipocortin inhibits the phospholipase A<sub>2</sub> activity and inhibits mRNA that is responsible for IL-1 formation. These events exert anti-inflammatory, immunosuppressant, antiproliferative action and anti-mitogenic effects (Kwatra and Mukhopadhyay, 2018). The selection of a steroidal drug is based on the severity of the condition and potency of steroids. The steroids are grouped into 7 classes based on the potency as shown in **Table 3** (Ramanunny et al., 2020).

**Table 3.** Classification of corticosteroid based on the potency

<b>Class</b>	<b>Potency</b>	<b>Drugs</b>
<b>Class I</b>	Super potent	Clobetasol propionate 0.05% w/w Halobetasol propionate 0.05% w/w
<b>Class II</b>	High potent	Betamethasone dipropionate 0.05% w/w Halcinonide 0.1% w/w
<b>Class III</b>	Upper mid-strength	Fluticasone propionate 0.05% w/w, Betamethasone valerate 0.1% w/w
<b>Class IV</b>	Mid-strength	Mometasone furoate 0.1% w/w
<b>Class V</b>	Lower mid-strength	Fluocinolone acetonide 0.01% w/w
<b>Class VI</b>	Mild	Desonide 0.05% w/w, Fluocinolone acetonide 0.01% w/w
<b>Class VII</b>	Least potent	Hydrocortisone acetate 0.5% w/w - 2.5% w/w

The main side effects of corticosteroids on the epidermis are photosensitivity, atrophy, loss of skin barrier, hypo or hyperpigmentation while on the dermis the effects are delayed wound healing, telangiectasia, and ulceration. The most serious impact of corticosteroid usage is the increased susceptibility to infections and also the rebound flares on withdrawal of the therapy (Mehta et al., 2016).

**2.4.1.8. Vitamin D analogues:** Calcipotriene, Calcitriol, Tacalcitol are the synthetic vitamin D analogues mostly used in conjugation with corticosteroids to reduce its hypercalcemic side effects and to enhance its efficacy (Gerritsen et al., 2001) The antipsoriatic activity is exerted by hindering in the production of S100 proteins especially psoriasin (S100A7) and koebnerisin (S100A15) thereby Th-17 mediated release of cytokine from keratinocytes are reduced (Hegyí et al., 2012).

**2.4.1.9. Pyrimidine antagonist:** 5-Fluorouracil (5-FU), an antimetabolite inhibits the synthesis of DNA and processing of RNA which leads to diminished epidermal proliferation. 5-FU (5% w/w) ointment base was applied topically along with the occlusive dressing for localized resistant plaque psoriasis. This contributes towards rapid epithelialization and prolonged relapse period (Tsuji and Sugai, 1972).

All the aforementioned synthetic drugs in their conventional dosage form have shown challenges related to increased dosing frequency causing side effects as well as decreased patient compliances, limited drug penetration leading to lesser therapeutic efficacy (Jindal et al., 2020). The psoriatic lesions require repeated long term treatment approaches to prevent the recurrence of the condition. However, the possibilities for long term treatment with synthetic drugs are limited due to their side effects. Hence, alternative therapy with herbal drugs is preferred for long term psoriasis treatment. The benefits of herbal drugs have been reported since ancient times, and still, they are being used to treat psoriasis with not many lethal issues. Moreover, there are many reports wherein it is observed that patients are well responded to these therapies. The main advantage of herbal therapy is lesser side effects, multidirectional mechanism of action and cost-effectiveness (Bhuchar et al., 2012; Dabholkar et al., 2021; Deng et al., 2013, 2014).

## **2.4.2. Herbals**

All the traditional systems of medicine utilize herbs in their therapy and provide relatively safer treatment options with diminished side effects. The herbs with medicinal values provide a rationale for treating many chronic external and internal diseases with considerable benefits and reduced toxicity. Now the use of herbs was enormously increased but the development of these plant ingredients into dosage forms needs improvement. Some of the herbal extracts and essential oils which are subjected to pre-clinical antipsoriasis activity are mentioned as follows:

### **2.4.2.1. Herbs for psoriasis**

**2.4.2.1.1. *Nigella sativa*** (black cumin) seeds were extracted with 95% v/v ethanol and its antipsoriasis activity was studied on the mouse tail model using tazarotene gel (0.1% w/w) as the standard therapy. The extract and gel were applied to the respective group of mouse tail once daily (at least 2 h in contact with the skin) for 14 days. The degree of epidermal differentiation and orthokeratosis obtained with extract treatment were significant and equivalent to the standard gel treatment (Dwarampudi et al., 2012).

**2.4.2.1.2. *Rubia cordifolia*** roots were extracted with ethanol and fractioned with hexane, ethyl acetate, n-butanol, and water. Later the ethyl acetate fraction (1% w/v, 2% w/v, 5% w/v) was formulated into a gel and applied to the mouse tail. The treatment with extract gel was compared to standard dithranol gel (1% w/w). The treatment was carried out by applying the gel twice a day, 7 times a week for 4 consecutive weeks. It was reported that 5% w/v ethyl acetate fraction contained gel showed an increase in the granular layer thickness and keratinocytes differentiation which was equivalent to the standard therapy (Lin et al., 2010).

**2.4.2.1.3. *Smilax china*** rhizomes were extracted with methanol and the flavonoid “quercetin” was isolated. The lower dose of methanolic extract was 100 mg/kg and the higher dose was 200 mg/kg). Similarly, for quercetin, it was 25 mg/kg and 50 mg/kg body weight of the rat. The methanolic extract and isolated quercetin were formulated into the cream and applied on the mouse tail and the standard used was retinoic acid cream (0.005% w/w). The treatment regimen was to apply once daily, 5 times a week for 2 weeks. After the treatment, the isolated quercetin showed significant orthokeratosis with changes in the epidermal thickness as compared to the methanolic extract (Vijayalakshmi et al., 2012b).

**2.4.2.1.4. *Thespesia populne*** barks were extracted using ethanol, petroleum ether, butanol, ethyl acetate. From the extracts, three compounds were isolated, represented as TpS-2 (steroid), TpF-1, and TpF-2 (flavanoids). All extracts and isolated compounds were formulated into the cream and applied on the mouse tail model using Retino-A (Tretinoin) cream as the standard. The application regimen of all formulations was once daily, 5 times a week for 2 weeks. After the treatment of parakeratosis, the isolated flavonoid compounds showed more orthokeratosis compared to the extract (Shrivastav et al., 2009).

**2.4.2.1.5. *Cassia tora*** methanolic leaf extract, oil in water cream of methanolic extract in different concentrations (0.05% w/w, 0.1% w/w, and 0.2% w/w) and standard tretinoin (0.05% w/w) were applied to different rat groups that are irradiated on the dorsal skin surface (UV B induced psoriasis). Treatment with both extract and formulated creams exhibited antipsoriatic activity with a significant reduction in epidermal thickness (Singhal and Kansara, 2012).

**2.4.2.1.6. *Kigelia africana*** stem, fruit, and leaf were extracted with methanol and hexane and formulated into an ointment containing 50, 100, 200 mg/mL of each extract and applied on the mouse tail model once daily in the morning with a contact period of 2-3 h for 2 weeks. The methanolic stem extract exhibited the highest antipsoriasis activity among the extracts as it exhibited prominent orthokeratosis in the parakeratotic mouse tail (Oyedeki and Bankole-Ojo, 2012).

**2.4.2.1.7. *Solanum xanthocarpum*** ethanolic stem extract was formulated into gel at different concentrations (2.5% w/w, 5% w/w, 10% w/w) for topical treatment. Also, the extract was administered orally at three different doses (100 mg/kg, 200 mg/kg and 400 mg/kg) by suspending in carboxymethylcellulose (0.5% w/v). Both topical and oral doses were administered to IMQ induced model for evaluating its antipsoriasis potential. The antipsoriasis effect was found to be more prominent with topical treatment (10% w/w) than the oral (200 and 400 mg/kg). The reduction in the scores of PASI and significant inhibition in the levels of biomarkers such as TNF- $\alpha$ , IL-1 $\beta$ , IL-6 and IL-17 demonstrated enhanced therapeutic efficacy of extract in treating psoriasis (Parmar et al., 2017).

**2.4.2.1.8. *Annona squamosa*** seeds were macerated with petroleum ether to obtain *Annona squamosa* seed oil (ASO). The antipsoriasis activity of ASO was demonstrated in oxazolone induced psoriasis model and results of histological examination was compared with standard clobetasol propionate (0.05% w/w) cream. A marked reduction in the erythema, edema and ear

thickness was observed with percentage efficacy of 82.0% for ASO and 92.50% clobetasol propionate cream treatment. This non-significant difference in the results proved the potential of ASO in reducing the severity of psoriasis (Bhoir et al., 2019).

**2.4.2.1.9. *Pongamia pinnata*** hydroalcoholic leaf extract was formulated into a gel. The effectiveness of the formulated gel to treat psoriasis conditions was demonstrated in IMQ induced model. The reduction in the epidermal thickness and PASI scoring confirmed the recovery from psoriasis condition. However, the histopathological studies demonstrated the ability of formulated gel to regain tissue (greater collagen content, keratinization, angiogenesis, fibroblast proliferation) in comparison to the control group (Wadher et al., 2021).

The herbal formulations which are under clinical trials (Herman and Herman, 2016) are as follows:

- a) *Mahonia aquifolium* extract 10% w/w cream
- b) *Hypericum perforatum* 5% w/w ointment
- c) Refined *Indigo naturalis* extract in oil
- d) *Indigo naturalis* (1.4% w/w) ointment
- e) Aloe vera (70% w/w aloe mucilage) cream
- f) Capsaicin cream (*Capsicum frutescens*)
- g) *Curcuma longa* hydroalcoholic extract in microemulgel

The major challenge associated with herbal extracts is the identification of particular phytoconstituents that are responsible for the said activity. This is the major reason for the dominance of synthetic treatment over phytotherapy. However, the exploration of phytoconstituents offers the benefits of proper characterization and evaluation for pharmacological activities. Some of the phytoconstituents that have been reported for antipsoriasis activity during their cell line, preclinical, and clinical studies are reported in **Table 4**.

**Table 4.** Isolated phytoconstituents with its mode of action

<b>Chemical component</b>	<b>Evaluation (cell line / preclinical/clinical)</b>	<b>Mode of action</b>	<b>References</b>
<b>Psoralen [8-methoxy psoralen]</b>	Clinical studies	Inhibition of epidermal DNA synthesis and thereby cell division	(Briffa and Warin, 1979)
<b>Camptothecin</b>	Preclinical studies (Mouse tail model)	Inhibition of proliferation and induction of differentiation	(Huang and Lin, 1996)
<b>Hypericin</b>	Cell line studies (Mouse epithelial)	Photosensitizer ,induces desquamation and erosions	(Kamuhabwa et al., 1999)
<b>Fumaric acid esters</b>	Clinical studies	Inhibition of T cell activity via induction of apoptosis	(Harries et al., 2005)
<b>Gossypol (-)</b>	Cell line studies (Keratinocytes)	Anti-proliferative and antioxidant activity	(Dodou et al., 2005)
<b>Koumine</b>	Preclinical studies (Mouse tail model)	Inhibition of epidermal cell proliferation, promote the formation of granular cells, decrease serum IL-2 levels	(Zhang et al., 2005)
<b>Curcumin</b>	Clinical studies	Selective phosphorylase kinase inhibitor, reducing inflammation through inhibition of NFκB	(Traub and Marshall, 2007)
<b>Artesunate</b>	Cell line studies (Keratinocytes)	Antiproliferative action by regulating the expression of CXCR2 and enhanced secretion of TGF β1	(Jin et al., 2007)
<b>iso-Camptothecin</b>	Cell line studies (Keratinocytes)	Inhibits keratinocyte proliferation, induces apoptosis and downregulates telomerase	(Lin et al., 2008a)
<b>Embelin</b>	Preclinical studies (TPA induced mouse ear edema)	Inhibition of IL-1β and TNF-α and subsequent blockade of leukocyte accumulation	(Kumar et al., 2011)
<b>Galangin</b>	Preclinical studies (IMQ induced mouse model)	Inhibition of NF-κB, ↓ pro-inflammatory cytokine level and ↑ anti-inflammatory cytokine level, restored level of antioxidant markers	(Sangaraju et al., 2021)

#### 2.4.2.2. Oils

Among various types of oils, essential oil is being commonly used in aromatherapy and for inhalation therapy. But it can also be used as a complementary (second line) therapy for psoriasis. Mostly these oils provide soothing effects on the skin with some therapeutic activities.



**2.4.2.2.1. Tea tree oil (TTO):** TTO is obtained by steam distillation of the leaves and terminal branchlets of *Melaleuca alternifolia* (Myrtaceae). It contains terpinen-4-ol which has potent anti-inflammatory properties. It prevents infection of the affected area, stimulates the immune system and provides support to maintain healthy skin. It also exerts antibacterial, antifungal, antiviral and antipsoriasis activities (Carson et al., 2006; Pazyar and Yaghoobi, 2012).

**2.4.2.2.2. Rose geranium oil:** It is obtained by steam distillation of leaves and stem of *Pelargonium graveolens* belongs to Geraniaceae family. The major constituents are citronellol (29.13%), geraniol (12.62%), and citronellyl formate (8.06%). It possesses anti-inflammatory, antidepressant, antiseptic, wound-healing, antibacterial, and antifungal activities (Boukhatem et al., 2013).

**2.4.2.2.3. Lavender oil:** It is obtained by the steam distillation of flowers of *Lavendula angustifolia* belongs to Lamiaceae family. The major components include linalyl acetate and linalool. The essential oil has shown rapid absorption through the skin and exhibited antibacterial, antifungal and cytotoxic effects. The cytotoxic effect can be used in psoriasis treatment (Cavanagh and Wilkinson, 2002; Prashar et al., 2004; Rai et al., 2020).

**2.4.2.2.4. Kalonji oil (black seed oil):** It is obtained from the seeds of *Nigella sativa* belonging to Ranunculaceae family. The oil was reported to possess anti-inflammatory, antioxidant and immunostimulatory activities. The topical application of this oil on IMQ induced psoriasis mouse model has shown inhibition of inflammation and improvement in the epidermal and dermal skin layers (Okasha et al., 2018). These histopathological changes highlight the ability of this oil to be used as adjuvant therapy for psoriasis. In another study, a combination of Tacrolimus and Kalonji oil in nanoemulgel formulation has shown a significant reduction in the level of serum cytokines indicating the efficacy of the above-said combination therapy (Sahu et al., 2018).

**2.4.2.2.5 Matricaria recutita (chamomilla) oil:** It is obtained from the flowers of *Matricaria recutita* Linn belonging to Asteraceae family. The oil was reported to contain terpenoids,  $\alpha$ -bisabolol and its oxides, azulenes such as chamazulene. Chamazulene has shown anti-inflammatory activity by inhibiting lipoxygenase and leukotriene B<sub>4</sub> as well as shown antimicrobial activity against *Staphylococcus* and *Candida* species (Singh and Tripathy, 2014). Moreover, the  $\alpha$ -bisabolol has also shown anti-inflammatory activity in carrageenan-induced rat paw edema model (Murthi et al., 2012; Petronilho et al., 2012).

**2.4.2.2.6. Medium chain triglycerides (MCT):** It is colorless/ pale yellow liquid oil synthesized by esterification reaction of the medium-chain fatty acids that are obtained from coconut oil or palm oil with glycerol. Chemically, it is a mixture of caprylic acid (C8) and capric acid (C10) in the ratio of 60:40 (v/w). It has been widely explored as carrier oil along with essential oils due to its soothing, conditioning, hydrating and protective action. Hence, it has been used in aromatherapy as well as in massage therapy. However, its anti-inflammatory activity (Yu et al., 2019), antioxidant activity (Li et al., 2015), antimicrobial activity (Lavery et al., 2015), wound healing (Magalhães et al., 2008), and antibacterial activity (Petschow et al., 1996) are well explored. These therapeutic effects prove its potential in treating skin disease.

Apart from these mentioned herbs and oils, still, a number of herbal components are reported for psoriasis. Among them, some have been explored well and some are yet to be explored. However, the researchers are exploiting these herbal extracts, isolated phytoconstituents and essential oils into dosage forms.

The most widely explored herbal resource is *Curcuma longa* (Turmeric). The major phytoconstituent is curcuminoids that inhibit the expression of VEGF and iNOS, suppression of IL-1 $\beta$ , IL-6, TNF- $\alpha$ , inhibition of NF- $\kappa$ B and mitogen-activated protein kinase (MAPK) pathway in keratinocytes (Chen and Zhang, 2004; Cho et al., 2007). Thus, turmeric microgel has been developed and subjected to clinical trial studies (Sarafian et al., 2015). Similarly, *Indigo naturalis* contains indirubin which inhibited the expression of IL-17 A and JAK3/STAT-3 in the psoriasis model (Xie et al., 2018). In one of the research studies, *Indigo naturalis* ointment containing 1.4% w/w indigo and 0.16% w/w of indirubin was subjected to a clinical trial for the treatment of recalcitrant psoriasis. Approximately 74% of the treated patients have shown a significant ( $p < 0.01$ ) reduction in the percentage of psoriasis plaque area (38%) in comparison to vehicle ointment (Lin et al., 2008b). Later, *Indigo naturalis* containing oil named “Lindioil” was also found to be effective in nail psoriasis. A marked reduction in the nail psoriasis severity index was observed after 12 weeks of treatment with Lindioil (Lin et al., 2014). Similar to these herbals, an emerging plant species belonging to Zingiberaceae family is AG.

AG rhizomes have been extensively used in traditional systems of medicine as anti-inflammatory, antibacterial (Latha et al., 2009b), antifungal (Jantan et al., 2003) agents and for the treatment of various ailments such as bronchitis, rheumatism, dysentery and fever (Namsa et

al., 2009). These activities are contributed by the phytoconstituents present in the extract. The reported phytoconstituents present in the extract are ACA, 1'-acetoxyeugenol acetate, p-coumaryl diacetate, palmitic acid, 9-octadecanoic acid, eugenol, galangin, sesquiphellandrene, p-hydroxyl cinnamaldehyde, chrysin, ellagic acid and gallic acid (Kaur et al., 2010; Li et al., 2020a; Nampoothiri et al., 2015; Oonmetta-aree et al., 2006; Sangaraju et al., 2021). Among these components, ACA, chemically a phenylpropanoid is reported as a potent molecule with numerous pharmacological activities.

Some noteworthy contributions from previous research work reporting its therapeutic activities are the protective role of ACA as gastroprotective (Matsuda et al., 2003b) and xenobiotic (Tanaka et al., 1997). Later on, several pharmacological activities such as antitumor (Baradwaj et al., 2017) , antiobesity (Narukawa et al., 2010), antimicrobial (Phongpaichit et al., 2006), antiallergic (Matsuda et al., 2003a), antidementia (Kojima-Yuasa et al., 2016) and antioxidant (Mahae and Chaiser, 2009) activities have been demonstrated.

All the above mentioned therapeutic activities highlight the importance of AGE and its phytoconstituents. Salee *et al.* reported the antipsoriasis activity of ethanolic extract of AG in HaCaT cell lines. A reduction in the expression of colony stimulating factor (CSF)-1 and NF- $\kappa$ B inferred its possibilities in treating psoriasis conditions (Salee et al., 2011). This study also emphasized the presence of ACA and its ability to ameliorate psoriasis. Several research studies have reported the anti-proliferative role of ACA. Ito *et al.* demonstrated the induction of apoptosis in myeloid leukemia cells through mitochondrial and Fas-mediated dual mechanism and with the production of reactive oxygen species (Ito et al., 2004). However, this plant has not been explored to its best even though a number of pharmacological activities have been reported.

Considering the reported activities of AG, further exploitation of the herbal extract into a dosage form can lead to translational research in psoriasis treatment.

## **2.5. Herb of choice - AG**

AG is a perennial herb that is a native of Indonesia widely distributed in the southern region of Western Ghats in India. The most commonly used parts of the plant are rhizomes and seeds. The rhizomes are cylindrical branched and prominent with round warts and fine annulations.

Externally, it is reddish-brown in colour and internally orangish-yellow. It gives a pleasant aromatic odour with a sweet and pungent taste.

### **2.5.1. Taxonomy of the plant**

The taxonomical classification of the plant AG is presented below in **Table 5** (Kress et al., 2005).

**Table 5.** Taxonomical classification

<i>Alpinia galanga</i>	
Kingdom	Plantae
Phylum	Magnoliophyta
Class	Liliopsida
Order	Zingiberales
Family	Zingiberaceae
Subfamily	Alpinioideae
Tribe	Alpiniaiea
Genus	<i>Alpinia</i>
Species	<i>galanga</i>

### **2.5.2. Phytochemistry and bioactive components**

Phytochemicals are secondary metabolites that are synthesized through various biosynthetic pathways. The variations in geographical features, climatic conditions and cultivation procedures have shown distinction in the phytochemical composition of the plant. The phytochemical investigation of various parts of AG has been reported for the presence of different classes of compounds such as phenolic compounds and terpenes (Namdeo and Kale, 2015).

Phenolic compounds are biosynthesized by the shikimate pathway (Santos-Sánchez et al., 2019). Some phenolic compounds reported in AG are categorized as flavonoids eg. galangin, kaempferol, kaempferide (Tungmunnithum et al., 2020), phenylpropanoids such as ACA, 1'-acetoxyeugenol acetate, 1'-hydroxychavicol acetate, lignans e.g. galanganal, galanganols A, B and C (Morikawa et al., 2005). The next class of compound present in AG rhizomes is terpenes, which is biosynthesized by the mevalonate pathway (Dubey et al., 2003). Mostly, terpenes are

found in the essential oil of AG, and they are chemically present as monoterpenes, sesquiterpenes and diterpenes such as 1,8-cineole,  $\alpha$ -pinene,  $\beta$ -pinene, fenchyl acetate,  $\beta$ -bisabolene,  $\beta$ -carophyllene, and  $\beta$ -selinene. These compounds are the contributors of aroma, hence widely used in food and medicinal industries (Chudiwal et al., 2010).

Several techniques have been explored for extraction and/or chemical profiling of phytochemicals in AG which include conventional methods and advanced/modern techniques. Most widely used conventional method for extraction utilizes solvents of different polarity. Non-polar solvents are used for extraction of lipophilic bioactive components and polar solvents for hydrophilic bioactive components (Vlietinck et al., 2006). Some of the extraction methods used are maceration, percolation, heat assisted reflux, soxhlet extraction, microwave-assisted extraction (MAE), etc. After completion of extraction with the selected method, the compounds are separated and identified by advanced techniques, which include chromatography such as thin layer chromatography (TLC), high performance liquid chromatography (HPLC), high performance thin layer chromatography (HPTLC), GC, column chromatography (CC) and spectroscopy such as ultraviolet-visible (UV-Vis) spectroscopy, infrared spectroscopy (IR), nuclear magnetic resonance (NMR), MS and/or combination of chromatographic-spectroscopic techniques includes GC-MS, LC-MS, LC-MS/MS, ultra-high performance liquid chromatography coupled with quadrupole/time-of-flight mass spectroscopy (UPLC-QTOF-MS) (Sasidharan et al., 2011).

Huang *et al.* used similar maceration procedure using methanol as the solvent for extraction. After obtaining viscous methanolic residue, CC was done using silica gel as stationary phase and mixture of dichloromethane: methanol as mobile phase to separate out various fractions present in the extract. A total of 8 fractions were obtained, which were re-fractionated and purified using various solvent system such as hexane and acetone (at varying ratio of 100:1, 90:1, 70:1) and dichloromethane: methanol (50:1). This led to isolation of 19 compounds from the extract. Among them, a new phenylalkanoide, 1-dehydro-3-hydro[2]-gingerdione was identified and structural elucidation was done with  $^1\text{H-NMR}$ ,  $^{13}\text{C-NMR}$  and IR spectroscopy. Other 18 known compounds reported were 3 sesquiterpenes (zerumbone, zerumbone epoxide,  $\alpha$ -humulene), 5 benzenoids (p-hydroxybenzoic acid, vanillin, vanillic acid, syringaldehyde, ferulic acid, 2 steroids ( $\beta$ -sitosterone, stigmasta-4,22-di-3-one), 8 flavonoids (kaempferol-3-O-methylether,

kaempferol-3,4'-O-dimethylether, kaempferol-3-O-rhamnoside, kaempferol-3-O-(2''-O-acetyl) rhamnoside, kaempferol-3-O-(3''-O-acetyl) rhamnoside, kaempferol-3-O-(4''-O-acetyl) rhamnoside, kaempferol-3-O-(2'',4''-O-diacetyl) rhamnoside, kaempferol-3-O-(3'',4''-O-diacetyl) rhamnoside (Huang et al., 2018).

Similarly, Baradwaj *et al.* reported maceration along with continuous shaking procedure. The finely powdered rhizomes were soaked with hexane and kept in a shaker for 24 h. After careful filtration, the filtrate was concentrated on rotary evaporator to obtain a residue and re-dissolved the residue in methanol and centrifuged to collect the supernatant. Later, ACA (0.378% w/w) was identified in the methanol soluble component of hexane extract by HPLC analysis (Baradwaj et al., 2017). Zhou *et al.* also used maceration with a shaking procedure to extract out AG rhizome's components. Similar procedure was adopted with only change in the selected solvent. Instead of hexane, 80% v/v ethanol was used to soak powdered rhizome and kept it in shaker for 24 h at room temperature. After 24 h, mixture was centrifuged to collect the supernatant. The supernatant was concentrated using rotary evaporator. The residue was freeze dried to obtain powder which was dissolved in water and successively partitioned with solvent of different polarity such as n-hexane, chloroform, ethyl acetate, n-butanol and ethanol. However, in the study only hexane and chloroform fraction were later subjected to normal phase CC followed by reverse phased HPLC. HPLC analysis of hexane and chloroform fractions identified 6 peaks and 8 peaks respectively. Later, their analysis using UPLC-QTOF-MS confirmed that the major components in the fractions are hydroxycinnamaldehyde, cinnamaldehyde, coumaryl alcohol and ACA (Zhou et al., 2021).

Latha *et al.* carried out cold percolation of AG rhizome with acetone for 12 h and the procedure was repeated 5 times. Each time the filtrate was concentrated and finally reddish syrupy extract was obtained. CC of the syrupy extract was done by gradient elution technique with hexane-acetone mixture and eluted out the bioactive compounds. The isolated fractions were purified, identified and characterized by HPTLC, GC, <sup>1</sup>H NMR, <sup>13</sup>C NMR. The obtained compound was confirmed as ACA (3.26%) (Latha et al., 2009a). Similar to this study, another researcher carried out percolation of AG rhizomes with hexane for 7 days. The residue obtained after hexane based extraction was subsequently percolated with ethyl acetate, acetone and methanol. Among these solvent fractions, acetone fraction was analyzed by CC, TLC and NMR techniques. Their results confirmed that the eluted compound was p-hydroxycinnamaldehyde (Phitak et al., 2009).

Powdered AG rhizome was sequentially extracted using non-polar solvents, starting with hexane, followed by chloroform and ethyl acetate using soxhlet extractor for 48 h. The obtained extract was concentrated using rotary evaporator. The isolation and identification of individual components in the fractions was done by vacuum LC using silica gel G as stationary phase and hexane/ethyl acetate (0-100%, v/v gradient elution) as mobile phase. Several fractions were obtained from each extract using different solvent systems and identification of components in the individual fraction was done by semi-preparative reverse phased HPLC. In hexane fraction, methyl eugenol (0.5%), p-coumaryl diacetate (0.5%), ACA (1.3%), p-coumaryl diacetate (0.2%), 1'-acetoxyeugenol acetate (0.5%), trans-p-acetoxycinnamyl alcohol (0.2%) were isolated. Chloroform fraction gave isolation of 3 compounds, trans-3,4-dimethoxycinnamyl alcohol (1.07%), p-hydroxybenzaldehyde (0.35%), p-hydroxycinnamaldehyde (0.57%), whereas trans-p-coumaryl alcohol (0.4%), galangin (0.85%), trans-p-coumaric acid (1.16%), and galanganol B (2.5%) were isolated from ethyl acetate fraction (Kaur et al., 2010).

All the above said extraction process has reported various phytoconstituents with different solvents. The yield of the phytoconstituents and solvents used for extraction plays a significant role in pharmaceutical product development. Hence, solvent selection is given more importance. Class III solvents are accepted in pharmaceuticals as they are non-toxic solvents showing no health hazards (Kay et al., 2021). Hence, phytoconstituents extracted out using non-toxic solvents were focused further and their beneficial role in various pharmacological activities is considered.

### **2.5.3. Pharmacological activities of AGE**

#### **2.5.3.1. Antioxidant**

A study by Juntachote and Berghofer indicated antioxidant potential of AGE at neutral pH having the capacity to maintain their heat-stability at 80 °C for 1 h. The extract exhibited superoxide anion scavenging activity with strong reducing power in a concentration-dependent manner. These activities were reported due to various antioxidants present in rhizome extract such as vitamin C (7.87 mg %), vitamin E (0.0042 mg %), total carotenes (0.64 mg %), total xanthophylls (1.05 mg %), tannins (17.7 mg %) and phenolics (63.4 mg %). This study also indicated the potential of ethanolic extract of AG to act as radical scavenger as well a lipooxygenase inhibitor. The lipooxygenase inhibition was exerted through Fe<sup>2+</sup> inhibitory activity

of AGE. The extract interacted with ferric ion at the active site of the enzyme leading to enzyme inactivation (Juntachote and Berghofer, 2005). Hydro-ethanolic (50%) extract has shown antioxidant activity with highest 1,1-diphenyl-2-picrylhydrazyl (DPPH) free radical scavenging ability and oxygen radical absorbance capacity (ORAC) value in comparison to its water extract and essential oil. The IC<sub>50</sub> value of ethanolic extract was 10.66 mg/mL and reported with highest concentration of total phenolic content (TPC) (31.49 mg gallic acid equivalent (GAE)/g) and flavonoids (13.78 mg CE/g). Among the phenolic compounds, the major antioxidant component in ethanolic extract was reported as ACA (10.56 mg/g extract) and catechin (1.74 mg/g extract) (Mahae and Chaiseri, 2009). In another study, methanolic leaf extract of AG has indicated TPC of 392 ± 50 mg/GAE/100 g and ascorbic acid equivalent antioxidant activity (AEAC) of 90 mg AA/100g by Folin-Ciocalteu and DPPH radical-scavenging assays respectively whereas rhizomes have lesser TPC of 214 mg GAE/100 g and higher AEAC of 168 mg AA/100 g. Also, Ferrous ion chelating (FIC) activity of AG leaves were 20 times higher than that of rhizomes (Chan et al., 2008).

Further studies were carried on methanolic leaves and rhizomes extract, in which crude methanolic extract leaves reported higher TPC than in rhizomes whereas AEAC values were found comparable for both the extracts. Later, non-polymeric phenolic content (NPC) and polymeric tannin (PT) fractions were separated from their crude leaves and rhizomes extract and their TPC and AEAC activity were evaluated. The percentage yield of NPC fractions in both leaves and rhizomes were higher (66-74%) than that of PT fractions (0.5-6.0%), suggesting phenolic compounds as the major components. However, PT fraction from AG rhizome reported highest TPC (155 ± 6 mg GAE /100 g of extract) and AEAC (143 ± 6 mg AA/g of extract) (Chan et al., 2011). In another study, the antioxidant activity of ethanolic extract of AG rhizomes was demonstrated by modified β-carotene bleaching method (coupled oxidation of β-carotene and linoleic acid) which was found to be 70.3%. Higher antioxidant activity of extract was correlated to higher TPC (40.9 mg GAE/g) in the extract (Mayachiew and Devahastin, 2008). Nampoothri *et al.* also demonstrated the correlation of phenolic content in AG for antioxidant activity. LC-MS/MS technique was used for identification and quantification of phenolic compounds in AG and later demonstrated their free radical quenching activity. In this study, TPC of AG was recorded as 15.50 ± 0.95% and LC-MS/MS technique identified two major phenolic compounds i.e. gallic and ellagic acids. Further, free radical scavenging activity of the AGE was determined



by DPPH, 2,2'-azino-bis(3-ethylbenzothiazoline-6-sulfonate) (ABTS) and total antioxidant activity (TAA) assay methods and  $IC_{50}$  values obtained from each methods are recorded as  $21.26 \pm 0.2 \mu\text{g/mL}$ ,  $25.54 \pm 0.1 \mu\text{g/mL}$  and  $11.60 \pm 0.1 \mu\text{g/mL}$  respectively (Nampoothiri et al., 2015). The study concluded that the phenolic compounds in AG have free radical scavenging activity against oxygen species ( $O_2$ ,  $H_2O_2$ ,  $OH$ ) and nitrogen species ( $NO$ ,  $NO_2$ ).

### **2.5.3.2. Anticancer activity**

Cytotoxicity study of ethanolic extract of AG rhizome on normal fibroblast cell line (NIH-3T3 cells) has shown low cytotoxic effect in normal cells compared to the cancer cells.  $IC_{50}$  of ethanolic extract in NIT-3T3 cells at 24 and 48 h were  $620.5 \mu\text{g/mL}$  and  $666.6 \mu\text{g/mL}$  respectively (Sandra et al., 2017) whereas at  $100 \mu\text{g/mL}$  concentration,  $69 \pm 3.91\%$  of the PC-3 cell (prostate cancer cell line) underwent apoptosis showing higher cytotoxic effect on cancer cells (Suja and Chinnaswamy, 2008). Similarly, cytotoxic and apoptotic effect of ethanolic extract of AG rhizome in cultured human breast carcinoma cell line (MCF-7) and non-malignant cell line (MRC-5) were evaluated after three consecutive application of the extract. A dose-dependent decrease in cell viability and morphological changes in malignant cells were observed.  $IC_{50}$  of MCF-7 was recorded as  $400 \pm 11.7$  and  $170 \pm 5.9 \mu\text{g/mL}$  at 24 h and 48 h respectively. However, no morphological changes or change in cell viability were observed for MCF-5 cell line (Samarghandian et al., 2014b). *In vivo* anticancer activity of ethanolic extract of AG root (red galangal) was demonstrated in breast adenocarcinoma cells transplanted in female strain of C3H mice. At higher oral dose of  $675 \text{ mg/kg}$  of body weight, AGE has inhibited cell proliferation and decreased tumor volume suggesting its anticancer activity in the inoculated breast carcinoma cells (Asri and Winarko, 2016). In another study ACA extracted from AG root exerted antiproliferative activity by inhibiting NF- $\kappa$ B activation. It also suppressed the expression of cyclin D and interrupted G1 to S phase transition in the cell cycle which subsequently resulted in tumor volume reduction (Sethi et al., 2008).

Nur *et al.* evaluated chemotherapeutic and anti-ageing potential of ethanolic extract of AG on 4T1 (metastatic breast cancer) cells and NIH-3T3. The cytotoxicity and migratory effects on 4T1 were analyzed by 3-(4,5-dimethylthiazol-2-yl)-2,5-diphenyltetrazolium bromide (MTT assay) and scratch wound healing cell migration-based assay respectively and anti-ageing effect on NIH-3T3 was analyzed by senescence-associated beta (SA- $\beta$ ) galactosidase (Nur et al., 2020).

AGE exhibited cytotoxicity at IC<sub>50</sub> of 135 µg/mL on 4T1 cells but no cytotoxicity was observed in NIH-3T3 fibroblast cells. This confirmed the selective cytotoxicity towards 4T1 cells and enhanced cytotoxicity of AGE (100 µg/mL) was reported when used in combination with doxorubicin (100 nM). Cell cycle profiling showed G2/M cell accumulation with AG alone whereas combination of AG (100 µg/mL) and doxorubicin increased the cell population in G2/M phase (increase in senescent cells) but caused no apoptosis. AGE stimulated cell cycle arrest with induction of senescence in 4T1 cells alone with increase in reactive oxygen species level. In addition to this, AGE has shown anti-metastasis activity by suppressing matrix metalloproteinase (MMP)-9 expressions and also inhibited the migration of 4T1 cells. However, AGE on NIH-3T3 produced anti-senescence effect with no interference on reactive oxygen species suggesting its potential as anti-ageing agent (Nur et al., 2020)

Chrysin, a flavonoid isolated from AG rhizomes was found with selective cytotoxicity towards human lung cancer cells and murine lymphoma cells with a sparing effect on normal fibroblast cells and lymphocytes. Induction of late stage apoptosis was observed in a dose and time dependent manner by the activation of caspase-3, poly adenosine diphosphate (ADP) ribose polymerase and Bcl-2. During the cell cycle analysis, the accumulation of S-phase cells has been reported due to G1/S phase transition blockade. During *in vivo* antitumor activity studies carried out in Dalton's lymphoma ascites (DLA) mice, it was reported that there is a reduction in tumor volume, hence increased the lifespan of mice (52.6%) at a dose of 1.3 mg/kg. A synergistic effect of chrysin and cyclophosphamide in chemoprotection was also observed. The study suggested about the possibility for dose reduction of cyclophosphamide when used in combination with chrysin (Lakshmi et al., 2019). Similar to this study, anti-metastatic property of galangin was reported due to the inhibition of cell migration and MMP expression (Chien et al., 2015).

### **2.5.3.3. Anti-inflammatory activity**

Several *in vivo* anti-inflammatory models have been used to demonstrate anti-inflammatory potential of AGE and its essential oils. Among these models, carrageenan-induced paw edema model has shown involvement of various inflammatory mediators in its developmental stages. Hence, it is widely used to access the anti-inflammatory activity of AG. In one of the studies, carrageenan induced pleurisy rats were orally treated with 2 selected doses (250 mg/kg, 500 mg/kg) of AG rhizome extract as well as indomethacin as standard (10 mg/kg). After 4 h of

treatment, extract treated group has shown 40.90% and 50.0% inhibition of paw edema where standard indomethacin treated group has shown 75% inhibition of paw edema (Sharma et al., 2015). Similar to this study, lower doses of ethanolic extract of AG rhizome extract (100, 200, and 400 mg/kg) and indomethacin (10 mg/kg) also exhibited anti-inflammatory activity in carrageenan-induced pleurisy rat model. The volume of pleural exudates and leukocyte influx was significantly decreased in both AG and indomethacin treated groups. The percentage inhibition of inflammation after AG treated group and indomethacin standard groups were 69.6% and 78.4% respectively. The results of these studies revealed that AG exerts anti-inflammatory activity similar to that of indomethacin by partly preventing prostaglandin biosynthesis via cyclooxygenase (COX) blockade (Subash et al., 2016).

Recently, George *et al.* investigated molecular anti-inflammatory mechanism of AG ethanolic extract in lipopolysaccharide (LPS) stimulated RAW 264.7 cells. Pretreatment with AGE blocked LPS induced activation of toll like receptor-4 specifically through the inhibition of NF- $\kappa$ B translocation and JAK/STAT. AGE also down regulated the release of pro-inflammatory mediators such as IL-6, TNF, NO, reactive oxygen species and also inflammatory enzymes such as iNOS, COX-2, MMP-9. It is important to notice that along with down-regulation of these mediators, stimulation of anti-inflammatory mediators such as IL-10 has occurred. It is also reported that pretreatment with AGE particularly inhibited LPS induced phosphorylation of Janus kinase, P38, I $\kappa$ B- $\alpha$  and STAT. These cascades of up-regulation and down-regulation play a significant role in anti-inflammatory activity. Polyphenolic compounds in AGE might be responsible for exerting anti-inflammatory activity through multiple molecular pathways (George et al., 2021).

#### **2.5.3.4. Antipsoriasis activity**

*In vitro* antipsoriasis effect of ethanolic extract of AG rhizomes was carried out in HaCaT keratinocyte cell lines. The cell lines were pretreated with pro-inflammatory cytokines, TNF- $\alpha$  (10 ng/mL) and IFN- $\gamma$  (10 ng/mL) followed by treatment with extract. Further these were evaluated for the expression of NF- $\kappa$ B signaling biomarkers by semi-quantitative reverse transcriptase-polymerase chain reaction and reporter gene assay. Ethanolic extract of AG reported IC<sub>50</sub> at 6.30  $\mu$ g/mL and reduced the expression of NF- $\kappa$ B signaling biomarkers via increased expression of TNFAIP3 and decreased mRNA expression of CD40, CSF-1 and NF-

$\kappa$ B2 (Saelee et al., 2011). AG rhizomes contain ACA which has been reported to have NF- $\kappa$ B inhibition (Ito et al., 2005). The down-regulation of NF- $\kappa$ B pathway by the extract reflected its potential in treatment of diseases involving inflammation and hyperproliferation like psoriasis. Similarly, galangin demonstrated antipsoriasis activity on IMQ induced psoriasis-like inflammation in BALB/c mice. Application of anionic emulsifying cream of galangin 1% w/w and 2% w/w for six consecutive days has shown marked reduction in the IMQ induced PASI, skin and ear thickness, dose-dependent decrease in circulatory neutrophils, lymphocytes and monocytes, decrease in myeloperoxidase level, restoration of anti-oxidative enzyme level by regulating nuclear factor-erythroid 2 related factor 2 (Nrf2)/ heme oxygenase-1 signaling, decreased production of pro-inflammatory cytokines such as TNF- $\alpha$ , IL-6, IL-17, IL-23, IL-1 $\beta$  whereas increased anti-inflammatory cytokines IL-10. Also, treatment with galangin at 1% w/w and 2% w/w has increased phosphorylation of I $\kappa$ B- $\alpha$  in the cytoplasmic fraction and decreased the accumulation of NF- $\kappa$ B (p65) in the nucleus. Modulation in protein levels of pro-inflammatory mediators of COX-2 and iNOS were observed in IMQ alone treated mice and galangin treated mice. These observations directed that galangin exerts protective role through up-regulation of anti-inflammatory and antioxidant markers against psoriasis (Sangaraju et al., 2021).

#### ***2.5.3.5. Gastroprotective effect***

In one of the studies, oral administration of 500 mg/kg ethanolic extract of AG significantly reduced gastric mucosal damage induced by pyloric ligation and hypothermic stress in rats. It also exhibited cytoprotective effect against destruction caused by 80% ethanol, 0.6 M hydrochloric acid (HCl), 0.2 M sodium hydroxide (NaOH) and 25% NaOH. Pretreatment with extract also prevented hypothermic and stress-induced gastric mucus depletion. Mastuda *et al.* demonstrated gastroprotective effect of AG rhizome and presence of ACA and 1'-acetoxyeugenol acetate significantly protected ethanol induced gastric mucosal lesions with an ED<sub>50</sub> of 0.61 mg/kg. It also prevented 0.6 M HCl and aspirin induced gastric lesion in mucosa. The outcomes of study suggested the involvement of endogenous prostaglandin and intracellular glutathione in the protection of gastric mucosa. Further, structural activity relationship reported that 1'-acetoxy group in these compounds are responsible for protection of mucosa (Matsuda et al., 2003b).

#### **2.5.3.6. Neuroprotective effect**

Amyloid  $\beta_{(25-35)}$  peptide increases acetylcholinesterase and monoamine oxidase level in the synaptic cleft and creates oxidative stress-induced Alzheimer's type amnesia. Ethanolic AGE has been reported to improve cognitive function by decreasing the elevated acetylcholinesterase and monoamine oxidase enzymes. The antioxidant enzyme in AGE also decreases the oxidative stress generated free radicals. Assessment of step-down inhibitory avoidance assessment and water maze behavioral studies indicated increased hippocampal memory as well accelerated other cognitive functions (Hanish Singh et al., 2011). Further, investigation was carried out to identify the potential bioactive component in various fractions of the extract that ameliorated amnesia. Chloroform fraction of AG rhizomes was identified with the presence of 1'-acetoxyeugenol acetate that exerted a similar anti-amnesic effect. Improvement in brain integrity was achieved through free radical scavenging activity and increased  $\text{Na}^+\text{K}^+\text{ATPase}$  activity (Singh et al., 2011a).

Ethanolic extract of AG rhizomes was administrated as intra-peritoneal (i.p) injection at a dose of 5 and 10 mg/kg, once daily for 3 days after 45 min in transient middle cerebral artery occlusion (MCAO) - induced ischaemic rats. After treatment, amelioration of motor coordination and locomotor functions were demonstrated in the rotarod test, angle board and grip test. A significant increase in their latency to fall, stand and hold was observed in comparison to the control group which showed neuroprotective effect of AG. Further, histological examination of treated rats at a dose of 5 and 10 mg/kg indicated reduction in the contralateral hemispheric infarction volume of 380 and 190  $\text{mm}^3$  respectively whereas the infarct area of MCAO induced control group was 455  $\text{mm}^3$ . This observation confirmed that the bioactives in AG rhizomes scavenge the free radicals of oxygen and hydroxyl groups that are extensively generated in ischemia and reperfusion phases resulting in cerebral injuries (Farkhondeh et al., 2020). In another study, neuroprotective effect of ethanolic extract of AG rhizome was reported in neurodegeneration in rat hippocampus by kainic acid. Administration of AGE (200 mg/kg) for two weeks before and two weeks after kainic acid injection lowered the expression of glial fibrillary acidic protein with significantly higher density of neuron. The increase in the neuron density indicated new brain cell growth, which confirmed their recovery from neurodegeneration (Sriraksa et al., 2020).

### **2.5.3.7. Antimicrobial activity**

Antimicrobial activity of AG was extensively studied by various *in vitro* experiments. Essential oils and extracts obtained from AG have potential antimicrobial activity against various types of microbes such as bacteria, fungi and parasites. Oonmetta-aree *et al.* demonstrated cytological effects of ethanolic extract of AG rhizome on *S.aureus* (gram positive). AGE acted on the outer cell membrane of the gram-positive bacteria, damaged its membrane integrity and resulted in release of nucleic acid, ribosomes and proteins out of the cell causing cell coagulation. However, hydrophobic nature of the extract could not penetrate the LPS constituted cell wall of the gram negative bacteria. Hence, extract was not effective against gram-negative bacteria. The study finding reported that ethanolic extract of AG rhizome contained ACA and also exhibited antimicrobial activity against *S.aureus* 209P with minimum inhibitory concentration (MIC) of 0.32 mg/mL and minimum bactericidal concentration (MBC) of 1.3 mg/mL (Oonmetta-aree *et al.*, 2006). Previous reports revealed that ester of acetic acid in ACA are responsible for antibacterial activity. The dissociation of ester from acetic acid occurred in solution and released undissociated acetate group which get penetrated into the lipid bilayer of microbes and released protons into the cell cytoplasm. The release of protons increased the cytosol resulting in denaturation of protein and coagulation of cell content (Huang *et al.*, 1986; Marquis *et al.*, 2003). It was concluded that the antimicrobial activity of AG rhizome is apparently related to the bioactive components present in its extract.

In another study, Mayachiew and Devahastin performed antimicrobial activity of ethanolic extract of AG rhizome using disc diffusion method against *S.aureus* (ATCC 25923). Later, agar dilution method was carried out against same strains and reported MIC value and MBC value to be 0.78 mg/mL and 2.34 mg/mL respectively. However, the major component reported in the extract was 1, 8-cineole. The variation in the bioactive components and strain tested might be the reason for variation in MIC and MBC values. However, study finding showed that MBC to MIC ratio was less than 4 which confirmed the bactericidal potential of extract towards *S.aureus* (Mayachiew and Devahastin, 2008). Recently, ACA isolated from AG rhizome has demonstrated antibacterial activity with MIC of 0.313 mg/mL and MBC of 0.625 mg/mL against multidrug resistant *S.aureus* SJTUF 20758. ACA significantly affected bacterial membrane and inhibited protein expressions that are associated with cell wall and membrane synthesis, osmotic

regulation, bacterial adhesion and invasion. These inhibitory effects confirmed antibacterial potential of AG extract (Zhang et al., 2021).

#### **2.5.3.8. Antiallergic/antiasthmatic activities**

Among the nine phenyl propanoids isolated from 80% aqueous acetone extract of AG rhizome, 1'-S- ACA and 1'-S-1'-acetoxyeugenol acetate are considered as novel inhibitors of allergic reactions. These natural anti-allergic compounds have shown inhibitory effect on the antigen IgE mediated release of  $\beta$ -hexosaminidase, TNF- $\alpha$  and IL-4. The inhibitory activity of 1'-S-ACA and 1'-S-1'-acetoxyeugenol acetate were reported with IC<sub>50</sub> of 15 mM and 19 mM respectively which was stronger than the synthetic antiallergic compounds, tranilast and ketotifen fumarate. The structural activity relationship of both these natural compounds reported stronger inhibition on degranulation due to 1' and 4-acetoxy groups. Further, *in vivo* studies on passive cutaneous anaphylaxis mice model has demonstrated dose-dependent (6.25-50 mg/kg) inhibition in the leakage of Evans blue dye after 30 min of addition of IgE allergens. Leakage of dye expressed as % of control confirmed higher potency of both natural compounds than tranilast (Matsuda et al., 2003a). The structural requirement of 1'-S- ACA and ability to act against type-1 allergic reactions led to the development of more stable and potent analogue of acetoxybenzhydrol, that is chemically known as 4-(methoxycarbonyloxyphenylmethyl)phenyl acetate. This acetoxybenzhydrol analogue also strongly inhibited antigen-IgE-mediated TNF- $\alpha$  and IL-4 production (Yasuhara et al., 2009). In another study, ACA isolated from AG rhizomes ameliorated ovalbumin-induced asthma in BALB/c mice. Dose dependent suppression of eosinophil infiltration and decreased level of IgE was observed in ACA treated group. However, at higher dose of 50 mg/kg/day, recovery from the ovalbumin induced changes such as airway remodeling, goblet-cell hyperplasia, eosinophil infiltration and mucus plugs were confirmed from the histopathological analysis of lungs. In addition, ACA decreased Th-2 cytokines such as IL-4 and IL-13 which were overexpressed with the induction of asthma and suppressed the release of Th-1 cytokines IL-12 $\alpha$  and interferon- $\gamma$ . The ability of ACA to act on immune and inflammatory pathway suggested the antiasthmatic activity (Seo et al., 2013). Similarly, galangin also inhibited ovalbumin induced overexpression of IL-4, IL-13, reduced eosinophil infiltration, goblet cell hyperplasia, expression of iNOS synthase and vascular cell adhesion protein-1 levels in lung tissue. Apart from these, galangin inhibited TNF- $\alpha$  induced NF- $\kappa$ B activation pathway by

blocking p65 nuclear translocation as well as inhibited the activation of I $\kappa$ B kinase  $\beta$  (Zha et al., 2013).

All these reported pharmacological activities showed the potential of ethanolic AGE to act on multiple signaling pathways. In a nutshell, the phytoconstituents reported in the ethanolic extract of AG include ACA, p-coumaryl diacetate, palmitic acid, acetoxyeugenol acetate, 9-octadecanoic acid and traces of eugenol,  $\beta$ -bisabolene,  $\beta$ -farnesene and sesquiphellandrene (Oonmetta-aree et al., 2006), galangin (Sangaraju et al., 2021). All these bioactives are known to exert specific therapeutic activities. However, the pungent principle, ACA has reported numerous therapeutic activities in particular such as antioxidant, antitumor, antimicrobial, anti-inflammatory, and antipsoriasis.

Structural activity relationship study has confirmed the presence of basic phenylpropanoid structure containing para or ortho substitution of acetoxy and 1-acetoxy propenyl groups at the benzene ring respectively. These functional groups are present in ACA and are involved in various activation and inhibition mechanisms such as inhibition of xanthine oxidase activity, inhibition of nitric oxide synthase expression, inhibition of translocation of NF- $\kappa$ B, activation of AMPK signaling pathway and induction of apoptosis via mitochondrial/Fas-mediated mechanism (In et al., 2012; Kojima-Yuasa and Matsui-Yuasa, 2020). These multiple mechanisms of action of ACA have shown its potential role in prevention of various life threatening diseases (Kojima-Yuasa and Matsui-Yuasa, 2020).

Other phenyl propanoid phytoconstituents such as p-coumaryl diacetate have reported anti-inflammatory and antioxidant activities (Yu et al., 2009) where as 1'-acetoxyeugenol acetate have antimycobacterial activity (Roy et al., 2012), anticancer (Aun et al., 2011; Hasima et al., 2010) and neuro-protective effect (Chellammal et al., 2019)

Apart from these phenylpropanoids, some of the flavonoids such as galangin (Sangaraju et al., 2021) and chrysin (Li et al., 2020a) present in *Alpinia* species are reported with antipsoriasis activity. Hence, to obtain whole benefit of these phytoconstituents, AGE has been selected for topical formulation developed.

During formulation development, it is essential to quantify the phytoconstituents present in the extract. ACA is one of the potent phenylpropanoid with the aforementioned therapeutic activity



and is present in major portion of the ethanolic extract. However, ACA is susceptible to hydrolytic degradation and results in the formation of 1'-hydrochavicol acetate, p-coumaryl diacetate, p-acetoxy cinnamic alcohol (Yang and Eilerman, 1999) . These degradation products are not as potent as ACA. Hence, to obtain the therapeutic potential of the ACA, it is essential to protect them from aqueous environment. In concern to overcome this challenge, NANE was proposed to be developed instead of aqueous nanoemulsion. NANE could provide protection to ACA as well as other components in AG formulation. In addition to this, it also ensures stability while transporting across/into the skin membrane by entrapping the drug in the emulsion droplets. Therefore, in the present study, ACA has been used as the marker compound for carrying out quantification of extract as well as used for characterization and evaluation of NANE. In addition to this, using ACA as marker will also ensure the efficiency of NANE to protect ACA in the formulation.

#### **2.5.4. Selection of marker**

Among the phytoconstituents present in the ethanolic extract of AG rhizomes, ACA was selected as the marker compound in view of its therapeutic potential and for confirmation of its stability within the developed formulation.

#### **2.5.5. ACA profile**

The profile of ACA is mentioned below in **Table 6** (Chouni and Paul, 2018; PubChem).

**Table 6.** ACA profile

Characteristic	Description
Drug name	1'-acetoxychavicol acetate
IUPAC name	[4-[(1S) -1-acetyloxy prop-2-enyl] phenyl] acetate
Chemical structure	
Synonym	D, L-1'- acetoxy chavicol acetate, galangal acetate
Molecular weight	234.251 g/mol
Molecular formula	C <sub>13</sub> H <sub>14</sub> O <sub>4</sub>
Physical appearance	White crystalline powder
Melting point	68 °C
Boiling point	325.4 °C
Log P	2.2
Solubility	Soluble in dimethyl sulphoxide (20 mg/mL), ethanol (20 mg/mL), dimethylformamide (14 mg/mL), practically insoluble in water (0.12 g/L)
Storage	Protected from light and store in a cool place
Category	Anticancer, anti-plasmodium, anti-allergic, antiulcer
Mechanism of action	Inhibition of NF-κB

All the above mentioned features are significant for developing a topical delivery system. However, the major challenge with AGE is the prerequisite to preserve the stability of the phytoconstituents. To explore AGE along with potential activities of ACA, it is important to find a suitable dosage form that prevent ACA degradation and deliver extract to the targeted site.

Typical outcome for topical application of synthetic drugs and/or herbal medicines is the ability to bypass its exposure to vital organs. Yet, the major challenge is the ineffectiveness to attain desired concentration even after direct application to the targeted site. The upper layer of the skin with hard keratinization makes drug delivery more difficult and challenging (Elias, 1981). The application of conventional dosage form exerts low permeability through the skin hence limit its penetration. Some of the reasons that account for these issues are related to the drug-specific problem such as solubility, permeability and stability. These drug-related properties do not comply with the structural arrangements in the skin that result in inefficacy of the medication and non-compliance by the patient (Ramanunny et al., 2021c).

However, significant interest in topical administration has urged researchers and scientist to tackle issues related to conventional dosage forms and to introduce a newly designed drug delivery system. The basic understanding of the molecular target for a particular disease and techniques reliable for adopting innovative formulation strategies resolves the challenges of topical drug delivery (Das Kurmi et al., 2017).

## **2.6. Novel carrier systems explored for topical delivery**

A wide variety of novel carriers systems are developed to overcome the challenges in topical delivery. The selection of the carrier system is based on the type of skin diseases, degree of penetration and retention capacity. A diverse set of lipid-based carriers, such as vesicular systems, micelles, nanoparticles and micro/nanoemulsions have shown increasing attention in drug delivery to the psoriatic skin. The selected therapeutic moiety has been extensively integrated with the suitable carrier system for effective dermal delivery of the drugs (Pradhan et al., 2013; Ramanunny et al., 2021b). The types of colloidal nanocarriers explored for psoriasis with their remarkable outcomes in delivering both synthetic drugs and herbals to various sites in the psoriatic skin has been emphasized in **Table 7** (Ramanunny et al., 2021c).

**Table 7.** Colloidal novel drug delivery systems for psoriasis

S.No.	Drug moiety	Formulation design	Composition	Mechanistic evaluation	Outcomes	References
1	Methotrexate	Niosomes	Chitosan gel	Skin sensitivity testing by human repeated insult patch test	Better absorption and penetration of methotrexate through the skin and improved patient compliance by ↓ in the dosage regimen to once-daily application	(Lakshmi et al., 2007)
2	Methoxsalen	Microemulsion	Soyabean oil, egg phosphatidylcholine, ethanol, chitosan.	<i>Ex vivo</i> permeation studies in human cadaver skin	Prolonged effect, avoid first-pass metabolism, ↓ in adverse effect, ↑ retention on the skin, large contact area of drug	(Behera et al., 2010)
3	Betamethasone dipropionate and salicylic acid	Microemulsion	Oleic acid: Sefsol (1.5:1), Tween 80, isopropyl alcohol	<i>In vivo</i> anti-inflammatory studies using Wistar rat carrageenan-induced paw edema model	↑ permeation with sustained release of betamethasone across the skin	(Baboota et al., 2011)
4	Betamethasone dipropionate	Nanoemulgel	Babchi oil: Eucalyptus oil mixture (1:1), Tween 80, ethanol, carbopol	<i>In vitro</i> permeation studies in rat abdominal skin	↑ permeation of the drug with ↓ in dosing frequency, and sustained drug release for the desired period. Eucalyptus oil provided antiseptic action and prevented microbial infection of the skin	(Alam et al., 2012)

<b>5</b>	Dithranol	Dendrimers	Propylene imine dendrimers	<i>In vivo</i> studies in nude albino rats by tape stripping method	Improved bioavailability, ↑ in drug permeation and retention in the targeted site without staining the adjacent cells	(Agrawal et al., 2013)
<b>6</b>	Aceclofenac and capsaicin	Nanomiemugel	Olive oil, Miglycol, Polysorbate 80, Transcutol, vitamin E (TPGS), propylene glycol (PPG), Pluronic F-127, EDTA, ethanolamine, carbopol	<i>In vivo</i> studies in IMQ-induced plaque psoriasis in C57BL/6 mice model	↑skin permeation of aceclofenac and capsaicin improved therapeutic response Improved skin contact time, hydration of the skin due to the occlusive effect	(Somagoni et al., 2014)
<b>7</b>	Cyclosporin	Polymeric micellar	Methoxy-poly(ethylene glycol) di-(hexyl-substituted polylactide) (MPEG-dihexPLA) with Nile red labelled analogue	<i>In vitro</i> skin permeation studies in porcine skin and human skin	Biodegradable and biocompatible nanosized polymeric micelles ↑aqueous solubility with deeper penetration	(Lapteva et al., 2014)
<b>8</b>	Methotrexate	Nanostructured lipid carrier	Witespol S51, oleic acid, Polysorbate 60	<i>In vitro</i> skin permeation studies using porcine ear skin	↑ drug loading with better stability and deeper drug penetration into the skin	(Pinto et al., 2014)
<b>9</b>	Psoralen	Ethosomes	Lipoid S 100, ethanol	<i>In vivo</i> microdialysis studies	↑ permeation and skin deposition of psoralen, ↓ toxicity and improvement in the efficacy of long-term psoralen treatment.	(Zhang et al., 2014)
<b>10</b>	Leflunomide	Nanoemulgel	Capryol 90, Cremophor EL, Transcutol HP, Pluronic F127	<i>Ex vivo</i> permeation studies in rat abdominal skin	Nanosized emulgel provided bioadhesiveness with high drug penetration	(Pund et al., 2015)

<b>11</b>	Tacrolimus and curcumin	Liposphere gel	Egg lecithin, Tricaprin, Tween 80, Cremophor RH 40, HPMC	<i>In vivo</i> psoriasis assessment in IMQ psoriatic plaque model	Liposphere facilitated ease of application with spreadability and maximum retention on the skin Drug combinations provided synergistic effect and ↑ therapeutic efficacy	(Jain et al., 2016)
<b>12</b>	Tacrolimus	Composite hydrogel	MPEG-hexPLA, carbopol, citrate buffer	<i>In vivo</i> studies in IMQ-induced psoriasis model	Hydrogel rapidly evaporated, leaving no residual film formation and efficiently delivered a high payload of the drug into the inflamed cells, ↓ dose and frequency of dosing	(Gabriel et al., 2016)
<b>13</b>	Acitretin - aloe emodin	Nanogel	Dimethyl sulphoxide, methanol, chitin, rhodamine B	<i>In vivo</i> antipsoriatic activity in Perry's mouse tail model	Nanosized spherical particles, ↑ in drug penetration and retention in the deeper layers of the skin, reported additive effect with nanogel	(Divya et al., 2016)
<b>14</b>	Fusidic acid	Liposomes	Phospholipid 90G, Span 80	<i>In vivo</i> studies in mouse tail model	Fusidic acid liposomal system provided favourable changes in the barrier properties of the skin, and facilitated delivery by targeting the molecule to the site	(Wadhwa et al., 2016)
<b>15</b>	Diacerein	Niosome	Span 60, cholesterol	<i>In vitro</i> skin penetration studies using rat skin model	Niosomal formulation has high ability to deliver diacerein to the viable epidermis layer with a smaller amount of diacerein penetrated into the dermis layer	(Moghddam et al., 2016)

<b>16</b>	Triamcinolone	Nanostructured lipid carriers	Compritrol® 888 ATO, Miglycol 812, Poloxamer 188	<i>In vitro</i> skin distribution in goat skin	Selective drug deposition in the epidermis, ↓ side effects and prolonged drug release to the targeted site minimizing the dose-dependent side effects	(Pradhan et al., 2017)
<b>17</b>	Tazarotene	Proniosomal gel	Span 60, stearylamine, cholesterol, lecithin	<i>In vitro</i> release and permeation studies in Wister rat skin <i>In vivo</i> skin histological studies in male Albino NMRI mice tail model	Fusion of the vesicles with the intercellular lipid of the stratum corneum causes ↑ permeation, prolonged release of the entrapped drug at the local site, ↑ residence time of the drug for a longer duration with lesser irritancy	(Prasad and Chaurasia, 2017)
<b>18</b>	Thymoquinone	Liposphere gel	Egg lecithin, Tricaprin, Tween 80, Cremophor RH 40, HPMC	<i>In vivo</i> IMQ-induced psoriatic plaque model	Deeper skin penetration, slow-release and skin compatibility have potential anti-inflammatory and anti-psoriasis activity	(Jain et al., 2017)
<b>19</b>	Methotrexate and Etanercept	Solid lipid nanoparticulate hydrogel	Cetyl palmitate, polysorbate 80, carbopol	<i>Ex vivo</i> human skin permeation studies in both healthy and psoriasis skin	Combination therapy provided synergistic effect with ↑bioavailability of methotrexate and retention in the skin.	(Ferreira et al., 2017)
<b>20</b>	Vitamin D3	Polymeric nanosphere (tyroSphere)	Polyethylene glycol, desaminotyrosyl-tyrosine octyl ester, suberic acid	<i>Ex vivo</i> skin distribution studies in dermatomed human skin	↑ drug loading and binding efficiencies with sustained drug release. Vitamin D3 was actively protected from hydrolysis and photodegradation thereby significantly ↑ stability of vitamin D3 in the topical formulation	(Ramezanli et al., 2017)

21	Methoxypsoralen	Niosomal hydrogel	Span 60, Span 80, carboxymethyl cellulose	<i>In vitro</i> skin permeation and deposition studies with dorsal skin of Wister rat	Nanosized niosomes offered ↑ drug deposition and skin permeation	(Kassem et al., 2017)
22	Methotrexate	Nanostructured lipid carrier	Glyceryl monostearate, oleic acid, ethanol, acetone	<i>In vitro</i> drug release and drug deposition studies using Wister rat skin	Nanostructured lipid carrier improved drug loading capacity and a good ability to reduce the drug expulsion on storage. Close contact with stratum corneum with occlusion suggested depot effect on the upper skin layer	(Tripathi et al., 2018)
23	Methotrexate	Nanogel	Chitin, Rhodamine	<i>In vivo</i> studies in IMQ mice model	Chitosan hydrogel ↑ drug residence due to its bioadhesion property as well as ↑ penetration	(Panonnumma 1 and Sabitha, 2018)
24	Methoxypsoralen	Nanoemulsion thickened hydrogel	Clove oil, Pluronic F68, chitin/sweet fennel oil, Cremophor RH 40, chitin,	<i>In vitro</i> permeation studies using synthetic cellulose acetate membrane	Clove oil with Pluronic F68, and chitosan led to ↓ skin permeation and ↑ skin retention. PUVA therapy ↑ efficacy and ↓ systemic exposure to the drug	(Barradas et al., 2018)
25	Acitretin	Niosomes	Cholesterol, Span 60, HPMC	<i>In vivo</i> psoriasis studies in Swiss albino rats mouse tail model	↑ drug permeation and deposition into deeper skin layers, but diminished systemic absorption	(Hashim et al., 2018)
26	Methotrexate	Nanoemulsion	Chaulmoogra oil, Tween 80, ethanol	<i>In vivo</i> studies on IMQ psoriasis model	↑ skin permeation with effective skin retention and ↓ systemic toxicity	(Rajitha et al., 2019)



27	Curcumin	Ethosomes	Hyaluronic acid, propylene glycol, chloesterol, 1,2distearoyl-sn-glycero-3-phosphoethanolamine-N-[amino(polyethylene glycol)-2000], hydrogenated soyabean phospholipids	<i>In vivo</i> studies in IMQ psoriasis model	Targeted delivery of curcumin to CD44 protein, ↓ drug leakage, slow release of the loaded curcumin and improvement in stability	(Zhang et al., 2019)
28	Methotrexate - salicylic acid	Ethosomes	Methotrexate, salicylic acid, soyalecithin, ethanol, water, Carbopol 934	<i>In vivo</i> studies in IMQ-induced psoriasis model	Slow, prolonged release of methotrexate, ↓ in hyperkeratosis and parakeratosis indicated the sign of recovery	(Chandra et al., 2019)
29	Ethylenediamine	Dendrimers	Polyamidoamine (PAMAM), ethylenediamine	Flow cytometric analysis of keratinocytes and fibroblast cells	Dose-dependent inhibition of cell proliferation	(Czarnomysy et al., 2019)
30	Dithranol	Dendrimers	Dithranol, PAMAM dendrimer, ethyl cellulose, polyvinyl alcohol, dichloromethane, sodium metabisulphate, distilled water	<i>In vitro</i> release studies and pharmacokinetic studies	↑ permeability across the skin and prolonged release of the drug	(Tripathi et al., 2019)

31	Methotrexate	Gold nanoparticles	Aqueous solution of chloroauric solution, 3-mercapto-1-propansulfonate	<i>In vivo</i> studies in IMQ-induced psoriasis like mice model	↓ keratinocyte hyperproliferation, epidermal thickness and ↓ inflammatory infiltrate was observed in <i>in vivo</i> studies	(Fratoddi et al., 2019)
32	Poly(phosphorhydrazone) capped with azabisphosphonate	Dendrimers	Poly(phosphorhydrazone), azabisphosphonate	<i>In vivo</i> studies in IMQ induced mice model	↑ therapeutic efficacy	(Jebbawi et al., 2020)
33	Curcumin, thymoquinone, and resveratrol	Nanoemulgel	Oleic acid, Tween 80, polyethylene glycol (PEG) 200, water, Carbopol 940	<i>In vivo</i> studies in IMQ induced mice model	Drug combination in emulgel has shown ↑ retention and improved therapeutic efficacy	(Khatoon et al., 2021)
34	Clobetasol propionate	Microsponges based gel	Eurdragit RS 100, dichloromethane, water, polyvinyl alcohol, 1% triethylcitrate	<i>In vivo</i> studies in mouse tail model	Maximum drug payload, ↓ permeation into systemic circulation, ↓ side effects, ↑ orthokeratosis in comparison to plain Clobetasol propionate gel	(Devi et al., 2020)
35	Clobetasol propionate	Squarticles	3.2% w/v Pluronic® F68, double-distilled water, soy phosphotidycholine	<i>In vivo</i> studies in UV induced psoriasis model	Spherical globules of the squarticles has shown 2.7 folds ↑ in drug retention in comparison to the marketed formulation	(Dadwal et al., 2020)
36	miR210 antisense	Nanocarrier gel	Reconstituted high-density lipoprotein, carbomer U20, propylene glycol, glycerol, distilled water, triethanolamine	<i>In vivo</i> studies in IMQ induced mice model and reverse transcription quantitative polymerase chain reaction	↓ expression of miR-210 was observed in nanocarriers gel treated group as compared to the control group and ↓ infiltration of Th1 and Th17 cells in the skin lesion was observed with	(Feng et al., 2020)

					nanocarrier gel	
37	Cyclosporine	Niosomes-gel	Cholesterol, span 60 and carbopol 940	<i>In vivo</i> studies on IMQ induced psoriasis like mice model	↑drug permeation rate and ↑ skin deposition obtained with niosomal gel as compared to cyclosporine suspension. ↓ in the PASI scores, and ↑ efficacy of the optimized formulation	(Pandey et al., 2021)
38	Fluocinolone acetonide with salicylic acid	Nanostructured lipid carrier gel	Carbopol 934, sodium hydroxide	<i>In vivo</i> studies on IMQ-induced psoriasis like mice model	Fluocinolone loaded nanostructured lipid carrier gel and plain salicylic acid containing novel gel showed deeper penetration and prolonged action. Better anti-psoriasis activity with improvement in the phenotypic as well as histopathological characteristics of psoriatic skin as compared to conventional gel formulation. ↓ TNF- $\alpha$ , IL22, and IL-17, and ↑ anti-psoriatic efficacy	(Pradhan et al., 2021b)
39	Rosmarinic acid	Transethosome gel	L- $\alpha$ phosphatidylcholine cholesterol, sodium deoxycholate, dicethyl phosphate, chloroform, methanol	IMQ- induced psoriasis-like skin inflammation in mice model	↓ in punch edema and ↓ in TNF- $\alpha$ and IL-6 showed effectiveness of the transethosome gel	(Rodríguez-Luna et al., 2021)

40	Calcipotriol	NLC loaded nanogel	Hydrogenated palm oil, olive oil, methyl alcohol, acetone, Poloxamer 188, Lipoid S100	<i>In vivo</i> studies in mouse tail model	1.57 folds ↑ in drug retention in SC where as 3.67 folds ↑ in viable layers was observed with NLC as compared to pure drug which shows improved therapeutic efficacy	(Pradhan et al., 2021a)
41	Apremilast	Solid lipid nanocarriers loaded hydrogel	Precirol ATO5, Kolliphor CS 12, Carbopol 974P	<i>Ex vivo</i> permeation and dermatopharmacokinetics studies	<i>Ex vivo</i> studies confirmed ↑ permeation and retention. Dermatopharmacokinetic studies confirmed 2 folds higher retention of apremilast loaded solid lipid nanocarriers, in the epidermis and 5-folds higher in dermis	(Rapalli et al., 2021)
42	Resveratrol	Spanlastics	Span 60, Brij 35, Cremophor EL, Carbopol 934	<i>In vivo</i> studies on IMQ-induced psoriasis mice model	Improvement in erythema and scaling after treatment with least changes in mRNA gene expression of inflammatory cytokines	(Elgewelly et al., 2022)

Amongst these novel drug delivery systems, nanoemulsions have shown enhanced efficacy in treating topical skin conditions. The characteristics feature of nanoemulsions such as fluidic nature, smaller droplet size, protective nature to deliver components (irritants, volatile components, high molecular weight components), maximized skin cell interaction and permeation across the stratum corneum contributed towards versatile application in dermatological conditions (Rai et al., 2018; Shakeel et al., 2012). The non-toxic and non-irritant nature of this colloidal system has preferred its application over the vesicular system (Chawla et al., 2019). Depending on the composition of the selected colloidal system, modification in the diffusivity of the strata can occur that results in local or systemic drug action. The suitability of the system to incorporate different polar components in the same single-phase solution facilitates the solubilization of both hydrophilic and hydrophobic drugs. The increase in the thermodynamic activity of the drug may favour its partitioning in the skin and enhance the permeation rate (Muzaffar et al., 2013; Shukla et al., 2018).

## **2.7. Nanoemulsions**

Nanoemulsions are colloidal dispersion that forms an isotropic system with heterogeneous components. The system contains two immiscible liquids that are stabilized at their interface by emulsifier or with a mixture of emulsifier and co-emulsifier. In nanoemulsions, the free energy of the colloidal dispersion is higher than the free energy of the individual phases making the system thermodynamically unstable. However, this system ensures thermokinetic stability due to the higher energy barrier between the phases (McClements, 2012; Ramanunny et al., 2022).

Now the classical concept of emulsions contains oil and water phases has been replaced with a relatively polar non-aqueous solvent system to produce anhydrous/NANEs (Peterson and Hamill, 1968). Though the concept of non-aqueous emulsions in the conventional emulsion size range is not new, the scientific literature is sparse on non-aqueous emulsions in the nano-size range (Sakthivel et al., 1999; Suitthimeathegorn et al., 2005). There is a scarcity of knowledge pertaining to the range of pharmaceutically relevant oily and polar phases as well as surfactants that would lead to formulation of a stable, safe and elegant formulation of NANEs (Suitthimeathegorn et al., 2007). The basic concept in this unique delivery system is the mixing of two immiscible phases devoid of any aqueous phase to create nano-sized droplets of one in the continuous phase constituted by the other. The aqueous phase is generally replaced with either

polyols or other polar liquid phases (LinVerma et al., 2017). The two immiscible phases generally constitute oily phases of different polarity. This system is generally introduced for incorporation of drugs that are labile towards hydrolytic or oxidative degradation such as cholecalciferol, ascorbic acids, astaxanthin (ASX) etc. making it a suitable dosage form for application. These features show that incorporation of AG (herb of choice) extract containing ACA into NANE prevent the chances for hydrolytic degradation (Yang and Eilerman, 1999). Hence, this aqueous free delivery system can preserve the activity of ACA by protecting ACA within the delivery system.

### **2.7.1. Preparation of NANEs**

First critical step in the fabrication of NANEs is the selection of different components of the system. Key components of the system include oil phase, non-aqueous polar phase and emulsifiers (**Figure 3**) on which the stability, drug loading and globule size of the system depends. Although emulsions with polar continuous phase such as dimethyl sulphoxide (DMSO), N, N'-dimethyl formamide (DMF) and formamide are nearer to aqueous phase in terms of polarity and are extensively reported, yet they are not utilized for pharmaceutical applications much because of their reported toxicity (Cameron and Sherrington, 1996; Chen et al., 1988). As not much literature is available on this aspect, the selection of the three essential components i.e. oily phase, polar phase and surfactants is generally done based on the previously reported excipients while those that have been hitherto unexplored, have also been tried, though less frequently.

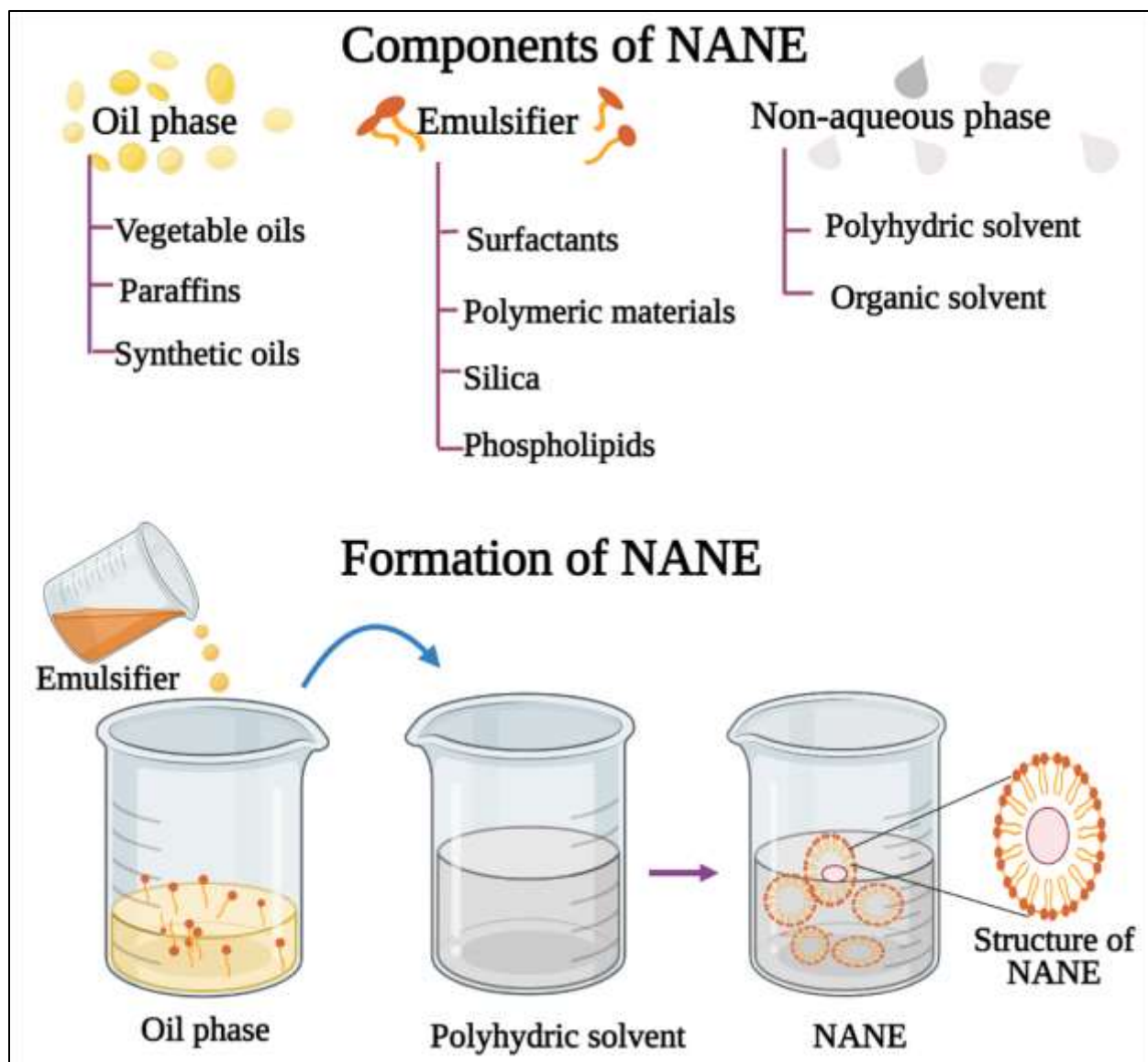


**Figure 3.** Schematic representation of components and structure of NANE

**2.7.1.1. Oil/oleaginous phase:** This phase represents the lipophilic portion of the nanoemulsions and is generally selected based on the solubility of the active moiety in it, if the drug is oil soluble. However, for the drugs that are soluble in polar phase, the choice of this phase is based on its interaction with the polar phase. Apart from this, choice of oil phase also depends on the site of administration, hydrophilic-lipophilic balance (HLB) as well as potential activity of the oil. Generally, the oil phase is selected from the following sources:

#### **2.7.1.1.1. Vegetable oils**

A number of vegetable oils have been reported in the preparation of NANEs with varying degree of success. Castor oil in silicone oil microemulsions were initially prepared to study their rheological properties in electric field (Ha and Yang, 2000). Looking at their remarkable stability, they were explored as vehicles for lipophilic drugs like dexamethasone and dehydroepiandrosterone for their controlled release (Jaitely et al., 2004; Suitthimeathegorn et al., 2005). These emulsions were found to improve the mean residence time and elimination half-life of dexamethasone as compared to its aqueous emulsion (Suitthimeathegorn et al., 2007).

Rottke *et al.* (Rottke et al., 2014) formulated oil in oil emulsion of nonivamide in castor oil-silicone oil with droplet size in the range of 1.1 to 1.8  $\mu\text{m}$ , for long term treatment of chronic pruritus. The results of the permeation study demonstrated constant permeation of drug through porcine skin for 10 h. Castor oil has also been successfully used in the preparation of NANEs of cholecalciferol with cyclomethicone and PEG/PPG-18/18 dimethicone as surfactants (Payghan, 2016). Being resistant to oxidative degradation, saturated oils are preferred over unsaturated oils in the preparation of NANEs of drugs prone to oxidative degradation (Maszewska et al., 2018).

Olive oil was used with glycerin by Hamill and Petersen in the mid-1960s for preparation of non-aqueous emulsions in the higher size range (Hamill et al., 1965; Hamill and Petersen, 1966a, b). Interestingly, olive oil has been used both as oily phase as well as polar phase based on the polarity characteristics of the second phase. One such study where it is used as a polar phase is reported by Payghan *et al.* for delivery of piroxicam while the oily phase is composed of liquid paraffin (Payghan et al., 2012). Jadhav *et al.* prepared glycerine in olive oil micro-emulsion cream of griseofulvin which was found to stabilize the drug more than its aqueous emulsion (Jadhav et al., 2015b).

#### **2.7.1.1.2. Paraffins**

Paraffins are extensively used in cosmetic and biomedical applications because of their inert nature and penetration into the upper skin layers resulting in prolonged lubricating effect (Petry et al., 2017). Liquid paraffin was used as oily phase in the preparation of non-aqueous emulsions of piroxicam along with other oil phases (Payghan et al., 2012). Non-aqueous micro-emulsions of PEG 400/ paraffin oil were found to show satisfactory stability when prepared using PBut-Block-P2VP block copolymers (Atanase and Riess, 2015).



### 2.7.1.1.3. Synthetic oils

These are chemically synthesized oils that may either be used as oily phase or polar phase. Silicone oils are polysiloxane polymers made up of siloxane units. These have been frequently used in preparation of non-aqueous emulsions. Lin *et al.* prepared polyol-in-silicone anhydrous emulsions of deoxyarbutin which proved to enhance the drug stability as compared to its conventional emulsions (Lin et al., 2011). In US patent US5587149A, Punto *et al.* have revealed the art of preparing non-aqueous emulsions of vitamin C using silicone oils. These were claimed to be suitable to be filled into soft gelatin capsules (Punto et al., 1996).

Lin *et al.* prepared polyol-in-silicone anhydrous emulsions of deoxyarbutin which proved to enhance the drug stability as compared to its conventional emulsions (Lin et al., 2011). Octyl and decyl glycerate was used as the oily phase to solubilize the highly lipophilic ASX for its topical delivery (Sun et al., 2019). The resulting formulation proved to be stable and was able to facilitate the permeation of ASX in skin while the systemic absorption was low.

Some of the widely utilized synthetic oils for the formulation of nanoemulsions are summarized in **Table 8**. These oil/emulsifiers have been widely explored in aqueous nanoemulsions and self-emulsifying drug delivery system. These agents, therefore, can be explored in formulation of NANEs.

**Table 8.** Enlist few synthetic oils utilized in the fabrication of nanoemulsions

Brand Name	Chemical Name	HLB	Reference
<b>Capmul MCM</b>	Caprylic/Capric Glyceride	5.0-6.0	(ABITEC; Urmaliya et al., 2016)
<b>Caproyl® PGMC</b>	Propylene glycol monocaprylate type(I)	6.0	(Pandey and Kohli, 2018)
<b>Caproyl®90</b>	Propylene glycol monocaprylate type(II)	5.0	(Patel et al., 2016)
<b>Labrafac™ lipophile WL1349</b>	MCT	1.0	(Heurtault et al., 2009)
<b>Labrafac™ PG</b>	Propylene glycol dicaprolate/dicaprate	1.0	(Gattefossé, 2008a; Modi and Patel, 2011)
<b>Labrafil®M1944CS</b>	Oleoyl polyoxyl-6-glycerides	9.0	(Gattefossé, 2008b)
<b>Labrafil®M2130CS</b>	Lauroyl polyoxyl-6-glycerides	9.0	(Gattefossé, 2008c)
<b>Lauroglycol™ 90</b>	Propylene glycol monolaurate type (II)	3.0	(Sosnowska et al., 2017)
<b>Lauroglycol™ FCC</b>	Propylene glycol monolaurate type (I)	5.0	(Gattefossé, 2008d; Thakur et al., 2018)
<b>Maisine®CC</b>	Glyceryl monolinoleate	1.0	(Gattefossé, 2008e; Soliman et al., 2021)
<b>Peceol™</b>	Glyceryl monooleate (Type40)	1.0	(Gattefossé, 2008f; Jakab et al., 2018)

<b>Plurol® Diisostearique</b>	Polyglyceryl-3-diisostearate	4.5	(Kim et al., 2019)
<b>Plurol®Oleique CC497</b>	Polyglyceryl-3-dioleate	3.0	(Gattefossé, 2008g; Janković et al., 2016)

### 2.7.1.2. Non-aqueous polar phase

In conventional emulsions, the aqueous phase represents the hydrophilic part of the emulsion system. However, in NANEs, water is substituted with non-aqueous polar solvent of pharmaceutically acceptable grade, viz., polyhydric or organic solvents. Commonly employed polar solvents are generally those containing hydroxyl groups which could be alcohol, glycol, polyhydric alcohol or mixtures thereof. Some examples of polyhydroxy solvents used in NANEs are glycerin, PEG, propylene glycol, silicone oil, etc. Their selection is generally based on their immiscibility with the selected dispersed phase and the site of application. Glycerol has been used as the polar solvent in a number of reports (Lin et al., 2011; Sun et al., 2019). Polydimethyl siloxane was used as a polar phase by Rottke *et al.* for the formulation of non-aqueous emulsion of nonivamide (Rottke et al., 2014). In US patent US5110606A, the art of preparing palatable formulations was revealed by dissolving the drug in propylene glycol and dispersing this solution in fatty ester (Geyer and Tuliani, 1992). Propylene glycol was also employed for preparation of non-aqueous nanoemulsions of flavanones isolated from *Eysenhardtia platycarpa*. Formulation was found to be successful in sustained release of flavanones and promoted their permeation through the skin (Dominguez-Villegas et al., 2014).

Atanase and Reiss reported the preparation of stable non-aqueous emulsions by using PEG 400 and paraffin oil (Atanase and Riess, 2015). Powell *et al.* revealed a method of preparation of non-aqueous emulsions using a range of polar solvents including ethylene glycol, ethanol, propyl alcohol, iso-propyl alcohol, propylene glycol, dipropylene glycol, tripropylene glycol, butylene glycol, iso-butylene glycol, methyl propane diol, glycerin, sorbitol, PEG, PPG mono alkyl ethers, polyoxyalkylene copolymers and mixtures thereof (Powell and Kasson, 2001).

A blend of quercetin, dipropylene glycol, and glycerol was used as the dispersed phase in an oil phase containing a low HLB emulsifier and cetostearyl alcohol for preparation of oil in oil emulsions as a component of the non-aqueous self-double-emulsifying drug delivery system (Wang et al., 2016).

### **2.7.1.3. Surfactants**

Surfactants are amphiphiles with a hydrophilic head and lipophilic tail that may exhibit multifunctionality as a solubilizer, stabilizer, or emulsifier. The selection of suitable surfactants for NANEs in proper quantity plays a significant role in determining the stability of the system.

The most widely accepted method for the selection of surfactants is based on the HLB value required for the system. HLB value represents a numerical system that arranges molecules as per their relative hydrophilicity or lipophilicity (Zheng et al., 2015). Non-ionic surfactants with HLB values around 12 were found to stabilize oil dispersed in formamide emulsion (Cameron and Sherrington, 1996).

Nature of surfactants plays a significant role in the formulation of emulsions. Several ionic (anionic or cationic) and non-ionic surfactants have been reported in the emulsification of the glycerin-olive oil binary system. Some anionic surfactants like 2-amino-2-methyl-1,3-propanediol (Hamill and Petersen, 1966b), trisaminomethane, ethanolamine, triethanolamine and ammonia gas, etc. and cationic surfactants like cetyl pyridinium chloride, stearyl trimethyl ammonium chloride and stearyl methyl benzyl ammonium chloride were reported to be successful in emulsification of the binary system leading to formation of stable emulsions (McMahon et al., 1963). Non-ionic surfactants such as sorbitan monolaurate (Span 20), sorbitan monopalmitate (Span 40), sorbitan monooleate (Span 80), polyoxyethylene sorbitan monolaurate (Tween 20), polyoxyethylene sorbitan monopalmitate (Tween 40), polyoxyethylene sorbitan monooleate (Tween 80), glyceryl monostearate have been preferred either individually or in combination to obtain stable emulsions (Peterson and Hamill, 1968). Hence non-ionic surfactants are preferred over ionic surfactants in pharmaceutical manufacturing (Kale and Deore, 2017).

### **2.7.1.4. Polymeric materials**

Polymeric materials such as polybutadiene-*b*-poly(ethylene oxide) (PB-PEO) and poly(ter-butyl styrene)-poly(ethylene oxide) (PtBuS-PEO) diblock copolymers (Riess et al., 2004) act as emulsifier and stabilizer in NANE system. These particles form a sheath around the emulsion droplets resulting in highly rigid shell-like structures with higher adsorption energy. The interfacial modification by polymeric particles ensures better stability of emulsion as well as

preserved drug characteristic features. The nature of stabilizer used in the emulsion plays a key role in the permeation and absorption of the emulsion across the skin stratum.

Cross-linked poly(N-isopropylacrylamide-co-2-acrylamido-2-methylpropane sulfonic acid) microgels functionalized with a nonionic polymerisable surfactant (polyoxyethylene 4-nonyl-2-propyl-phenyl maleate ester) (Amro, 2013). Microgel-stabilised non-aqueous emulsions were successfully used to prepare stable non-aqueous emulsions of formamide in paraffin oil.

#### **2.7.1.5. Silica**

Hydrophobic silica nanoparticles possessing 50% silanol groups have been reported to stabilize the Pickering nanoemulsions of aspirin composed of olive oil and glycerine [63]. Silica encapsulated droplets have shown higher adhesion on the skin structure that results in enhanced penetration of the drug moiety (Frelichowska et al., 2009). This type of emulsions is well suited for encapsulation of both hydrophilic and lipophilic drugs. A combination of polymeric surfactant and kaolinite solid particles was used for preparation of silicon oil - in - glycerin emulsions (Tawfeek et al., 2014). Another advanced modification of Pickering emulsions, in the form of oil/oil/oil emulsions was reported using two-stage method. Stage 1 involved the preparation of a simple emulsion while in stage 2, the primary oil in oil emulsion, was re-emulsified into another immiscible oil phase (Dyab and Al-Haque, 2013).

#### **2.7.1.6. Phospholipids**

Phospholipids are natural emulsifiers which may be anionic, cationic or zwitterions based on the size and functional head attached to the fatty acid chain. They have been successfully used for preparation of nanoemulsions. In an early report on non-aqueous microemulsion, Friberg and Podzimek found the emulsion stability to increase with increase in concentration of lecithin which was used as an emulsifier (Friberg and Podzimek, 1984). A promising alternative treatment for cutaneous Leishmaniasis was established by de Mattos *et al.* using a newly synthesized chalcone, (E)-3-(3-nitrophenyl)-1-(3,4,5-trimethoxyphenyl)prop-2-en-1-one, which has lower water solubility. This synthetic chalcone loaded nanoemulsion was stabilized with a combination of soya lecithin and polysorbate 20. It was found to exhibit excellent physicochemical properties, stability and therapeutic efficacy with higher activity against *Leishmaniasis amazonensis* (de Mattos et al., 2015).

## **2.7.2. Methods of preparation**

Method of preparation employed plays a significant role in the formulation of nanoemulsions with desirable stability. The formulation development of nanoemulsions involves two steps that occur simultaneously. Firstly, hydrodynamic break down of the dispersed phase into dispersion medium occurs with the application of extensive shear. The applied shear breaks the coarse droplets into small spherical droplets of characteristically small radius. Secondly, the emulsifier modifies the interfacial tension of the system based on steric hindrance, repulsive forces or van der Waals force of attraction (Tadros et al., 2004).

Several methods have been employed for the formulation of these emulsions including various high energy and low energy methods. The basic principles involved in preparation techniques and their merits and demerits are discussed in the following section. As the literature on preparation of NANEs is limited and methods of preparation for aqueous and non-aqueous emulsions are similar, methods are explained by using examples from aqueous emulsions also.

### **2.7.2.1. High energy method/ Mechanical process**

In this class, a high degree of shear force is applied to break the forces of attraction that exist within each of the liquid phases. The external force can be in the form of pressure, shear or frequency waves that reduces the surface tension and in turn, reduces the droplet size into the nano-scale.

**2.7.2.1.1. Rotor-stator stirring method:** In this method, a stationary rotor known as “stator” and the high-speed rotor are used to generate shear among the fluids. Rotor-stator with an 18 mm head, operating at 13,000 rpm was used for 2-3 min to prepare stable non-aqueous emulsions of formamide/toluene using a series of nonionic polymerisable nonyl phenol ethoxylates as surfactants (Dyab et al., 2013) The fluids at the center of the rotor experience less velocity compared to the fluid at the periphery. The velocity differences create the shear force. The extremely high shear zone thus created, converts larger droplets to smaller droplets. However, this method is generally used for batch production with a major concern of the maintenance of the droplet size in the nanometric range (below 200 -300 nm) (Koroleva and Yurtov, 2012).

**2.7.2.1.2. High-pressure homogenization method:** In this technique, fluid under high pressure (100-350 MPa) is forced to move through a homogenizer valve where the fluid gets

depressurized (10-20 MPa) and moves to a low-pressure area. The differential pressure experienced by the fluid initiates the droplet size reduction. This is accomplished by a combination of three mechanisms i.e. shear, turbulence and cavitation. The fluid motion into the homogenizer valve creates shear forces that disrupt the droplets and initiate the size reduction. The velocity gradient is generated inside the homogenizer valve which results in a turbulent flow of the fluid. This turbulence creates kinetic energy in the form of eddies and heat which, in turn, enable the mixing of the fluid and reduces the droplet size. The cavitation of the liquid is observed near the orifice of the homogenizer valve due to the pressure variation in the flowing liquid. The pressure reduces abruptly but experiences higher velocity resulting in cavitation (Martínez-Monteaudo et al., 2017).

In this high energy method,  $10^8$ - $10^{10}$  W Kg<sup>-1</sup> energy density (Gupta et al., 2016) is supplied for a short time to obtain small homogenous droplets. The higher the number of homogenization cycles, the narrower is the size range of droplets obtained. This method is most preferable for the preparation of nanoemulsions due to very low batch to batch variation and ease of scale up (Patel and Joshi, 2012). The reported limitation of this process is the increased temperature and energy consumption that might lead to degradation of thermolabile compounds (Cinar, 2017). Jadhav *et al.* formulated griseofulvin (0.5% w/w) NANEs by employing the homogenization method using the immiscible phase composition of olive oil in glycerin (Jadhav et al., 2015b). A similar technique was employed by Payghan *et al.* for loading cholecalciferol in the castor oil-silicone oil system (Payghan, 2016). An interesting improvisation of the method in the form of “syringe in syringe” technique was introduced for the formulation of nonivamide emulsion where homogenization was achieved by transferring the content from one syringe to the other approximately 70 times (Rottke et al., 2014).

**2.7.2.1.3. Ultrasonic emulsification:** The powerful ultrasound frequency of 16-100 Hz generated mechanically or electrically, is used for emulsification in this technique. Probe sonication was used to produce oil in oil emulsions of castor oil in silicone oil in micron size range by Jaitely *et al.* (Jaitely et al., 2004). These high frequency ultrasound vibrations enter the liquid mixture leading to physical and chemical changes explained by the cavitation phenomenon. The efficiency of cavitation is based on the intensity of the ultrasonic frequency. On the application of low acoustic ultrasonic waves, stable cavitation occurs, which is represented by a vibrating

bubble exhibiting oscillation of small amplitude. However, high-intensity waves produce unstable cavitation represented by bubbles of nearly double their size. For achieving efficient cavitation, the ultrasound frequency of the sound waves should be equivalent to the oscillating frequency of the bubbles (Canselier et al., 2002). This method is widely employed for small volume preparations at the laboratory scale. Droplet size of the dispersed phase is reported to be highly dependent on the concentration of surfactants (Yukuyama et al., 2016). Generation of ultrasound frequency by probe sonication was employed by Jaitely *et al.* for formulating <sup>3</sup>H-Dexamethasone and <sup>3</sup>H dehydroepiandrosterone NANEs in castor oil-silicone system which was further subjected to optimization (Jaitely et al., 2004). Campos *et al.* employed sonication technique for developing nystatin loaded NANE in Labrafac® lipophile-propylene glycol (Campos et al., 2012). Similar technique was employed for loading flavanones into NANE for providing anti-inflammatory activity (Dominguez-Villegas et al., 2014).

**2.7.2.1.4. Microfluidization:** In this technique, emulsification is based on the principle of stress, shear deformation and cavitation. In microfluidizer, coarse emulsion enters the interaction chamber from two opposite microchannels with high pressure and velocity, resulting in collisions generating a high shear. This results in the formation of emulsion droplets with uniform size distribution. The stability and the type of emulsion formed depend on the wettability of the emulsion components to the channel wall. Hence, selection of microchannel material as well as emulsifiers plays a crucial role in deciding the emulsion type (Villalobos-Castillejos et al., 2018). This technique is usually selected for generation of smaller droplets. Jo *et al.* investigated the effect of microfluidization conditions such as microfluidizer pressure and number of cycles on droplet size of  $\beta$ -carotene nanoemulsions. When the microfluidizer pressure and number of cycles were increased from 20 to 120 MPa and 1 to 3 cycles respectively, a marked reduction in droplet size from 416.0 to 97.2 nm was observed (Jo and Kwon, 2014). However, some of the limitations of this method include higher manufacturing costs, chances of clogging of microchannels and longer emulsification time leading to coalescence of droplets, resulting eventually in the formation of larger droplets (Yukuyama et al., 2016).

#### **2.7.2.2. Low-pressure homogenization**

This technique has shown considerable advantages over the high energy process, especially in the product development on a large scale and subsequent commercialization. It ensures the

stability of the encapsulated product with the least energy consumption and is considered a non-destructive process (Khan et al., 2018).

**2.7.2.2.1. Phase inversion emulsification method:** In the phase inversion method, the transformation of one emulsion type to the other type occurs. This is achieved either by varying the composition or temperature of the system. The method requires low energy input of  $10^3$ -  $10^5$  W kg (Gupta et al., 2016) which can be achieved by the simple batch stirrer.

**2.7.2.2.1.1. Phase inversion by composition (PIC):** The method is based on the concept of phase inversion point where the interfacial tension is lowered and the small droplets are formed with the expenditure of lower energy. At the phase inversion point, major change in the surfactant arrangement occurs at the interface of the immiscible phases which reverts the dispersed phase of the system to become the continuous phase and *vice versa* (Preziosi et al., 2013). The ease of scale-up and low expenditure procedure are the major advantages of this method but utmost care is required during the addition of one phase to the other phase. Formation of liquid crystals or mid-range microemulsion phases are major limitations in this method (Yukuyama et al., 2016). Dyab *et al.* formulated aspirin loaded PEs using high shear homogenization technique. Later on, multiple emulsions were formed by the catastrophic phase inversion (CPI) emulsification method. A simple olive oil in glycerin emulsion was formed at the phase volume of 0.4 and CPI was observed in between the phase volume of 0.4 to 0.5 resulting in multiple olive oil- glycerin - olive oil emulsion (Dyab et al., 2018).

**2.7.2.2.1.2. Phase inversion by temperature (PIT):** In this method, phase inversion is brought about by change in the temperature. Initially, macroemulsion is prepared at a higher temperature then it is cooled down to room temperature. During this passage from higher to lower temperature, the system reaches phase inversion temperature. At this point, transformation of dispersed phase to continuous phase takes place to form an emulsion with reduced size and greater surface area (Preziosi et al., 2013). This method is limited to temperature-sensitive non-ionic surfactants such as polyethoxylated surfactants. The final nanoemulsion so formed, should be stored at a temperature far from PIT to avoid instability issues (Maali and Mosavian, 2013).

**2.7.2.2.2. Membrane emulsification:** Membrane emulsification is a static emulsification method. In this, a microporous membrane of uniform pore diameter is used. Shirasu porous glass



membrane is used under pressure (Joseph and Bunjes, 2014) and this membrane is permeated by the dispersed phase which forms droplets of dimensions close to those of the membrane pore diameter. These are then dispersed uniformly into the continuous phase. Selection of membrane, in this process, is very crucial. A hydrophilic membrane is selected for oil in water emulsion and hydrophobic membrane for water in oil emulsion. This method focuses on the droplet formation whereas other high shear methods are droplet disruption methods. Hence this method ensures uniformly sized dispersed phase droplets with higher stability (Sotoyama et al., 1999). Features like ease in scale-up, good reproducibility of results and efficient energy utilization make this technique useful at industrial as well as laboratory scale. Generally, tubular micro-porous glass (Nakashima, 1991), uncoated or titania oxide coated ceramic  $\alpha$ -Al<sub>2</sub>O<sub>3</sub> membranes are used (V. Schröder, 1999). However, one major constraint in the industrial scale-up is related to low dispersed phase flux through the membrane which influences the submicron droplet formation (Joscelyne and Trägårdh, 2000).

**2.7.2.2.3. Microchannel emulsification method:** The method is a modification of the membrane emulsification method. In this method, instead of the membrane, microchannel arrays fabricated on silicon chips are employed. Based on the size of the microchannel array system, a monodisperse emulsion is generated with droplet diameter in microns and size variation less than 5 % (Tan et al., 2018). Recently straight-through microchannel emulsification was used to prepare monodisperse O/W emulsions stabilized by natural emulsifiers like hydrophilically modified lecithin and whey protein isolate (Ma et al., 2020).

**2.7.2.2.4. Spontaneous emulsification:** In this method, optically transparent nanoemulsion is formed spontaneously by mixing the nonpolar phase/surfactant mixture by titration into the polar medium with constant stirring. The droplet size and stability of the emulsion is highly dependent on the composition of oil phase (single oil or if required combination of oils), surfactant to oil ratio, and co-solvent (Gulotta et al., 2014).

**2.7.2.2.5. Solvent evaporation method:** In this technique, an organic solvent is used to solubilize the drug and further mixed with surfactant. The emulsion gets formed with the addition of the continuous phase. Then the organic solvent is evaporated resulting in encapsulation of the drug (Kale and Deore, 2017). This low energy method was employed by Meng *et al.* for developing microencapsulated oxalic acid (OA) NANE where acetone was used as the volatile solvent

(Meng et al., 2017). Similar technique was employed by Suitthimeathegorn *et al.* for loading <sup>3</sup>H-Dexamethasone into castor oil-silicone NANE using absolute ethanol as the solvent (Suitthimeathegorn et al., 2007).

Among these methods of preparation, most suitable preparation technique has to be selected. The selected methods play a significant role in the formation of NANE which ultimately ensures the protection of encapsulated drug.

### **2.7.3. Mechanism of drug encapsulation in NANEs**

NANEs are colloidal dispersion system with the potential to encapsulate highly lipophilic drugs. Generally, the lipophilic drugs are solubilized in the selected oil phase (having maximum solubility). Upon mixing of oil phase with surfactant-co-surfactant ( $S_{mix}$ ) and dispersion medium, emulsification process begins. During the process, the lipophilic drug stays inside the oil droplets. The oily matrix protects the encapsulated drug from the environmental stress conditions such as oxidation and hydrolytic degradation (Jafari et al., 2017). In case of Pickering emulsions, where the traditional surfactant is substituted with solid particles such as silica nanoparticles, clay etc., and the drug is encapsulated within the oil matrix where solid particles accumulate at the interface of the immiscible phase. This ensures efficient stabilization of the system as well as prevention of drug degradation (Yang et al., 2017). The solubility of drug in surfactant also allows the drug to be partially dispersed outside the core of the micelles. Entrapment efficacy of a drug depends not only on the solubility and hydrophobicity of drug but also other physicochemical properties such as its molecular weight, melting point etc. Schematic representation of drug encapsulation in NANEs and Pickering NANEs is shown in **Figure 4**.

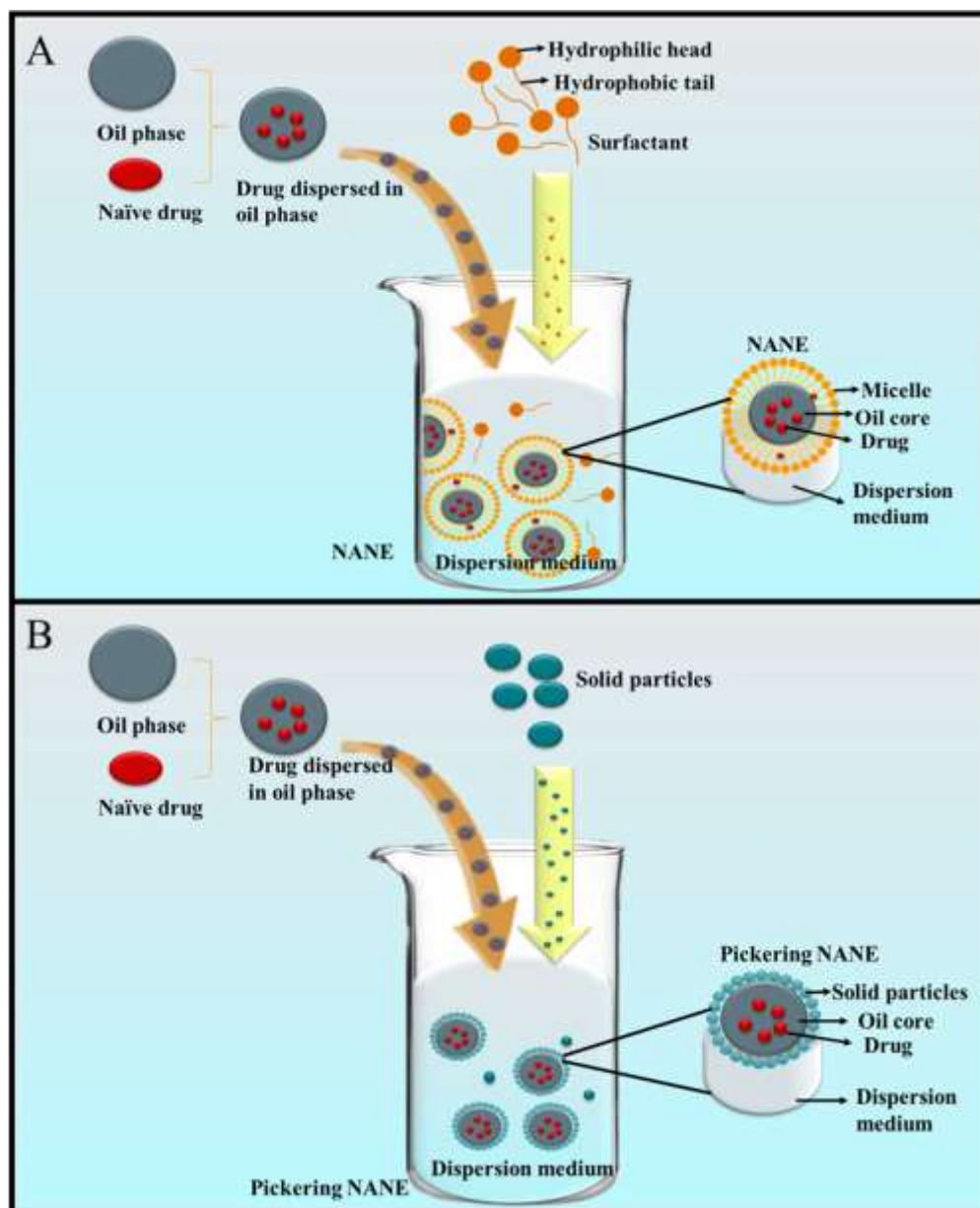


**Figure 4.** Schematic representation of drug encapsulation A) NANEs B) Pickering NANEs

#### 2.7.4. NANE explored for preservation of drug stability

The unique composition of the NANE helps in preservation of drug's characteristic features as well as stabilizes the system. Therefore, this system has been explored in pharmaceuticals, cosmeceuticals and nutraceuticals (Garg et al., 2016). Some NANEs explored so far are summarized in **Table 9**.

Table 9. NANE explored so far for delivery of drugs

Drug candidates	Benefits of NANE	Formulation composition	Type of studies	Study outcomes	Reference
<b><sup>3</sup>H-Dexamethasone and <sup>3</sup>H-Dehydroepiandrosterone</b>	<ul style="list-style-type: none"> <li>• Provide reservoir/depot effect</li> <li>• For controlled release of drug</li> <li>• Incorporation of lipophilic molecules</li> </ul>	DP: Castor oil Surfactant: Triton X 100 DM: Silicone oil	<i>In vitro</i> release studies using dialysis membrane	<ul style="list-style-type: none"> <li>• Slow and controlled release of drugs</li> <li>• Depot effect on intramuscular administration</li> <li>• ↓ frequency of administration</li> </ul>	(Jaitely et al., 2004)
<b>Dexamethasone</b>	<ul style="list-style-type: none"> <li>• Provided depot effect/reservoir effect</li> <li>• Incorporation of poorly water soluble compound</li> </ul>	DP: Castor oil Surfactant: Cyclomethicone/PEG/PPG-18/18 dimethicone DM: Silicone oil	<i>In vivo</i> studies in rats	<ul style="list-style-type: none"> <li>• ↓ peak plasma concentration with longer T<sub>max</sub></li> <li>• Sustained drug release of the drug</li> <li>• Slower absorption of the drug</li> <li>• Deposit of emulsion observed after 48 h confirmed depot effect</li> </ul>	(Suitthimeathegorn et al., 2007)
<b>Deoxyarbutin</b>	<ul style="list-style-type: none"> <li>• In aqueous solution, it decomposes to hydroquinone</li> <li>• A stable vehicle that delay degradation</li> </ul>	DP: Propylene glycol, glycerin Surfactants: Cetyl dimethicone copolyol DM: Cyclomethicone, stearyl dimethicone, isostearyl isostearate	Stability studies	<ul style="list-style-type: none"> <li>• Delayed degradation of deoxyarbutin to hydroquinone at 25°C and 45°C</li> <li>• Effective in melasma</li> </ul>	(Lin et al., 2011)
<b>Nystatin</b>	<ul style="list-style-type: none"> <li>• Enhanced penetration of non-polar and high molecular weight Nystatin</li> </ul>	DP: Labrafac® lipophile Surfactant : Labrasol, Plurol oleique Solvent : Transcutol P DM: Propylene glycol	<i>Ex vivo</i> permeation studies in porcine mucosa	<ul style="list-style-type: none"> <li>• Stable NANE effective against <i>Candida albicans</i></li> <li>• Approximately 50% of drug release after 6 h of permeation study</li> <li>• Effective for mucositis</li> </ul>	(Campos et al., 2012)
<b>Flavanones isolated from <i>Eysenhardtia platycarpa</i> leaves</b>	<ul style="list-style-type: none"> <li>• Improved permeation and retention of the poorly water soluble flavanones</li> </ul>	DP: Labrafac ® lipophile Surfactant : Labrasol, Plurol oleique DM: Propylene glycol	<i>In vivo</i> anti-inflammatory studies in mice	<ul style="list-style-type: none"> <li>• Better permeation across the skin</li> <li>• Maintenance of skin integrity</li> <li>• Used for topical treatment of anti-inflammatory</li> </ul>	(Dominguez-Villegas et al., 2014)

				condition	
<b>Nonivamide</b>	<ul style="list-style-type: none"> <li>To deliver highly lipophilic synthetic analogue of capsaicin</li> <li>To exhibit higher substantivity on the skin during the application interval.</li> </ul>	DP: Polydimethyl siloxane Surfactant: Dispersion of silicone (1:1) DM: Castor oil	<i>Ex vivo</i> permeation studies using pig ear skin	<ul style="list-style-type: none"> <li>Constant permeation rate was observed for 10 h</li> <li>↓ frequency of application</li> <li>To treat chronic pruritus</li> </ul>	(Rottke et al., 2014)
<b>Ascorbic acid</b>	<ul style="list-style-type: none"> <li>To prevent the degradation of ascorbic acid to dehydro ascorbic acid in presence of water</li> </ul>	DP: Glycerin Surfactant: Glyceryl monostearate DM: Mineral oil	<i>Ex vivo</i> drug permeation and retention studies using abdominal rat skin	<ul style="list-style-type: none"> <li>Stable NANE with slow permeation and enhanced retention</li> <li>Improved anti-wrinkle activity</li> </ul>	(Shirke et al., 2015)
<b>Griseofulvin</b>	<ul style="list-style-type: none"> <li>Dermal penetration and bioavailability</li> <li>Improve stability of griseofulvin</li> </ul>	DP: Glycerin Surfactant: Glyceryl monostearate Co-surfactant: Ethanol DM: Olive oil	Stability studies	<ul style="list-style-type: none"> <li>A stable NANE obtained with single surfactant rather than using a combination of surfactants.</li> <li>Hydrophobic surfactants were more efficient than hydrophilic surfactants</li> </ul>	(Jadhav et al., 2015a)
<b>Cholecalciferol</b>	<ul style="list-style-type: none"> <li>For controlled drug delivery</li> <li>To prevent the degradation of cholecalciferol</li> </ul>	DP: Silicone oil Surfactant: Cyclomethicone DM: Castor oil	<i>In vitro</i> drug release using artificial membrane	<ul style="list-style-type: none"> <li>Emulsion was stable at room temperature</li> <li>Preferred for psoriasis condition</li> </ul>	(Payghan, 2016)
<b>Progesterone, <math>\alpha</math>-tocopherol and lycopene</b>	<ul style="list-style-type: none"> <li>To improve the topical delivery of highly lipophilic drugs that are sparingly soluble in water</li> </ul>	DP: Isopropyl myristate, tributyrin, oleic acid Surfactant: Brij 95, vitamin E- D- $\alpha$ -tocopherol PEG 1000 succinate, ethanol DM: Propylene glycol	<i>In vitro</i> penetration studies on porcine ear skin and drug release studies on cellophane membrane	<ul style="list-style-type: none"> <li>Improved drug delivery into viable skin layers by 2.5 to 38 folds</li> <li>Increase in drug lipophilicity, enhanced penetration magnitude into viable skin layer</li> </ul>	(Carvalho et al., 2017)
<b>Aspirin</b>	<ul style="list-style-type: none"> <li>To reduce the adverse effects of drug.</li> <li>Silica nanoparticles on the droplets acts as a barrier that prevent its direct exposure to</li> </ul>	DP: Olive oil Surfactant: Silica nanoparticles DM: Glycerin	<i>In vitro</i> release studies	<ul style="list-style-type: none"> <li>Simple and multiple NANE</li> <li>Maximized stability with silica nanoparticles</li> <li>↑ release rate of aspirin</li> </ul>	(Dyab et al., 2018)

<b>ASX</b>	digestive environment <ul style="list-style-type: none"> <li>To improve ASX solubility</li> <li>To prevent degradation of ASX in presence of the dissolved oxygen in water</li> </ul>	DP: Octyl and decyl glycerates Surfactant: Soya lecithin, Tween 80 DM: Glycerin	<i>In vivo</i> studies using male rats	<ul style="list-style-type: none"> <li>Improved the chemical stability</li> <li>Prolonged antioxidant activity</li> <li>Better permeation across the skin</li> </ul>	(Sun et al., 2019)
------------	--	---	--	--	--------------------

### 2.7.5. Patented non-aqueous emulsions

Patent search for non-aqueous emulsions has been carried out and very few patents reported which are tabulated in **Table 10**

**Table 10.** Patents on non-aqueous emulsions

Patent No	Claim	Reference
<b>US5110606A</b>	Art of preparing palatable formulations was revealed by dissolving the drug in propylene glycol and dispersing this solution in fatty ester	(Geyer and Tuliani, 1992)
<b>US5587149A</b>	Art of preparing non-aqueous emulsions of vitamin C using silicone oils. These were claimed to be suitable to be filled into soft gelatin capsules	(Punto et al., 1996)
<b>EP0940423A3</b>	Emulsions of silicones with non- aqueous hydroxylic solvents.	(Powell and Kasson, 2001)

### **2.7.6. Stabilization of nanoemulsions**

The basic understanding of the relationship between the composition and physicochemical properties of the nanoemulsions helps in understanding the mechanism of nanoemulsion stabilization and its related instability issues.

#### **2.7.6.1. Factors involved**

The key factors that influence the stability of any nanoemulsion include droplet size, surface charge and droplet distribution. The nature and amount of emulsifier chosen as well as the preparation method employed collectively determine the droplet size and associated factors. It is the brownian motion of the droplets that freely suspends them in the dispersion medium. Hence, the effect of the gravitational force on the droplets is negligible and minimizes the sedimentation rate (Rai et al., 2018). Nature of the emulsifier determines the surface charge of the droplets and the uniformity of distribution. If the selected emulsifier is ionic, it exerts charge to the droplets and imparts repulsive force (Davis, 1990) among the droplets creating an electro-kinetic potential termed as zeta potential. The magnitude of zeta potential determines the stability of the colloidal system. Higher magnitude of zeta potential such as more than  $\pm 30$  mV are reported to result in better stability (Eid et al., 2013). Hydrogen bond donor-acceptor ability of the constituents also affects the stability of NANEs. The solvents that are similar in polarity and structural properties to that of water show the ability to solvate surfactant through hydrogen bonding (Imhof and Pine, 1997). Hence, in brief, the stabilization of nanoemulsion depends on various inter and intra molecular attractive and repulsive forces (Ramanunny et al., 2022).

#### **2.7.6.2. Associated stability problems**

The major stability problems encountered in nanoemulsions include droplet aggregation such as flocculation, coalescence, and Ostwald ripening leading to creaming/sedimentation, and finally phase separation. The emulsifier forms an adsorption layer around the droplets which creates steric interface and maximizes the repulsive forces. When the attractive force replaces the repulsive force, droplets move towards each other and physical contact causes aggregation. This phenomenon is known as flocculation. The so formed floccules, however, redisperse on shaking. On the other hand, physical contact among the droplets initiates droplet growth, which causes the rupture of the emulsifier layer and droplets merge to form a bigger droplets resulting in

coalescence. It is practically difficult to distinguish between flocculation and coalescence (Pawignya et al., 2019).

The differential density of droplets and dispersion medium determines the stability issues. If the dispersed droplets possess lower density in comparison to the dispersion medium, they tend to move upward. This phenomenon is known as creaming. The droplets with higher density experience higher gravitational pull and move downward. This is termed as sedimentation. The difference in chemical potential that exists between droplets and the Laplace pressure generated at the curved interface explains the frequency of Ostwald ripening (Singh et al., 2017). When the potential is higher in smaller droplets, the mass transfer occurs resulting in the larger droplet. The smaller droplets merge with larger once gradually with time, resulting in giant droplets. This is the major issue faced in the formulation development of nanoemulsion termed as Ostwald ripening (Nazarzadeh et al., 2013). The instability problems associated with nanoemulsions are briefly represented in **Figure 5**.



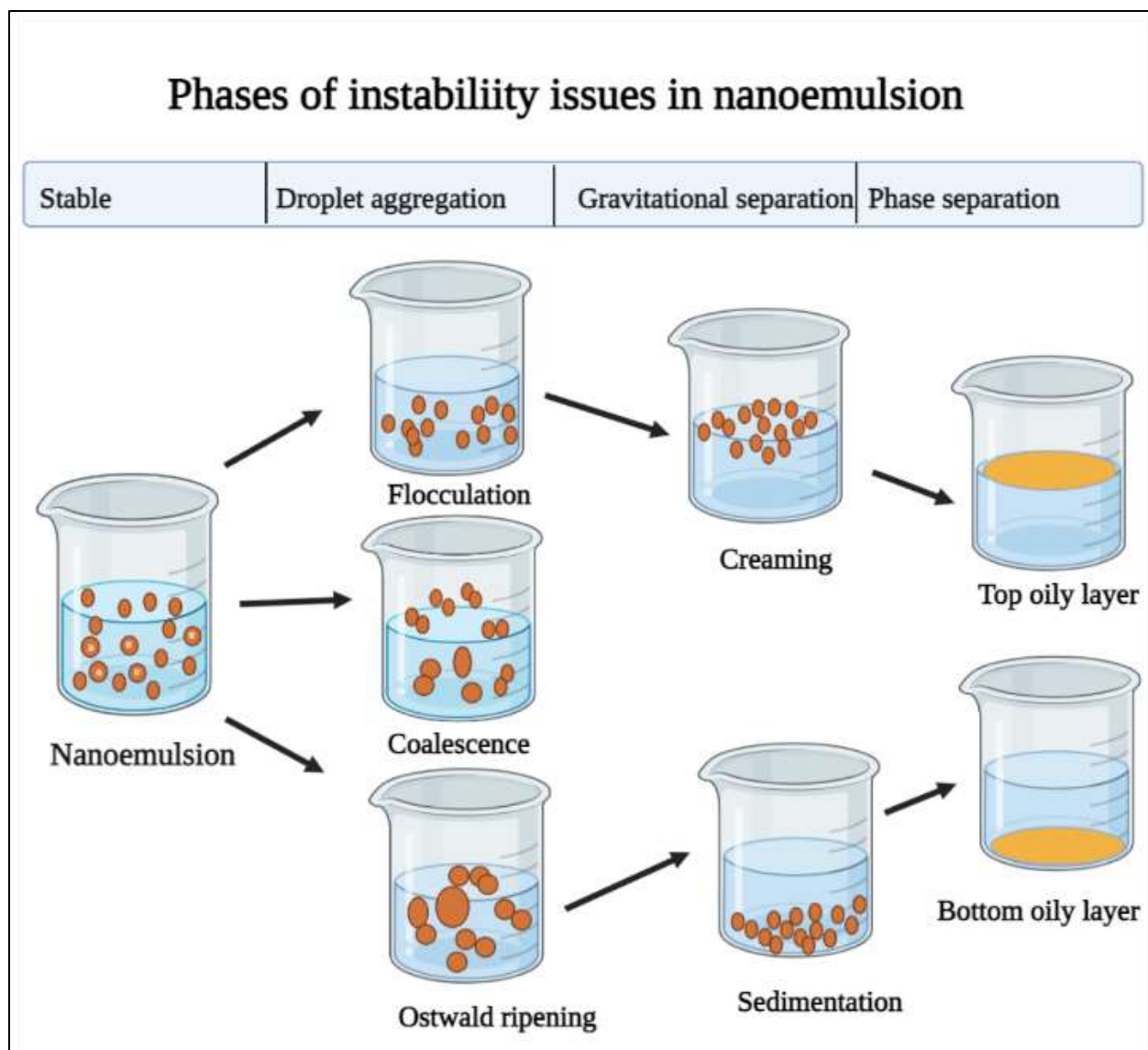


**Figure 5.** Phases of instability issues in nanoemulsions

The instability issues of NANEs need to be addressed for preparation of formulations with optimum shelf life. Addition of high-density hydrophobic materials before homogenization helps to overcome the gravitational separation and hence prevents creaming/sedimentation related problems. Addition of highly insoluble oil, preferably long-chain triglycerides prior to homogenization prevents droplet aggregation and Ostwald ripening (Maphosa and Jideani, 2018). The added insoluble oil generates entropy within the system that exerts an effect on the curvature of the droplets. Chen *et al.* in 2016 studied the effect of both long and MCT, bean oil and MCT oil on the stability of eugenol nanoemulsion. In the study, it was observed that Ostwald ripening could be avoided and maximum stability of emulsion was achieved at an effective

concentration of about 30% w/w strength of triglyceride. Thus, the stability of the formulated nanoemulsions is reported to depend on the interfacial tension and droplet size that may be achieved by the appropriate selection of triglyceride concentration (Chen et al., 2016).

These studies show the significant role of each component in the development of a stable nanoemulsion. The selection of suitable components as well as adequate mixing of each component in appropriate volume and concentration is too crucial in assuring stability of nanoemulsion. Hence, the critical analysis of various process and product development parameters needs to be carried out using optimization technique.

## **2.8. Quality by design approach for optimization**

Quality by design (QbD) is a systematic approach that sets a predefined objective and incorporates scientific knowledge for better management and control of product and process variables to ensure quality product at the end of the manufacturing process (Lawrence et al., 2014). Hence, these approaches incorporate scientific knowledge, results from design of experiment (DoE) and uses quality risk management. This approach was approved by the European Medicines Agency and United States Food and Drug Administration (FDA). Further improvement in the QbD objectives has been done through International Conference on Harmonisation (ICH) of Technical Requirements for Registration of Pharmaceuticals for Human Use. ICH introduced the guidelines such as ICH Q8 (Pharmaceutical Development) (Administration, 2020), ICH Q9 (Quality Risk Management) (Food and Administration, 2006), ICH Q10 (Pharmaceutical Quality System)(Administration, 2006) to build better understanding of QbD into formulation development. The implementation of this approach in pharmaceutical product development helps to monitor each stages of the product development and ensures quality based product (Zhang and Mao, 2017).

The better understanding of these element in QbD explains the life cycle management in product development (Cunha et al., 2020)

1) Quality target product profile (QTPP): The characteristics required for a final product that are related to quality, safety and efficacy are considered which include route of administration, pharmaceutical dosage form, drug delivery system, strength, stability, sterility, packing containers/closures.

2) Critical quality attributes (CQAs): Identify the parameters that have impact on the quality of the final product. This parameter is closely related to the physical, chemical, biological, microbiological characteristic of excipients, drug substances, in-process materials, and drug products that has to be selected on the basis of their range, limits or distribution.

3) Critical material attributes (CMAs): Determine the properties of materials that can ensure quality in the final product. The selection of excipients, drugs and other materials of standard quality can guarantee high quality in the final product.

4) Critical process parameters (CPPs): These are the production parameters that affect CQAs. The process parameters that interfere in the quality of product have to be monitored and controlled.

### **2.8.1. Steps involved in QbD implementation**

The implementation of QbD approach in pharmaceutical product development involves the following steps:

a) Define and identify the parameters that influence product performance and quality (QTPP, CMAs, CPPs, and CQAs)

b) Identify risk parameters using risk assessment

c) Establish DoE to associate CMAs and CPPs to CQAs

d) Development of control strategy to identify the causes of variability

e) Life cycle management for continuous monitoring and improving of manufacturing process

### **2.9. DoE**

An analytical tool with systematic methodology to determine the relationship between input factor affecting the process and their effect on the desired output (response). In simplest words it is the “cause and effect” relationship. A well-organized methodology is adopted in DoE based optimization and the sequence are mentioned as follows (Beg et al., 2019; Durakovic, 2017):

Step 1: Set the product development objective

The most importance step in the initial stage of product development is to describe the objective. The parameters that influence CQAs are screened to identify independent process and product variables that are directly linked to the safety and efficacy of product.

Step 2: Selection of independent variables (factors) and dependent variables (responses).

In this step identification of CMAs related with the product and CPPs associated with processes involved in the product development. These are considered as the input variables and their effect on CQAs is recorded as the response. Thus, the selection of independent variables (CMAs and/or CPPs) is crucial as they provide meaningful link to the CQAs and QTPP. Among the possible input variables, more influential input variables are selected based on the screening design such as Fractional Factorial Design (FFD), Plackett-Burman Design (PBD) and Taguchi Design (TD). Later, more experimental studies are conducted to demonstrate the effect of various factors and their interaction on the responses. This helps to point out the broad range of factors to be included in the experiment design.

Step 3: Selection of experimental design

The most appropriate experimental design for optimization is selected in response to the product development objective and identified CMAs and /or CPPs. Some of the response surface designs used in optimization are Central Composite Design (CCD), Box Behnken Design (BBD), Factorial Design (FD), D-Optimal Design, and Mixture Design. The selection of suitable design among them, type of factors, number of factors and their levels such as high, medium and low are considered as significant for successful optimization. Further, evaluation of their respective responses provides better understanding towards formulation development.

Step 4: Optimization of final formulation

Execution of the DoE design generates suitable data and further statistical evaluation of these data anticipates an appropriate model. The model relates the response variables to different levels of the input variables. Further, numerical and graphical optimization of the selected variables and responses are accomplished to finalize the optimized product(s) and/or processes.

Step 5: Validation and scale-up

In this stage, predicted response of the design model is validated. The predicted responses obtained from the surface methodology is critically analyzed and evaluated experimentally. This is the final confirmatory run to obtain the optimized formulation. Further, scale-up and production levels can be set forth.

### **2.9.1 Application of DoE**

DoE approach has been extensively used to optimize the product quality with minimum experimentation and investment. This statistical tool can be used in various types of system, process and product design, development and optimization. This tool helps in early detection of basic parameters such as variation in manufacturing processes, raw material characteristics, product design, production techniques, etc. that influences product quality and reliability. In this era, DoE approach has been used in various technology-driven industries to ensure process capability, product quality and product/process improvement in the optimized product (Durakovic, 2017).

In present research work, DoE approach has been employed in extraction process as well as in formulation development for ensuring the reliability and quality of the process and product respectively. Hence, few studies that have utilized DoE for extraction and formulation development are summarized in **Table 11** and **Table 12** respectively.

**Table 11.** Design explored for extraction optimization by ultrasound-assisted technique

S.No.	Plant part	Design	Experimental run	Independent variable	Dependent variable	Optimization outcome	References
1	<i>Rheum moorcroftianum</i> rhizomes	BBD	29	<ul style="list-style-type: none"> <li>• Vessel diameter</li> <li>• Sample to solvent ratio</li> <li>• Extraction temperature</li> </ul>	<ul style="list-style-type: none"> <li>• Polyphenolic content</li> <li>• Antioxidant activity</li> </ul>	<ul style="list-style-type: none"> <li>• 12 polyphenolic compounds were obtained under optimized condition</li> <li>• Optimized extraction was carried out using a vessel of 6 cm diameter containing 1:28.42 g/mL of sample in 40% v/v of acetone with 0.2 N HCl. Sonication was carried out at 37 °C under frequency of 50 kHz for 10 min</li> <li>• Effect of each factors on antioxidant assays were different indicated different mechanism of action of the identified polyphenolic compounds</li> <li>• Experimental values for the responses were close to the predicted values</li> </ul>	(Pandey et al., 2018)
2	<i>Gentiana lutea</i> root	CCD	30	<ul style="list-style-type: none"> <li>• Extraction time</li> <li>• Ethanol concentration</li> <li>• Solid to solvent ratio</li> <li>• Extraction temperature</li> </ul>	<ul style="list-style-type: none"> <li>• Isogentisin</li> <li>• Gentiopicroside</li> <li>• Total polyphenols</li> </ul>	<ul style="list-style-type: none"> <li>• Optimal parameters for extraction of maximum content of isogentisin <math>4.81 \pm 0.09</math> mg/g dried weight, gentiopicroside (<math>21.45 \pm 0.22</math> mg/g dried weight), total phenolic content (<math>36.55 \pm 0.31</math> mg GAE/g dried weight) were carried out using 49% ethanol at sample: solvent ratio of 1:42 g/mL for 31 min at 80°C.</li> <li>• Predicted values were close to the experimental values</li> </ul>	(Živković et al., 2019)
3	<i>Cynara cardunculus</i> leaves	BBD	17	<ul style="list-style-type: none"> <li>• Solid: liquid ratio</li> <li>• Amplitude</li> <li>• Temperature</li> </ul>	<ul style="list-style-type: none"> <li>• Extraction yield (mg of cynaropicrin/g dry weight)</li> <li>• Cynaropicrin concentration (mg)</li> </ul>	<ul style="list-style-type: none"> <li>• At optimal conditions of solid/liquid ratio (1:27), amplitude (67%) and temperature (44 °C), average yield and concentration of cynaropicrin was <math>23.90 \pm 0.14</math> mg/g dried weight and <math>192.51 \pm</math></li> </ul>	(Brás et al., 2020)

					cynaropicrin /g extract)	6.96 mg/g extract respectively.	
4	<i>Momordica charantia</i> (bitter guard) fruit	CCD	20	<ul style="list-style-type: none"> <li>• Temperature</li> <li>• Time</li> <li>• Bitter guard to solvent</li> </ul>	<ul style="list-style-type: none"> <li>• Total phenolics content</li> <li>• Antioxidant activity</li> <li>• Soluble proteins content</li> </ul>	<ul style="list-style-type: none"> <li>• No statistical difference between experimental data and predicted values</li> <li>• Using 0.3 g/L of bitter guard / solvent at 68.4 °C for 11.6 min yielded 12.5 ± 4 mg GAE/g , 68.2 ± 2% and 41 ± 4 mg/1000mL, for total polyphenols, antioxidant activity and total soluble proteins respectively.</li> <li>• The experimentally determined values were close to the predicated value</li> </ul>	(Chakraborty et al., 2020)
5	<i>Cuphea glutinosa</i> leaves	FFD (Screening design)	16	<ul style="list-style-type: none"> <li>• Ethanol concentration</li> <li>• Plant:solvent ratio</li> <li>• Number of extractions</li> <li>• Extraction time</li> <li>• Particle size</li> </ul>	<ul style="list-style-type: none"> <li>• Miquelianin peak area</li> </ul>	<ul style="list-style-type: none"> <li>• Time 60 min, plant:solvent 1:60 (w/v) and particle size ≤ 180 µm were screened</li> <li>• Pareto results has shown statistically no significant difference except in ethanol concentration</li> <li>• Dong's algorithm explained the effect of number of extractions on miquelianin peak area</li> </ul>	(Santos et al., 2020)
		CCD	13	<ul style="list-style-type: none"> <li>• Number of extractions</li> <li>• Ethanol concentration</li> </ul>	<ul style="list-style-type: none"> <li>• Miquelianin peak area</li> </ul>	<ul style="list-style-type: none"> <li>• Optimized extraction parameters such as 5 times extraction, using 38% ethanol resulted in average content of miquelianin of 1.03%, represented an increased yield of 29.02% of miquelianin with regard to the non-optimized and validated method</li> </ul>	
6	<i>Amaranthus caudatus L</i> flower	CCD	18	<ul style="list-style-type: none"> <li>• Time</li> <li>• Ultrasonic power</li> </ul>	<ul style="list-style-type: none"> <li>• Amaranthine</li> <li>• Isoamaranthine</li> <li>• Total betacyanins</li> </ul>	<ul style="list-style-type: none"> <li>• A maximum of 1.92% w/w of extract, 55.2 ± 0.6 mg/g plant material of amaranthine, 19.4 ± 0.3 mg/g plant material of isoamaranthine and total 77.6 mg/g of total betacyanins were obtained with 13.3 min sonication at 500 W</li> </ul>	(Roriz et al., 2021)

**Table 12.** Design explored for optimization of nanoemulsion

Drugs	Design	No of experimental run	Independent variable	Dependent variable	Optimization outcome	References
-	CCD	18	<ul style="list-style-type: none"> <li>• Homogenizing pressure</li> <li>• Oil content</li> <li>• Number of passes</li> </ul>	<ul style="list-style-type: none"> <li>• Sauter mean diameter (SMD)</li> <li>• Polydispersity index (PDI)</li> </ul>	<ul style="list-style-type: none"> <li>• Nanoemulsion containing 2% w/w of emulsifier was optimized at pressure of 856.5 bar, oil content of 5% v/v and number of pass 4. At this optimal condition, SMD and PDI were 176.1 nm and 0.163 respectively</li> </ul>	(Galooyak and Dabir, 2015)
Clove oil	Taguchi	9	<ul style="list-style-type: none"> <li>• Clove oil concentration</li> <li>• Emulsifier concentration</li> <li>• Mixed HLB</li> <li>• Ultrasonication time</li> </ul>	<ul style="list-style-type: none"> <li>• Droplet size</li> <li>• Zeta potential</li> <li>• PDI</li> </ul>	<ul style="list-style-type: none"> <li>• By optimizing clove oil concentration (15 %), emulsifier concentration (2.5% w/w), mixed HLB (9), ultrasonication time (450 min), nanoemulsion with droplet size of <math>32.2 \pm 2.3</math> nm, PDI <math>0.38 \pm 0.06</math> and zeta potential of <math>-40.7 \pm 2.04</math> mV was obtained</li> </ul>	(Shahavi et al., 2016)
Curcumin	BBD	15	<ul style="list-style-type: none"> <li>• Surfactant concentration</li> <li>• Number of cycles</li> <li>• Pressure</li> </ul>	<ul style="list-style-type: none"> <li>• Droplet size</li> </ul>	<ul style="list-style-type: none"> <li>• At optimized conditions of 350 bar pressure, 5 cycles and 1% w/w surfactant concentration, a stable curcumin encapsulated palm oil based nanoemulsion with 275.5 nm droplet was obtained</li> </ul>	(Raviadaran et al., 2018)
ASX- $\alpha$ -tocopherol	BBD	15	<ul style="list-style-type: none"> <li>• Ultrasonic intensity</li> <li>• Sonication time</li> <li>• Temperature</li> </ul>	<ul style="list-style-type: none"> <li>• Droplet size</li> <li>• PDI</li> <li>• Zeta potential</li> <li>• ASX content</li> </ul>	<ul style="list-style-type: none"> <li>• Optimal conditions of ultrasonic intensity (90%), sonication time (10 min), and temperature (20 °C) resulted in nanoemulsion with droplet size of 217.81 nm, PDI of 0.11, zeta potential of -15.76 mV and ASX content 1.07 mg/mL</li> <li>• Experimentally obtained values were similar to the predicted values</li> </ul>	(Shanmugapriya et al., 2018)



<b>Sulconazole (SCZ)</b>	CCD	12	<ul style="list-style-type: none"> <li>• Ratio of oil:mixed-surfactant</li> <li>• Proportion of aqueous phase</li> </ul>	<ul style="list-style-type: none"> <li>• Encapsulation efficiency(EE)</li> <li>• Drug loading</li> <li>• Particle size</li> <li>• Zeta potential</li> </ul>	<ul style="list-style-type: none"> <li>• Optimized proportion of Capryol 90 (5.4%), labrasol (28.9%), 1,2-propanediol (14.4%) and aqueous phase (51.3%) resulted in satisfactory SCZ-nanoemulsion with particle size of <math>52.3 \pm 3.8</math> nm, PDI of <math>0.205 \pm 0.02</math>, zeta potential of <math>23.3 \pm 1.2</math> mV, % drug loading of <math>0.47 \pm 0.05\%</math> and EE of <math>87.1 \pm 3.2\%</math></li> </ul>	(Yang et al., 2019)
<b>Cinnamon</b>	BBD	17	<ul style="list-style-type: none"> <li>• Sonication time</li> <li>• Temperature</li> <li>• Tween 80 concentration</li> </ul>	<ul style="list-style-type: none"> <li>• Droplet size</li> <li>• PDI</li> <li>• Viscosity</li> </ul>	<ul style="list-style-type: none"> <li>• Optimum condition of sonication time 266 s, temperature at <math>4.82</math> °C, and Tween 80 concentration at 3% w/w produced stable nanoemulsion with minimum droplet size, PDI and optimum viscosity</li> </ul>	(Pongsumpun et al., 2020)
<b>Nitrendipine</b>	BBD	17	<ul style="list-style-type: none"> <li>• Oil</li> <li>• Surfactant</li> <li>• Co-surfactant</li> </ul>	<ul style="list-style-type: none"> <li>• Globule size</li> <li>• Drug content</li> <li>• Zeta potential</li> </ul>	<ul style="list-style-type: none"> <li>• Optimized composition of oil (27.11%), surfactant (58.56%) and co-surfactant (39.07%) resulted in formulation with globule size of <math>20.43 \pm 1.50</math> nm, drug content of <math>97.05 \pm 1.77\%</math> and zeta potential of <math>-15.45 \pm 0.35</math> mV</li> </ul>	(Sharma et al., 2020)
<b>Brazilian red propolis benzophenone-rich extract (BZP)</b>	BBD	15	<ul style="list-style-type: none"> <li>• Phospholipid egg lecithin concentration</li> <li>• DOTAP concentration</li> <li>• BZP extract concentration</li> </ul>	<ul style="list-style-type: none"> <li>• Droplet size</li> <li>• Zeta potential</li> <li>• Association efficiency</li> </ul>	<ul style="list-style-type: none"> <li>• Optimal formulation contained 182 mg of lecithin, 21 mg DOTAP and 6.7 mg of BZP resulted in a nanoemulsion with an average droplet size of <math>140.56 \pm 5.22</math> nm, zeta potential of <math>+60.72 \pm 3.07</math> and association efficiency of <math>99.55 \pm 1.09\%</math></li> </ul>	(Fasolo et al., 2020)
<b>Naringenin</b>	BBD	17	<ul style="list-style-type: none"> <li>• Capryol 90</li> <li>• <math>S_{mix}</math> (Tween 20 and Transcutol P)</li> <li>• Purified water</li> </ul>	<ul style="list-style-type: none"> <li>• Droplet size</li> <li>• PDI</li> <li>• Zeta potential</li> </ul>	<ul style="list-style-type: none"> <li>• Optimized formulation containing combination of 6% oil, 41% <math>S_{mix}</math> and 53% aqueous phase</li> <li>• Optimized formulation had</li> </ul>	(Akrawi et al., 2020)

---

<b>Cinnamon</b>	BBD	17	<ul style="list-style-type: none"> <li>• Sonication time</li> <li>• Temperature</li> <li>• Tween 80 concentration</li> </ul>	<ul style="list-style-type: none"> <li>• Droplet size</li> <li>• PDI</li> <li>• Viscosity</li> </ul>	<p>smaller droplet size of 14.14 nm and PDI of 0.279</p> <ul style="list-style-type: none"> <li>• Optimum condition of sonication time 266 s, temperature at 4.82 °C, and Tween 80 concentration at 3% w/w produced stable nanoemulsion with minimum droplet size, PDI and maximum viscosity</li> </ul> <p>(Pongsumpun et al., 2020)</p>
<b>Kojic Monooleate (KMO)</b>	CCD	20	<ul style="list-style-type: none"> <li>• Time of high shear</li> <li>• Speed of high shear</li> <li>• Speed of stirrer</li> </ul>	<ul style="list-style-type: none"> <li>• Droplet size</li> </ul>	<ul style="list-style-type: none"> <li>• KMO nanoemulsion obtained under the optimized conditions such as time of high shear (8.04 min), speed of high shear (4905.42 rpm), and speed of stirrer (271.77 rpm) has shown droplet size of 103.97 nm</li> <li>• ANOVA results has shown <math>p &lt; 0.0001</math> indicating significant model</li> </ul> <p>(Roselan et al., 2020)</p>

---

# Chapter 3



---

## **Rationale of the study**

---

## **Chapter 3**

### **Rationale of the study**

#### **3.1. Hypothesis**

Numerous therapeutics agents are available for the treatment of psoriasis. However, the treatment strategies based on conventional dosage forms are not suitable for long term use due to their side effects. Most of the existing treatments reduced the signs or symptoms of psoriasis. But being an autoimmune disease, frequency of appearance of psoriasis lesions are fast and mostly occur with mild triggering of the immune system. Nowadays, biologics are most preferred for the treatment of psoriasis and it was found to show better recovery with lesser side effects. The major limitation is the cost of the biologics which is too expensive for a common man to afford. Hence, it is important to find treatment strategies that need to be therapeutically effective and affordable.

Thorough literature search has shown the importance of herbals in psoriasis treatment. Traditional systems of medicine have been explored well in India since years ago. Among them Ayurveda treatment utilized herbals in the different dosage forms such as “Avleha”, “Lepa Kalpana”, “Churna”, “Asava”.

The major limitation of these dosage forms are the paucity in standardization of drugs (related to dosage form development) as well as the gradual recovery from the disease (related to therapeutic effectiveness). These reduced the demand for herbal dosage forms as compared to allopathic medicines.

Nowadays, advancement in technology utilizes the concept of translational research by incorporating herbal (extract or isolated phytoconstituents) into novel drug delivery systems. This translational research can promote the alternative and traditional system of medicine specially Ayurveda into a new phase. Combinational approach with herbal can be a better treatment strategy for psoriasis.

*In vitro* antipsoriasis activity of ethanolic extract of AG rhizomes on HaCaT keratinocyte cell line reported down-regulation of NF- $\kappa$ B pathway *via* increased expression of TNFAIP 3 and decreased mRNA expression of CD- 40. The study has also emphasized the importance of ACA which is present in the ethanolic extract of AG (Saelee et al., 2011).

Structural activity relationship of ACA has reported the presence of basic phenylpropanoid structure, which containing 1-acetoxy propenyl and acetoxy groups at 1' and 4 positions on the benzene ring respectively. These groups are responsible for various activation and inhibition mechanisms such as inhibition of xanthine oxidase activity, inhibition of nitric oxide synthase expression, inhibition of translocation of NF- $\kappa$ B, activation of AMPK signaling pathway and induction of apoptosis via mitochondrial/Fas- mediated mechanism (In et al., 2012; Kojima-Yuasa and Matsui-Yuasa, 2020; Ramanunny et al., 2021a).

Owing to the pharmacological benefits of potential phytoconstituents present in the extract, it was thought to develop a topical formulation with AGE. However, delivering an extract through a conventional topical formulation has certain limitations such as low bioavailability, poor penetration and inadequate drug retention. Hence, developing a nanoemulsion can overcome the aforementioned challenges. It is important to note that ethanolic extract of AG rhizomes contained ACA, which possesses aqueous degradation. It would be a major challenge while developing an aqueous nanoemulsion of AGE. This problem can be overcome by developing a NANE, a delivery system free from aqueous environment. Therefore, in the present study formulating AGE loaded NANE could provide protection to ACA as well as other components in AGE formulation (**Figure 6**). In addition to this, it also ensures stability of all components specially ACA, while transporting across/into the skin membrane by entrapping the drug in the emulsion droplets.

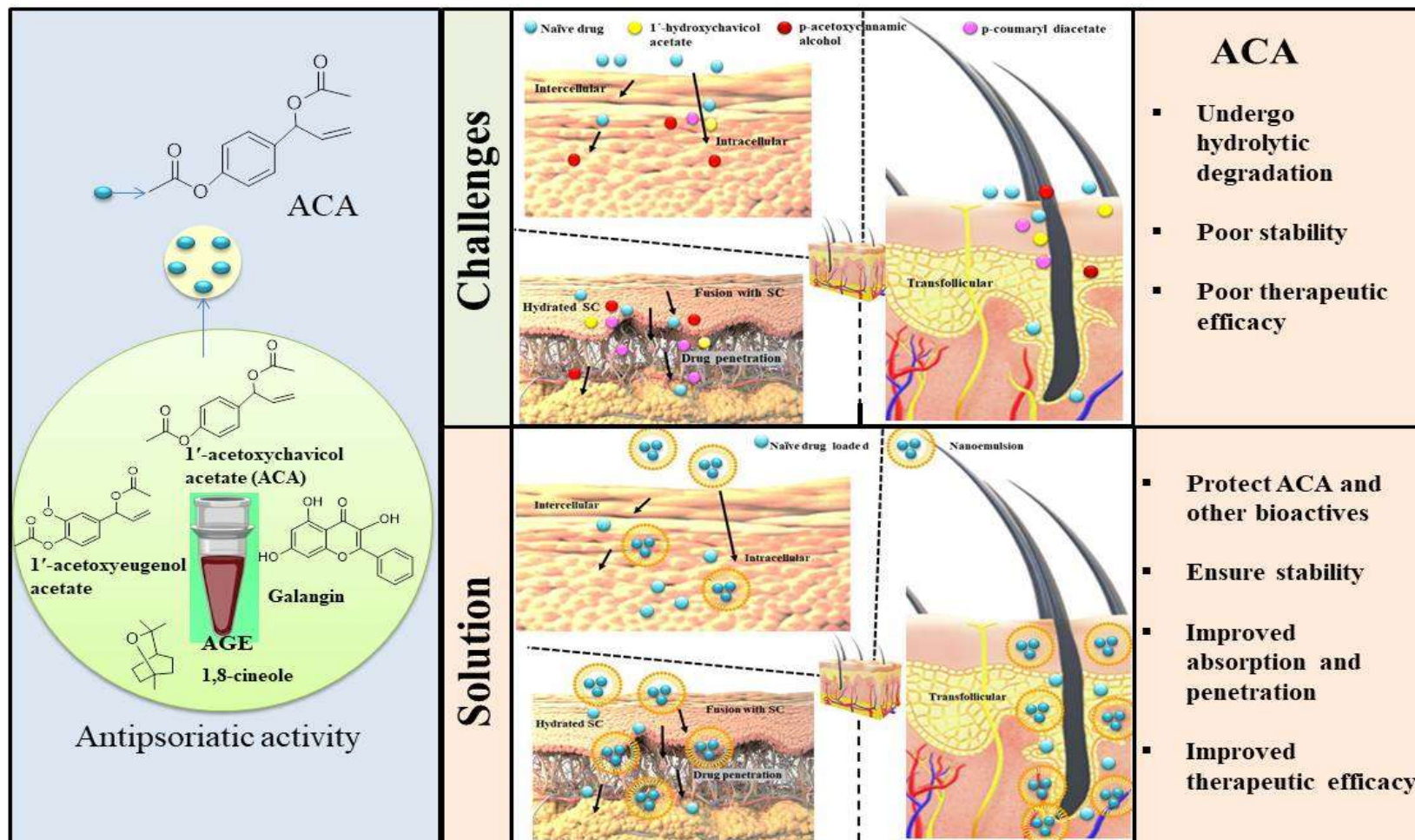


Figure 6. Hypothesis of the research

In a nutshell, the aim of the study is to develop a NANE loaded with ethanolic extract of AG for the effective treatment of psoriasis in IMQ induced mouse model. In the present study, ACA has been used as the marker compound for carrying out quantification of extract during characterization and evaluation of NANE. In addition to this, using ACA as a marker will also ensure the efficiency of NANE to protect ACA in the formulation.

### **3.2. Aim**

Formulation development, optimization and evaluation of *Alpinia galanga* extract loaded nanoemulsion.

### **3.3. Objective**

The objectives of the research proposal are as follows:

- 1) To prepare an ethanolic extract of *Alpinia galanga* rhizomes
- 2) To formulate and characterize nanoemulsion of *Alpinia galanga* extract
- 3) To evaluate the developed formulation for anti-psoriatic activity using animal model

# Chapter 4



---

## Experimental work

---



## Chapter 4

### Experimental work

#### 4.1. Materials and Instruments

##### 4.1.1. Materials

The list of materials used throughout the study was listed in **Table 13** along with the respective source(s).

**Table 13.** Various materials employed in the research work

Material (s)	Source(s)
1'-acetoxychavicol acetate (ACA)	LKT Laboratories Inc. USA
Absolute ethanol	Suzhou Yacoo Laboratories, China
Acetone	Loba Chemie Pvt. Ltd., India
Acetonitrile HPLC grade	Rankem, Avantor Performance Materials India Ltd., India
Almond oil	Central Drug House Pvt. Ltd., India
Ammonia solution	Loba Chemie Pvt. Ltd., India
Betamethasone valerate skin cream BP (Betnovate®)	GlaxoSmithKline Pharmaceuticals Ltd., India
Buffer capsules pH 4.0 ± 0.05	Merck Specialities Pvt. Ltd., India
Buffer capsules pH 7.0 ± 0.05	Merck Specialities Pvt. Ltd., India
Capmul MCM	Abitec Cooperation, USA
Capryol 90	Gattefosse Pvt. Ltd., India
Carbopol 934 Extra pure	Loba Chemie Pvt. Ltd., India
Castor oil	Central Drug House Pvt. Ltd., India
Chloroform	Loba Chemie Pvt. Ltd., India
Conc. Sulphuric acid	Loba Chemie Pvt. Ltd., India
Cremophor RH 40	Himedia Lab Pvt. Ltd., India
Dialysis membrane-110 (LA395)	Himedia Lab Pvt. Ltd., India
Diethyl ether	Loba Chemie Pvt. Ltd., India
Dimethicone	Supreme silicones, India
Formaldehyde	Loba Chemie Pvt. Ltd., India

Ferric chloride	Loba Chemie Pvt. Ltd., India
Formic acid	Qualigens fine chemicals, India
Glycerine 98% (glycerin)	Central Drug House Pvt. Ltd., India
Hexane	Central Drug House Pvt. Ltd., India
Hydrochloric acid	Loba Chemie Pvt. Ltd., India
Imiquimod cream 5% w/w (Imiquad cream)	Glenmark Pharmaceuticals Ltd., India
Iodine resublimed	Loba Chemie Pvt. Ltd., India
Isopropyl alcohol	Loba Chemie Pvt. Ltd., India
Isopropyl myristate (IPM)	KP Manish Global Ingredients Pvt. Ltd., India
Labrafac PG	Gattefosse Pvt. Ltd., India
Labrafil M 1944CS	Gattefosse Pvt. Ltd., India
Labrasol	Gattefosse Pvt. Ltd., India
Methanol HPLC grade	Loba Chemie Pvt. Ltd., India
Millipore water (in-house)	Bio-Age Equipment Ltd., India
Millon's reagent	Quali-Tech Fine Chemicals, India
Molisch reagent	Sisco Research Laboratories Pvt. Ltd., India
Olive oil	Central Drug House Pvt. Ltd., India
Palmester 3595 (MCT oil)	KP Manish Global Ingredients Pvt. Ltd., India
Peanut oil	Central Drug House Pvt. Ltd., India
Polyethylene glycol 400	Loba Chemie Pvt. Ltd., India
Potassium dihydrogen orthophosphate anhydrous purified	Central Drug House Pvt. Ltd., India
Potassium iodide	Loba Chemie Pvt. Ltd., India
Rhodamine B	Loba Chemie Pvt. Ltd., India
Sesame oil	Central Drug House Pvt. Ltd., India
Silicone oil	Supreme Silicones, India
Sodium bicarbonate	Loba Chemie Pvt. Ltd., India
Sodium chloride 99.5% extra pure	Loba Chemie Pvt. Ltd., India
Sodium hydroxide	Loba Chemie Pvt. Ltd., India

Sodium nitroprusside	Loba Chemie Pvt. Ltd., India
Sodium phosphate dibasic anhydrous 98% purified	Loba Chemie Pvt. Ltd., India
Span 60	S.D. Fine-Chem. Ltd., India
Span 80	S.D. Fine-Chem. Ltd., India
Transcutol P	Gattefosse Pvt. Ltd., India
Triton X 100	Himedia Lab Pvt. Ltd., India
Tween 20	Himedia Lab Pvt. Ltd., India
Tween 60	Loba Chemie Pvt. Ltd., India
Tween 80	Loba Chemie Pvt. Ltd., India
Veet hair removal cream	Reckitt Benckiser, India

**4.1.2. Instruments and equipment**

The list of instruments and equipment used in various stages of research work were enlisted in **Table 14** along with its model/manufacturer details.

**Table 14.** List of instruments and equipment used in various stages of work

<b>Instruments/equipment</b>	<b>Model/Manufacturer details</b>
Analytical balance	AX200 Shimadzu Analytical Pvt. Ltd., India
Cyclone mixer	REMI CM 101, India
Digital ultrasonic cleaner	LMUC-4 Labman Scientific Instruments Serial No: L10321, India
Diode array detector	SPD-M20A Shimadzu, Japan
GC-MS	TQ8040 NX Shimadzu, Japan
Hot air oven	Q-5247, Navyug, India
Muffle furnace	Bionics Scientific, India
Nylon membrane filter (0.45 $\mu\text{m}$ )	Millipore, Germany
Nylon syringe filter (0.22 $\mu\text{m}$ )	Millipore, Germany
Nanoparticle size analyzer	Malvern Zetasizer, Nano ZS90, Malvern Panalytical Ltd., UK
Optical microscope	KYOWA, Getner Instruments Pvt. Ltd., Japan
pH meter	Phan, Lab India, India
Rotary evaporator	IKA®RV8, IKA® India Pvt. Ltd., India
Rotational Rheometer	Model RheolabQC, Anton Paar, Austria
Sieves 22, 44, 66	Bhushan Engineering and Scientific Traders, India
Tissue homogenizer	REMI RQ-1, India
Walk in Stability chambers	REMI-WSC 100, India
Transmission electron microscopy	JEM-2100 plus Electron microscope, Jeol Ltd., Japan
Ultracentrifuge	REMI, RM-12C, REMI Elektrotechnik Ltd., India

Ultrafine Liquid chromatograph (UFLC) equipped with degasser unit and pump system	DGU-20 A5 prominence degasser with LC-20AD/T prominence Liquid Chromatograph Shimadzu, Japan
UV Spectrophotometer	UV-1800, Shimadzu Co.Ltd., Kyoto, Japan

## **4.2. Methods**

### **4.2.1. Collection of AG plant and its rhizomes**

The fresh whole plant of AG inclusive of its flowers and rhizomes were collected from “*Pattarethu Traders*” Vayyattupuzha, Pathanamthitta, Kerala, India. The sample specimen was identified by Dr. Abraham Mathew, Assistant Professor in the Department of Botany at St. Peters College, Kolenchery, Kerala, India. A voucher specimen [SPC-H-3085] of leaves, flowers and rhizomes were deposited into the herbarium of St. Peters College, Kolenchery, Kerala, India.

### **4.2.2. Physicochemical standardization of powdered rhizomes**

The physicochemical standardization of the powdered rhizomes was carried out to identify and assess the quality of phytoconstituents. All the parameters (mentioned as per section 4.2.2.1-4.2.2.6) were evaluated in triplicate which is described in following subsections: (George and Joseph, 2013; Kadam et al., 2012; Putranti et al., 2018; Shalavadi, 2018)

**4.2.2.1. Loss on drying:** Powdered rhizomes (1.5 g) were accurately weighed in a tared porcelain dish and dried in a hot air oven at 105°C to obtain a constant weight. The dishes were kept in a desiccator to achieve room temperature, then their weights were recorded. The percentage loss on drying was calculated by the **Eq. (4.1)**.

$$\text{Loss on drying (\%)} = \frac{\text{Weight loss of the sample (g)}}{\text{Weight of the powdered rhizomes (g)}} \times 100 \quad \text{Eq. (4.1)}$$

**4.2.2.2. Total ash value:** Powdered rhizomes (2 g) was accurately weighed and transferred into a silica crucible and incinerated by gradually increasing the temperature not exceeding 450°C in a muffle furnace until they are carbon-free. The resultant ash was cooled and weighed to obtain a constant weight. The percentage ash value was calculated by the **Eq. (4.2)**.

$$\text{Ash value (\%)} = \frac{\text{Mean weight of ash (g)}}{\text{Weight of powdered rhizomes (g)}} \times 100 \quad \text{Eq. (4.2)}$$

The total ash obtained was equally divided into three portions and then acid-insoluble ash value, water soluble ash value and sulphated ash value was performed.

**4.2.2.3. Acid-insoluble ash value:** To one portion of the ash obtained from total ash value test, 25 mL of dilute hydrochloric acid (2 M) was added and boiled for 5 min. The insoluble matter obtained was collected in a crucible or ashless filter paper, ignited and weighed. The percentage

yield of acid insoluble ash value was calculated with reference to the air-dried powdered rhizomes using **Eq. (4.3)**.

$$\text{Acid – insoluble ash value (\%)} = \frac{\text{Weight of acid insoluble ash (g)}}{\text{Weight of powdered rhizomes (g)}} \times 100 \quad \text{Eq. (4.3)}$$

**4.2.2.4. Water soluble ash value:** To the second portion of the ash obtained from total ash value test, 25 mL of water was added and boiled for 5 min, then collected the soluble matter in a crucible, ignited and weighed. The percentage water soluble ash value was calculated with reference to air-dried powdered rhizomes using **Eq. (4.4)**.

$$\text{Water soluble ash (\%)} = \frac{\text{Weight of total ash (g)}}{\text{Weight of powdered rhizomes (g)}} \times 100 \quad \text{Eq. (4.4)}$$

**4.2.2.5. Sulphated ash value:** The third portion of the ash obtained from total ash value test was moistened with 1 mL of concentrated sulphuric acid, then heated gently until white fumes are no longer evolved. Then, it was ignited at 800°C until black particles disappear. The crucible was cooled and then weighed. The procedure was continued twice until two successive weighings differ by not more than 0.5 mg.

**4.2.2.6. Extractive value:** This was carried out to determine the nature of chemical constituent present in the crude drug.

**4.2.2.6.1. Alcohol soluble extractive value:** The coarsely powdered rhizomes (5 g) were accurately weighed and macerated with 100 mL of 95% v/v ethanol in a stoppered flask for 24 h. The content of the flask was shaken frequently for 6 h using mechanical shaker, maintained at  $37 \pm 0.2^\circ\text{C}$  and 100 rpm. Then the stoppered flask was kept undisturbed for the next 18 h. After completion of 24 h maceration, the filtrate was filtered out. Then, filtrate was subjected to evaporation at  $105^\circ\text{C}$  until dryness in a tared dish. The extractive value was calculated as % w/w with reference to air-dried rhizomes as shown in **Eq.(4.5)** (Pawar and Jadhav, 2016).

$$\text{Extractive value} = \frac{\text{Weight of the dried extract (g)}}{\text{Weight of air dried rhizomes (g)}} \times 100 \quad \text{Eq. (4.5)}$$

**4.2.2.6.2. Water-soluble extractive value:** The coarsely powdered rhizomes (5 g) were accurately weighed and macerated with 100 mL of chloroform water I.P in a stoppered flask for 24 h. The stoppered flask was shaken frequently for 6 h using mechanical shaker, maintained at  $37 \pm 0.2^\circ\text{C}$  and 100 rpm and then kept undisturbed for the next 18 h. After completion of 24 h, the content

was filtered and the filtrate was collected in a tared dish. The dish was subjected to evaporation at 105°C until a dried mass is obtained. Extractive value was calculated as per **Eq. (4.5)** in terms of % w/w with reference to air-dried rhizomes

#### **4.2.3. Preparation of the extract**

The pulverized rhizomes were subjected to ultrasonication assisted maceration process using absolute ethanol for 24 h with intermittent shaking using a mechanical shaker. The method was adapted from Onmetta-aree *et al.* with modification. The dried rhizomes were weighed and absolute ethanol was added to it. The ratio of solute to solvent was 1:10. The mixture was sonicated in an ultrasound bath cleanser (40 kHz) for 20 min and then kept aside in the dark for 6 h with intermittent shaking. Then, the mixture was filtrated and marc was pressed. Afterwards, the combined filtrate was subjected to evaporation using a rotary evaporator at 65 rpm by maintaining the temperature at 40°C. The resultant concentrate was stored in the refrigerator (Onmetta-aree *et al.*, 2006).

#### **4.2.4. Phytochemical screening of the extract**

The ethanolic extract was subjected to preliminary phytochemical screening for analyzing the presence of the metabolites present in it (Dixit *et al.*, 2014; Malik *et al.*, 2016; Subash *et al.*, 2013).

The following tests were carried out:-

- i) Test for phenolic compounds (Ferric chloride test): Small quantity of extract was dissolved in 2 mL of distilled water, then few drops of 10% w/v aqueous ferric chloride solution was added. Blue or green color showed the presence of phenolic compounds.
- ii) Test for proteins and free amino acids (Millon's Reagent): Few mL of the extract was diluted with 5 mL of distilled water and the solution was filtered. To 2 mL of filtrate, 5 drops of Millon's reagent was added. The formation of red precipitate indicated the presence of proteins and amino acids.
- iii) Test for the acidic compound: To 2 mL of extract, 1 mL of sodium bicarbonate solution was added. Evolution of effervescence indicated the presence of acidic compounds.
- iv) Test for carbohydrate (Molisch test): To 2 mL of the ethanolic extract, 2 to 3 drops of Molisch reagent was added and shaken vigorously. Then, 1 mL of concentrated sulphuric acid was added along the sides of the test tubes. Formation of reddish-violet ring at the junction of the layers indicated the presence of carbohydrate.



- v) Test for glycosides (Legal's test): The ethanolic extract (2 mL) was made alkaline with 10% w/v NaOH. To this alkaline extract solution, freshly prepared sodium nitroprusside solution was added. The presence of blue colored solution indicates the presence of glycoside.
- vi) Test for alkaloids (Wagner's test): The ethanolic extract (5 mL) was taken in test tube and evaporated to dryness. To the dried residue, 5 mL of 2% v/v of HCl was added, then saturated with sodium chloride solution. The saturated solution was filtered and to the filtrate, Wagner's reagent was added. Formation of reddish-brown precipitate indicates the presence of alkaloids
- vii) Test for tannins: Few mL of the extract was boiled with 10 mL of water and filtered. Then to the filtrate, few drops of 0.1% w/v of ferric chloride were added. Presence of brownish green or blue-black colour indicates the presence of tannins.
- viii) Test for terpenoids and steroids (Salkowski test): To 2 mL of the concentrated extract 2 mL of chloroform was added. To one portion of extract, 3 mL of concentrated sulphuric acid was added slowly and carefully to form a layer. The appearance of reddish-brown coloration at the interface shows the presence of steroids. To the other portion of extract, chloroform was added and heated to dryness in a water bath. To the dried extract, 3 mL of concentrated sulphuric acid was added and heated for 10 minutes in a water bath. The appearance of the grey color indicated the presence of terpenoids
- ix) Test for flavonoids: To 0.5 mL of the extract, 5 mL of ammonia was added, followed by the addition of 1 mL of concentrated sulphuric acid. The presence of yellow coloration in the solution that disappeared on standing, indicated the presence of flavonoids.
- x) Test for saponins: To 2 mL of the extract, 5 mL of water was added and shaken vigorously to observe for a stable persistent froth. Then, to this water mixture, 3 to 4 drops of olive oil was added and the mixture was shaken vigorously to observe for the resultant emulsion formed.

#### **4.2.5. GC-MS of AGE**

AGE was subjected to GC-MS analysis for the detection of volatile phytoconstituents that might be present in the ethanolic extract. This spectral analysis was also carried out to confirm the presence of ACA, which is reported to be a semi-volatile component. The qualitative analysis of the ethanolic extract was performed using GC-MS (Shimadzu model TQ8040 NX) having GC-

2030 analyzer attached with a flame ionization detector and SH-Rxi-5Sil MS column (30m X 0.25 mm X 0.25 $\mu$ m) maintained at an oven temperature set with initial temperature of 35 °C, later heated to injection temperature of 250 °C where temperature increment was done at a rate of 10 °C /min and hold time of 10 min was preset. The linear flow velocity of 36.3 cm/sec and column flow of 1.02 mL/min at a pressure of 48.9 kPa was maintained. The splitless injection mode was chosen using helium as the carrier gas at rate of 1.5 mL/min. The ionization potential used was 60 eV with a maximum scan rate of 20,000 amu/sec. The GCMS solution™ software was used for acquisition of chromatography and mass spectroscopy of the isolated compounds are obtained from the Mass Spectral Library 2017(APAWLY-9781119376743 NIST).

#### **4.2.6. Analytical method development and validation of ACA by reverse phase high performance liquid chromatography (RP-HPLC)**

The chromatographic method was developed using Nucleodur C18 Column [Macherey Nagel, 250 mm  $\times$  4.6 mm i.d., 5 $\mu$ m] as stationary phase and acetonitrile (solvent A) : 0.1% v/v aqueous formic acid (solvent B) (60:40, v/v) as the mobile phase (Chua et al., 2017). The method was developed using standard ACA procured from M/s LKT labs, USA. An injection volume of 20  $\mu$ L was used for detection of component at a flow rate of 1 mL/min with  $\lambda_{\text{max}}$  of 218 nm. The data acquisition was done using LC solution software (Ramanunny et al., 2021a).

##### **4.2.6.1. Preparation of standard ACA solution**

###### **4.2.6.1.1. Preparation of standard stock solution**

Standard ACA procured from LKT lab (USA) was used for the preparation of standard stock solution. ACA (5 mg) was accurately weighed using an electronic balance and dissolved in 5 mL of HPLC grade methanol. Then, the final volume was adjusted up to 10 mL with methanol to obtain a standard stock solution of 500  $\mu$ g/mL concentration.

###### **4.2.6.1.2. Preparation of working standards for calibration curve**

To develop a calibration curve, a suitable aliquot (8.0 mL) from the stock solution was withdrawn and the final volume was made up to 16 mL using HPLC grade methanol to obtain a concentration of 250  $\mu$ g/mL. This served as the working standard. Further, five dilutions were prepared from the working standard by taking the aliquot of 1.0, 2.0, 3.0, 4.0, 5.0 mL, and final dilution was made up to 5.0 mL with HPLC grade methanol to obtain a concentration of 50, 100, 150, 200, and 250  $\mu$ g/mL respectively. Six injections were given for each concentration and the mean area was calculated. The samples were analyzed at the determined  $\lambda_{\text{max}}$  of 218 nm. The

calibration curve was obtained by plotting concentration ( $\mu\text{g/mL}$ ) on the  $x$ -axis and mean area ( $\text{cm}^2$ ) on the  $y$ -axis

#### **4.2.6.2. Analytical method validation**

The developed analytical method was validated following Q2 [R1] guidelines established by the International Council for Harmonization of Technical Requirements for Pharmaceuticals for Human Use (ICH Harmonised Tripartite, 2005). The system suitability parameters such as peak purity index, theoretical plate, height equivalent to theoretical plate (HETP), tailing factor are considered for evaluating the system performance.

##### **4.2.6.2.1. Linearity and range**

The linearity of the developed method was evaluated using five concentrations of ACA (50, 100, 150, 200, and 250  $\mu\text{g/mL}$ ). The linear least square regression analysis demonstrated the linearity of the method by plotting these five concentrations on the  $x$ -axis and mean peak area of each concentration on the  $y$ -axis. The regression equation obtained from the plot establishes slope, intercept, and correlation coefficient ( $r^2$ ).

##### **4.2.6.2.2. Accuracy**

The accuracy of the developed method was determined by calculating the drug recovery at three levels of method concentration. The method concentration was selected from the mid concentration of the calibration plot. Middle quality control [MQC] concentration represents 100% of the mid concentration of the calibration plot and its 80% and 120% represents lower quality control [LQC] concentration and higher quality control [HQC] concentration respectively. The three levels of concentration were prepared by withdrawing suitable aliquots of 2.4, 3.0 and 3.6 mL from the working standard solution and volume was made up to 5.0 mL using HPLC grade methanol, hence the final concentration was 120  $\mu\text{g/mL}$  [LQC], 150  $\mu\text{g/mL}$  [MQC] and 180  $\mu\text{g/mL}$  [HQC] respectively. The samples were injected in hexaplicate and the mean % recovery of ACA was calculated using **Eq. (4.7)**:

$$\text{Percentage recovery} = \frac{\text{Actual concentration recovered}}{\text{Theoretical concentration}} \times 100 \quad \text{Eq. (4.7)}$$

##### **4.2.6.2.3. Precision**

The precision of the developed method was performed at two levels i) repeatability (intraday) and ii) intermediate precision studies. The repeatability of the method was evaluated by injecting

hexaplicate of selected sample concentrations i.e., LQC, MQC, and HQC on the same day under similar experimental conditions (intraday) and the intermediate precision data were evaluated similarly with the LQC, MQC and HQC concentration with hexaplicate injection on different days [inter-day] and by different analyst [inter-analyst] respectively under similar experimental conditions. The average peak area was recorded and % RSD of responses was calculated by using the following **Eq. (4.8)**:

$$\% \text{ RSD} = \frac{\text{Standard deviation of the average peak area}}{\text{Average peak area}} \times 100 \quad \text{Eq. (4.8)}$$

#### **4.2.6.2.4. Limit of detection (LOD) and limit of quantification (LOQ)**

The slope of the calibration curve [s] and standard deviation [ $\sigma$ ] of the responses were used in determination of the LOD and LOQ. The calculation was done as per the following **Eq. (4.9)** and **(4.10)**.

$$\text{LOD} = 3.3 \times \frac{\sigma}{s} \quad \text{Eq. (4.9)}$$

$$\text{LOQ} = 10 \times \frac{\sigma}{s} \quad \text{Eq. (4.10)}$$

#### **4.2.6.2.5. Robustness**

The robustness of the developed method was assessed under the established experimental conditions with minor alterations in the selected parameters i.e., altering the flow rate, ratio of mobile phase composition, and wavelength. The methods are discussed below in section 4.2.6.2.5.1 to 4.2.6.2.5.3.

##### **4.2.6.2.5.1. Change in flow rate**

The change in flow rate was evaluated with MQC concentration of the sample at three different flow rates i.e. 0.8, 1.0, and 1.2 mL/min in hexaplicate. The % RSD of the sample at three different levels of flow rates was calculated.

##### **4.2.6.2.5.2. Change in composition of mobile phase**

The change in the ratio of mobile phase composition was evaluated with MQC concentration of the sample at three different ratios of acetonitrile: 0.1% formic acid in water such as 55:45,

60:40, and 65:35 (v/v). The % RSD of the sample at three different ratios of the mobile phase was calculated.

#### **4.2.6.2.5.3. Change in wavelength**

The change in flow rate was evaluated with MQC concentration of the sample at three different wavelengths i.e. 216, 218, 220 nm in hexaplicate. The % RSD of the samples at three different levels of flow rates was calculated.

#### **4.2.6.2.6. Specificity**

The specificity of the developed method was evaluated using ethanolic extract of AG under similar experimental conditions used for the elution of standard ACA. The retention time and chromatogram of the isolated ACA from AGE solution was compared with standard ACA. Further, purity index and quantitative estimation of the isolated ACA from the extract was evaluated.

### **4.2.7. Preliminary screening of parameters - Factorial experiment**

#### **4.2.7.1. Selection of solvent for extraction of ACA from AG rhizomes**

Selection of best suitable solvent plays a significant role in isolating a compound with maximum yield. The main criterion of solvent selection is based on the nature of phytoconstituents that have to be isolated. Some previously reported isolation processes for ACA have given priority to organic solvents that belongs to class III such as acetone (Latha et al., 2009a), absolute ethanol (Oonmetta-aree et al., 2006), 50% ethanol in water (v/v), and 50% acetone in water (v/v) (Wong et al., 2009). Thus, these four solvents were selected to evaluate isolation efficiency of these solvents in producing better yield of ACA. Other parameters selected for extraction are solid to solvent ratio 1:10, mean particle size 328.3  $\mu\text{m}$ , extraction time of 6 h at room temperature (25  $^{\circ}\text{C}$ ). The method of extraction was carried out by modified ultrasonication assisted maceration process (as per section 4.2.3). All the extracts obtained after extraction procedure were subjected to rotary evaporation. The oily concentrate obtained after evaporation was further analyzed by validated HPLC method at 218 nm. The amount of ACA in each extract was analyzed with the help of calibration curve.

#### **4.2.7.2. Effect of temperature on extraction process**

The effect of temperature on extraction was carried out by placing different set of extraction at 25  $^{\circ}\text{C}$ , 50  $^{\circ}\text{C}$  and 100  $^{\circ}\text{C}$  by modified ultrasonication assisted maceration process (mentioned in

section 4.2.3). In all the set up mean particle size of the powdered rhizomes were 328.3  $\mu\text{m}$ ; solid to solvent ratio was 1:10 and extraction time of 6 h. All the extracts were concentrated by rotary evaporator and analyzed by validated HPLC at 218 nm to determine the amount of ACA in each of the extract.

#### **4.2.7.3. Effect of mean particle size on extraction**

The effect of mean particle size on extraction was carried out by reducing the particles size of AG rhizomes. The size reduction was done using ball mill operating at a critical rotation speed of 80 rpm for 2 h. After passing the powdered rhizomes through sieve 66, sieve 44 and sieve 22 separately, the mean particle size is then measured by optical microscopy. The size of the particles were recorded as 254.9  $\mu\text{m}$  (sieve 66), 328.3  $\mu\text{m}$  (sieve 44) and 692.40  $\mu\text{m}$  (sieve 22). On the basis of size analysis, the solid (powdered rhizomes of selected particle size) to solvent ratio of 1: 10 was selected for the extraction process. The extraction process was carried out at 25 °C by ultrasonication assisted maceration process for 6 h. All the set of extracts were subjected to rotary evaporation followed by HPLC analysis for the determination of the amount of ACA in each extract.

#### **4.2.7.4. Effect of solid to solvent ratio on extraction**

The effect of solid to solvent ratio on extraction was carried out by keeping plant ratio constant with varying volume of the solvent. The selected volume of solvent are 10 mL, 30 mL, and 50 mL with mean particle size of the powdered rhizomes at 328.3  $\mu\text{m}$  and extraction carried out at 25 °C by ultrasonication assisted maceration process for 6 h. The amount of ACA in each of the extract was analyzed by HPLC method at 218 nm.

#### **4.2.7.5. Effect of time on extraction**

The effect of time on extraction was carried out by placing 5 sets of extraction process for 6, 12, 24, 48, and 72 h with similar experimental conditions. The solid to solvent ratio of 1:10, mean particles size of 328.3  $\mu\text{m}$  and modified ultrasonication assisted maceration process at 25 °C was maintained. The amount of ACA in each extract was analyzed by developed HPLC method.

#### **4.2.7.6. Effect of extraction steps**

The number of extraction steps required for complete extraction of ACA was determined by setting up the solid to solvent ratio of 1:10 with mean particles size of 328.3  $\mu\text{m}$  and extraction

carried out at 25 °C by ultrasonication assisted maceration process for 6 h (as per 4.2.3 section). After 6 h, the solid-solvent mixture was filtered and marc was pressed to collect the whole solvent. Then, the marc was again soaked with 10 mL of absolute ethanol, sonicated for 15 min and extraction process continued for 6 h (total time 12 h). After the prescribed time, the steps described above are repeated again for 6 h (total time 18 h). All the 3 set of extracts obtained were analyzed by HPLC to determine the amount of ACA extracted out.

Based on the amount of ACA extracted out in each of the above preliminary screening studies, the parameters influencing the amount of ACA was determined and further optimization of the extraction process was carried out by RSM.

#### **4.2.8. Optimization of the extraction process**

On the basis of the factorial experiments carried out, the process variables ( $X_1$ : sieve number represents the particle size ( $\mu\text{m}$ );  $X_2$ : solid to solvent ratio (g/mL) with fixed quantity of solid content (g) were optimized by CCD design of response surface methodology using Design Expert Software at three levels [ $X_1$  at 22(-1), 44 (0), 66 (+1) and  $X_2$  at 1:10 (-1), 1: 30 (0), 1:50 (+1)]. The amount of isolated ACA is the response (Y), which is determined by RP-HPLC method. The experimental design consists of thirteen experimental runs with five replicates at the center point to estimate the precision of the method. All the sets of extraction were carried out by modified ultrasonication assisted maceration process (as per section 4.2.3). The optimal extraction parameters are evaluated on account of the response obtained. For approximating the function, the second-order polynomial equation was used for quadratic model as shown in **Eq. (4.11)**.

$$Y = \beta_0 + \beta_1 X_1 + \beta_2 X_2 + \beta_{12} X_1 X_2 + \beta_{11} X_1^2 + \beta_{22} X_2^2 + \text{experimental error} \quad \text{Eq. (4.11)}$$

Where  $\beta_0$  is the model constant, Y represents predicted response,  $X_1$  and  $X_2$  represents independent variables,  $\beta_1$  and  $\beta_2$  represents linear coefficient,  $\beta_{12}$  represents cross-product coefficient,  $\beta_{11}$  and  $\beta_{22}$  represents quadratic coefficient.

The efficiency of the applied model was estimated using a statistical analysis of the data by analysis of variance (ANOVA) and the fit quality of the model equation. The coefficient of regression ( $R^2$ ), F value, and probability value confirms the response fit to the quadratic model. The  $p$ -value less than 0.05 indicate the significant effect of variables on responses.

On the basis of the obtained responses, a new set of variables were obtained from the design which serves as the optimized extraction parameters. Further, a set of extraction process was carried out in triplicate to validate the optimized extraction parameters.

#### **4.2.9. Preformulation studies**

Preformulation studies are carried out to understand the physicochemical characteristic features of the active substances and excipients before moving into the various phases of formulation development (Jones, 2018).

##### **4.2.9.1. Screening of components for NANE**

The foremost step carried out in the formulation development is the screening of the suitable components such as oil, surfactant and co-surfactant on the basis of solubility testing.

###### **4.2.9.1.1. Excipient screening**

The solubility study of AGE was carried out to select the most suitable oil, surfactant and cosurfactant for formulating a NANE. In this study, solubility of AGE was analyzed on the basis of the amount of AGE solubilized in the particular system which was later quantified by HPLC. It is also important to visually examine whole mixture to find out the clarity of the mixture.

A known excess amount of AGE (100 mg) was added into 1 mL of various oils [Capryol 90, Palmester 3595 (MCT oil), Labrafac PG, Labrafil M 1944 CS, Labrasol, isopropyl myristate (IPM), almond oil, castor oil, sesame oil, olive oil, peanut oil, Capmul MCM], surfactants [Tween 80, Span 80, Tween 20, Span 20, Cremophor RH 40, Triton-X100, Dimethicone] and co-surfactants [Transcutol P, propylene glycol, PEG 400] in a glass stoppered vials. All the mixtures were separately vortexed for 2 min using cyclone mixer. The vials were kept at  $37 \pm 0.5$  °C in a shaking water bath for 72 h to attain equilibrium. After the specified time, the samples were centrifuged at 10,000 g for 15 min to separate the undissolved matter from the saturated solution (Pandey et al., 2020a). The obtained supernatants were quantified using developed HPLC method at 218 nm after serial dilution with suitable solvents.

###### **4.2.9.1.2. Solvent selection**

The solubility study of AGE was carried out in various solvents, buffers and combination of solvent system. Similar procedure (as per section 4.2.9.1.1) was followed with selected solvents such as distilled water, Glycerin, absolute ethanol, 10% absolute ethanol in water (v/v), 50%



absolute ethanol in water (v/v), methanol, 10% methanol in water (v/v), 50% methanol in water (v/v), phosphate buffer pH 6.8, phosphate buffer pH 7.4, phosphate buffered saline (PBS) pH 7.4 and mixed phosphate buffer pH 5.5. Further, a combination system of mixed phosphate buffer (pH 5.5) and absolute ethanol at different ratio (1:1, 5:1, 9:1) were mixed together and solubility of ACA was analyzed by the developed HPLC method.

#### **4.2.9.2 Selection of oil phase and non-aqueous polar phase**

On the basis of solubility studies, it was observed that most of the edible oils such as olive oil, IPM, almond oil, sesame oil and among solvents, glycerin have shown less solubility of AGE. But edible oils are not much preferred for use in the formulation due to their tendency to get rancid upon storage (Chime et al., 2014). Hence, preference was given to glycerin which is widely explored as non-aqueous polar phase in NANE (Lin et al., 2011; Sun et al., 2019).

The selection of oil phase and non-aqueous polar phase for NANE was carried out by visual examination of phase separation between them. On the basis of the solubility study, the selected oils which have shown higher solubility were mixed thoroughly with non-aqueous polar phase (glycerin) at a ratio of 1:1. The mixture was observed for phase separation after 2, 4, 6 and 24 h. On the basis of phase separation with the selected oil, oil phase and non-aqueous polar phase were selected.

#### **4.2.10. Formulation of AGE loaded NANE**

AGE loaded NANEs were prepared using a modified spontaneous emulsification method (Guttoff et al., 2015; Saberi et al., 2013). AGE (100 mg) containing weight equivalent to 3.89 % w/w of ACA was mixed thoroughly with the selected ratio of oil, followed by the addition of  $S_{mix}$ .  $S_{mix}$  resembles the mixture of surfactant and co-surfactant. The mixture was vortexed for 2 minutes to obtain a clear, homogenous phase. To the homogenous phase, glycerin (polar phase) was added instantaneously and vortexed for 10 minutes followed by ultra-sonication in a bath sonicator (40 kHz) for 5 min.

#### **4.2.11. Preliminary screening of formulations based on emulsification**

On the basis of the solubility further screening was initiated for selecting oil phase, surfactants, co-surfactants and non-aqueous polar phase for further studies.

Initial set of formulation batches (F) were prepared using Capryol 90 as the selected oil phase, Tween 80 as surfactant and Transcutol P as co-surfactant. The ratio of oil phase was set from 1 to 9 and surfactant-cosurfactant ( $S_{\text{mix}}$ ) ratio was varied from 1:1, 1:2 and 2:1 to prepare 27 prototypes (F<sub>1</sub>- F<sub>27</sub>). Glycerin was added into selected oil- $S_{\text{mix}}$  mixture in order to form emulsion. However, none of the compositions formed a stable emulsion.

New formulation prototypes (N) were designed by replacing surfactant Tween 80 with Cremophor RH 40 and preceded without the addition of co-surfactant. Therefore, the prepared emulsion composition contained Capryol 90 as the selected oil phase, Cremophor RH 40 as surfactant, glycerin as the non-aqueous polar phase. A total of 27 prototypes (N<sub>1</sub>- N<sub>27</sub>) were prepared by varying the ratio of oil phase (1:9) and surfactant-cosurfactant ( $S_{\text{mix}}$ ) ratio (1:1, 1:2 and 2:1). Among these 27 batches, 2 compositions (N<sub>25</sub> and N<sub>26</sub>) formed stable emulsion. Based on this observation, further 81 formulation prototypes (E) were prepared using  $S_{\text{mix}}$  containing Cremophor RH 40-Transcutol P. Hence, the prototype (E) contained Capryol 90, Cremophor RH 40, Transcutol P and glycerin. However, all the prepared batches from E<sub>1</sub>- E<sub>81</sub> have shown phase separation.

The emulsion composition with Capryol 90 was not satisfactory hence new formulation prototype (M) was designed by replacing Capryol 90 with MCT oil, which has also shown better solubility. Prototype (M) contained MCT oil, Cremophor RH 40, Transcutol P and glycerin. A total of 81 formulations, M<sub>1</sub>- M<sub>81</sub> were prepared. All the batches were physically examined for physical changes that would lead to phase separation.

#### **4.2.12. Phase behavior study using pseudo-ternary phase diagram (p-TPD)**

On the basis of the solubility studies, selected oil (MCT oil), surfactant (Cremophor RH 40), co-surfactant (Transcutol P) and non-aqueous polar phase (glycerin) were used to construct the p-TPD. The mixture of Cremophor RH 40 and Transcutol P were used as  $S_{\text{mix}}$ . The ratio of oil phase was varied as 1:9 and  $S_{\text{mix}}$  was prepared by varying the ratio from 1:1, 1:2 and 2:1 and glycerin was used as the non-aqueous polar phase. A total of 81 formulation prototypes (M<sub>1</sub>- M<sub>81</sub>) were prepared as represented in **Table 15**. By choosing each components on the three vertices (oil phase,  $S_{\text{mix}}$  and non-aqueous polar phase), three p-TPDs were plotted using Todd

Thompson Triplot software 4.1.2.version. The plot categorized NANEs either as stable NANEs or unstable (phase separation) NANEs on the basis of their physical appearance.

On the basis of the area covered in the p-TPD, appropriate concentration range of components was selected. Further, interaction effects of selected components on the physicochemical properties of NANEs were studied with the help of DoE.

**Table 15.** Composition of formulation by varying the ratio of oil,  $S_{mix}$  and non-aqueous polar phase

Formulation code	MCT oil (1:1)	* $S_{mix}$ (1:1)	Glycerin	Formulation code	MCT oil (1:1)	$S_{mix}$ (1:1)	Glycerin	Formulation code	MCT oil (1:1)	$S_{mix}$ (1:1)	Glycerin
M1	90	2.5:2.5	5	M28	90	1.6:1.6	6.6	M55	90	3.3:33	3.3
M2	80	5.0:5.0	10	M29	80	3.3:3.3	1.33	M56	80	6.6: 6.6	6.6
M3	70	7.5:7.5	15	M30	70	5.0:5.0	20.0	M57	70	10.0:10.0	10.0
M4	60	10.0:10.0	20	M31	60	6.6:6.6	26.6	M58	60	13.3:13.3	13.3
M5	50	12.5:12.5	25	M32	50	8.3:8.3	33.3	M49	50	16.6:16.6	16.6
M6	40	15.0:15.0	30	M33	40	10.0:10.0	40.0	M60	40	20.0:20.0	20.0
M7	30	17.5:17.5	35	M34	30	11.6:11.6	46.6	M61	30	23.3:23.3	23.3
M8	20	20.0:20.0	40	M35	20	13.0:13.0	53.2	M62	20	26.6:26.6	26.6
M9	10	22.5:22.5	45	M36	10	15.0:15.0	60.0	M63	10	30.0:30.0	30.0
			$S_{mix}$ (1:2)				$S_{mix}$ (1:2)				$S_{mix}$ (1:2)
M10	90	1.6:3.3	5.0	M37	90	1.1:2.2	6.6	M64	90	2.2:4.4	3.3
M11	80	3.3:6.6	10	M38	80	2.2:4.4	1.33	M65	80	4.4:8.8	6.6
M12	70	5.0:10.0	15	M39	70	3.3: 6.6	20.0	M66	70	6.6:13.2	10.0
M13	60	6.6:13.3	20	M40	60	4.4:8.8	26.6	M67	60	8.8:17.7	13.3
M14	50	8.3:16.6	25	M41	50	5.5:11.0	33.3	M68	50	11.1:22.2	16.6
M15	40	10.0:20.0	30	M42	40	6.6:13.3	40.0	M69	40	13.3:26.6	20.0
M16	30	11.6:23.3	35	M43	30	7.7: 15.5	46.6	M70	30	15.5:31.0	23.3
M17	20	13.3:26.6	40	M44	20	8.8:17.7	53.2	M71	20	17.7:35.4	26.6
M18	10	15.0:30.0	45	M45	10	10.0:20.0	60.0	M72	10	20.0:40.0	30.0
			$S_{mix}$ (2:1)				$S_{mix}$ (2:1)				$S_{mix}$ (2:1)
M19	90	3.3:1.6	5.0	M46	90	2.2:1.1	6.6	M73	90	4.4:2.2	3.3
M20	80	6.6:3.3	10	M47	80	4.4:2.2	1.33	M74	80	8.8:4.4	6.6
M21	70	10.0:5.0	15	M48	70	6.6: 3.3	20.0	M75	70	13.2: 6.6	10.0
M22	60	13.3:6.6	20	M49	60	8.8:4.4	26.6	M76	60	17.7: 8.8	13.3
M23	50	16.6:8.3	25	M50	50	11.0: 5.5	33.3	M77	50	22.2:11.1	16.6
M24	40	20.0:10.0	30	M51	40	13.3: 6.6	40.0	M78	40	26.6:13.3	20.0
M25	30	23.3:11.6	35	M52	30	15.5: 7.7	46.6	M79	30	31.0:15.5	23.3
M26	20	26.6:13.3	40	M53	20	17.7:8.8	53.2	M80	20	35.4:17.7	26.6
M27	10	30.0:15.0	45	M54	10	20.0:10.0	60.0	M81	10	40.0:20.0	30.0

\*  $S_{mix}$ : Cremophor RH 40: Transcutol P

#### 4.2.13. Experimental design for optimization of NANEs

The p-TPD represented stable NANEs at larger concentration range of components. It helped in scrutinizing the range/region of compositions that could offer the nanoemulsion upon formulation. This p-TPD has further helped in utilizing DoE for narrowing as well as optimizing the best formulations that could offer desirable formulation attributes. On the basis of upper and lower limits of each components such as oil (20-30% v/v), surfactant (15-35 % v/v), cosurfactant (15-35 % v/v) and glycerin (23- 26 % v/v), optimization of the NANEs were carried out by a randomized statistical screening approach. A three-level, four factor BBD was applied (Kassem et al., 2020). In this design, the independent variables were the varying ratios of oil phase ( $X_1$ ), surfactant ( $X_2$ ), co-surfactant ( $X_3$ ) and continuous phase ( $X_4$ ). These components are represented in the design at their high (+) level and low (-) level as shown in **Table 16** to optimize the composition of the NANEs. The effect of each one of the selected factors at their coded levels were evaluated with respect to the response variables (dependent variables) such as droplet size ( $Y_1$ ), zeta potential ( $Y_2$ ), % drug loading ( $Y_3$ ), % cumulative drug permeation at 6 h ( $Y_4$ ) and % drug retention in the skin after 6 h ( $Y_5$ ). Considering the number of independent variables and their levels, 29 experimental runs were designed using BBD as shown in **Table 17**.

**Table 16.** Experimental levels of independent variables

Independent variables	Low level (-)	High level (+)
$X_1$ - Oil phase (MCT oil)	20	30
$X_2$ -Surfactant (Cremophor RH 40)	15	35
$X_3$ -Co-surfactant (Transcutol P)	15	35
$X_4$ - Non-Aqueous polar phase (Glycerin)	23	26

Level are expressed in % v/v

These experimental runs were used to evaluate the main effect, interaction effect and quadratic effect of the independent variables on dependent variables. Design Expert software was used to evaluate the effect of these independent variables. The linear **Eq. (4.12)** and quadratic **Eq. (4.13)** models were generated by the Design Expert software (version 11). These equations represented the effect of each independent variables on selected dependent variables (i.e. response), which were analyzed statistically through analysis of variance (ANOVA).

$$Y = \beta_0 + \beta_1X_1 + \beta_2X_2 + \beta_3X_3 + \beta_4X_4 \quad \text{Eq. (4.12)}$$

$$Y = \beta_0 + \beta_1 X_1 + \beta_2 X_2 + \beta_3 X_3 + \beta_4 X_4 + \beta_{12} X_1 X_2 + \beta_{13} X_1 X_3 + \beta_{14} X_1 X_4 + \beta_{23} X_2 X_3 + \beta_{24} X_2 X_4 + \beta_{34} X_3 X_4 + \beta_{11} X_1^2 + \beta_{22} X_2^2 + \beta_{33} X_3^2 + \beta_{44} X_4^2 \quad \text{Eq. (4.13)}$$

Y indicated measured response of the dependent variable;  $\beta_0$  is the intercept;  $\beta_1$  to  $\beta_{44}$  are the regression co-efficient;  $X_1$ ,  $X_2$ ,  $X_3$  and  $X_4$  are independent variables.

The responses obtained for the dependent variables were analyzed statistically (ANOVA). The design expert software has generated 3D-response surface plots and 2D-contour plots to evaluate the effects of independent variables on dependent variables. On the basis of the evaluation of the response parameters, optimized composition (AGE NANE) was obtained from the design and further validation of the composition was done by carrying out the experiment in the laboratory (Mittal et al., 2021). The non-significant variation ( $p > 0.05$ ) between the experimental responses and observed responses confirmed the optimized composition.

**Table 17.** Composition of NANEs containing oil phase,  $S_{\text{mix}}$  and non-aqueous polar phase

<b>Run</b>	<b>Factor 1 MCT oil</b>	<b>Factor 2 Cremophor RH 40</b>	<b>Factor 3 Transcutol P</b>	<b>Factor 4 Glycerin</b>
1	25	35	25	23.0
2	20	35	25	24.5
3	30	25	25	26.0
4	20	15	25	24.5
5	30	35	25	24.5
6	20	25	15	24.5
7	25	25	35	23.0
8	30	15	25	24.5
9	25	25	15	26.0
10	25	15	25	23.0
11	25	25	25	24.5
12	25	35	15	24.5
13	25	25	25	24.5
14	20	25	25	23.0
15	25	25	25	24.5
16	30	25	25	23.0
17	25	35	35	24.5
18	25	15	35	24.5
19	30	25	15	24.5
20	25	25	25	24.5
21	25	15	25	26.0
22	25	25	15	23.0
23	25	35	25	26.0
24	30	25	35	24.5
25	25	25	25	24.5
26	20	25	35	24.5
27	25	15	15	24.5
28	25	25	35	26.0
29	20	25	25	26.0

Factors are expressed in % v/v

#### **4.2.14. Characterization of developed AGE NANEs**

The characterization of the developed AGE NANEs was carried out to evaluate the physicochemical properties of the formulation.

##### **4.2.14.1. Droplet size analysis and PDI**

The formulated AGE NANEs were subjected to evaluation of droplet size and PDI using Zeta sizer. The samples were filled in disposable cuvettes and dynamic light scattering was measured at 90° (side scatter) at a target temperature of 25 °C. Millipore water was used as the diluting solvent (Kassem et al., 2020). Each sample was analyzed in triplicate and mean data with standard deviation were recorded.

##### **4.2.14.2. Zeta potential**

The zeta potential of the AGE NANEs was also evaluated using Zeta sizer using different cuvette. The samples were filled into omega cuvette that was maintained at a target temperature of 25 °C. The sample cell was diluted with water and adjusted with 200 V. Zeta potential of each samples were recorded in triplicate (Kassem et al., 2020).

##### **4.2.14.3. Drug loading**

All the NANEs containing AGE (100 mg) were diluted in suitable volume (5 mL) of HPLC grade methanol and vortexed it for 2 min. Then the samples were centrifuged at 10,000 g for 10 min. Afterwards, the supernatant was taken and filtered using syringe filter (0.22 µm). A suitable volume of the supernatant (20 µL) was injected into HPLC to evaluate % drug loading. % Drug loading was calculated using **Eq. (4.14)** (Khursheed et al., 2022)

$$\% \text{ Drug loading} = \frac{\text{Weight of the entrapped drug inside the formulation}}{\text{Total weight of formulation}} \times 100 \quad \text{Eq. (4.14)}$$

##### **4.2.14.4. Thermodynamic stability testing of the selected AGE NANEs**

To confirm the stability of selected AGE NANEs, thermodynamic stability studies were conducted. The formulations were subjected to different stress conditions like heating-cooling cycle at 4 °C and 40 °C, alternatively for 2 days to complete the cycle. The samples were subjected to 3 cycles and confirmed the stability of the formulation by visual examination (Chandrasekaran, 2015). Also, the selected AGE NANEs were subjected to freeze thaw cycle i.e.



two extreme temperatures  $-21\text{ }^{\circ}\text{C}$  and  $25\text{ }^{\circ}\text{C}$  for 24 h. Each set of samples was subjected to three cycles (Shafiq et al., 2007). Absence of phase separation after three freeze-thaw cycles confirmed the thermodynamic stability of the formulation. The formulated NANEs were subjected to centrifugation at  $3500\text{ g}$  for 30 min (Shafiq et al., 2007). The absence of turbidity or phase separation indicated the stability of formulations.

#### **4.2.14.5 Optical microscopy of AGE NANE**

The microscopic examination of dye mixed AGE NANE helped in identifying the nature of the dispersed phase and continuous phase. In this study, optimized batch AGE NANE was mixed with methylene blue (cationic dye) which gets solubilized in glycerin. When observed under microscope, if the droplets appeared blue colour with a colourless background, then it meant that the formed emulsion have polar phase as the dispersed phase and oil phase as the continuous phase. In contrast, the formation of blue background and colourless globules indicated that the oil phase is the dispersed phase and non-aqueous polar phase (glycerin) formed the continuous phase (Savrikar and Lagad, 2010).

#### **4.2.14.6. High resolution transmission electron microscopy (HR-TEM)**

Morphological analysis of the dispersed oil globules was carried out using HR-TEM. It was operated at an accelerating voltage of 200 kV with a resolution of 0.194 nm (point) and magnification of 15, 000,00 lakh (Max). Optimized AGE NANE (100  $\mu\text{L}$ ) was diluted with 100 mL of millipore water and a drop of the diluted sample was placed on the carbon coated copper grid and allowed to stand for one minute. Then, the excess amount of the sample was removed to perform negative staining with 2% w/v of phosphotungstic acid. The grid was air dried and thin sample specimen was analyzed and images were recorded (Khatoon et al., 2021).

#### **4.2.14.7. Refractive index, pH and viscosity**

The refractive index of the optimized AGE NANE was evaluated by Abbe's refractometer at  $25 \pm 0.5\text{ }^{\circ}\text{C}$ . A drop of AGE NANE was placed on the prism and refractive index of AGE NANE was noted from the refractive scale. The measurements are done in triplicate. The pH of optimized AGE NANE was determined with the help of calibrated pH meter in triplicate at  $25 \pm 0.5\text{ }^{\circ}\text{C}$ . The glass electrode of the pH meter was cleaned well and dipped into 4 mL of the optimized AGE NANE. The pH of formulation recorded on the digital display meter was noted (Khatoon et al., 2021). Viscosity of the optimized AGE NANE was measured with the help of Rotational

rheometer. The sample was placed into the sample holder having 1 mL capacity and it was fitted with probe. The testing of the sample was performed at  $25 \pm 0.5$  °C with a controlled shear rate from 10 to 100  $s^{-1}$ . The viscosity of the formulation was noted and the relationship between viscosity and shear shear rate was represented to determine the type of flow (Pukale et al., 2020).

#### **4.2.14.8. Spreadability**

Spreadability of the AGE NANE was evaluated in triplicate using previously reported method with slight modification (Algahtani et al., 2020; Dantas et al., 2016). Approximately, 100  $\mu$ L of the AGE NANE was kept at the centre of a glass plate (48 mm wide, 146 mm length) having a circle with diameter of 10 mm. Then another plate of similar dimension was placed over the first plate. A known quantity of weight (50 g) was placed on to the upper plate for 1 min. The spreading profile of the nanoemulsion was determined by measuring the diameter of the circle after applying weight. The spreadability of the formulation  $E_i$  ( $mm^2$ ) was expressed by measuring the diameter in mm and applying the **Eq. (4.15)** (Deuschle et al., 2015).

$$E_i = d^2 \left( \frac{\pi}{4} \right) \quad \text{Eq. (4.15)}$$

Spreadability factor (Sf) was calculated using the following **Eq. (4.16)** (Deuschle et al., 2015) .

$$Sf = \frac{A}{W} \quad \text{Eq. (4.16)}$$

Where A is the area in  $mm^2$  and W is the weight in g.

#### **4.2.14.9. *In vitro* diffusion studies and release kinetics**

##### **4.2.14.9.1. *In vitro* diffusion studies**

*In vitro* diffusion studies of AGE *per se* and AGE NANE were performed using a vertical Franz diffusion cell having a thermostatic water bath system attached with it. The dialysis membrane-110 having molecular weight cutoff value of 12,000-14,000 Dalton with pore size of 2.4 nm was used. The membrane was washed thoroughly in running water. Then, the membrane was soaked in diffusion medium which comprises of 1:1 ratio of mixed phosphate buffer (pH 5.5): absolute ethanol for 30 h. The receptor compartment was filled with diffusion medium which was maintained at a temperature of  $32 \pm 0.5$  °C with a stirring speed of 550 rpm using a magnetic stirrer (Moolakkadath et al., 2018). The dialysis membrane was placed carefully in between the receptor compartment and donor compartment. The samples were placed onto the donor compartment and aliquots were periodically withdrawn at suitable time interval of 0.5, 1.0, 2.0,

4.0, 6.0, 8.0, 12.0, 24.0, 30.0 h. During each withdrawal, a fresh volume of diffusion medium was replaced into the receptor compartment to maintain sink condition. Then each aliquot was subjected to HPLC analysis (Ramanunny et al., 2021a).

#### **4.2.14.9.2. Release kinetic**

On the basis of the diffusion study, the release kinetic of the drug was evaluated with respect to five models including zero-order, first-order, Higuchi, Korsmeyer-Peppas and Hixson-Crowell. Each model was evaluated with the help of a graph made on the basis of the theoretical equation as shown in the **Eq. (4.17)** (zero order; graph represents percentage cumulative drug released on y-axis and time on x-axis), **Eq. (4.18)** (first-order plot represents ln cumulative drug remaining on y-axis and time on x-axis), **Eq. (4.19)** (Higuchi model represents percentage cumulative drug released versus square root of time), **Eq. (4.20)** (Korsmeyer- Peppas model, plot represents log percentage cumulative drug released versus log time), and **Eq. (4.21)** (Hixson-Crowell model, graph shows cube root of drug remaining versus time). The coefficient of regression ( $r^2$ ) value was determined from the plotted graph and best- fit model was selected based on the  $r^2$  (Khursheed et al., 2021). All the above described model Eqs. **(4.17-4.21)** is mentioned as follows:

$$Q_0 - Q_t = k_0 \quad \text{Eq. (4.17)}$$

$$\ln(Q_0/Q_t) = -k_1 t \quad \text{Eq. (4.18)}$$

$$Q_t = kt^{1/2} \quad \text{Eq. (4.19)}$$

$$Q_t/Q_\infty = kt^n \quad \text{Eq. (4.20)}$$

$$Q_0^{1/3} - Q_t^{1/3} = k_{HCT} t \quad \text{Eq. (4.21)}$$

where “ $Q_0$ ” is the initial amount of ACA in NANE, “ $Q_t$ ” is the amount of ACA loaded NANE permeated, “ $k_0$ ” resembles the zero-order rate constant, “ $k_1$ ” is the first-order constant, “ $k$ ” is the constant reflecting the design variables of the system, “ $Q_t/Q_\infty$ ” is the fraction of drug released over time, “ $n$ ” is the release exponent, “ $k_{HCT}$ ” is the Hixson-Crowell rate constant and “ $t$ ” is the time (Musa et al., 2017).

#### 4.2.14.10. *Ex vivo* skin permeation and retention studies

##### 4.2.14.10.1. Collection and preparation of skin specimen

Porcine ear skin was collected from slaughterhouse (Vishal meat shop, Phagwara) and cleaned thoroughly under running water. The hairs on the skin were removed using Veet hair removing cream (Reckitt Benckiser, India). The dorsal ear skin was carefully separated from cartilage using sterile surgical blade no: 11. The isolated skin samples were cleaned with cotton pads that are soaked with 0.9% w/v of sodium chloride solution. Then samples were dried using cloth, packed in an aluminium foil and stored at -20 °C until use but not longer than a month (Pantelić et al., 2018)

##### 4.2.14.10.2. *Ex vivo* permeation studies

The *ex vivo* permeation studies were carried out in the porcine ear skin having a surface area of 2.54 cm<sup>2</sup>. Prior to the experimentation, the skin was soaked in the mixed phosphate buffer (pH 5.5) : ethanol (1:1) for 1 h. Then, the skin was carefully placed in between the cells of the Franz diffusion cell. The outer skin surface faces the donor compartment and inner skin surface rest on the receptor compartment, which is in contact with the diffusion medium. The medium was gently stirred at 550 rpm and the temperature was maintained at 32 ± 1 °C using a thermostatically controlled magnetic stirrer. The samples were placed in the donor compartment. An aliquot of 1 mL was withdrawn from the receptor compartment at regular time intervals of 0.5, 1.0, 2.0, 4.0, 6.0, 8.0, 12.0, 24.0, 30.0 h and during each withdrawal, an equal volume of the fresh medium was replaced. The amount of ACA permeated at each selected time was quantified using the developed HPLC method. The cumulative amount of drug permeated through the skin per unit area was calculated from the obtained drug concentration using the **Eq. (4.19) - (4.25)**.

$$Q_1 = \frac{C_1 V_c}{P} \quad \text{Eq. (4.22)}$$

$$Q_2 = \frac{C_2 V_c + C_1 V_u}{P} \quad \text{Eq. (4.23)}$$

$$Q_3 = \frac{C_3 V_c + C_1 V_u + C_2 V_u}{P} \quad \text{Eq. (4.24)}$$

$$Q_{30} = \frac{C_{30} V_c + \dots + C_1 V_u}{P} \quad \text{Eq. (4.25)}$$

Where “C<sub>1</sub>”, “C<sub>2</sub>”, “C<sub>3</sub>” ..... “C<sub>30</sub>” represents the drug concentration (µg/mL) of the samples withdrawn at different time (“t<sub>1</sub>, t<sub>2</sub>, t<sub>3</sub> ..... t<sub>30</sub>”), “V<sub>c</sub>” is the volume of the receptor cell, “V<sub>u</sub>” volume of the receptor medium withdrawn at different time (“t<sub>1</sub>, t<sub>2</sub>, t<sub>3</sub> ..... t<sub>30</sub>”) and “P” is the surface area of the diffusion cell available for drug diffusion (Pantelić et al., 2018).

The data obtained from these studies are graphically represented as cumulative drug amount (“Q<sub>i</sub>”) permeated through unit surface area versus time. The linear portion of the plot determined the slope which represents the steady state flux (“J”). Permeability coefficient was calculated using the **Eq. (4.26)** (Rajitha et al., 2019).

$$P = \frac{J}{C} \quad \text{Eq. (4.26)}$$

Where C is the concentration of the drug applied in the donor compartment.

Enhancement ratio of flux (ER<sub>flux</sub>) was calculated using **Eq. (4.27)**.

$$ER_{\text{flux}} = \frac{\text{Flux of AGE NANE}}{\text{Flux of AGE per se}} \quad \text{Eq. (4.27)}$$

#### **4.2.14.10.3. Drug retention studies**

After 24 h of *ex vivo* permeation studies, the amount of drug deposited in the porcine skin was determined by careful removal of the skin specimen from the receptor cell. The skin specimen was washed with water to remove excess extract/formulation present on the outer surface of the skin. The skin specimen was cut into small pieces and homogenized with 10 mL of HPLC methanol using tissue homogenizer. The sample was kept aside for 12 h to complete the extraction of drug and subjected to centrifugation at 10,000 g for 15 min. The supernatant was collected and analyzed using the developed HPLC method (Li et al., 2020b; Pandey et al., 2020b).

#### **4.2.14.11. Depth of Penetration - Confocal laser scanning microscopy (CLSM)**

CLSM was used for analyzing the depth of penetration of NANE into the skin stratum. Similar to the *ex vivo* skin permeation studies (as per section 4.2.14.10.2), the skin specimens were placed in between the donor and receptor compartments. Only difference in this procedure was the addition of fluorescent dye loaded NANE (Sahu et al., 2018). For determination of depth of penetration, Rhodamine B aqueous dispersion (RAD) (0.1% w/v) and NANE loaded with Rhodamine B (R-NANE) instead of AGE were prepared. The study was conducted by placing each sample

separately on the donor compartment and receptor compartment filled with mixed phosphate buffer (pH 5.5) and ethanol in the ratio of 1:1. After 24 h of permeation study, the skin specimens were washed thoroughly with water and fixed in 10% formalin. Later the skin samples were sectioned into 20  $\mu\text{m}$  slices and fixed on glass slides. The sections were observed under confocal microscope having an argon laser beam with excitation at 540 nm and emission at 625 nm respectively. A comparison in the depth of penetration of RAD and R-NANE were evaluated (Khatoon et al., 2021).

#### **4.2.14.12. Stability studies**

The stability studies of optimized AGE NANE were carried out at accelerated stability testing  $40 \pm 2^\circ\text{C}/75 \pm 5\%$  RH. The measured volume of the formulations were filled in the specific glass containers and stored at the mentioned storage condition. The optimized sample was also analyzed in triplicate prior (0 month) to the storage into various conditions. At the end of three months and six months, the aged samples were analyzed and results were compared with freshly prepared AGE NANE for evaluating change in physical nature of the NANE, globule size, zeta potential, % drug loading, % cumulative amount of drug permeated and % drug retained after 24 h (Zothanpuii et al., 2020). The samples were analyzed in triplicate and their mean data with S.D. was recorded and results obtained were compared with the results of freshly prepared sample stored at 0 month.

#### **4.2.15. Pharmacodynamic studies**

After characterization of the optimized AGE NANE, pharmacodynamics studies were performed to evaluate the functional response and dose-response effect on suitable experimental model. In this research, anti-angiogenic activity was carried out in Hen's egg test-chorioallantoic membrane (HET-CAM) model, acute dermal toxicity was carried out in SD rats and antipsoriasis activity was carried out in IMQ induced mouse model.

##### **4.2.15.1 HET-CAM test for anti-angiogenic activity**

HET-CAM test was performed in accordance with the previously reported procedure with certain variations (Khatoon et al., 2021; Kota et al., 2018). The test began with the collection of 5 days old fertilized chicken eggs from a nearby hatchery (Sahota hatchery, Jalandhar Cantt). The collected eggs were rubbed with 70% ethanol (v/v) and dried to avoid the chances of

inflammation. The eggs were divided into 6 groups each containing 3 eggs. Each egg was observed under light to differentiate the air sac. A small hole was pricked on the outer eggshell where the air sac is present for the removal of albumin (2 mL). Then, the hole was covered with parafilm to avoid contamination and again incubated at  $37 \pm 0.5^\circ\text{C}$  for 24 h. At the end of 24 h incubation (6 days), an opening was made in the air sac side of the egg and the initial number of blood vessels in each egg was noted. Before administration of the test samples, image of blood vessels present in the egg was captured. The samples were administered to each group simultaneously as mentioned in **Table 18**. After administration of the samples, the opened area was tightly covered with the parafilm and incubated again for 24 h (Khatoon et al., 2021) .

**Table 18.** Dosing pattern in HET-CAM test

Group No.	Group	Samples for administration (per egg)
Group I	Normal control	100 $\mu\text{L}$ of 0.9 % w/v sodium chloride
Group II	Positive control	100 $\mu\text{L}$ of 0.1% w/v betamethasone valerate cream
Group III	Negative control	300 $\mu\text{g}$ /egg of pyruvic acid
Group IV	AGE <i>per se</i>	100 $\mu\text{L}$ of 0.1% w/v of AGE
Group V	NANE-B	100 $\mu\text{L}$ of 0.1% w/v of blank formulation
Group VI	AGE NANE	100 $\mu\text{L}$ of 0.1% w/v of AGE loaded NANE

On the 7<sup>th</sup> day, the parafilm covering was removed and the number of blood vessels after treatment was recorded and images of those blood vessels in the egg after treatment were captured. The anti-angiogenesis activity of the samples was determined by calculating the percentage inhibition of blood vessels using the **Eq. (4.27)** (Pachava, 2017).

$$\% \text{ inhibition of blood vessels} = \frac{\text{No. of blood vessels in CAM before treatment} - \text{No. of blood vessels in CAM after treatment}}{\text{No. of blood vessels in CAM before treatment}} \times 100$$

**Eq. (4.27)**

#### **4.2.15.2. Acute dermal toxicity study**

The acute dermal toxicity of the developed AGE NANE was performed by following Organization of Economic Co-operation and Development (OECD) guideline, No.402. Healthy adult female Sprague Dawley rats of approximately 200-300 g weight were purchased from National Institute of Pharmaceutical Education and Research (NIPER), Mohali. All the animals were acclimatized to laboratory conditions by providing plastic cages with rice husk bedding at a temperature of  $25 \pm 2^\circ\text{C}$  with 45% RH. During this period, 12 h light and 12 h dark cycles were

maintained in the housing with the help of artificial lighting. The animals were supplemented with pellet food and purified water *ad libitum*. All the experimental procedures were conducted after the approval of Institutional Animal Ethical Committee (IAEC) and approval number is LPU/IAEC/2021/80.

Fur was removed from the dorsal back of the Sprague Dawley rats 24 h prior to the start of study. Hair removal was done from approximately 10% of the body surface area using hair remover cream to avoid any abrasion on the skin. The animals were divided into 3 groups having 1 animal each in one group to perform range finding study followed by main study with 3 groups having 2 animal each in one group (OECD, 2017). Markings were done on each animal for identification of individual animals in the respective groups. The rats of group I (in range finding study) and group IV (in main study) received a dose of 200 mg/kg, group II (in range finding study) and group V (in main study) received a dose of 1000 mg/kg and group III (in range finding study) and group VI (in main study) received a dose of 2000 mg/kg. The protocol is mentioned in **Table 19**. All the treated rats were observed for changes in skin and fur, eyes, mucous membrane, sleep pattern, respiratory, circulatory, autonomic and central nervous system activity, behaviour pattern, toxic reactions and mortality for a total period of 14 days. The body weight of all the animals was determined before initiation of treatment as well as after completion of treatment. All the observations were recorded systematically (Raghuwanshi et al., 2019).

In addition to the above-stated observations, treated sites were observed at 24, 48 and 72 h after removal of the formulations using Draize criteria (Draize, 1944). The details of Draize scoring system is mentioned in **Table 20**. This observation further avoided the requirement for separate *in vivo* skin irritation study. The data obtained after observation were tabulated to provide details for *in vivo* skin irritation study.



**Table 19.** Details of dosing in acute dermal toxicity studies

Range finding study		
Group	Number of animals	Dose (mg/kg)
I	1	200
II	1	1000
III	1	2000
Main study		
IV	2	200
V	2	1000
VI	2	2000

**Table 20.** Draize scoring system

Description of erythema or edema	Scoring
<b>Erythema</b>	
No erythema	0
Very slight erythema	1
Well-defined erythema	2
Moderate to severe	3
Severe erythema	4
<b>Edema</b>	
No edema	0
Very slight edema	1
Slight edema with raised margin	2
Moderate edema with raised margin (1mm)	3
Severe edema with raised margin (>1 mm), extending beyond the exposed surface	4

Note: The interpretation of scoring ;< 2 : slight irritation; 2-4: moderately irritation and >4: severely irritation

#### **4.2.15.3. Antipsoriatic activity in IMQ induced mouse model**

IMQ induced psoriasis model is one of the most reliable preclinical research model for psoriasis. However, mostly reported limitation of the model is the sensitivity to genetic variation in the mice as reported by Badanthadka et al. In order to demonstrate the reported variation of disease severity and stability of IMQ induced psoriasis model, Badanthadka et al. selected three different strains of mice (BALB/c, C57BL/6 and Swiss albino). In all the selected strains, IMQ was applied which resulted in psoriasis induction that was confirmed from their increased PASI

scoring and body weight alterations. Among the selected strains, Swiss albino mice was found to have stable and severe psoriasis in comparison to than other strains (Badanthadka et al., 2021).

Hence, Swiss albino mice strain was selected for induction of psoriasis using topical application of IMQ. Even though it is the drug of choice for the treatment of external genital and perianal warts, topical application of IMQ also reported to induce psoriasis plaques in mice, that closely resembled psoriasis conditions in human (Na Takuathung et al., 2018; Tyring, 1998). IMQ is an immune response modifier that specifically acts as a stimulator and gets activated through toll-like receptor-7/8. Apart from activation of toll-like receptor, studies in toll-like receptor-7 knock out mice reported development of acanthosis upon IMQ treatment. Another study with Aldara (an IMQ cream brand) vehicle alone activated keratinocyte inflammasome (Walter et al., 2013). Different brands of IMQ cream have shown variable histological features (Luo et al., 2016). All these studies highlight the multifactorial mechanism of IMQ, which is therefore best model for induction of psoriasis which is caused by multiple factors. Hence, Swiss albino mice were selected as the animal strain and IMQ was selected as the drug for psoriasis induction.

The antipsoriasis activity of the developed and optimized AGE NANE at lower and higher doses was evaluated using IMQ induced mouse model after the approval from IAEC (approval number: LPU/IAEC/2021/80).

As per the study protocol, Swiss albino mice of either sex weighing approximately 20-30 g were purchased from NIPER, Mohali. All the collected animals were acclimatized in our laboratory conditions by providing plastic cages with rice husk bedding at a temperature of  $25 \pm 2^\circ\text{C}$  with 45% RH. During this period, 12 h light and 12 h dark cycles were maintained in the housing with the help of artificial lighting. The animals were fed with pellet food and purified water *ad libitum* (Khurana et al., 2020).

#### **4.2.15.3.1. Induction of psoriasis lesion**

Swiss albino mice were divided into 7 groups, each group containing six mice. The hairs on the dorsal back surface of the mice ( $6.25\text{ cm}^2$ ) as well as on the dorsal surface of the right ear were removed using hair removing cream. Initial body weight of all the animals was noted. Then, the lesions were developed by administering once daily a dose of 62.5 mg of 5% w/w IMQ cream that was equivalent to 3.125 mg of drug. The dosing was done in the morning. Except group I (normal control), all groups were exposed to IMQ for development of psoriasis lesion on the

dorsal back skin as well as dorsal side of the right ear. The selected dosing was applied to the shaved dorsal back skin (50 mg of IMQ cream) and right ear (12.5 mg of IMQ cream) for 7 consecutive days (Khurana et al., 2020) (Rajitha et al., 2019). After 7 days of induction, treatment began and continued for consecutive 7 days. The details of the dosing carried out in the study design are mentioned in **Table 21** and **Figure 7** represented diagrammatic representation of study design. During the treatment period, all mice were carefully observed for measuring the degree of irritation or redness.

**Table 21.** Experimental details for animal study

<b>Group No.</b>	<b>Groups</b>	<b>Treatment</b>	<b>Dosage and route of administration</b>	<b>n= no: of animals</b>
<b>I</b>	Normal control	Normal saline (no induction)	To be applied topically once daily to the shaved dorsal surface for 5 times in a week	6
<b>IMQ induced psoriasis (5% w/w IMQ cream daily for 7 consecutive days)</b>				
<b>II</b>	Experimental control	IMQ induced psoriasis (no treatment)	5% w/w, to be applied topically on dorsal surface of the body once daily for 7 consecutive days	6
<b>III</b>	Positive control	Marketed Betamethasone cream on psoriasis skin	0.1% w/w to be applied topically once daily for 7 consecutive days after induction of psoriasis	6
<b>IV</b>	NANE-B	Blank formulation on psoriasis skin	To be applied topically once daily for 7 consecutive days after induction of psoriasis	6
<b>V</b>	AGE <i>per se</i>	AGE on psoriasis skin	0.1% w/w to be applied topically topically using normal saline as vehicle once daily for 7 consecutive days after induction of psoriasis	6
<b>VI</b>	AGE NANE <sub>L</sub>	Optimized AGE NANE low dose on psoriasis skin	0.05% w/w to be applied topically once daily for 7 consecutive days after induction of psoriasis	6
<b>VII</b>	AGE NANE <sub>H</sub>	Optimized AGE NANE high dose on psoriasis skin	0.10% w/w to be applied topically once daily for 7 consecutive days after induction of psoriasis	6

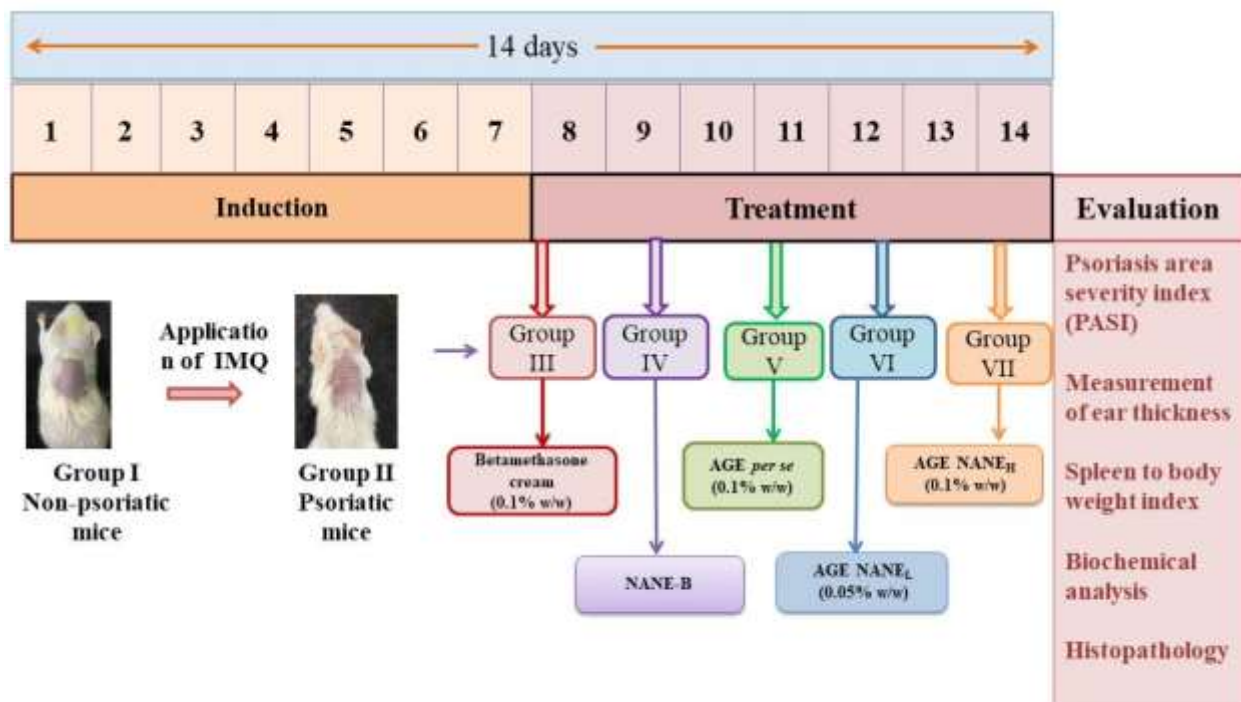


Figure 7. Diagrammatic representation of study design

#### 4.2.15.3.2. Evaluation parameters for antipsoriatic activity

##### 4.2.15.3.2.1. PASI

PASI scoring tool was used to evaluate the severity of inflammation. The scoring tool included parameters such as erythema, scaling and thickness (roughness). The scoring scale used in the study is represented based on the Physician Global Assessment severity scale as written below (Pascoe and Kimball, 2015):

0: Clear, 1: Almost clear (slight), 2: Moderate, 3: Marked and 4: Severe.

The PASI scoring was recorded on the initial day (1<sup>st</sup> day) before the induction of psoriasis and then on the third day, sixth day (the induction of psoriasis), followed by ninth day, twelfth day and fourteenth day (treatment period). The percentage reduction in PASI scoring after treatment (14<sup>th</sup> day) was compared with the scoring before treatment begun i.e. on 6<sup>th</sup> day of psoriasis induction. Images of the dorsal skin were captured before psoriasis induction (1<sup>st</sup> day), after

induction of psoriasis (7<sup>th</sup> day) and after completion of treatment (14<sup>th</sup> day). Then, all the mice were euthanized for further evaluations (Khurana et al., 2020).

#### ***4.2.15.3.2.2. Ear thickness***

The ear thickness measurement was carried out using vernier calliper by keeping left ear as control and disease-induced right ear for measuring the extent of inflammation. After treatment images of the right ear from all the groups were captured (Sahu et al., 2018).

#### ***4.2.15.3.2.3. Spleen to body weight index***

Once the treatment period was over, the body weight of all mice were noted. After euthanasia, the spleen was collected, cleaned thoroughly with PBS (pH 7.4) and weighed. Images of the collected spleen were captured, then spleen to body weight index was calculated (Domala et al., 2020).

#### ***4.2.15.3.2.4. Histopathology***

On completion of the treatment period, mice were taken and anaesthetized in a glass jar containing cotton balls previously soaked with diethyl ether, then euthanized by cervical dislocation. Then, the dorsal back and ear skin were removed immediately and rinsed with normal saline for evaluating the pathological changes in the skin specimens. After removal of dorsal and ear skin were fixed in 10% formalin. The skin samples were stained with hematoxylin and eosin and finally mounted on the glass slides. The prepared slides were examined under microscope at a total magnification of 100x and 400x and various features such as acanthosis, appearance of parakeratosis and hyperkeratosis, vascularity, mononuclear cell infiltration, microabscess were recorded with the help of a pathologist (blind analysis). The scoring are rated with the help of following scale (Sun et al., 2017).

0- No inflammation

1- Mild acanthosis with low infiltration of inflammatory cells.

2- Mild to moderate thickening of epidermis with mononuclear cell infiltration.

3- Severe acanthosis and rich vascularity with an abundance of mononuclear infiltration.

4- Very severe acanthosis with the microabscess

Photomicrograph of the dorsal skin and ear were captured using 100x microscopic magnification and measured at 100 µm scale. All the aforementioned features were keenly observed and recorded using 400x magnification.

#### **4.2.15.3.3. Biochemical estimation of the antioxidant activity in the dorsal skin tissue**

After 14 days of *in vivo* studies on IMQ induced mouse model, a portion of the dorsal skin tissue from the sacrificed mice of each sample group were washed in normal saline and cut into small parts. These samples were homogenized in phosphate buffer (pH 6.5) using tissue homogenizer. Homogenized tissues were later centrifuged for 10 min in a freeze centrifuge at 10,000 g. The supernatant obtained was separated and used for the estimation of antioxidant markers in the tissue homogenate. The antioxidant markers estimated were superoxide dismutase (SOD) (Spitz and Oberley, 1989), catalase (CAT) (Mueller et al., 1997) and reduced glutathione (GSH), lipid peroxidation by measuring content of malondialdehyde (MDA) (Valenzuela, 1991).

##### **4.2.15.3.3.1. Estimation of SOD**

The supernatant obtained from the tissue homogenate was added into the mixture containing 500 mM of sodium carbonate solution (20  $\mu$ L), 0.3% Triton X-100 (2 mL), 1.0 mM of ethylenediamine tetraacetic acid (20  $\mu$ L), 10 mM of hydroxylamine (5 mL) and distilled water (178 mL). Into this mixture, 20  $\mu$ L of nitro blue tetrazolium (240  $\mu$ M) was added and the optical density of the reaction mixture was measured at 560 nm for total 3 min with a time interval of 1 min. The rate of increase in the measured optical density was considered as the SOD activity. The final concentration of SOD determined using a standard calibration curve was expressed in U/mL (Agrawal et al., 2020).

##### **4.2.15.3.3.2. Measurement of CAT activity**

A measured volume of tissue homogenate supernatant (20  $\mu$ L) was added to 1 mL of hydrogen peroxide solution (10 mM) into the cuvette. The reduction in the optical density of this reaction mixture was measured at 240 nm. The rate of decrease in the optical density after addition of tissue homogenate was noted from the time of addition till the completion of reaction. Approximately 3 min was considered as an indicator of CAT activity present in the tissue samples. The final concentration of catalase was determined by using a standard calibration curve and concentration was expressed in moL/min/mL (Agrawal et al., 2020).

##### **4.2.15.3.3.3. Estimation of GSH**

The estimation of GSH content in the tissue homogenate was determined using Ellman's reagent which is chemically 5,5'-dithio-bis(2-nitrobenzoic acid) (DTNB) (Rahman et al., 2006).

The tissue homogenate (20  $\mu$ L) was treated with 1 mM DTNB solution (180  $\mu$ L) at room temperature which resulted in yellow colouration. The optical density of the reaction mixture was measured at 412 nm and concentration of GSH was expressed as  $\mu$ g/mg of protein. The final concentration was determined by using standard calibration curve (Agrawal et al., 2020).

#### **4.2.15.3.3.4. Estimation of TBARS**

The extent of lipid peroxidation in the tissue homogenate was determined by measuring MDA content which represents the level of thiobarbituric acid reactive substances (TBARS) and concentration is expressed as nmol MDA eq./g of the tissue at 37°C. For estimation of MDA, a reaction mixture containing 1 mL of tissue homogenate, 1 mL of trichloroacetic acid (10%) and 1 mL of thiobarbituric acid (0.67%) were mixed together and incubated in boiling water for 45 min. After the specified time, the reaction mixture was cooled and centrifuged at 10,000 g for 10 min. The supernatant obtained was extracted with 4 mL of n-butanol. The pink coloured n-butanol layer was separated and absorbance was measured at 532 nm. The final concentration was determined from the standard calibration curve. The measurement of TBARS indicated extends of lipid peroxidation (Agrawal et al., 2020; Sangaraju et al., 2021).

#### **4.2.15.4. Statistical analysis**

All the experimental data obtained from the study are statistically analyzed. The obtained data are expressed as mean  $\pm$  standard error of mean (SEM). The data are statistically assessed using analysis of variance (one-way and two-way ANOVA) or Tukey's multiple comparisons test, Bonferroni posttest using GraphPad Prism version 7.0 ( GraphPad software Inc.,USA). The results obtained were compared with normal control and experimental control which is expressed in terms of " $\alpha$ " indicates  $p < 0.001$ ; " $\beta$ " indicates  $p < 0.01$ ; " $\gamma$ " indicates  $p < 0.05$ ; " $\psi$ " indicates  $p > 0.05$  with respect to normal control. Similarly, "a" indicates  $p < 0.001$ ; "b" indicates  $p < 0.01$ ; "c" indicates  $p < 0.05$ ; "d" indicates  $p > 0.05$  with respect to experimental control.

# Chapter 5



---

## Results and Discussion

---



## Chapter 5

### Results and Discussion

#### 5.1. Collection of AG plant and its rhizomes

The collected AG plant along with its parts was submitted for authentication that is shown in **Figure 8**.

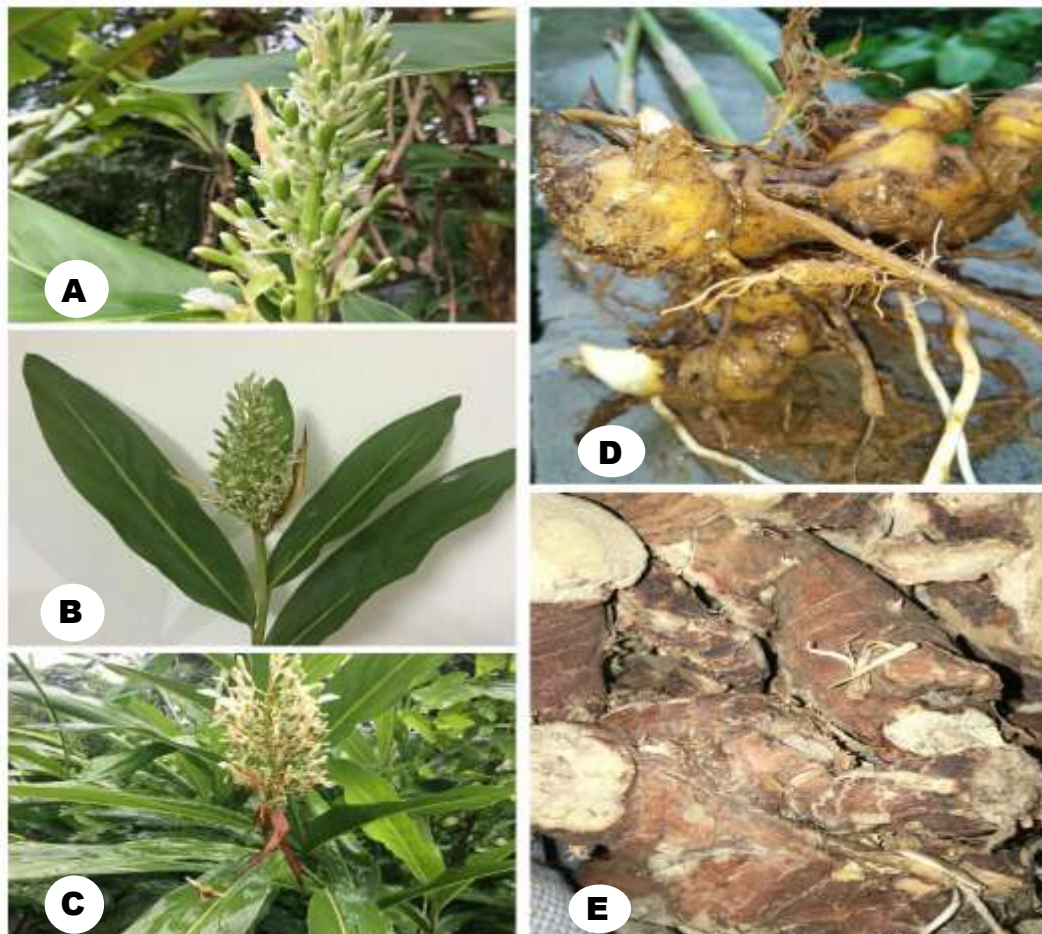


**Figure 8.** Various parts of AG (A) Flower, (B) Specimen for herbarium, (C) Plant collected for authentication, (D) Fresh rhizomes of the collected plant, (E) Dried rhizomes for research work

#### 5.2. Authentication of the collected plant

The authentication of the plant was confirmed by Dr. Abraham Mathew, Assistant Professor, Department of Botany, St Peters College, Kolenchery, Kerala. A certificate was issued (Annexure I) confirming that the collected plant is *Alpinia galanga* (L) Sw. belonging to the

family Zingiberaceae. Further, a plant specimen was deposited in the Herbarium of the College with specimen number SPC-H-3085 as shown in **Figure 9**.



**Figure 9.** Herbarium of AG

### 5.3. Physicochemical evaluation of powdered rhizomes

The physicochemical parameters were evaluated to ensure the quality of the powdered rhizome which has to be used further for extraction. The results obtained are reported in **Table 22**.

**Table 22.** Physicochemical evaluation of the powdered rhizomes

S.No.	Parameters	Observation (% w/w)	Reported (% w/w)
1	Loss on drying	6.33 ± 0.92	4.65
2	Total ash value	4.69 ± 1.01	4.10
3	Acid insoluble ash value	1.07 ± 0.02	1.25
4	Water soluble ash value	2.77 ± 0.21	4.66
5	Sulphated ash value	6.50 ± 0.11	3.66
6	Alcohol soluble extractive value	6.72 ± 0.13	8.20
7	Water soluble extractive value	13.28 ± 1.12	15.30

The physicochemical parameters are mainly evaluated for judging the purity and quality of the drug. All the physicochemical parameters were evaluated and results closely complied with the reported results (Kadam et al., 2012). Also, observed results were within the limit mentioned in the Ayurvedic Pharmacopoeia of India (India, 2008).

### 5.4. Preparation of the extract

Ultrasonication assisted maceration process was carried out using absolute ethanol. The solid to solvent ratio was 1:10 and the yield of the extract was  $3.49 \pm 1.09\%$  w/w of dried rhizome.

### 5.5. Phytochemical screening of the extract

The obtained ethanolic extract was subjected to preliminary phytochemical screening for the analysis of reported metabolites. The observations are shown in **Figure 10** which helped in analyzing the metabolites present in the ethanolic extract. The results of the phytochemical screening are tabulated in **Table 23**.

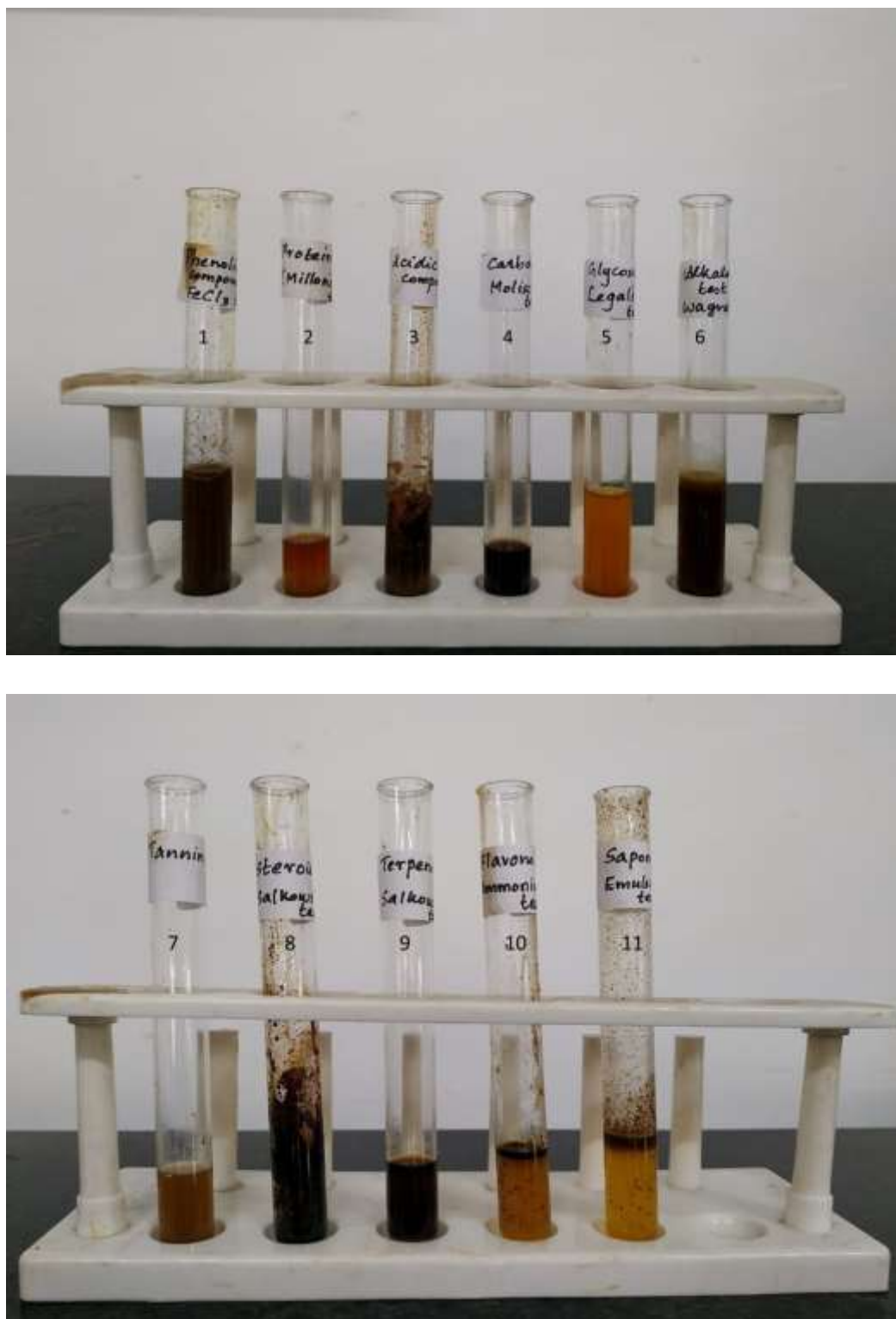


**Figure 10.** Observation of phytochemical screening study for (1) Phenolic compounds (2) Protein (3) Acidic compounds (4) Carbohydrates (5) Glycosides (6) Alkaloids (7) Tannins (8) Steroids (9) Terpenoids (10) Flavonoids (11) Saponins

**Table 23.** Phytochemical screening of the ethanolic AGE

S.No	Chemical Test	Observation	Inference
1	Phenolic compounds (Ferric chloride test)	Appearance of green colored solution	+
2	Protein and amino acids (Millons test)	No red precipitate	-
3	Acidic compounds (Bicarbonate test)	Evolution of effervescence	+
4	Carbohydrates (Molisch test)	Reddish violet ring at the junction of two layers	+
5	Glycosides (Legal's Test)	No red colouration	-
6	Alkaloids (Wagner's Test)	Appearance of reddish brown precipitate	+
7	Tannins (Ferric chloride test)	No brownish-green or a blue-black colour	-
8	Steroids (Salkowski Test)	No reddish brown colouration at the interface	-
9	Terpenoids (Salkowski Test)	No grey colouration	-
10	Flavonoids (Ammonia test)	Appearance of yellowish coloration, disappears on standing	+
11	Saponins (Emulsion test)	No persistent froth or emulsion formation	-

Note: (+) indicates the presence of the compound

(-) indicates the absence of the compound

The phytochemical screening of the ethanolic extract has confirmed the presence of alkaloids, carbohydrates, phenolic compounds, acidic compounds and flavonoids. These observations point towards the chemistry of phytoconstituents present in it. Some of the previously reported studies have identified the individual bioactive compounds in AG rhizome extract which included phenolic compounds, basically phenylpropanoids like ACA, 1'-acetoxyeugenol acetate, p-coumaryl diacetate, p-hydroxy cinnamaldehyde (Verma et al., 2011), flavonoids like galangin, kaempferol, quercetin, myricetin (Tungmunnithum et al., 2020), alkaloids such as berberine, some terpenoids such as 1,8-cineole,  $\alpha$ -terpineol, etc.

Among these compounds, ACA being a phenylpropanoid (Ye and Li, 2006) contained 1' and 4 substituted 1-acetoxy propenyl and acetoxy groups at the benzene ring. These functional groups exerted various mechanism of action such as inhibition of translocation of NF- $\kappa$  B (Batra et al., 2012; Murakami et al., 2000), activation of AMPK signaling pathway (Ohnishi et al., 2012) etc. In the earlier research studies, the potential protective role of ACA as gastroprotective (Matsuda et al., 2003b) and xenobiotic protective (Tanaka et al., 1997) has been proved. Later, several pharmacological activities such as antitumor (Baradwaj et al., 2017), antiobesity (Narukawa et al., 2010), antimicrobial (Phongpaichit et al., 2006), antiallergic (Matsuda et al., 2003a),

antidementia (Kojima-Yuasa et al., 2016) and antioxidant (Mahae and Chaiseri, 2009) activities of ACA have been demonstrated. The ethanolic extract of AG was reported to have antipsoriatic activity on the HaCaT keratinocytes cell line. A significant reduction in the expression of NF- $\kappa$  B and CSF-1 with increased expression of TNFAIP3 resulted in the antipsoriatic activity and the study finding focused on the presence of ACA in the ethanolic extract that contributed towards the activity (Saelee et al., 2011).

Therefore, ACA was selected as the marker compound in the present study. Hence, for further identification and analysis of ACA in the extract, GC-MS analysis was carried out. GC-MS analysis identifies the volatile components present in the extract and ACA being semivolatile in nature, GC-MS analysis was preferred.

### **5.6. GC-MS**

GC-MS analysis of ethanolic AGE confirmed the presence of ACA in it. The elution of ACA was observed at 17.956 min in the chromatogram (**Figure 11**) and later MS analysis of AGE (**Figure 12A**) confirmed that the base peak and other mass fragmentation peaks obtained were similar to the MS spectrum of ACA (**Figure 12B**) obtained from its MS-library. The molecular weight of ACA was reported to be 234 and the fragmentation of its molecular mass into various fragments such as 43, 132, 150, 174, and 192. Among these fragments, base peak was found to be at 132 showing 100% relative intensity which was similar in the reference spectrum obtained from MS-library. Along with this peak, other fragmentation peaks obtained from AGE are also shown in the Figure 11A and all peaks comply with the reference MS-spectrum (**Figure 12B**).

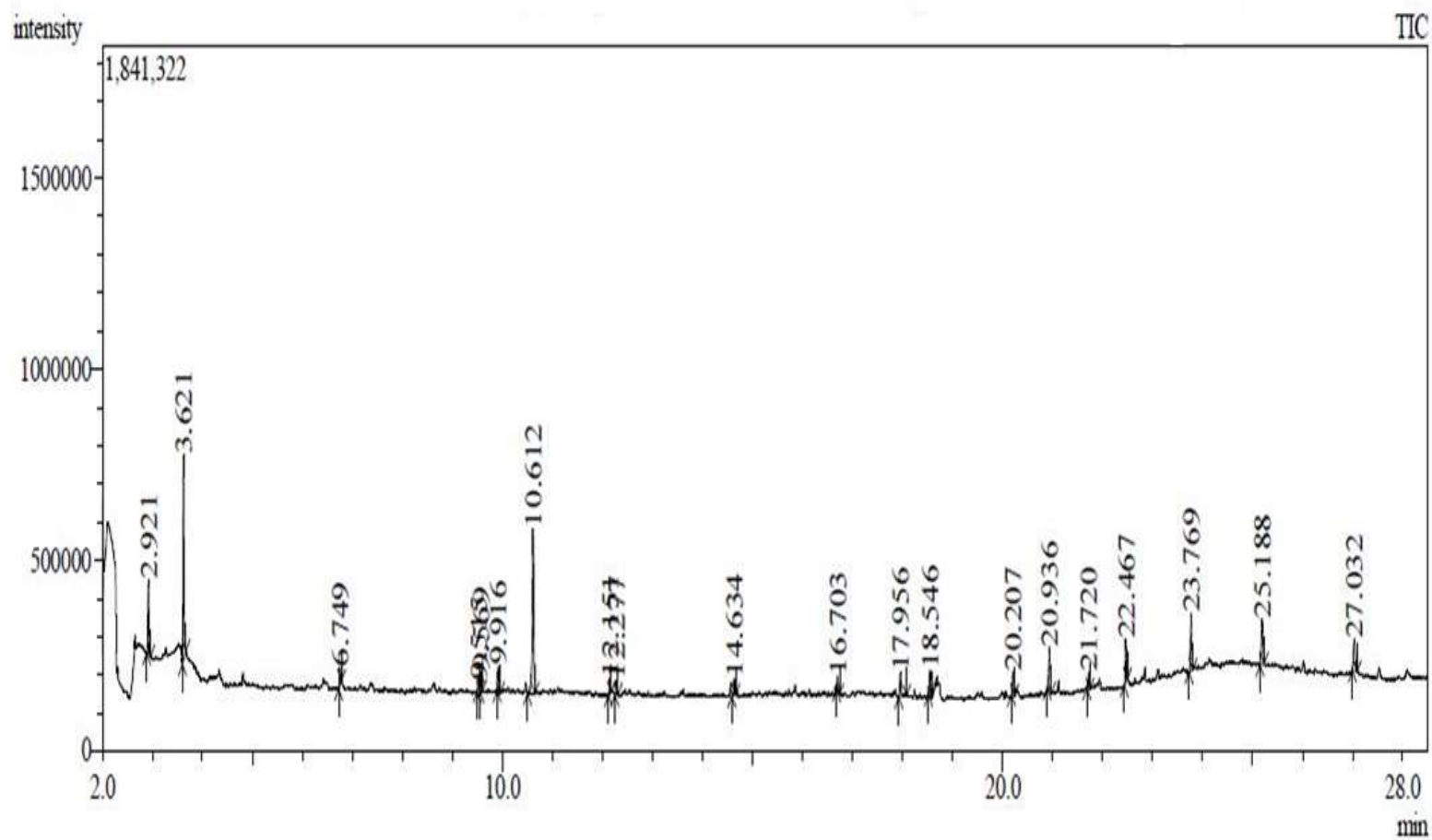
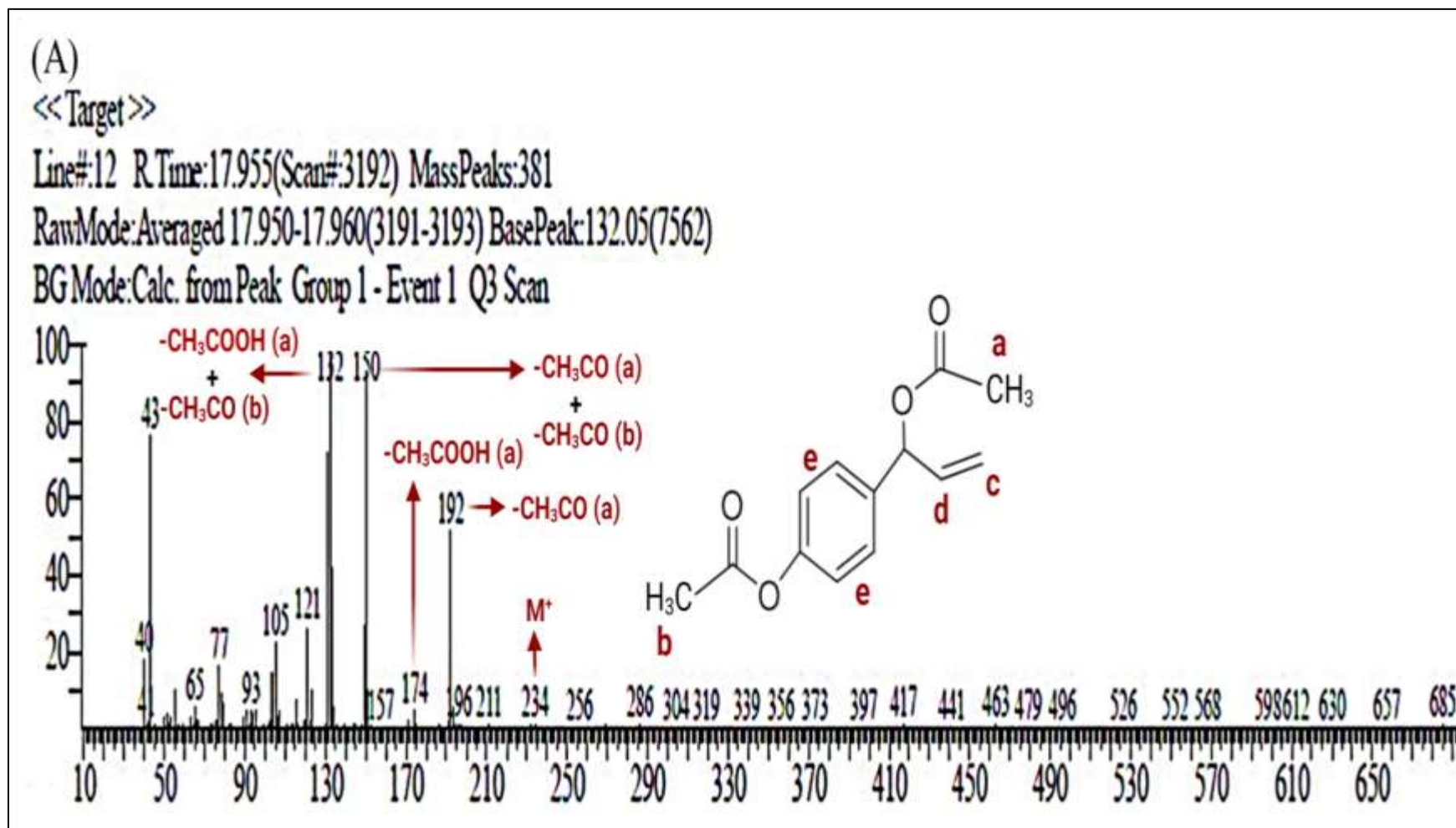


Figure 11. GC of AGE





(B)

Hit#:1 Entry:105868 Library:NIST17.lib

SI:92 Formula:C<sub>13</sub>H<sub>14</sub>O<sub>4</sub> CAS:52946-22-2 MolWeight:234 RetIndex:1664

CompName:(S)-4-(1-Acetoxyallyl)phenyl acetate

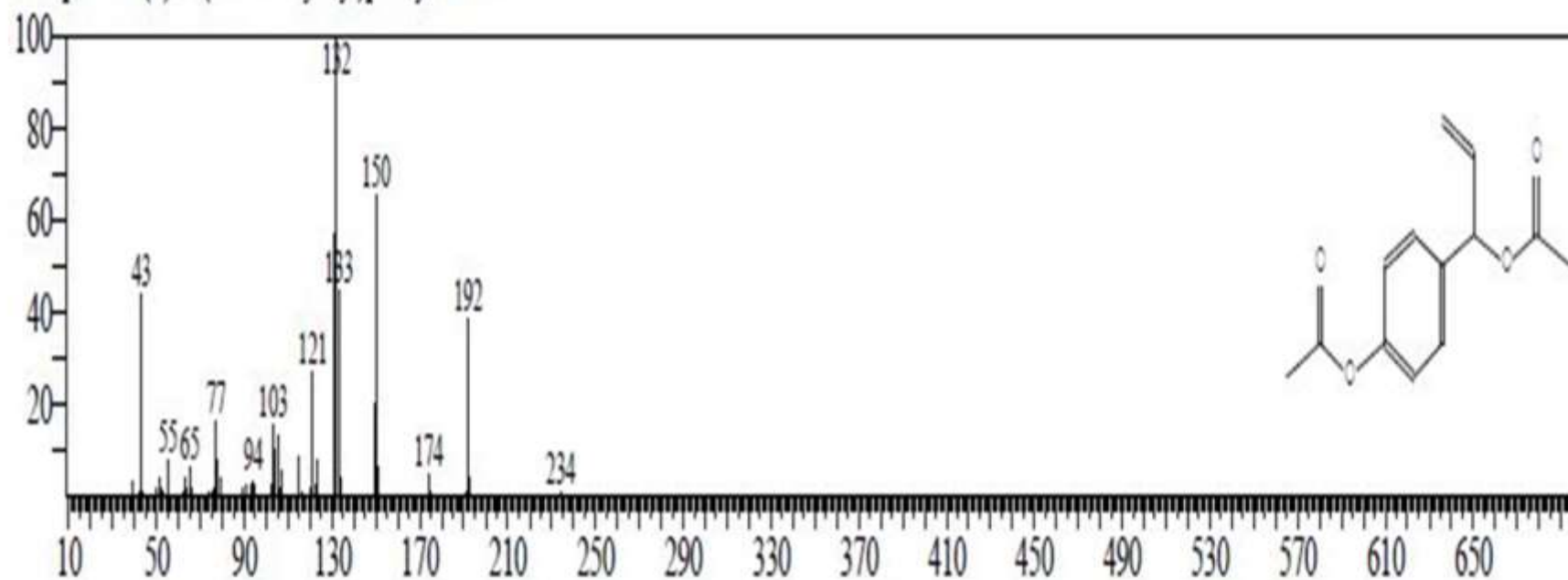


Figure 12. (A) Mass spectrum of eluted ACA from AGE (B) Mass spectra of ACA obtained from MS library

### **5.7 Analytical method development**

An analytical method is the major requisite for the identification and the content determination in the herbal extracts and its finished product. The suitability of the developed method and its repeatability in various fields of application has to be confirmed. Considering the method of chemical analysis for ACA in AG, few studies are described in the literature regarding methods for identification and further quantification. Baradwaj *et al.* 2017 reported a method by HPLC using a mobile phase of acetonitrile and water (60:40, v/v) to analyze the purified ACA obtained from the AG rhizomes. The reported method by Baradwaj *et al.* 2017 has shown the chromatographic profile of standard ACA and purified ACA from the extract. However, the presence of shoulder peak in the standard ACA and elution of two components from the extract were visible (Baradwaj *et al.*, 2017). However, the same mobile phase composition has been tried with the available chromatographic condition at a flow rate of 1 mL/min and detection wavelength at 218 nm ( $\lambda_{max}$  of ACA). With this method, a single broad peak was obtained as shown in **Figure 13 (A)** and elution of ACA was obtained at 7.23 min.

To obtain better elution of the compound, a mixture of 0.1% v/v aqueous orthophosphoric acid and acetonitrile was used in varying ratio. The chromatogram obtained was not satisfactory due to the appearance of shoulder peak as shown in **Figure 13 (B)**. Hence, another mobile phase composition comprising of 0.1% v/v aqueous orthophosphoric acid and methanol has been used for elution of ACA. The chromatogram obtained has shown shoulder peak as shown in **Figure 13(C)**. Therefore, alterations in the mobile phase composition have been done by removing orthophosphoric acid. A mobile phase composition of methanol and water has shown peak fronting and peak broadening at ratio 70:30, v/v and 60:40, v/v respectively (**Figure 13 D and E**).

Then, a mobile phase composition of acetonitrile and 0.1% v/v aqueous formic acid has been used for elution of ACA. The chromatogram obtained was single, sharp peak as shown in **Figure 13F**. This composition has been reported by Chua *et al.* 2017 for the identification and quantification of the ACA in *Chlorophytum borivilianum* (Chua *et al.*, 2017). In this method, the chromatographic profile of the extract was compared with the previously isolated ACA, which served as the standard. The reported method was satisfactory for the elution of ACA, however, lacked validation.

## Results and Discussion

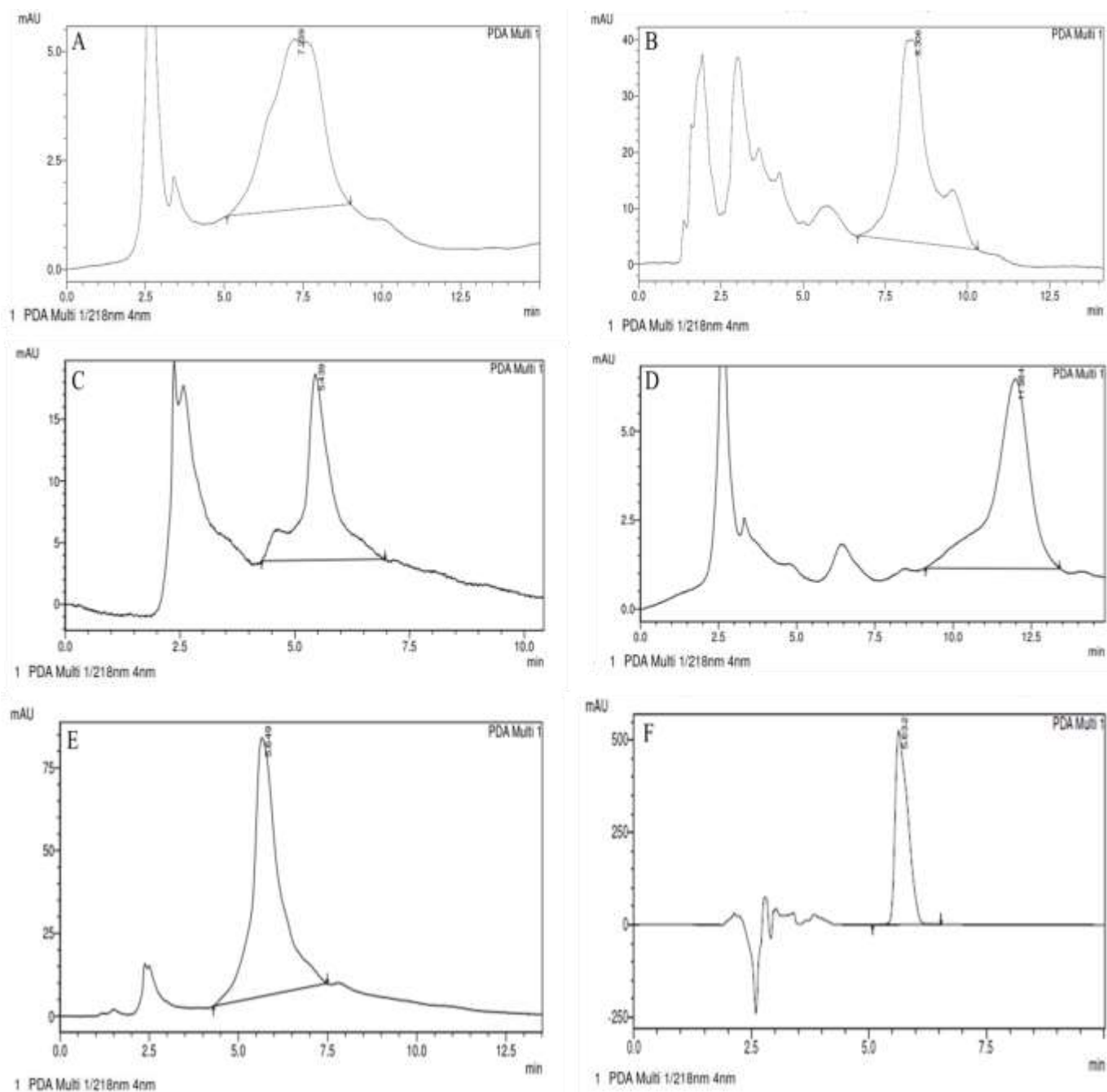


**Figure 13.** Chromatogram of ACA in (A) Acetonitrile: water (40:60, v/v) (B) 0.1% v/v Orthophosphoric acid in water: acetonitrile (50:50, v/v) (C) 0.1% v/v Orthophosphoric acid : methanol (30:70, v/v) (D) Methanol: water (70:30, v/v) (E) Methanol: water (60:40, v/v) (F) Acetonitrile: 0.1% v/v formic acid (60:40, v/v)

Therefore, a method was developed with a mobile phase composition of acetonitrile and 0.1% v/v formic acid in water (60:40 v/v). Isocratic elution was performed with 1 mL/min flow rate at the absorption maxima ( $\lambda_{\max}$ ) of 218 nm. The retention time of standard ACA (250 ppm) was recorded at 5.632 min and the chromatogram of standard ACA was recorded as shown in **Figure 14** (Ramanunny et al., 2021a).

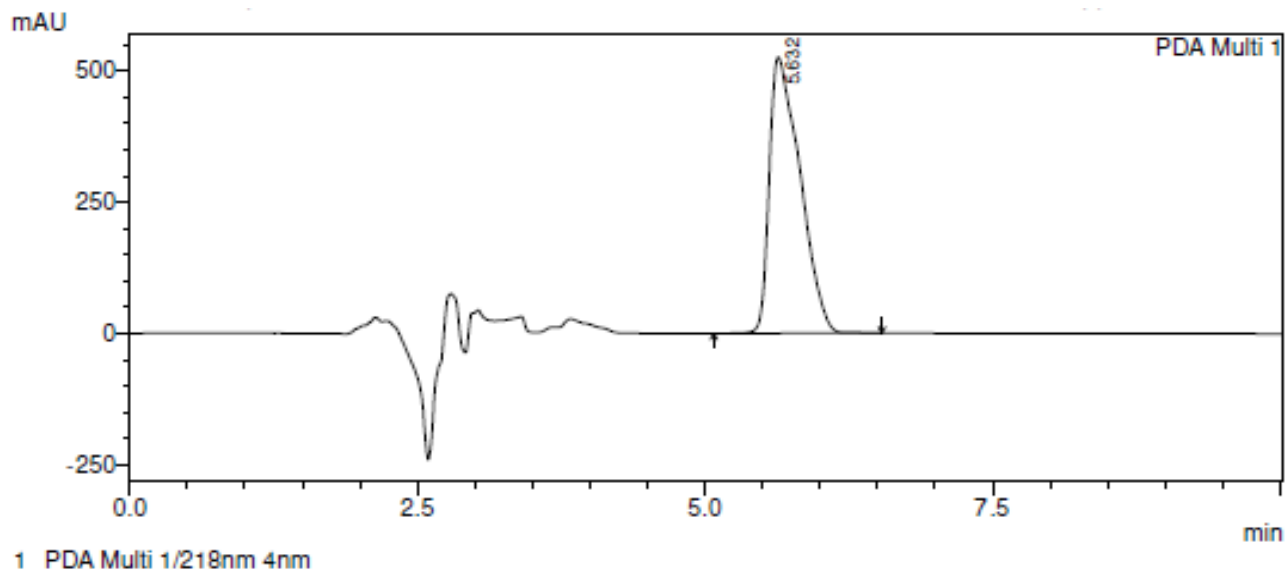


**Figure 14.** Chromatogram of standard ACA

### 5.8. Analytical Validation

Validation is an important parameter to justify the sensitivity, accuracy, precision and reproducibility of method. Hence, the developed HPLC method for quantification of ACA was validated as per ICH Q2 [R1] guidelines (ICH Harmonised Tripartite, 2005).

#### 5.8.1. Linearity and range

The calibration plot was constructed with the linear concentration of ACA ranging from 50, 100, 150, 200 and 250  $\mu\text{g/mL}$  by keeping the values of concentration on the  $x$ -axis and their mean peak area on the  $y$ -axis as shown in **Figure 15**. The plot represented good linearity, with the correlation coefficient ( $r^2$ ) value of 0.9987. The slope and intercept of the calibration plot are expressed in the linearity equation  $y = 37722x + 131819$ .

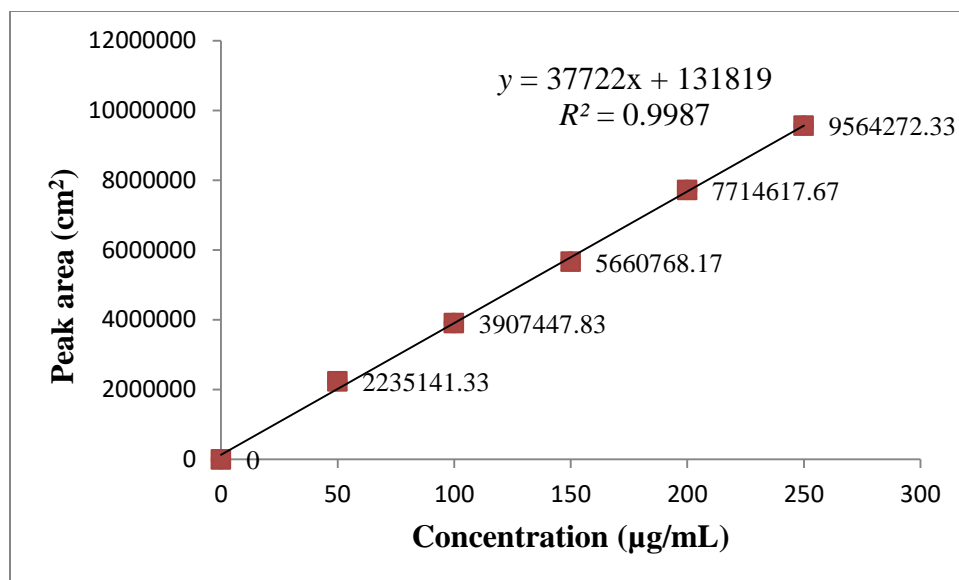


**Figure 15.** Calibration curve of standard ACA

### 5.8.2. Accuracy

The percentage recovery of ACA from the different levels of method concentration i.e. LQC, MQC, and HQC was evaluated. The data shown in **Table 24** revealed that the percentage recovery of ACA lies within the prescribed limit (95-105%) which indicates that the developed method is accurate.

### 5.8.3. Precision

The precision of the developed method was confirmed by repeatability (intraday) and intermediate precision (inter-day and inter-analyst) studies. The precision is expressed as the percentage relative standard deviation for each set of concentrations, LQC, MQC, and HQC. The precision results in **Table 25** shows % RSD less than 2 for all the sets of analysis performed. This confirms that the developed method was precise.

### 5.8.4. LOD and LOQ

The calculated values of LOD and LOQ were 12.58 µg/mL and 38.13 µg/mL respectively. This indicated that the developed method was sensitive.

The system performance was evaluated by measuring the system suitability parameter. The peak purity index of the standard ACA was obtained as 1.000 where no impurities were detected. The theoretical plate was recorded as 9626.36 (>2000) with an HETP of 15.58 and tailing factor was recorded as 1.07 ( $\leq 2$ ) (ICH Harmonised Tripartite, 2005).

#### **5.8.5. Robustness**

The minor variation in the experimental setup, such as a change in the flow rate (0.8, 1.0, and 1.2 mL/min), change in the ratio of mobile phase composition (55:45, 60:40, 65:35 v/v) and change in wavelength (216, 218, 220) was evaluated for the selected concentration (MQC) as shown in **Table 26**. The % RSD for all sets of analysis was less than 2% that has confirmed the robustness of the developed method.

#### **5.8.6. Specificity**

The specificity of the RP-HPLC method was evaluated by the comparative analysis of the peak retention time of standard ACA with the isolated ACA. The chromatogram of standard ACA and isolated ACA from the AGE were recorded at 5.63 min and 5.46 min respectively as represented in **Figure 16 (a) and (b)**. Since, no significant deviation was observed in the retention times of the standard and isolated ACA, the developed method was found to be specific. The peak purity index of the isolated ACA was evaluated and confirmed the absence of impurities (**Figure 17**). This also inferred the absence of interference of the other phytoconstituents during elution of the ACA (Ramanunny et al., 2021a).

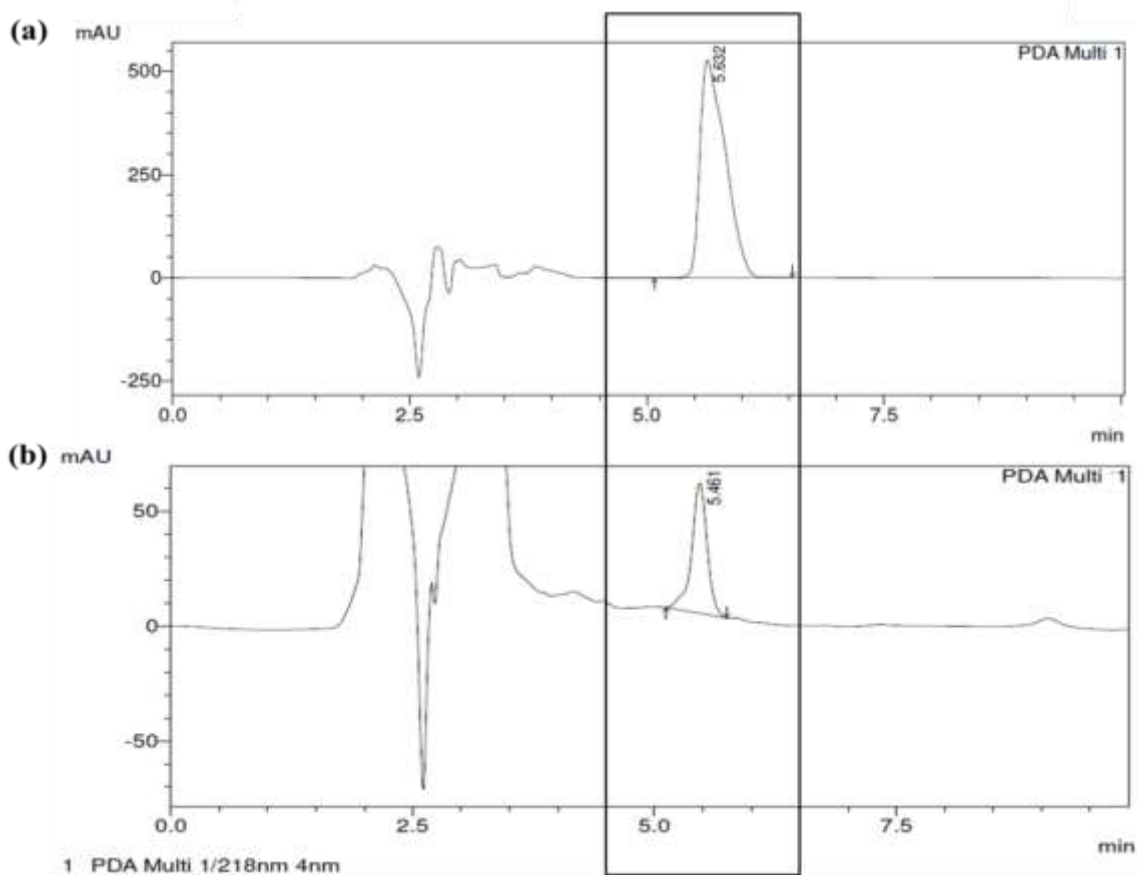


Figure 16. Comparison of retention time of standard ACA and isolated ACA from AGE

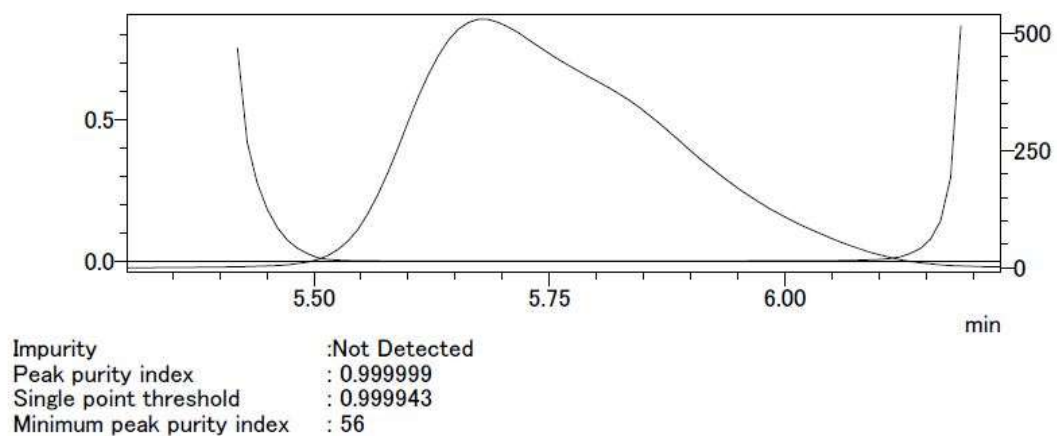


Figure 17. Peak purity index of isolated ACA from ethanolic extract

**Table 24.** Accuracy results based on the percentage recovery of ACA

	<b>Theoretical concentration (<math>\mu\text{g/mL}</math>)</b>	<b>Mean peak area (<math>\pm</math>) S.D. (<math>\text{cm}^2</math>)</b>	<b>Recovered concentration (<math>\mu\text{g/mL}</math>)</b>	<b>% Recovery</b>
<b>Accuracy</b>	120	4502660.85 $\pm$ 31437.71	122.86	102.38
	150	5669647.33 $\pm$ 32317.97	153.79	102.53
	180	6767054.67 $\pm$ 39917.42	182.88	101.60



Table 25. Precision results

Parameter	Level	Concentration ( $\mu\text{g/mL}$ )	Area ( $\text{cm}^2$ ) ( $n=6$ )						Mean area ( $\text{cm}^2$ )	S.D. ( $\pm$ )	% RSD
<b>Repeatability</b>											
<b>Intra-day</b>	LQC	120	4536994	4621341	4598765	4576541	4621023	4598123	4592131.17	35383.40	0.77
	MQC	150	5743211	5698287	5712312	5781932	5776324	5598762	5718471.33	67471.34	1.18
	HQC	180	6654312	6745321	6617823	6782312	6654212	6734214	6698032.33	64673.98	0.97
<b>Intermediate precision</b>											
<b>Inter-day</b>											
<b>Day 1</b>	LQC	120	4602957	4529008	4665059	4678751	4698778	4676473	4641838.67	64165.21	1.38
	MQC	150	5676432	5589601	5700213	5685816	5640187	5715328	5667930.50	46013.18	0.81
	HQC	180	6578243	6698724	6774398	6656981	6675625	6574983	6659826.67	75830.89	1.14
<b>Day 2</b>	LQC	120	4703592	4679189	4778213	4678751	4576331	4585068	4666857.33	69435.29	1.49
	MQC	150	5774422	5678792	5689115	5879021	5790179	5668907	5746739.33	82640.24	1.44
	HQC	180	6892341	6798942	6674825	6766442	6772134	6647833	6758753.83	88369.95	1.31
<b>Day 3</b>	LQC	120	4715371	4632187	4683019	4775208	4512281	4665331	4663900.50	88769.76	1.90
	MQC	150	5566338	5589601	5679119	5534219	5689841	5629783	5614817.83	62401.00	1.11
	HQC	180	6712849	6699489	6679883	6768012	6652484	6678218	6698489.17	39784.96	0.59
<b>Inter-analyst</b>											
<b>Analyst 1</b>	LQC	120	4689892	4665971	4753032	4569327	4734891	4643298	4676069.50	66549.48	1.42
	MQC	150	5775892	5456898	5699348	5662314	5686548	5580976	5643663.67	110980.30	1.97
	HQC	180	6798357	6875437	6678544	6643098	6589326	6564985	6691625.50	121825.55	1.82
<b>Analyst 2</b>	LQC	120	4728544	4721343	4717905	4702431	4509654	4671245	4675187.00	83619.52	1.79
	MQC	150	5643267	5587321	5563814	5793125	5755217	5686173	5671486.17	91099.89	1.61
	HQC	180	6792141	6742897	6702189	6693218	6721874	6772176	6737416.83	39163.97	0.58
<b>Analyst 3</b>	LQC	120	4751273	4702379	4743982	4775208	4668793	4678540	4720029.17	43017.77	0.91
	MQC	150	5656766	5709504	5568216	5621396	5575439	5678645	5634994.33	56784.11	1.01
	HQC	180	6810217	6774439	6685432	6714532	6664325	6787518	6739410.50	59540.47	0.88

**Table 26.** Robustness

Parameter	Level	Concentration ( $\mu\text{g/mL}$ )	Area ( $\text{cm}^2$ ) ( $n=6$ )						Mean area ( $\text{cm}^2$ )	S.D. ( $\pm$ )	% RSD
<b>Change in flow rate (<math>\text{mL min}^{-1}</math>)</b>											
0.8	MQC	150	6327654	6319874	6327541	6400213	6398543	6321678	6349250.50	38956.03	0.61
1.0	MQC	150	5779801	5819059	5823154	5798132	5892134	5720932	5805535.33	56333.69	0.97
1.2	MQC	150	5576921	5523080	5499852	5497623	5589341	5532659	5536579.33	38666.10	0.70
<b>Change in mobile phase ratio</b>											
55/45	MQC	150	5837745	5846912	5808963	5820808	5828234	5878435	5836849.50	24251.28	0.42
60/40	MQC	150	5613774	5614691	5508961	5621432	5628231	5627822	5602485.17	46231.97	0.83
65/35	MQC	150	5598673	5579085	5509832	5432187	5499879	5698325	5552996.83	92915.99	1.67
<b>Change in wavelength</b>											
216 nm	MQC	150	5863212	5798987	5812435	5880208	5798731	5821328	5829150.17	34475.60	0.59
218 nm	MQC	150	5612785	5624315	5590871	5610923	5532171	5467821	5573147.67	61160.61	1.09
220 nm	MQC	150	5543675	5498892	5476854	5476841	5467896	5532187	5499390.83	31765.55	0.57

### 5.9. Preliminary screening of parameter for extraction process

The initial screening studies were carried out to select the most suitable factors that influence the yield of ACA in the extract.

#### 5.9.1. Selection of solvent for extraction of ACA from AG rhizomes

Among the solvents selected, a higher content of ACA was obtained with 50% ethanol in water (v/v) ( $1.50 \pm 1.18\%$  w/w of dried rhizome). However, the elution peak of ACA was observed with substantial shoulder, which infers the possibility for decomposition of ACA. Yang and Eilerman, 1999 reported hydrolytic decomposition reaction of ACA into 1'-hydroxy chavicol, *p*-coumayl diacetate, and *p*-acetoxy cinnamic alcohol (Yang and Eilerman, 1999). Considering the quality and quantity of the ACA in the AG extract, absolute ethanol ( $1.48 \pm 1.09\%$  w/w of dried rhizome) was selected as a solvent for the further extraction process. The amount of ACA obtained during the preliminary screening of solvents from each extract was calculated and tabulated in **Table 27**.

**Table 27.** Selection of solvent based on the amount of ACA in the extract

Solvents	% yield (% w/w)	Area (cm <sup>2</sup> )			Mean area (cm <sup>2</sup> )	Amount of ACA in extract (% w/w)
Acetone	5.93	1617210	2000598	2091051	1902953.33	$1.06 \pm 1.12$
Absolute ethanol	5.05	2744466	2511223	2472248	2575979.00	$1.48 \pm 1.09$
50% v/v acetone	26.56	4384190	4411028	4621953	4472390.33	$1.31 \pm 1.03$
50% v/v ethanol	19.43	7721430	7899330	7767511	7796090.33	$1.50 \pm 1.18$

#### 5.9.2. Effect of temperature on extraction process

The effect of temperature on the yield of isolated ACA was evaluated at varying temperature such as 25°C, 50°C and 100°C. The ACA elution peak was detected only with the extraction carried out at 25°C which clearly infers that extraction at higher temperature 50°C and 100°C is not suitable for further studies. The amount of ACA isolated from each extract was calculated and tabulated in **Table 28**.

**Table 28.** Effect of temperature on the amount of ACA in the extract

Temperature (°C)	% yield (% w/w)	Area (cm <sup>2</sup> )			Mean area (cm <sup>2</sup> )	Amount of ACA in extract (% w/w)
25°C	6.90	3341887	3112593	2755117	3069865.67	$1.36 \pm 0.11$

50°C	7.02	-	-	-	-	-
100°C	8.23	-	-	-	-	-

### 5.9.3. Effect of mean particle size on extraction

Various sieves such as sieve 66, sieve 44 and sieve 22 were selected to evaluate the effect of mean particle size on the yield of ACA. The mean particle size of the powdered rhizomes was measured by optical microscopy. The mean particle size obtained from selected sieve number 22, 44, and 66 were recorded as 692.4 μm, 328.3 μm, and 254.9 μm respectively. The amount of ACA obtained with three different particle sizes was recorded in **Table 29**. The variation in the amount of ACA was significant when the particle size was varied. Hence, this parameter needs to be considered in the optimization of the extraction process.

**Table 29.** Effect of mean particle size on the amount of ACA

Mean particle size (μm)	% yield (% w/w)	Area (cm <sup>2</sup> )			Mean area (cm <sup>2</sup> )	Amount of ACA in extract (% w/w)
692.4	6.9	3622510	3267556	3278879	3389648.33	0.71 ± 0.17
328.3	4.62	3213377	3401198	3365793	3326789.33	2.02 ± 0.21
254.9	1.63	2318144	2334921	2333181	2328749.67	1.69 ± 0.11

### 5.9.4. Effect of solid to solvent ratio on extraction

The effect of solid to solvent ratio on the amount of ACA isolated was carried out by varying solvent volume. The solvent volume such as 10 mL, 30 mL and 50 mL were found to have significant involvement in the extraction. The amount of ACA isolated from the extract is tabulated in **Table 30**. The amount of ACA extracted out showed a significant variation with the solvent volume; hence this parameter has to be considered in optimization of the extraction process.

**Table 30.** Effect of solid to solvent ratio on amount of ACA

Volume of solvent (mL)	% yield (% w/w)	Area (cm <sup>2</sup> )			Mean area (cm <sup>2</sup> )	Amount of ACA in extract (% w/w)
10	5.04	2665339	2661932	2669532	2665601.00	0.99 ± 1.02
30	7.10	2711890	2766517	2844738	2774381.67	3.17 ± 0.91
50	3.75	3481051	3218649	3314687	3338129.00	1.61 ± 1.07

**5.9.5. Effect of time on extraction**

The effect of extraction time on amount of ACA was evaluated by varying the extraction time period (6, 12, 24, 48, and 72 h) whereas other experimental conditions were kept similar. The amount of ACA in the extract was found to be higher after 6 h of extraction. However, keeping for longer duration couldn't show any improvement in the amount of ACA. It was found that the amount of ACA was found to be reduced when it is in longer contact with ethanol. This confirmed that ethanol have effect on ACA as reported by Yang and Eilerman (Yang and Eilerman, 1999). The results are tabulated in **Table 31**.

**Table 31.** Effect of time on the amount of ACA

Time (h)	% yield (% w/w)	Area (cm <sup>2</sup> )			Mean area (cm <sup>2</sup> )	Amount of ACA in extract (% w/w)
6	9.24	3252671	3278156	3341872	3290899.67	2.99 ± 1.14
12	6.72	3175283	3802363	3149222	3375622.67	2.31 ± 1.21
24	16.77	2401474	2436119	2631320	2489637.67	2.22 ± 0.12
48	15.59	1464128	1738234	1713456	1638606.00	1.89 ± 0.14
72	16.54	1693385	1511712	1868823	1691306.67	1.23 ± 0.16

**5.9.6. Effect of extraction steps**

The number of extraction steps required for complete extraction of ACA was determined by placing the same set of plant material for 3 consecutive 6 h. After each 6 h, 10 mL of the fresh solvent was added and amount of ACA extracted out was obtained and tabulated in **Table 32**. The amount of ACA extracted out after 6 h was 2.52 ± 1.11% w/w of dried rhizome which is significantly higher yield compared to the other two experimental set up. Hence, a single step 6 h extraction process is preferred for further experimental studies.

**Table 32.** Number of extraction steps on amount of ACA extraction

Time (h)	% yield (% w/w)	Area (cm <sup>2</sup> )			Mean area (cm <sup>2</sup> )	Amount of ACA in extract (% w/w)
6	6.82	3060213	3350214	3206612	3205680.67	2.52 ± 1.11
12	4.03	2557233	2554031	2644320	2585195.67	0.71 ± 0.12
24	4.42	1897472	1837011	1895417	1876633.33	0.22 ± 0.16

### **5.10. Optimization of the extraction process**

Among the various set of experiments carried out, the sieve number and solid to solvent ratio has shown more prominent influence on the yield of ACA in the AG extract. To evaluate the effect of selected process variables i.e sieve number and solid to solvent ratio on the response (Y1) i.e. yield of isolated ACA, CCD was designed. The study design contained 13 runs at 3 levels for enhancing the yield of ACA content in the AG extract. **Table 33** presents the process variables and experimentally observed responses for the isolated ACA content from AG extract.

As per the applied CCD design, 13 experiments were performed for extraction in which 5 were replicates of the center point. The replication of the samples was done to confirm the precision of the experimental run. The response corresponding to the selected variable was observed within the range of 0.83 to 4.06% w/w of dried rhizomes. The ratio of maximum to minimum responses was found to be 4.92. This value was less than 10 hence, power transformation was not done. The experimental results were adjustable to the quadratic polynomial model and ANOVA was carried out to estimate the effects of the selected variables, their interaction and the statistical significance of the model. The results of fit summary and ANOVA for the quadratic model are summarized in **Table 34** and **35** respectively. The coefficient of regression ( $R^2$ ),  $F$  value and probability values indicated that the response fit the quadratic model. The adjusted ( $R^2$ ) value of 0.931 and predicted ( $R^2$ ) value of 0.809 were in reasonable agreement since the difference is less than 0.2 and the results of ANOVA represented the  $p$ -value which was less than 0.05 that indicated a good estimation of the tested response and the quadratic model was significant. The lack of fit tests represented  $p$ -value greater than 0.05 (insignificant), hence the model is significant that infers the efficiency of the selected model.

Hence, the final mathematical equation obtained for the response Y from the CCD design is shown in **Eq. (5.1)**.

$$Y = +3.73 + 0.3060X_1 + 0.0218X_2 + 0.0518 X_1X_2 - 1.05X_1^2 - 1.24X_2^2 \quad \text{Eq. (5.1)}$$

The overall quadratic model, individual and interaction effects of process variables such as  $X_1$ : sieve number ( $\mu\text{m}$ ), and  $X_2$ : solid to solvent ratio (g/mL) is represented in the equation with the positive sign indicating the agonist effect of the selected variables. A synergistic effect of sieve

number and solvent volume was observed on the amount of isolated ACA from the extract. The perturbation plot (**Figure 18A**) obtained for the effect of  $X_1$  and  $X_2$  indicated more influence of  $X_1$  on the yield of ACA than that of  $X_2$ . The 3D response surface plot was well constructed to express the interaction effect of the variables in the polynomial equation as shown in **Figure 18 B**. The plot revealed a linear increase in the yield of ACA with increasing the values of  $X_1$  and  $X_2$ . The optimal extraction parameters were selected from the Design-Expert software to maximize the responses. The optimized process variables to obtain maximum responses were sieve number 44 and fixed solid content of 1 g with 30 mL of solvent volume.

A graphical optimization method adopted to optimize the process variable is expressed as an overlay plot in **Figure 19**. The CCD model predicted to select sieve number 44 and solvent volume of 30 mL to obtain a higher yield of AG rhizome extract with ACA of 3.73% w/w of dried rhizomes. Using the predicted values of factor  $X_1$  and  $X_2$ , the isolation process was carried out in triplicate and the amount of ACA isolated was found to be  $3.89 \pm 0.23\%$  w/w of dried rhizomes. Hence the  $p$ -value found between predicted and observed values was 0.42 which is more than 0.05 indicated non-significant differences.

**Table 33.** CCD with process variables and experimentally observed responses of the extracts

S.No	Factor 1 X <sub>1</sub> : sieve number (micrometer)	Factor 2 X <sub>2</sub> : solid to solvent (g/mL)	Response 1 Y: Amount of ACA (% w/w of dried rhizomes)
1	44	30	4.06
2	22	50	0.83
3	44	30	3.47
4	44	1.72	1.23
5	22	10	0.91
6	44	30	3.84
7	75.11	30	1.79
8	66	10	1.87
9	44	58.28	1.33
10	44	30	3.42
11	66	50	1.18
12	12.89	30	1.55
13	44	30	3.87



**Table 34.** Fit summary for the amount of ACA (Y)

<b>Fit summary</b>					
<b>Source</b>	<b>Sequential <math>p</math>-value</b>	<b>Lack of fit <math>p</math>-value</b>	<b>Adjusted <math>R^2</math></b>	<b>Predicted <math>R^2</math></b>	
	Y	Y	Y	Y	Y
<b>Linear</b>	0.8058	0.0018	-0.1493	-0.5186	-
<b>2FI</b>	0.9417	0.0013	-0.2762	-1.1978	-
<b>Quadratic</b>	<0.0001	0.2820	0.9315	0.8092	-
<b>Cubic</b>	0.1269	0.7149	0.9579	0.9326	-
<b>Sequential Model Sum of Squares (Type 1)</b>					
<b>Source</b>	<b>Sum of Squares</b>	<b>Df</b>	<b>Mean square</b>	<b>F-value</b>	<b>p-value</b>
<b>Mean vs Total</b>	69.9062	1	69.9063	-	-
<b>Linear vs Mean</b>	0.7529	2	0.3764	0.2206	0.8058
<b>2FI vs Linear</b>	0.0107	1	0.0107	0.0056	0.9417
<b>Quadratic vs 2FI</b>	16.3397	2	8.1698	80.2718	< 0.0001
<b>Cubic vs Quadratic</b>	0.4005	2	0.2002	3.2090	0.1269
<b>Residual</b>	0.3120	5	0.0624	-	-
<b>Total</b>	87.7219	13	6.7478	-	-
<b>Lack of Fit Tests</b>					
<b>Linear</b>	16.7623	6	2.7937	37.1965	0.0018
<b>2FI</b>	16.7516	5	3.3503	44.6073	0.0013
<b>Quadratic</b>	0.4120	3	0.1373	1.8285	0.2820
<b>Cubic</b>	0.0116	1	0.0116	0.1538	0.7149
<b>Pure Error</b>	0.3004	4	0.0751	-	-
<b>Model Summary Statistics</b>					
<b>Source</b>	<b>Std. Dev.</b>	<b><math>R^2</math></b>	<b>Adjusted <math>R^2</math></b>	<b>Predicted <math>R^2</math></b>	<b>PRESS</b>
<b>Linear</b>	1.3062	0.0423	-0.1493	-0.5186	27.0556
<b>2FI</b>	1.3765	0.0429	-0.2762	-1.1977	39.1543
<b>Quadratic</b>	0.3190	0.9600	0.9315	0.8092	3.3993
<b>Cubic</b>	0.2497	0.9825	0.9580	0.9321	1.2088

Table 35. ANOVA for quadratic model

Response 1: Amount of ACA						
Source	Sum of Squares	Df	Mean Square	F-value	p-value	
Model	17.1000	5	3.4206	33.60	< 0.0001	Significant
X <sub>1</sub> -sieve number	0.7490	1	0.7490	7.36	0.0301	
X <sub>2</sub> - solvent volume	0.0038	1	0.0038	0.04	0.8520	
X <sub>1</sub> X <sub>2</sub>	0.0107	1	0.0107	0.10	0.7551	
X <sub>1</sub> <sup>2</sup>	7.6579	1	7.6578	75.24	< 0.0001	
X <sub>2</sub> <sup>2</sup>	10.7733	1	10.7732	105.85	< 0.0001	
Residual	0.7124	7	0.1018	-	-	
Lack of fit	0.4120	3	0.1373	1.83	0.2820	Not significant
Pure Error	0.3004	4	0.0751	-	-	
Cor Total	17.8157	12	-	-	-	

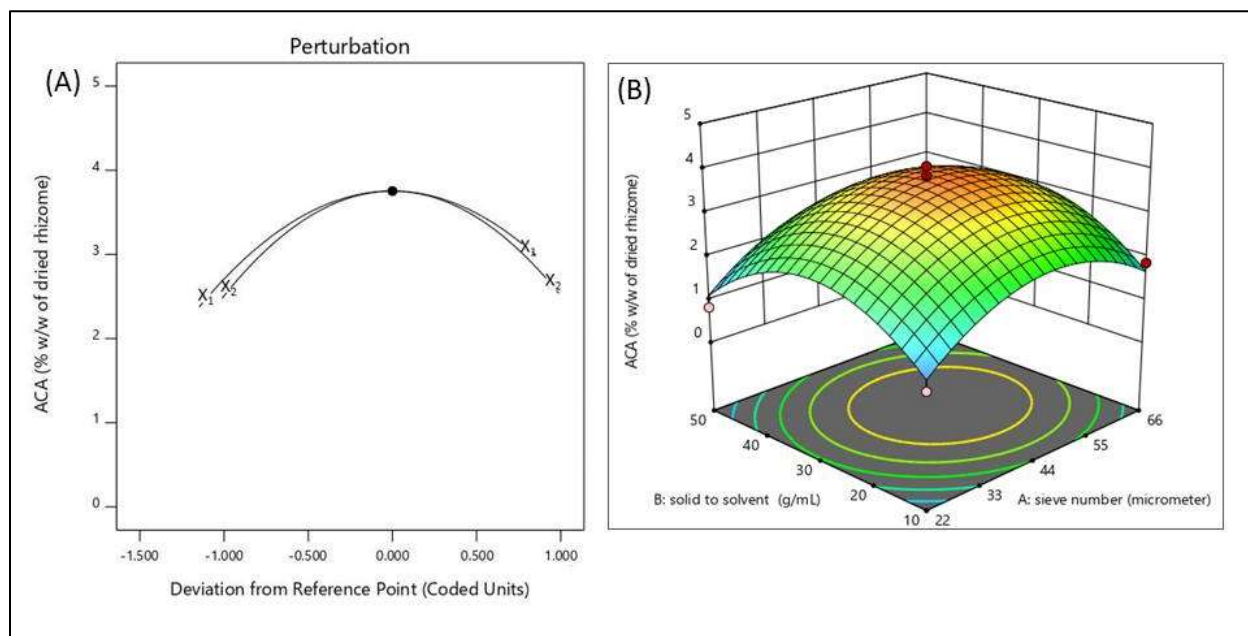
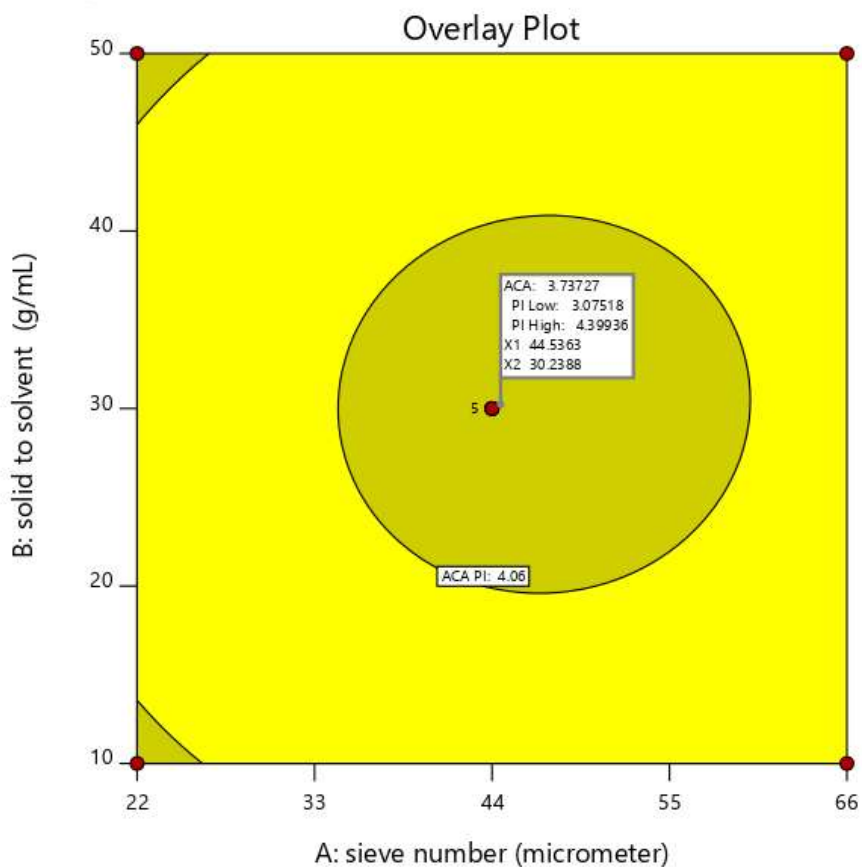


Figure 18. (A) Perturbation plot represents influence of variable X<sub>1</sub> and X<sub>2</sub> on the yield of ACA (B) 3D-response surface plot represents the effect of sieve number and solvent volume on the yield of ACA



**Figure 19.** Overlay plot represents the optimized parameters for the effective extraction of ACA

## 5.11. Preformulation studies

### 5.11.1. Screening of components for nanoemulsion

#### 5.11.1.1. Excipient solubility

The solubility of AGE (ACA) in selected components of NANE such as oil, surfactant, and co-surfactant was carried out to choose the best suitable components. Selection of components was based on the amount of ACA solubilized in each component which was analyzed by developed HPLC method. Visual examination of various oil-AGE mixtures was also carried out to find out the possibility for sedimentation of extract.

Both natural (MCT oil, IPM, almond oil, castor oil, sesame oil, olive oil, peanut oil) and synthetic oils (Capryol 90, Labrafac PG, Labrafil M 1944 CS, Labrasol Capmul MCM) were included in the study to analyze the solubility profile of AGE (ACA).

The results of solubility of AGE (ACA) in selected oils and surfactants are shown in **Figure 20** and **Figure 21** respectively.

The solubility of AGE (ACA) in each of the selected oil was recorded in their decreasing order of solubility as follows:

Capryol 90 ( $96.8 \pm 1.56\%$ ) > MCT oil ( $92.8 \pm 1.20\%$ ) > Capmul MCM ( $84.6 \pm 1.29\%$ ) > Labrasol ( $59.5 \pm 1.54\%$ ) > Labrafil M 1944 CS ( $46.01 \pm 1.34\%$ ) > Labrafac PG ( $7.6 \pm 0.6\%$ ) > Castor oil ( $3.4 \pm 1.58\%$ ) > Sesame oil ( $1.6 \pm 0.2\%$ ) > Almond oil ( $1.50 \pm 0.89\%$ ) > Olive oil ( $1.10 \pm 0.12\%$ )

The solubility of AGE in most of the selected vegetable oils and glycerin was found to be less than 2%.

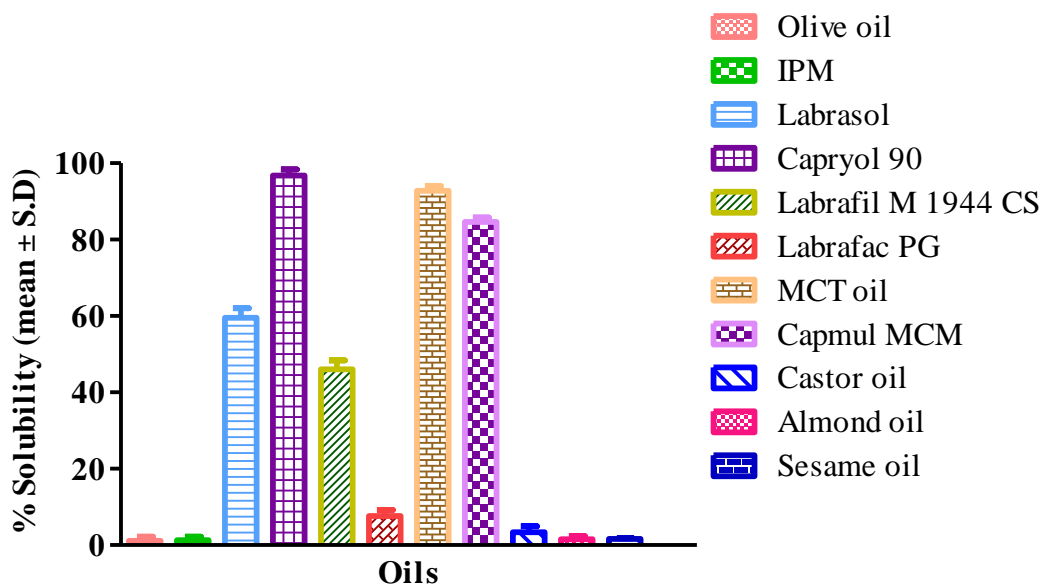


**Figure 20.** Solubility profile of AGE (ACA) in various oils

The selection of surfactant and co-surfactant are crucial in the development of a stable NANE. Hence, “Generally Recognized-as-Safe” (GRAS) surfactants and co-surfactants that are non-irritant for dermal application were selected for solubility studies.

The solubility of AGE (ACA) in various surfactant/co-surfactant was found to decrease in the following order:

Surfactants:

Tween 80 ( $89.7 \pm 3.23\%$ ) > Cremophor ( $88.8 \pm 2.32\%$ ) > Tween 20 ( $83.8 \pm 3.23\%$ ) > Triton X-100 ( $58.57 \pm 1.43\%$ ) > Span 20 ( $43.91 \pm 2.4\%$ ) > Span 80 ( $33.95 \pm 2.40\%$ ) > Dimethicone ( $1.71 \pm 0.12\%$ )

Co-surfactants:

Transcutol P ( $90.89 \pm 2.65\%$ ) > PEG 400 ( $75.90 \pm 1.95\%$ ) > Propylene glycol ( $15.45 \pm 2.10\%$ )

The obtained results indicated that the maximum % solubility of AGE (ACA) was found in Capryol 90 followed by MCT and Capmul MCM (among selected oils). Among the surfactant, maximum % solubility of AGE (ACA) was obtained with Tween 80 followed by Cremophor RH 40. Likewise, Transcutol P has shown maximum solubility in comparison to other co-surfactant (propylene glycol, PEG 400). Hence, Capryol 90, MCT oil and Capmul MCM were considered for oil phase, Tween 80 and Cremophor RH 40 were selected as surfactant and Transcutol P as cosurfactant for further development of various NANE prototypes.

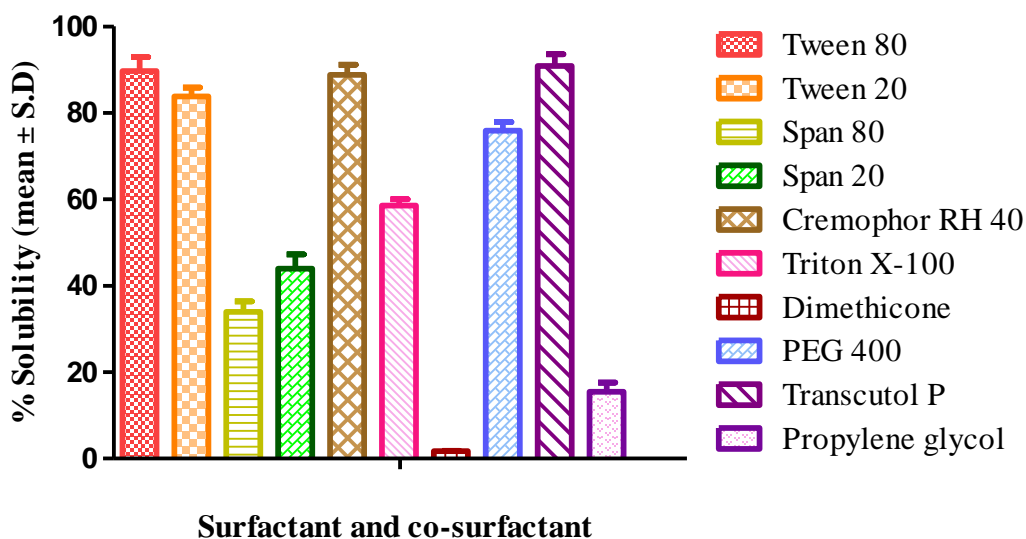


**Figure 21.** Solubility of AGE (ACA) in various surfactant and co-surfactant

**5.11.1.2. Solvent system**

Apart from the selection of oils and surfactants, it is essential to select the most suitable solvent system to carry out the *in vitro* evaluation of the developed formulation. On the basis of the solubility of the extract (ACA) in various solvent systems, the most suitable solvent system was selected. The solubility of AGE (ACA) in solvents (distilled water, glycerin, absolute ethanol, 10% v/v ethanol in water, 50% v/v ethanol in water, methanol, 10% v/v methanol in water, 50% v/v methanol in water) and buffer (phosphate buffer pH 6.8, phosphate buffer 7.4, PBS pH 7.4 and mixed phosphate buffer pH 5.5) were carried out. Solubility profile of AGE (ACA) in absolute ethanol was found out to be more in comparative to other solvents. Similarly, mixed phosphate buffer pH 5.5 has shown better solubility as compared to other selected buffers (phosphate buffer pH 6.8, phosphate buffer 7.4, PBS pH 7.4 and mixed phosphate buffer pH 5.5). % Solubility profile of AGE (ACA) in various solvent systems is shown in **Figure 22**.

% Solubility of AGE (ACA) in various solvents is represented in their decreasing order:

Absolute ethanol ( $98.51 \pm 2.12\%$ ) > methanol ( $97.87 \pm 3.23\%$ ) > pH 5.5 : ethanol (1:1) ( $47.98 \pm 2.13\%$ ) > 50% ethanol ( $26.87 \pm 3.21\%$ ) > 50% methanol ( $22.34 \pm 3.20\%$ ) > PB pH 5.5 : ethanol (5:1) ( $27.16 \pm 4.11\%$ ) > mixed PB pH 5.5 (  $25.23 \pm 4.15\%$ ) > PB pH 6.8 ( $19.13 \pm 2.43\%$ ) > 10% ethanol ( $15.32 \pm 2.43\%$ ) > 10% methanol ( $13.67 \pm 3.43\%$ ) > PB pH 7.4 ( $10.32 \pm 2.53\%$ ) > PB pH 5.5: ethanol (9:1) ( $10.12 \pm 3.15\%$ ) > PBS pH 7.4 ( $9.21 \pm 2.09\%$ ) > Distilled water ( $2.2 \pm 0.98\%$ ) > glycerin ( $0.99 \pm 0.88\%$ ).

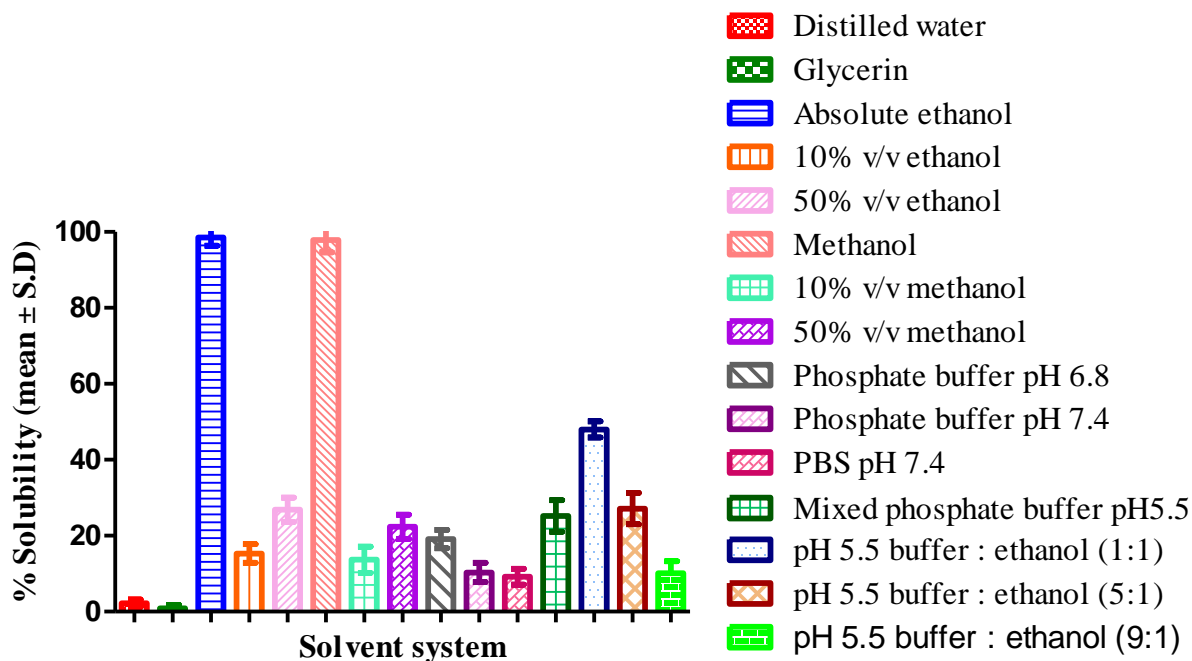


**Figure 22.** Solubility profile of AGE (ACA) in various solvent systems

Solubility profile of AGE (ACA) in absolute ethanol was found to be more in comparison to other solvents. Whereas among the buffer system, mixed phosphate buffer pH 5.5 has shown better solubility as compared to other selected buffers (phosphate buffer pH 6.8, phosphate buffer 7.4, PBS pH 7.4 and mixed phosphate buffer pH 5.5). Among the combination system, absolute ethanol and mixed phosphate buffer pH 5.5 (1:1) have shown maximum solubility of extract (ACA).

Even though absolute ethanol has shown maximum solubility of AGE (ACA), it is mostly used as a co-surfactant due to its ability to enhance drug penetration across the skin. Bommanna *et al.* demonstrated that the skin treated with pure ethanol for 30 min has shown penetration of ethanol across the intercellular lipid bilayer with the removal of measurable quantities of the barrier material. However, the changes induced in the skin with short contact (30 min) of ethanol was found to be reversed within 24 h (Bommanna *et al.*, 1991). In addition, ethanol alone is not preferred as an *in vitro* diffusion/permeation medium for longer duration (24-48 h) study. The exposure of skin to ethanol for longer duration is reported with intercellular lipid bilayer rearrangement or disordered arrangement which cannot be mimicked in the physiological

conditions, which is normally maintained at acidic pH which ranges from 4.8 to 5.6 (Proksch, 2018). Hence, a combination of solvents containing ethanol and mixed phosphate buffer (pH 5.5) [Absolute ethanol and buffer (1:1)] was selected for the evaluation of the developed formulations. Similar type of buffer solvent system i.e. phosphate buffer (pH 5.5) and ethanol in the ratio of 7:3 (v/v) was used for *in vitro* release studies of 8-methoxypsoralen loaded niosomes (Kassem et al., 2017). Similarly to this study, hydroethanolic solution (1:1) was used to evaluate release profile of loratadine loaded nanoemulsion. The selection of the media in the receptor compartment is based on the solubilization capacity of the drug and the selected medium is used further to carry out the *in vitro* and *ex vivo* evaluation where the medium has to be maintained at sink condition for better prediction of the release kinetics (Sarheed et al., 2020).

#### **5.11.2. Selection of oil phase and non-aqueous polar phase**

The phase separation was used as a tool for selection of oil phase and non-aqueous phase. The oils (Capryol 90, MCT oil, Capmul MCM) and non-aqueous polar phase (glycerin) were mixed in 1:1 ratio and observed for phase separation. Among the selected oils, Capryol 90 and MCT oil has shown phase separation with glycerin within a short span of time (i.e. 2 h) whereas, Capmul MCM with glycerin took 4 h to show phase separation. In one of the studies, the moisturizing efficacy of humectant (glycerol or 1, 2-hexanediol) for dry skin syndrome was evaluated in presence of various oils and solvents such as MCT oil, water and mixture of MCT oil and isopropyl alcohol. No moisturizing effect was obtained when glycerin was mixed with MCT oil and it was mainly due to the immiscibility between glycerol and MCT oil (Sagiv et al., 2001). Hence, for further formulation development, Capryol 90/MCT oil was selected as oil phase and glycerin was selected as non-aqueous polar phase.

#### **5.11.3. Formulation of AGE loaded NANE**

Modified spontaneous nanoemulsion formation method was chosen for the formulation of AGE loaded NANE [30]. This selected low energy method is mostly preferred and it can be prepared by either mixing of an organic phase containing surfactant to the aqueous phase under magnetic stirring (Saber et al., 2013), or oil phase containing surfactant was mixed with polar phase by aqueous titration method (Yildirim et al., 2017). In both cases, the droplet size in the emulsion



can be adjusted by manipulating the composition ratio of non-polar (oil) and/polar phase as well as surfactant to oil ratio (Gulotta et al., 2014).

But, in this study, a slight modification was done in the mixing sequence. AGE was mixed with the oil phase using a cyclone mixer, followed by the addition of  $S_{\text{mix}}$  into the oil phase and mixed carefully using cyclone mixer. After the formation of oil-surfactant mixer, non-aqueous polar phase was added into it and mixed spontaneously using a cyclone mixer to form NANE. An additional step of 5 min sonication was carried out using an ultrasound bath cleaner (40 kHz) to remove the air bubbles, which also assisted in droplet size reduction.

#### **5.11.4. Screening of emulsification efficiency**

Selected surfactant and co-surfactant which has shown maximum solubility of AGE (ACA) were investigated further to determine the emulsifying efficiency with the selected oil phase. To determine the emulsification efficiency various nanoemulsion compositions were prepared by the method described in section 4.2.10. The surfactant-cosurfactant system having the maximum potential to emulsify the selected oil phase was analyzed based on the ability to form a single-phase system after attaining equilibrium.

Preliminary screening study was carried out using various oil phase,  $S_{\text{mix}}$  and non-aqueous polar phase. Firstly, designated formulation batch was “F” which was prepared using Capryol 90 as dispersed phase with varying ratio of surfactant and co-surfactant such as Tween 80 and Transcutol P respectively in the ratio of 1:1, 1:2, and 2:1 using glycerin as the non-aqueous polar phase. But, phase separation in all the 27 batches ( $F_1 - F_{27}$ ) was observed as shown in **Figure 23**.

Even though, the solubilization capacity of AGE in Tween 80 was higher, it was later excluded from the formulation composition as it has shown phase separation upon mixing with Capryol 90.

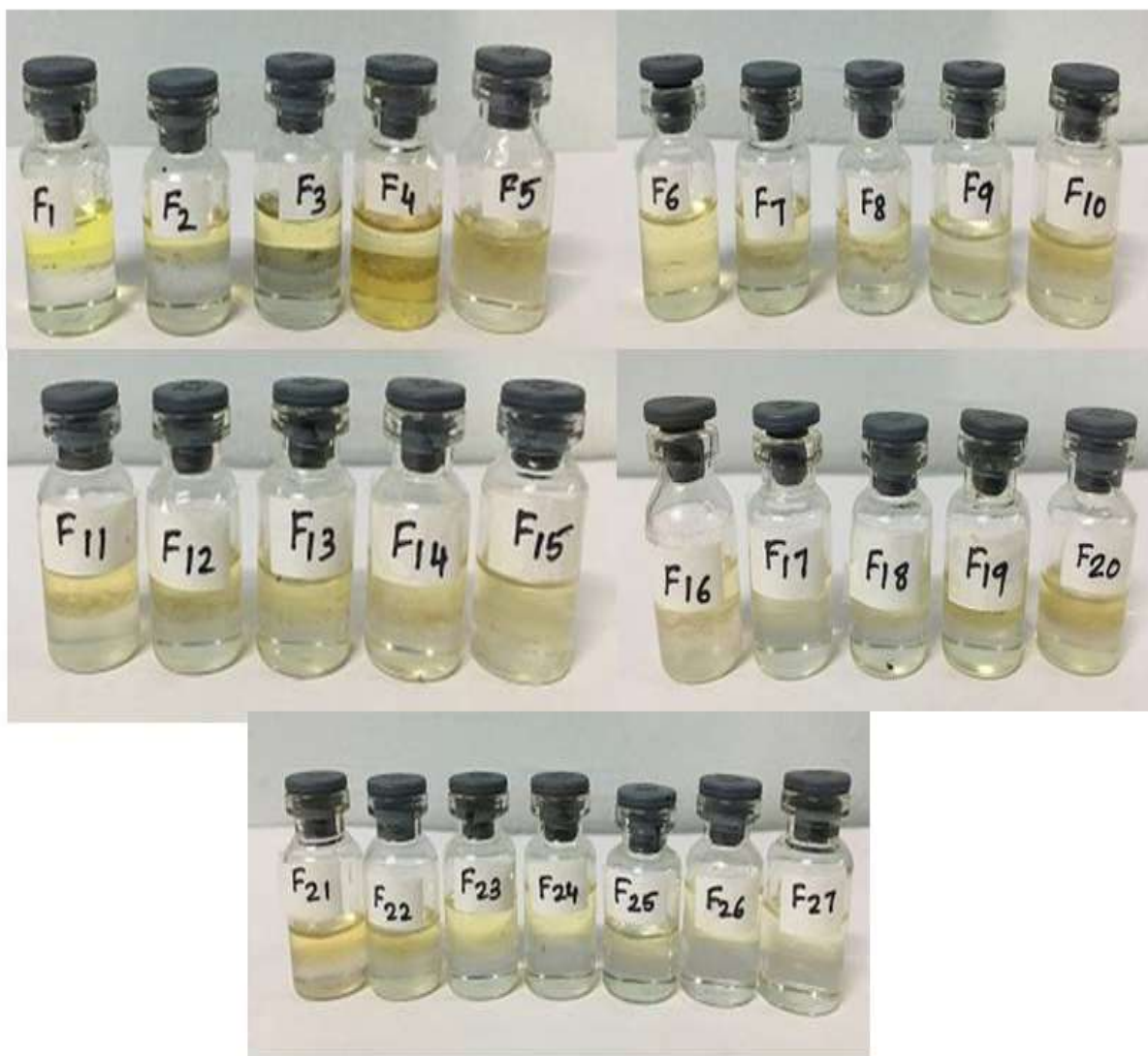


**Figure 23.** Preliminary screening designated as "F". F<sub>1</sub> - F<sub>27</sub> formulations containing S<sub>mix</sub> as Tween 80 and Transcutol P, Capryol 90 as oil phase and glycerin as non-aqueous polar phase.

Secondly screened batch was designated as "N" that contained Capryol 90 as dispersed phase, Cremophor RH 40 as surfactant and glycerin as non-aqueous polar phase. In this method, only surfactant was used and 27 formulations (N<sub>1</sub>-N<sub>27</sub>) were prepared by varying the oil ratio from 9:1 and by varying ratio of surfactant and non-aqueous polar phase. Amongst all (N<sub>1</sub>-N<sub>27</sub>), the formulations "N<sub>25</sub>" and "N<sub>26</sub>" were transparent with no phase separation and rest all formulations have phase separation as shown in **Figure 24**.

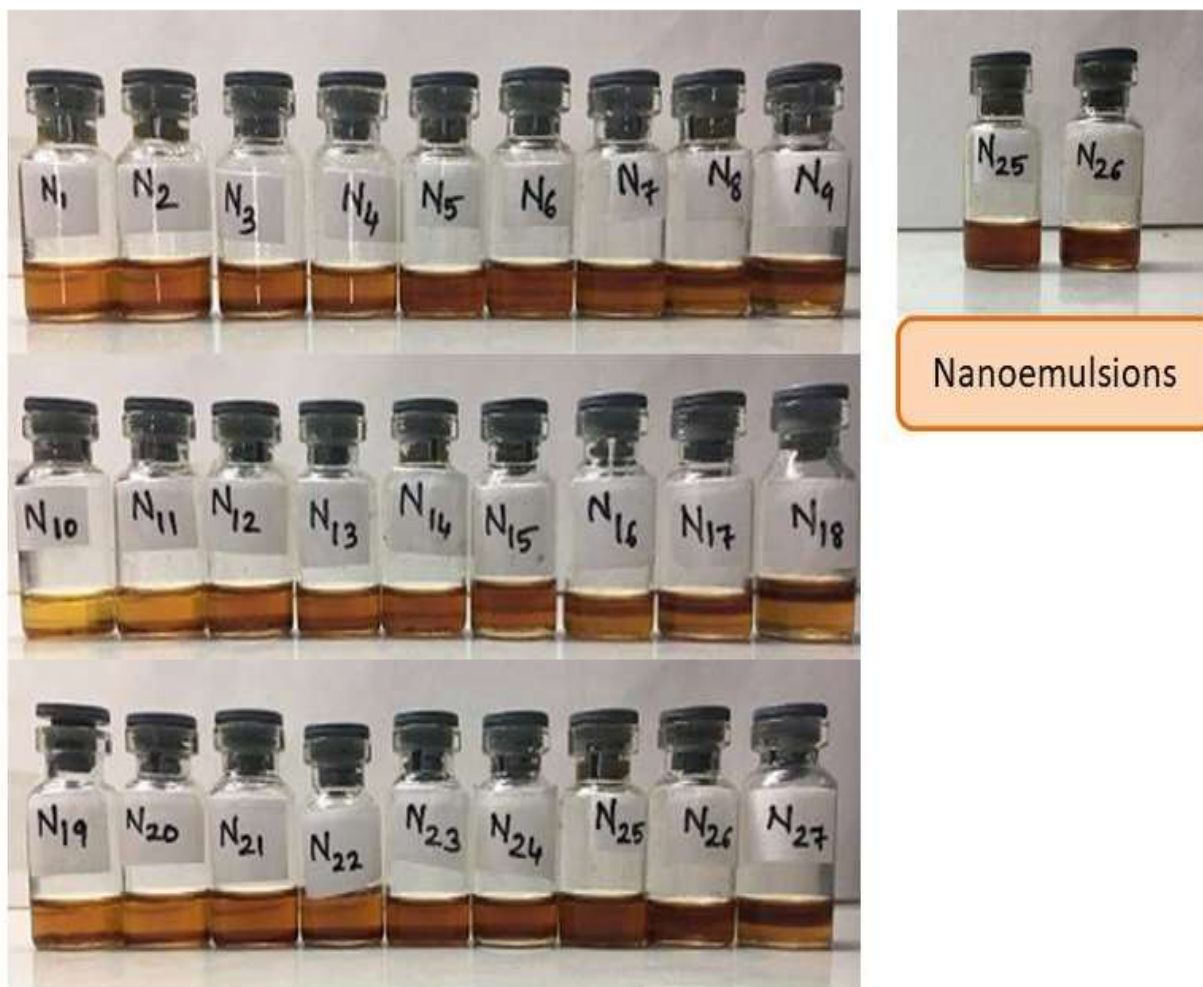


**Figure 24.** Preliminary screening designated as “N”. N<sub>1</sub> - N<sub>27</sub> formulations with Capryol 90 as oil phase, Cremophor RH 40 as surfactant and glycerin as non-aqueous polar phase

On the basis of the above observation, a new formulation prototype (designated as “E”) was carried out with the addition of co-surfactant. A mixture of Cremophor RH 40 and Transcutol P were prepared in different ratio (1:1, 1:2, and 2:1) with a varying ratio of Capryol 90 (1:9) as the dispersed phase and glycerin as the non-aqueous polar phase. In these batches, slow phase separation was observed and none of the formulation was stable as shown in **Figure 25**.





**Figure 25.** Preliminary screening designated as “E”. E<sub>1</sub> - E<sub>81</sub> with Capryol 90 as oil phase, glycerin as non-aqueous polar phase, Cremophor RH 40 and Transcutol P as S<sub>mix</sub>.

All the above said formulation prototype were not satisfactory with respect to stability. Hence, a formulation prototype “M” was prepared using MCT oil instead of Capryol 90 and all other components such as S<sub>mix</sub> as Cremophor RH 40 -Transcutol P and glycerin as non-aqueous polar phase were kept similar as prototype “E”. Using this composition, 81 formulations (M<sub>1</sub> - M<sub>81</sub>) were prepared (**Figure 26**).





**Figure 26.** Preliminary screening designated as “M”. M<sub>1</sub> - M<sub>81</sub> formulations having MCT oil as oil phase, glycerin as non-aqueous polar phase, Cremophor RH 40 and Transcutol P as S<sub>mix</sub>.

Among these 81 formulations, 4 formulations (M<sub>70</sub>, M<sub>71</sub>, M<sub>79</sub> and M<sub>80</sub>) prepared with S<sub>mix</sub> ratio of 1:2 and 2:1 (**Figure 27**) were transparent nanoemulsion and rest others have shown phase separation. Hence, this composition at their particular ratio was considered for further studies. Overall study details with regard to preliminary screening for formulation development are summarized in **Table 36**.



**Figure 27.** Selected NANE designated as M<sub>70</sub>, M<sub>71</sub>, M<sub>79</sub> and M<sub>80</sub>

**Table 36.** Summary of the preliminary screening studies for emulsification efficiency

<b>Preliminary screening batch code</b>	<b>Oil phase</b>	<b>Surfactant /cosurfactant</b>	<b>Non-aqueous polar phase</b>	<b>Inference</b>
<b>F (F<sub>1</sub>- F<sub>27</sub>)</b>	Capryol 90	Tween 80 /Transcutol P	Glycerin	Phase separation in all the formulations (F <sub>1</sub> - F <sub>27</sub> )
<b>N (N<sub>1</sub>- N<sub>27</sub>)</b>	Capryol 90	Cremophor RH 40	Glycerin	Among N <sub>1</sub> - N <sub>27</sub> formulations, N <sub>25</sub> and N <sub>26</sub> formed transparent single phase system
<b>E (E<sub>1</sub>- E<sub>81</sub>)</b>	Capryol 90	Cremophor RH 40/ Transcutol P	Glycerin	Phase separation in all the formulations (E <sub>1</sub> - E <sub>81</sub> )
<b>M (M<sub>1</sub>- M<sub>81</sub>)</b>	MCT oil	Cremophor RH 40/ Transcutol P	Glycerin	Among M <sub>1</sub> - M <sub>81</sub> formulation, M <sub>70</sub> , M <sub>71</sub> , M <sub>79</sub> and M <sub>80</sub> were transparent single phase system

#### 5.11.5. Construction of p-TPD

A total of 81 formulation prototypes were prepared by varying the ratio of oil phase and S<sub>mix</sub> (1:1, 1:2 and 2:1). The composition of these formulations is shown in **Table 13** (section 4.2.12). The p-TPD developed for these prototypes are shown in **Figure 27(A-C)**.

The results revealed that among 81 NANE prototypes, S<sub>mix</sub> (1:1) formulations have shown complete phase separation (**Figure 28A**), whereas, two formulations from S<sub>mix</sub> 1:2 (M<sub>70</sub> and M<sub>71</sub>) (**Figure 28B**) and 2:1 (M<sub>79</sub> and M<sub>80</sub>) (**Figure 28C**) prototypes formed clear and transparent emulsion. In the p-TPD, the transparent NANE are represented as red stars. From p-TPD, it was inferred that S<sub>mix</sub> have more significant impact on the stability and transparency of the emulsion. It was also observed that the oil composition was almost the same for the formed stable NANE. Hence, for better insight of these excipients on various formulation attributes such as droplet size, zeta potential, % drug loading, % cumulative drug permeation, and % drug retention were investigated using DoE.



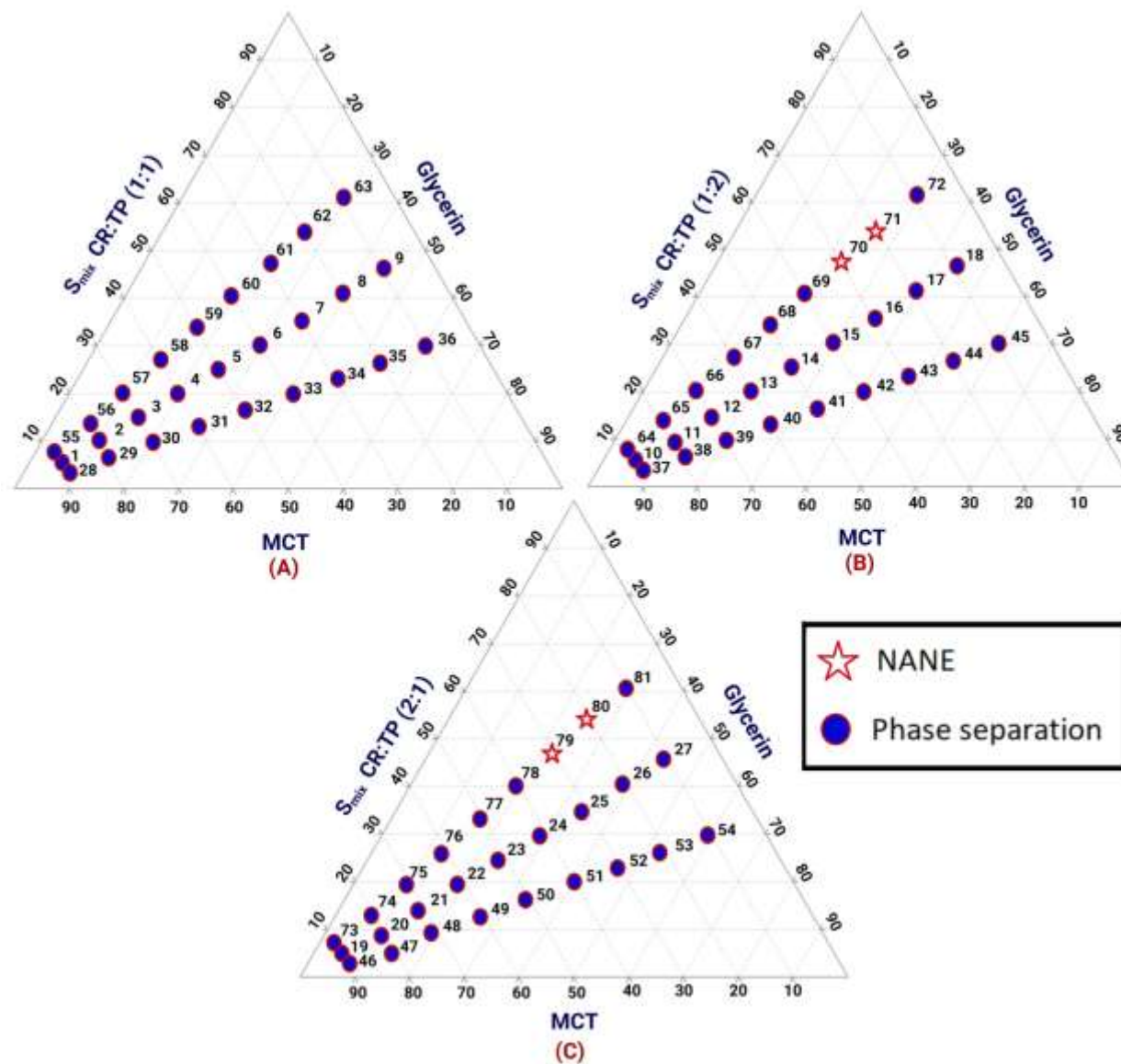


Figure 28. p-TPD for (A)  $S_{mix}$  1:1 (B)  $S_{mix}$  1:2 (C)  $S_{mix}$  2:1

### 5.11.6. Optimization of AGE loaded NANE

#### 5.11.6.1 DoE

BBD was applied and 29 experimental trial runs were conducted to evaluate the effect of selected variables such as oil ( $X_1$ ), surfactant ( $X_2$ ), co-surfactant ( $X_3$ ), and non-aqueous polar phase ( $X_4$ ) on NANEs specific responses such as droplet size ( $Y_1$ ), zeta potential ( $Y_2$ ), % drug loading ( $Y_3$ ), % cumulative drug permeated in 6 h ( $Y_4$ ), and % drug retained after 6 h ( $Y_5$ ). The responses for each of the 29 experimental trial runs are shown in **Table 37**. **Figure 29** represented 29 formulations (FM<sub>1</sub>- FM<sub>29</sub>) that were developed as per the suggested compositions from the design. All the formulations were homogenous clear with no sign of phase separation.



**Figure 29.** Formulation prototype designated as “FM” and 29 formulations (FM1 to FM29) obtained as per BBD design

**Table 37.** Optimization of NANE based on the selected factors (X1- X4) for specific responses (Y1- Y5) using BBD

Run	Factor X <sub>1</sub> : MCT oil	Factor X <sub>2</sub> : Cremophor RH 40	Factor X <sub>3</sub> : Transcutol P	Factor X <sub>4</sub> : Glycerin	Response Y <sub>1</sub> : Droplet size (nm)	Response Y <sub>2</sub> : Zeta potential (mV)	Response Y <sub>3</sub> : Drug loading (%)	Response Y <sub>4</sub> : % Cumulative drug permeation in 6h (%)	Response Y <sub>5</sub> : % Drug retained after 6 h (%)
1	25	35	25	23.0	109.24	-1.7	98.99	22.49	27.46
2	20	35	25	24.5	84.53	-2.1	100.01	26.98	29.23
3	30	25	25	26.0	108.00	-5.2	84.01	39.77	17.90
4	20	15	25	24.5	113.70	-5.5	66.02	36.67	33.30
5	30	35	25	24.5	92.98	-1.9	90.28	38.80	31.39
6	20	25	15	24.5	63.51	-9.1	87.02	19.81	19.87
7	25	25	35	23.0	126.77	-10.9	57.35	32.20	15.68
8	30	15	25	24.5	106.57	-8.3	73.36	23.24	35.38
9	25	25	15	26.0	90.60	-7.9	87.10	25.29	15.02
10	25	15	25	23.0	102.71	-3.0	71.31	37.08	12.44
11	25	25	25	24.5	77.93	-4.8	81.58	48.55	57.54
12	25	35	15	24.5	58.10	-1.4	94.65	27.48	31.32
13	25	25	25	24.5	98.73	-3.9	86.34	44.95	56.16
14	20	25	25	23.0	81.81	-4.9	99.12	28.09	34.07
15	25	25	25	24.5	99.78	-5.9	82.90	41.72	49.03
16	30	25	25	23.0	114.33	-3.4	87.90	26.51	29.56
17	25	35	35	24.5	102.68	-8.3	83.99	36.95	19.22
18	25	15	35	24.5	105.85	-10.2	67.03	33.85	26.22
19	30	25	15	24.5	98.86	-5.3	93.99	29.22	30.80
20	25	25	25	24.5	80.34	-3.1	85.36	46.03	50.96
21	25	15	25	26.0	99.49	-10.4	64.97	32.13	17.58
22	25	25	15	23.0	84.47	-4.4	99.45	23.24	24.91
23	25	35	25	26.0	94.13	-3.6	99.41	43.24	12.47
24	30	25	35	24.5	91.30	-13.1	69.36	34.76	36.69
25	25	25	25	24.5	99.78	-5.2	93.01	53.61	50.85
26	20	25	35	24.5	90.93	-9.7	61.98	41.48	30.60
27	25	15	15	24.5	117.78	-10.7	56.60	20.21	12.33
28	25	25	35	26.0	104.91	-12.3	58.75	54.87	19.67
29	20	25	25	26.0	91.35	-5.6	88.36	33.83	19.68

As suggested by BBD design, the varied responses for  $Y_1$  (58.1 to 126.77 nm),  $Y_2$  (-13.1 to -1.4 mV),  $Y_3$  (56.6 to 100.01%),  $Y_4$  (19.81 to 54.87%), and  $Y_5$  (12.33 to 57.54%) were obtained. From the obtained data, the ratio of maximum to minimum for all the responses i.e.  $Y_1$ ,  $Y_2$ ,  $Y_3$ ,  $Y_4$  and  $Y_5$  were 2.181, 9.357, 1.766, 2.769 and 4.666 respectively. As all these values of maximum to minimum ratio were less than 10, hence power transformation was not required. The obtained experimental results were adjusted to the polynomial model and ANOVA was carried out to estimate the effect of selected variables, their interaction and statistical significance of the model. The results of the fit summary and ANOVA are summarized in **Table 38**. On the basis of the results obtained, it was observed that responses  $Y_1$  and  $Y_3$  have shown linear model whereas  $Y_2$ ,  $Y_4$  and  $Y_5$  have shown quadratic model. The adjusted  $R^2$  and predicted  $R^2$  values were in reasonable agreement ( $R^2$  value  $<0.2$ ) and the results of the statistical evaluation of the responses indicated  $p$ -value less than 0.05, which indicated good correlation of the tested responses. The lack of fit test represented  $p$ -value greater than 0.05, which is insignificant value that inferred the efficiency of the selected models.

**Table 38.** Results of regression analysis for the selected responses

Responses	Model	Adequate precision	R <sup>2</sup>	Adjusted R <sup>2</sup>	Predicted R <sup>2</sup>	S.D.	% CV	F-value	*p-value	**Lack of fit
Y1	Linear	6.7565	0.4023	0.3027	0.1108	12.69	13.18	4.04	0.0121	0.4241
Y2	Quadratic	13.6912	0.9392	0.8785	0.7129	1.18	18.86	15.45	<0.0001	0.4582
Y3	Linear	13.2235	0.6646	0.6087	0.4891	8.75	10.71	11.89	<0.0001	0.0779
Y4	Quadratic	12.8062	0.9359	0.8718	0.7579	3.46	10	14.6	<0.0001	0.8624
Y5	Quadratic	12.6369	0.9347	0.8693	0.6708	4.78	16.38	14.3	<0.0001	0.2759

Values of adjusted R<sup>2</sup> and predicted R<sup>2</sup> should be in reasonable agreement that their difference should be less than 0.2

\*p value less than 0.05 indicated model to be significant

\*\*For the selected model to be fit, lack of fit value should be insignificant i.e value more than 0.05

The applied design represented the effect of responses  $Y_1, Y_2, Y_3, Y_4,$  and  $Y_5$  in the form of mathematical equation represented in **Eq. (5.2-5.6)**.

$$Y_1 = +96.25 + 7.18 * X_1 - 8.70 * X_2 + 9.09 * X_3 - 2.57 * X_4 \quad \text{Eq. (5.2)}$$

$$Y_2 = -4.58 - 0.0250 * X_1 + 2.43 * X_2 - 2.14 * X_3 - 1.39 * X_4 + 0.750 * X_1 X_2 - 1.80 * X_1 X_3 - 0.2750 * X_1 X_4 - 1.85 * X_2 X_3 + 1.37 * X_2 X_4 + 0.5250 * X_3 X_4 - 0.3517 * X_1^2 + 0.5233 * X_2^2 - 4.00 * X_3^2 - 0.2517 * X_4^2 \quad \text{Eq. (5.3)}$$

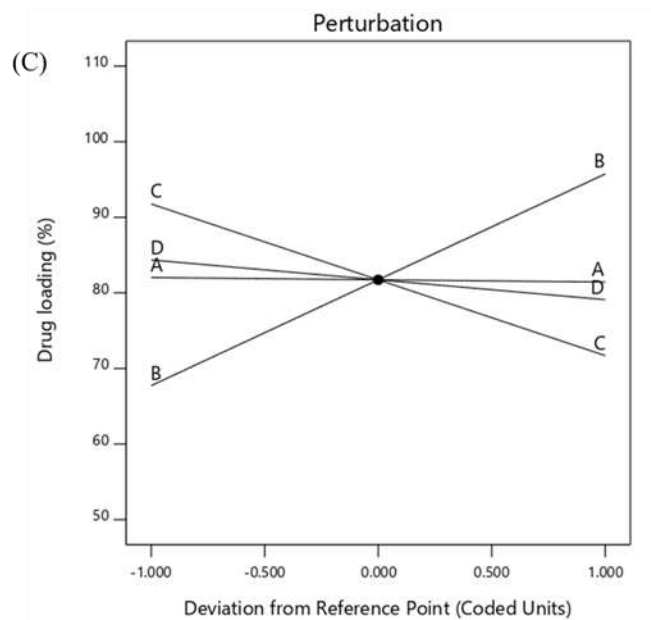
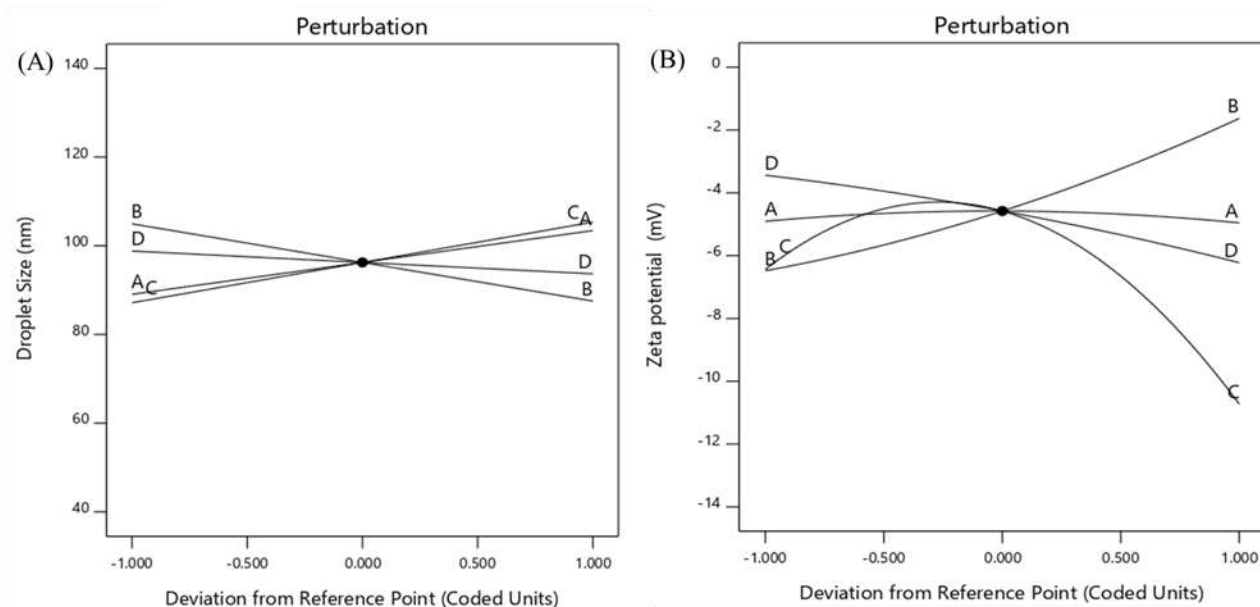
$$Y_3 = +81.73 - 0.3008 * X_1 + 14.00 * X_2 - 10.03 * X_3 - 2.63 * X_4 \quad \text{Eq. (5.4)}$$

$$Y_4 = +46.97 + 0.4548 * X_1 + 1.06 * X_2 + 7.41 * X_3 + 4.96 * X_4 + 6.31 * X_1 X_2 - 4.03 * X_1 X_3 + 1.88 * X_1 X_4 - 1.04 * X_2 X_3 + 6.42 * X_2 X_4 + 5.15 * X_3 X_4 - 8.10 * X_1^2 - 8.10 * X_2^2 - 8.07 * X_3^2 - 5.65 * X_4^2 \quad \text{Eq. (5.5)}$$

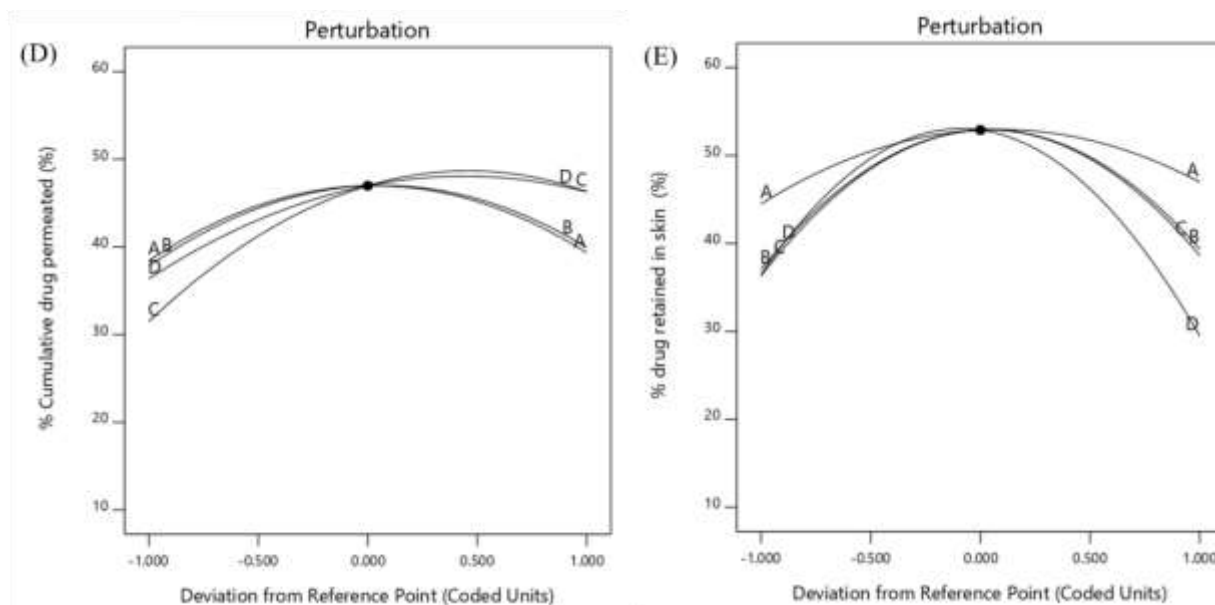
$$Y_5 = +52.91 + 1.25 * X_1 + 1.15 * X_2 + 1.15 * X_3 - 3.84 * X_4 + 0.0197 * X_1 X_2 - 1.21 * X_1 X_3 + 0.6870 * X_1 X_4 - 6.50 * X_2 X_3 - 5.03 * X_2 X_4 + 3.47 * X_3 X_4 - 7.18 * X_1^2 - 14.69 * X_2^2 - 15.44 * X_3^2 + 19.93 * X_4^2 \quad \text{Eq. (5.6)}$$

The comparison of the factor coefficients in the coded equations is useful for identification of the relative impact of the factors. The positive sign and negative sign in the polynomial equation represented the synergistic and antagonistic effect of each selected variable ( $X_1, X_2, X_3, X_4$ ) on the respective responses ( $Y_1, Y_2, Y_3, Y_4, Y_5$ ). The droplet size in the NANE has shown a linear effect (**Eq. 5.2**) with the selected variables. In case of droplet size ( $Y_1$ ), an increase in its size was observed with an increase in concentration of  $X_1$  and  $X_3$  whereas its value was decreased with increase in concentration of  $X_2$  and  $X_4$ . The zeta potential ( $Y_2$ ) has shown quadratic effect with the selected variables, hence their interaction effects also played a significant role in determining the responses. Response  $Y_2$  showed an increase in zeta potential with decrease in  $X_1, X_3,$  and  $X_4$  whereas, it showed an increase in zeta potential with increase in  $X_2$  (**Eq. 5.3**). The % drug loading ( $Y_3$ ) increased with increase in  $X_2$ , whereas it increased with decrease in  $X_1, X_3,$  and  $X_4$  (**Eq.5.4**). The % cumulative drug permeation ( $Y_4$ ) showed an increase in its value with increase of all the factors  $X_1, X_2, X_3,$  and  $X_4$  (**Eq. 5.5**). The % drug retained after 6 h ( $Y_5$ ) showed an increase in its value with increase in  $X_1, X_2,$  and  $X_3$  whereas, factor  $X_4$  had an antagonistic effect on drug retention (**Eq. 5.6**). Along with these informations obtained from the polynomial equation, it is important to identify the influence/ interaction of each factor on the responses.

The perturbation plots for all the responses are shown in **Figure 30 (A-E)**. In the perturbation plot, factors  $X_1$ ,  $X_2$ ,  $X_3$ , and  $X_4$  are represented as A, B, C and D, respectively. **Figure 30A** for droplet size has shown dominant effect of  $X_1$  and  $X_3$  on  $Y_1$  droplet size. The droplet size in the NANEs was found to be increased with an increase in the concentration of  $X_1$  and  $X_3$  whereas decreased with increase in concentration of  $X_2$  and  $X_4$ . These outcomes clearly emphasized the role of surfactant in reducing the droplet size. The surfactant is added to reduce the surface tension between the two phases, which thereby reduces the chance for agglomeration of small droplets (Mehmood et al., 2018). The perturbation plot (**Figure 30B**) for zeta potential has shown a decrease in magnitude with increase in  $X_1$ ,  $X_3$ , and  $X_4$  whereas  $X_2$  has shown predominant effect with increased magnitude of zeta potential. **Figure 30C** revealed that drug loading has shown linear effect of the selected factors on the responses. Factor  $X_2$  has shown the most dominant role in drug loading whereas  $X_1$ ,  $X_3$ , and  $X_4$  have shown a minimum effect on drug loading. In case of percentage cumulative drug permeated (**Figure 30D**), the results indicated that maximum effect obtained was with  $X_3$  and  $X_4$  whereas,  $X_1$  and  $X_2$  exhibited minimum effect. In case of % drug retention,  $X_1$  and  $X_4$  have shown prominent effects as shown in **Figure 30E**. The increase in volume of  $X_1$  has shown enhanced drug retention whereas,  $X_4$  has shown decreased retention. Whereas, factors  $X_2$  and  $X_3$  exhibited minimum effects on drug retention.







Note: In the plot A represents the factor  $X_1$ ; B represents the factor  $X_2$ ; C represents the factor  $X_3$ ; D represents the factor  $X_4$ .

**Figure 30.** Perturbation plot (A) Droplet size (B) Zeta potential (C) % Drug loading (D) % Cumulative drug permeated (E) % Drug retained in skin.

The polynomial equations obtained from the BBD design aided in the generation of 2D contour plots and 3D response surface plots. These plots further helped in understanding the design by visualizing the response surface with respect to the selected factors.

**Figure 31(A-F)** and **Figure 32(A-F)** deciphered that increase in the concentration of  $X_1$  and  $X_3$  has shown increase in droplet size whereas, increase in  $X_2$  decreased the droplet size. These effects suggested using lower concentration of both  $X_1$  and  $X_3$  and a higher concentration of  $X_2$  for the formation of NANE in the nano-size range. The reduction in droplet size with increase in concentration of  $X_2$  can be explained by the emulsifying capacity and smaller molecular packing arrangement of Cremophor RH 40.

Zeng *et al.* demonstrated the importance of surfactant packing parameters in formulating nanoemulsion. Some of the selected surfactant included in the study was Tween 80, Tween 20, Cremophor RH 40 and Cremophor EL. Nanoemulsion containing Cremophor RH 40 has shown smaller droplet size in comparison to Cremophor EL. Both Cremophor grades are surfactants with non-polar tail groups, however Cremophor RH 40 has shown a higher degree of polymerization and expected to have a smaller packing capacity than Cremophor EL which might be the reason for formation of fine droplets (Zeng *et al.*, 2017b). The nature of co-surfactant was found to influence the droplet size. The addition of short-chain alcohol as co-surfactant was found to influence the emulsification efficiency of surfactant and droplet size formation. Zeng *et al.* reported the instability of nanoemulsion with an increase in concentration of co-surfactant (Zeng *et al.*, 2017b). This study has shown the importance of selection of co-surfactant and the ratio of surfactant to co-surfactant in obtaining a stable nanoemulsion.

In the prepared NANE, Transcutol P was used as co-surfactant and the addition of higher concentration of Transcutol P was found to increase the droplet size. This effect has demonstrated the requirement for an optimum concentration of surfactant and co-surfactant to produce NANE with fine droplets and better stability. Hence, selection of an optimum ratio of surfactant to cosurfactant can produce a nanoemulsion with fine droplets and better stability.

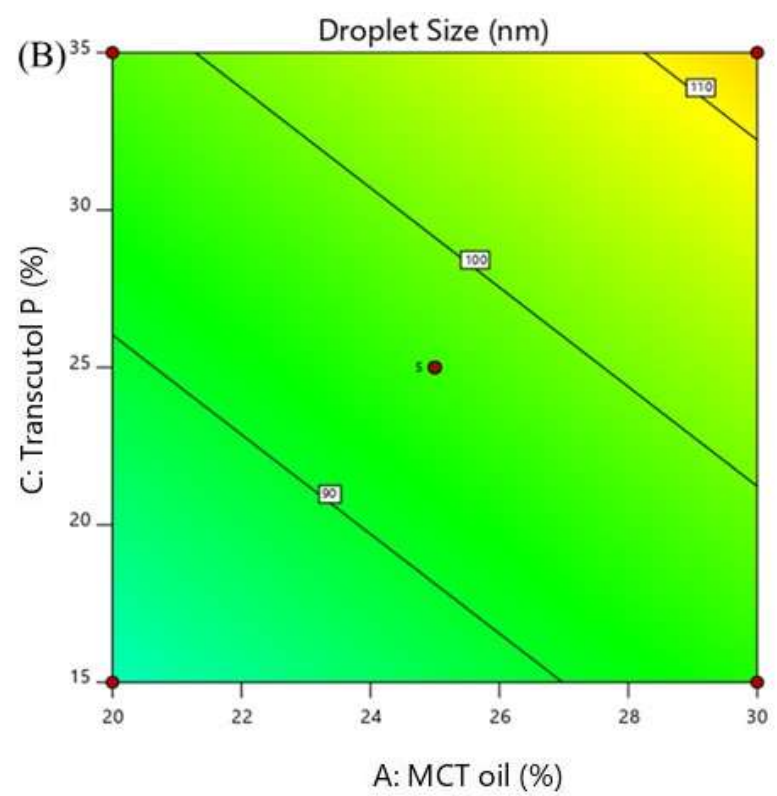
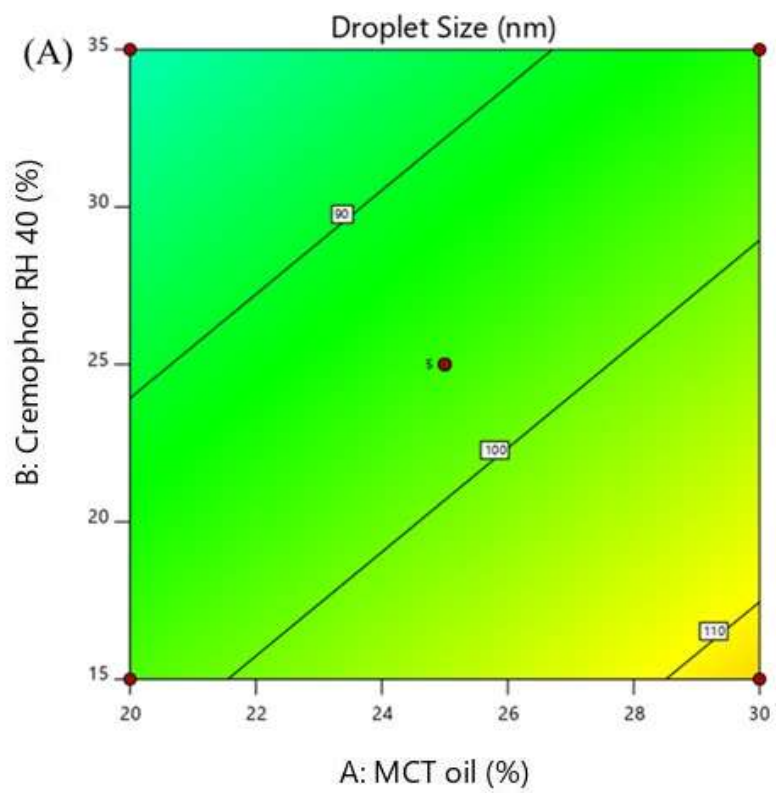
The 2D contour plots and 3D response surface plots for zeta potential are shown in **Figure 33(A-F)** and **Figure 34(A-F)** respectively. The increase in the magnitude of the zeta potential (-

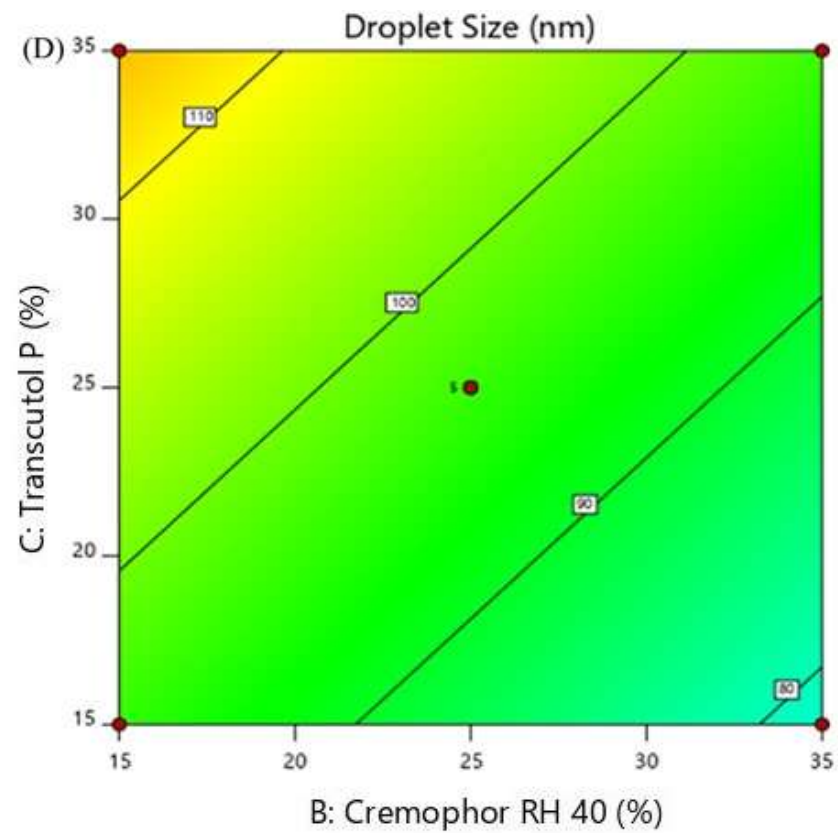
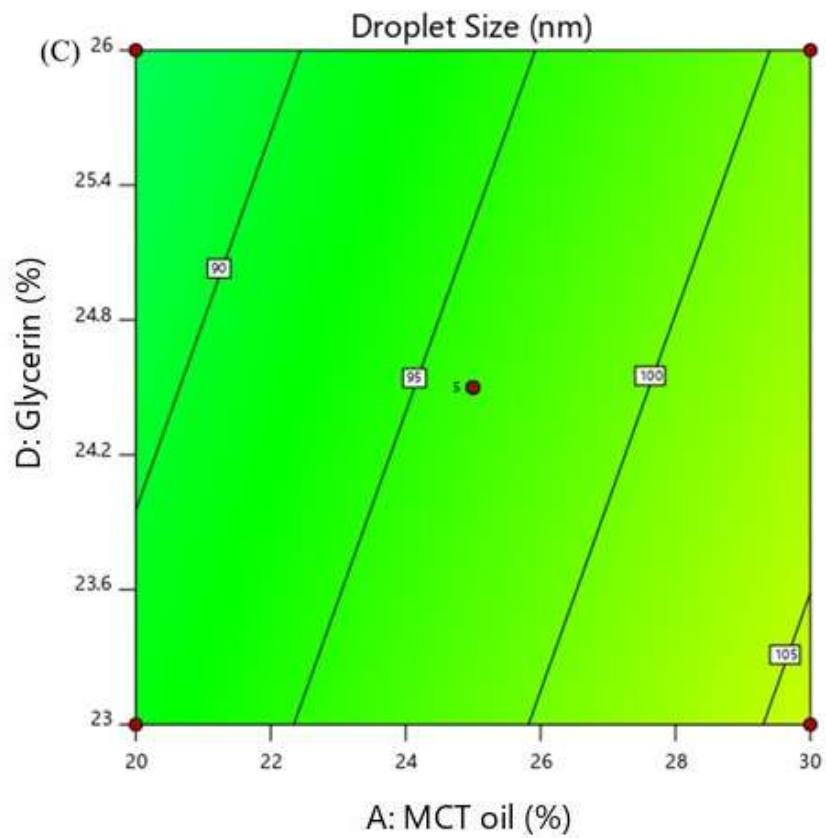
13.1mV) was observed with an increase in  $X_1$ ,  $X_3$  and  $X_4$  whereas an increase in the concentration of  $X_2$  decreased the magnitude of the zeta potential (-1.4 mV). The interaction of components such as  $X_1X_3$ ,  $X_1X_4$  and  $X_2X_3$  has shown decrease in the zeta potential with increase in their concentration. However, the charge on the droplets depends upon nature of selected surfactant and co-surfactant. The presence of non-ionic surfactant imparted neutral charge and their interaction with the other components in the system imparted charge but not as much as ionic surfactant. For instance, Mishra *et al.* reported zeta potential of Zaltropren loaded microemulsion to be -11.2 mV in which a combination of Cremophor RH 40 and Transcutol P were used as  $S_{mix}$ . This study has reported the ability of negatively charged droplets to prevent aggregation and provided better stability (Mishra et al., 2016). In the present study, the same combination of Cremophor RH 40 and Transcutol P might be imparting negative charge to the droplets and providing stability.

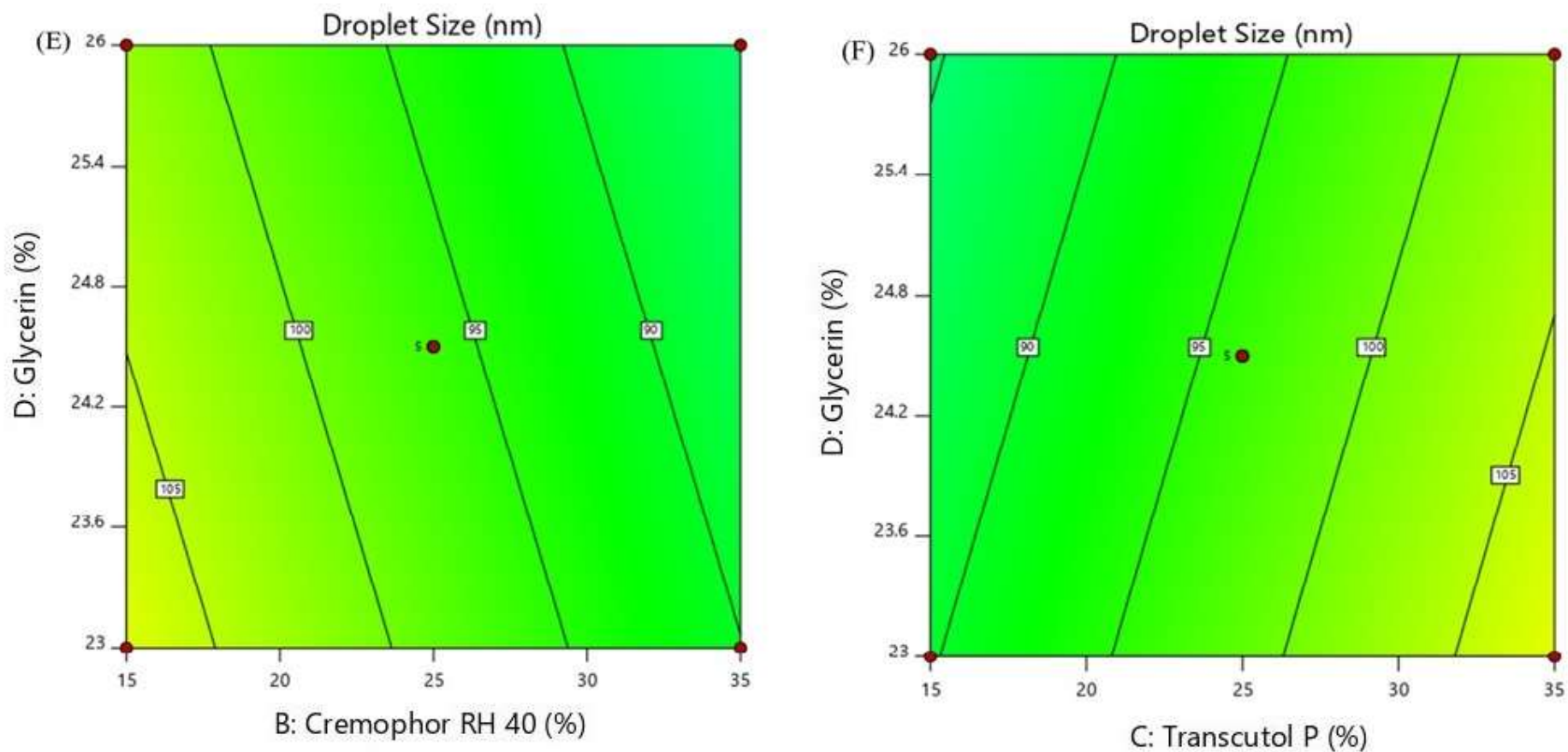
The constructed 2D contour plot and 3D response surface plot for drug loading are shown in **Figures 35(A-F)** and **36(A-F)**, respectively. A linear increase in drug loading was observed with an increase in concentration of  $X_1$ ,  $X_2$  and  $X_4$ . However, an increase in concentration of  $X_3$  has shown decreased drug loading. Hence, selection of optimum ratio of surfactant to co-surfactant is crucial to ensure higher loading capacity of the extract which later interferes in the release studies. Therefore, in this study, the selection of suitable ratio of Cremophor RH 40 to Transcutol P is significant.

The 2D contour plot and 3D response surface plot for % cumulative drug permeated in 6 h are shown in **Figures 37(A-F)** and **38(A-F)**, respectively. It was observed that the interaction effects of  $X_1X_2$ ,  $X_1X_4$ ,  $X_2X_4$  and  $X_3X_4$  are dominant and revealed maximum % cumulative drug permeation at an optimal level of  $X_1$ ,  $X_2$ ,  $X_3$ , and  $X_4$ .

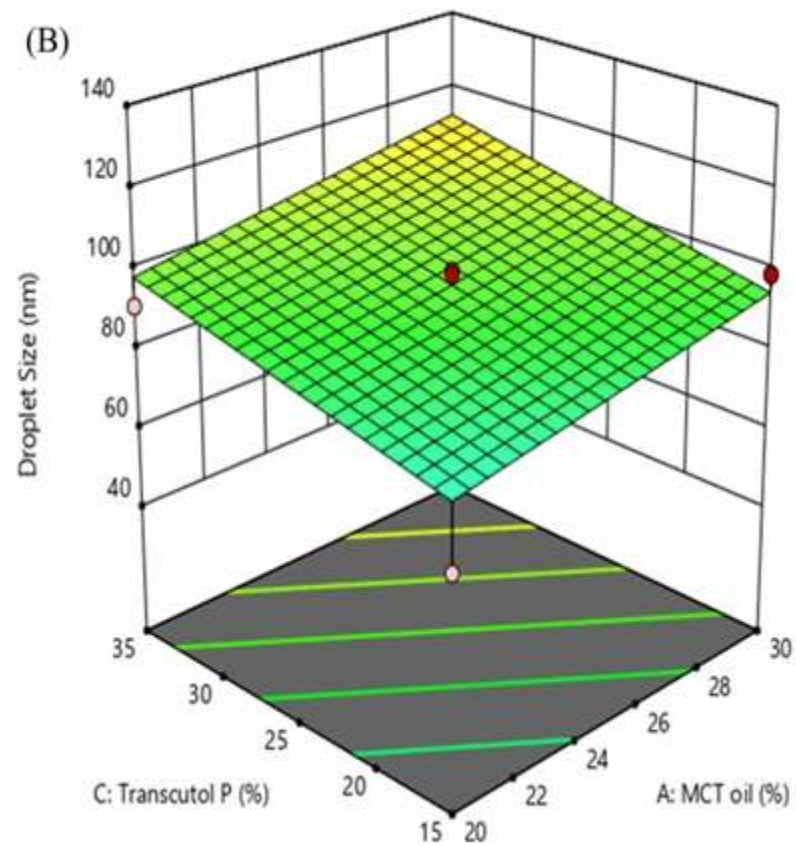
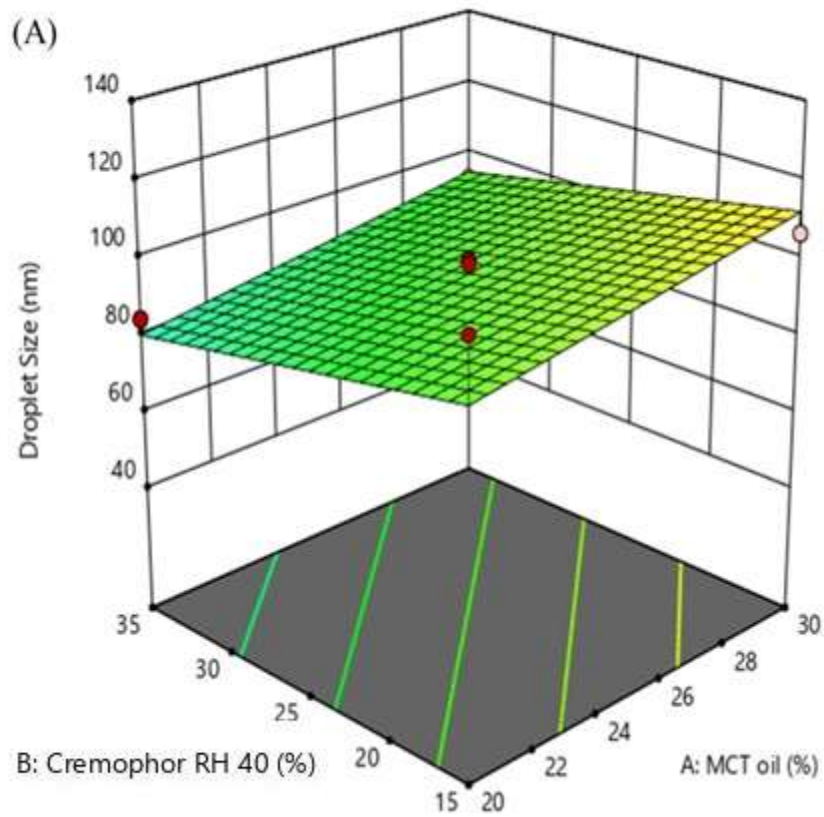
The 2D contour plot and 3D response surface plot for % drug retention after 6 h are shown in **Figure 39(A-F)** and **Figure 40(A-F)**, respectively. Interaction effect was dominant and it was observed that interaction between  $X_1X_2$ ,  $X_1X_4$ ,  $X_2X_4$  and  $X_3X_4$  suggested that maximum % drug retention was obtained at an optimal level of  $X_1$ ,  $X_2$ ,  $X_3$ , and  $X_4$ . All these effects confirmed the crucial role of each variable in the formation of stable NANEs.

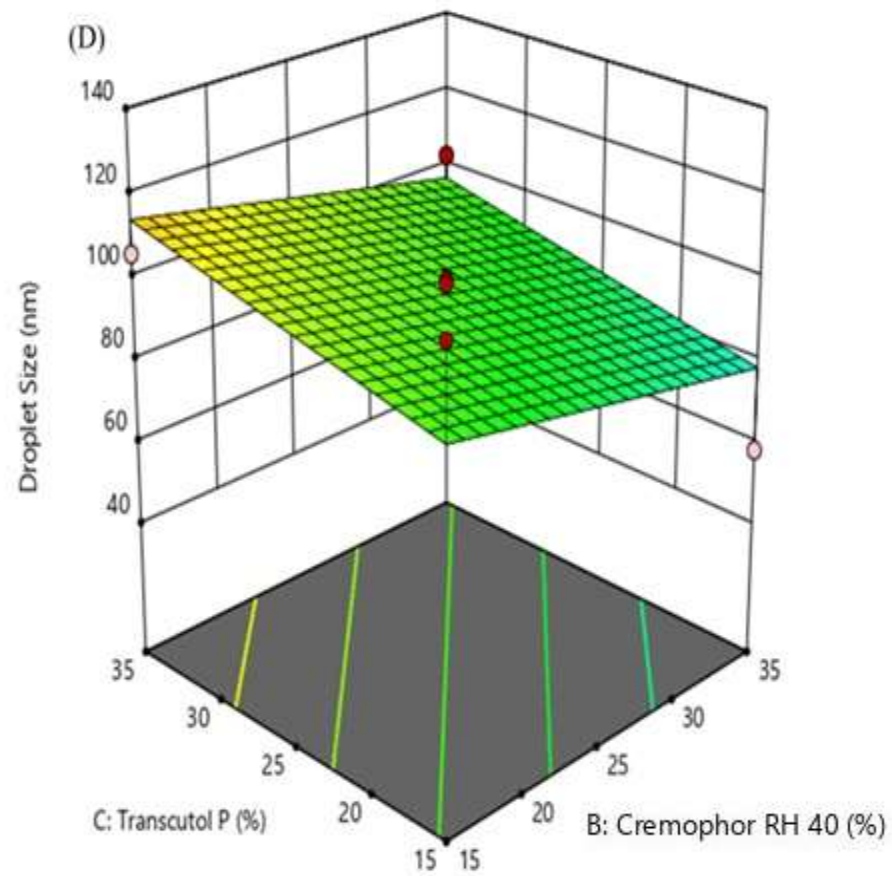
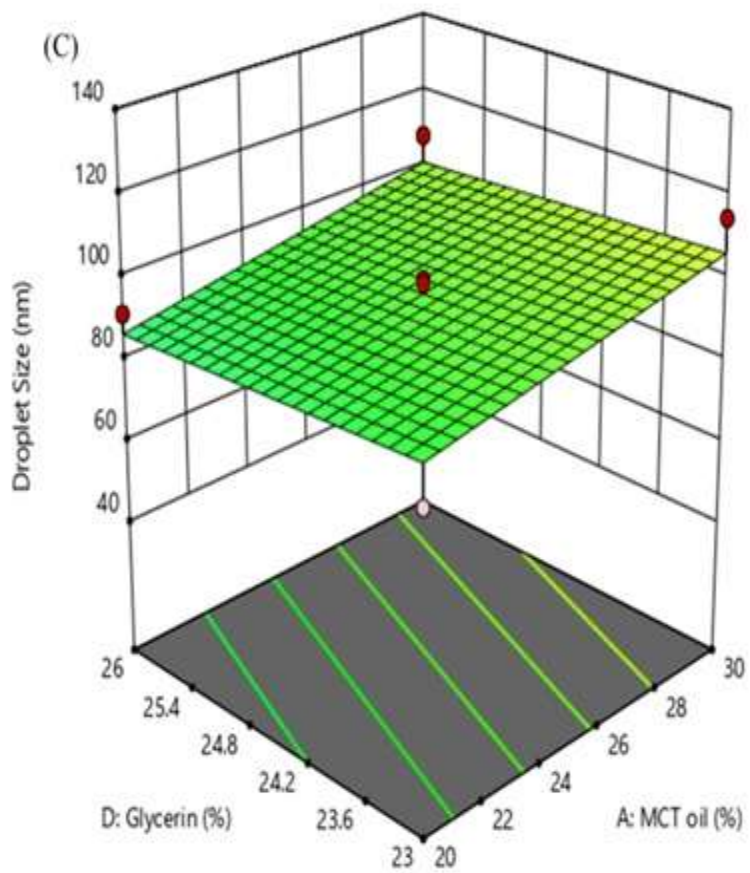




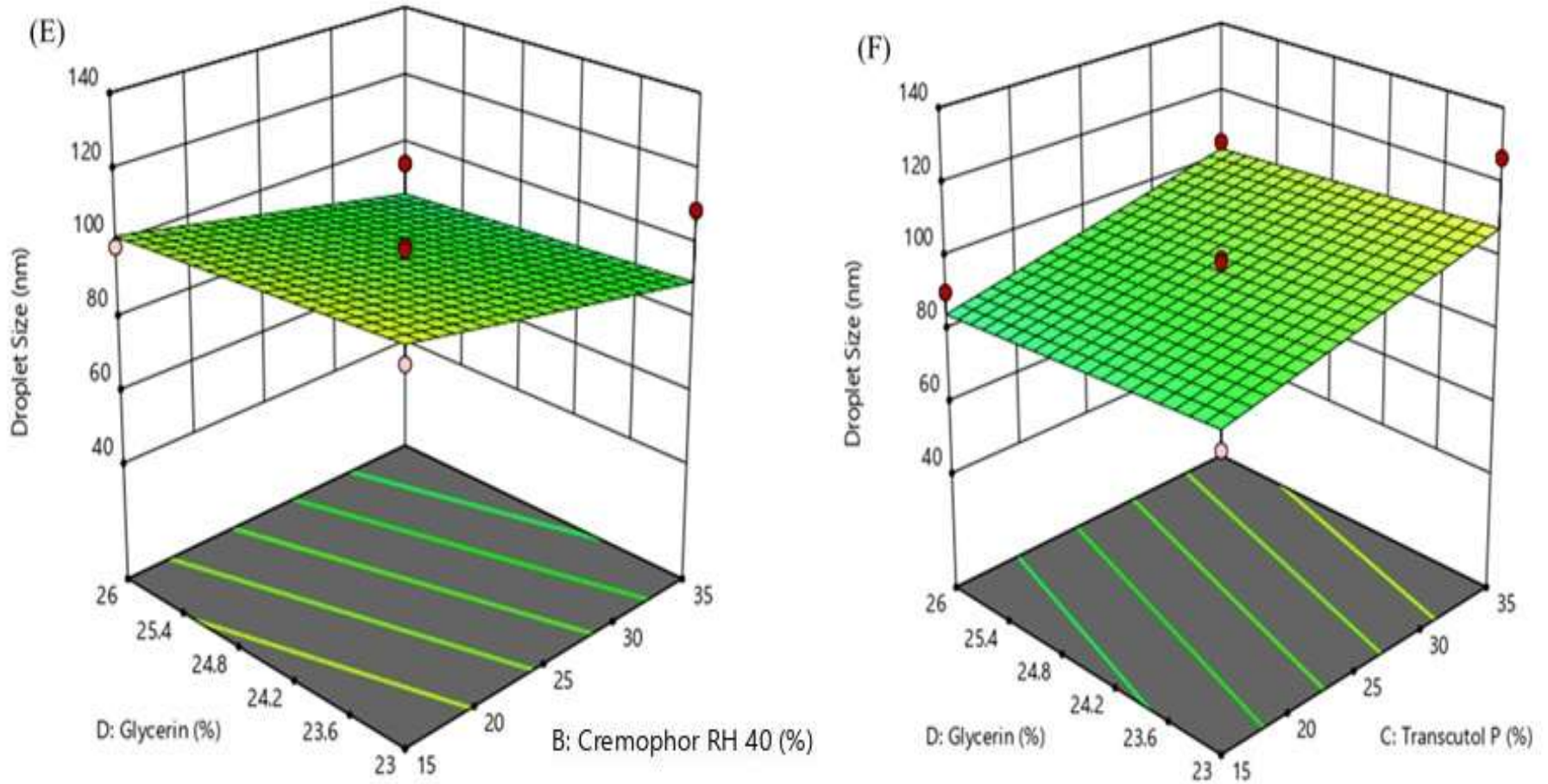


**Figure 31.** Contour plots for the effect of (A) MCT oil and Cremophor RH 40 (B) MCT oil and Transcutol P (C) MCT oil and Glycerin (D) Cremophor RH 40 and Transcutol P (E) Cremophor RH 40 and Glycerin (F) Transcutol P and Glycerin on droplet size

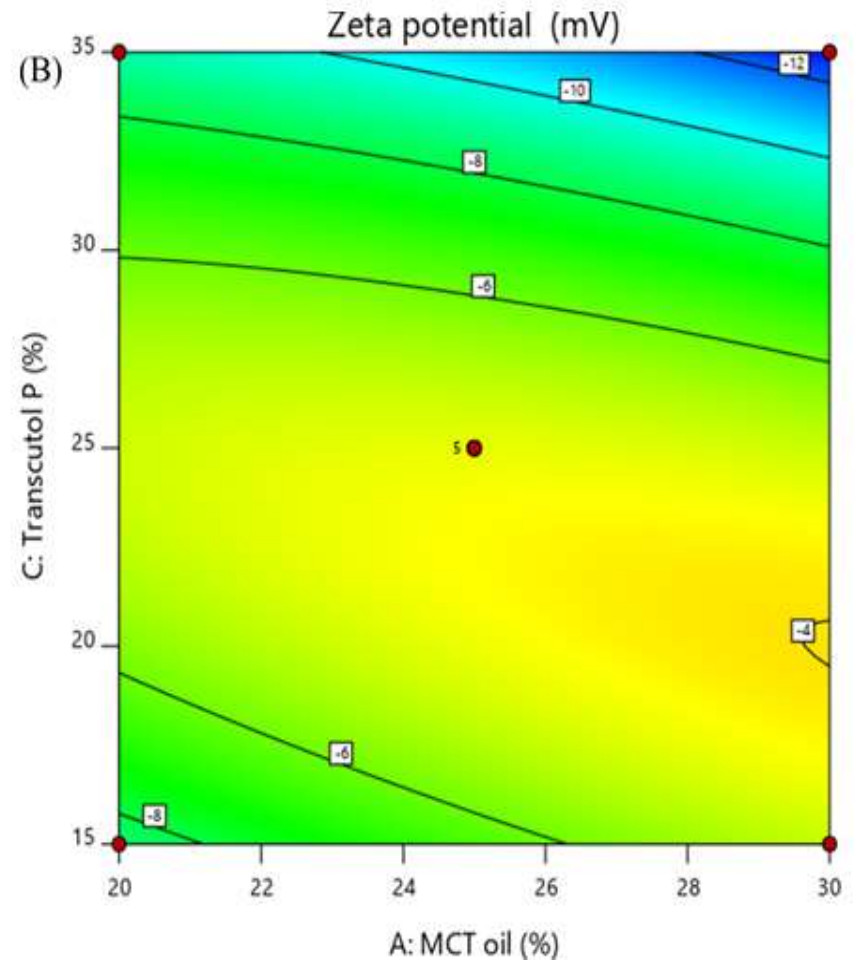
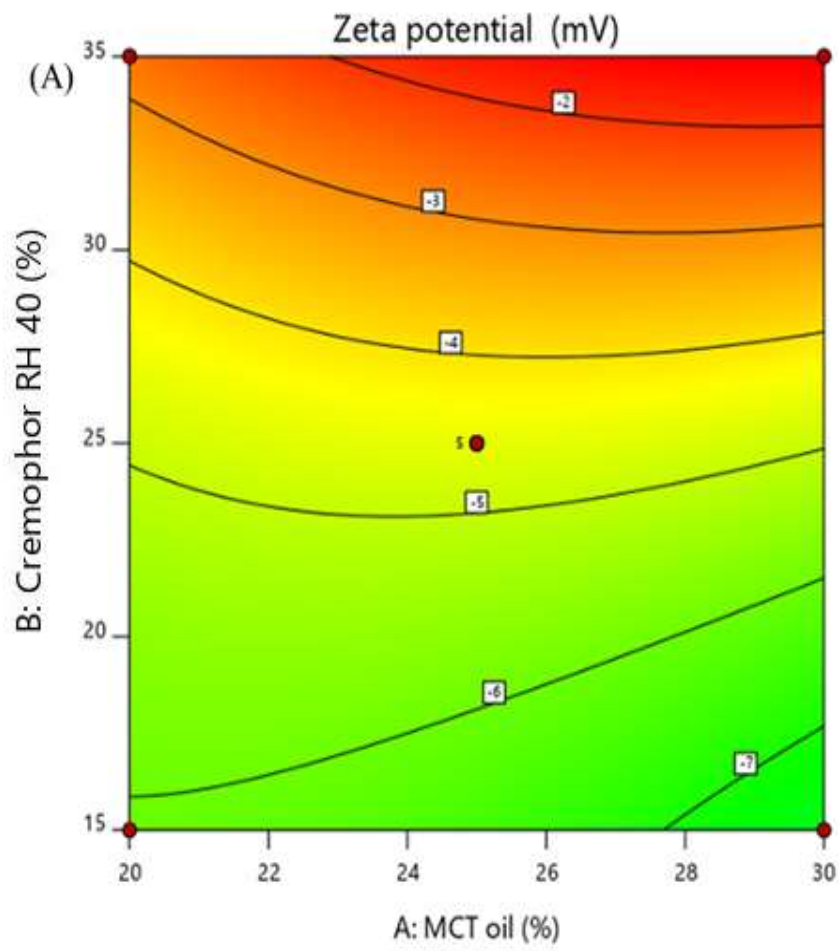


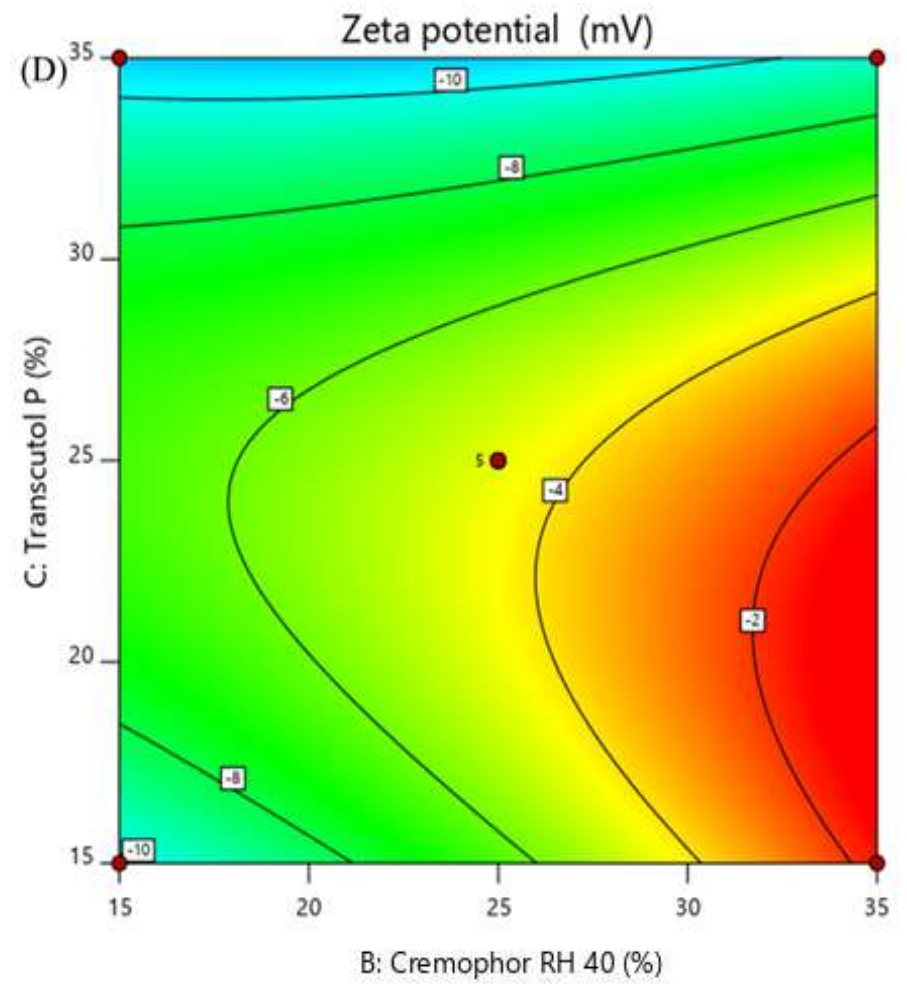
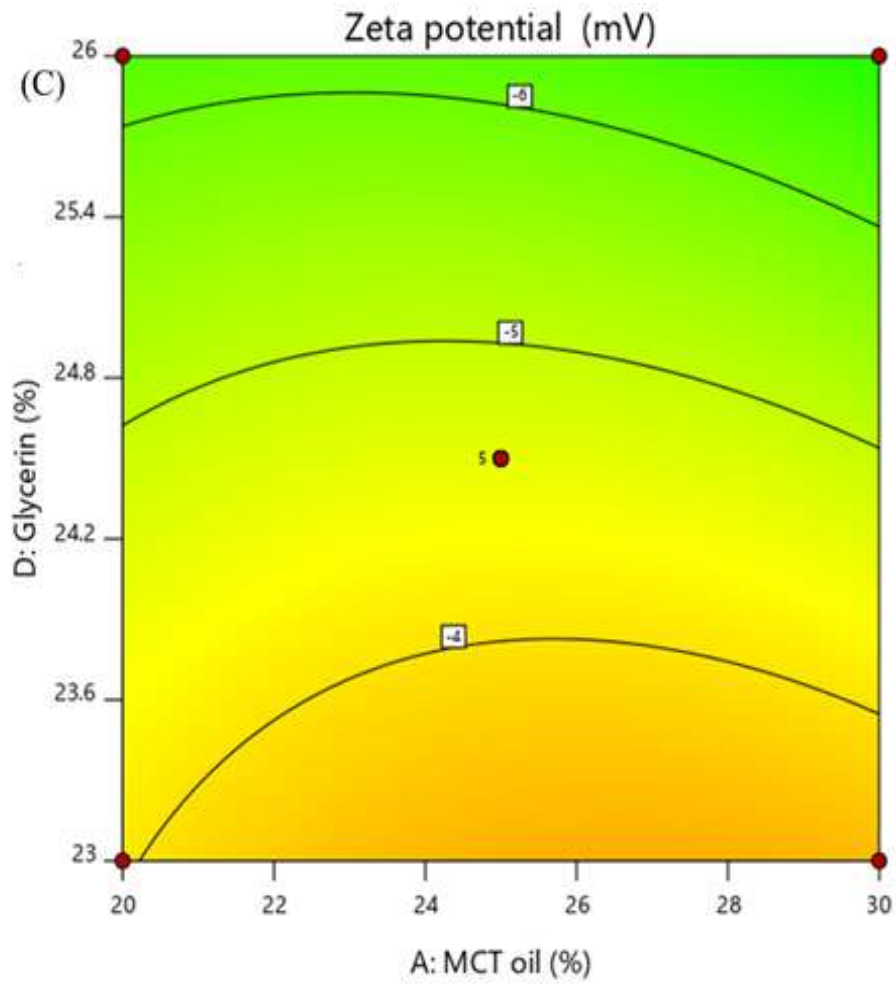


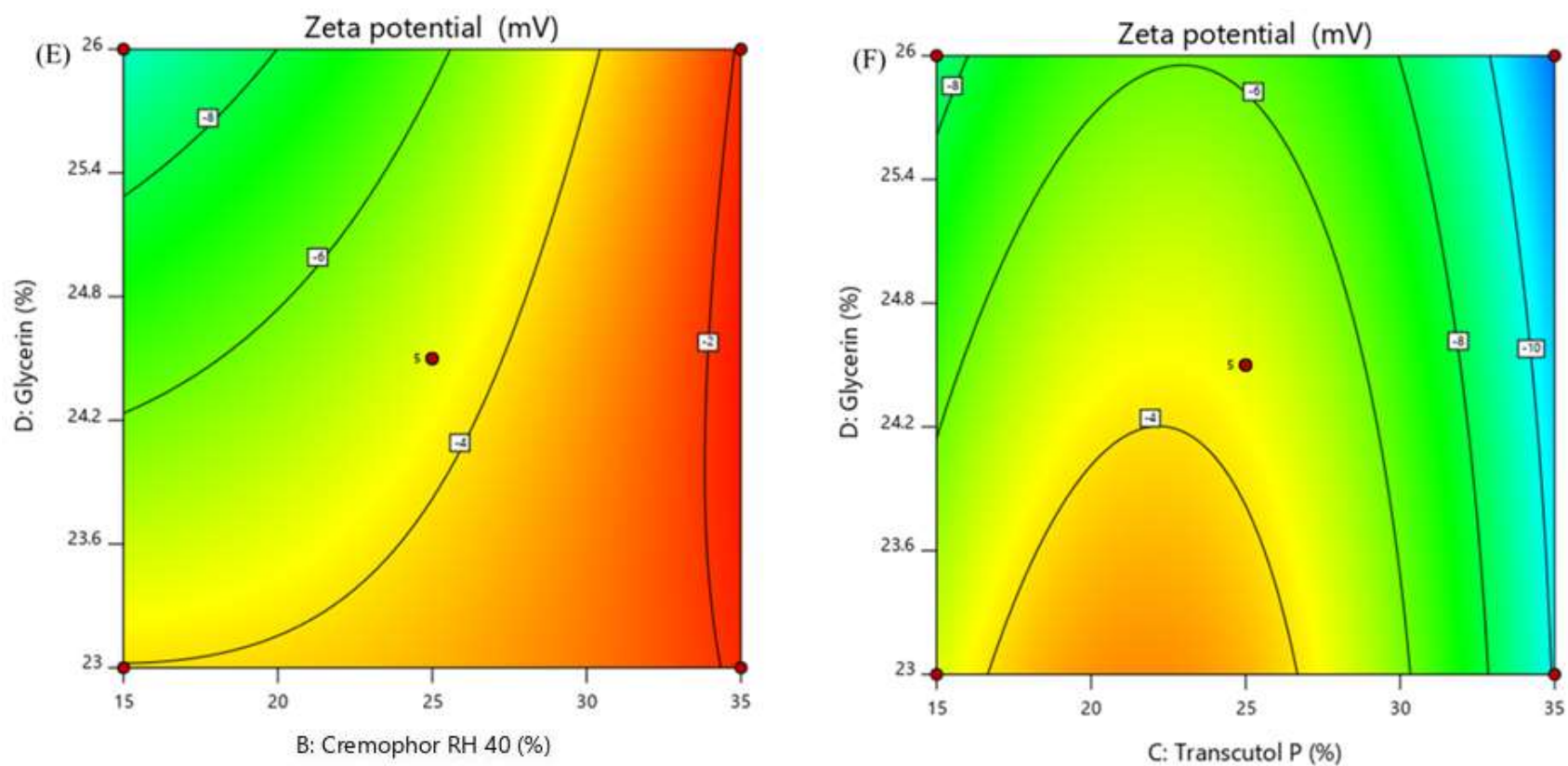




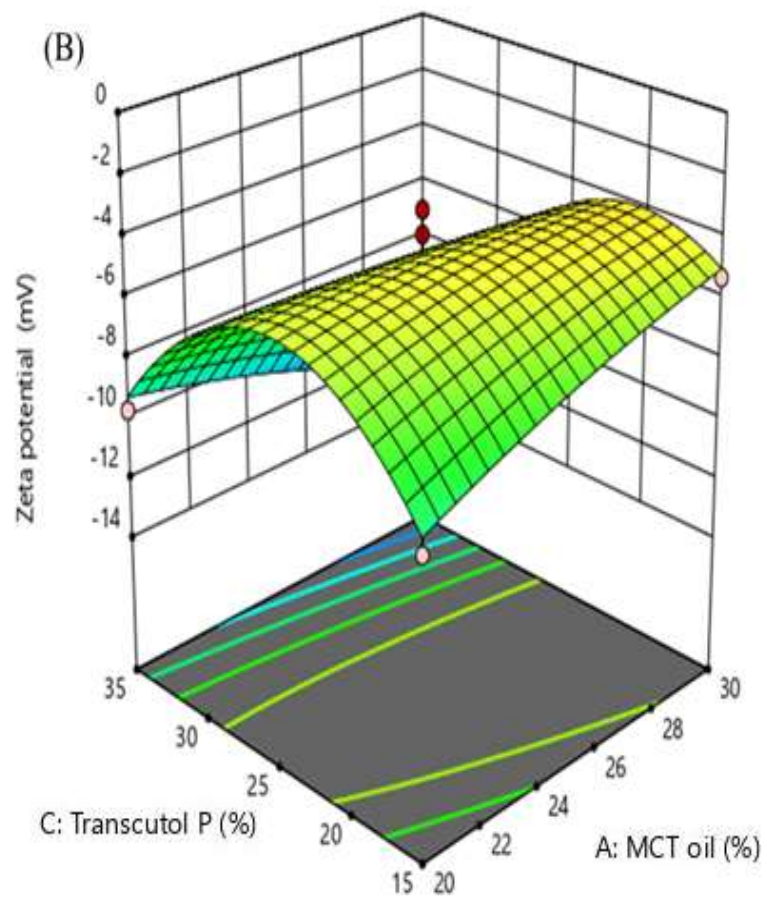
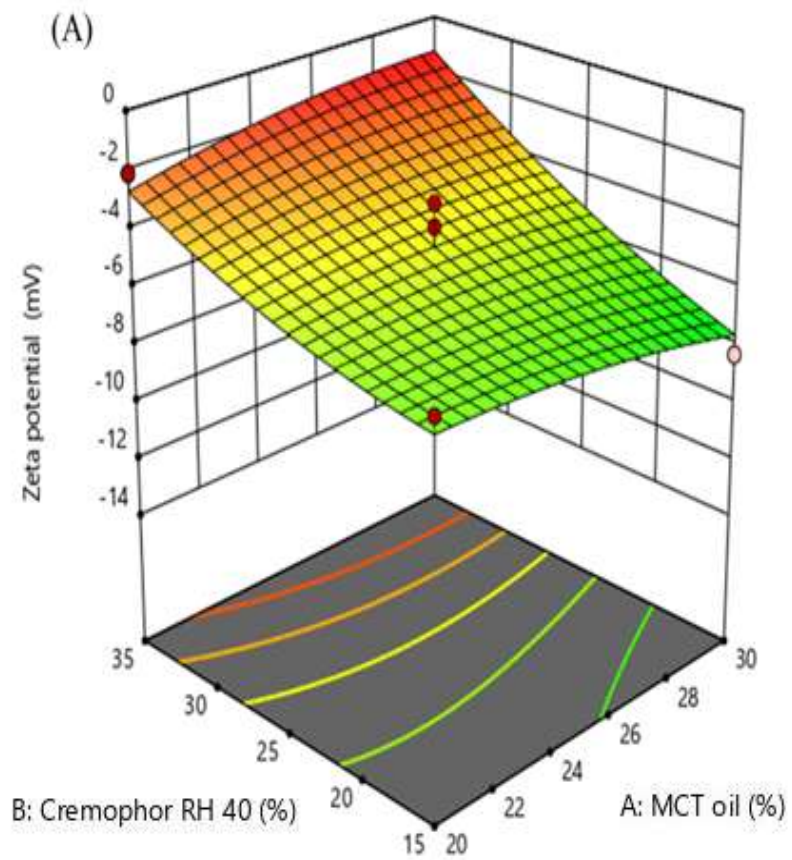
**Figure 32.** 3D response surface plot for the effect of (A) MCT oil and Cremophor RH 40 (B) MCT oil and Transcutol P (C) MCT oil and Glycerin (D) Cremophor RH 40 and Transcutol P (E) Cremophor RH 40 and Glycerin (F) Transcutol P and Glycerin on droplet size

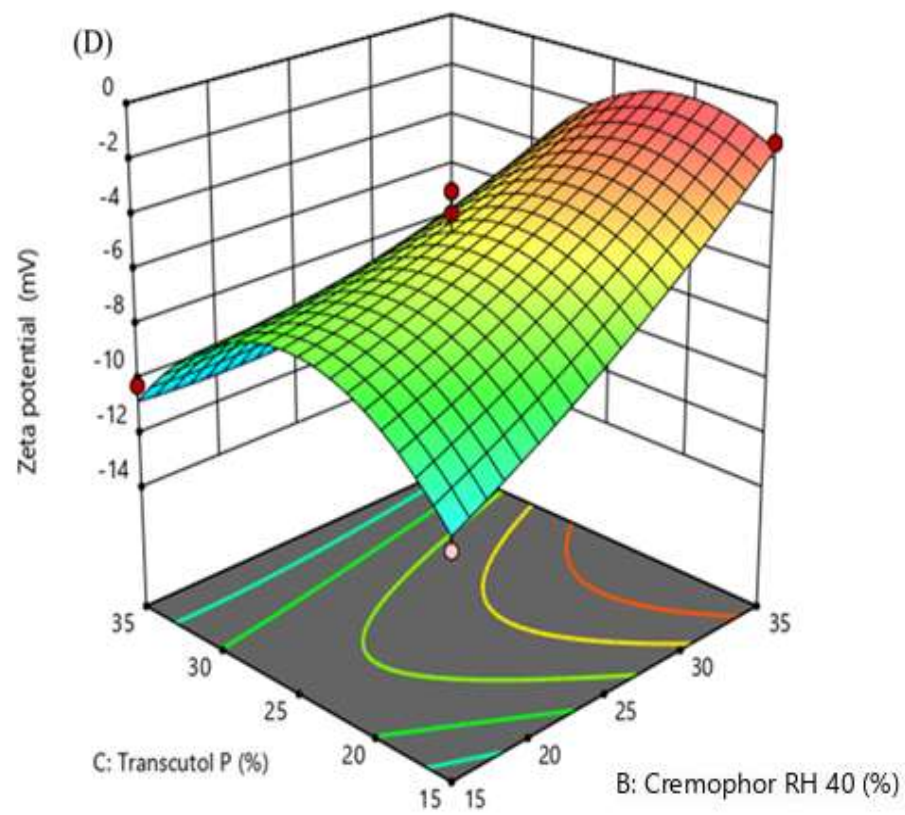
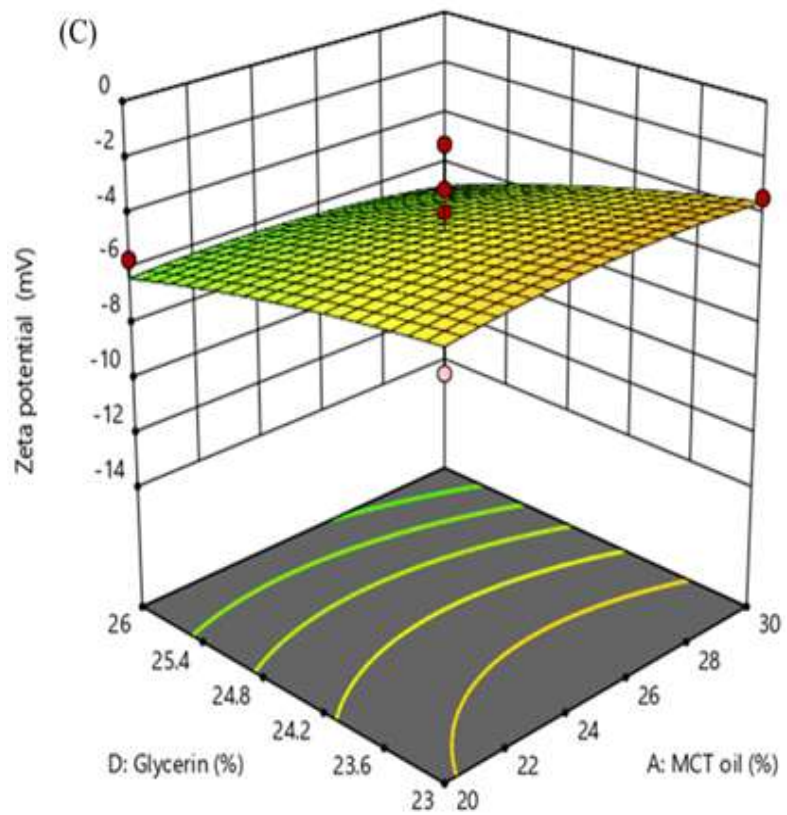


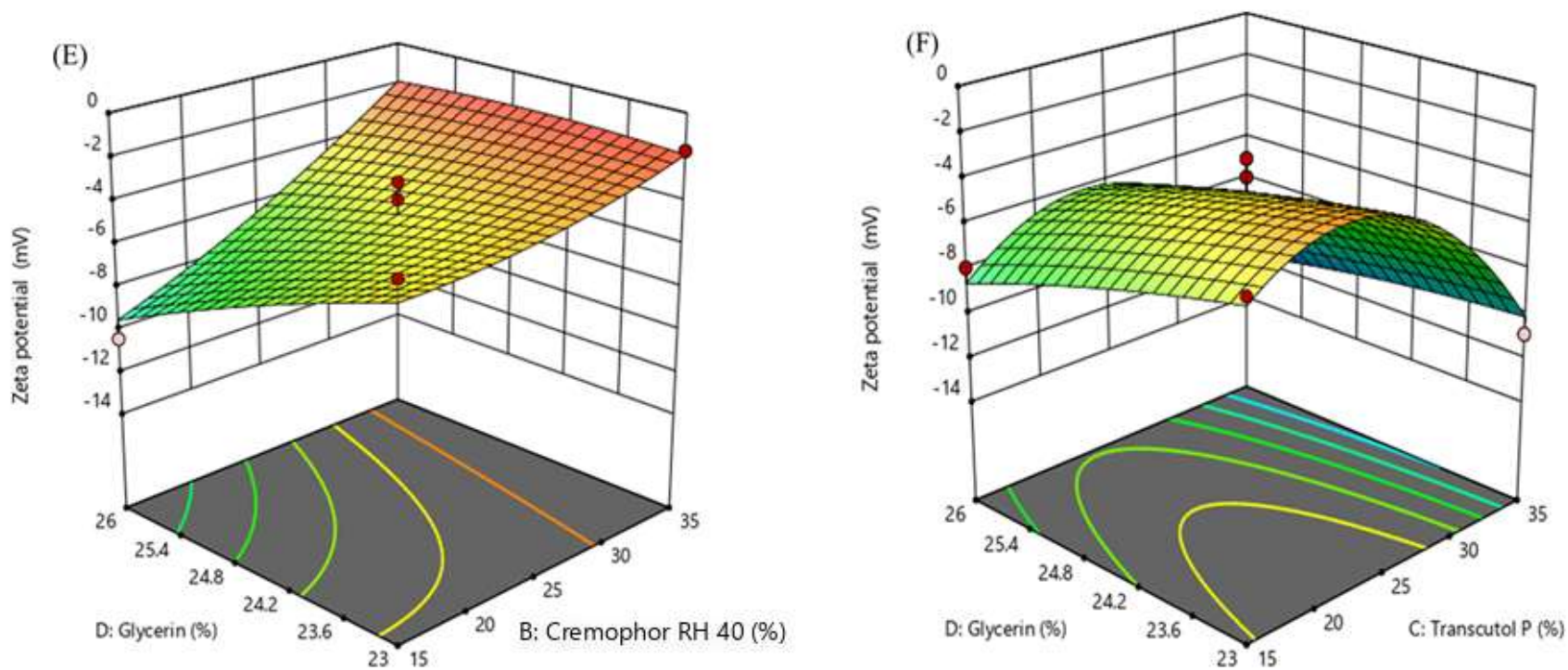




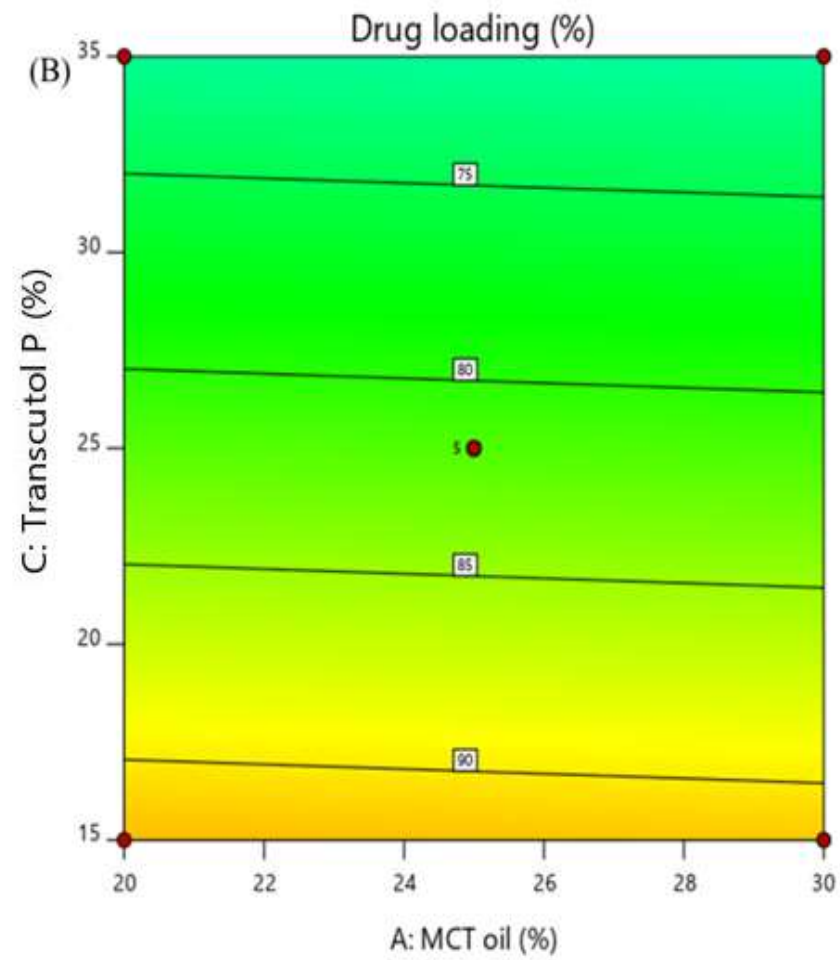
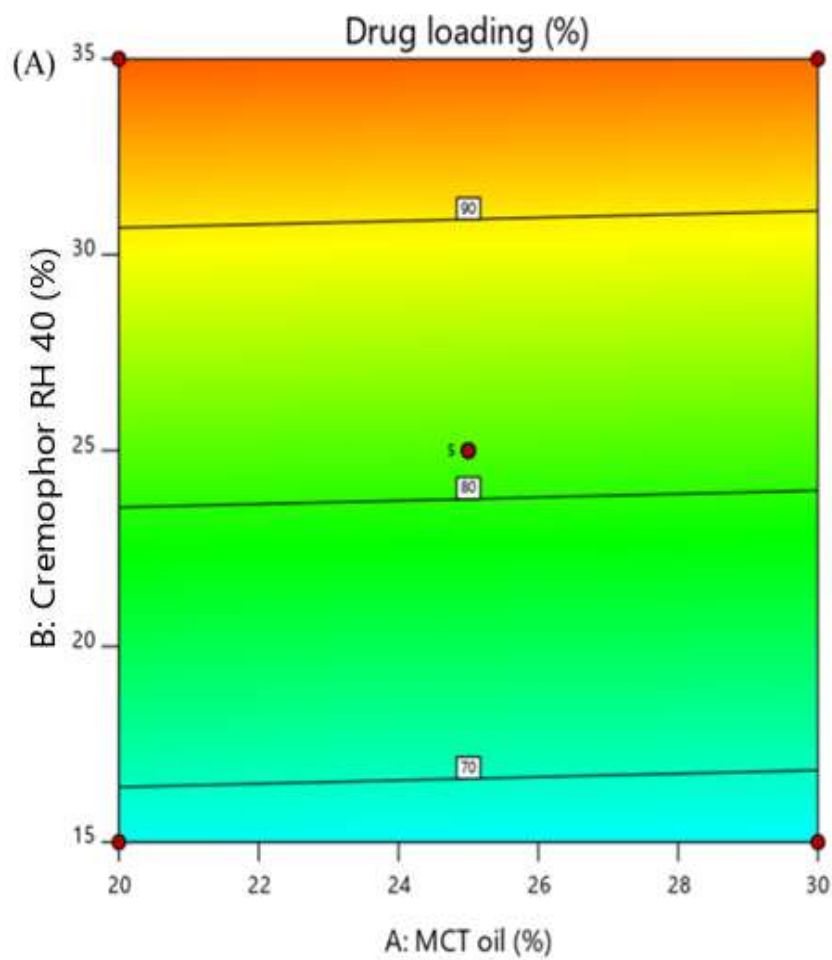
**Figure 33.** Contour plots for the effect of (A) MCT oil and Cremophor RH 40 (B) MCT oil and Transcutol P (C) MCT oil and Glycerin (D) Cremophor RH 40 and Transcutol P (E) Cremophor RH 40 and Glycerin (F) Transcutol P and Glycerin on zeta potential



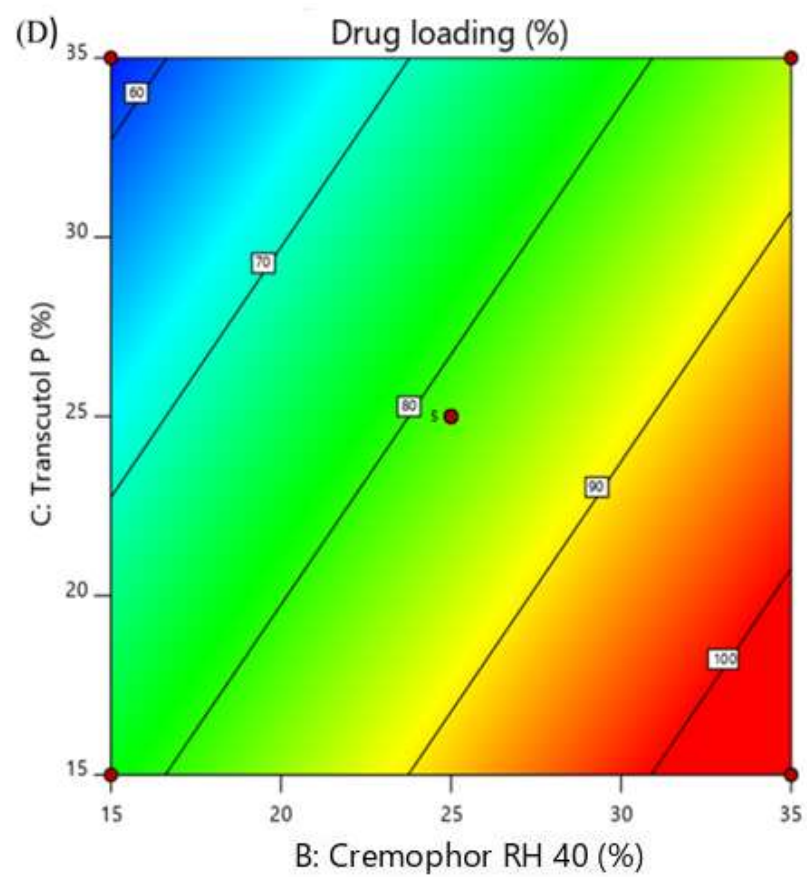
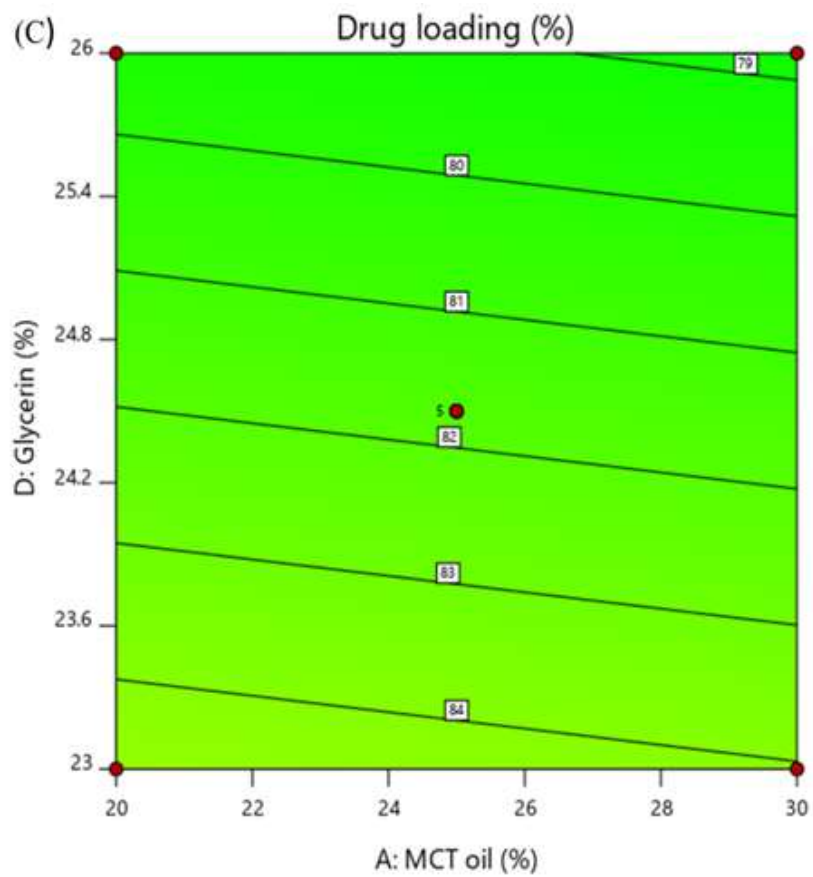


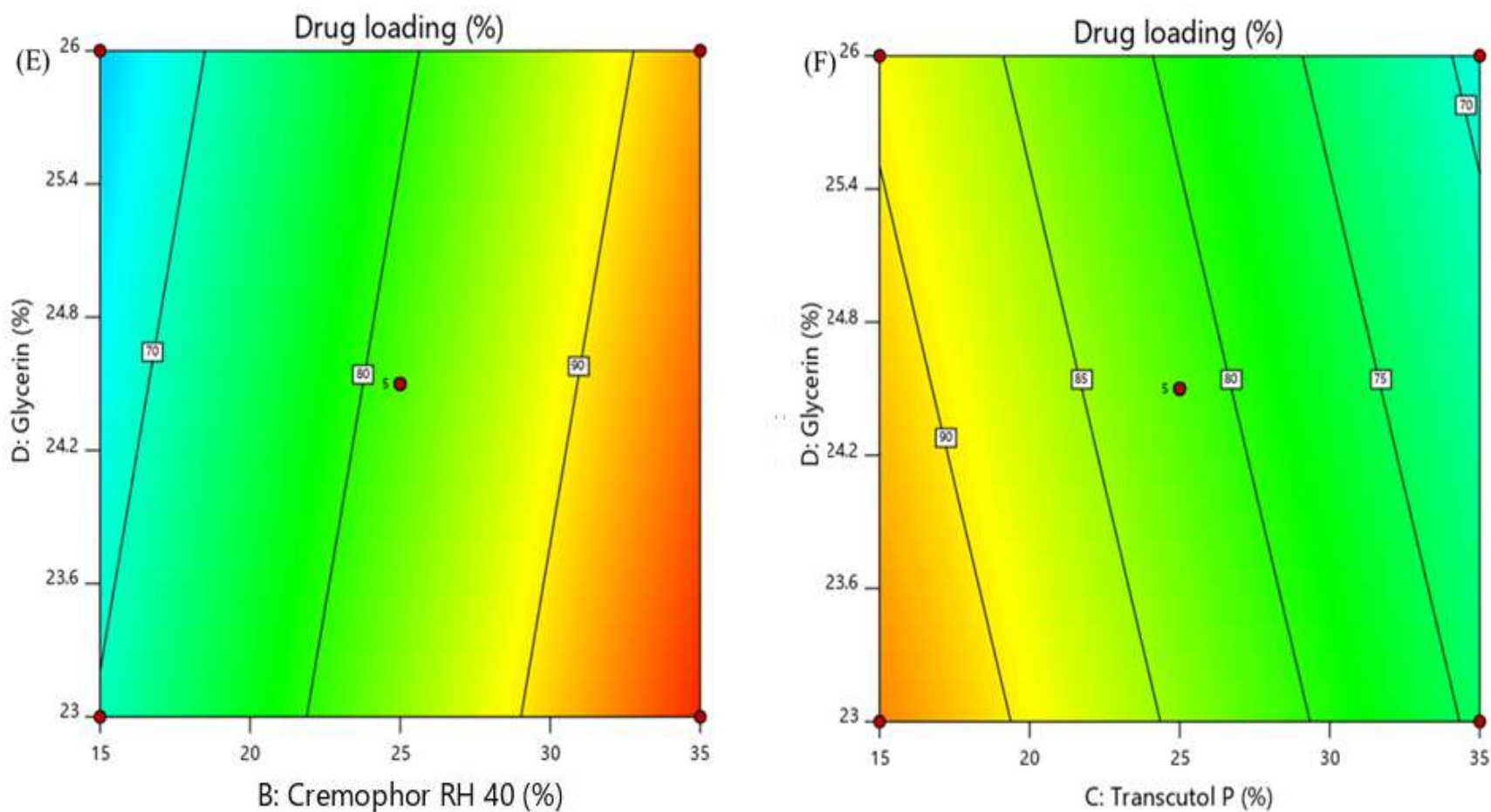


**Figure 34.** 3D response surface plot for the effect of (A) MCT oil and Cremophor RH 40 (B) MCT oil and Transcutol P (C) MCT oil and Glycerin (D) Cremophor RH 40 and Transcutol P (E) Cremophor RH 40 and Glycerin (F) Transcutol P and Glycerin on zeta potential

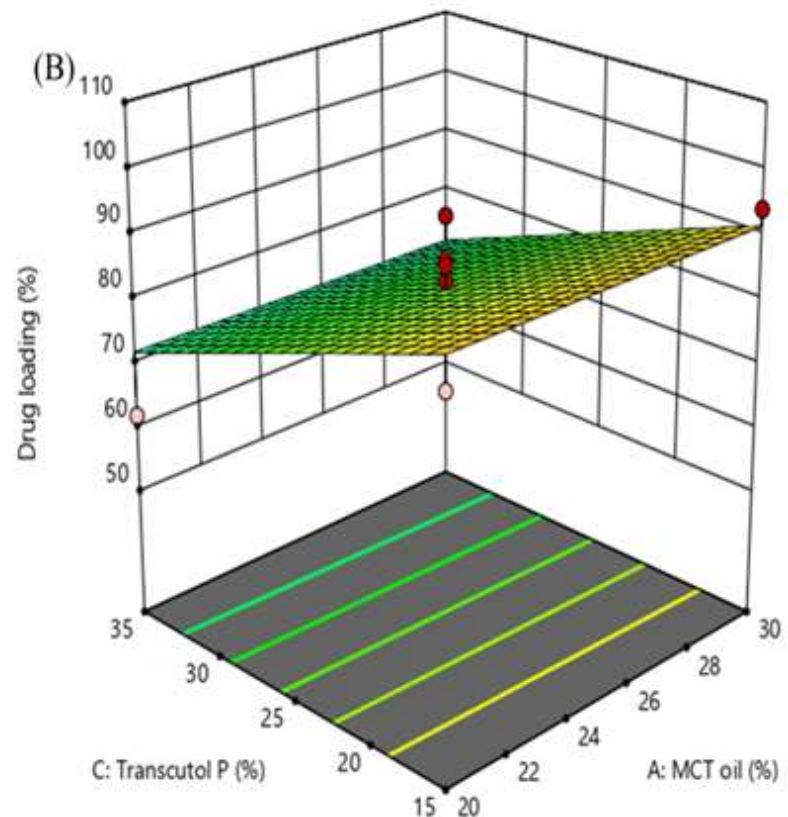
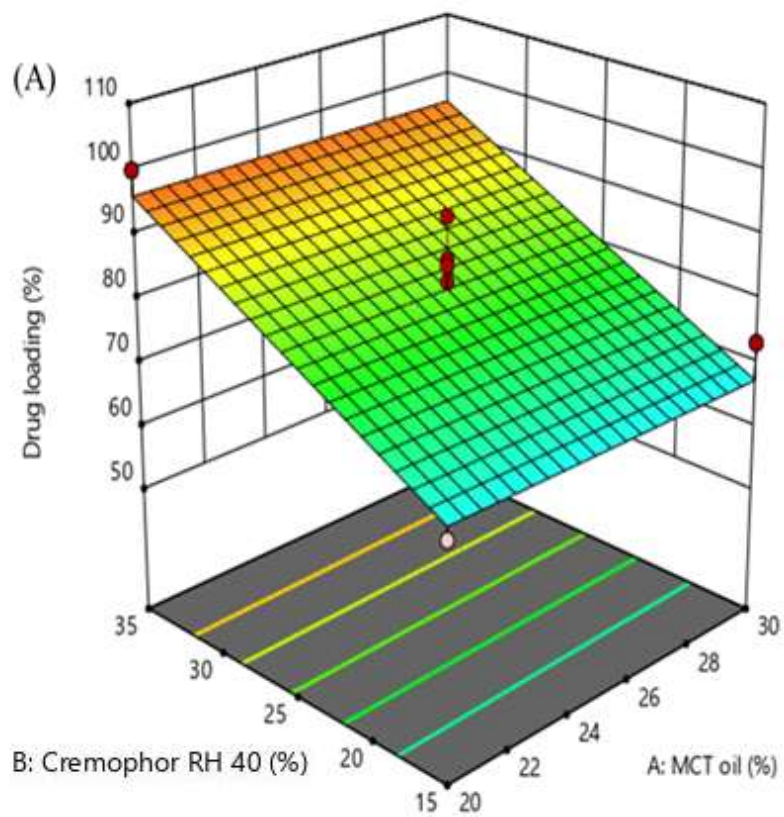


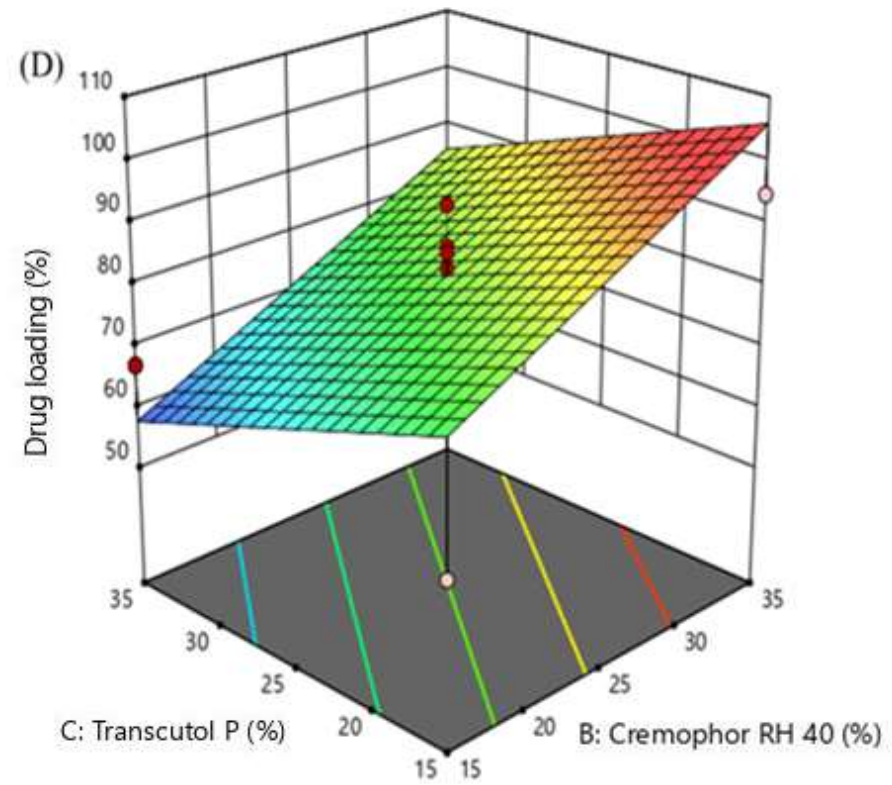
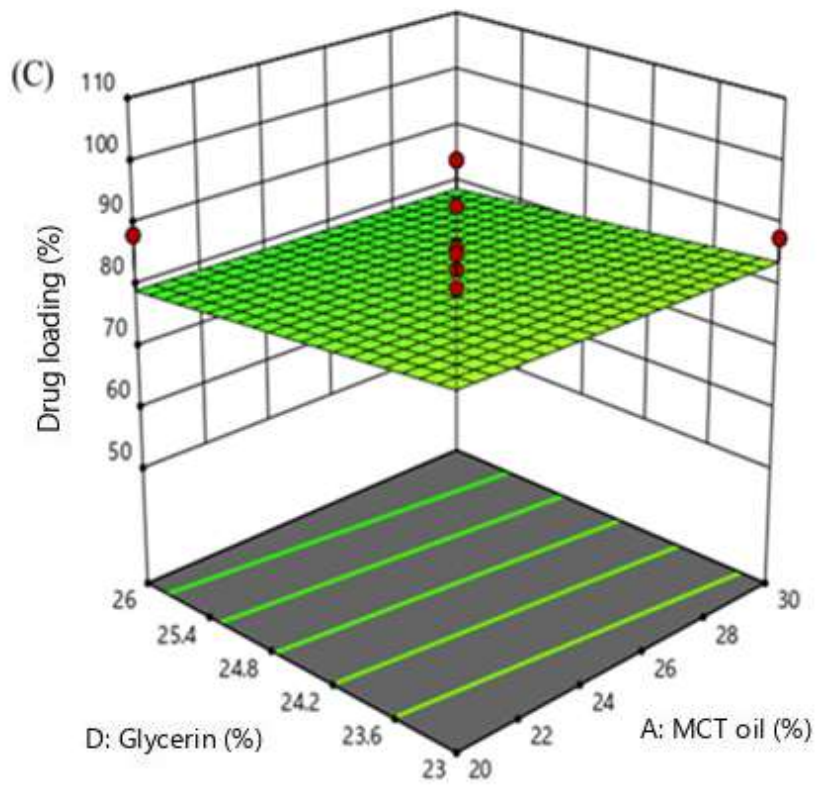


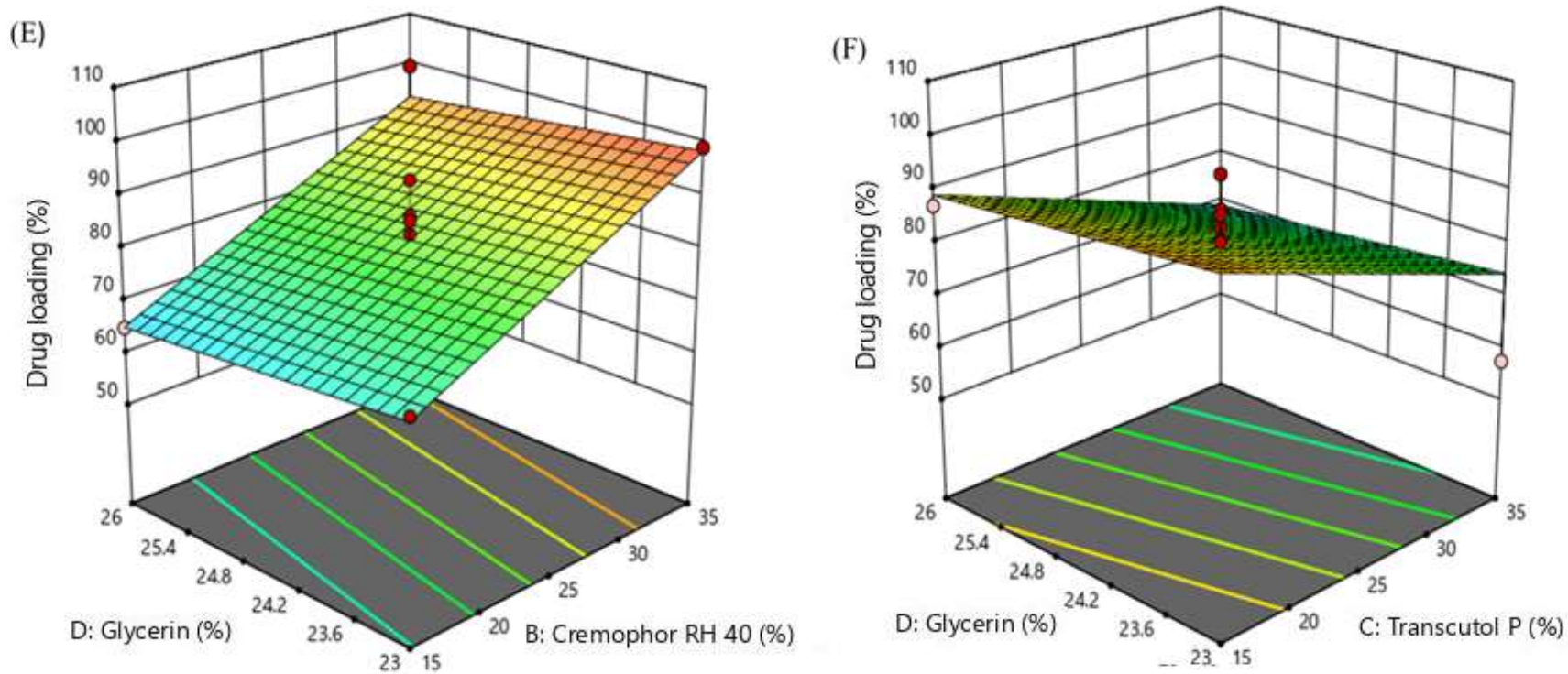




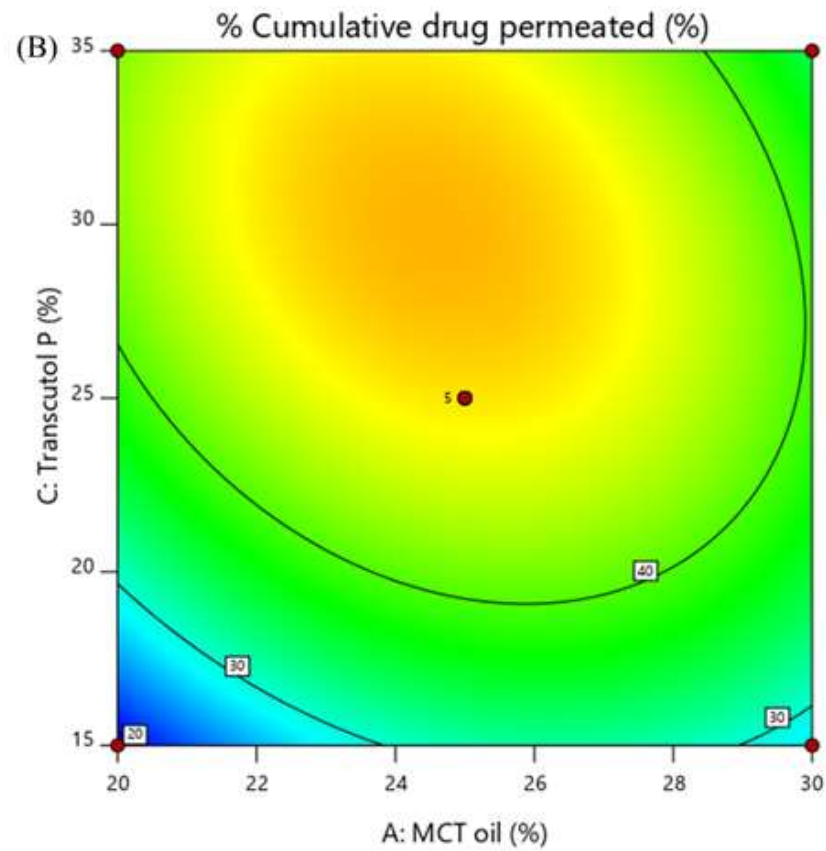
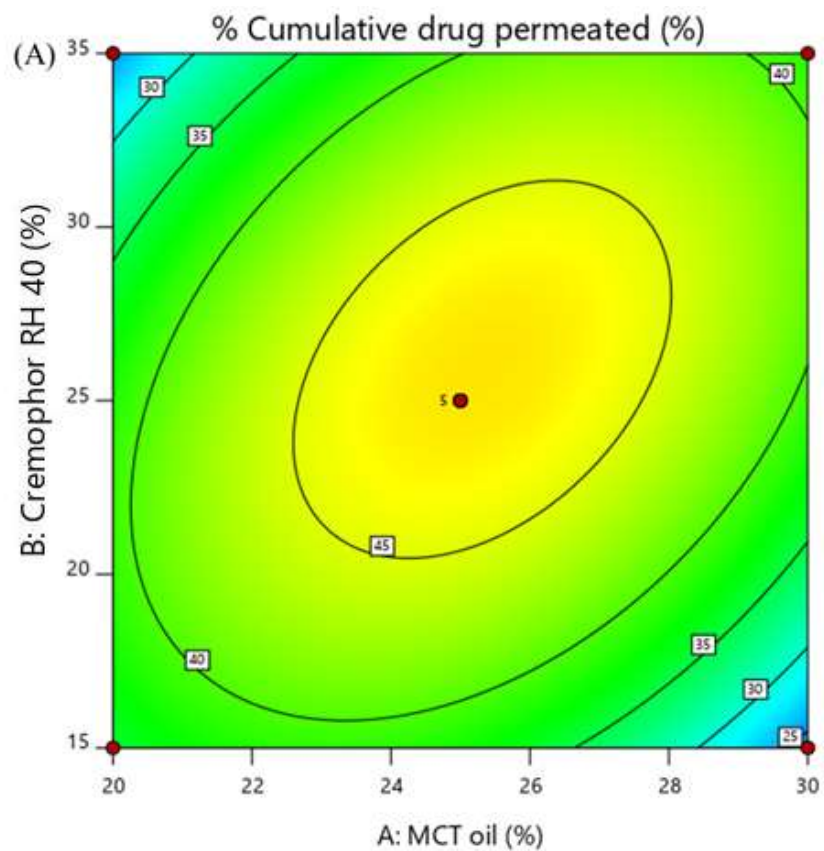
**Figure 35.** Contour plots for the effect of (A) MCT oil and Cremophor RH 40 (B) MCT oil and Transcutol P (C) MCT oil and Glycerin (D) Cremophor RH 40 and Transcutol P (E) Cremophor RH 40 and Glycerin (F) Transcutol P and Glycerin on drug loading

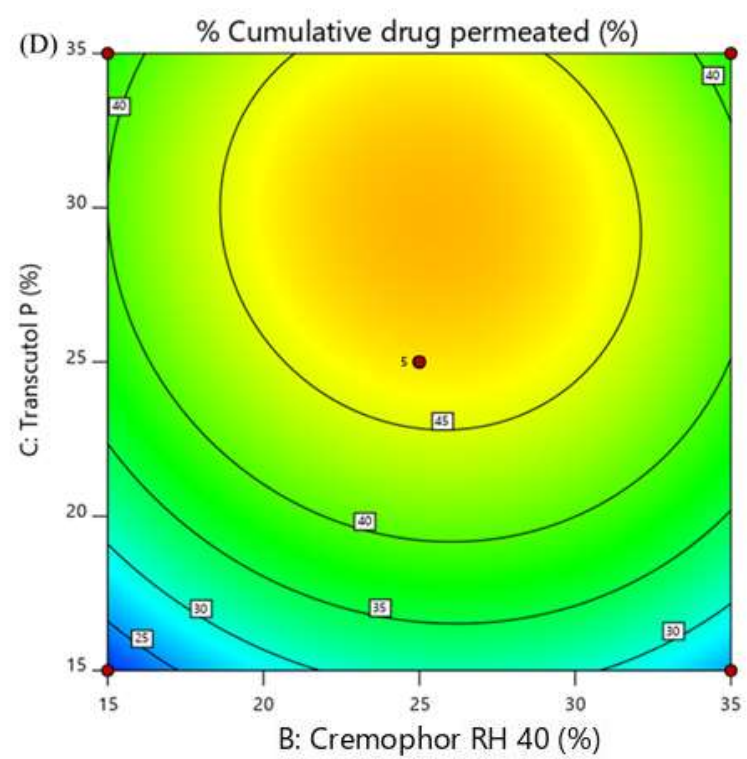
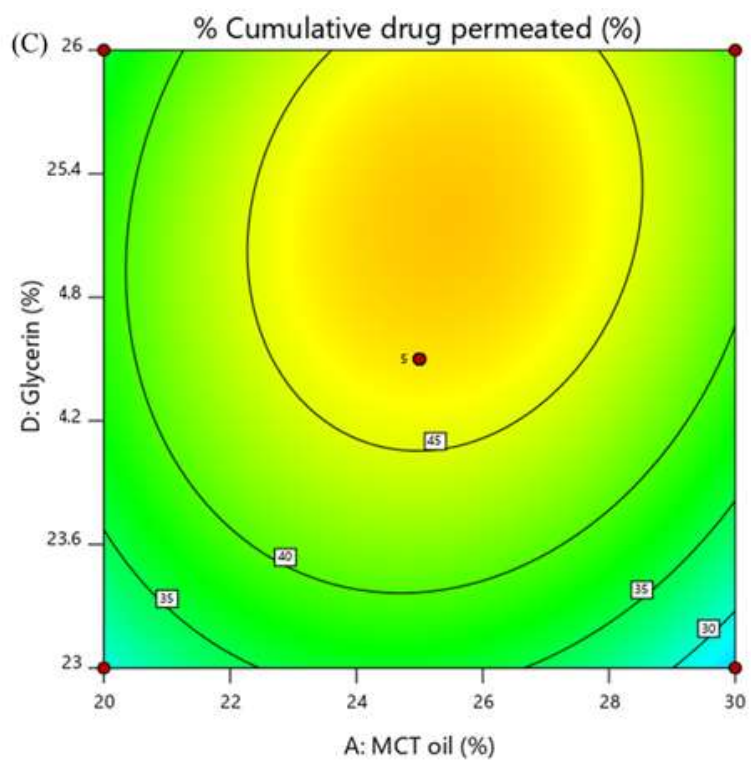


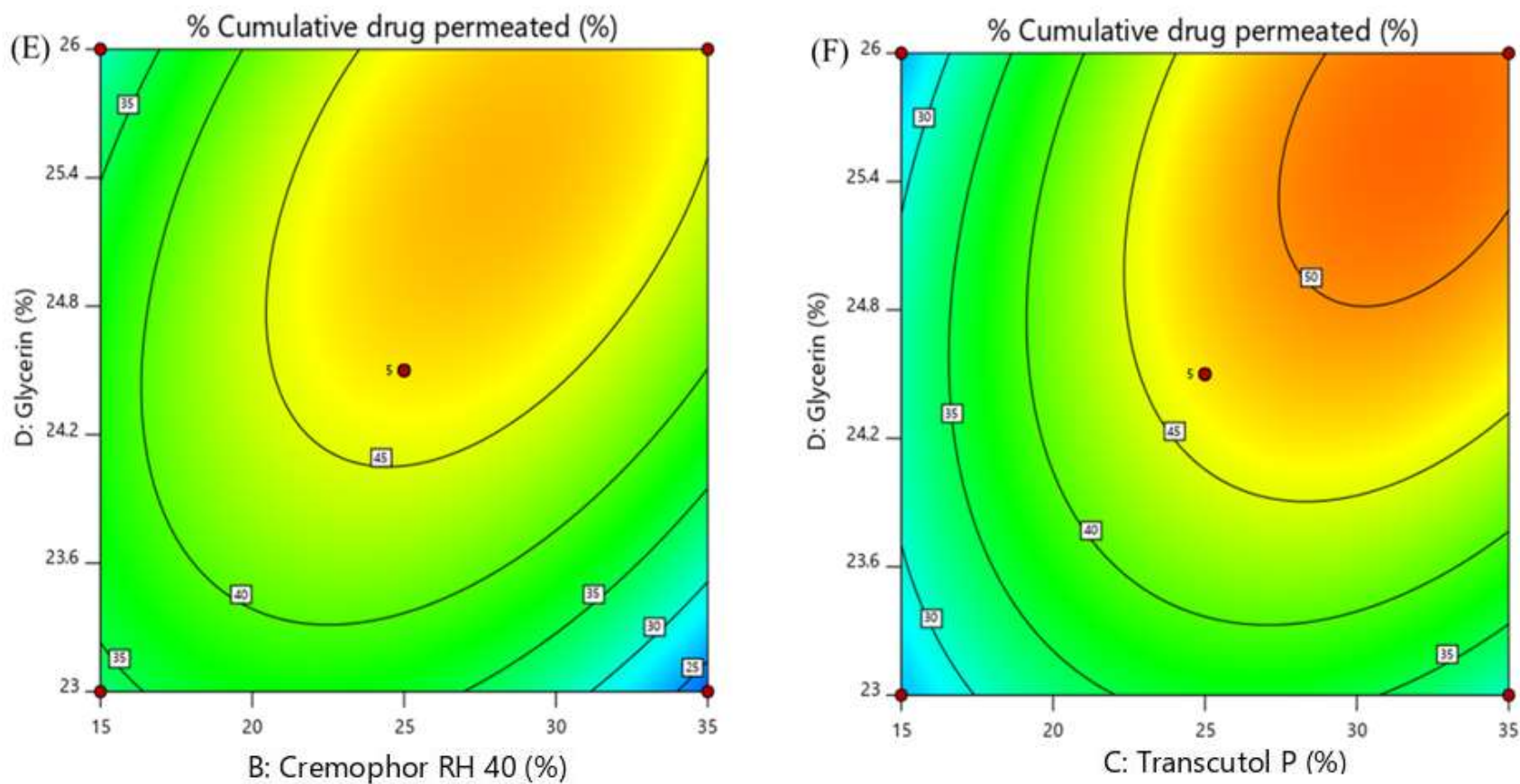




**Figure 36.** 3D response surface plot for the effect of (A) MCT oil and Cremophor RH 40 (B) MCT oil and Transcutol P (C) MCT oil and Glycerin (D) Cremophor RH 40 and Transcutol P (E) Cremophor RH 40 and Glycerin (F) Transcutol P and Glycerin on drug loading

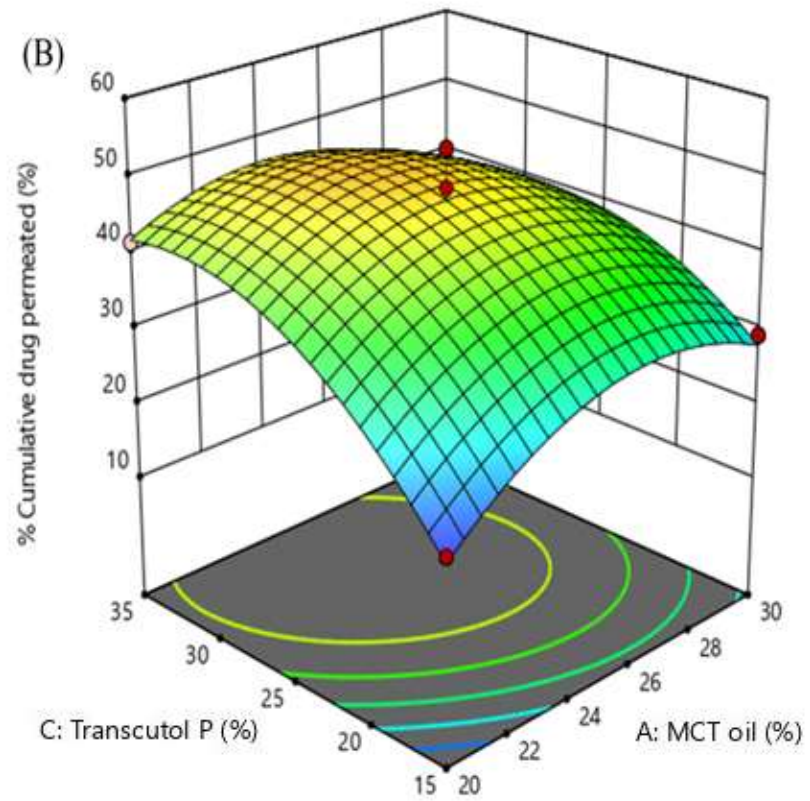
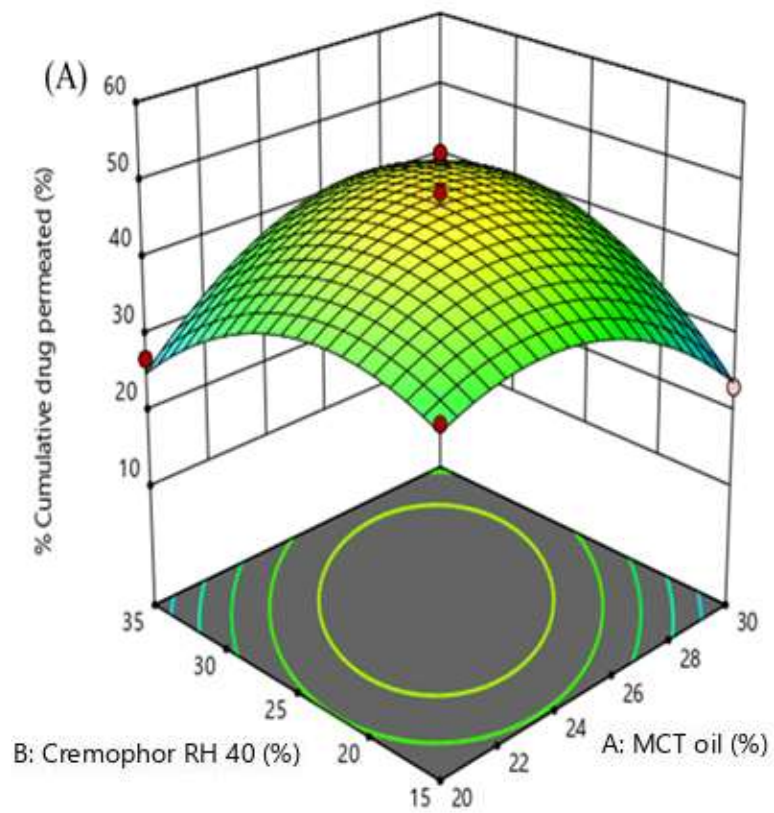


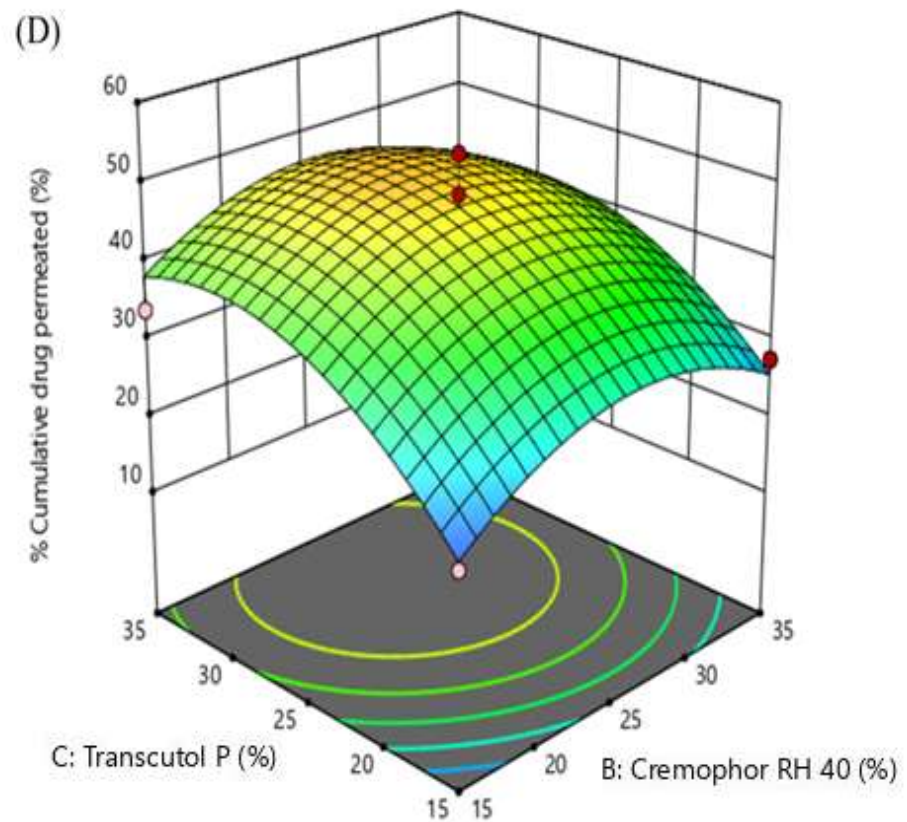
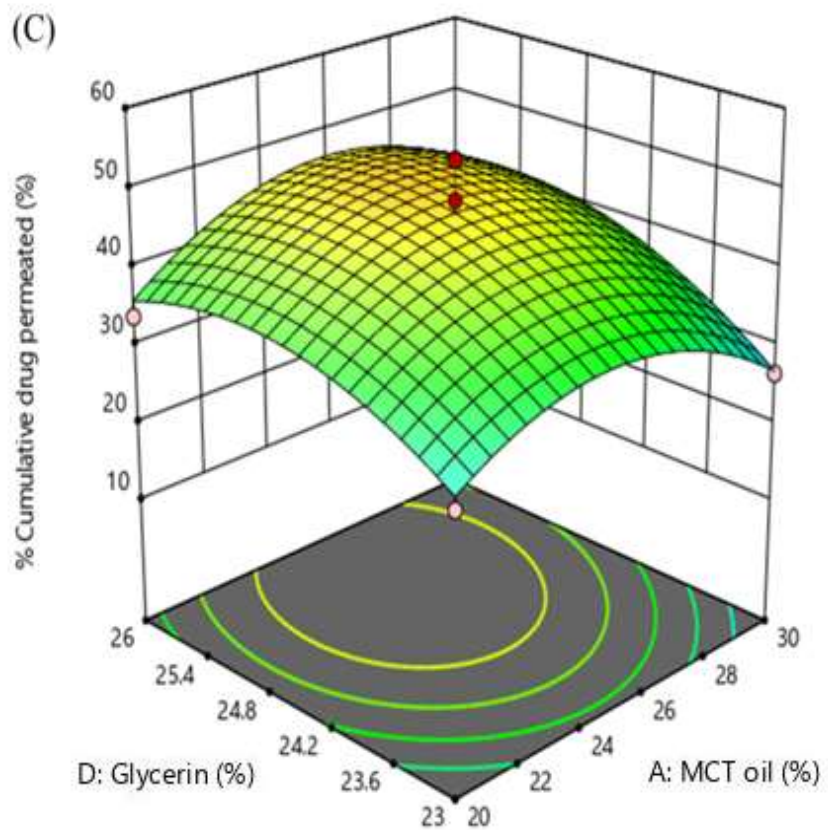


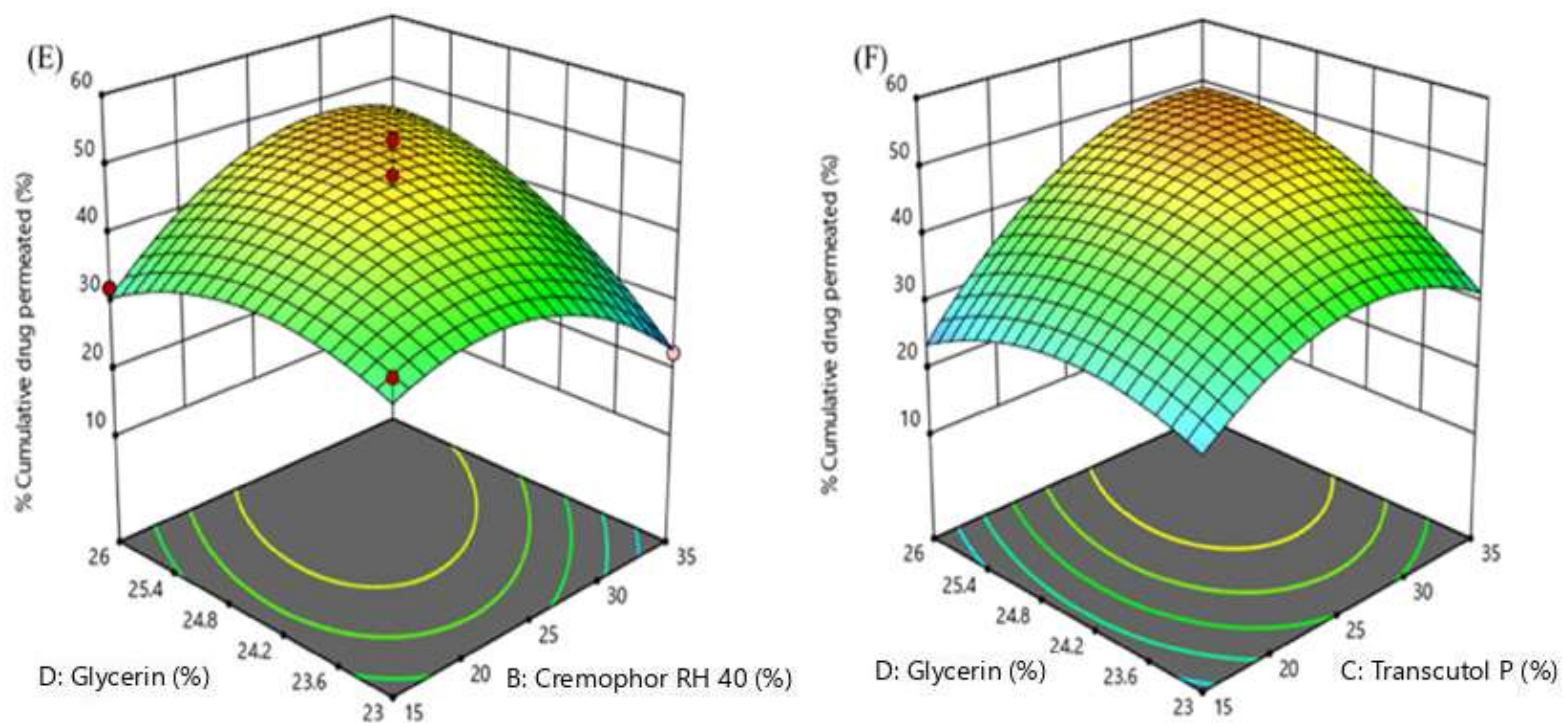


**Figure 37.** Contour plots for the effect of (A) MCT oil and Cremophor RH 40 (B) MCT oil and Transcutol P (C) MCT oil and Glycerin (D) Cremophor RH 40 and Transcutol P (E) Cremophor RH 40 and Glycerin (F) Transcutol P and Glycerin on % cumulative drug permeated

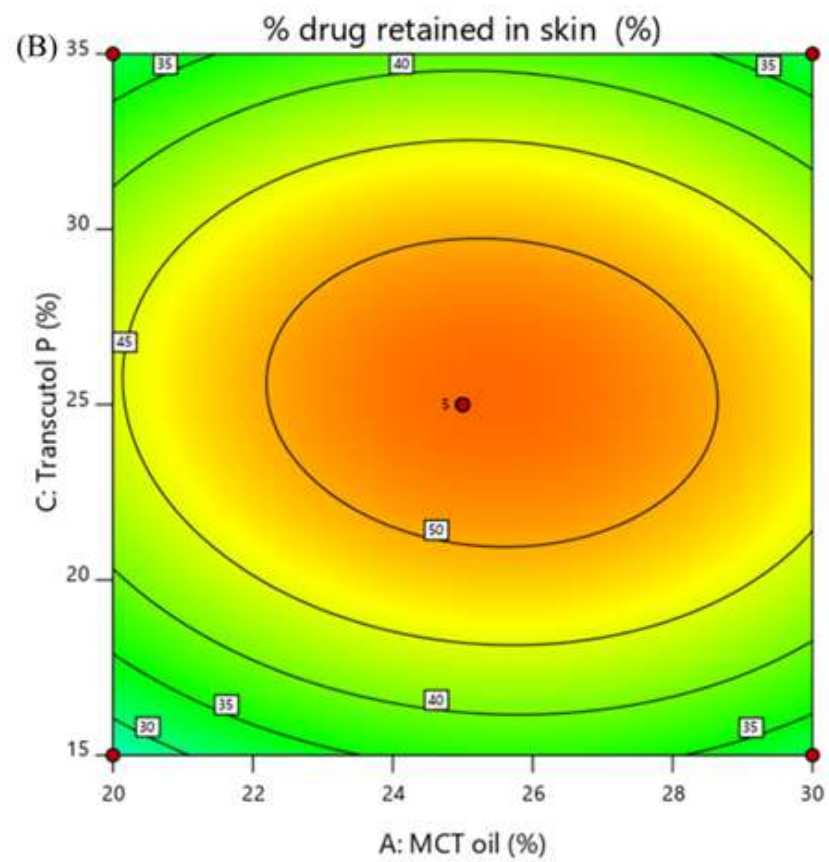
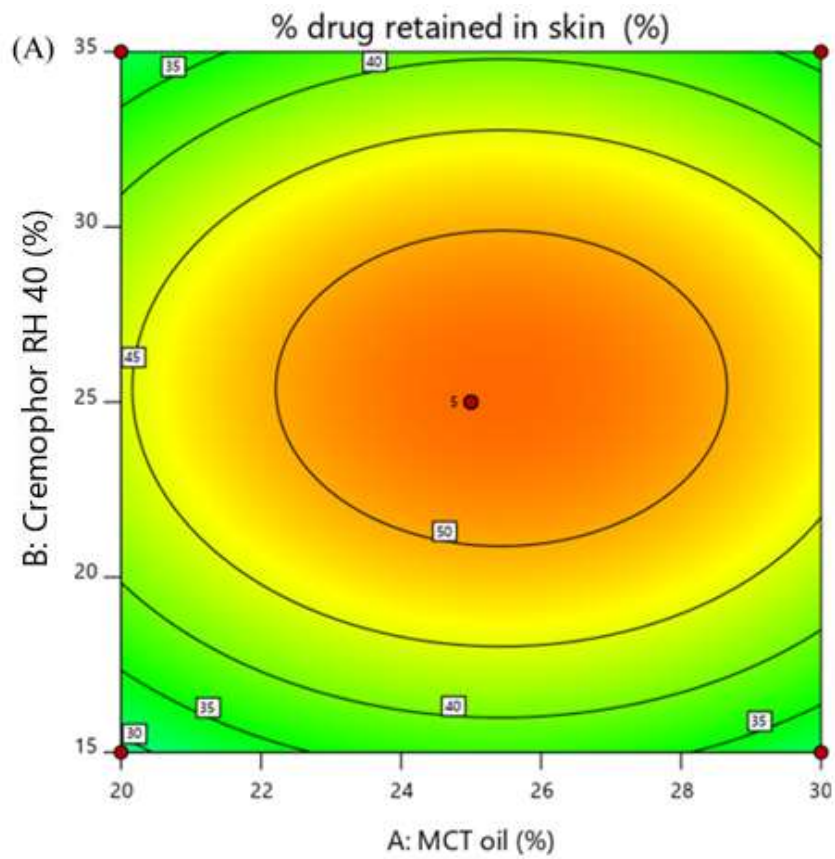


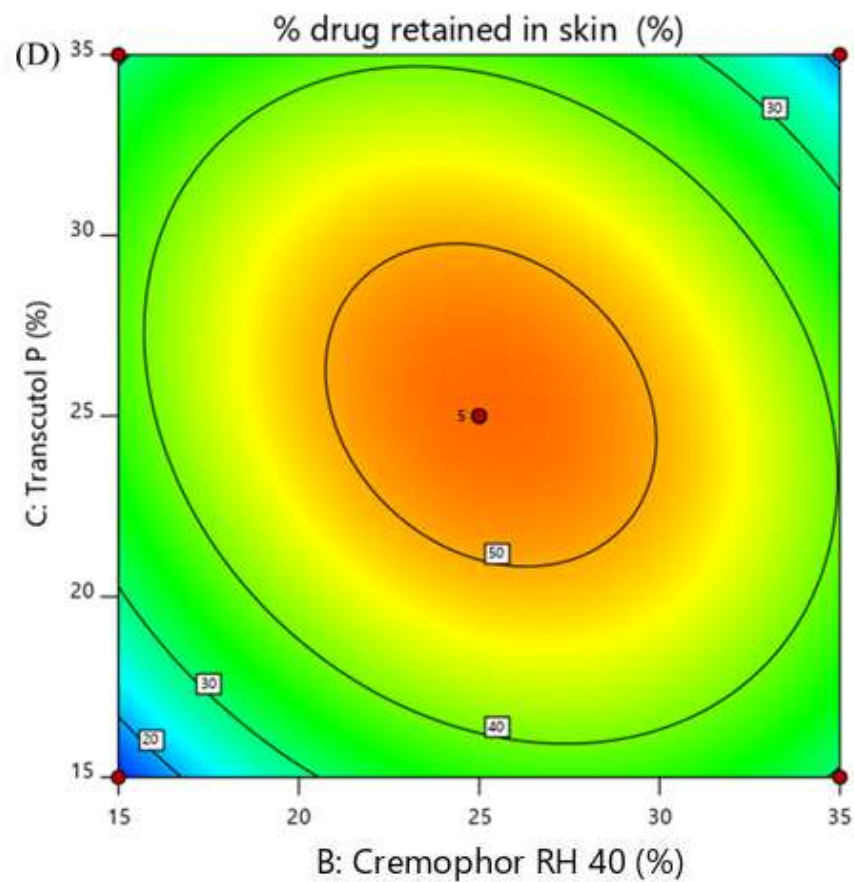
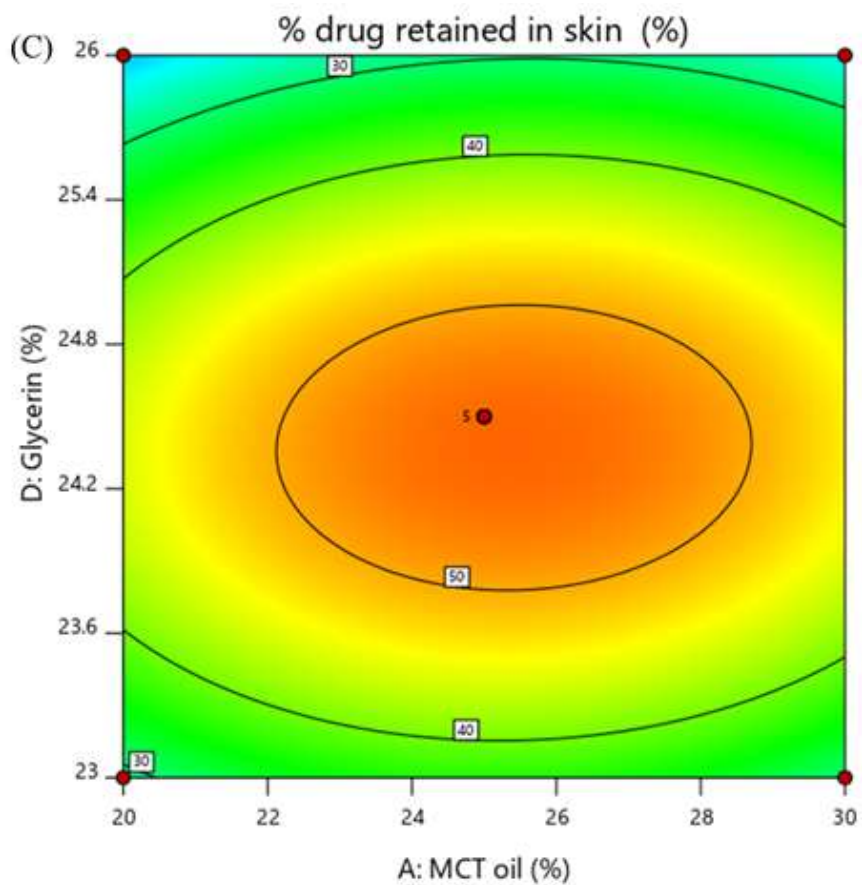


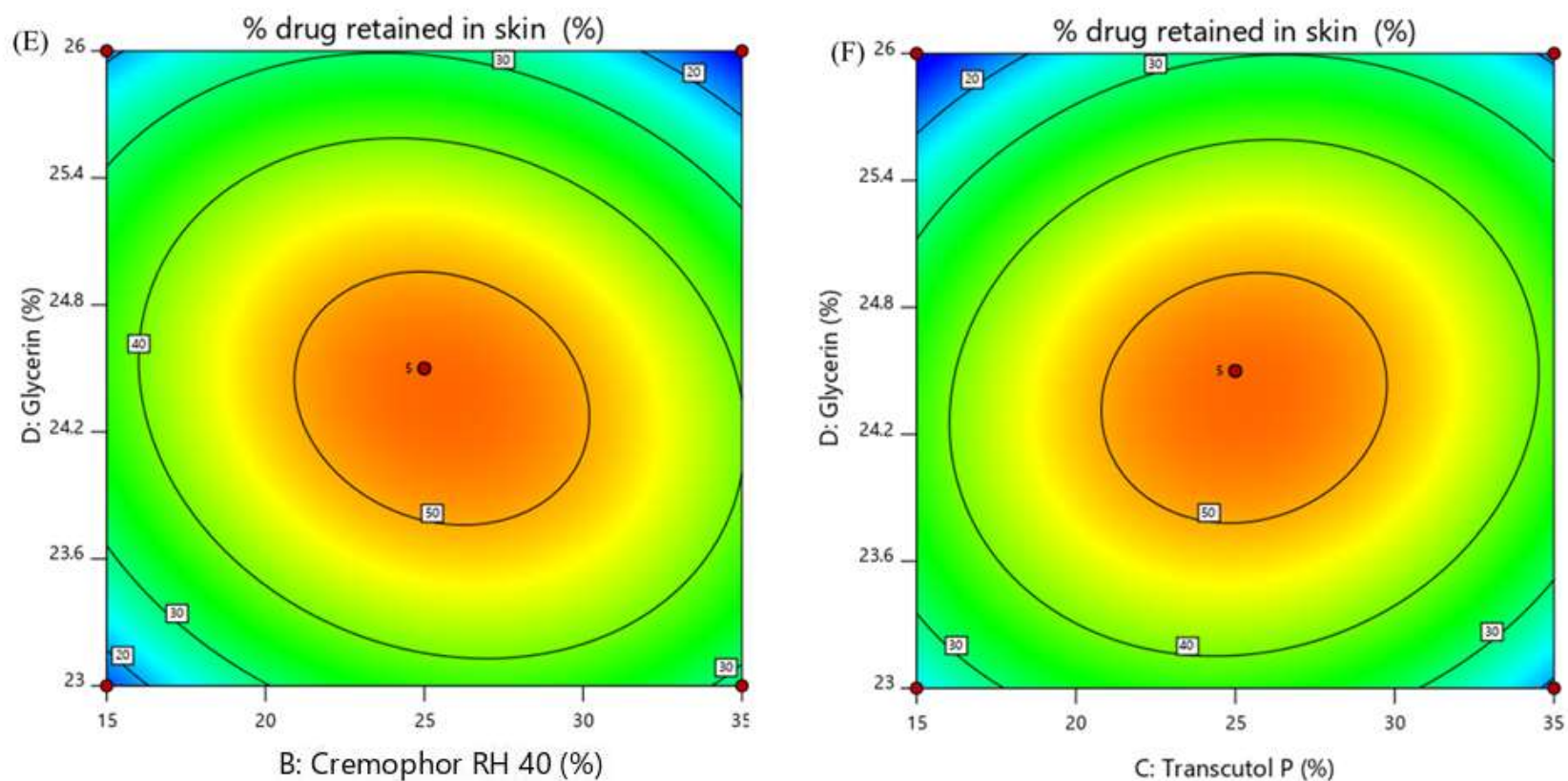




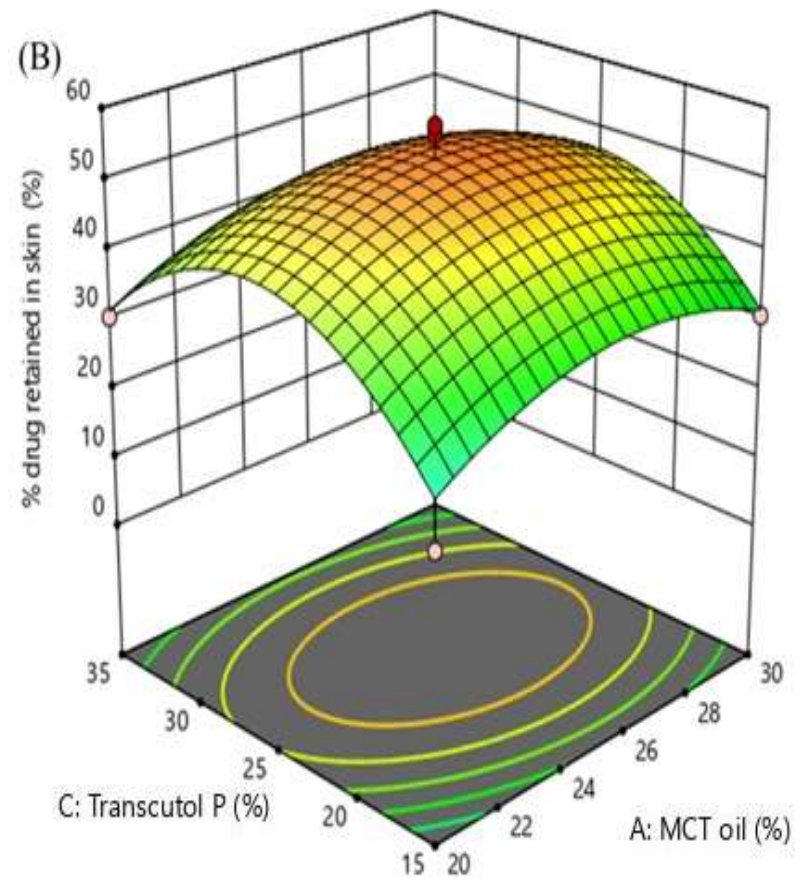
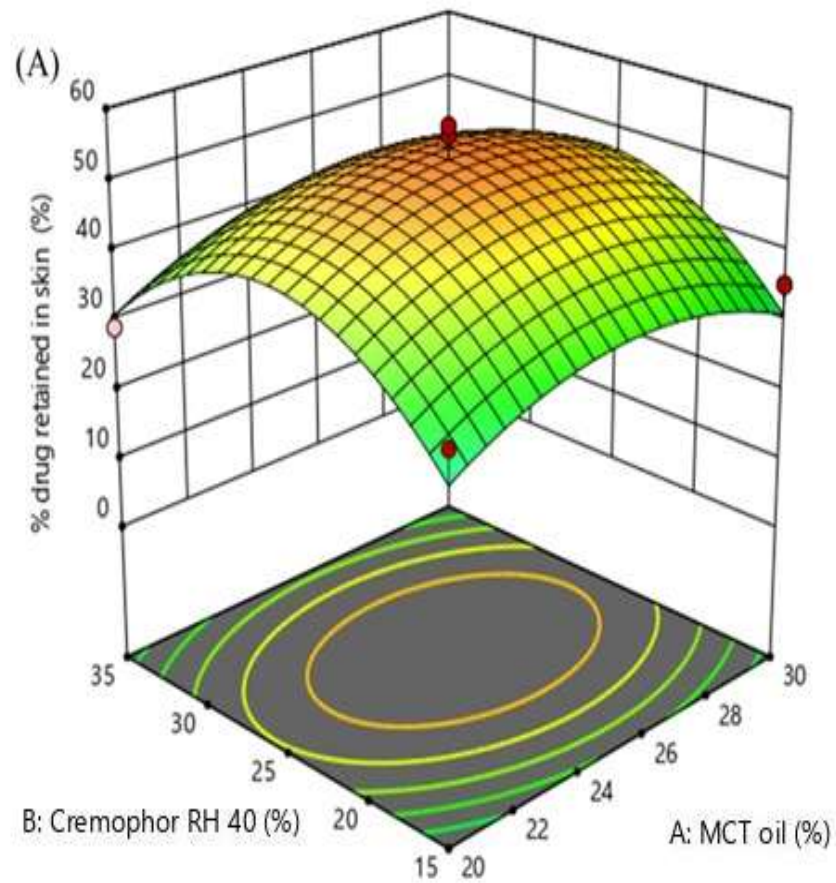
**Figure 38.** 3D response surface plot for the effect of (A) MCT oil and Cremophor RH 40 (B) MCT oil and Transcutol P (C) MCT oil and Glycerin (D) Cremophor RH 40 and Transcutol P (E) Cremophor RH 40 and Glycerin (F) Transcutol P and Glycerin on % cumulative drug permeated

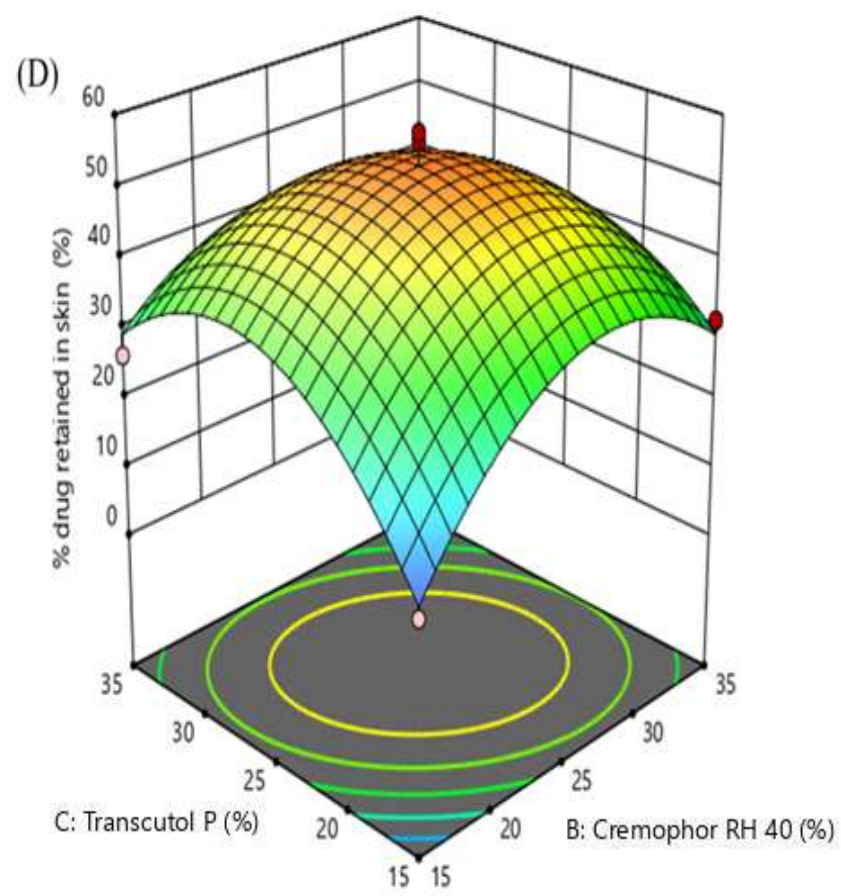
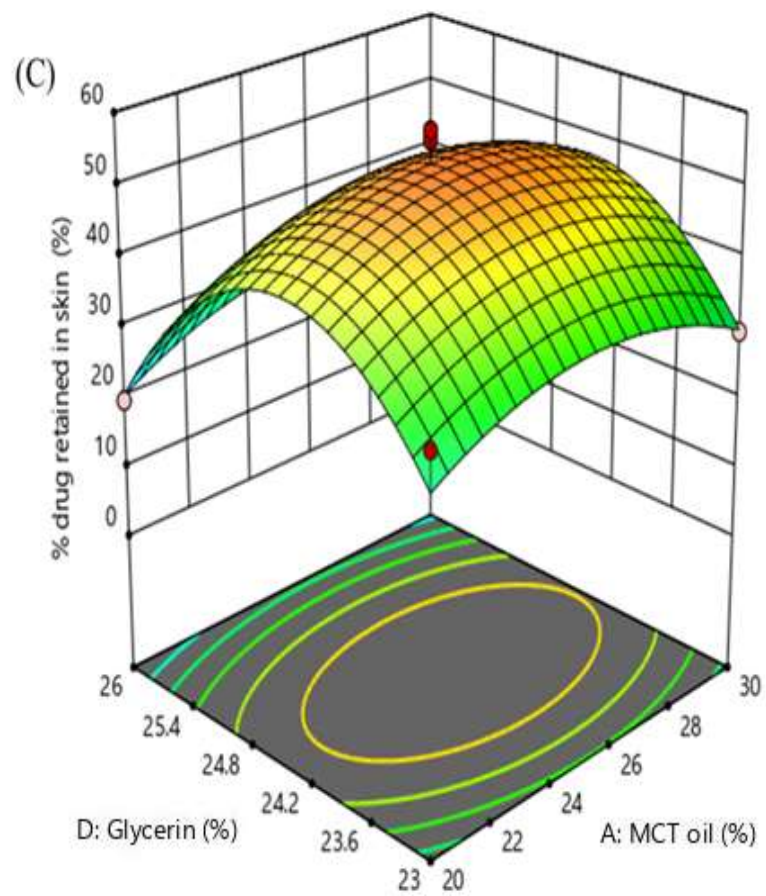






**Figure 39.** Contour plots for the effect of (A) MCT oil and Cremophor RH 40 (B) MCT oil and Transcutol P (C) MCT oil and Glycerin (D) Cremophor RH 40 and Transcutol P (E) Cremophor RH 40 and Glycerin (F) Transcutol P and Glycerin on % drug retained in the skin







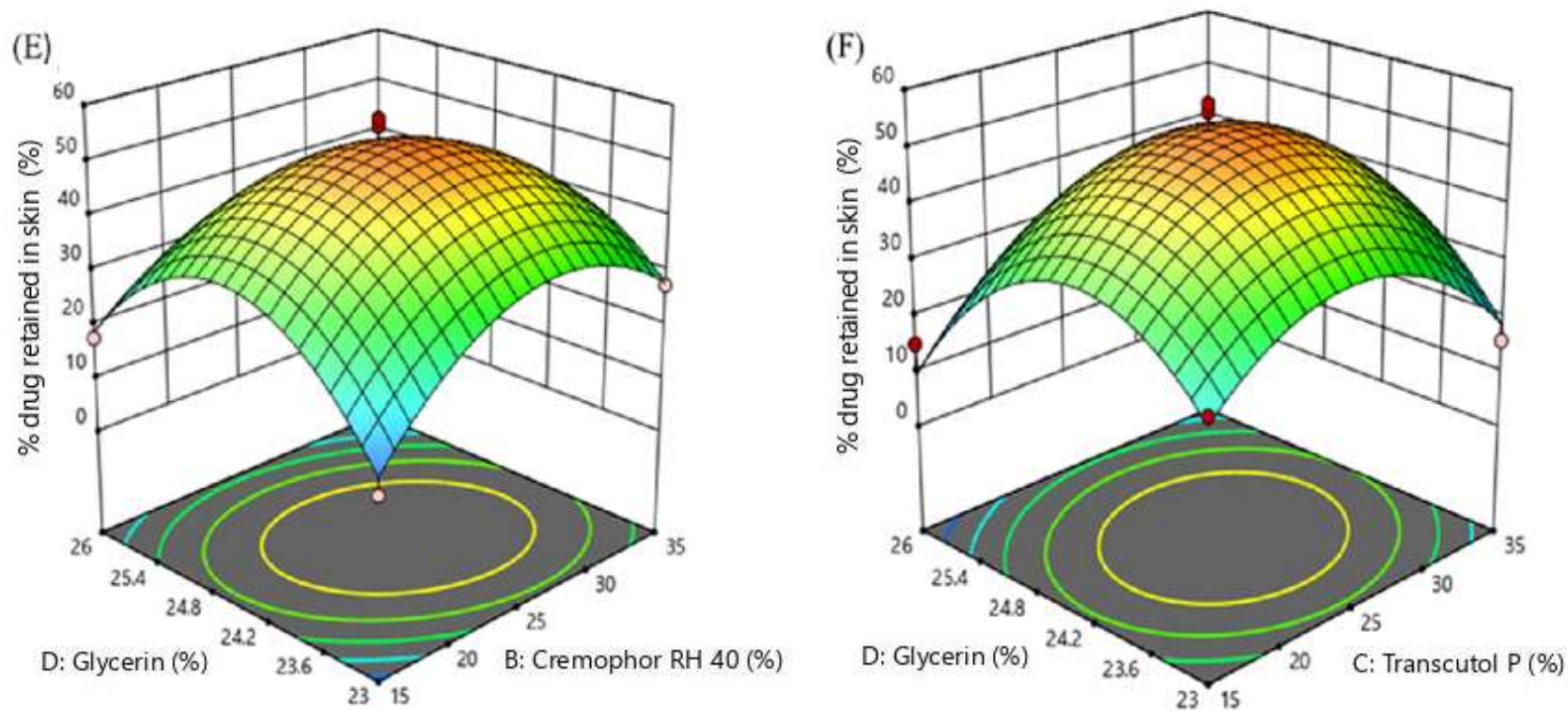


**Figure 40.** 3D response surface plot for the effect of (A) MCT oil and Cremophor RH 40 (B) MCT oil and Transcutol P (C) MCT oil and Glycerin (D) Cremophor RH 40 and Transcutol P (E) Cremophor RH 40 and Glycerin (F) Transcutol P and Glycerin on % drug retained in the skin.

Graphical optimization of NANE was carried out by considering the effects of each factor ( $X_1$ ,  $X_2$ ,  $X_3$ , and  $X_4$ ) on the respective responses. The predicted response ranges were as follow -  $Y_1$  : 54.44 to 101.82 nm;  $Y_2$  : -8.46 to -3.32 mV;  $Y_3$ : 80.14 to 112.83%;  $Y_4$  : 12.28 to 27.33 %;  $Y_5$  : 22.24 to 43.06 %. The predicted optimized composition for the formulation obtained through BBD for the selected four factors were 20 % v/v of  $X_1$ , 29 % v/v of  $X_2$ , 16 % v/v of  $X_3$  and 24 % v/v of  $X_4$ . An overlay plot represented the optimized parameters and the predicted responses with their limits as shown in **Figure 41**. Using the predicted values of  $X_1$ ,  $X_2$ ,  $X_3$ , and  $X_4$ , a new formulation AGE NANE (1000  $\mu$ L) was prepared using  $X_1$  (224  $\mu$ L),  $X_2$ , (326  $\mu$ L),  $X_3$  (180  $\mu$ L) and  $X_4$  (270  $\mu$ L) and all the responses were evaluated in triplicate. The obtained value for  $Y_1$  was  $60.81 \pm 18.88$  nm;  $Y_2$  was  $-7.99 \pm 4.14$  mV;  $Y_3$  was  $96.99 \pm 0.398\%$ ;  $Y_4$  was  $26.98 \pm 1.03\%$  and  $Y_5$  was  $32.87 \pm 1.98\%$ . The  $p$ -value between the predicted responses and observed responses were higher than 0.05 which indicated a non-significant difference. This confirmed the reproducibility of the optimized method. The optimized AGE NANE is shown in **Figure 42** and it was found to be transparent. Further, characterization of the optimized AGE NANE was carried out.

Design-Expert® Software  
Factor Coding: Actual

**Overlay Plot**

- Droplet Size
- PI Low
- PI High
- Zeta potential
- PI Low
- PI High
- Drug loading
- PI Low
- PI High
- % Cumulative drug permeated
- PI Low
- PI High
- % drug retained in skin
- PI Low
- PI High

X1 = A: MCT oil  
X2 = B: Cremophor RH 40

**Actual Factors**

C: Transcutol P = 16.6207  
D: Glycerin = 24.3395

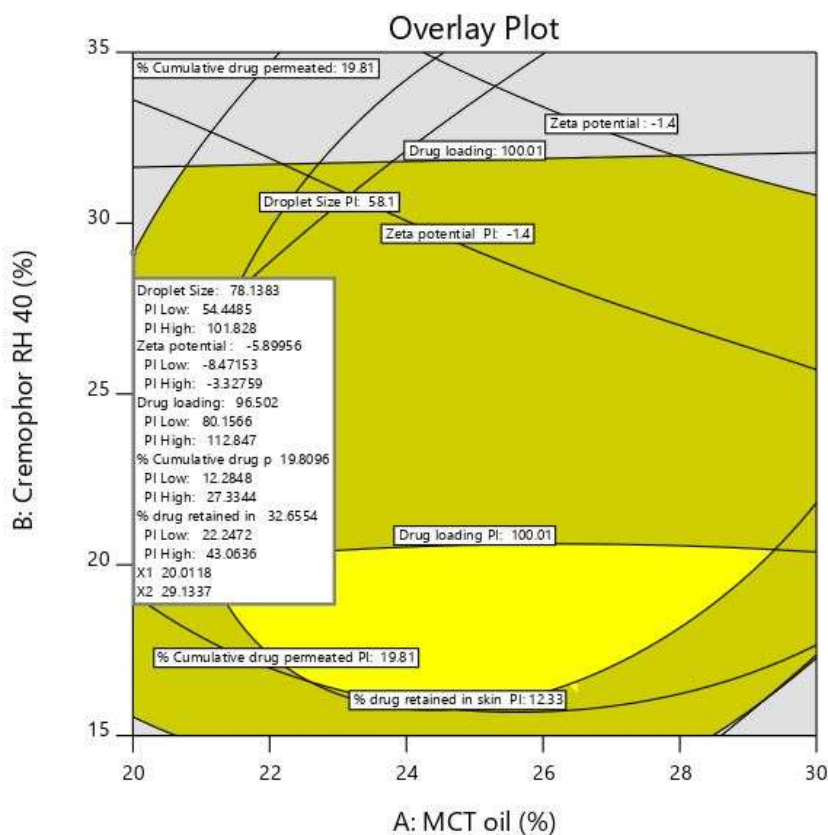


Figure 41. Overlay plot represents the optimized parameters for obtaining nanoemulsion



**Figure 42.** Optimized AGE NANE

### **5.11.7. Characterization of AGE loaded NANE**

#### ***5.11.7.1. Droplet size analysis and PDI***

Optimized AGE NANE was found to be transparent having a droplet size of  $60.81 \pm 18.88$  nm and a uniform PDI of 0.113 (**Figure 43**). The uniformity in the droplet size and narrow size unimodal distribution of globules were observed which showed the ability of surfactant to form a closely packed film at the interface of two immiscible phases. This observation account to smaller droplet size which helps in further stabilization of the developed NANEs.

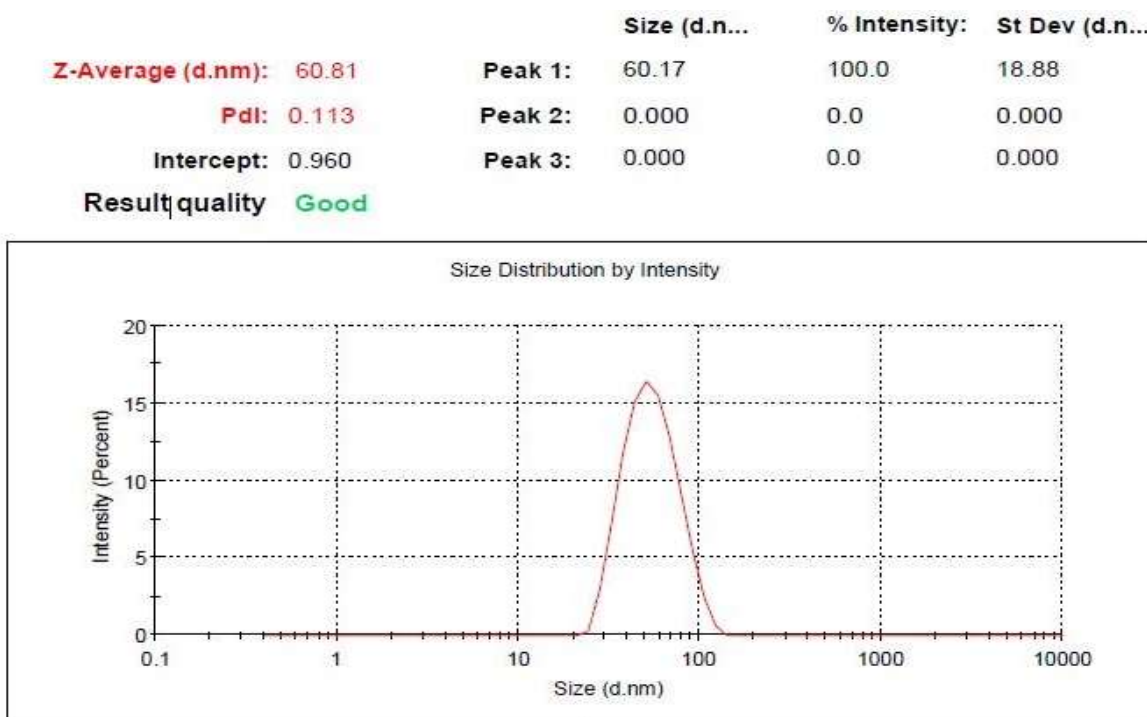


**Figure 43.** Globule size analysis and PDI of optimized AGE NANE

**5.11.7.2. Zeta potential**

The surface charge of the droplets and the electrostatic force between these charged globules decreases the possibilities of coalescence. Zeta potential is a parameter that determines the stability of the formulation. The zeta potential of the NANE was found to be  $-7.99 \text{ mV} \pm 4.14 \text{ mV}$  (**Figure 44**). In the developed formulation, the presence of fatty acids in the MCT oil, chemically caprylic/capric acid triglyceride that generally imparts a surface charge to the droplets. The negative charge on the droplet prevents agglomeration of the nanosized droplets.

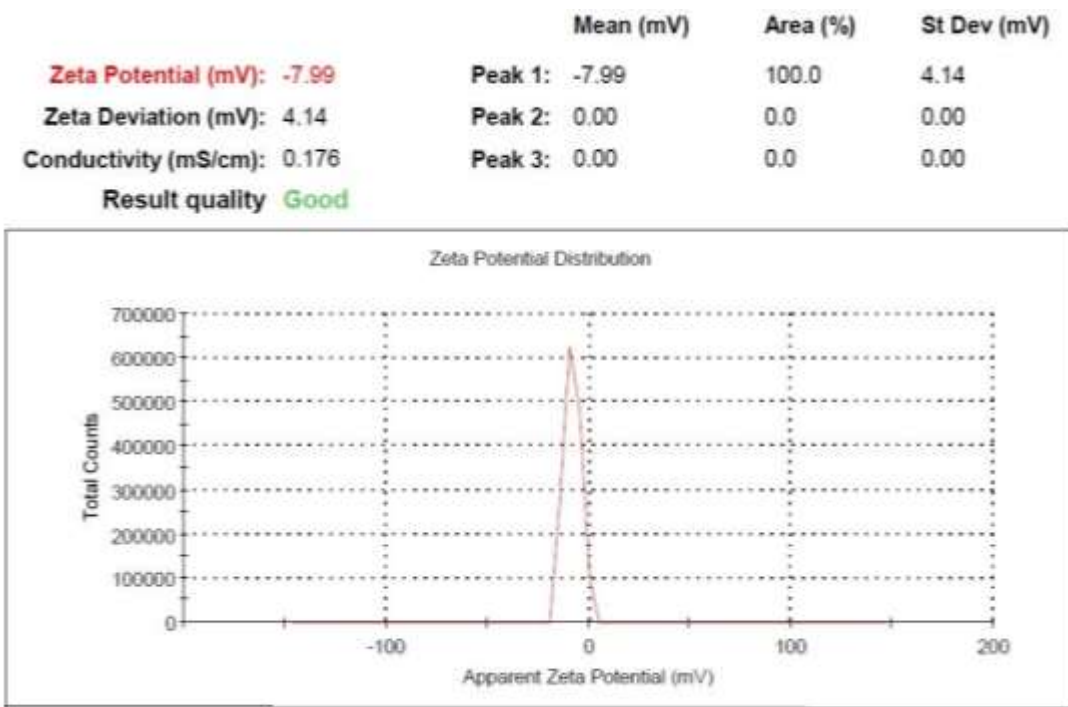


**Figure 44.** Zeta potential of optimized AGE NANE

#### **5.11.7.3. Drug loading**

The maximum drug loading capacity of the optimized AGE NANE was found to be  $96.99 \pm 0.398\%$ .

#### **5.11.7.4. Thermodynamic stability testing of the selected NANE**

AGE NANE was subjected to different thermodynamic stability testing such as heating-cooling cycle, centrifugation test and freeze-thaw cycle and no physical instabilities like creaming, cracking and coalescence occur which indicated that the optimized formulation is thermodynamically stable.

#### **5.11.7.5. Optical microscopy of AGE NANE**

The microscopic examination of methylene blue mixed AGE NANE was carried out to identify the nature of dispersed phase and continuous phase as shown in **Figure 45**. The image represented dark blue continuous background with colourless globules dispersed in it. This confirmed that the optimized AGE NANE have oil phase (MCT oil) as the dispersed phase and non-aqueous polar phase (glycerin) as the continuous phase.



**Figure 45.** Optical microscopy of methylene blue loaded AGE NANE

#### **5.11.7.6 HR-TEM**

The morphological characterization of the optimized AGE NANE carried out with HR-TEM is shown in **Figure 46**. The images represented spherical shape droplets and the measured average size of the droplets ( $65.40 \pm 23.07$  nm) complies with the results of droplet size analysis as mentioned in 4.4. The HR-TEM images clearly exhibited nanosize ( $< 100$  nm) spherical globules with no agglomeration.

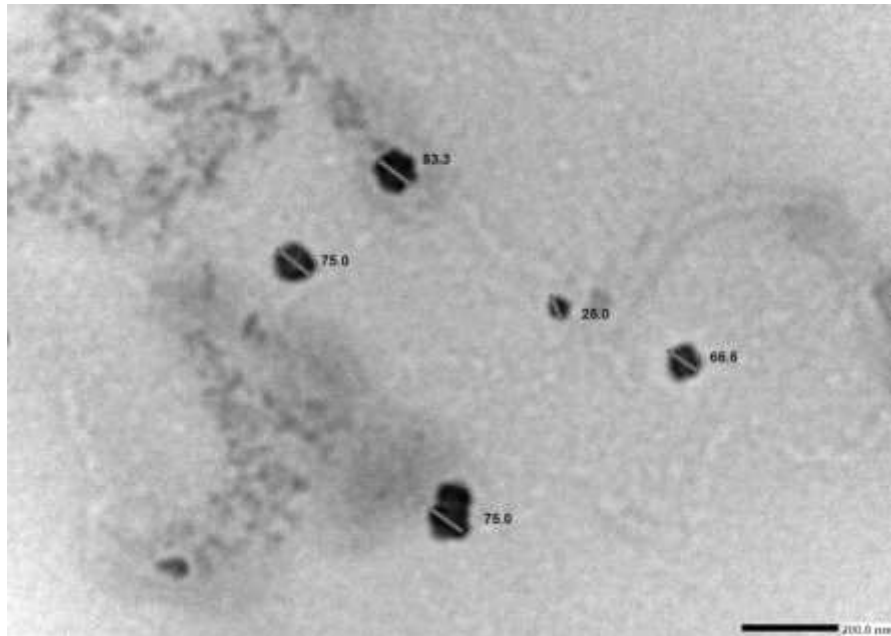


**Figure 46.** HR-TEM image of the optimized AGE NANE

**5.11.7.7. Refractive index, pH and viscosity**

Refractive index is an optical property measured to determine the isotropic nature of the nanoemulsion. Apart from this, the measurement represented the chemical interaction among the components in the formulation (Kotta et al., 2015). The mean value of refractive index of the optimized AGE NANE was found to be  $1.451 \pm 0.01$  which was similar to the refractive index of glycerin (1.467) indicating isotropic nature of the nanoemulsion.

The normal pH of the healthy skin stratum is 4.1 to 5.8 and formulations with this pH have shown no skin irritation (Proksch, 2018). The optimized AGE NANE was reported to have a pH of  $5.88 \pm 0.02$  which is acceptable to be applied on the skin without causing any irritation. The viscosity of the optimized NANE measured at 25°C was found to be 1450 mPa.s and torque was reported to be 0.203 mNm. **Figure 47** represents the viscosity versus shear rate plot which indicated decrease in the viscosity with increase in shear rate. The result exhibited shear-thinning property, which indicated its ability to be applied on the skin when stress is applied (Kong et al., 2018).

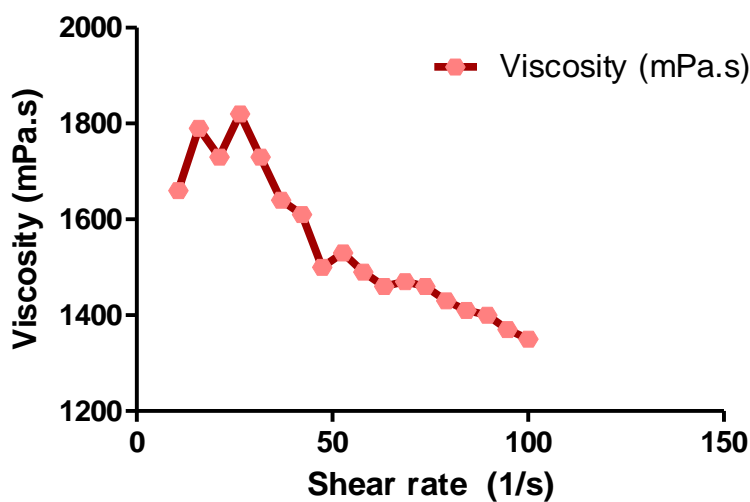


**Figure 47.** Relationship between viscosity and shear rate



#### **5.11.7.8. Spreadability**

The spreadability of the topical formulation determines its ability to adhere to the site of application. In this study, spreadability of the optimized AGE NANE was found to be  $1685.39 \pm 42.14$  mm and spreadability factor was  $33.70 \pm 0.84$  mm<sup>2</sup>g<sup>-1</sup>. The increase in diameter with the application of weight showed the ability of the NANE to be easily applied on the skin with mild stress. The pseudoplastic behavior of the nanoemulsion confirmed by viscosity measurement is in agreement with the spreadability behavior of the nanoemulsion (Deuschle et al., 2015).

#### **5.11.7.9. In vitro drug diffusion studies**

The diffusion study of the AGE (ACA) from AGE NANE and AGE *per se* were performed using dialysis membrane. The *in vitro* diffusion studies of the ACA from the AGE *per se* have shown initial rapid release followed by constant release. The release of ACA from AGE *per se* and AGE NANE were insignificant (*p*-value obtained was 0.2172) till 6 h. The presence of ethanol in the AGE might be the reason for initial burst release. However, the optimized AGE NANE was found to show slow and controlled release of ACA after 6 h till 30 h. This release was significant (*p*-value was 0.0369) in comparison to the ACA release from the AGE *per se*. The initial amount of ACA released from AGE *per se* and AGE NANE was found to be  $760.88 \pm 15.54$  µg/cm<sup>2</sup> and  $716.53 \pm 18.76$  µg/cm<sup>2</sup> respectively. However, the amount of ACA release from extract *per se* and AGE NANE at 30 h were recorded as  $1140.54 \pm 12.93$  µg/cm<sup>2</sup> (29.32± 1.98%) and  $3217.80 \pm 11.98$  µg/cm<sup>2</sup> (82.72 ± 2.48%), respectively. The graphical representation of the % cumulative amount of drug released versus time is shown as **Figure 48**.

Hence, the *in vitro* diffusion rate of ACA from optimized NANE was fitted into different mathematical release model and results are listed in **Table 37**. On the basis of the correlation coefficient value; the best fit model for release was selected. The optimized AGE NANE was found to fit zero-order release pattern as the highest r<sup>2</sup> value of 0.9738 was obtained with zero-order equation. This shows that NANE acts as a reservoir for AGE and ACA was released from the inner phase to the outer phase and then further released into skin stratum. Therefore, the drug release followed zero-order kinetics and also delivered the drug in a sustained manner for prolonged period. The exponential value obtained for the release study from Korsmeyer-Peppas

model was less than 0.5 i.e. 0.3539, hence the release mechanism was reported to follow Fickian transport mechanism (Musa et al., 2013).

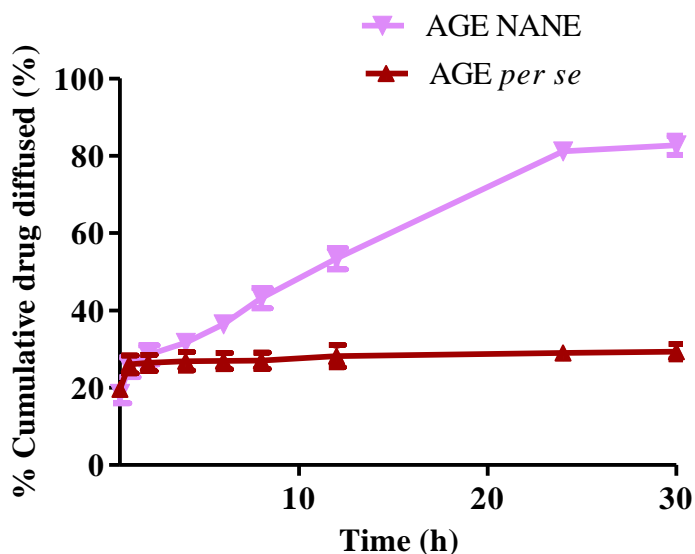


**Figure 48.** Comparison of % cumulative drug diffused from AGE *per se* and AGE NANE with respect to time

Hence, the *in vitro* diffusion rate of ACA from optimized NANE was fitted into different mathematical release model as shown in **Figure 49 (A-E)** and results are listed in **Table 39**. On the basis of the correlation coefficient value; the best fit model for release was selected. The optimized AGE NANE was found to fit to zero order release pattern as highest  $r^2$  of 0.9738 was obtained with zero order equation. This shows that NANE acts as a reservoir for AGE and drug was released from the inner phase to the outer phase and then further release into the skin stratum. Therefore, the drug release followed zero-order kinetics and also delivered the drug in a sustained manner for prolonged period. The exponential value obtained for the release study from Korsmeyer-Peppas model was less than 0.5 i.e. 0.3539, hence the release mechanism was reported to follow Fickian transport mechanism (Musa et al., 2013)

**Table 39.** Kinetic release model and correlation coefficient ( $r^2$ ) for optimized AGE NANE

<b>Kinetic model</b>	<b>(<math>r^2</math>)</b>
<b>Zero order</b>	0.9738
<b>First-order</b>	0.9618
<b>Higuchi model</b>	0.9580
<b>Korsmeyer- Peppas model</b>	0.9354
<b>Hixson-Crowell model</b>	0.9707

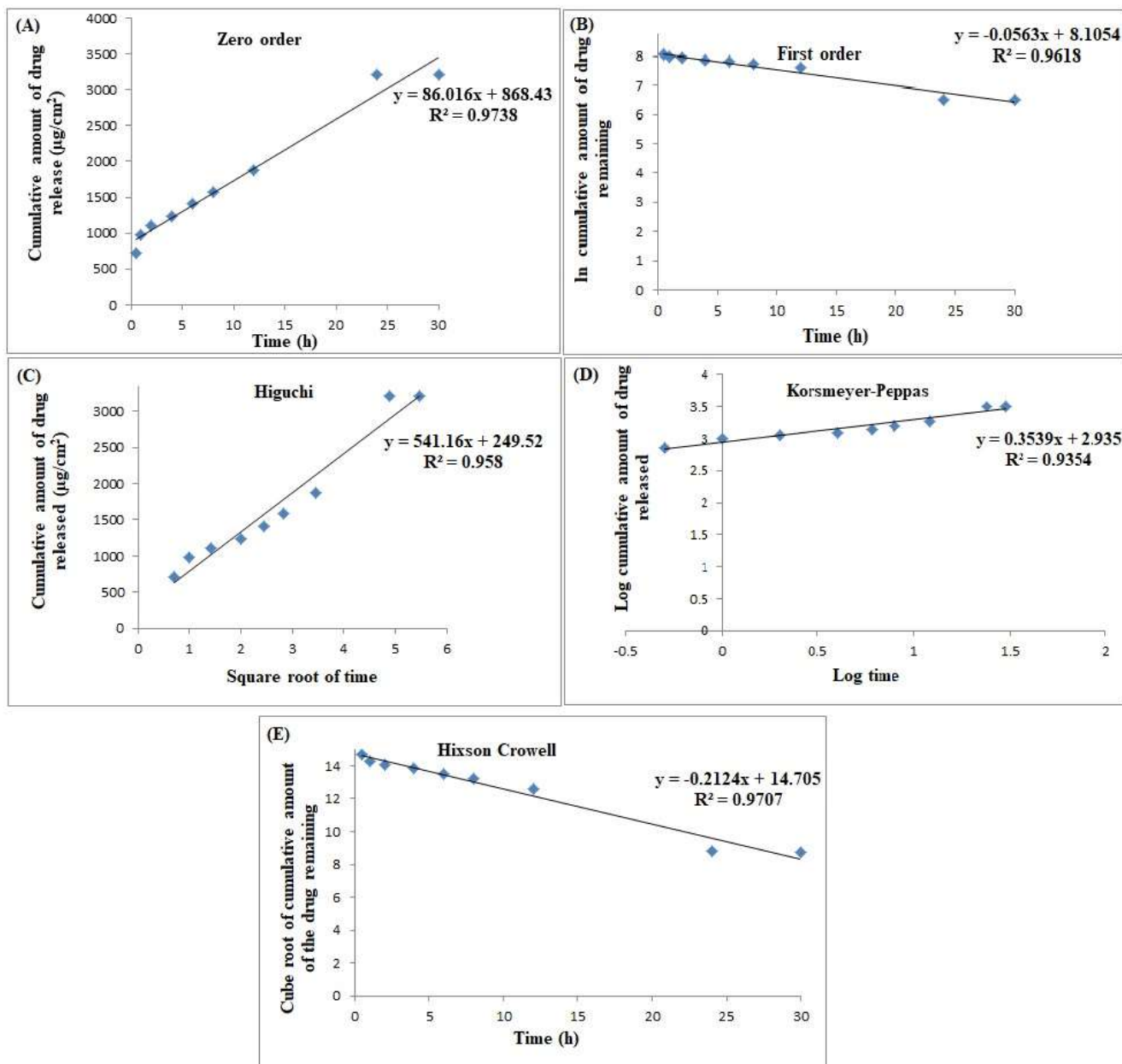


**Figure 49.** Prediction of kinetic release model for optimized AGE NANE (A) Zero-order kinetics-Percentage cumulative drug released versus time (B) First-order kinetics- ln cumulative drug remaining versus time (C) Higuchi model-Percentage cumulative drug released versus square root of time (D) Korsmeyer- Peppas model- Log percentage cumulative drug released versus log time (E) Hixson-Crowell- Cube root of cumulative amount of drug remaining versus time

**5.11.7.10. Ex vivo skin permeation studies**

The *ex vivo* permeation studies for AGE *per se* and AGE NANE were performed using porcine ear skin. The morphological and structural similarity of porcine skin to human skin resulted in selection of porcine skin for permeation studies (Neupane et al., 2020). The steady state flux was determined by plotting graph between cumulative amount of drug permeated versus time and comparing their results among each other is shown in **Figure 50**. The skin permeation rate of AGE *per se* and AGE NANE was non-significant ( $p$  value is 0.4943) in the initial period of drug release (till 6 h). Later, a significant permeation rate ( $p$  value is 0.0430) was observed till 30 h. After 24 h, a plateau was observed in permeation rate that indicated the achievement of equilibrium. Almost  $3123.32 \pm 100.95 \mu\text{g}/\text{cm}^2$  of the ACA was released from AGE NANE within 30 h whereas from AGE *per se*, release of ACA was found to be  $1026.60 \pm 41.53 \mu\text{g}/\text{cm}^2$  only.

The flux for AGE NANE and AGE *per se* at the end of 30 h was found to be  $125.58 \pm 8.36 \mu\text{g}/\text{cm}^2 \text{ h}^{-1}$  and  $12.02 \pm 1.64 \mu\text{g}/\text{cm}^2 \text{ h}^{-1}$  respectively. The enhancement ratio reported 10-folds increase in the flux for AGE NANE when compared to AGE *per se*. The higher permeation rate of NANE across the stratum corneum highly depends upon the physicochemical nature of the formulation which includes the globule size of the droplet as well as the interaction of components in the formulation with the stratum corneum. Among the components, permeation enhancer such as Transcutol P causes extraction of the lipid bilayer, thereby modifying the penetration pathway in the stratum. The permeability coefficient of AGE NANE was found to be  $3.228 \times 10^{-2} \pm 0.0004 \text{ cm h}^{-1}$  that was higher in comparison to the permeability coefficient of the AGE *per se* ( $3.09 \times 10^{-3} \pm 0.0003 \text{ cm h}^{-1}$ ). These results confirmed the active role of permeation enhancers in delivering the drug into the stratum corneum.

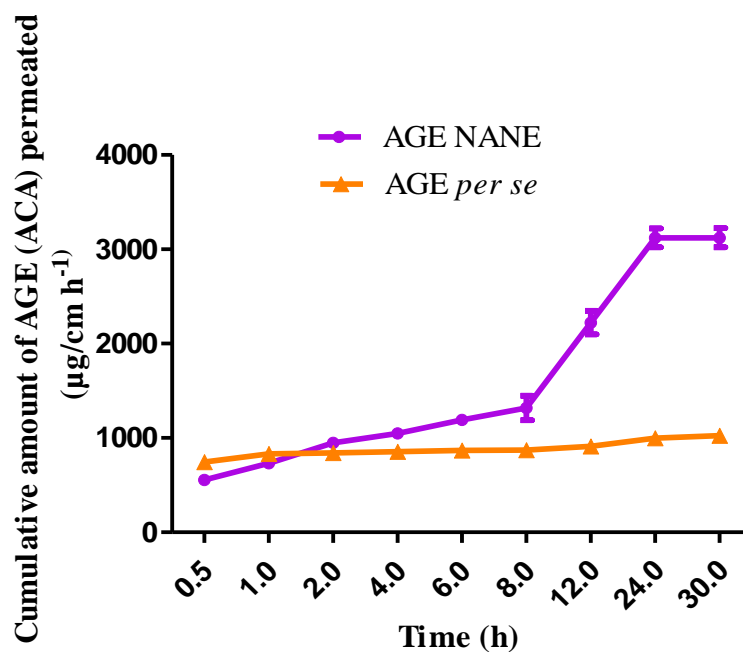


**Figure 50.** Comparison of cumulative amount of AGE (ACA) permeated through porcine ear skin with respect to time

#### 5.11.7.11. Drug retention studies

The amount of drug retained in the skin after application of optimized AGE NANE for 30 h was  $732.56 \pm 86.39 \mu\text{g}/\text{cm}^2$  which was higher in comparison to the AGE *per se* ( $221.56 \pm 54.56 \mu\text{g}/\text{cm}^2$ ). The higher retention in the skin stratum confirmed the penetration of nanosized formulation, into/across stratum corneum where they strongly interact with lipid matrix and proteins and they reside in the dermis.

#### 5.11.7.12. CLSM

The significant advantage of CLSM is the ability to visualize the depth of penetration of the fluorescent probe within a tissue sample. This visual examination depicts the mechanism of penetration of the drug in the skin strata. The first stage in the sample analysis is to carry out the permeation study of the samples using a fluorescent probe, followed by visualization of the fluorescent probe in the subjected tissue sample using the microscopic technique. Rhodamine B was selected as the fluorescent probe in the study. The selected probe is a lipophilic basic dye with red

fluorescence. The selection of this dye was based on the similarity of log P value of rhodamine B (1.95) with ACA (2.2) (Iyer and Eddington, 2019; PubChem).

Both RAD and R-NANE were prepared and *ex vivo* permeation studies were carried out for 24 h. In this study, the skin samples treated with RAD and R-NANE appeared as red coloured fluorescence. The intensity of the fluorescence signal was measured to analyze the mechanism of skin penetration and depth of drug uptake through the skin.

The depth of penetration and mechanism involved in cellular uptake of RAD and R-NANE was demonstrated in **Figure 51a and 51b** respectively. R-NANE has shown highly intense fluorescent signal both in viable epidermis and dermis. However, RAD has shown highly intense fluorescence limiting to upper layer of stratum corneum and lesser intense fluorescence in the deeper skin stratum. Furthermore, R-NANE has shown bright red fluorescence in the skin appendages representing its ability to participate in transfollicular transport mechanism.

The deeper and better penetration of NANE into various layers of skin's strata and possible reasons of penetration into skin are explained with respect to the components present in the NANE. Firstly, presence of Transcutol P, which is a penetration enhancer, modifies the orderly arranged-lipid bilayer and multi-lamellar skin structure. Secondly, the presence of oils in the NANE provides lubricant effect to the tough keratinized skin stratum enabling the NANE to cross the skin stratum.

Similar conclusion was reported by Khatoon et al. 2021. The study demonstrated rhodamine B assisted penetration study of nanoemulsion containing three bioactive components curcumin, resveratrol, and thymoquinone. The study concluded that aqueous dispersion of rhodamine B has shown lesser penetration into skin strata and remained at the upper layer of the stratum even after 24 h whereas rhodamine B loaded nanoemulsion has shown higher fluorescent intensity both in the viable epidermis and dermis (Khatoon et al., 2021).

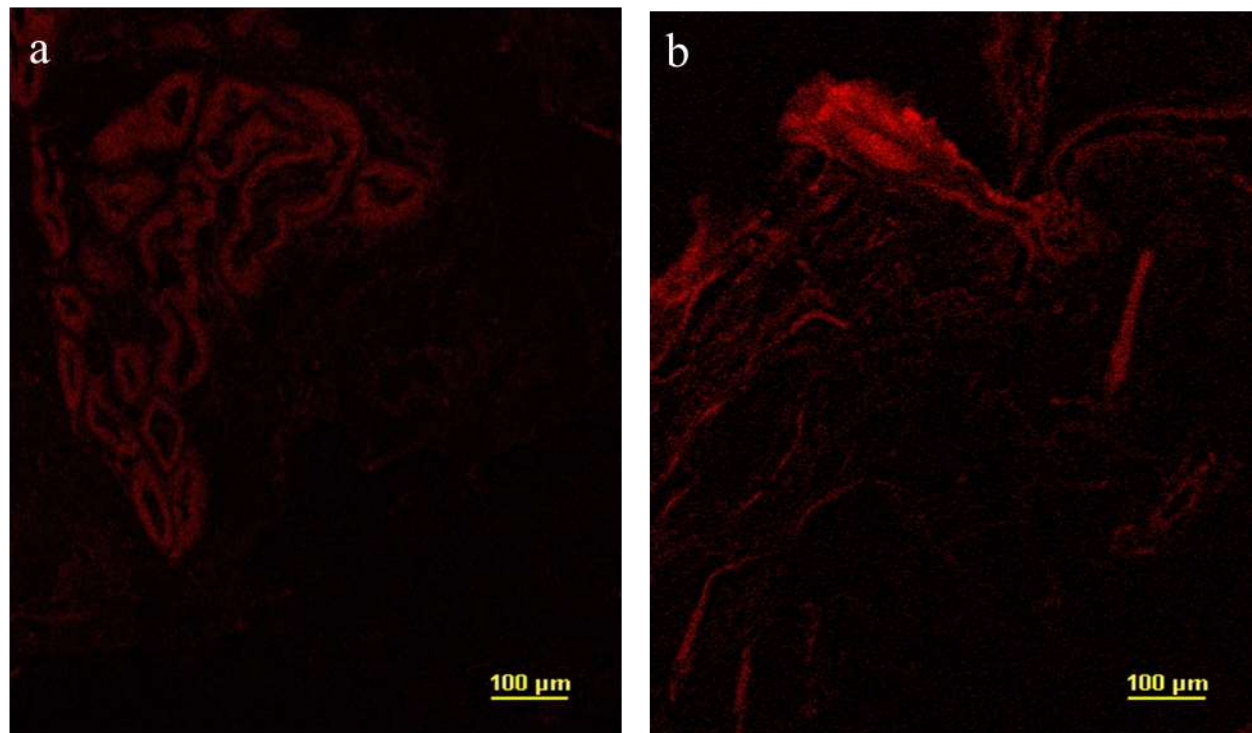


**Figure 51.** CLSM in porcine skin (a) RAD (b) R-NANE

#### *5.11.7.13. Stability studies*

The stability studies of AGE NANE were carried out at accelerated condition of  $40 \pm 2^\circ\text{C} / 75 \pm 5\%$  RH for a period of 6 months. The results of various parameters such as physical appearance, droplet size, zeta potential, drug loading, % cumulative drug permeated and % drug retained for aged AGE NANE are recorded as shown in **Table 40**.

AGE NANE stored at accelerated condition ( $40 \pm 2^\circ\text{C} / 75 \pm 5\%$  RH) for 3 months and 6 months have shown insignificant difference ( $p > 0.05$ ) in comparison to the freshly prepared AGE NANE. The freshly prepared AGE NANE was analyzed and droplet size was recorded as ( $60.81 \pm 1.75$  nm), zeta potential ( $7.39 \pm 1.35$  mV), and % drug loading ( $96.56 \pm 1.15\%$ ). The % cumulative drug permeated in 24 h was found to be  $83.67 \pm 1.75\%$  and % drug retention after 24 h was recorded as  $10.65 \pm 1.02\%$ .

Overall, stability studies showed that the optimized AGE NANE was found to be stable at  $40 \pm 2^\circ\text{C} / 75 \pm 5\%$ .



**Table 40.** Stability studies for AGE NANE and results of various parameters

Time (months)	Physical appearance	Droplet size (nm) (mean ± S.D.)	Zeta potential (mean ± S.D.)	% Drug loading (mean ± S.D.)	% Cumulative drug permeated (mean ± S.D.) after 24 h	% Drug retained (mean ± S.D.)
0	Homogenous phase	60.81 ± 1.75	-7.39 ± 1.25	96.56 ± 1.15	83.67 ± 1.75	10.65 ± 1.02
<b>40 ± 2°C (75 ± 5 % RH)</b>						
3	Homogenous phase	63.14 ± 1.53	-7.06 ± 1.14	95.11 ± 1.13	81.32 ± 3.12	11.59 ± 1.27
6	Homogenous phase	64.98 ± 1.54	-7.00 ± 1.03	94.63 ± 1.36	79.21 ± 2.87	12.88 ± 1.56

## 5.12. Pharmacodynamic studies

### 5.12.1. HET-CAM test for anti-angiogenic activity

An abnormality in angiogenesis is involved in the early stages of psoriasis progression. During keratinocyte proliferation, infiltration of multiple immune cells, as well as several angiogenic mediators such as vascular endothelial growth factor (VEGF), TNF, angiopoietin, IL-8, IL-17, hypoxia-inducible factors, are involved in the formation of skin lesions. These pro-angiogenic mediators promote micro-vascularization and vasodilation, preparing the skin for hyperproliferation.

The anti-angiogenic activity of the prepared samples was examined on the HET-CAM model. A comparison of the blood vessel formation/ inhibition is clearly represented in before and after treatment images shown in **Figure 52(A-F)**.

**Figure 52(A)** normal control group which showed normal development of capillary network which include primary and secondary blood vessels. However, primary blood vessels were more prominent before treatment whereas after the addition of 0.9% w/v of normal saline (after treatment), along with primary blood vessels mild rise in secondary blood vessels was observed. This inferred the occurrence of normal angiogenesis during developmental stage of an embryo.

**Figure 52(B)** represents positive control where marketed formulation (Betamethasone valerate (0.1% w/w) was applied. It was observed that primary blood vessels were more prominent along with few secondary blood vessels in the CAM before treatment. After treatment with betamethasone significant disappearance of primary blood vessels and secondary blood vessels

were observed showing the antiangiogenesis activity of the applied formulation. Observation from this study complies with the results of Lemus *et al.* They demonstrated antiangiogenesis effect of betamethasone on CAM model. A significant reduction in the vascular density was observed after treatment with methylcellulose disc instilled with betamethasone (0.08µg/mL). This confirmed the inhibitory role of betamethasone on embryonic neovascularization (Lemus *et al.*, 2001).

In contrary to the above-said observation, **Figure 52(C)** showed a significant increase in the capillary network which included primary, secondary and tertiary blood vessels showing the ability of pyruvic acid to promote angiogenesis. Lee *et al.* reported presence of higher rate of pyruvic acid in the tumor cells that are formed as end product from the abnormal metabolic pathway. It was also observed that higher pyruvic acid content in the tumor cells modulated neovascularization in the endothelial cells resulting in the growth and proliferation of tumor cells (Lee *et al.*, 2001).

In **Figure 52(D)**, a significant reduction in the primary and secondary blood vessels was observed after treatment with AGE *per se*. This infers the ability of phytoconstituents in AGE to promote antiangiogenic activity. **Figure 52(E)** showed complete disturbance/ disruption of the blood vessels after treatment with blank formulation (NANE-B). However, it should be noted that either the observed blood vessels disappeared or no new blood vessels were formed. **Figure 52(F)** showed significant inhibition of new blood vessel formation as well as disappearance of the observed primary blood vessels confirming the antiangiogenic activity which was non-significant when compared with experimental group (Betamethasone treated) and AGE *per se* treated group.

On the basis of the aforementioned observation, anti-angiogenic activity of all the prepared samples was evaluated and % inhibition of blood vessels was recorded in **Table 41**. The results obtained were statistically analyzed by one-way ANOVA (Tukey test).

AGE NANE has shown significant anti-angiogenic activity in comparison to the AGE *per se* and experimental control (standard betamethasone) group ( $p < 0.001$ ). The AGE NANE exhibited 1.8 folds and 1.5 folds increase in anti-angiogenic activity with respect to AGE *per se* and standard

betamethasone respectively. Group E treated with blank formulation has shown slight disruption in the blood vessels, along with inhibition of new blood formation.

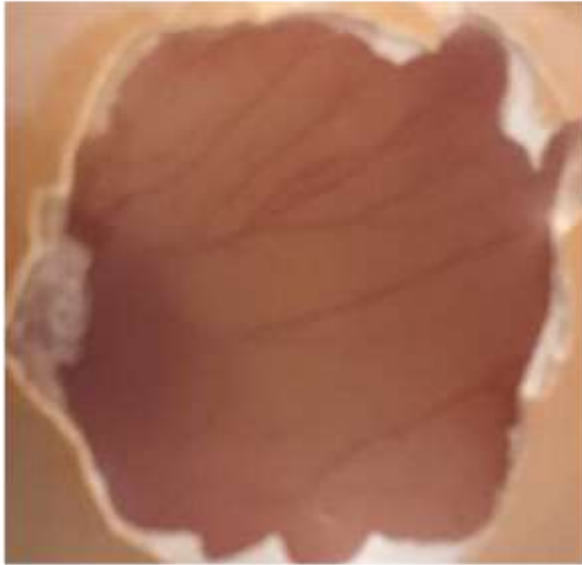
All these observations and results helped in understanding the anti-angiogenic effect of AGE NANE which is essential for the prevention of disease progression. This also confirmed that AGE NANE helps to prevent neo-vascularization that occurs in the early stages of psoriasis lesion development.

**Table 41.** Results of anti-angiogenic activity in HET-CAM

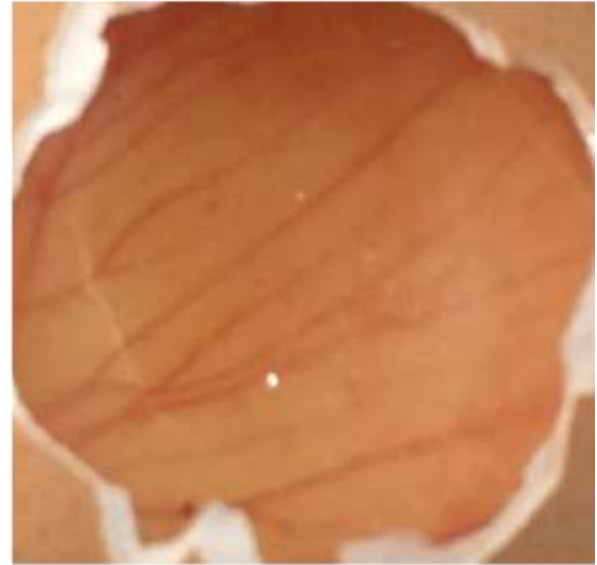
<b>Groups*</b>	<b>% inhibition of blood vessels</b>
Group A: Normal control	-42.466 ± 4.037
Group B: Positive control	33.193 ± 4.340
Group C: Negative control	-77.620 ± 7.427
Group D: AGE <i>per se</i>	28.876 ± 4.663
Group E: NANE-B	7.536 ± 4.001
Group F : AGE NANE	52.796 ± 7.314

Each group contain n=3 eggs; *p* <0.001 (one way ANOVA analysis)

(A) **Group A: Normal control**



**Before treatment**

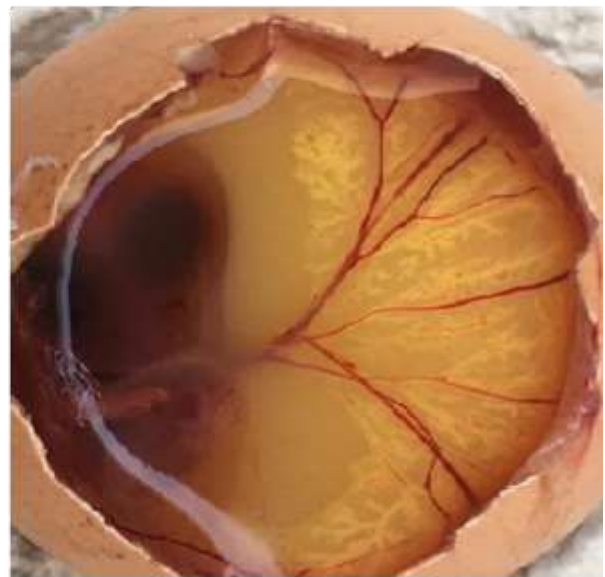


**After treatment**

(B) **Group B: Positive control**

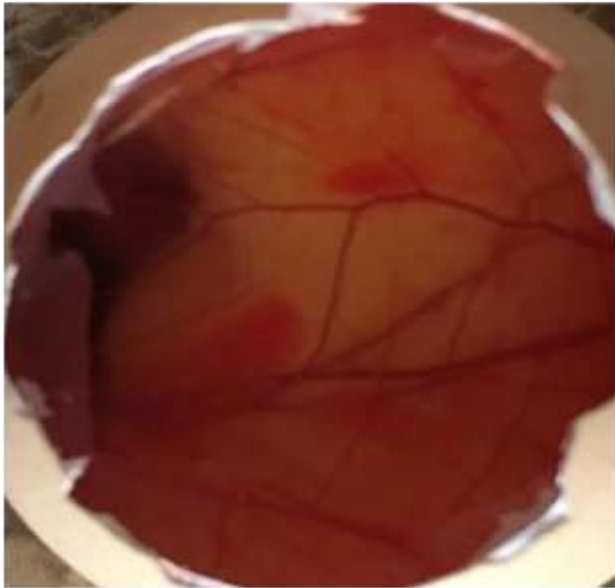


**Before treatment**

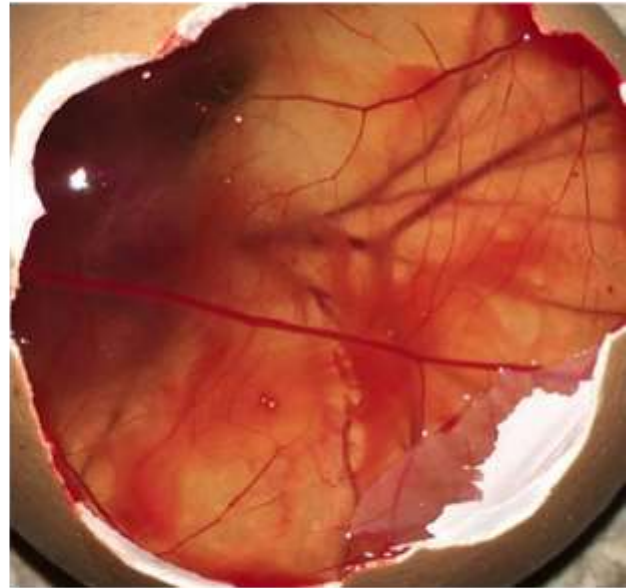


**After treatment**

(C) **Group C: Negative control**



**Before treatment**

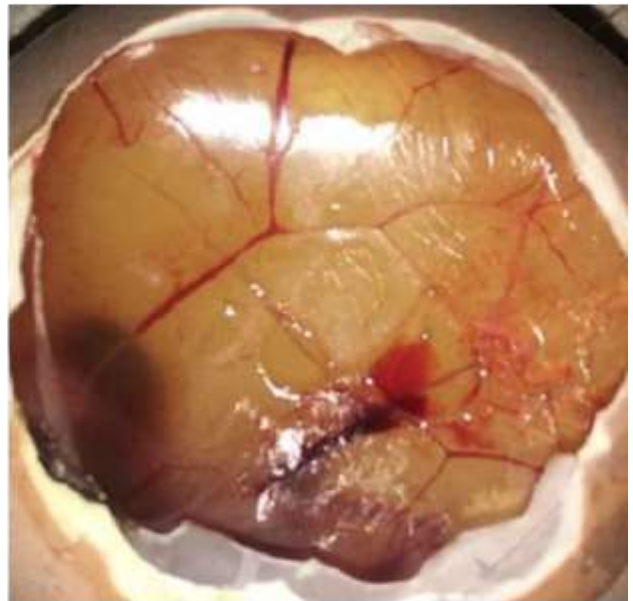


**After treatment**

(D) **Group D: AGE *per se***



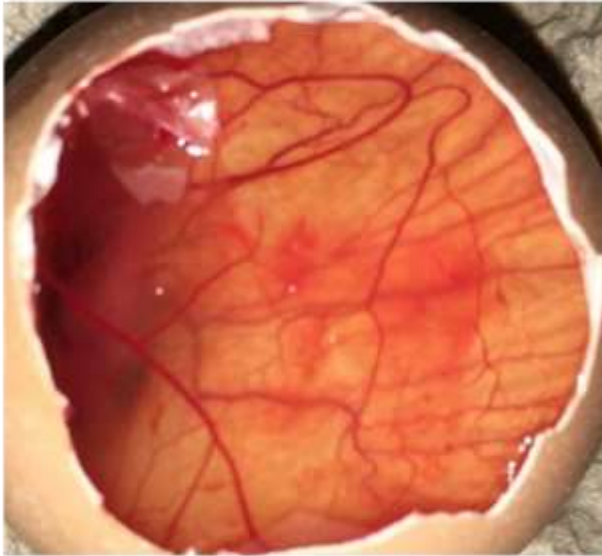
**Before treatment**



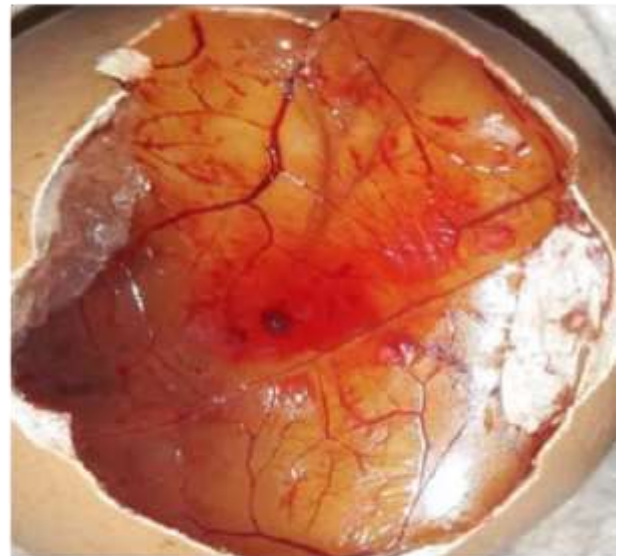
**After treatment**

(E)

**Group E: Blank NANE**



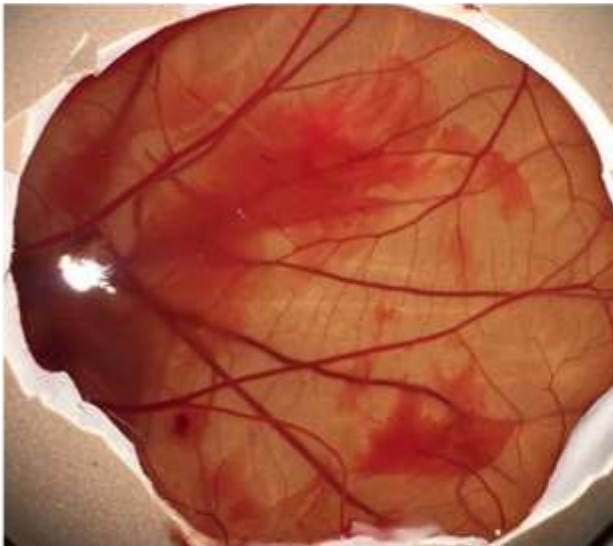
**Before treatment**



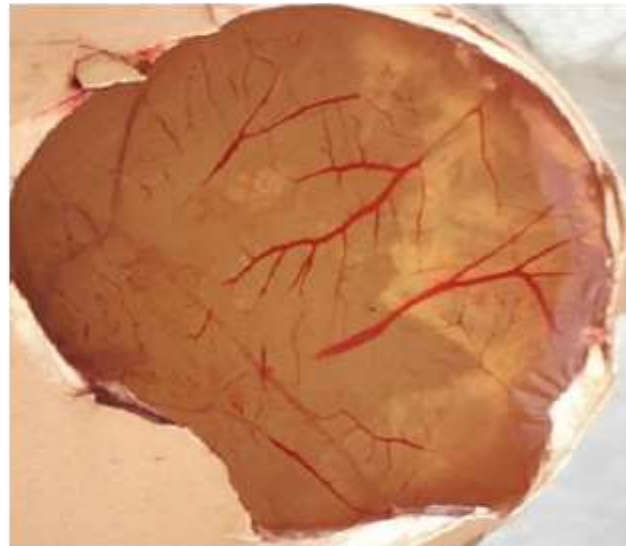
**After treatment**

(F)

**Group F : AGE NANE**



**Before treatment**



**After treatment**

**Figure 52.** A comparison of blood vessel formation (before treatment) and inhibition (after treatment) in the HET-CAM model (A) Normal control (B) Positive control (C) Negative control (D) AGE *per se* (E) Blank NANE (F) AGE NANE

**5.12.2. Acute dermal toxicity study**

Both range finding and main study have confirmed the safety of NANE at the lower (200 mg/kg) to higher doses (2000 mg/kg) of the AGE. None of the treated rats has shown changes in the skin, fur, eyes, mucous membrane, sleep pattern, respiratory, circulatory, autonomic and central nervous system activity, behaviour pattern, toxic reactions and mortality during the 14 days treatment. Hence, AGE NANE formulation was found to be safe at the selected doses of 200 mg/kg, 1000 mg/kg and 2000 mg/kg.

On the basis of the observation noted on 24, 48 and 72 h, Draize skin irritation scoring was assigned and systematically recorded observations for skin irritation study is shown in **Table 42**. None of the animals in the treatment groups have shown erythema or edema. Hence, the optimized AGE NANE was further selected for anti-psoriasis studies.

**Table 42.** Skin irritation study

Time (h)	Group /Dose	Animal code	Erythema	Edema
24	Group 1 (200mg/kg)	1	0	0
		2	0	0
	Group 2 (1000 mg/kg)	1	0	0
		2	0	0
	Group 3 (2000 mg/kg)	1	0	0
		2	0	0
48	Group 1 (200mg/kg)	1	0	0
		2	0	0
	Group 2 (1000 mg/kg)	1	0	0
		2	0	0
	Group 3 (2000 mg/kg)	1	0	0
		2	0	0
72	Group 1 (200mg/kg)	1	0	0
		2	0	0
	Group 2 (1000 mg/kg)	1	0	0
		2	0	0
	Group 3 (2000 mg/kg)	1	0	0
		2	0	0

### **5.12.3. Antipsoriatic activity in IMQ induced animal model**

As per the study protocol discussed in section 4.2.15.3.1., IMQ was applied in all animals (group II, group III, group IV, group V, group VI, group VII, except in group I animals). During the initial days of induction, erythema was more prominent during 1<sup>st</sup> and 2<sup>nd</sup> day and later on 3<sup>rd</sup> to 6<sup>th</sup> day scaling and thickness were observed. After 7 consecutive days of IMQ application (psoriasis scales were formed), the treatment for psoriatic plaques were initiated with respective formulations for consecutive 7 days. The sign of transformation of the phenotypic characteristic of normal skin to psoriasis skin (induction of psoriasis) and later degree of recovery from psoriasis to normal skin (treatment period) were visually analyzed as shown in **Figure 53** and later further scoring of the psoriasis condition was performed with PASI scoring (results shown in section 5.12.3.1.1).



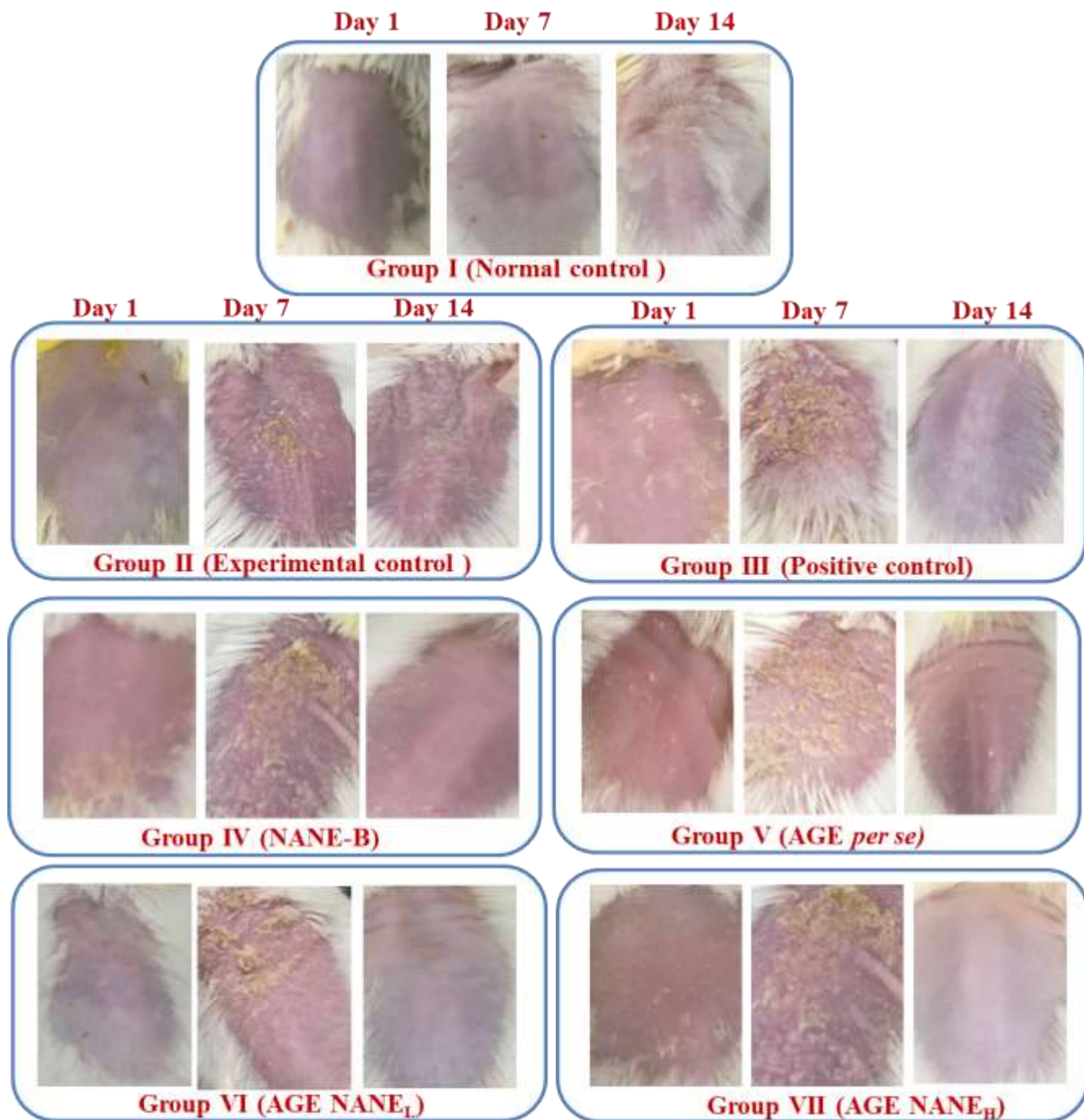


**Figure 53.** Phenotypic variations observed in all the groups (I-VII) before induction (1st day), after induction (7th day) and after treatment (14th day)

*5.12.3.1. Evaluation parameters for antipsoriatic activity*

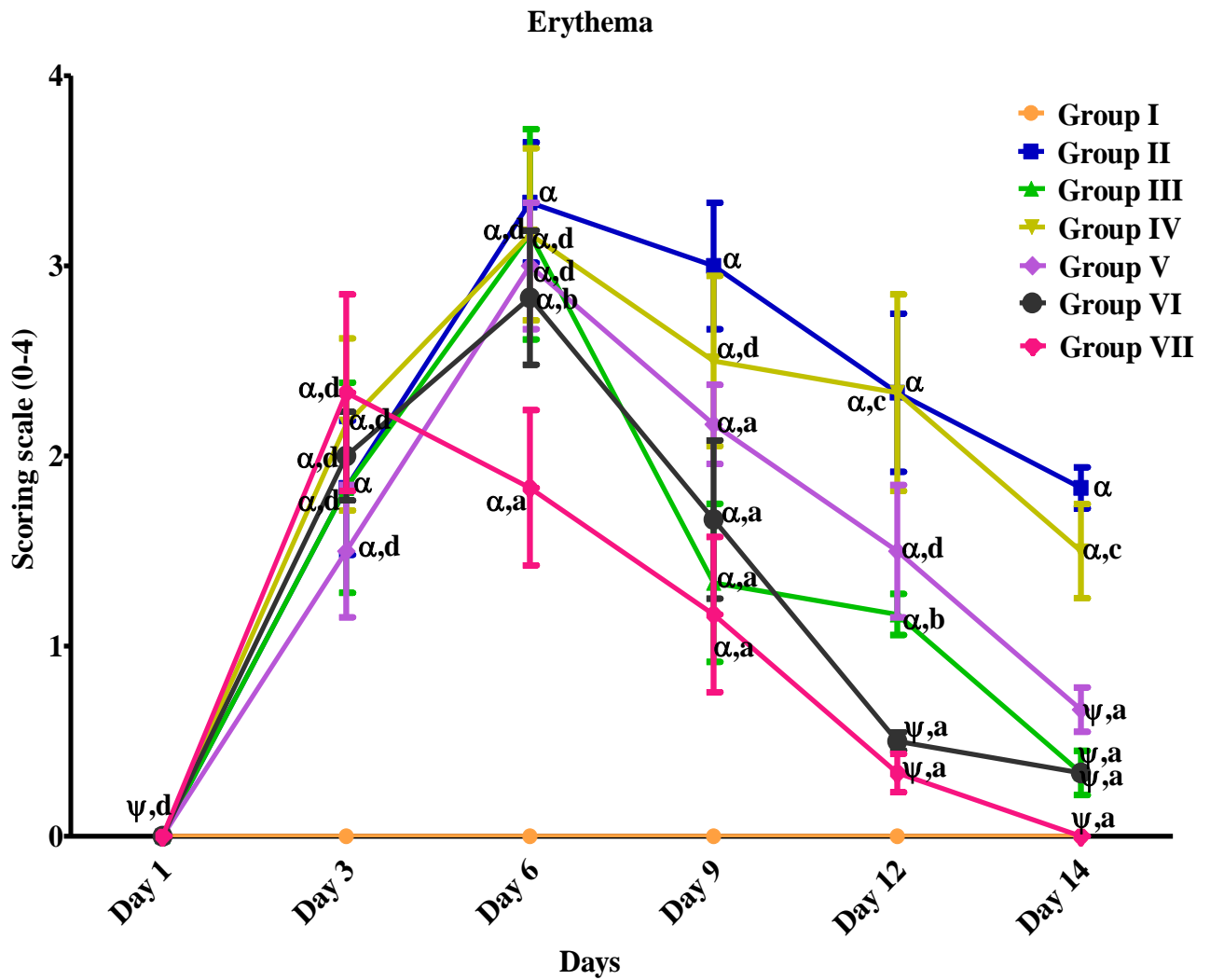
*5.12.3.1.1. PASI*

The application of IMQ on dorsal skin and right ear pinna has shown psoriasis-like features on the skin from second day onwards. The severity of the condition began with severe erythema on second day, followed by the development of scales on 3<sup>rd</sup> day. Once the scale formation occurred, then the erythema subsided and skin became rough which was considered as thickness. The PASI scoring on the dorsal skin surface was gradually increased when it is exposed to IMQ in the psoriasis induction period (7 days). Except group I (normal control), all other groups (II to VII) were exposed to IMQ and a significant increase in the PASI scoring ( $p < 0.001$ ) was reported in group II- VII (i.e all IMQ treated groups) as compared to group I (normal control).

Efficacy of the developed AGE NANE on IMQ-induced mice model was studied. The topical application of low dose (AGE NANE<sub>L</sub> 0.05% w/w) and high dose (AGE NANE<sub>H</sub> 0.1% w/w) of the AGE NANE have shown significant reduction ( $p < 0.001$ ) in the phenotypic features such as skin lesions, scales, thickness and erythema. The observed results with both doses were comparable with that of group III (positive control) which confirmed dose-independent effect of AGE NANE. The marked reduction in the PASI scoring displayed with AGE NANE denoted the healing effect which was confirmed further by histopathology (results shown in 5.12.3.1.4.).

The PASI scoring for all the groups from day 1 to day 14 was analyzed statistically using two way ANOVA (Bonferroni posttest) and results are shown in **Figure 54 (A-D)** which specify the scoring from 0 to 4 for erythema, scaling, skin thickness whereas cumulative PASI scoring was done from 0-12.

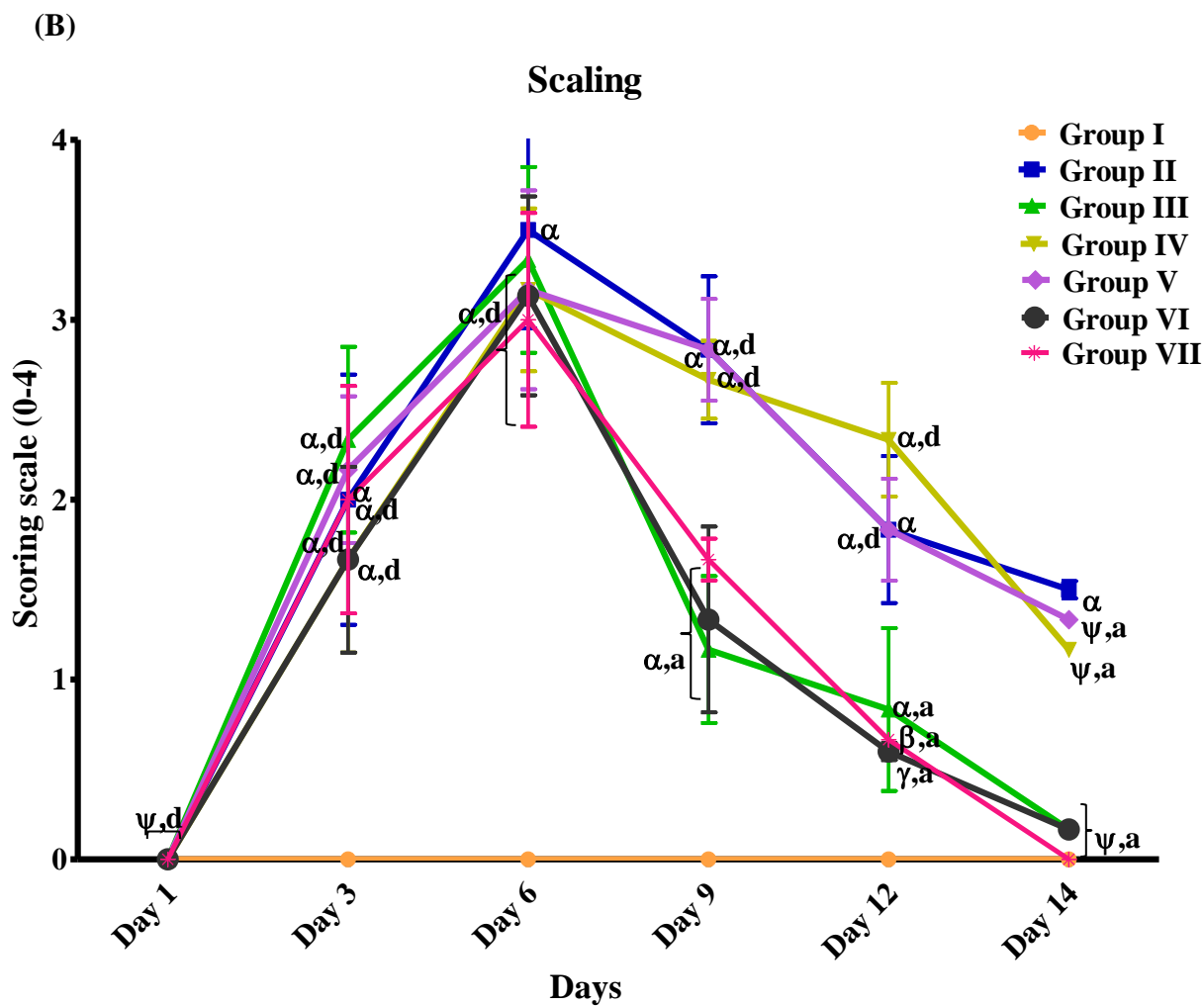
(A)



Data expressed as mean  $\pm$  standard error of mean (SEM). Each group comprises of six mice (n=6)

\* $\alpha$  ( $p < 0.001$ ),  $\beta$  ( $p < 0.01$ ),  $\gamma$  ( $p < 0.05$ ),  $\psi$  (non-significant) with respect to normal control (group I)

\* a ( $p < 0.001$ ), b ( $p < 0.01$ ), c ( $p < 0.05$ ), d (non-significant) with respect to experimental control (group II)

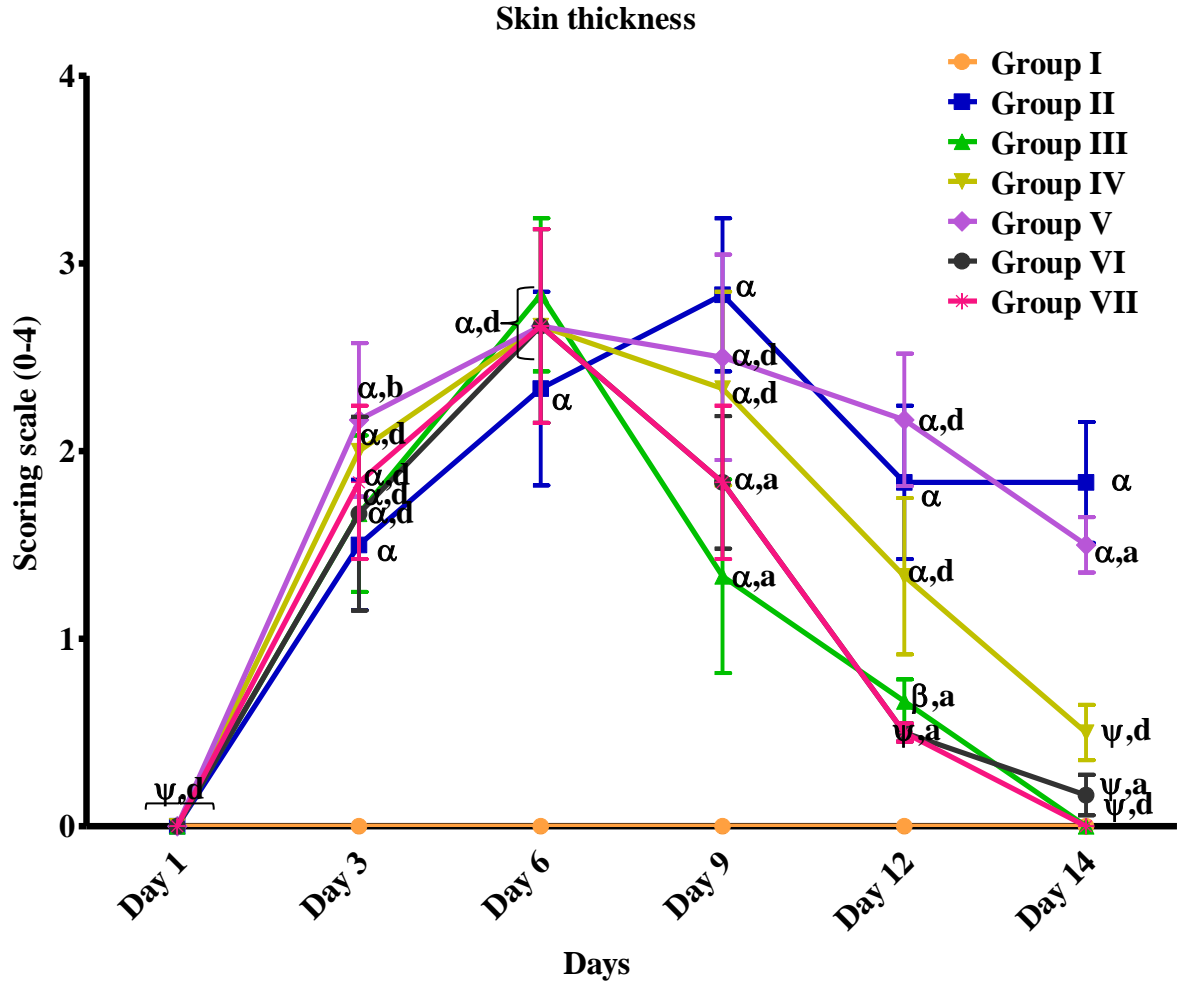


Data expressed as mean  $\pm$  standard error of mean (SEM). Each group comprises of six mice ( $n=6$ )

\* $\alpha$  ( $p < 0.001$ ),  $\beta$  ( $p < 0.01$ ),  $\gamma$  ( $p < 0.05$ ),  $\psi$  (non-significant) with respect to normal control (group I)

\*a ( $p < 0.001$ ), b ( $p < 0.01$ ), c ( $p < 0.05$ ), d (non-significant) with respect to experimental control (group II)

(C)



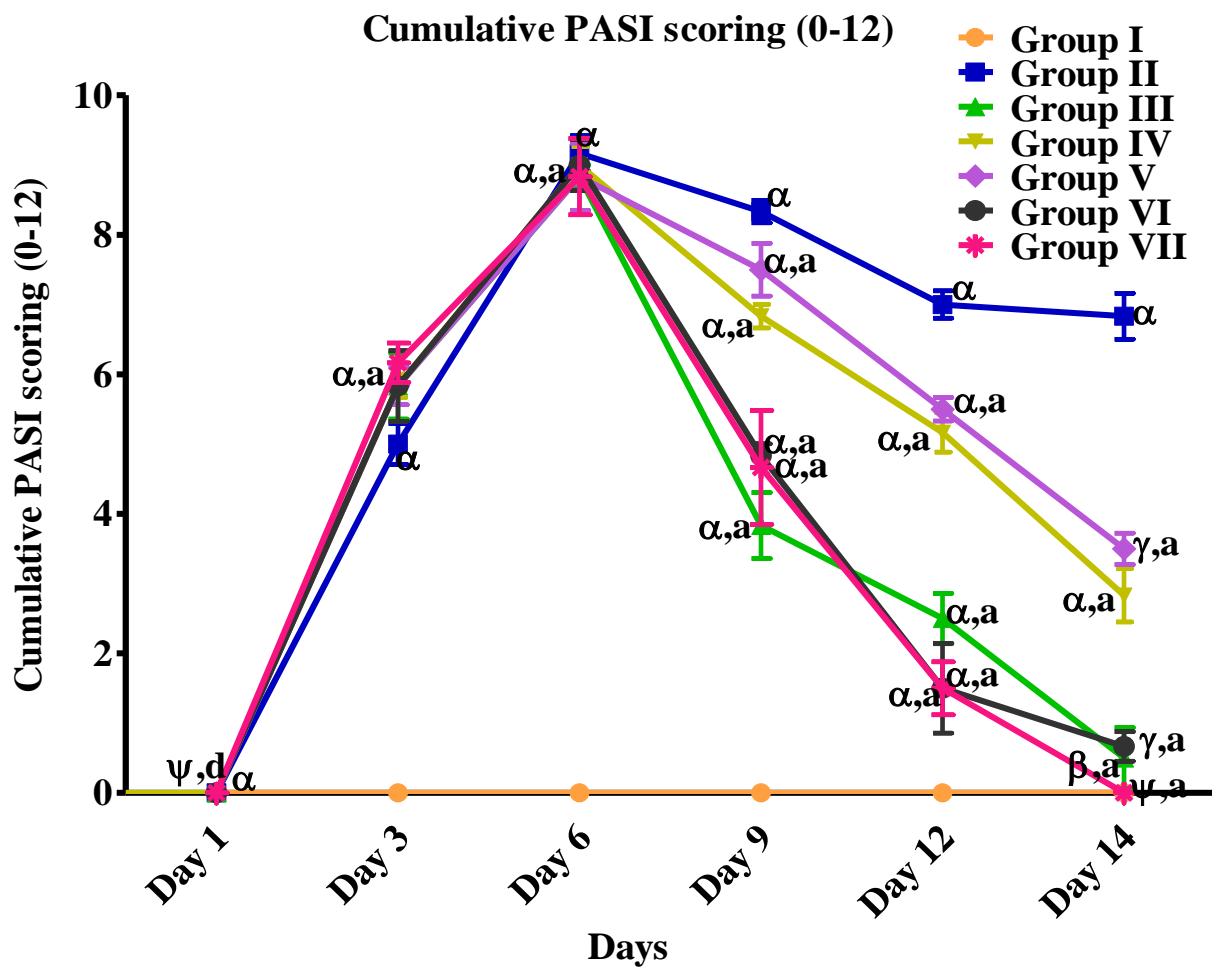
Data expressed as mean  $\pm$  standard error of mean (SEM). Each group comprises of six mice (n=6).

\* $\alpha$  ( $p < 0.001$ ),  $\beta$  ( $p < 0.01$ ),  $\gamma$  ( $p < 0.05$ ),  $\psi$  (non-significant) with respect to normal control (group I)

\*a ( $p < 0.001$ ), b ( $p < 0.01$ ), c ( $p < 0.05$ ), d (non-significant) with respect to experimental control (group II)

Statistical analysis carried out by Bonferroni posttest

(D)



Data expressed as mean  $\pm$  standard error of mean (SEM). Each group comprises of six mice (n=6)

\* $\alpha$  ( $p < 0.001$ ),  $\beta$  ( $p < 0.01$ ),  $\gamma$  ( $p < 0.05$ ),  $\psi$  (non-significant) with respect to normal control (group I)

\*a ( $p < 0.001$ ), b ( $p < 0.01$ ), c ( $p < 0.05$ ), d (non-significant) with respect to experimental control (group II)

Statistical analysis carried out by Bonferroni posttest

**Figure 54.** PASI scoring in IMQ induced psoriasis mice model during the study (A) Erythema (B) Scaling (C) Skin thickness (D) Cumulative PASI scoring.

**5.12.3.1.2. Ear thickness**

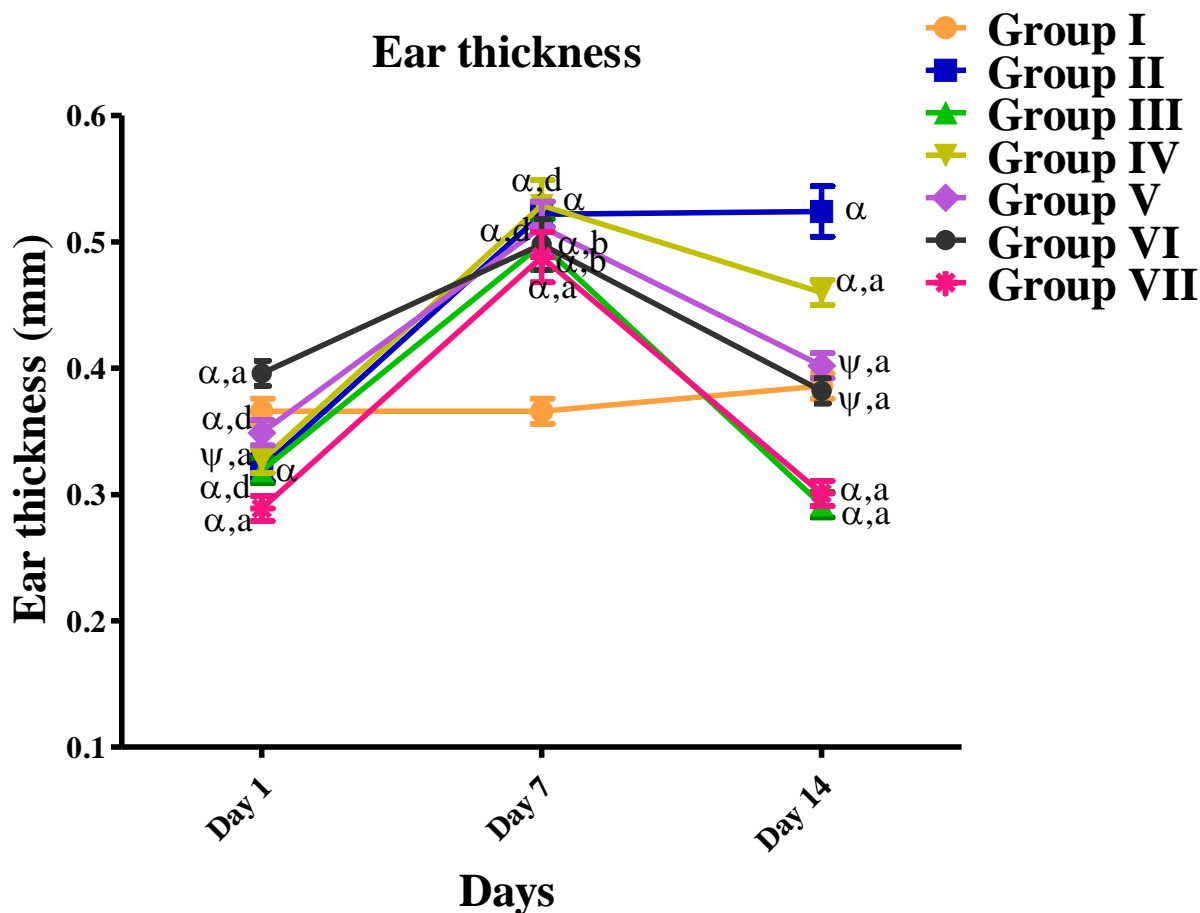
The topical application of IMQ (12.5 mg) for 7 consecutive days only on mice's right ear resulted in an increase in thickness which was considered as the index of skin inflammation. A significant reduction in ear thickness was observed when treated with group III (positive control), group VI (AGE NANE<sub>L</sub>), group VII (AGE NANE<sub>H</sub>) and the results were significant ( $p < 0.001$ ) with respect to group II (experimental control group) whereas insignificant difference was observed with respect to group I (normal control).

This confirmed a decrease in the degree of inflammation in the ear after treatment. A non-significant difference ( $p > 0.05$ ) in the ear thickness was observed after treatment in group III (positive control group), groups VI and VII (AGE NANE<sub>L</sub> and AGE NANE<sub>H</sub>) as compared to group I. The group's IV and V have shown slight reduction in the ear thickness as compared to group II (experimental control group). The phenotypic changes on the ear of all groups (I to VII) after treatment on 14<sup>th</sup> day are represented in Figure 55. It was observed that in group II (experimental control), blood vessels were more prominently visible confirming vascular changes that might be either due to neo-angiogenesis or increased endothelial cell markers that occur during psoriasis lesion development (Jabeen et al., 2020). However, all the groups which have received treatment (III, IV, V, VI, and VII) showed normal phenotypic features with slightly reddish blood vessels similar to that in group I (normal control). In terms of erythema, scales and thickness, only groups IV and V were observed with very slight powdery white scales and reported insignificant differences with respect to group I ( $p > 0.05$ ) whereas all other treatment received groups (III, VI, VII) were observed to be similar to that of group I ( $p < 0.001$ ). The graphical representation of the variation in ear thickness during the study period in all groups (I to VII) is represented in **Figure 56**.



**Figure 55.** Morphological changes observed on mice right ear in all groups after treatment i.e on 14th day





Data expressed as mean  $\pm$  standard error of mean (SEM). Each group comprises of six mice (n=6)  
 \* $\alpha$  ( $p < 0.001$ ),  $\beta$  ( $p < 0.01$ ),  $\gamma$  ( $p < 0.05$ ),  $\psi$  (non-significant) with respect to normal control (group I)  
 \*a ( $p < 0.001$ ), b ( $p < 0.01$ ), c ( $p < 0.05$ ), d (non-significant) with respect to experimental control (group II)

**Figure 56.** Graphical representation of variation in ear thickness during study period

### 5.12.3.1.3. Spleen to body weight index

IMQ is an immune activator that exacerbates psoriasis by activation of immune cells. Studies have reported the pathogenic mechanism, role of IL-23/IL-17 axis, and an increase in splenic Th-17 cells. This resulted in an increase in spleen weight with respect to body weight.

Topical application of IMQ for induction of psoriasis resulted in the enlargement of the spleen as shown in **Figure 57**. The spleen length and weight were significantly ( $p < 0.001$ ) increased in group II (experimental control group) as compared to normal control. However, significant ( $p < 0.001$  and  $p < 0.01$ ) reduction in spleen to body weight index was observed in group III (positive

control), group V (AGE *per se*), group VI (AGE NANE<sub>L</sub>) and group VII (AGE NANE<sub>H</sub>) in comparison to the group II as shown in **Figure 58**. Group IV has shown slightly higher spleen weight to body weight index ( $p < 0.05$ ) in comparison to group II (experiment control). However, the results were found non-significant ( $p > 0.05$ ) with respect to the group I (normal control). This showed that reduction in spleen to body weight index is a time-dependent recovery process.

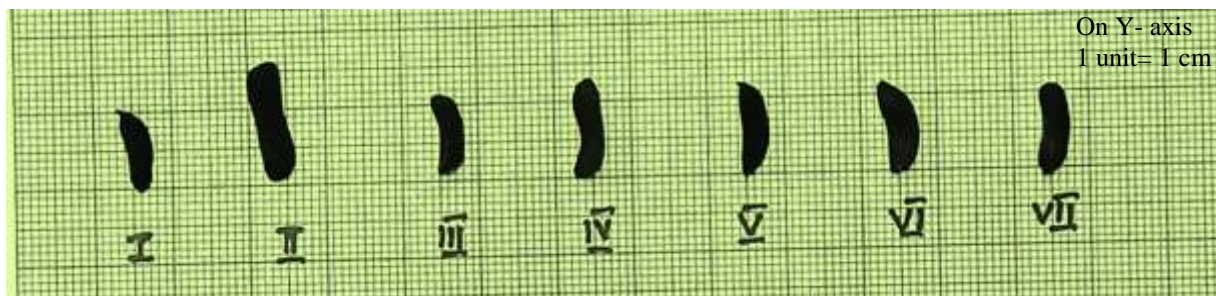
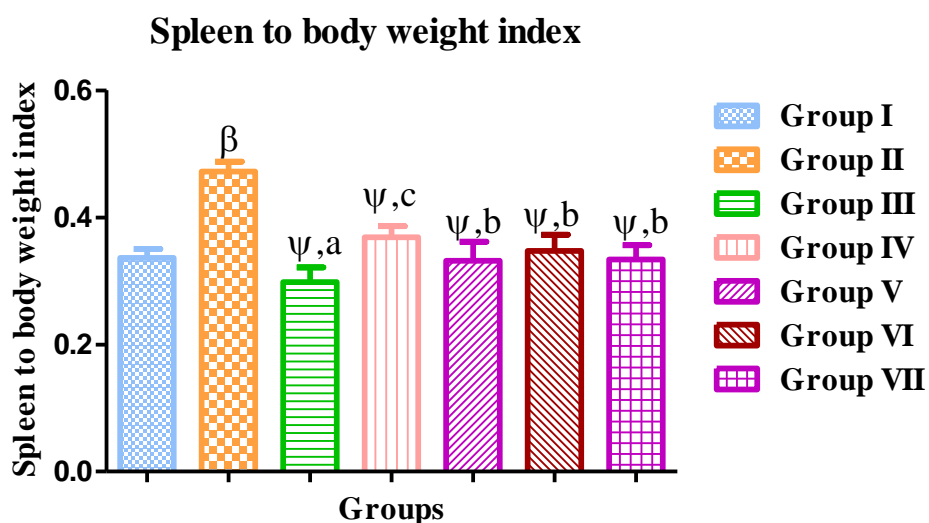


**Figure 57.** Effect of IMQ and various treatments applied on spleen length



Data expressed as mean  $\pm$  standard error of mean (SEM). Each group comprises of six mice (n=6)

\*a ( $p < 0.001$ ),  $\beta$  ( $p < 0.01$ ),  $\gamma$  ( $p < 0.05$ ),  $\psi$  (non-significant) with respect to normal control (group I)

\* a ( $p < 0.001$ ), b ( $p < 0.01$ ), c ( $p < 0.05$ ), d (non-significant) with respect to experimental control (group II)

**Figure 58.** IMQ induced splenomegaly and effect of treatment on spleen to body weight index

**5.12.3.1.4. Histopathology**

After completion of 14 days study, animals were sacrificed and their dorsal skin from the back and ear was removed. Each skin specimen was later stained and fixed with hematoxylin and eosin and observed at 100 x and 400 x magnification. The pathological changes observed in the skin specimens are recorded and images of dorsal skin and ear skin are shown in **Figure 59 (I-VII)** and **Figure 60 (I-VII)**.

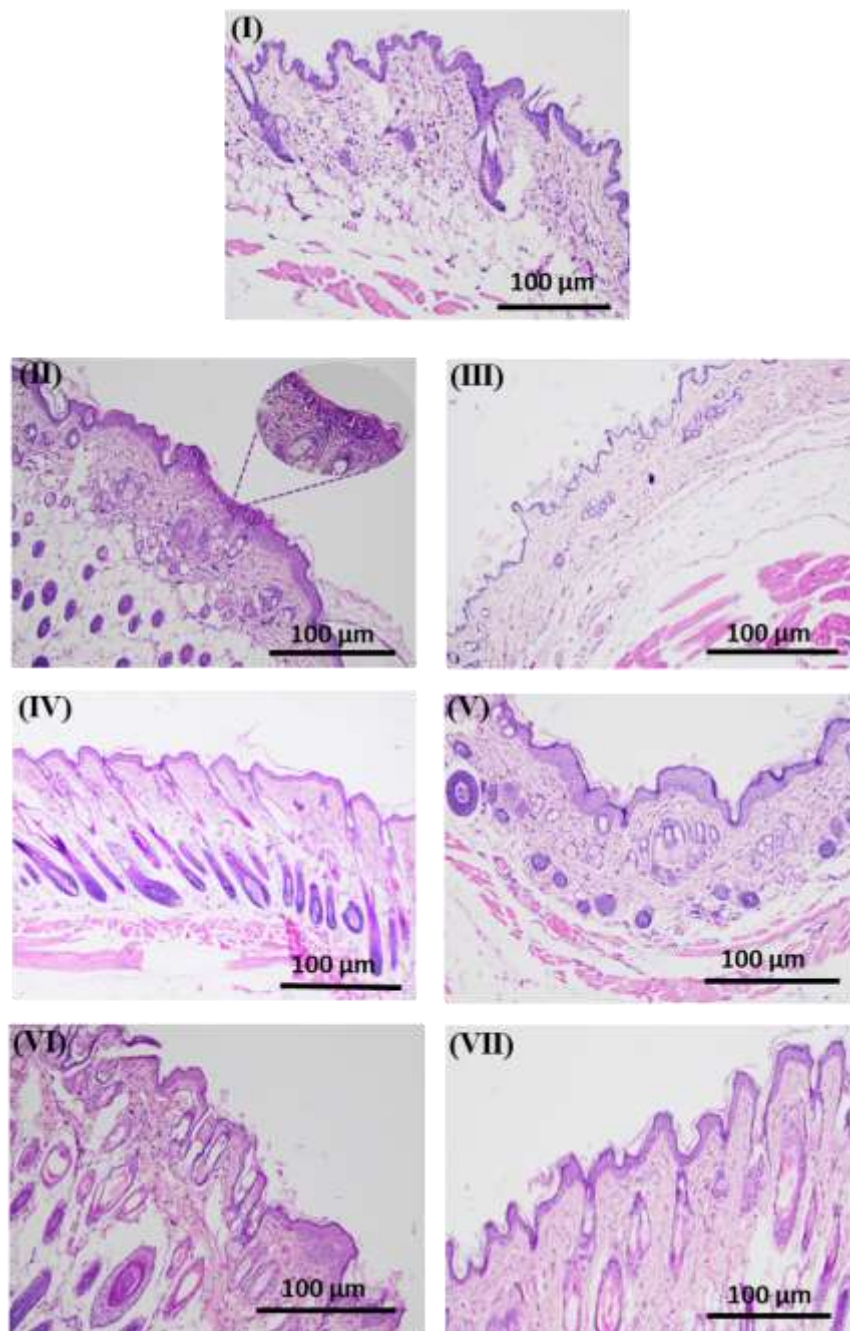
**Figure 59 I** represented group I (normal control) showing the characteristic features of normal skin. The normal skin has shown intact orthokeratotic stratum corneum and thin layered epidermis with normal level of keratin deposition. Other salient features observed include dermal papilla and hair shaft. On the contrary, group II (experimental control group) (**Figure 59 II**) has shown acanthosis and formation of hyperkeratotic as well as parakeratotic cells. The epithelial cells are reported with accumulation of neutrophils, which indicated the activation of the innate and adaptive immune system.

Group III (positive control group) shown in **Figure 59 III** reported a very thin epidermis in comparison to normal skin histology. This clearly pointed towards the reported side effects of corticosteroids (skin atrophy)(Del Rosso and Friedlander, 2005). Along with these changes, no hair follicles were found in the dermis. But the hyperkeratosis and parakeratosis of psoriatic skin disappeared with the treatment. Apart from skin thinning, all other histology features resembled that of the normal skin, this inferred the recovery from psoriasis condition. **Figure 59 IV** represented group IV (NANE-B) treatment with blank formulation has shown similar features of normal skin, however more immature hair follicles and shaft were observed in the dermis, and they are protruding towards the epidermis. These features concluded the potential of natural oil and other components in the formulation to support skin nourishment and hair growth (Das et al., 2020). These characteristic features were also visually observed on the dorsal skin of group IV (NANE-B). The skin appeared to be more shining and smooth with slight degree of redness and scales at the end of the treatment. These observations suggested the requirement of therapeutic moiety in the formulation to diminish the reported psoriatic features.

**Figure 59 V** showed that group V treated with AGE *per se*. Thickened epidermis was observed, however, no neutrophil infiltration in the epithelial cells of the thickened epidermis inferred

delay in recovery from psoriatic lesions. **Figure 59 VI** represented group VI treated low dose (AGE NANE<sub>L</sub>) has shown variation in the epidermal thickness. Both normal epidermal thickness, as well as thickened stratum corneum with few hyperkeratotic cells was observed in these groups whereas **Figure 59 VII** showed group VII treated with AGE NANE<sub>H</sub> (high dose), which has shown similar histology of normal skin with a thin epidermal layer having normal level of keratin deposition. By the end of 12<sup>th</sup> day, the disappearance of psoriatic lesions and scales were observed in these treatment groups.

These observations showed the therapeutic efficacy of the developed AGE NANE both at low and high doses. The recovery of psoriatic lesions to normal skin was found to be dose-dependent. The histological changes after application of AGE *per se* (group V) suggested that long term application of the extract could offer better therapeutic benefits. Similarly, group VI (AGE NANE<sub>L</sub>) has shown 50% recovery in epidermal thickness, whereas group VII (AGE NANE<sub>H</sub>) has shown almost complete recovery which is evident from the morphological as well as histological photomicrograph.



Groups are represented with notation: I: group I (normal control); II: group II (experimental control); III: group III (positive control); IV: group IV (NANE-B); V: group V (AGE *per se*); VI: group VI (AGE NANE<sub>L</sub>) and VII: group VII (AGE NANE<sub>H</sub>).

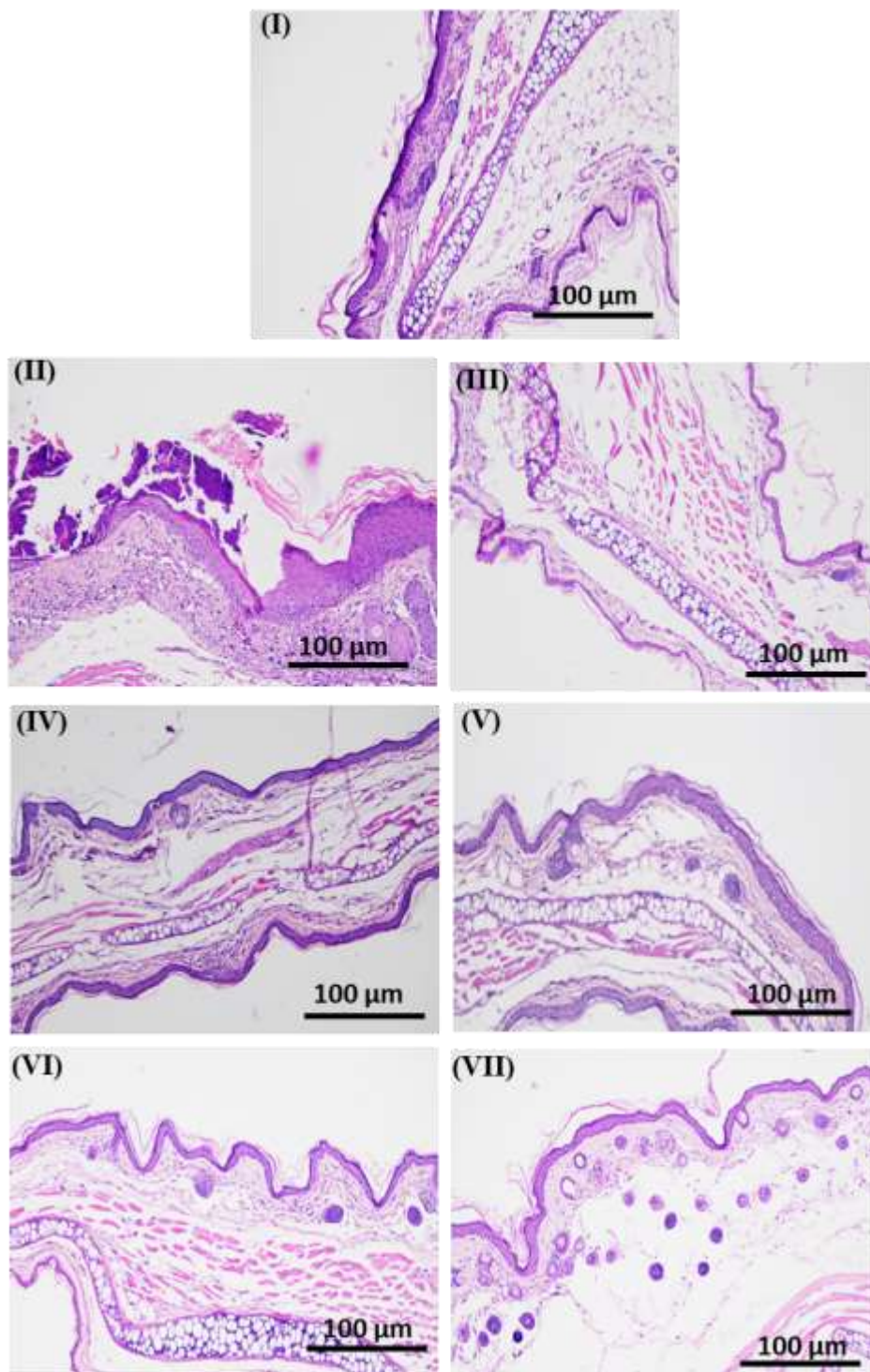
**Figure 59.** Photomicrograph showing histopathology of dorsal skin of groups (I-VII)

Similar to the changes in the dorsal skin, **Figure 60 I** show the histology of ear skin from group I (normal control) which represented normal features including epidermis, muscles and cartilage. **Figure 60 II** represented group II (experimental control) where more prominent neutrophil infiltration in the epidermis and dermis was observed. The parakeratotic cells were observed clearly through a total of magnification 400x and these features confirmed the induction of psoriasis with IMQ.

**Figure 60 III** represents group III (positive control group) where skin thinning was observed in dorsal skin. However, keratin deposition was slightly higher in the ear section than that of the dorsal skin section.

Group IV (blank formulation, **Figure 60 IV**) and group V (AGE *per se*, **Figure 60 V**) have shown slightly thicker epidermis than that of the normal control. However, neutrophil infiltration was observed in group V and the obtained result was found contrary to the observation of no neutrophils in the dorsal skin. Group VI (AGE NANE<sub>L</sub>) and group VII (AGE NANE<sub>H</sub>) resumed to normal orthokeratotic skin, with no sign of hyperkeratosis or parakeratosis (as shown in **Figure 60 VI** and **60VII**). However, these features were predominantly observed in psoriasis induced skin without treatment (Group II).

All these observations manifested the effectiveness of the developed AGE NANE at low and high doses. It is important to note that with marketed betamethasone formulation (0.01% w/w), skin thinning was observed, which reduced the skin barrier integrity. This is a mostly reported side effect of steroidal treatment (Danby et al., 2014).



Groups are represented with notation: I: group I (normal control); II: group II (experimental control); III: group III (positive control); IV: group IV (NANE-B); V: group V (AGE *per se*); VI: group VI (AGE NANE<sub>L</sub>) and VII: group VII (AGE NANE<sub>H</sub>)

**Figure 60.** Photomicrograph showing histopathology of dorsal ear skin of groups (I-VII)

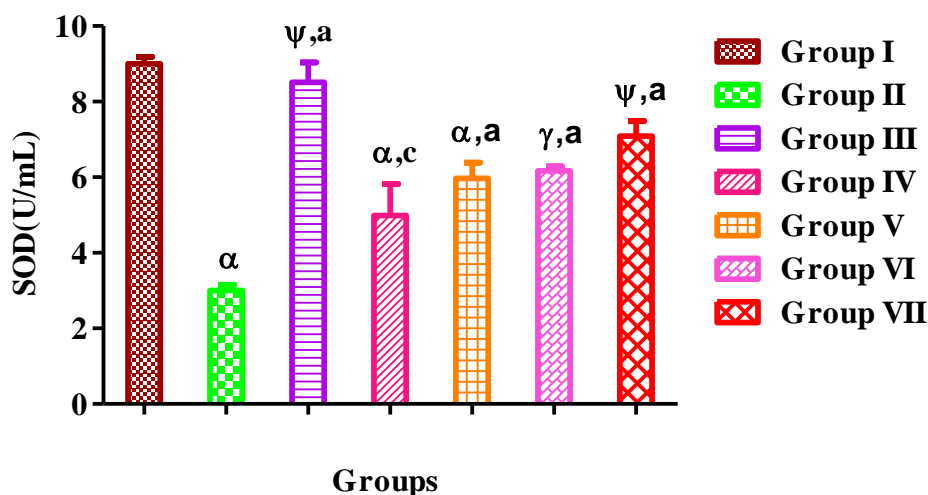
**5.12.3.1.5. Biochemical estimation of the antioxidant activity in the dorsal skin tissue**

Oxidative stress is also a triggering stimulus that plays a significant role in hyperproliferation and activation of immune cells. Along with these changes, oxidative stress generates reactive oxygen species imbalance and impairment in antioxidant enzyme levels which results in molecular abnormalities and irregular redox signaling. Numerous literatures have reported relation between redox imbalance and psoriasis lesion occurrence. During this condition, a remarkable increase in oxidative stress markers occur and antioxidant enzymes such as SOD, GSH, TBARS and catalase activities and their enzyme levels are affected /compromised (Kadam et al., 2010)

**5.12.3.1.5.1. Estimation of SOD**

SOD is a metalloenzyme that converts superoxide anion into hydrogen peroxide. In psoriasis, reduced SOD level was reported with epidermal hyperproliferation. **Figure 61** showed the effect of treatment on SOD level in each group (I-VII). Our study findings also exhibited significant ( $p < 0.001$ ) reduction in SOD level in psoriasis induced group II in comparison to normal control. In contrast to group II, group III, V, VI and VII have shown significant ( $p < 0.001$ ) restoration of SOD level when treated with AGE NANE at 0.05% and 0.1% w/w. In group IV (NANE-B), a slightly significant difference in SOD level was observed with respect to Group I whereas a non-significant difference was observed with respect to group II. This confirmed that when hyper proliferation subsides, SOD level increases. Hence results confirmed the effectiveness of the group VII treatment with formulated NANEs which is similar to group III (positive control).



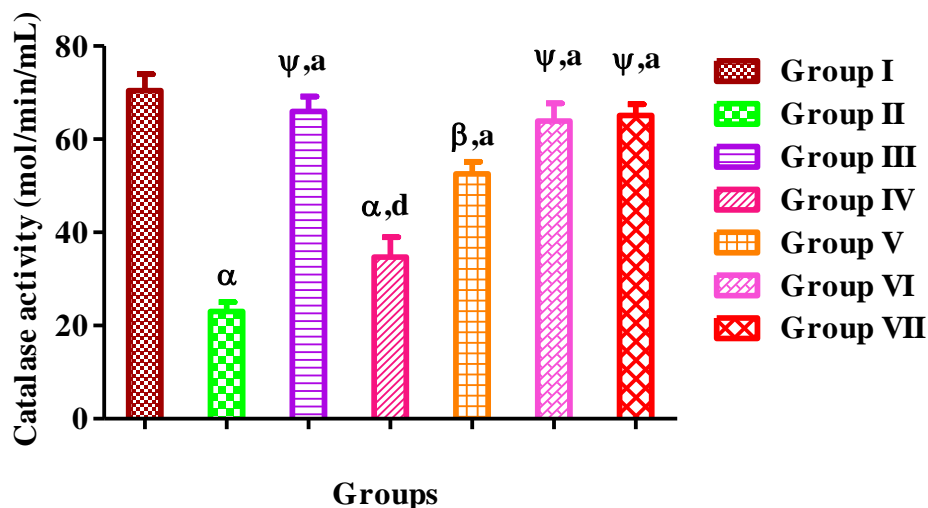


Data expressed as mean  $\pm$  standard error of mean (SEM). Each group comprises of six mice (n=6); \* $\alpha$  ( $p < 0.001$ ),  $\beta$  ( $p < 0.01$ ),  $\gamma$  ( $p < 0.05$ ),  $\psi$  (non-significant) with respect group I (normal control); \* a ( $p < 0.001$ ), b ( $p < 0.01$ ), c ( $p < 0.05$ ), d (non-significant) with respect to group II (experimental control).

**Figure 61.** Effect of treatment on SOD level

#### 5.12.3.1.5.2. Measurement of CAT activity

Reactive oxygen species such as superoxide anion ( $O_2^-$ ), hydrogen peroxide ( $H_2O_2$ ), hydroxyl radicals ( $OH^\cdot$ ) (Hoidal, 2001) exacerbate inflammatory conditions and their effect on psoriasis skin was analyzed by measuring the status of antioxidant enzyme (catalase) level. **Figure 62** showed the effect of treatment on catalase activity in the psoriasis induced mice model. Groups III, VI and VII have shown non-significance differences ( $p > 0.05$ ) in the level of catalase as compared to the group I (normal control). However, the effectiveness of the formulation was confirmed from the significant increase ( $p < 0.001$ ) in the catalase level when compared to group II (experimental control). Group V has shown a significant difference in the catalase activity with respect to group I ( $p < 0.01$ ) and group II ( $p < 0.001$ ), whereas group IV has shown insignificant differences with respect to group I and group II.

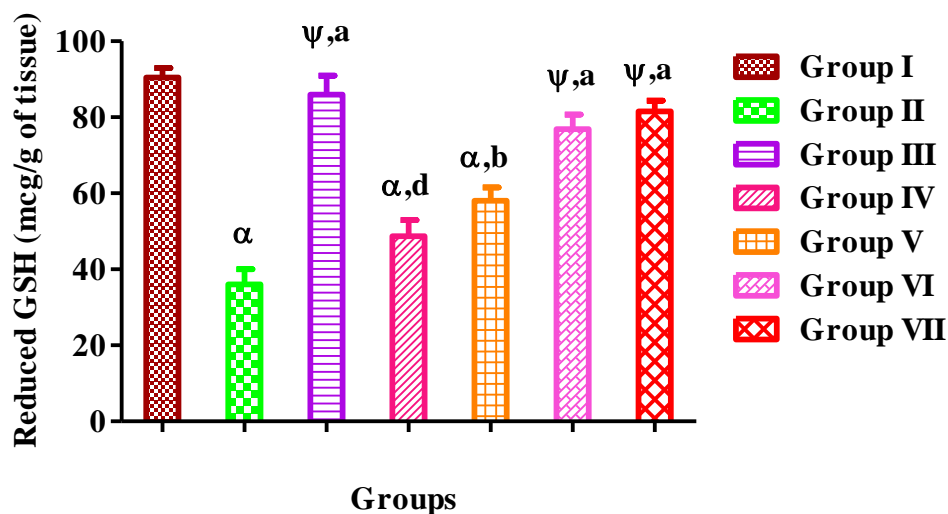


Data expressed as mean  $\pm$  standard error of mean (SEM). Each group comprises of six mice (n=6); \* $\alpha$  ( $p < 0.001$ ),  $\beta$  ( $p < 0.01$ ),  $\gamma$  ( $p < 0.05$ ),  $\psi$  (non-significant) with respect group I (normal control); \* a ( $p < 0.001$ ), b ( $p < 0.01$ ), c ( $p < 0.05$ ), d (non-significant) with respect to group II (experimental control)

**Figure 62.** Effect of treatment on catalase activity

#### 5.12.3.1.5.3. Estimation of GSH

Elevated oxidative stress aggravates psoriasis which results in depletion of GSH level. Hence depletion in GSH level is considered as a biomarker for estimating the stress level (Kumar et al., 2021). Effect of treatment on GSH level is shown in **Figure 63**. Mice of groups III, VI and VII have shown better recovery in GSH level which have shown non-significant differences ( $p > 0.05$ ) when compared with the group I (normal control). However, GSH level of these three groups (III, VI and VII) have shown significant difference ( $p < 0.001$ ) when compared with group II (experimental control group). These results confirmed the therapeutic effectiveness of the formulated NANEs. In case of group IV, significant difference in the level of GSH was observed with respect to normal control and insignificant difference in the level of GSH with respect to group II. This infers that the presence of therapeutic moiety is essential for decreasing the elevated GSH level. In group V, GSH level was found to be significantly less with respect to groups I. This suggested that if extract as such is used then long term treatment is required to provide effective treatment.



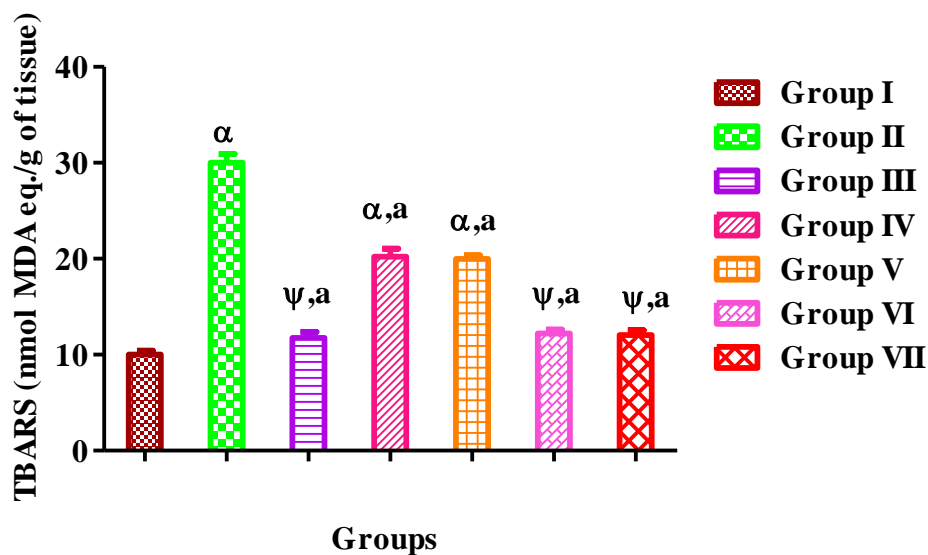
Data expressed as mean  $\pm$  standard error of mean (SEM). Each group comprises of six mice ( $n=6$ ); \* $\alpha$  ( $p < 0.001$ ),  $\beta$  ( $p < 0.01$ ),  $\gamma$  ( $p < 0.05$ ),  $\psi$  (non-significant) with respect group I (normal control); \* a ( $p < 0.001$ ), b ( $p < 0.01$ ), c ( $p < 0.05$ ), d (non-significant) with respect to group II (experimental control).

**Figure 63.** Effect of treatment on reduced GSH level

#### 5.12.3.1.5.4. Estimation of TBARS

Studies have reported the occurrence of lipid peroxidation in psoriatic skin which is measured from the increased level of TBARS (Drewa et al., 2002; Solak Tekin et al., 2007). TBARS assay quantitatively measured malondialdehyde (MDA), which is an end product of polyunsaturated fatty acids that are formed during the oxidation of lipid substrates. Hence, an increased level of TBARS is reported in psoriasis condition (Tampa et al., 2017).

The effectiveness of the treatment was analyzed based on the decreased level of TBARS. In this study, **Figure 64** shows a significant decrease in the level of TBARS after treatment in mice of groups III, VI and VII in comparison to group II (experimental control) and insignificant difference was observed in comparison to the normal control as shown in Fig 62. This clearly confirmed the effectiveness of the AE NANEs and their involvement in lipid peroxidation status of the skin. Both, group IV and V have shown significant differences ( $p < 0.001$ ) in the level of TBARS with respect to group I and group II



Data expressed as mean  $\pm$  standard error of mean (SEM). Each group comprises of six mice (n=6). \* $\alpha$  ( $p < 0.001$ ),  $\beta$  ( $p < 0.01$ ),  $\gamma$  ( $p < 0.05$ ),  $\psi$  (non-significant) with respect group I (normal control); \* a ( $p < 0.001$ ), b ( $p < 0.01$ ), c ( $p < 0.05$ ), d (non-significant) with respect to group II (experimental control)

**Figure 64.** Effect of treatment on TBARS

The normalized level of antioxidant enzymes and decrease in lipid peroxidation caused by NANEs has helped in treating psoriasis. Moreover, the effect of marketed formulation (group III) and group VII on antioxidant enzymes was found similar. Overall, the results of biochemistry and histopathology indicated that the developed AGE NANEs (group VI and VII) have shown excellent antipsoriatic activity.

# Chapter 6



---

## Conclusion and future perspective

---

## Chapter 6

### Conclusion and future perspective

The present study was designed to utilize the holistic approach of herbal remedies for treatment of psoriasis. AGE contains many phytoconstituents that are used for treatment of various diseases such as diarrhoea, stomach-ache, flatulence, abdominal discomfort, abnormal menstruation inflammatory disorders, rheumatism, neurodegenerative diseases and diabetes (Achuthan and Padikkala, 1997). However, among the phytoconstituents, ACA has been reported with inhibition of NF- $\kappa$ B expression and hence emphasized to play a crucial role in psoriasis treatment. The major problem associated with ACA includes their aqueous instability (i.e undergo hydrolytic degradation) and semi-volatility during long term storage hence reduces the therapeutic effectiveness. Hence, to improve the stability of ACA present in AGE has been loaded into NANE. Hence, AGE loaded NANE was formulated and optimization of the composition was carried out by BBD. The observed experimental values of responses were found to be in excellent agreement with predicted values. The average droplet size, zeta potential, % drug loading, % cumulative drug permeation and % drug retention in the skin were analyzed. Further, thermodynamic stability studies and accelerated stability studies confirmed the stability of the optimized AGE NANE. The viscosity and spreadability of AGE NANE was in agreement with the criteria for a topical application

The *in vitro* release kinetic and *ex vivo* permeation studies of AGE NANE were carried out and the amount of ACA released was analyzed using developed HPLC method. The results of release studies reported zero-order release profile and *ex vivo* studies on porcine skin has shown 10-folds increase in flux of AGE NANE in comparison to AGE *per se*. Hence, optimized AGE NANE was subjected to acute dermal toxicity studies (also obtained results for skin irritation study) and further, therapeutic efficacy of the NANE was evaluated using IMQ induced mouse model. The results of *in vivo* pharmacodynamic study conducted for 14 days showed excellent recovery from developed psoriatic lesions with AGE NANE in a dose-dependent manner. In AGE *per se* treated group, only a slight reduction in the psoriatic lesions was observed which showed that AGE is not effective this might be due to its poor permeation.

## *Conclusion and future perspective*

The blank NANE (NANE<sub>B</sub>) has shown skin nourishment effect, which confirmed the usefulness of the composition to regain the shiny skin texture. Both, MCT oil and glycerin in the formulation have emollient effect which might be the reason for skin moisturizing property. However, psoriasis lesions were present in the form of powdery scales which pointed towards the need for therapeutic moiety.

PASI scoring, spleen to body weight index, ear thickness, histological examination of dorsal skin's and antioxidant enzyme assay reported the complete recovery of psoriatic lesions in group III and group VII. However, it should be noted at this stage that treatment with marketed corticosteroid (group III) has shown skin thinning in comparison to normal skin (Group I), which is the main side effect of steroidal treatment. But treatment with AGE NANE (both low and high dose) has shown better recovery without any side effects.

Overall, the study entailed the successful development of AGE NANE for treatment of psoriasis. The developed composition was found to be safe and effective, ensuring long term use without considerable side effects. This provide benefits to the patients to utilize the “traditional system of medicine” (herbal extract) in a suitable dosage form. This dosage form improves patient compliances and herbal ingredients overcome the major challenges of synthetic drugs. Due to these advantages, demand for herbal based pharmaceuticals and cosmeceuticals are increasing specially for skin diseases.

The method used for formulation development as well the excipients used in them is routinely used in the laboratory. The developed method does not involve any complex processes or equipments. Hence, the method is reproducible and scale-up challenges are minimized making technology transfer easier from small scale (laboratory) to industrial scale. This ensures that the production cost can minimize and hence effective formulation can be made available at affordable cost. This research also provides direction to the researchers who have keen interest to exploit herbals into novel drug delivery systems.

# Chapter 7



---

## Bibliography

---



- (IFPA), I.F.o.P.A., 2021. International Federation of Psoriasis Associations, Sweden. <https://ncdalliance.org/international-federation-of-psoriasis-associations-ifpa>, Accessed on Oct 26,2021
- ABITEC, ABITEC Personal Care Products—A perfect balance between science and nature, pp. 1-13. <https://www.abiteccorp.com/media/2887/personal-care-brochure.pdf>-, Accessed on Aug 13,2020
- Achuthan, C., Padikkala, J., 1997. Hypolipidemic effect of *Alpinia galanga* (Rasna) and *Kaempferia galanga* (Kachoori). Indian J Clin Biochem 12, 55-58.
- Administration, U.F.a.D., 2020. Q8(R2) Pharmaceutical Development. Center for Drug Evaluation and Research; Center for Biologics Evaluation and Research, Rockville, MD.
- Agrawal, U., Mehra, N.K., Gupta, U., Jain, N., 2013. Hyperbranched dendritic nano-carriers for topical delivery of dithranol. J. Drug Target. 21, 497-506.
- Agrawal, Y.O., Mahajan, U.B., Mahajan, H.S., Ojha, S., 2020. Methotrexate-loaded nanostructured lipid carrier gel alleviates imiquimod-induced psoriasis by moderating inflammation: Formulation, optimization, characterization, in-vitro and in-vivo studies. Int. J. Nanomed 15, 4763.
- Akrawi, S.H., Gorain, B., Nair, A.B., Choudhury, H., Pandey, M., Shah, J.N., Venugopala, K.N., 2020. Development and optimization of naringenin-loaded chitosan-coated nanoemulsion for topical therapy in wound healing. Pharmaceutics 12, 893.
- Al-Yahya, M., Rafatullah, S., Mossa, J., Ageel, A., Al-Said, M., Tariq, M., 1990. Gastric antisecretory, antiulcer and cytoprotective properties of ethanolic extract of *Alpinia galanga* Willd in rats. Phytother Res 4, 112-114.
- Alam, M.S., Ali, M.S., Alam, N., Alam, M.I., Anwer, T., Imam, F., Ali, M.D., Siddiqui, M.R., Shamim, M., 2012. Design and characterization of nanostructure topical gel of betamethasone dipropionate for psoriasis. J App Pharm Sci 2, 148.
- Algahtani, M.S., Ahmad, M.Z., Ahmad, J., 2020. Nanoemulsion loaded polymeric hydrogel for topical delivery of curcumin in psoriasis. J Drug Deliv Sci Technol. 59, 101847.
- AlShobaili, H.A., Shahzad, M., Al-Marshood, A., Khalil, A., Settin, A., Barrimah, I., 2010. Genetic background of psoriasis. Int. J. Health Sci. 4, 23.
- Amro, K., 2013. Microgel-stabilised non-aqueous emulsions. RSC Adv. 3, 25662-25665.

- Asri, A., Winarko, S., 2016. Antiproliferative Activity by Ethanolic Extract of Red *Alpinia galanga* (L) Willd in Inoculated Breast Carcinoma Cells of C3H Mice. *J. adv. med. pharm. sci*, 1-9.
- Atanase, L.I., Riess, G., 2015. PEG 400/Paraffin oil non-aqueous emulsions stabilized by P But-Block-P 2 VP block copolymers. *J. Appl. Polym. Sci.* 132.
- Aun, L.L., Azmi, M.N., Ibrahim, H., Awang, K., Nagoor, N.H., 2011. 1' S-1'-acetoxyeugenol acetate: a novel phenylpropanoid from: *Alpinia conchigera*: enhances the apoptotic effects of paclitaxel in MCF-7 cells through NF- $\kappa$ B inactivation. *Anticancer Drugs* 22, 424-434.
- Baboota, S., Alam, M.S., Sharma, S., Sahni, J.K., Kumar, A., Ali, J., 2011. Nanocarrier-based hydrogel of betamethasone dipropionate and salicylic acid for treatment of psoriasis. *Int. J. Pharm. Investig.* 1, 139.
- Badanthadka, M., D'Souza, L., Salwa, F., 2021. Strain specific response of mice to IMQ-induced psoriasis. *J Basic Clin Physiol Pharmacol.* 32, 959-968.
- Baradwaj, R., Rao, M., Kumar, T.S., 2017. Novel purification of 1'S-1'-Acetoxychavicol acetate from *Alpinia galanga* and its cytotoxic plus antiproliferative activity in colorectal adenocarcinoma cell line SW480. *Biomed. Pharmacother.* 91, 485-493.
- Barradas, T.N., Senna, J.P., Cardoso, S.A., e Silva, K.G.d.H., Mansur, C.R.E., 2018. Formulation characterization and in vitro drug release of hydrogel-thickened nanoemulsions for topical delivery of 8-methoxypsoralen. *Mater. Sci. Eng. C* . 92, 245-253.
- Batra, V., Syed, Z., Gill, J.N., Coburn, M.A., Adegboyega, P., DiGiovanni, J., Mathis, J.M., Shi, R., Clifford, J.L., Kleiner-Hancock, H.E., 2012. Effects of the tropical ginger compound, 1'-acetoxychavicol acetate, against tumor promotion in K5. Stat3C transgenic mice. *J. Exp. Clin. Cancer Res.* 31, 1-14.
- Beg, S., Rahman, M., Kohli, K., 2019. Quality-by-design approach as a systematic tool for the development of nanopharmaceutical products. *Drug Discov. Today* 24, 717-725.
- Behera, J., Keservani, R.K., Yadav, A., Tripathi, M., Chadoker, A., 2010. Methoxsalen loaded chitosan coated microemulsion for effective treatment of psoriasis. *Int. J. Drug Deliv.* 2.
- Berg, M.-H.H., Carrasco, D., 2017. Injection site reactions to biologic agents used in psoriasis and psoriatic arthritis. *J Drugs Dermatol.* 16, 695-698.
- Bhoir, S.S., Vishwapathi, V., Singh, K.K., 2019. Antipsoriatic potential of *Annona squamosa* seed oil: An in vitro and in vivo evaluation. *Phytomedicine* 54, 265-277.

- Bhuchar, S., Katta, R., Wolf, J., 2012. Complementary and alternative medicine in dermatology. *Am. J. Clin. Dermatol.* 13, 311-317.
- Bommannan, D., Potts, R.O., Guy, R.H., 1991. Examination of the effect of ethanol on human stratum corneum in vivo using infrared spectroscopy. *J Control Release* 16, 299-304.
- Boukhatem, M.N., Kameli, A., Ferhat, M.A., Saidi, F., Mekarnia, M., 2013. Rose geranium essential oil as a source of new and safe anti-inflammatory drugs. *Libyan J. Med.* 8, 22520.
- Boutet, M.-A., Nerviani, A., Gallo Afflitto, G., Pitzalis, C., 2018. Role of the IL-23/IL-17 axis in psoriasis and psoriatic arthritis: the clinical importance of its divergence in skin and joints. *Int. J. Mol. Sci* 19, 530.
- Brás, T., Paulino, A.F., Neves, L.A., Crespo, J.G., Duarte, M.F., 2020. Ultrasound assisted extraction of cynaropicrin from *Cynara cardunculus* leaves: Optimization using the response surface methodology and the effect of pulse mode. *Ind Crops Prod* 150, 112395.
- Briffa, D.V., Warin, A., 1979. Photochemotherapy in psoriasis: a review. *J R Soc Med* 72, 440-446.
- Cameron, N.R., Sherrington, D.C., 1996. Non-aqueous high internal phase emulsions. Preparation and stability. *J. Chem. Soc., Faraday trans.* 92, 1543-1547.
- Campos, F.F., Campmany, A.C.C., Delgado, G.R., Serrano, O.L., Naveros, B.C., 2012. Development and characterization of a novel nystatin-loaded nanoemulsion for the buccal treatment of candidosis: Ultrastructural effects and release studies. *J. Pharm. Sci.* 101, 3739-3752.
- Canselier, J., Delmas, H., Wilhelm, A., Abismail, B., 2002. Ultrasound emulsification—an overview. *J Dispers Sci Technol* 23, 333-349.
- Carson, C., Hammer, K., Riley, T., 2006. *Melaleuca alternifolia* (tea tree) oil: a review of antimicrobial and other medicinal properties. *Clin. Microbiol. Rev.* 19, 50-62.
- Carvalho, V.F., de Lemos, D.P., Vieira, C.S., Migotto, A., Lopes, L.B., 2017. Potential of non-aqueous microemulsions to improve the delivery of lipophilic drugs to the skin. *AAPS PharmSciTech* 18, 1739-1749.
- Cavanagh, H.t.t., Wilkinson, J.t., 2002. Biological activities of lavender essential oil. *Phytother Res.* 16, 301-308.

- Chakraborty, S., Uppaluri, R., Das, C., 2020. Optimization of ultrasound-assisted extraction (UAE) process for the recovery of bioactive compounds from bitter melon using response surface methodology (RSM). *Food Bioprod. Process.* 120, 114-122.
- Chan, E.W., Ng, V.P., Tan, V.V., Low, Y.Y., 2011. Antioxidant and antibacterial properties of *Alpinia galanga*, *Curcuma longa*, and *Etilingera elatior* (Zingiberaceae). *Pharmacogn. J.* 3, 54-61.
- Chan, E.W.C., Lim, Y.Y., Wong, L., Lianto, F.S., Wong, S., Lim, K., Joe, C., Lim, T., 2008. Antioxidant and tyrosinase inhibition properties of leaves and rhizomes of ginger species. *Food Chem.* 109, 477-483.
- Chandra, A., Aggarwal, G., Manchanda, S., Narula, A., 2019. Development of topical gel of methotrexate incorporated ethosomes and salicylic acid for the treatment of psoriasis. *Pharm Nanotechnol* 7, 362-374.
- Chandra, A., Senapati, S., Roy, S., Chatterjee, G., Chatterjee, R., 2018. Epigenome-wide DNA methylation regulates cardinal pathological features of psoriasis. *Clin. Epigenetics* 10, 1-16.
- Chandrasekaran, N., 2015. Nanoemulsion formation and characterization by spontaneous emulsification: Investigation of its antibacterial effects on *Listeria monocytogenes*. *Asian J. Pharm.* 9, 23-28.
- Chawla, P., Kumar, N., Kaushik, R., Dhull, S.B., 2019. Synthesis, characterization and cellular mineral absorption of nanoemulsions of *Rhododendron arboreum* flower extracts stabilized with gum arabic. *J Food Sci Technol* 56, 5194-5203.
- Chellammal, H.S.J., Veerachamy, A., Ramachandran, D., Gummadi, S.B., Manan, M.M., Yellu, N.R., 2019. Neuroprotective effects of 1 $\delta$ -1-acetoxyeugenol acetate on A $\beta$  (25-35) induced cognitive dysfunction in mice. *Biomed. Pharmacother.* 109, 1454-1461.
- Chen, H., Jin, X., Li, Y., Tian, J., 2016. Investigation into the physical stability of a eugenol nanoemulsion in the presence of a high content of triglyceride. *RSC Adv.* 6, 91060-91067.
- Chen, H., Zhang, Y., 2004. Effects of curcuma on expression of CD45RO, VEGF and iNOS in psoriatic lesions. *Chin J Dermatol Venerol Integ Trad W Med* 3, 198-201.
- Chen, J.L., Fayerweather, W.E., Pell, S., 1988. Cancer incidence of workers exposed to dimethylformamide and/or acrylonitrile. *J Occup Med.* 30, 813-818.

- Chien, S.T., Shi, M.D., Lee, Y.C., Te, C.C., Shih, Y.W., 2015. Galangin, a novel dietary flavonoid, attenuates metastatic feature via PKC/ERK signaling pathway in TPA-treated liver cancer HepG2 cells. *Cancer Cell Int* 15, 15.
- Chime, S., Kenechukwu, F., Attama, A., 2014. Nanoemulsions—advances in formulation, characterization and applications in drug delivery. IntechOpen Limited, London, United Kingdom.
- Cho, J.-W., Lee, K.-S., Kim, C.-W., 2007. Curcumin attenuates the expression of IL-1 $\beta$ , IL-6, and TNF- $\alpha$  as well as cyclin E in TNF- $\alpha$ -treated HaCaT cells; NF- $\kappa$ B and MAPKs as potential upstream targets. *Int. J. Mol. Med.* 19, 469-474.
- Chouni, A., Paul, S., 2018. A review on phytochemical and pharmacological potential of *Alpinia galanga*. *Pharmacogn. J.* 10.
- Chua, B., Abdullah, Z., Pin, K.Y., Abdullah, L.C., Choong, T.S.Y., Yusof, U.K., 2017. Isolation, structure elucidation, identification and quantitative analysis of 1'-acetoxychavicol (ACA) from the roots of chlorophytum borivilianum (SAFED MUSLI). *J Eng Sci Technol* 12, 198-213.
- Chudiwal, A., Jain, D., Somani, R., 2010. *Alpinia galanga* Willd.—An overview on phyto-pharmacological properties. *Indian J Nat Prod Resour.* 1, 143-149.
- Cinar, K., 2017. A review on nanoemulsions: preparation methods and stability. *Trakya Univ. J. Eng. Sci* 18, 73-83.
- Cunha, S., Costa, C.P., Moreira, J.N., Lobo, J.S., Silva, A.C., 2020. Using the quality by design (QbD) approach to optimize formulations of lipid nanoparticles and nanoemulsions: A review. *Nanomed.: Nanotechnol. Biol. Med.*, 102206.
- Czarnomysy, R., Bielawska, A., Bielawski, K., 2019. Effect of 2nd and 3rd generation PAMAM dendrimers on proliferation, differentiation, and pro-inflammatory cytokines in human keratinocytes and fibroblasts. *Int J Nanomedicine* 14, 7123-7139.
- Dabholkar, N., Rapalli, V.K., Singhvi, G., 2021. Potential herbal constituents for psoriasis treatment as protective and effective therapy. *Phytother Res* 35, 2429-2444.
- Dadwal, A., Mishra, N., Rawal, R.K., Narang, R.K., 2020. Development and characterisation of clobetasol propionate loaded Squarticles as a lipid nanocarrier for treatment of plaque psoriasis. *J Microencapsul.* 37, 341-354.

- Danby, S., Chittock, J., Brown, K., Albenali, L., Cork, M., 2014. The effect of tacrolimus compared with betamethasone valerate on the skin barrier in volunteers with quiescent atopic dermatitis. *Br. J. Dermatol. Suppl.* 170, 914-921.
- Dantas, M.G.B., Reis, S.A.G.B., Damasceno, C.M.D., Rolim, L.A., Rolim-Neto, P.J., Carvalho, F.O., Quintans-Junior, L.J., Almeida, J.R.G.d.S., 2016. Development and evaluation of stability of a gel formulation containing the monoterpene borneol. *Sci. World J.* 2016, 7394685.
- Das Kurmi, B., Tekchandani, P., Paliwal, R., Rai Paliwal, S., 2017. Transdermal drug delivery: opportunities and challenges for controlled delivery of therapeutic agents using nanocarriers. *Curr. Drug Metab.* 18, 481-495.
- Das, S., Lee, S.H., Chow, P.S., Macbeath, C., 2020. Microemulsion composed of combination of skin beneficial oils as vehicle: Development of resveratrol-loaded microemulsion based formulations for skin care applications. *Colloids Surf. B* 194, 111161.
- Davis, S., 1990. *Phospholipid Stabilised Emulsions for Parenteral Nutrition and Drug Delivery.* Springer, Boston, MA.
- de Mattos, C.B., Argenta, D.F., de Lima Melchiades, G., Cordeiro, M.N.S., Tonini, M.L., Moraes, M.H., Weber, T.B., Roman, S.S., Nunes, R.J., Teixeira, H.F., 2015. Nanoemulsions containing a synthetic chalcone as an alternative for treating cutaneous leishmaniasis: optimization using a full factorial design. *Int. J. Nanomedicine* 10, 5529-5542.
- Del Rosso, J., Friedlander, S.F., 2005. Corticosteroids: options in the era of steroid-sparing therapy. *JAAD* 53, S50-S58.
- Deng, S., May, B.H., Zhang, A.L., Lu, C., Xue, C.C., 2013. Topical herbal medicine combined with pharmacotherapy for psoriasis: a systematic review and meta-analysis. *Arch. Dermatol.* 305, 179-189.
- Deng, S., May, B.H., Zhang, A.L., Lu, C., Xue, C.C., 2014. Topical herbal formulae in the management of psoriasis: systematic review with meta-analysis of clinical studies and investigation of the pharmacological actions of the main herbs. *Phytother Res.* 28, 480-497.
- Deuschle, V.C.K.N., Deuschle, R.A.N., Bortoluzzi, M.R., Athayde, M.L., 2015. Physical chemistry evaluation of stability, spreadability, in vitro antioxidant, and photo-protective capacities of topical formulations containing *L.* leaf extract. *Braz. J. Pharm. Sci.* 51, 63-75.
- Dev, K., Sahoo, D., Shahi, D.S., 2017. Psoriasis: A review. *Int. J. Pharm. Sci. Res* 2, 46-51.

- Devi, N., Kumar, S., Prasad, M., Rao, R., 2020. Eudragit RS100 based microsponges for dermal delivery of clobetasol propionate in psoriasis management. *J Drug Deliv Sci Technol.* 55, 101347.
- Di Meglio, P., Nestle, F.O., 2017. Immunopathogenesis of psoriasis, *Clinical and basic immunodermatology.* Springer, Switzerland, pp. 373-395.
- Divakaran, S., Hema, P., Nair, M., Nair, C., 2013. Antioxidant capacity and radioprotective properties of the flavonoids galangin and kaempferide isolated from *Alpinia galanga* L.(Zingiberaceae) against radiation induced cellular DNA damage. *Int. J. Radiat. Res.* 11, 81-89.
- Divya, G., Panonnummal, R., Gupta, S., Jayakumar, R., Sabitha, M., 2016. Acitretin and aloe-emodin loaded chitin nanogel for the treatment of psoriasis. *Eur J Pharm Biopharm.* 107, 97-109.
- Dixit, A., Rohilla, A., Dixit, J., Singh, V., 2014. Qualitative analysis of various plant extracts of *Alpinia officinarum*. *IJPCBS* 4, 505-508.
- Dodou, K., Anderson, R.J., Lough, W.J., Small, D.A., Shelley, M.D., Groundwater, P.W., 2005. Synthesis of gossypol atropisomers and derivatives and evaluation of their anti-proliferative and anti-oxidant activity. *Bioorg. Med. Chem.* 13, 4228-4237.
- Dogra, S., Mahajan, R., 2016. Psoriasis: Epidemiology, clinical features, co-morbidities, and clinical scoring. *Indian Dermatol.* 7, 471.
- Dogra, S., Yadav, S., 2010. Psoriasis in India: Prevalence and pattern. *Indian J Dermatol Venereol Leprol.* 76, 595.
- Domala, A., Bale, S., Godugu, C., 2020. Protective effects of nanoceria in imiquimod induced psoriasis by inhibiting the inflammatory responses. *Nanomedicine* 15, 5-22.
- Dominguez-Villegas, V., Clares-Naveros, B., Garcia-Lopez, M.L., Calpena-Campmany, A.C., Bustos-Zagal, P., Garduno-Ramirez, M.L., 2014. Development and characterization of two nanostructured systems for topical application of flavanones isolated from *Eysenhardtia platycarpa*. *Colloids Surf B Biointerfaces* 116, 183-192.
- Draize, J.H., 1944. Methods for the study of irritation and toxicity of substances applied topically to the skin and mucous membranes. *J. Pharmacol. Exp. Ther.* 82, 377-390.
- Drewa, G., Krzyżyńska-Malinowska, E., Woźniak, A., Protas-Drozd, F., Mila-Kierzenkowska, C., Rozwodowska, M., Kowaliszyn, B., Czajkowski, R., 2002. Activity of superoxide dismutase and catalase and the level of lipid peroxidation products reactive with TBA in patients with psoriasis. *Med. Sci. Monit.* 8, BR338-BR343.

- Dubey, V.S., Bhalla, R., Luthra, R., 2003. An overview of the non-mevalonate pathway for terpenoid biosynthesis in plants. *J Biosci* 28, 637-646.
- Durakovic, B., 2017. Design of experiments application, concepts, examples: State of the art. *Period. Eng. Nat. Sci* 5, 421-439.
- Duvic, M., Nagpal, S., Asano, A.T., Chandraratna, R.A., 1997. Molecular mechanisms of tazarotene action in psoriasis. *J. Am. Acad. Dermatol.* 37, S18-S24.
- Dwarampudi, L.P., Palaniswamy, D., Muruganantham Nithyanantham, P., 2012. Antipsoriatic activity and cytotoxicity of ethanolic extract of *Nigella sativa* seeds. *Pharmacogn. Mag.* 8, 268.
- Dyab, A.K., Al-Haque, H.N., 2013. Particle-stabilised non-aqueous systems. *RSC Adv.* 3, 13101-13105.
- Dyab, A.K., Atta, A.M., El-Mahdy, G.A., 2013. Non-Aqueous Emulsions Stabilised by Nonionic Nonyl Phenol Ethoxylate Reactive Polymerisable Surfactants. *Int. J. Electrochem. Sci* 8, 9868-9885.
- Dyab, A.K., Mohamed, L.A., Taha, F., 2018. Non-aqueous olive oil-in-glycerin (o/o) Pickering emulsions: Preparation, characterization and in vitro aspirin release. *J Dispers Sci Technol.* 39, 890-900.
- Eid, A.M., Elmarzugi, N.A., El-Enshasy, H.A., 2013. Development of avocado oil nanoemulsion hydrogel using sucrose ester stearate. *J. Appl. Pharm.* 3, 145.
- Elgewelly, M.A., Elmasry, S.M., El Sayed, N.S., Abbas, H., 2022. Resveratrol-Loaded Vesicular Elastic Nanocarriers Gel in Imiquimod-Induced Psoriasis Treatment: In Vitro and In Vivo Evaluation. *Journal of Pharmaceutical Sciences* 111, 417-431.
- Elias, P.M., 1981. Lipids and the epidermal permeability barrier. *Arch. Dermatol.* 270, 95-117.
- Farhangian, M.E., Feldman, S.R., 2015. Immunogenicity of biologic treatments for psoriasis: therapeutic consequences and the potential value of concomitant methotrexate. *Am. J. Clin. Dermatol.* 16, 285-294.
- Farkhondeh, T., Azimi-Nezhad, M., Samini, F., Pourbagher-Shahri, A.M., Samarghandian, S., 2020. Neuroprotective effect of *Alpinia galanga* against middle cerebral artery occlusion-induced ischemia in rat. *Biointerface Res Appl Chem* 10, 6273-6281.
- Fasolo, D., Pippi, B., Meirelles, G., Zorzi, G., Fuentesfria, A.M., von Poser, G., Teixeira, H.F., 2020. Topical delivery of antifungal Brazilian red propolis benzophenones-rich extract by means



of cationic lipid nanoemulsions optimized by means of Box-Behnken Design. *J Drug Deliv Sci Technol.* 56, 101573.

Feng, H., Wu, R., Zhang, S., Kong, Y., Liu, Z., Wu, H., Wang, H., Su, Y., Zhao, M., Lu, Q., 2020. Topical administration of nanocarrier miRNA-210 antisense ameliorates imiquimod-induced psoriasis-like dermatitis in mice. *J. Dermatol.* 47, 147-154.

Ferreira, M., Barreiros, L., Segundo, M.A., Torres, T., Selores, M., Lima, S.A.C., Reis, S., 2017. Topical co-delivery of methotrexate and etanercept using lipid nanoparticles: a targeted approach for psoriasis management. *Colloids Surf. B: Biointerfaces* 159, 23-29.

Fluhr, J.W., Cavallotti, C., Berardesca, E., 2008. Emollients, moisturizers, and keratolytic agents in psoriasis. *Clin. Dermatol.* 26, 380-386.

Food, Administration, D., 2006a. Guidance for industry: Q9 Quality risk management. Food and Drug Administration, Rockville, MD.(Online.) <http://www.fda.gov/downloads/Drugs/GuidanceComplianceRegulatory-Information/Guidances/ucm073511.pdf>., Accessed on Sept 04, 2020.

Food, Administration, D., 2006b. Guidance for industry: Quality systems approach to pharmaceutical cGMP regulations. Pharmaceutical CGMPs. <https://www.fda.gov/regulatory-information/search-fda-guidance-documents/quality-systems-approach-pharmaceutical-current-good-manufacturing-practice-regulations>. Accessed on July 06, 2020.

Fratoddi, I., Benassi, L., Botti, E., Vaschieri, C., Venditti, I., Bessar, H., Samir, M.A., Azzoni, P., Magnoni, C., Costanzo, A., Casagrande, V., Federici, M., Bianchi, L., Pellacani, G., 2019. Effects of topical methotrexate loaded gold nanoparticle in cutaneous inflammatory mouse model. *Nanomedicine* 17, 276-286.

Frelichowska, J., Bolzinger, M.A., Valour, J.P., Mouaziz, H., Pelletier, J., Chevalier, Y., 2009. Pickering w/o emulsions: drug release and topical delivery. *Int J Pharm* 368, 7-15.

Friberg, E., Podzimek, M., 1984. A non-aqueous microemulsion. *Colloid & Polymer Science* 262, 252-253.

Furue, K., Ito, T., Tsuji, G., Kadono, T., Nakahara, T., Furue, M., 2018. Autoimmunity and autoimmune co-morbidities in psoriasis. *Immunology* 154, 21-27.

Gabriel, D., Mugnier, T., Courthion, H., Kranidioti, K., Karagianni, N., Denis, M.C., Lapteva, M., Kalia, Y., Möller, M., Gurny, R., 2016. Improved topical delivery of tacrolimus: a novel composite hydrogel formulation for the treatment of psoriasis. *J Control Release* 242, 16-24.

- Galooyak, S.S., Dabir, B., 2015. Three-factor response surface optimization of nano-emulsion formation using a microfluidizer. *J. Food Sci. Technol.* 52, 2558-2571.
- Garg, V., Gupta, R., Kapoor, B., Singh, S.K., Gulati, M., 2016. Application of self-emulsifying delivery systems for effective delivery of nutraceuticals, *Emulsions*. Elsevier, pp. 479-518.
- Gattefossé, 2008a. Labrafac™ PG, Lyon, France, p. Propylene glycol dicaprolate/dicaprate. <https://www.gattefosse.com/pharmaceuticals-products/labrafac-pg>, Accessed on July 20,2020.
- Gattefossé, 2008b. Labrafil® M 1944 CS, Lyon, France, pp. Oleoyl polyoxyl-6 glycerides. <https://www.gattefosse.com/pharmaceuticals-products/labrafil-m-1944-cs>, Accessed on July 20,2020.
- Gattefossé, 2008c. Labrafil® M 2130 CS, Lyon,France, pp. Lauroyl polyoxyl-6 glycerides. <https://www.gattefosse.com/pharmaceuticals-products/labrafil-m-2130-cs>, Accessed on July 20,2020.
- Gattefossé, 2008d. Lauroglycol™ FCC, Lyon, France, p. Propylene glycol monolaurate (type I). <https://www.gattefosse.com/pharmaceuticals-products/lauroglycol-fcc>, Accessed on July 20,2020.
- Gattefossé, 2008e. Maisine® CC, Lyon, France, p. Glyceryl monolinoleate. <https://www.gattefosse.com/pharmaceuticals-products/maisine-cc>, Accessed on July 20,2020.
- Gattefossé, 2008f. Peceol™, p. Glyceryl monooleate (Type 40). <https://www.gattefosse.com/pharmaceuticals-products/peceol>, Accessed on July 20,2020.
- Gattefossé, 2008g. Plurol® Oleique CC 497, Lyon, France, pp. Polyglyceryl-3 dioleate. <https://www.gattefosse.com/pharmaceuticals-products/plurol-oleique-cc-497>, Accessed on July 20,2020.
- Gelmetti, C., 2009. Therapeutic moisturizers as adjuvant therapy for psoriasis patients. *Am. J. Clin. Dermatol.* 10, 7-12.
- George, G., Shyni, G.L., Abraham, B., Nisha, P., Raghu, K.G., 2021. Downregulation of TLR4/MyD88/p38MAPK and JAK/STAT pathway in RAW 264.7 cells by *Alpinia galanga* reveals its beneficial effects in inflammation. *J Ethnopharmacol* 275, 114132.
- George, M., Joseph, L., 2013. Pharmacognostical and phytochemical characterization of Pimento leaves. *Glob J Pharmacol* 7, 75-80.
- Gerritsen, M., Van de Kerkhof, P., Langner, A., 2001. Long-term safety of topical calcitriol 3 µg g<sup>-1</sup> ointment. *Br. J. Dermatol.* 144, 17-19.

- Geyer, R.P., Tuliani, V., 1992. Non-aqueous microemulsions for drug delivery. Google Patents.
- Gisondi, P., Del Giglio, M., Girolomoni, G., 2017. Treatment approaches to moderate to severe psoriasis. *Int. J. Mol. Sci* 18, 2427.
- Goyal, R., Macri, L.K., Kaplan, H.M., Kohn, J., 2016. Nanoparticles and nanofibers for topical drug delivery. *J Control Release* 240, 77-92.
- Gudjonsson, J.E., Karason, A., Runarsdottir, E.H., Antonsdottir, A.A., Hauksson, V.B., Jónsson, H.H., Gulcher, J., Stefansson, K., Valdimarsson, H., 2006. Distinct clinical differences between HLA-Cw\* 0602 positive and negative psoriasis patients—an analysis of 1019 HLA-C-and HLA-B-typed patients. *J. Invest. Dermatol.* 126, 740-745.
- Gulotta, A., Saberi, A.H., Nicoli, M.C., McClements, D.J., 2014. Nanoemulsion-based delivery systems for polyunsaturated ( $\omega$ -3) oils: formation using a spontaneous emulsification method. *J. Agric. Food Chem.* 62, 1720-1725.
- Gupta, A., Eral, H.B., Hatton, T.A., Doyle, P.S., 2016. Nanoemulsions: formation, properties and applications. *Soft Matter* 12, 2826-2841.
- Guttoff, M., Saberi, A.H., McClements, D.J., 2015. Formation of vitamin D nanoemulsion-based delivery systems by spontaneous emulsification: factors affecting particle size and stability. *Food Chem.* 171, 117-122.
- Ha, J.-W., Yang, S.-M., 2000. Rheological responses of oil-in-oil emulsions in an electric field. *J Rheol* 44, 235-256.
- Hamill, R.D., Olson, F.A., Petersen, R.V., 1965. Some interfacial properties of a nonaqueous emulsion. *J. Pharm. Sci.* 54, 537-540.
- Hamill, R.D., Petersen, R.V., 1966a. Effect of surfactant concentration on the interfacial viscosity of a nonaqueous system. *J Pharm Sci* 55, 1274-1277.
- Hamill, R.D., Petersen, R.V., 1966b. Effects of aging and surfactant concentration on the rheology and droplet size distribution of a nonaqueous emulsion. *J Pharm Sci* 55, 1268-1274.
- Hanish Singh, J.C., Alagarsamy, V., Sathesh Kumar, S., Narsimha Reddy, Y., 2011. Neurotransmitter metabolic enzymes and antioxidant status on Alzheimer's disease induced mice treated with *Alpinia galanga* (L.) Willd. *Phytother Res* 25, 1061-1067.
- Harries, M., Chalmers, R., Griffiths, C., 2005. Fumaric acid esters for severe psoriasis: a retrospective review of 58 cases. *Br. J. Dermatol.* 153, 549-551.

- Hashim, I.I.A., El-Magd, N.F.A., El-Sheakh, A.R., Hamed, M.F., Abd El, A.E.-G.H., 2018. Pivotal role of Acitretin nanovesicular gel for effective treatment of psoriasis: ex vivo–in vivo evaluation study. *Int. J. Nanomedicine* 13, 1059.
- Hasima, N., Aun, L.I.L., Azmi, M.N., Aziz, A.N., Thirthagiri, E., Ibrahim, H., Awang, K., 2010. 1' S-1'-Acetoxyeugenol acetate: a new chemotherapeutic natural compound against MCF-7 human breast cancer cells. *Phytomedicine* 17, 935-939.
- Hegyi, Z., Zwicker, S., Bureik, D., Peric, M., Koglin, S., Batycka-Baran, A., Prinz, J.C., Ruzicka, T., Schaubert, J., Wolf, R., 2012. Vitamin D analog calcipotriol suppresses the Th17 cytokine–induced proinflammatory S100 “alarmins” psoriasin (S100A7) and koebnerisin (S100A15) in psoriasis. *J. Invest. Dermatol.* 132, 1416-1424.
- Heng, J.Y., Thielmann, F., Williams, D.R., 2006. The effects of milling on the surface properties of form I paracetamol crystals. *Pharm Res* 23, 1918-1927.
- Herman, A., Herman, A.P., 2016. Topically used herbal products for the treatment of psoriasis–mechanism of action, drug delivery, clinical studies. *Planta Med.* 82, 1447-1455.
- Heurtault, B., Saulnier, P., Benoit, J.-P., Proust, J.-E., Pech, B., Richard, J., 2009. Lipid nanocapsules, preparation process and use as medicine. *Google Patents* . US8057823B2.
- Hoidal, J.R., 2001. Reactive oxygen species and cell signaling. *Am. J. Respir. Cell Mol.* 25, 661-663.
- Huang, G., Kao, C., Li, W., Huang, S., Li, H., Chen, C., 2018. A New Phenylalkanoid from the Rhizomes of *Alpinia galanga*. *Chem. Nat. Compd.* 54, 1072-1075.
- Huang, L., Forsberg, C.W., Gibbins, L.N., 1986. Influence of External pH and Fermentation Products on *Clostridium acetobutylicum* Intracellular pH and Cellular Distribution of Fermentation Products. *Appl Environ Microbiol* 51, 1230-1234.
- Huang, T., Lin, X., 1996. Effects of camptothecin on proliferation and differentiation of keratinizing epithelium. *Chin J Dermatol Venereol* 10, 325-327.
- ICH Harmonised Tripartite, G., 2005. Validation of analytical procedures: text and methodology Q2 (R1), International conference on harmonization, Geneva, Switzerland. [https://database.ich.org/sites/default/files/Q2\(R1\)%20Guideline.pdf](https://database.ich.org/sites/default/files/Q2(R1)%20Guideline.pdf), Accessed on Dec 12, 2019.
- IFPA, G.l.i.f.p.d., 2021. Inside Psoriatic Disease: Diabetes. [https://ifpa-pso.com/wp-content/uploads/2021/04/Inside-Psoriatic-Disease\\_Diabetes.pdf](https://ifpa-pso.com/wp-content/uploads/2021/04/Inside-Psoriatic-Disease_Diabetes.pdf), Accessed on Aug 16, 2021.

- Imhof, A., Pine, D.J., 1997. Stability of Nonaqueous Emulsions. *J Colloid Interface Sci* 192, 368-374.
- In, L.L., Arshad, N.M., Ibrahim, H., Azmi, M.N., Awang, K., Nagoor, N.H., 2012. 1'-Acetoxychavicol acetate inhibits growth of human oral carcinoma xenograft in mice and potentiates cisplatin effect via proinflammatory microenvironment alterations. *BMC Complement Altern. Med.* 12, 1-14.
- India, A.P.I., 2008. *Ayurvedic Pharmacopoeia Kulanjan(Rz), India, Part I, Vol. 5* p. 107. <http://www.ayurveda.hu/api/API-Vol-5.pdf>, Accessed on May 13, 2019
- Ito, K., Nakazato, T., Xian, M.J., Yamada, T., Hozumi, N., Murakami, A., Ohigashi, H., Ikeda, Y., Kizaki, M., 2005. 1'-Acetoxychavicol acetate is a novel nuclear factor  $\kappa$ B inhibitor with significant activity against multiple myeloma in vitro and in vivo. *Cancer Res.* 65, 4417-4424.
- Iyer, M.A., Eddington, D., 2019. Storing and releasing rhodamine as a model hydrophobic compound in polydimethylsiloxane microfluidic devices. *Lab Chip* 19, 574-579.
- Jabeen, M., Boisgard, A.-S., Danoy, A., El Kholti, N., Salvi, J.-P., Boulieu, R., Fromy, B., Verrier, B., Lamrayah, M., 2020. Advanced characterization of imiquimod-induced psoriasis-like mouse model. *Pharmaceutics* 12, 789.
- Jadhav, C., Kate, V., Payghan, S.A., 2015a. Investigation of effect of non-ionic surfactant on preparation of griseofulvin non-aqueous nanoemulsion. *Journal of Nanostructure in Chemistry* 5, 107-113.
- Jadhav, C., Kate, V., Payghan, S.A., 2015b. Investigation of effect of non-ionic surfactant on preparation of griseofulvin non-aqueous nanoemulsion. *J Nanostructure Chem.* 5, 107-113.
- Jafari, S.M., Paximada, P., Mandala, I., Assadpour, E., Mehrnia, M.A., 2017. Encapsulation by nanoemulsions, *Nanoencapsulation technologies for the food and nutraceutical industries.* Elsevier, pp. 36-73.
- Jain, A., Doppalapudi, S., Domb, A.J., Khan, W., 2016. Tacrolimus and curcumin co-loaded liposphere gel: Synergistic combination towards management of psoriasis. *J Control Release* 243, 132-145.
- Jain, A., Pooladanda, V., Bulbake, U., Doppalapudi, S., Rafeeqi, T.A., Godugu, C., Khan, W., 2017. Liposphere mediated topical delivery of thymoquinone in the treatment of psoriasis. *Nanotechnol. Biol. Med.* 13, 2251-2262.

- Jaiswal, M., Dudhe, R., Sharma, P., 2015. Nanoemulsion: an advanced mode of drug delivery system. *3.3 Biotech* 5, 123–127
- Jaitely, V., Sakthivel, T., Magee, G., Florence, A., 2004. Formulation of oil in oil emulsions: potential drug reservoirs for slow release. *J Drug Deliv Sci Technol.* 14, 113-117.
- Jakab, G., Fulop, V., Bozo, T., Balogh, E., Kellermayer, M., Antal, I., 2018. Optimization of Quality Attributes and Atomic Force Microscopy Imaging of Reconstituted Nanodroplets in Baicalin Loaded Self-Nanoemulsifying Formulations. *Pharmaceutics* 10, 275.
- Janković, J., Djekic, L., Dobričić, V., Primorac, M., 2016. Evaluation of critical formulation parameters in design and differentiation of self-microemulsifying drug delivery systems (SMEDDSs) for oral delivery of aciclovir. *Int. J. Pharm.* 497, 301-311.
- Janssen, A., Scheffer, J., 1985. Acetoxychavicol acetate, an antifungal component of *Alpinia galanga*. *Planta Med.* 51, 507-511.
- Jantan, I.b., Yassin, M.S.M., Chin, C.B., Chen, L.L., Sim, N.L., 2003. Antifungal activity of the essential oils of nine Zingiberaceae species. *Pharm. Biol.* 41, 392-397.
- Jebbawi, R., Oukhrib, A., Clement, E., Blanzat, M., Turrin, C.O., Caminade, A.M., Lacoste, E., Fruchon, S., Poupot, R., 2020. An Anti-Inflammatory Poly(PhosphorHydrazone) Dendrimer Capped with AzaBisPhosphonate Groups to Treat Psoriasis. *Biomolecules* 10, 949.
- Jin, H., Zhang, R., Gao, Y., 2007. Effect of artesunate on keratinocyte cultured in vitro. *Chin. J. Trad. Med. Sci. Tech* 14, 176-178.
- Jindal, S., Awasthi, R., Singhare, D., Kulkarni, G.T., 2020. Topical delivery of Tacrolimus using liposome containing gel: An emerging and synergistic approach in management of psoriasis. *Med. Hypotheses* 142, 109838.
- Jo, Y.-J., Kwon, Y.-J., 2014. Characterization of  $\beta$ -carotene nanoemulsions prepared by microfluidization technique. *Food Sci. Biotechnol.* 23, 107-113.
- Jones, T.M., 2018. Preformulation studies, *Pharmaceutical Formulation: The Science and Technology of Dosage Forms* pp. 1-41.
- Joscelyne, S.M., Trägårdh, G., 2000. Membrane emulsification—a literature review. *J. Membr. Sci.* 169, 107-117.
- Joseph, S., Bunjes, H., 2014. Evaluation of Shirasu Porous Glass (SPG) membrane emulsification for the preparation of colloidal lipid drug carrier dispersions. *Eur J Pharm Biopharm* 87, 178-186.

- Juntachote, T., Berghofer, E., 2005. Antioxidative properties and stability of ethanolic extracts of Holy basil and Galangal. *Food Chem.* 92, 193-202.
- Kadam, D.P., Suryakar, A.N., Ankush, R.D., Kadam, C.Y., Deshpande, K.H., 2010. Role of oxidative stress in various stages of psoriasis. *Indian J Clin Biochem.* 25, 388-392.
- Kadam, P., Yadav, K., Deoda, R., Navasare, V., Shivatare, R., Patil, M., 2012. Pharmacognostical evaluation of root of *Alpinia galanga* Willd. *Int J Pharm.* 2, 426-431.
- Kadukkattil Ramanunny, A., Singh, S.K., Wadhwa, S., Gulati, M., Kapoor, B., Khursheed, R., Kuppusamy, G., Dua, K., Dureja, H., Chellappan, D.K., 2022. Overcoming hydrolytic degradation challenges in topical delivery: Non-aqueous nano-emulsions. *Expert Opin Drug Deliv.* 19, 23-45.
- Kalb, R.E., Fiorentino, D.F., Lebwohl, M.G., Toole, J., Poulin, Y., Cohen, A.D., Goyal, K., Fakharzadeh, S., Calabro, S., Chevrier, M., 2015. Risk of serious infection with biologic and systemic treatment of psoriasis: results from the Psoriasis Longitudinal Assessment and Registry (PSOLAR). *JAMA Dermatol.* 151, 961-969.
- Kale, S.N., Deore, S.L., 2017. Emulsion micro emulsion and nano emulsion: a review. *Sys. Rev. Pharm.* 8, 39.
- Kamuhabwa, A.R., Roelandts, R., de Witte, P.A., 1999. Skin photosensitization with topical hypericin in hairless mice. *J. Photochem. Photobiol. B, Biol.* 53, 110-114.
- Kassem, A.A., Abd El-Alim, S.H., Asfour, M.H., 2017. Enhancement of 8-methoxypsoralen topical delivery via nanosized niosomal vesicles: Formulation development, in vitro and in vivo evaluation of skin deposition. *Int J Pharm.* 517, 256-268.
- Kassem, M.A., Ghalwash, M.M., Abdou, E.M., 2020. Development of nanoemulsion gel drug delivery systems of cetirizine; factorial optimisation of composition, in vitro evaluation and clinical study. *J. Microencapsul.* 37, 413-430.
- Kaur, A., Singh, R., Dey, C.S., Sharma, S.S., Bhutani, K.K., Singh, I.P., 2010. Antileishmanial phenylpropanoids from *Alpinia galanga* (Linn.) Willd. *Indian J Exp Biol* 48, 314-317.
- Kay, J., Thomas, R., Gruenhagen, J., Venkatramani, C.J., 2021. Simultaneous quantitation of water and residual solvents in pharmaceuticals by rapid headspace gas chromatography with thermal conductivity detection (GC-TCD). *J Pharm Biomed Anal* 194, 113796.

- Khan, W., Ansari, V.A., Hussain, Z., Siddique, N.F., 2018. Nanoemulsion: A Droplet Nanocarrier System for Enhancing Bioavailability of Poorly Water Soluble Drugs. *Res J Pharm Technol.* 11, 5191-5196.
- Khatoon, K., Ali, A., Ahmad, F. J., Hafeez, Z., Rizvi, M., Akhter, S., & Beg, S. 2021. Novel nanoemulsion gel containing triple natural bio-actives combination of curcumin, thymoquinone, and resveratrol improves psoriasis therapy: in vitro and in vivo studies. *Drug Deliv. Transl. Res.*, 11, 1245-1260.
- Khurana, B., Arora, D., Narang, R.K., 2020. QbD based exploration of resveratrol loaded polymeric micelles based carbomer gel for topical treatment of plaque psoriasis: In vitro, ex vivo and in vivo studies. *J Drug Deliv Sci Technol.* 59, 101901.
- Khursheed, R., Singh, S.K., Kumar, B., Wadhwa, S., Gulati, M., Awasthi, A., Vishwas, S., Kaur, J., Corrie, L., Arya, K., 2022. Self-nanoemulsifying composition containing curcumin, quercetin, *Ganoderma lucidum* extract powder and probiotics for effective treatment of type 2 diabetes mellitus in streptozotocin induced rats. *Int. J. Pharm.* 612 121306.
- Khursheed, R., Singh, S.K., Wadhwa, S., Gulati, M., Kapoor, B., Jain, S.K., Gowthamarajan, K., Zacconi, F., Chellappan, D.K., Gupta, G., 2021. Development of mushroom polysaccharide and probiotics based solid self-nanoemulsifying drug delivery system loaded with curcumin and quercetin to improve their dissolution rate and permeability: State of the art. *Int. J. Biol. Macromol.* 2021 744-757.
- Kim, D.S., Cho, J.H., Park, J.H., Kim, J.S., Song, E.S., Kwon, J., Giri, B.R., Jin, S.G., Kim, K.S., Choi, H.G., Kim, D.W., 2019. Self-microemulsifying drug delivery system (SMEDDS) for improved oral delivery and photostability of methotrexate. *Int J Nanomedicine* 14, 4949-4960.
- Kojima-Yuasa, A., Matsui-Yuasa, I., 2020. Pharmacological Effects of 1'-Acetoxychavicol Acetate, a Major Constituent in the Rhizomes of *Alpinia galanga* and *Alpinia conchigera*. *J Med Food* 23, 465-475.
- Kojima-Yuasa, A., Yamamoto, T., Yaku, K., Hirota, S., Takenaka, S., Kawabe, K., Matsui-Yuasa, I., 2016. 1'-Acetoxychavicol acetate ameliorates age-related spatial memory deterioration by increasing serum ketone body production as a complementary energy source for neuronal cells. *Chem. Biol. Interact.* 257, 101-109.



- Kong, W., Salim, N., Masoumi, H.R.F., Basri, M., Da Costa, S.S., Ahmad, N., 2018. Optimization of Hydrocortisone-Loaded Nanoemulsion Formulation Using D-Optimal Mixture Design. *Asian J. Chem.* 30, 853-858.
- Koroleva, M.Y., Yurtov, E.V., 2012. Nanoemulsions: the properties, methods of preparation and promising applications. *Russ. Chem. Rev.* 81, 21-43.
- Kota, K., Sharma, S., Ragavendhra, P., 2018. Study of antiangiogenic activity of “aqueous extract of *Nigella sativa* seeds” in chick chorioallantoic membrane (CAM) model. *Int J Adv Med.* 5.
- Kotta, S., Khan, A.W., Ansari, S., Sharma, R., Ali, J., 2015. Formulation of nanoemulsion: a comparison between phase inversion composition method and high-pressure homogenization method. *Drug Deliv. Transl. Res.* 22, 455-466.
- Kress, W.J., Liu, A.Z., Newman, M., Li, Q.J., 2005. The molecular phylogeny of *Alpinia* (Zingiberaceae): a complex and polyphyletic genus of gingers. *Am. J. Bot.* 92, 167-178.
- Kumar, G.K., Dhamotharan, R., Kulkarni, N.M., Mahat, M.Y.A., Gunasekaran, J., Ashfaque, M., 2011. Embelin reduces cutaneous TNF- $\alpha$  level and ameliorates skin edema in acute and chronic model of skin inflammation in mice. *Eur. J. Pharmacol.* 662, 63-69.
- Kumar, S., Prasad, M., Rao, R., 2021. Topical delivery of clobetasol propionate loaded nanosponge hydrogel for effective treatment of psoriasis: Formulation, physicochemical characterization, antipsoriatic potential and biochemical estimation. *Mater. Sci. Eng. C.* 119, 111605.
- Kwatra, G., Mukhopadhyay, S., 2018. Topical corticosteroids: pharmacology, A treatise on topical corticosteroids in dermatology. Springer, pp. 11-22.
- Lakshmi, P., Devi, G.S., Bhaskaran, S., Sacchidanand, S., 2007. Niosomal methotrexate gel in the treatment of localized psoriasis: phase I and phase II studies. *Indian J Dermatol Venereol Leprol.* 73, 157.
- Lakshmi, S., Suresh, S., Rahul, B., Saikant, R., Maya, V., Gopi, M., Padmaja, G., Remani, P., 2019. In vitro and in vivo studies of 5, 7-dihydroxy flavones isolated from *Alpinia galanga* (L.) against human lung cancer and ascetic lymphoma. *Med Chem Res.* 28, 39-51.
- Lapteva, M., Santer, V., Mondon, K., Patmanidis, I., Chiriano, G., Scapozza, L., Gurny, R., Möller, M., Kalia, Y.N., 2014. Targeted cutaneous delivery of ciclosporin A using micellar

nanocarriers and the possible role of inter-cluster regions as molecular transport pathways. *J Control Release* 196, 9-18.

Latha, C., Shriram, V.D., Jahagirdar, S.S., Dhakephalkar, P.K., Rojatkar, S.R., 2009a. Antiplasmodial activity of 1'-acetoxychavicol acetate from *Alpinia galanga* against multi-drug resistant bacteria. *J Ethnopharmacol* 123, 522-525.

Latha, C., Shriram, V.D., Jahagirdar, S.S., Dhakephalkar, P.K., Rojatkar, S.R., 2009b. Antiplasmodial activity of 1'-acetoxychavicol acetate from *Alpinia galanga* against multi-drug resistant bacteria. *J Ethnopharmacol* 123, 522-525.

Lavery, G., Gilmore, B., Jones, D., Coyle, L., Folan, M., Breathnach, R., 2015. Antimicrobial efficacy of an innovative emulsion of medium chain triglycerides against canine and feline periodontopathogens. *J Small Anim Pract* 56, 253-263.

Lawrence, X.Y., Amidon, G., Khan, M.A., Hoag, S.W., Polli, J., Raju, G., Woodcock, J., 2014. Understanding pharmaceutical quality by design. *AAPS J.* 16, 771-783.

Lebwohl, M., Ali, S., 2001. Treatment of psoriasis. Part 1. Topical therapy and phototherapy. *J. Am. Acad. Dermatol.* 45, 487-502.

Lebwohl, M., Thaçi, D., Warren, R., 2021. Addressing challenges associated with long-term topical treatment and benefits of proactive management in patients with psoriasis. *J. Eur. Acad. Dermatol.* 35, 35-41.

Lee, C.-H., Hwang, S.T.-Y., 2012. Pathophysiology of chemokines and chemokine receptors in dermatological science: a focus on psoriasis and cutaneous T-cell lymphoma. *Dermatologica Sin.* 30, 128-135.

Lee, M.-S., Moon, E.-J., Lee, S.-W., Kim, M.S., Kim, K.-W., Kim, Y.-J., 2001. Angiogenic activity of pyruvic acid in in vivo and in vitro angiogenesis models. *Cancer Res.* 61, 3290-3293.

Lemus, D., Dabancens, A., Illanes, J., Fuenzalida, M., Guerrero, A., Lopez, C., 2001. Antiangiogenic effect of betamethasone on the chick chorioallantoic membrane stimulated by TA3 tumor supernatant. *Biol. Res.* 34, 227-236.

Li, H.-J., Wu, N.-L., Pu, C.-M., Hsiao, C.-Y., Chang, D.-C., Hung, C.-F., 2020a. Chrysin alleviates imiquimod-induced psoriasis-like skin inflammation and reduces the release of CCL20 and antimicrobial peptides. *Sci. Rep.* 10, 1-13.

Li, K., Armstrong, A.W., 2012. A review of health outcomes in patients with psoriasis. *Dermatol. Clin.* 30, 61-72.

- Li, Q., Li, F., Qi, X., Wei, F., Chen, H., Wang, T., 2020b. Pluronic® F127 stabilized reduced graphene oxide hydrogel for the treatment of psoriasis: In vitro and in vivo studies. *Colloids Surf. B: Biointerfaces* 195, 111246.
- Li, Y., Zhang, H., Yang, L., Zhang, L., Wang, T., 2015. Effect of medium-chain triglycerides on growth performance, nutrient digestibility, plasma metabolites and antioxidant capacity in weanling pigs. *Anim Nutr.* 1, 12-18.
- Liang, Y., Sarkar, M.K., Tsoi, L.C., Gudjonsson, J.E., 2017. Psoriasis: a mixed autoimmune and autoinflammatory disease. *Curr. Opin. Immunol.* 49, 1-8.
- Lin, C.C., Yang, C.H., Chang, N.F., Wu, P.S., Chen, Y.S., Lee, S.M., Chen, C.W., 2011. Study on the stability of deoxyArbutin in an anhydrous emulsion system. *Int J Mol Sci* 12, 5946-5954.
- Lin, J., Liu, X., Bao, Y., Hou, S., An, L., Lin, X., 2008a. Effects of isocamptothecin, a novel camptothecin analogue, on proliferation, apoptosis and telomerase activity in HaCaT cells. *Exp. Dermatol* 17, 530-536.
- Lin, Y.-K., Chang, C.-J., Chang, Y.-C., Wong, W.-R., Chang, S.-C., Pang, J.-H.S., 2008b. Clinical assessment of patients with recalcitrant psoriasis in a randomized, observer-blind, vehicle-controlled trial using indigo naturalis. *Arch. Dermatol.* 144, 1457-1464.
- Lin, Z., Jiao, B., Che, C., Zuo, Z., Mok, C., Zhao, M., Ho, W., Tse, W., Lam, K., Fan, R., 2010. Ethyl acetate fraction of the root of *Rubia cordifolia* L. inhibits keratinocyte proliferation in vitro and promotes keratinocyte differentiation in vivo: potential application for psoriasis treatment. *Phytother Res.* 24, 1056-1064.
- LinVerma, S., Vaishnav, Y., K Verma, S., K Jha, A., 2017. Anhydrous Nanoemulsion: An Advanced Drug Delivery System for Poorly Aqueous Soluble Drugs. *Current Nanomedicine (Formerly: Recent Pat Nanomed)* 7, 36-46.
- Lowes, M.A., Bowcock, A.M., Krueger, J.G., 2007. Pathogenesis and therapy of psoriasis. *Nature* 445, 866-873.
- Luo, D.Q., Wu, H.H., Zhao, Y.K., Liu, J.H., Wang, F., 2016. Different imiquimod creams resulting in differential effects for imiquimod-induced psoriatic mouse models. *Exp Biol Med (Maywood)* 241, 1733-1738
- Ma, Z., Zhao, Y., Khalid, N., Shu, G., Neves, M.A., Kobayashi, I., Nakajima, M., 2020. Comparative study of oil-in-water emulsions encapsulating fucoxanthin formulated by microchannel emulsification and high-pressure homogenization. *Food Hydrocoll.*, 105977.

- Maali, A., Mosavian, M.H., 2013. Preparation and application of nanoemulsions in the last decade (2000–2010). *J Dispers Sci Technol.* 34, 92-105.
- Magalhães, M.S.F., Fechine, F.V., Macedo, R.N.d., Monteiro, D.L.S., Oliveira, C.C., Brito, G.A.d.C., Moraes, M.E.A.d., Moraes, M.O.d., 2008. Effect of a combination of medium chain triglycerides, linoleic acid, soy lecithin and vitamins A and E on wound healing in rats. *Acta Cir. Bras.* 23, 262-269.
- Mahae, N., Chaiser, S., 2009. Antioxidant activities and antioxidative components in extracts of *Alpinia galanga* (L.) Sw. *Agric. Nat. Resour.* 43, 358-369.
- Mahajan, R., Handa, S., 2013. Pathophysiology of psoriasis. *Indian J Dermatol Venereol Leprol.* 79, 1.
- Mahesh, K.V., Singh, S.K., Gulati, M., 2014. A comparative study of top-down and bottom-up approaches for the preparation of nanosuspensions of glipizide. *Powder technology* 256, 436-449.
- Malik, T., Pandey, D.K., Roy, P., Okram, A., 2016. Evaluation of Phytochemicals, Antioxidant, Antibacterial and Antidiabetic Potential of *Alpinia galanga* and *Eryngium foetidum* Plants of Manipur (India). *Pharmacogn. J.* 8, 459-464
- Maphosa, Y., Jideani, V.A., 2018. Factors affecting the stability of emulsions stabilised by biopolymers, *Science and Technology Behind Nanoemulsions.* IntechOpen, pp. 65-81.
- Marquis, R.E., Clock, S.A., Mota-Meira, M., 2003. Fluoride and organic weak acids as modulators of microbial physiology. *FEMS Microbiol. Rev.* 26, 493-510.
- Martínez-Monteaudo, S.I., Yan, B., Balasubramaniam, V., 2017. Engineering process characterization of high-pressure homogenization—from laboratory to industrial scale. *Food Eng. Rev.* 9, 143-169.
- Maszewska, M., Florowska, A., Dluzewska, E., Wroniak, M., Marciniak-Lukasiak, K., Zbikowska, A., 2018. Oxidative stability of selected edible oils. *Molecules* 23, 1746.
- Matsuda, H., Ando, S., Morikawa, T., Kataoka, S., Yoshikawa, M., 2005. Structure–activity relationships of 1' S-1'-acetoxychavicol acetate for inhibitory effect on NO production in lipopolysaccharide-activated mouse peritoneal macrophages. *Bioorg Med Chem Lett.* 15, 1949-1953.

- Matsuda, H., Morikawa, T., Managi, H., Yoshikawa, M., 2003a. Antiallergic principles from *Alpinia galanga*: structural requirements of phenylpropanoids for inhibition of degranulation and release of TNF-alpha and IL-4 in RBL-2H3 cells. *Bioorg Med Chem Lett* 13, 3197-3202.
- Matsuda, H., Pongpiriyadacha, Y., Morikawa, T., Ochi, M., Yoshikawa, M., 2003b. Gastroprotective effects of phenylpropanoids from the rhizomes of *Alpinia galanga* in rats: structural requirements and mode of action. *Eur J Pharmacol* 471, 59-67.
- Mayachiew, P., Devahastin, S., 2008. Antimicrobial and antioxidant activities of Indian gooseberry and galangal extracts. *LWT* 41, 1153-1159.
- McClements, D.J., 2012. Nanoemulsions versus microemulsions: terminology, differences, and similarities. *Soft matter* 8, 1719-1729.
- McMahon, J., Hamill, R., Petersen, R., 1963. Emulsifying effects of several ionic surfactants on a nonaqueous immiscible system. *J. Pharm. Sci.* 52, 1163-1168.
- Mehmood, T., Ahmed, A., Ahmad, A., Ahmad, M.S., Sandhu, M.A., 2018. Optimization of mixed surfactants-based  $\beta$ -carotene nanoemulsions using response surface methodology: an ultrasonic homogenization approach. *Food Chem.* 253, 179-184.
- Mehta, A.B., Nadkarni, N.J., Patil, S.P., Godse, K.V., Gautam, M., Agarwal, S., 2016. Topical corticosteroids in dermatology. *Indian J Dermatol Venereol Leprol.* 82.
- Meier, M., Sheth, P.B., 2009. Clinical spectrum and severity of psoriasis, Management of psoriasis. Karger Publishers, pp. 1-20.
- Meng, F., Wang, S., Wang, Y., Liu, H., Huo, X., Ma, H., Ma, Z., Xiong, H., 2017. Microencapsulation of oxalic acid via oil-in-oil (O/O) emulsion solvent evaporation. *Powder Technol.* 320, 405-411.
- Mishra, R., Prabhavalkar, K.S., Bhatt, L.K., 2016. Preparation, optimization, and evaluation of Zaltoprofen-loaded microemulsion and microemulsion-based gel for transdermal delivery. *J. Liposome Res.* 26, 297-306.
- Mittal, S., Ali, J., Baboota, S., 2021. Enhanced anti-psoriatic activity of tacrolimus loaded nanoemulsion gel via omega 3-Fatty acid (EPA and DHA) rich oils-fish oil and linseed oil. *J Drug Deliv Sci Technol.* 63, 102458.
- Modi, J.D., Patel, J.K., 2011. Nanoemulsion-based gel formulation of aceclofenac for topical delivery. *Int. J. Pharm. Pharm. Sci.* 1, 6-12.

- Moghddam, S.R.M., Ahad, A., Aqil, M., Imam, S.S., Sultana, Y., 2016. Formulation and optimization of niosomes for topical diacerein delivery using 3-factor, 3-level Box-Behnken design for the management of psoriasis. *Mater. Sci. Eng. C* . 69, 789-797.
- Moolakkadath, T., Aqil, M., Ahad, A., Imam, S.S., Iqbal, B., Sultana, Y., Mujeeb, M., Iqbal, Z., 2018. Development of transethosomes formulation for dermal fisetin delivery: Box–Behnken design, optimization, in vitro skin penetration, vesicles–skin interaction and dermatokinetic studies. *Artif Cells Nanomed Biotechnol.* 46, 755-765.
- Morikawa, T., Ando, S., Matsuda, H., Kataoka, S., Muraoka, O., Yoshikawa, M., 2005. Inhibitors of nitric oxide production from the rhizomes of *Alpinia galanga*: structures of new 8–9' linked neolignans and sesquiolignan. *Chem. Pharm. Bull.* 53, 625-630.
- Mueller, S., Riedel, H.-D., Stremmel, W., 1997. Determination of catalase activity at physiological hydrogen peroxide concentrations. *Anal. Biochem.* 245, 55-60.
- Murakami, A., Toyota, K., Ohura, S., Koshimizu, K., Ohigashi, H., 2000. Structure- Activity Relationships of (1'S)-1'-Acetoxychavicol Acetate, a major constituent of a Southeast Asian condiment plant *Languas galanga*, on the inhibition of tumor-promoter-induced Epstein-Barr Virus activation. *J. Agric. Food Chem.* 48, 1518-1523.
- Murti, K., Panchal, M.A., Gajera, V., Solanki, J., 2012. Pharmacological properties of *Matricaria recutita*: a review. *Pharmacologia* 3, 348-351.
- Musa, S.H., Basri, M., Masoumi, H.R.F., Karjiban, R.A., Abd Malek, E., Basri, H., Shamsuddin, A.F., 2013. Formulation optimization of palm kernel oil esters nanoemulsion-loaded with chloramphenicol suitable for meningitis treatment. *Colloids Surf. B: Biointerfaces* 112, 113-119.
- Musa, S.H., Basri, M., Masoumi, H.R.F., Shamsudin, N., Salim, N., 2017. Enhancement of physicochemical properties of nanocolloidal carrier loaded with cyclosporine for topical treatment of psoriasis: in vitro diffusion and in vivo hydrating action. *Int. J. Nanomedicine* 12, 2427.
- Muzaffar, F., Singh, U., Chauhan, L., 2013. Review on microemulsion as futuristic drug delivery. *Int J Pharm Pharm Sci* 5, 39-53.
- Na Takuathung, M., Wongnoppavich, A., Panthong, A., Khonsung, P., Chiranthanut, N., Soonthornchareonnon, N., Sireeratawong, S., 2018. Antipsoriatic effects of Wannachawee recipe on imiquimod-induced psoriasis-like dermatitis in BALB/c Mice. *Evid.-Based Complementary Altern. Med.* 2018, 7931031.

- Nakashima, T., 1991. Membrane emulsification by microporous glass. *Key Eng. Mater.* 61, 513-516.
- Namdeo, A.G., Kale, V.M., 2015. Comparative pharmacognostic and phytochemical investigation of two *Alpinia* species from Zingiberaceae Family. *World J Pharm Res* 4, 1417-1432.
- Nampoothiri, S.V., Esakkidurai, T., Pitchumani, K., 2015. Identification and quantification of phenolic compounds in *Alpinia galanga* and *Alpinia calcarata* and its relation to free radical quenching properties: a comparative study. *J. Herbs Spices Med. Plants* 21, 140-147.
- Namsa, N.D., Tag, H., Mandal, M., Kalita, P., Das, A., 2009. An ethnobotanical study of traditional anti-inflammatory plants used by the Lohit community of Arunachal Pradesh, India. *J Ethnopharmacol* 125, 234-245.
- Narukawa, M., Koizumi, K., Iwasaki, Y., Kubota, K., Watanabe, T., 2010. Galangal pungent component, 1'-acetoxychavicol acetate, activates TRPA1. *Biosci Biotechnol Biochem* 74, 1694-1696.
- Nazarzadeh, E., Anthonypillai, T., Sajjadi, S., 2013. On the growth mechanisms of nanoemulsions. *J Colloid Interface Sci* 397, 154-162.
- Neupane, R., Boddu, S.H., Renukuntla, J., Babu, R.J., Tiwari, A.K., 2020. Alternatives to biological skin in permeation studies: Current trends and possibilities. *Pharmaceutics* 12, 152.
- Nola, I., Kostovic, K., Kotrulja, L., Lugovic, L., 2003. The use of emollients as sophisticated therapy in dermatology. *Acta Dermatovenerol Croat* 11, 80-87.
- Nur, F.N.F., Nugraheni, N., Salsabila, I.A., Haryanti, S., Da'i, M., Meiyanto, E., 2020. Revealing the reversal effect of galangal (*Alpinia galanga L.*) extract against oxidative stress in metastatic breast cancer cells and normal fibroblast cells intended as a co-chemotherapeutic and anti-ageing agent. *Asian Pac J Cancer Prev.* 21, 107.
- OECD, 2017. OECD Guidelines for the Testing of Chemicals, Section 4, 402.
- Ohnishi, R., Matsui-Yuasa, I., Deguchi, Y., Yaku, K., Tabuchi, M., Munakata, H., Akahoshi, Y., Kojima-Yuasa, A., 2012. 1'-acetoxychavicol acetate inhibits adipogenesis in 3T3-L1 adipocytes and in high fat-fed rats. *Am J Chin Med* 40, 1189-1204.
- Okasha, E.F., Bayomy, N.A., Abdelaziz, E.Z., 2018. Effect of topical application of black seed oil on imiquimod-induced psoriasis-like lesions in the thin skin of adult male albino rats. *Anat.* 301, 166-174.

- Oonmetta-aree, J., Suzuki, T., Gasaluck, P., Eumkeb, G., 2006. Antimicrobial properties and action of galangal (*Alpinia galanga* Linn.) on *Staphylococcus aureus*. LWT 39, 1214-1220.
- Oyedeji, F.O., Bankole-Ojo, O.S., 2012. Quantitative evaluation of the antipsoriatic activity of sausage tree (*Kigelia africana*). Afr. J. Pure Appl. Chem. 6, 214-218.
- Pachava, V.R., Krishnamurthy, P.T., Dahabal, S.P., Wadhvani, A., Chinthamaneni, P.K., 2017. Anti-angiogenesis potential of ethyl acetate extract of *Moringa oleifera* Lam leaves in chick chorioallantoic membrane (CAM) Assay. J. Nat. Prod. Plant Resour. 7, 18-22.
- Pandey, A., Belwal, T., Sekar, K.C., Bhatt, I.D., Rawal, R.S., 2018. Optimization of ultrasonic-assisted extraction (UAE) of phenolics and antioxidant compounds from rhizomes of *Rheum moorcroftianum* using response surface methodology (RSM). Ind Crops Prod. 119, 218-225.
- Pandey, K., 2020. An overview on promising nanotechnological approaches for the treatment of psoriasis. Recent Pat Nanotechnol. 14, 102-118.
- Pandey, N.K., Singh, S.K., Gulati, M., Kumar, B., Kapoor, B., Ghosh, D., Kumar, R., Khursheed, R., Awasthi, A., Kuppusamy, G., 2020a. Overcoming the dissolution rate, gastrointestinal permeability and oral bioavailability of glimepiride and simvastatin co-delivered in the form of nanosuspension and solid self-nanoemulsifying drug delivery system: A comparative study J Drug Deliv Sci Technol. 60, 102083.
- Pandey, S.S., Maulvi, F.A., Patel, P.S., Shukla, M.R., Shah, K.M., Gupta, A.R., Joshi, S.V., Shah, D.O., 2020b. Cyclosporine laden tailored microemulsion-gel depot for effective treatment of psoriasis: In vitro and in vivo studies. Colloids and Surfaces B: Biointerfaces 186, 110681.
- Pandey, S.S., Shah, K.M., Maulvi, F.A., Desai, D.T., Gupta, A.R., Joshi, S.V., Shah, D.O., 2021. Topical delivery of cyclosporine loaded tailored niosomal nanocarriers for improved skin penetration and deposition in psoriasis: Optimization, ex vivo and animal studies. J Drug Deliv Sci Technol. 63, 102441.
- Pandey, V., Kohli, S., 2018. Lipids and Surfactants: The Inside Story of Lipid-Based Drug Delivery Systems. Crit Rev Ther Drug Carrier Syst 35, 99-155.
- Panonnummal, R., Sabitha, M., 2018. Anti-psoriatic and toxicity evaluation of methotrexate loaded chitin nanogel in imiquimod induced mice model. Int. J. Biol. Macromol. 110, 245-258.
- Pantelić, I., Ilić, T., Marković, B., Savić, S., Lukić, M., Savić, S., 2018. A stepwise protocol for drug permeation assessment that combines heat-separated porcine ear epidermis and vertical diffusion cells. Hem. Ind. 72, 47-53.



- Parmar, K.M., Itankar, P.R., Joshi, A., Prasad, S.K., 2017. Anti-psoriatic potential of *Solanum xanthocarpum* stem in imiquimod-induced psoriatic mice model. *J Ethnopharmacol* 198, 158-166.
- Pascoe, V.L., Kimball, A.B., 2015. Seasonal variation of acne and psoriasis: a 3-year study using the Physician Global Assessment severity scale. *J. Am. Acad. Dermatol.* 73, 523-525.
- Patel, N., Nakrani, H., Raval, M., Sheth, N., 2016. Development of loteprednol etabonate-loaded cationic nanoemulsified in-situ ophthalmic gel for sustained delivery and enhanced ocular bioavailability. *Drug Deliv* 23, 3712-3723.
- Patel, R.P., Joshi, J.R., 2012. An overview on nanoemulsion: a novel approach. *Int J Pharm Sci Res.* 3, 4640.
- Patravale, V.B., Date, A.A., Kulkarni, R.M., 2004. Nanosuspensions: a promising drug delivery strategy. *J Pharm Pharmacol* 56, 827-840.
- Pawar, S., Jadhav, M., 2016. Determination of extractive value and phytochemical analysis of *Bacopa monnieri* (L). *Int. J. Pharmaceut. Clin. Res.* 8, 1222-1229.
- Pawignya, H., Kusworo, T.D., Pramudono, B., 2019. Kinetic modeling of flocculation and coalescence in the system emulsion of water-xylene-terbutyl oleyl glycosides. *Bull. Chem. React. Eng. Catal.* 14, 60-68.
- Payghan, S., Kate, V., Purohit, S., Bhandari, A., 2012. Effect of aging conditions on the dissolution and diffusion stability of non aqueous emulsion. *Inventi Rapid: Pharm Tech.*
- Payghan, S.A., 2016. Effect of formulation variables on physicochemical properties of cholecalciferol non-aqueous nanoemulsion. *Asian J Pharm* 10.
- Pazyar, N., Yaghoobi, R., 2012. Tea tree oil as a novel antipsoriasis weapon. *Skin Pharmacol. Physiol.* 25, 162-163.
- Peterson, R., Hamill, R.D., 1968. Studies on non aqueous emulsions. *J. Soc. Cosmet. Chem* 19, 627-640.
- Petronilho, S., Maraschin, M., Coimbra, M.A., Rocha, S.M., 2012. In vitro and in vivo studies of natural products: A challenge for their valuation. The case study of chamomile (*Matricaria recutita* L.). *Ind Crops Prod* 40, 1-12.
- Petry, T., Bury, D., Fautz, R., Hauser, M., Huber, B., Markowetz, A., Mishra, S., Rettinger, K., Schuh, W., Teichert, T., 2017. Review of data on the dermal penetration of mineral oils and waxes used in cosmetic applications. *Toxicol. Lett.* 280, 70-78.

- Petschow, B.W., Batema, R.P., Ford, L.L., 1996. Susceptibility of *Helicobacter pylori* to bactericidal properties of medium-chain monoglycerides and free fatty acids. *Antimicrob. Agents Chemother.* 40, 302-306.
- Phitak, T., Choocheep, K., Pothacharoen, P., Pompimon, W., Premanode, B., Kongtawelert, P., 2009. The effects of p-hydroxycinnamaldehyde from *Alpinia galanga* extracts on human chondrocytes. *Phytochemistry* 70, 237-243.
- Phongpaichit, S., Vuddhakul, V., Subhadhirasakul, S., Wattanapiromsakul, C., 2006. Evaluation of the antimycobacterial activity of extracts from plants used as self-medication by AIDS patients in Thailand. *Pharm. Biol.* 44, 71-75.
- Pinto, M.F., Moura, C.C., Nunes, C., Segundo, M.A., Lima, S.A.C., Reis, S., 2014. A new topical formulation for psoriasis: development of methotrexate-loaded nanostructured lipid carriers. *Int J Pharm* 477, 519-526.
- Pongsumpun, P., Iwamoto, S., Siripatrawan, U., 2020. Response surface methodology for optimization of cinnamon essential oil nanoemulsion with improved stability and antifungal activity. *Ultrason Sonochem* 60, 104604.
- Powell, V.V.V., Kasson, A.-E., 2001. Emulsions of silicones with non-aqueous hydroxylic solvents. Google Patents.
- Pradhan, M., Alexander, A., Singh, M.R., Singh, D., Saraf, S., Saraf, S., Yadav, K., 2021a. Statistically optimized calcipotriol fused nanostructured lipid carriers for effectual topical treatment of psoriasis. *J Drug Deliv Sci Technol.* 61, 102168.
- Pradhan, M., Singh, D., Singh, M.R., 2013. Novel colloidal carriers for psoriasis: current issues, mechanistic insight and novel delivery approaches. *J Control Release* 170, 380-395.
- Pradhan, M., Singh, D., Singh, M.R., 2017. Fabrication, optimization and characterization of Triamcinolone acetonide loaded nanostructured lipid carriers for topical treatment of psoriasis: Application of Box Behnken design, in vitro and ex vivo studies. *J Drug Deliv Sci Technol.* 41, 325-333.
- Pradhan, M., Yadav, K., Singh, D., Singh, M.R., 2021b. Topical delivery of fluocinolone acetonide integrated NLCs and salicylic acid enriched gel: A potential and synergistic approach in the management of psoriasis. *J Drug Deliv Sci Technol.* 61, 102282.
- Prasad, V., Chaurasia, S., 2017. Performance evaluation of non-ionic surfactant based tazarotene encapsulated proniosomal gel for the treatment of psoriasis. *Mater. Sci. Eng. C* . 79, 168-176.

- Prashar, A., Locke, I.C., Evans, C.S., 2004. Cytotoxicity of lavender oil and its major components to human skin cells. *Cell proliferation* 37, 221-229.
- Preziosi, V., Perazzo, A., Caserta, S., Tomaiuolo, G., Guido, S., 2013. Phase inversion emulsification. *Chem. Eng* 32.
- Prieto-Pérez, R., Cabaleiro, T., Daudén, E., Ochoa, D., Roman, M., Abad-Santos, F., 2013. Genetics of psoriasis and pharmacogenetics of biological drugs. *Autoimmune Dis.* 2013.
- Proksch, E., 2018. pH in nature, humans and skin. *J. Dermatol.* 45, 1044-1052.
- PubChem, NIH National Library of Medicine, National center for Biotechnology Information, 1-Acetoxychavicol acetate, USA. [https://pubchem.ncbi.nlm.nih.gov/compound/1\\_-Acetoxychavicol-acetate](https://pubchem.ncbi.nlm.nih.gov/compound/1_-Acetoxychavicol-acetate), Accessed on May 09, 2019.
- PubChem, Rhodamine B. <https://pubchem.ncbi.nlm.nih.gov/compound/Rhodamine-B>, Accessed on May 06, 2021.
- Pukale, S.S., Sharma, S., Dalela, M., kumar Singh, A., Mohanty, S., Mittal, A., Chitkara, D., 2020. Multi-component clobetasol-loaded monolithic lipid-polymer hybrid nanoparticles ameliorate imiquimod-induced psoriasis-like skin inflammation in Swiss albino mice. *Acta Biomater.* 115, 393-409.
- Pund, S., Pawar, S., Gangurde, S., Divate, D., 2015. Transcutaneous delivery of leflunomide nanoemulgel: Mechanistic investigation into physicochemical characteristics, in vitro anti-psoriatic and anti-melanoma activity. *Int J Pharm* 487, 148-156.
- Punto, L., Potini, C., Duque, P., Gould, E., 1996. Improved topical application emulsions. Google Patents.CA2211263A1, <https://patents.google.com/patent/CA2211263A1/en>, Accessed on June 25, 2020.
- Putranti, W., Dewi, N.A., Widiyastuti, L., 2018. Standardization of extract and characterization of emulgel formula of Lengkuas (*Alpinia Galanga* (L.) Willd) rhizome extract. *Jurnal Farmasi Sains dan Komunitas* 15, 81-91.
- Rabinow, B.E., 2004. Nanosuspensions in drug delivery. *Nat Rev Drug Discov* 3, 785-796.
- Raghuwanshi, N., Yadav, T.C., Srivastava, A.K., Raj, U., Varadwaj, P., Pruthi, V., 2019. Structure-based drug designing and identification of *Woodfordia fruticosa* inhibitors targeted against heat shock protein (HSP70-1) as suppressor for Imiquimod-induced psoriasis like skin inflammation in mice model. *Mater. Sci. Eng. C* . 95, 57-71.

- Rahman, I., Kode, A., Biswas, S.K., 2006. Assay for quantitative determination of glutathione and glutathione disulfide levels using enzymatic recycling method. *Nat. Protoc.* 1, 3159-3165.
- Rai, V.K., Mishra, N., Yadav, K.S., Yadav, N.P., 2018. Nanoemulsion as pharmaceutical carrier for dermal and transdermal drug delivery: Formulation development, stability issues, basic considerations and applications. *J Control Release* 270, 203-225.
- Rai, V.K., Sinha, P., Yadav, K.S., Shukla, A., Saxena, A., Bawankule, D.U., Tandon, S., Khan, F., Chanotiya, C.S., Yadav, N.P., 2020. Anti-psoriatic effect of *Lavandula angustifolia* essential oil and its major components linalool and linalyl acetate. *J Ethnopharmacol* 261, 113127.
- Rajitha, P., Shammika, P., Aiswarya, S., Gopikrishnan, A., Jayakumar, R., Sabitha, M., 2019. Chaulmoogra oil based methotrexate loaded topical nanoemulsion for the treatment of psoriasis. *J Drug Deliv Sci Technol.* 49, 463-476.
- Ramanunni, A., Singh, S.K., Parveen, S.K., Wadhwa, S., 2018. Psoriasis scoring and its outcome on the quality of human life: An updated review. *JETIR* 5, 849-856.
- Ramanunni, A.K., Wadhwa, S., Gulati, M., Gupta, S., Porwal, O., Jha, N.K., Gupta, P.K., Kumar, D., Prasher, P., Dua, K., 2021a. Development and validation of RP-HPLC method for 1'-Acetoxychavicol acetate (ACA) and its application in optimizing the yield of ACA during its isolation from *Alpinia galanga* extract as well as its quantification in nanoemulsion. *S. Afr. J. Bot.*
- Ramanunni, A.K., Wadhwa, S., Gulati, M., Singh, S.K., Kapoor, B., Dureja, H., Chellappan, D.K., Anand, K., Dua, K., Khursheed, R., 2021b. Nanocarriers for treatment of dermatological diseases: Principle, perspective and practices. *Eur. J. Pharmacol.* 890, 173691.
- Ramanunni, A.K., Wadhwa, S., Singh, S.K., Sharma, D.S., Khursheed, R., Awasthi, A., 2020. Treatment Strategies Against Psoriasis: Principle, Perspectives and Practices. *Curr. Drug Deliv.* 17, 52-73.
- Ramanunni, A.K., Wadhwa, S., Thakur, D., Singh, S.K., Kumar, R., 2021c. Treatment Modalities of Psoriasis: A Focus on Requisite for Topical Nanocarrier. *Endocr. Metab. Immune. Disord. Drug Targets.* 21, 418-433.
- Ramezanli, T., Kilfoyle, B.E., Zhang, Z., Michniak-Kohn, B.B., 2017. Polymeric nanospheres for topical delivery of vitamin D3. *Int J Pharm* 516, 196-203.

- Rapalli, V.K., Sharma, S., Roy, A., Alexander, A., Singhvi, G., 2021. Solid lipid nanocarriers embedded hydrogel for topical delivery of apremilast: In-vitro, ex-vivo, dermatopharmacokinetic and anti-psoriatic evaluation. *J Drug Deliv Sci Technol.* 63, 102442.
- Raviadaran, R., Chandran, D., Shin, L.H., Manickam, S., 2018. Optimization of palm oil in water nano-emulsion with curcumin using microfluidizer and response surface methodology. *LWT* 96, 58-65.
- Reynolds, N., Al-Daraji, W., 2002. Calcineurin inhibitors and sirolimus: mechanisms of action and applications in dermatology. *Clin. Exp. Dermatol.* 27, 555-561.
- Riess, G., Cheymol, A., Hoerner, P., Krikorian, R., 2004. Non-aqueous emulsions stabilized by block copolymers: application to liquid disinfectant-filled elastomeric films. *Adv Colloid Interface Sci* 108-109, 43-48.
- Rodríguez-Luna, A., Talero, E., Ávila-Román, J., Romero, A.M.F., Rabasco, A.M., Motilva, V., González-Rodríguez, M.L., 2021. Preparation and in vivo evaluation of rosmarinic acid-loaded transthesomes after percutaneous application on a psoriasis animal model. *AAPS PharmSciTech* 22, 1-18.
- Roriz, C.L., Xavier, V., Heleno, S.A., Pinela, J., Dias, M.I., Calhella, R.C., Morales, P., Ferreira, I.C., Barros, L., 2021. Chemical and bioactive features of *Amaranthus caudatus* L. flowers and optimized ultrasound-assisted extraction of betalains. *Foods* 10, 779.
- Roselan, M.A., Ashari, S.E., Faujan, N.H., Mohd Faudzi, S.M., Mohamad, R., 2020. An improved nanoemulsion formulation containing kojic monooleate: optimization, characterization and in vitro studies. *Molecules* 25, 2616.
- Rottke, M., Lunter, D.J., Daniels, R., 2014. In vitro studies on release and skin permeation of nonivamide from novel oil-in-oil-emulsions. *Eur J Pharm Biopharm* 86, 260-266.
- Roy, S.K., Pahwa, S., Nandanwar, H., Jachak, S.M., 2012. Phenylpropanoids of *Alpinia galanga* as efflux pump inhibitors in *Mycobacterium smegmatis* mc2 155. *Fitoterapia* 83, 1248-1255.
- Runne, U., Kunze, J., 1982. Short-duration ('minutes') therapy with dithranol for psoriasis: a new out-patient regimen. *Br. J. Dermatol.* 106, 135-139.
- Sabat, R., Philipp, S., Höflich, C., Kreutzer, S., Wallace, E., Asadullah, K., Volk, H.D., Sterry, W., Wolk, K., 2007. Immunopathogenesis of psoriasis. *Exp. Dermatol.* 16, 779-798.

- Saberi, A.H., Fang, Y., McClements, D.J., 2013. Fabrication of vitamin E-enriched nanoemulsions: factors affecting particle size using spontaneous emulsification. *J. Colloid Interface Sci.* 391, 95-102.
- Saelee, C., Thongrakard, V., Tencomnao, T., 2011. Effects of Thai medicinal herb extracts with anti-psoriatic activity on the expression on NF- $\kappa$ B signaling biomarkers in HaCaT keratinocytes. *Molecules* 16, 3908-3932.
- Sagiv, A.E., Dikstein, S., Ingber, A., 2001. The efficiency of humectants as skin moisturizers in the presence of oil. *Skin Res Technol.* 7, 32-35.
- Sahu, S., Katiyar, S.S., Kushwah, V., Jain, S., 2018. Active natural oil-based nanoemulsion containing tacrolimus for synergistic antipsoriatic efficacy. *Nanomedicine (Lond)* 13, 1985-1998.
- Sakthivel, T., Wan, K., Florence, A., 1999. Formulation of nonaqueous emulsions. *Pharm Sci* 1, 685-681.
- Samarghandian, S., Afshari, J.T., Hosseini, M., 2014a. Antiproliferative activity and induction of apoptotic by ethanolic extract of *Alpinia galanga* rhizome in human breast carcinoma cell line. *BMC Complement Altern. Med.* 14, 1-9.
- Samarghandian, S., Hadjzadeh, M.A., Afshari, J.T., Hosseini, M., 2014b. Antiproliferative activity and induction of apoptotic by ethanolic extract of *Alpinia galanga* rhizome in human breast carcinoma cell line. *BMC Complement Altern Med* 14, 192.
- Sandra, F., Sudiono, J., Trisfilha, P., Pratiwi, D., 2017. Cytotoxicity of *Alpinia galanga* rhizome crude extract on NIH-3T3 cells. *Indones. Biomed. J.* 9, 23-28.
- Sangaraju, R., Alavala, S., Nalban, N., Jerald, M.K., Sistla, R., 2021. Galangin ameliorates imiquimod-induced psoriasis-like skin inflammation in BALB/c mice via down regulating NF- $\kappa$ B and activation of Nrf2 signaling pathways. *Int. Immunopharmacol* 96, 107754.
- Santos-Sánchez, N.F., Salas-Coronado, R., Hernández-Carlos, B., Villanueva-Cañongo, C., 2019. Shikimic acid pathway in biosynthesis of phenolic compounds. *Plant physiological aspects of phenolic compounds* 1.
- Santos, M.C., Koetz, M., Mendez, A.S., Henriques, A.T., 2020. Ultrasound-assisted extraction optimization and validation of ultra-performance liquid chromatographic method for the quantification of miquelianin in *Cuphea glutinosa* leaves. *Talanta* 216, 120988.

- Sarafian, G., Afshar, M., Mansouri, P., Asgarpanah, J., Raoufinejad, K., Rajabi, M., 2015. Topical turmeric microemulgel in the management of plaque psoriasis; a clinical evaluation. *Iran J Pharm Res* 14, 865.
- Sârbu, M.I., Mitran, M.I., Mitran, C.I., Limbău, A.M., Georgescu, S.R., 2017. Adverse reactions of biological therapies in patients with psoriasis. *J Mind Med Sci.* 4, 4-12.
- Sarheed, O., Shouqair, D., Ramesh, K., Khaleel, T., Amin, M., Boateng, J., Drechsler, M., 2020. Formation of stable nanoemulsions by ultrasound-assisted two-step emulsification process for topical drug delivery: Effect of oil phase composition and surfactant concentration and loratadine as ripening inhibitor. *Int J Pharm* 576, 118952.
- Sasidharan, S., Chen, Y., Saravanan, D., Sundram, K., Latha, L.Y., 2011. Extraction, isolation and characterization of bioactive compounds from plants' extracts. *Afr J Tradit Complement Altern Med.* 8
- Schleicher, S.M., 2016. Psoriasis: Pathogenesis, Assessment, and Therapeutic Update *Clin. Podiatr. Med. Surg.* 33, 355-366.
- Savrikar, S., Lagad, C., 2010. Study of preparation and standardization of 'Maadhutailika Basti' with special reference to emulsion stability. *Ayu* 31, 1.
- Schleicher, S.M., 2016. Psoriasis: Pathogenesis, Assessment, and Therapeutic Update *Clin. Podiatr. Med. Surg.* 33, 355-366.
- Schoket, B., Horkay, I., Kósa, Á., Paldeak, L., Hewer, A., Grover, P.L., Phillips, D.H., 1990. Formation of DNA adducts in the skin of psoriasis patients, in human skin in organ culture, and in mouse skin and lung following topical application of coal-tar and juniper tar. *J. Invest. Dermatol.* 94, 241-246.
- Seo, J.-W., Cho, S.-C., Park, S.-J., Lee, E.-J., Lee, J.-H., Han, S.-S., Pyo, B.S., Park, D.-H., Kim, B.-H., 2013. 1'-Acetoxychavicol acetate isolated from *Alpinia galanga* ameliorates ovalbumin-induced asthma in mice. *PLoS one* 8, e56447.
- Sethi, G., Sung, B., Aggarwal, B.B., 2008. Nuclear factor- $\kappa$ B activation: from bench to bedside. *Exp. Biol. Med.* 233, 21-31.
- Shafiq, S., Shakeel, F., Talegaonkar, S., Ahmad, F.J., Khar, R.K., Ali, M., 2007. Development and bioavailability assessment of ramipril nanoemulsion formulation. *Eur J Pharm Biopharm* 66, 227-243.

- Shahavi, M.H., Hosseini, M., Jahanshahi, M., Meyer, R.L., Darzi, G.N., 2016. Clove oil nanoemulsion as an effective antibacterial agent: Taguchi optimization method. *Desalin. Water Treat.* 57, 18379-18390.
- Shakeel, F., Shafiq, S., Haq, N., Alanazi, F.K., Alsarra, I.A., 2012. Nanoemulsions as potential vehicles for transdermal and dermal delivery of hydrophobic compounds: an overview. *Expert Opin Drug Deliv.* 9, 953-974.
- Shalavadi, M.H., 2018. Physicochemical and phytochemical screening of *Convolvulus pluricaulis* collected from Bagalkot, Karnataka. *Int. J. Green Pharm.* 12.
- Shanmugapriya, K., Kim, H., Saravana, P.S., Chun, B.-S., Kang, H.W., 2018. Astaxanthin-alpha tocopherol nanoemulsion formulation by emulsification methods: Investigation on anticancer, wound healing, and antibacterial effects. *Colloids Surf B Biointerfaces* 172, 170-179.
- Sharma, A., Singh, A., Harikumar, S., 2020. Development and optimization of nanoemulsion based gel for enhanced transdermal delivery of nitrendipine using box-behnken statistical design. *Drug Dev Ind Pharm.* 46, 329-342.
- Sharma, P.K., Singh, V., Ali, M., Kumar, S., 2015. Evaluation of Antinociceptive and Antiinflammatory Activities of Methanolic Extract of *Alpinia galanga* Rhizomes in Animal Models. *Int J Pharm Sci Res* 6, 3103-3108.
- Shirke, S., Kate, V., Tamboli, Z., Payghan, S., 2015. Nonaqueous emulsion based anti wrinkle preparation restrain vitamin C. *Literati J Pharm Drug Deliv Technol* 1, 37-50.
- Shrivastav, S., Sindhu, R., Kumar, S., Kumar, P., 2009. Anti-psoriatic and phytochemical evaluation of *Thespesia populnea* bark extracts. *Int J Pharm Pharm Sci* 1.
- Shukla, T., Upmanyu, N., Agrawal, M., Saraf, S., Saraf, S., Alexander, A., 2018. Biomedical applications of microemulsion through dermal and transdermal route. *Biomed. Pharmacother.* 108, 1477-1494.
- Singh, J.H., Alagarsamy, V., Diwan, P.V., Kumar, S.S., Nisha, J., Reddy, Y.N., 2011a. Neuroprotective effect of *Alpinia galanga* (L.) fractions on A $\beta$  (25–35) induced amnesia in mice. *J. Ethnopharmacol.* 138, 85-91.
- Singh, S.K., Srinivasan, K.K., Gowthamarajan, K., Singare, D.S., Prakash, D., Gaikwad, N.B., 2011b. Investigation of preparation parameters of nanosuspension by top-down media milling to improve the dissolution of poorly water-soluble glyburide. *Eur J Pharm Biopharm* 78, 441-446.



- Singh, K.K., Tripathy, S., 2014. Natural treatment alternative for psoriasis: a review on herbal resources. *J. Appl. Pharm.* 4, 114-121.
- Singh, Y., Meher, J.G., Raval, K., Khan, F.A., Chaurasia, M., Jain, N.K., Chourasia, M.K., 2017. Nanoemulsion: Concepts, development and applications in drug delivery. *J Control Release* 252, 28-49.
- Singhal, M., Kansara, N., 2012. Cassia tora Linn cream inhibits ultraviolet-B-induced psoriasis in rats. *ISRN dermatology* 2012.
- Slutsky, J.B., Clark, R., Remedios, A.A., Klein, P.A., 2010. An evidence-based review of the efficacy of coal tar preparations in the treatment of psoriasis and atopic dermatitis. *J Drugs Dermatol.* 9, 1258-1264.
- Solak Tekin, N., Tekin, I.O., Barut, F., Yilmaz Sipahi, E., 2007. Accumulation of oxidized low-density lipoprotein in psoriatic skin and changes of plasma lipid levels in psoriatic patients. *Mediators Inflamm.* 2007.
- Solans, C., Izquierdo, P., Nolla, J., Azemar, N., Garcia-Celma, M.J., 2005. Nano-emulsions. *Curr Opin Colloid Interface Sci.* 10, 102-110.
- Soliman, M., Salah, M., Fadel, M., Nasr, M., El-Azab, H., 2021. Contrasting the efficacy of pulsed dye laser and photodynamic methylene blue nanoemulgel therapy in treating acne vulgaris. *Arch Dermatol Res* 313, 173-180.
- Somagoni, J., Boakye, C.H., Godugu, C., Patel, A.R., Faria, H.A.M., Zucolotto, V., Singh, M., 2014. Nanomiengel-a novel drug delivery system for topical application-in vitro and in vivo evaluation. *PLoS One* 9, e115952.
- Sosnowska, K., Szymanska, E., Winnicka, K., 2017. Nanoemulsion with clotrimazole- Design and optimalization of mean droplet size using microfluidization technique. *Acta Pol Pharm.* 74, 519-526.
- Sotoyama, K., Asano, Y., Ihara, K., Takahashi, K., Doi, K., 1999. Water/oil emulsions prepared by the membrane emulsification method and their stability. *J. Food Sci.* 64, 211-215.
- Spitz, D.R., Oberley, L.W., 1989. An assay for superoxide dismutase activity in mammalian tissue homogenates. *Anal. Biochem.* 179, 8-18.
- Sriraksa, N., Kongsui, R., Thongrong, S., Surapinit, S., 2020. Neuroprotective effect of *Alpinia galanga* against neurodegeneration in the rat hippocampus induced by kainic acid. *Naresuan Phayao Journal* 13, 3-11.

- Subash, K., Bhaarathi, G.M., Rao, N.J., Cheriyan, B.V., 2013. Phytochemical screening and acute toxicity study of ethanolic extract of *Alpinia galanga* in rodents. *Int. j. med. health res.* 1, 93-100.
- Subash, K., Bhanu Prakash, G., Vijaya Chandra Reddy, K., Manjunath, K., Umamaheswara Rao, K., 2016. Anti-inflammatory activity of ethanolic extract of *Alpinia galanga* in carrageenan induced pleurisy rats. *Natl J Physiol Pharm Pharmacol.* 6, 468-470.
- Suitthimeathegorn, O., Jaitely, V., Florence, A.T., 2005. Novel anhydrous emulsions: Formulation as controlled release vehicles. *Int J Pharm* 298, 367-371.
- Suitthimeathegorn, O., Turton, J.A., Mizuuchi, H., Florence, A.T., 2007. Intramuscular absorption and biodistribution of dexamethasone from non-aqueous emulsions in the rat. *Int J Pharm* 331, 204-210.
- Suja, S., Chinnaswamy, P., 2008. Inhibition of in vitro cytotoxic effect evoked by *Alpinia galanga* and *Alpinia officinarum* on PC - 3 cell line. *Anc Sci Life* 27, 33-40.
- Sun, L., Liu, Z., Wang, L., Cun, D., Tong, H.H., Yan, R., Chen, X., Wang, R., Zheng, Y., 2017. Enhanced topical penetration, system exposure and anti-psoriasis activity of two particle-sized, curcumin-loaded PLGA nanoparticles in hydrogel. *J Control Release* 254, 44-54.
- Sun, R., Xia, N., Xia, Q., 2019. Non-aqueous nanoemulsions as a new strategy for topical application of astaxanthin. *J Dispers Sci Technol* 41, 1777-1788.
- Svensden, M.T., Feldman, S.R., Tiedemann, S.N., Sørensen, A.S.S., Rivas, C.M.R., Andersen, K.E., 2020. Limitations in health-care system resources affecting adherence of patient with psoriasis to topical drugs: A focus group study. *J. Psoriasis Psoriatic Arthritis* 5, 54-60.
- Tadros, T., Izquierdo, P., Esquena, J., Solans, C., 2004. Formation and stability of nano-emulsions. *Adv Colloid Interface Sci* 108-109, 303-318.
- Takeshita, J., Grewal, S., Langan, S.M., Mehta, N.N., Ogdie, A., Van Voorhees, A.S., Gelfand, J.M., 2017. Psoriasis and comorbid diseases: Epidemiology. *J Am Acad Dermatol* 76, 377-390.
- Tampa, M., Nicolae, I., Ene, C.D., Sarbu, I., Matei, C., Georgescu, S.R., 2017. Vitamin C and thiobarbituric acid reactive substances (TBARS) in psoriasis vulgaris related to psoriasis area severity index (PASI). *Revista de Chimie* 68, 43-47.
- Tan, T.B., Nakajima, M., Tan, C.P., 2018. Effect of polysaccharide emulsifiers on the fabrication of monodisperse oil-in-water emulsions using the microchannel emulsification method. *J. Food Eng.* 238, 188-194.

- Tanaka, T., Kawabata, K., Kakumoto, M., Makita, H., Matsunaga, K., Mori, H., Satoh, K., Hara, A., Murakami, A., Koshimizu, K., Ohigashi, H., 1997. Chemoprevention of azoxymethane-induced rat colon carcinogenesis by a xanthine oxidase inhibitor, 1'-acetoxychavicol acetate. *Jpn J Cancer Res* 88, 821-830.
- Tawfeek, A.M., Dyab, A.K., Al-Lohedan, H.A., 2014. Synergetic effect of reactive surfactants and clay particles on stabilization of nonaqueous oil-in-oil (o/o) emulsions. *J Dispers Sci Technol.* 35, 265-272.
- Thakur, K., Sharma, G., Singh, B., Jain, A., Tyagi, R., Chhibber, S., Katare, O.P., 2018. Cationic-bilayered nanoemulsion of fusidic acid: an investigation on eradication of methicillin-resistant *Staphylococcus aureus* 33591 infection in burn wound. *Nanomedicine (Lond)* 13, 825-847.
- Thakur, N., Garg, G., Sharma, P., Kumar, N., 2012. Nanoemulsions: a review on various pharmaceutical application. *Glob. J. Pharmacol.* 6, 222-225.
- Traub, M., Marshall, K., 2007. Psoriasis--pathophysiology, conventional, and alternative approaches to treatment. *Alternative medicine review* 12.
- Tripathi, P., Kumar, A., Jain, P.K., Patel, J.R., 2018. Carbomer gel bearing methotrexate loaded lipid nanocontainers shows improved topical delivery intended for effective management of psoriasis. *Int. J. Biol. Macromol.* 120, 1322-1334.
- Tripathi, P.K., Gorain, B., Choudhury, H., Srivastava, A., Kesharwani, P., 2019. Dendrimer entrapped micro sponge gel of dithranol for effective topical treatment. *Heliyon* 5, e01343.
- Tsuji, T., Sugai, T., 1972. Topically administered fluorouracil in psoriasis. *Arch. Dermatol.* 105, 208-212.
- Tungmunnithum, D., Tanaka, N., Uehara, A., Iwashina, T., 2020. Flavonoids profile, taxonomic data, history of cosmetic uses, anti-oxidant and anti-aging potential of *Alpinia galanga* (L.) Willd. *Cosmetics* 7, 89.
- Tyring, S., 1998. Immune response modification: imiquimod. *Aust. J. Dermatol.* 39, S11-13.
- Urmaliya, H., Gupta, M., Agrawal, A., Jain, N.K., Dubey, A., 2016. Formulation development and evaluation of microemulsion gel of ketoconazole as an antifungal agent. *Pharmacia: An. Int. J. of. Pharm. Sci.* 2, 120-130.
- Uva, L., Miguel, D., Pinheiro, C., Antunes, J., Cruz, D., Ferreira, J., Filipe, P., 2012. Mechanisms of action of topical corticosteroids in psoriasis. *Int. J. Endocrinol.* 2012.

- V. Schröder, H.S., 1999. Emulsification using microporous, ceramic membranes, in: 1), P.o.t.F.E.C.o.C.E.E. (Ed.), Florence, Italy, pp. 2491–2494.
- Valenzuela, A., 1991. The biological significance of malondialdehyde determination in the assessment of tissue oxidative stress. *Life Sci.* 48, 301-309.
- Verma, R.K., Garima, M., Pradeep, S., Jha, K., Khosa, R., 2011. *Alpinia galanga*-an important medicinal plant: a review. *Der Pharmacia Sinica* 2, 142-154.
- Verma, R.K., Mishra, G., Singh, P., Jha, K.K., Khosa, R.L., 2015. Anti-diabetic activity of methanolic extract of *Alpinia galanga* Linn. aerial parts in streptozotocin induced diabetic rats. *Ayu* 36, 91.
- Verma, S., Gokhale, R., Burgess, D.J., 2009. A comparative study of top-down and bottom-up approaches for the preparation of micro/nanosuspensions. *Int J Pharm* 380, 216-222.
- Vijayalakshmi, A., Ravichandiran, V., Velraj, M., Nirmala, S., Jayakumari, S., 2012. Screening of flavonoid “quercetin” from the rhizome of *Smilax china* Linn. for anti-psoriatic activity. *Asian Pac. J. Trop. Biomed.* 2, 269-275.
- Villalobos-Castillejos, F., Granillo-Guerrero, V.G., Leyva-Daniel, D.E., Alamilla-Beltrán, L., Gutiérrez-López, G.F., Monroy-Villagrana, A., Jafari, S.M., 2018. Fabrication of nanoemulsions by microfluidization, *Nanoemulsions*. Elsevier, pp. 207-232.
- Vlietinck, C.P., AJ, V.B.D., Maes, L., 2006. Anti-infective potential of natural products: How to develop a stronger in vitro ‘proof-of-concept’. *J Ethnopharmacol* 106, 290-302.
- Wadher, K., Dabre, S., Gaidhane, A., Trivedi, S., Umekar, M., 2021. Evaluation of antipsoriatic activity of gel containing *Pongamia pinnata* extract on Imiquimod-induced psoriasis. *Clin. Phytoscience* 7, 1-6.
- Wadhwa, S., Singh, B., Sharma, G., Raza, K., Katare, O.P., 2016. Liposomal fusidic acid as a potential delivery system: a new paradigm in the treatment of chronic plaque psoriasis. *Drug Deliv.* 23, 1204-1213.
- Walter, A., Schafer, M., Cecconi, V., Matter, C., Urosevic-Maiwald, M., Belloni, B., Schonewolf, N., Dummer, R., Bloch, W., Werner, S., Beer, H.D., Knuth, A., van den Broek, M., 2013. Aldara activates TLR7-independent immune defence. *Nat Commun* 4, 1560.
- Wang, Q., Hu, C., Zhang, H., Zhang, Y., Liu, T., Qian, A., Xia, Q., 2016. Evaluation of a new solid non-aqueous self-double-emulsifying drug-delivery system for topical application of quercetin. *J Microencapsul* 33, 785-794.

- Weinstein, G.D., Koo, J.Y., Krueger, G.G., Lebwohl, M.G., Lowe, N.J., Menter, M.A., Lew-Kaya, D.A., Sefton, J., Gibson, J.R., Walker, P.S., 2003. Tazarotene cream in the treatment of psoriasis: two multicenter, double-blind, randomized, vehicle-controlled studies of the safety and efficacy of tazarotene creams 0.05% and 0.1% applied once daily for 12 weeks. *J. Am. Acad. Dermatol.* 48, 760-767.
- Wong, L.F., Lim, Y.Y., Omar, M., 2009. Antioxidant and antimicrobial activities of some *Alpinia* species. *J. Food Biochem.* 33, 835-851.
- Xie, X.-j., Di, T.-t., Wang, Y., Wang, M.-x., Meng, Y.-j., Lin, Y., Xu, X.-l., Li, P., Zhao, J.-x., 2018. Indirubin ameliorates imiquimod-induced psoriasis-like skin lesions in mice by inhibiting inflammatory responses mediated by IL-17A-producing  $\gamma\delta$  T cells. *Mol. Immunol.* 101, 386-395.
- Yang, Q., Liu, S., Gu, Y., Tang, X., Wang, T., Wu, J., Liu, J., 2019. Development of sulconazole-loaded nanoemulsions for enhancement of transdermal permeation and antifungal activity. *Int. J. Nanomedicine* 14, 3955.
- Yang, X., Eilerman, R.G., 1999. Pungent principal of *Alpinia galangal* (L.) swartz and its applications. *J Agric Food Chem* 47, 1657-1662.
- Yang, Y., Fang, Z., Chen, X., Zhang, W., Xie, Y., Chen, Y., Liu, Z., Yuan, W., 2017. An overview of Pickering emulsions: solid-particle materials, classification, morphology, and applications. *Front. Pharmacol.* 8, 287.
- Yasuhara, T., Manse, Y., Morimoto, T., Qilong, W., Matsuda, H., Yoshikawa, M., Muraoka, O., 2009. Acetoxybenzhydrols as highly active and stable analogues of 1' S-1'-acetoxychavicol, a potent antiallergic principal from *Alpinia galanga*. *Bioorganic Med. Chem. Lett.* 19, 2944-2946.
- Ye, Y., Li, B., 2006. 1' S-1'-acetoxychavicol acetate isolated from *Alpinia galanga* inhibits human immunodeficiency virus type 1 replication by blocking Rev transport. *Journal of general virology* 87, 2047-2053.
- Yildirim, S.T., Oztop, M.H., Soyer, Y., 2017. Cinnamon oil nanoemulsions by spontaneous emulsification: Formulation, characterization and antimicrobial activity. *LWT* 84, 122-128.
- Yu, E.S., Min, H.J., Lee, K., Lee, M.S., Nam, J.W., Seo, E.K., Hong, J.H., Hwang, E.S., 2009. Anti-inflammatory activity of p-coumaryl alcohol- $\gamma$ -O-methyl ether is mediated through modulation of interferon- $\gamma$  production in Th cells. *Br. J. Pharmacol.* 156, 1107-1114.

- Yu, S., Go, G.-w., Kim, W., 2019. Medium chain triglyceride (MCT) oil affects the immunophenotype via reprogramming of mitochondrial respiration in murine macrophages. *Foods* 8, 553.
- Yukuyama, M., Ghisleni, D., Pinto, T., Bou-Chacra, N., 2016. Nanoemulsion: process selection and application in cosmetics—a review. *J Cosmet Sci.* 38, 13-24.
- Zeng, J., Luo, S., Huang, Y., Lu, Q., 2017a. Critical role of environmental factors in the pathogenesis of psoriasis. *J. Dermatol.* 44, 863-872.
- Zeng, L., Xin, X., Zhang, Y., 2017b. Development and characterization of promising Cremophor EL-stabilized o/w nanoemulsions containing short-chain alcohols as a cosurfactant. *RSC Adv.* 7, 19815-19827.
- Zha, W.-J., Qian, Y., Shen, Y., Du, Q., Chen, F.-F., Wu, Z.-Z., Li, X., Huang, M., 2013. Galangin abrogates ovalbumin-induced airway inflammation via negative regulation of NF- $\kappa$ B. *Evid.-Based Complementary Altern. Med.* 2013.
- Zhang, D., Zou, L., Wu, D.-T., Zhuang, Q.-G., Li, H.-B., Mavumengwana, V., Corke, H., Gan, R.-Y., 2021. Discovery of 1'-acetoxychavicol acetate (ACA) as a promising antibacterial compound from galangal (*Alpinia galanga* (Linn.) Willd). *Ind Crops Prod* 171, 113883.
- Zhang, L., Huang, C., Zhang, Z., Wang, Z., Lin, J., 2005. Therapeutic effects of koumine on psoriasis: an experimental study in mice. *Di Yi Jun Yi Da Xue Xue Bao. Academic journal of the first medical college of PLA* 2005 Chinese 25, 547-549.
- Zhang, L., Mao, S., 2017. Application of quality by design in the current drug development. *Asian J. Pharm. Sci.* 12, 1-8.
- Zhang, Y.-T., Shen, L.-N., Zhao, J.-H., Feng, N.-P., 2014. Evaluation of psoralen ethosomes for topical delivery in rats by using in vivo microdialysis. *Int J Nanomedicine* 9, 669.
- Zhang, Y., Xia, Q., Li, Y., He, Z., Li, Z., Guo, T., Wu, Z., Feng, N., 2019. CD44 assists the topical anti-psoriatic efficacy of curcumin-loaded hyaluronan-modified ethosomes: a new strategy for clustering drug in inflammatory skin. *Theranostics* 9, 48.
- Zheng, Y., Zheng, M., Ma, Z., Xin, B., Guo, R., Xu, X., 2015. Sugar fatty acid esters, Polar lipids. Elsevier, pp. 215-243.
- Zhou, C., Li, C., Siva, S., Cui, H., Lin, L., 2021. Chemical composition, antibacterial activity and study of the interaction mechanisms of the main compounds present in the *Alpinia galanga* rhizomes essential oil. *Ind Crops Prod* 165, 113441.

Živković, J., Janković, T., Menković, N., Šavikin, K., 2019. Optimization of ultrasound-assisted extraction of isogentisin, gentiopicroside and total polyphenols from gentian root using response-surface methodology. *Ind Crops Prod* 139, 111567.

Zothanpuii, F., Rajesh, R., Selvakumar, K., 2020. A Review on Stability Testing Guidelines of Pharmaceutical Products. *Asian J Pharm Clin Res* 13, 3-9.



---

# **Annexures**

---





**L**OVELY  
**P**ROFESSIONAL  
**U**NIVERSITY

*Transforming Education Transforming India*

**Center for  
Research Degree Programmes**

*LPU/CRDP/EC/290819/0103*

Dated: Thursday 29, Aug 2019

Arya K R  
Registration Number: 11815948  
Programme Name: Pharmaceutics

**Subject: Letter of Candidacy for Ph.D.**

Dear Candidate,

We are very pleased to inform you that the Department Doctoral Board has approved your candidacy for the Ph.D. Programme on Monday 20, May 2019 by accepting your research proposal entitled: "FORMULATION DEVELOPMENT, OPTIMIZATION AND EVALUATION OF ALPINIA GALANGA EXTRACT LOADED NANOEMULSION" under the supervision of Dr. Sheetu.

As a Ph.D. candidate you are required to abide by the conditions, rules and regulations laid down for Ph.D. Programme of the University, and amendments, if any, made from time to time.

We wish you the very best!!

In case you have any query related to your programme, please contact Centre of Research Degree Programmes.

HOS

Centre of Research Degree Programmes



POST GRADUATE & RESEARCH DEPARTMENT OF BOTANY

ST. PETERS COLLEGE KOLENCHERY

### PLANT IDENTIFICATION CERTIFICATE

This is to certify that Mrs. Arya K. R. (Full time PhD Scholar), Lovely Professional University, Phagwara, has approached me with a sample of plant specimen on which she intended to do her research work. I have identified and confirmed the Binomial name of the plant as *Alpinia galanga* (L) Sw. coming under the family Zingiberaceae.

She has also deposited the specimen in the Herbarium of the College and has been provided with the specimen Number SPC H-3085

Place: Kolenchery

Date: 22-07-2019



Dr. Abraham Mathew

Assistant Professor

Dept. of Botany

St. Peters College, Kolenchery

**CENTRAL ANIMAL HOUSE FACILITY (CAHF)**  
Lovely Institute of Technology (Pharmacy), Lovely Professional University  
Ludhiana- Jalandhar G.T. Road, Phagwara (Punjab), 144411  
Registration Number -954/PO/ReRcBiBu/S/06/CPCSEA

---

**CERTIFICATE**

This is to certify that the project titled "*Acute dermal toxicity study and antipsoriatic activity of Alpinia galanga extract loaded nano emulsion on experimental animals. (Thesis title: Formulation development, optimization and evaluation of Alpinia galanga extract loaded nano emulsion)*" has been approved by the IAEC.


Name of Principal Investigator: Dr. Sheetu

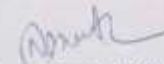
IAEC approval number: LPU/IAEC/2021/80


Date of Approval: 4<sup>th</sup> May 2021

Animals approved: 42 Swiss albino mice/BALB/c mice, Either sex and 9 SD/Wistar rats for a period of one year

Remarks if any: - NA

  
Dr. Monica Gulati

  
Dr. Navneet Khurana

  
Dr. Bimlesh Kumar

Biological Scientist,  
Chairperson IAEC

Scientist from different discipline

Scientist In-Charge of Animal House,  
Member Secretary IAEC

## List of publications, patents and presentations

### Publications related to research topic

- **Ramanunny, A.K.**, Singh, S.K., Wadhwa, S., Gulati, M., Kumar, B., Kumar, A., Almawash, S., Saq, A.A., Gowthamrajan, K., Dua, K., Singh, H., Vishwas, S., Khursheed, R., Parveen, S.R., Venkatesan, A., Paudel, K.R., Hansbr, P.M., Chellappan, D.K., **Topical non-aqueous nanoemulsion of *Alpinia galanga* extract for effective treatment in psoriasis: In vitro and in vivo evaluation**, Int. J Pharm. 121882
- **Ramanunny, A.K.**, Wadhwa, S., Gulati, M., Vishwas, S., Khursheed, R., Paudel, K.R., Gupta, S., Porwal, O., Alshahrani, S.M., Jha, N.K., Chellappan, D.K., Prasher, P., Gupta, G., Adams, J., Dua, K., Tewari, D., Singh, S.K. 2022. **Journey of *Alpinia galanga* from kitchen spice to nutraceutical to folk medicine to nanomedicine**. J Ethnopharmacol. 291,115144.
- **Ramanunny, A.K.**, Singh, S.K., Wadhwa, S., Gulati, M., Kapoor, B., Khursheed, R., Kuppusamy, G., Dua, K., Dureja, H., Chellappan, D.K., 2022. **Overcoming hydrolytic degradation challenges in topical delivery: Non-aqueous nano-emulsions**. Expert Opin Drug Deliv. 19, 23-45.
- **Ramanunny, A.K.**, Wadhwa, S., Gulati, M., Gupta, S., Porwal, O., Jha, N.K., Gupta, P.K., Kumar, D., Prasher, P., Dua, K., 2021. **Development and validation of RP-HPLC method for 1'-Acetoxychavicol acetate (ACA) and its application in optimizing the yield of ACA during its isolation from *Alpinia galanga* extract as well as its quantification in nanoemulsion**. S. Afr. J. Bot.
- **Ramanunny, A.K.**, Wadhwa, S., Thakur, D., Singh, S.K., Kumar, R., 2021. **Treatment modalities of psoriasis: A focus on requisite for topical nanocarrier**. Endocr. Metab. Immune. Disord. Drug Targets. 21, 418-433.
- **Ramanunny, A.K.**, Wadhwa, S., Gulati, M., Singh, S.K., Kapoor, B., Dureja, H., Chellappan, D.K., Anand, K., Dua, K., Khursheed, R., 2021. **Nanocarriers for treatment of dermatological diseases: Principle, perspective and practices**. Eur. J. Pharmacol. 890, 173691.

- **Ramanunny, A.K.**, Wadhwa, S., Singh, S.K., Sharma, D.S., Khursheed, R., Awasthi, A., 2020. **Treatment strategies against psoriasis: Principle, perspectives and practices.** Curr. Drug Deliv. 17, 52-73.

#### **Publications related to allied work**

- Khursheed, R., Singh, S.K., Kumar, B., Wadhwa, S., Gulati, M., Awasthi, A., Vishwas, S., Kaur, J., Corrie, L., **Arya, K.R.** and Kumar, R., 2021. Self-nanoemulsifying composition containing curcumin, quercetin, *Ganoderma lucidum* extract powder and probiotics for effective treatment of type 2 diabetes mellitus in streptozotocin induced rats. Int. J Pharm.121306.
- Sharma, D.S., Wadhwa, S., Gulati, M., **Kadukkattil Ramanunny, A.**, Awasthi, A., Singh, S.K., Khursheed, R., Corrie, L., Chitranshi, N., Gupta, V.K. and Vishwas, S., 2021. Recent advances in intraocular and novel drug delivery systems for the treatment of diabetic retinopathy. Expert Opin Drug Deliv.18,553-576.
- Khursheed, R., Singh, S.K., Wadhwa, S., Gulati, M., Kapoor, B., Awasthi, A., **K R, Arya**, Kumar, R., Pottoo, F.H., Kumar, V. and Dureja, H., 2021. Opening eyes to therapeutic perspectives of bioactive polyphenols and their nanoformulations against diabetic neuropathy and related complications. Expert Opin Drug Deliv. 18, 427-448.
- Khursheed, R., Singh, S.K., Wadhwa, S., Gulati, M., Awasthi, A., Kumar, R., **Ramanunny, A.K.**, Kapoor, B., Kumar, P. and Corrie, L., 2020. Exploring role of probiotics and *Ganoderma lucidum* extract powder as solid carriers to solidify liquid self-nanoemulsifying delivery systems loaded with curcumin. Carbohydr. Polym. 250, 116996.
- Kumar, R., Kumar, R., Khursheed, R., Awasthi, A., **Ramanunny, A.K.**, Kaur, J., Khurana, N., Singh, S.K., Khurana, S., Pandey, N.K. and Kapoor, B., 2020. Validated Reverse Phase - High-Performance Liquid Chromatography method for estimation of fisetin in self-nanoemulsifying drug delivery system. Assay Drug Dev.Technol, 18, 274-281.
- Awasthi, A., Vishwas, S., Corrie, L., Kumar, R., Khursheed, R., Kaur, J., Kumar, R., **Arya, K.R.**, Gulati, M., Kumar, B. and Singh, S.K., 2020. OUTBREAK of novel

- corona virus disease (COVID-19): Antecedence and aftermath. Eur.J. Pharmacol, 884, 173381.
- Khursheed, R., Singh, S.K., Wadhwa, S., Kapoor, B., Gulati, M., Kumar, R., **Ramanunny, A. K.**, Awasthi, A. and Dua, K., 2019. Treatment strategies against diabetes: Success so far and challenges ahead. Eur. J. Pharmacol. 862, 172625.

### Patents

- K R,Arya, Sheetu, Singh SK, Gulati M. A Novel Pharmaceutical Formulation of *Alpinia galanga* for skin infections. Application No: 202111059196, Dec 2021.

### Presentations

#### Poster presentations

- **Arya K R, Singh S K, Sheetu. “Possible Traditional and Alternative Therapies for the treatment of Psoriasis”**, Presented in “Recent Advancements in the Field of Pharmaceutical Sciences (RAPSCON-2019) held at Sri Sai College of Pharmacy, Amritsar, Punjab, 27<sup>th</sup> March, 2019.
- **Arya K R, Singh S K, Sheetu. “Phytochemical aspects and therapeutic perspective of *Alpinia galanga*”**, Presented in “International conference of Pharmacy (ICP-2019) held at Lovely Professional University, Phagwara, Punjab, 13<sup>th</sup>-14<sup>th</sup> Sept, 2019.

#### Oral presentations

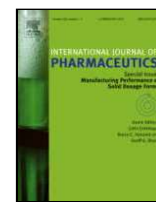
- **Arya K R, Singh S K, Sheetu, “Preliminary studies to identify suitable extraction method of 1’ Acetoxychavicol acetate from *Alpinia galanga* rhizome”**, Presented in “National Conference on Recent trends in Biomedical Sciences-2020” held at Lovely Professional University, Phagwara, Punjab, 2<sup>nd</sup> and 3<sup>rd</sup> July, 2021.
- **Arya K R, Singh S K, Sheetu, “Development and validation of RP-HPLC method for 1’-acetoxychavicol acetate (ACA) and its application in optimizing the yield of ACA during its isolation from *Alpinia galanga* extract**

**as well as its quantification in nanoemulsion**”, Presented in “International Conference on Plant Physiology and Biology” held at Lovely Professional University, Phagwara, Punjab, 10<sup>th</sup>-12<sup>th</sup> Sept, 2021.

- **Arya K R, Singh S K, Sheetu, “Evaluation of topical non-aqueous nano-emulsion of *Alpinia galanga* extract for effective treatment in psoriasis”** Presented in 9th International Congress for Society for Ethnopharmacology held in JSS Academy of Higher Education and Research, Mysuru, 22<sup>nd</sup> to 24<sup>th</sup> April, 2022.

### **Workshops**

- National Workshop on Advanced Instrumentation organized by “Lovely Professional University, Punjab” on 20<sup>th</sup> April 2019.
- Hands-on-Training for Managing the References using Endnote X<sub>9</sub> software organized by International Journal of Advance Study and Research Work held on April 23<sup>rd</sup>, 2020
- 2nd National Pharmacy Workshop on “Nanotechnology: An Effective Way to Improve Bioavailability and Bioactivity” organized by the faculty of pharmacy, Tishk International University, held on March 27, 2021.
- Short Term Course on Innovative Practices in Scientific Writing and Communication 2.0 organized by Lovely Professional University, Punjab held on July 26 to Aug 2, 2021.



## Topical non-aqueous nanoemulsion of *Alpinia galanga* extract for effective treatment in psoriasis: *In vitro* and *in vivo* evaluation

Arya Kadukkattil Ramanunny<sup>a</sup>, Sheetu Wadhwa<sup>a,\*</sup>, Bimlesh Kumar<sup>a</sup>, Monica Gulati<sup>a,b</sup>, Ankit Kumar<sup>a</sup>, Saud Almawash<sup>c</sup>, Ahmed Al Saqr<sup>d</sup>, Kuppusamy Gowthamarajan<sup>e</sup>, Harpreet Singh<sup>f</sup>, Sukriti Vishwas<sup>a</sup>, Rubiya Khursheed<sup>a</sup>, Shaik Rahana Parveen<sup>a</sup>, Aravindhanathan Venkatesan<sup>e</sup>, Keshav R Paudel<sup>g</sup>, Philip M Hansbro<sup>g</sup>, Dinesh Kumar Chellappan<sup>h</sup>, Kamal Dua<sup>b,i</sup>, Sachin Kumar Singh<sup>a,b</sup>

<sup>a</sup> School of Pharmaceutical Sciences, Lovely Professional University, Phagwara, Punjab 144411, India

<sup>b</sup> Faculty of Health, Australian Research Centre in Complementary and Integrative Medicine, University of Technology Sydney, Ultimo, NSW 2007, Australia

<sup>c</sup> Department of Pharmaceutical Sciences, College of Pharmacy, Shaqra University, Shaqra, Saudi Arabia

<sup>d</sup> Department of Pharmaceutics, College of Pharmacy, Prince Sattam Bin Abdulaziz University, Al-kharj 11942, Saudi Arabia

<sup>e</sup> Department of Pharmaceutics, JSS College of Pharmacy, JSS Academy of Higher Education and Research, Ooty, Nilgiris, Tamil Nadu, India

<sup>f</sup> Lovely Faculty of Applied Medical Sciences, Lovely Professional University, Phagwara, Punjab 144411, India

<sup>g</sup> Centre of Inflammation, Centenary Institute and University of Technology Sydney, Faculty of Science, School of Life Sciences, Sydney 2007, Australia

<sup>h</sup> Department of Life Sciences, School of Pharmacy, International Medical University, Kuala Lumpur 57000, Malaysia

<sup>i</sup> Discipline of Pharmacy, Graduate School of Health, University of Technology Sydney, Ultimo, NSW 2007, Australia

### ARTICLE INFO

#### Keywords:

*Alpinia galanga* extract  
Non-aqueous nanoemulsion  
Imiquimod induced mouse model  
PASI  
Box-Behnken design

### ABSTRACT

Non-aqueous nanoemulsion (NANE) of *Alpinia galanga* extract (AGE) was prepared using Palmester 3595 (MCT oil) as oil phase, Cremophor RH 40-Transcutol P® as surfactant-co-surfactant ( $S_{mix}$ ), and glycerin as non-aqueous polar continuous phase. The composition was optimized by applying three-level, four factor Box-Behnken design (BBD). The mean droplet size and zeta potential of the optimized AGE NANE was found to be  $60.81 \pm 18.88$  nm and  $-7.99 \pm 4.14$  mV, respectively. The *ex vivo* permeation studies of AGE NANE and AGE *per se* on porcine skin reported flux of  $125.58 \pm 8.36$   $\mu\text{g}/\text{cm}^2 \text{h}^{-1}$  and  $12.02 \pm 1.64$   $\mu\text{g}/\text{cm}^2 \text{h}^{-1}$ , respectively. Therefore, the enhancement ratio has shown 10-folds increase in the flux for AGE NANE when compared to extract *per se*. Later, confocal laser scanning microscopy confirmed that AGE NANE were able to penetrate into skin's stratum by *trans*-follicular transport mechanism. The stability studies of AGE NANE confirmed its stability at  $30 \pm 2$  °C/ $75 \pm 5$  % RH and  $5 \pm 3$  °C. The efficacy of AGE NANE was evaluated *in vivo* on imiquimod (IMQ) induced mouse model. The mice treated with low and high doses of AGE NANE (groups VI and VII) showed significant ( $p < 0.05$ ) amelioration of psoriasis. Results of histopathology indicated reduction in psoriasis area severity index in AGE NANE treated mice (group VI and group VII).

**Abbreviations:** ACA, 1'-acetoxychavicol acetate; AGE NANE<sub>H</sub>, *Alpinia galanga* extract loaded non-aqueous nanoemulsion high dose (0.1% w/w); AGE NANE<sub>L</sub>, *Alpinia galanga* extract loaded non-aqueous nanoemulsion low dose (0.05% w/w); AGE, *Alpinia galanga* extract; ANOVA, Analysis of variance; BBD, Box-Behnken design; CCD, Central Composite Design; CLSM, Confocal laser scanning microscopy; DoE, Design of Experiment; GSH, Reduced glutathione; HPLC, High performance liquid chromatography; HR-TEM, High resolution transmission electron microscopy; IMQ, imiquimod; IPM, Isopropyl myristate; MCT, Medium chain triglycerides; MDA, Malondialdehyde; NANE, Non-aqueous nanoemulsion; NANE-B, Blank non-aqueous nanoemulsion; PASI, Psoriasis area severity index; PBS, Phosphate buffered saline; PDI, Polydispersity; PEG 400, Polyethylene glycol 400; p-TPD, pseudo-ternary phase diagram; R<sup>2</sup>, coefficient of determination; RAD, Rhodamine B aqueous dispersion; R-NANE, Rhodamine B loaded NANE; S.D, Standard deviation; SEM, Standard error of mean;  $S_{mix}$ , Mixture of surfactant-co-surfactant; SOD, Superoxide dismutase; TBARS, Thiobarbituric acid reactive substances

\* Corresponding author at: School of Pharmaceutical Sciences, Lovely Professional University, Phagwara 144411, Punjab, India.

E-mail address: [sheetu.21001@lpu.co.in](mailto:sheetu.21001@lpu.co.in) (S. Wadhwa).

<https://doi.org/10.1016/j.ijpharm.2022.121882>

Received 23 December 2021; Received in revised form 20 May 2022; Accepted 27 May 2022  
0378-5173/© 20XX





ELSEVIER

Contents lists available at ScienceDirect

## South African Journal of Botany

journal homepage: [www.elsevier.com/locate/sajb](http://www.elsevier.com/locate/sajb)

## Development and validation of RP-HPLC method for 1'-Acetoxychavicol acetate (ACA) and its application in optimizing the yield of ACA during its isolation from *Alpinia galanga* extract as well as its quantification in nanoemulsion

Arya Kadukkattil Ramanunni<sup>a</sup>, Sheetu Wadhwa<sup>a</sup>, Monica Gulati<sup>a</sup>, Saurabh Gupta<sup>b</sup>, Omji Porwal<sup>c</sup>, Niraj Kumar Jha<sup>d</sup>, Piyush Kumar Gupta<sup>e</sup>, Deepak Kumar<sup>f</sup>, Parteek Prasher<sup>g</sup>, Kamal Dua<sup>h,i</sup>, Ahmed Al Saqr<sup>j</sup>, Saud Almawash<sup>k</sup>, Sachin Kumar Singh<sup>a,\*</sup>

<sup>a</sup> School of Pharmaceutical Sciences, Lovely Professional University, Phagwara 144411 Punjab, India

<sup>b</sup> Chitkara College of Pharmacy, Chitkara University, Punjab, India

<sup>c</sup> Department of Pharmacy, Tishk International University, Erbil, Kurdistan Region, Iraq

<sup>d</sup> Department of Biotechnology, School of Engineering & Technology (SET), Sharda University, Plot No.32-34 Knowledge Park III Greater Noida, Uttar Pradesh, 201310, India

<sup>e</sup> Department of Life Sciences, School of Basic Sciences and Research, Sharda University, Plot No. 32–34, Knowledge Park III, Greater Noida 201310, India

<sup>f</sup> Department of Pharmaceutical Chemistry, School of Pharmaceutical Sciences, Shoolini University, Solan 173229, India

<sup>g</sup> Department of Chemistry, University of Petroleum & Energy Studies, Energy Acres, Dehradun-248007, India

<sup>h</sup> Discipline of Pharmacy, Graduate School of Health, University of Technology Sydney, Ultimo NSW 2007, Australia

<sup>i</sup> Faculty of Health, Australian Research Centre in Complementary and Integrative Medicine, University of Technology Sydney, Ultimo, NSW 2007, Australia

<sup>j</sup> Department of Pharmaceutics, College of Pharmacy, Prince Sattam Bin Abdulaziz University, Al-kharj 11942, Saudi Arabia

<sup>k</sup> Department of Pharmaceutical Sciences, College of Pharmacy, Shaqra University, Shaqra, Saudi Arabia

## ARTICLE INFO

## Article History:

Received 8 August 2021

Revised 1 October 2021

Accepted 11 October 2021

Available online xxx

Edited by Dr V. Kumar

## Keywords:

1'-Acetoxychavicol acetate

RP-HPLC

Central composite design

ultrasonication

maceration

nanoemulsion.

## ABSTRACT

An isocratic RP-HPLC was developed and validated for isolation of 1'-Acetoxychavicol acetate (ACA) from *Alpinia galanga* extract (AGE). Nucleodur C18 column was used as the stationary phase and mixture of acetonitrile/0.1% formic acid in water (60/40, v/v) were used as mobile phase. The elution was carried out with a flow rate of 1 mL/min. Further, the method was validated as per ICH Q2 [R1] guidelines in terms of linearity, LOD, LOQ, recovery, precision and specificity. The validated method was utilized for two purposes i.e. optimizing the isolation of ACA from AGE and quantifying ACA's concentration and release from its nanoemulsion. To achieve high yield of ACA, Central composite design (CCD) was used to optimize sieve number and solid to solvent ratio. The retention time of standard and isolated ACA were found at 5.63 min and 5.46 min respectively. The results indicated that the validated method was linear, accurate, precise and specific. During optimization, excellent correlation was observed between practical yield ( $3.89 \pm 0.23\%$  w/w of dried rhizomes) and predicted yield ( $3.73\%$  w/w of dried rhizomes) of ACA with p value more than 0.05. The percentage of ACA loaded in the nanoemulsion was found to be  $99.12 \pm 0.39$ . The *in vitro* diffusion studies showed  $90.12 \pm 2.21\%$  release of ACA at the end of 24 h. It was concluded that the validated method has been successfully utilized to isolate the ACA from AGE and quantify the amount of ACA present in nanoemulsion.

© 2021 SAAB. Published by Elsevier B.V. All rights reserved.

**Abbreviations:** ACA, 1'-Acetoxychavicol acetate; AGE, *Alpinia galanga* extract; AMPK, Adenosine monophosphate-activated protein kinase; ANOVA, Analysis of variance; CCD, Central composite design; HQC, Higher quality control; ICH, International Council for Harmonisation of Technical requirements for Pharmaceuticals for Human Use; LOD, Limit of detection; LOQ, Limit of Quantification; LQC, Lower quality control; MQC, Middle quality control; NF-κ B, Nuclear Factor Kappa B; RSD, Relative standard deviation; SD, Standard deviation

\* Corresponding Author: Sachin Kumar Singh; School of Pharmaceutical Sciences, Lovely Professional University, Phagwara - 144411, Punjab, India

E-mail address: [singhsachin23@gmail.com](mailto:singhsachin23@gmail.com) (S.K. Singh).

<https://doi.org/10.1016/j.sajb.2021.10.012>

0254-6299/© 2021 SAAB. Published by Elsevier B.V. All rights reserved.

### 1. Introduction

1'-Acetoxychavicol acetate (ACA) is a phenylpropanoid found in the rhizomes and seeds of *Alpinia galanga* (AG). It is abundantly found in China, India and Southeast Asian countries where it is commonly known as "Greater galangal". The rhizomes are well known for its culinary uses such as spices, seasonings and flavor (Kojima-Yuasa and Matsui-Yuasa, 2020). In addition, it has been extensively used in traditional system of medicine as anti-inflammatory,



## Journey of *Alpinia galanga* from kitchen spice to nutraceutical to folk medicine to nanomedicine

Arya Kadukkattil Ramanunny<sup>a</sup>, Sheetu Wadhwa<sup>a</sup>, Monica Gulati<sup>a,b</sup>, Sukriti Vishwas<sup>a</sup>, Rubiya Khursheed<sup>a</sup>, Keshav Raj Paudel<sup>c,d</sup>, Saurabh Gupta<sup>e</sup>, Omji Porwal<sup>f</sup>, Saad M. Alshahrani<sup>g</sup>, Niraj Kumar Jha<sup>h</sup>, Dinesh Kumar Chellappan<sup>i</sup>, Parteek Prasher<sup>j</sup>, Gaurav Gupta<sup>k,l</sup>, Jon Adams<sup>b</sup>, Kamal Dua<sup>b,c,m</sup>, Devesh Tewari<sup>a</sup>, Sachin Kumar Singh<sup>a,b,\*</sup>

<sup>a</sup> School of Pharmaceutical Sciences, Lovely Professional University, Phagwara, 144411, Punjab, India

<sup>b</sup> Faculty of Health, Australian Research Centre in Complementary and Integrative Medicine, University of Technology Sydney, Ultimo, NSW, 2007, Australia

<sup>c</sup> Centre for Inflammation, Centenary Institute, Sydney, NSW, 2050, Australia

<sup>d</sup> School of Life Sciences, University of Technology Sydney, Ultimo, NSW, 2007, Australia

<sup>e</sup> Chitkara College of Pharmacy, Chitkara University, Punjab, India

<sup>f</sup> Department of Pharmacognosy, Faculty of Pharmacy, Tishk International University-Erbil, Kurdistan Region, Iraq

<sup>g</sup> Department of Pharmaceutics, College of Pharmacy, Prince Sattam Bin Abdulaziz University, Al-Kharj, 11942, Saudi Arabia

<sup>h</sup> Department of Biotechnology, School of Engineering & Technology (SET), Sharda University, Plot No.32-34 Knowledge Park III Greater Noida, Uttar Pradesh, 201310, India

<sup>i</sup> School of Pharmacy, International Medical University, Bukit Jalil, 57000, Kuala Lumpur, Malaysia

<sup>j</sup> Department of Chemistry, University of Petroleum & Energy Studies, Energy Acres, Dehradun, 248007, India

<sup>k</sup> School of Pharmacy, Suresh Gyan Vihar University, Mahal Road, Jagatpura, Jaipur, India

<sup>l</sup> Department of Pharmacology, Saveetha Dental College and Hospitals, Saveetha Institute of Medical and Technical Sciences, Saveetha University, Chennai, India

<sup>m</sup> Discipline of Pharmacy, Graduate School of Health, University of Technology Sydney, Ultimo, NSW, 2007, Australia

### ARTICLE INFO

#### Keywords:

*Alpinia galanga*  
Nutraceutical  
Nanomedicine  
Micropropagation  
Extraction

### ABSTRACT

**Ethanopharmacological importance:** *Alpinia galanga* (L.) Willd (AG), belonging to Zingiberaceae family is used as a spice and condiment in various culinary preparations of Indonesia, Thailand and Malaysia. It has been also used as a key ingredient in various traditional systems of medicine for the treatment of throat infection, asthma, urinary ailments, inflammation and rheumatism amongst other conditions. AG is widely used as a functional food and included in various preparations to obtain its nutraceutical and pharmacological benefits of its phytoconstituents such as phenyl propanoids, flavonoids and terpenoids. Over the past decades, several researchers have carried out systematic investigation on various parts of AG. Numerous studies on AG rhizomes have shown positive pharmacological effects such as anti-inflammatory, anticancer, antipsoriasis, antiallergic, neuroprotective and thermogenesis. Till date, no comprehensive review summarizing the exploitation of AG into nanomedicine has been published.

**Aim of the review:** This comprehensive review aims to briefly discuss cultivation methods, propagation techniques, extraction processes for AG. The ethnopharmacological uses and pharmacological activities of AG extracts and its isolates are discussed in detail which may contribute well in further development of novel drug delivery system (NDDS) i.e. future nanomedicine.

**Materials and methods:** Information about AG was collected using search engine tools such as Google, Google Scholar, PubMed, Google Patent, Web of Science and bibliographic databases of previously published peer-reviewed review articles and research works were explored. The obtained data sets were sequentially arranged for better understanding of AG's potential.

**Results:** More advanced genetic engineering techniques have been utilized in cultivation and propagation of AG for obtaining better yield. Extraction, isolation and characterization techniques have reported numerous phytoconstituents which are chemically phenolic compounds (phenyl propanoids, flavonoids, chalcones, lignans) and terpenes. Ethanopharmacological uses and pharmacological activity of AG are explored in numerous ailments,

\* Corresponding author. School of Pharmaceutical Sciences, Lovely Professional University, Phagwara, 144411, Punjab, India.

E-mail address: [singhsachin23@gmail.com](mailto:singhsachin23@gmail.com) (S.K. Singh).

<https://doi.org/10.1016/j.jep.2022.115144>

Received 9 December 2021; Received in revised form 9 February 2022; Accepted 22 February 2022

Available online 25 February 2022

0378-8741/© 2022 Elsevier B.V. All rights reserved.

## Overcoming hydrolytic degradation challenges in topical delivery: non-aqueous nano-emulsions

Arya Kadukkattil Ramanunni<sup>a,†</sup>, Sachin Kumar Singh<sup>a,†</sup>, Sheetu Wadhwa<sup>a</sup>, Monica Gulati<sup>a</sup>, Bhupinder Kapoor<sup>a</sup>, Rubiya Khursheed<sup>a</sup>, Gowthamarajan Kuppusamy<sup>b,c</sup>, Kamal Dua<sup>d,e</sup>, Harish Dureja<sup>f</sup>, Dinesh Kumar Chellappan<sup>g</sup>, Niraj Kumar Jha<sup>h</sup>, Piyush Kumar Gupta<sup>i</sup> and Sukriti Vishwas<sup>a</sup>

<sup>a</sup>School of Pharmaceutical Sciences, Lovely Professional University, Phagwara, India; <sup>b</sup>Department of Pharmaceutics, JSS College of Pharmacy, JSS Academy of Higher Education & Research, Ooty, Nilgiris, India; <sup>c</sup>Centre of Excellence in Nanoscience & Technology, JSS College of Pharmacy, JSS Academy of Higher Education & Research, Ooty, Nilgiris, India; <sup>d</sup>Discipline of Pharmacy, Graduate School of Health, University of Technology Sydney, Australia; <sup>e</sup>Faculty of Health, Australian Research Centre in Complementary and Integrative Medicine, University of Technology Sydney, Ultimo, Australia; <sup>f</sup>Department of Pharmaceutical Sciences, Maharshi Dayanand University, Rohtak, India; <sup>g</sup>Department of Life Sciences, School of Pharmacy, International Medical University, Kuala Lumpur, Malaysia; <sup>h</sup>Department of Biotechnology, School of Engineering & Technology (Set), Sharda University, Greater Noida, India; <sup>i</sup>Department of Life Sciences, School of Basic Sciences and Research, Sharda University, Greater Noida, India

### ABSTRACT

**Introduction:** Non-aqueous nano-emulsions (NANEs) are colloidal lipid-based dispersions with nano-sized droplets formed by mixing two immiscible phases, none of which happens to be an aqueous phase. Their ability to incorporate water and oxygen sensitive drugs without any susceptibility to degradation makes them the optimum dosage form for such candidates. In NANEs, polar liquids or polyols replace the aqueous phase while surfactants remain same as used in conventional emulsions. They are a part of the nano-emulsion family albeit with substantial difference in composition and application.

**Areas covered:** The present review provides a brief insight into the strategies of loading water-sensitive drugs into NANEs. Further advancement in these anhydrous systems with the use of solid particulate surfactants in the form of Pickering emulsions is also discussed.

**Expert opinion:** NANEs offer a unique platform for delivering water-sensitive drugs by loading them in anhydrous formulation. The biggest advantage of NANEs vis-à-vis the other nano-cargos is that they can also be prepared without using equipment-intensive techniques. However, the use of NANEs in drug delivery is quite limited. Looking at the small number of studies available in this direction, a need for further research in this field is required to explore this delivery system further.

### ARTICLE HISTORY

Received 2 April 2021  
Accepted 13 December 2021

### KEYWORDS

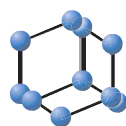
Non-aqueous nano-emulsions; water-sensitive drugs; high-pressure homogenization; Ostwald ripening; characterization techniques; Pickering emulsions

## 1. Introduction

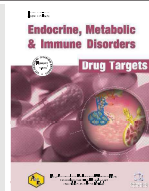
In the classical concept of emulsions, oil and water phases are dispersed in each other, whereas in anhydrous/non-aqueous nano-emulsions (NANEs), water is replaced with a non-aqueous solvent which is markedly more polar than the oily phase [1]. Though the concept of non-aqueous emulsions in the conventional emulsion size range is not new, the scientific literature is sparse regarding non-aqueous emulsions, especially in the nano-size range [2,3]. Not much information is available pertaining to the range of pharmaceutically relevant oily and polar phases as well as surfactants that would lead to formulation of a stable, safe and elegant formulation of NANEs [4]. The basic concept in this unique delivery system is the mixing of two non-aqueous immiscible phases to create nano-sized droplets of one, in the continuous phase constituted by the other. The aqueous phase is generally replaced with either polyols or other polar liquid phases [5]. An innovative modification in the system exists in the form of 'Pickering

emulsions' [6] where solid particles like hydrophobic silica nanoparticles are incorporated to provide better stability as compared to that provided by the surfactants or polymers [7]. Irreversible adsorption of highly energetic colloidal particles at the interface imparts stabilization to PEs. Their striking feature is the ability to bypass the adsorption-desorption phenomenon at the interface which is considered as the prime destabilization mechanism of the surfactant/polymer stabilized system [8]. The unique surfactant-free composition with preservation of drug character in a stabilized system renders them as a potential delivery system for pharmaceuticals, cosmeceuticals, and nutraceuticals [9].

Till date, aqueous nano-emulsions have been explored for drugs that are stable in aqueous medium. However, a number of bio-actives face the problem of hydrolytic as well as oxidative degradation while possessing excellent pharmaceutical potential. Some of the active ingredients that undergo aqueous degradation include cholecalciferol [10], ascorbic acid



# Treatment Modalities of Psoriasis: A Focus on Requisite for Topical Nanocarrier



Arya K. Ramanunni<sup>1</sup>, Sheetu Wadhwa<sup>1,\*</sup>, Divya Thakur<sup>2</sup>, Sachin K. Singh<sup>1</sup> and Rajesh Kumar<sup>1</sup>

<sup>1</sup>School of Pharmaceutical Sciences, Lovely Professional University, Phagwara, Punjab, India; <sup>2</sup>Department of Pharmaceutical Sciences and Drug Research, Punjabi University, Patiala, Punjab, India

**Abstract: Background and Objective:** Psoriasis is an autoimmune skin disease involving cascading release of cytokines activated by the innate and acquired immune system. The increasing prevalence rate of psoriasis demands for more appropriate therapy. The existing chemical moiety is promising for better therapeutic outcome, but the selection of a proper channel for administration has to be reviewed. Hence there is a need to select the most appropriate dosage form and route of administration for improving the curative rate of psoriasis.

## ARTICLE HISTORY

Received: January 09, 2020  
Revised: April 22, 2020  
Accepted: April 27, 2020

DOI:  
10.2174/1871530320666200604162258



CrossMark

**Results:** A total of 108 systematic reviews of research and review articles were conducted to make the manuscript comprehensible. The role of inflammatory mediators in the pathogenesis of the disease is discussed for a better understanding of the selection of pharmacotherapy. The older and newer therapeutic moiety with its mode of administration for psoriasis treatment has been discussed. With a comparative review on topical and oral administration of first-line drugs such as methotrexate (MTX), cyclosporine (CsA), and betamethasone, its benefits-liabilities in the selected routes were accounted for. Emphasis has also been paid on advanced nanocarriers for dermatologic applications.

**Conclusion:** For a better therapeutic outcome, proper selection of drug moiety with its appropriate administration is the major requisite. With the advent of nanotechnology, the development of nanocarrier for dermatologic application has been successfully demonstrated in positioning the systemically administered drug into topical targeted delivery. In a nutshell, to achieve successful treatment strategies towards psoriasis, there is a need to focus on the development of stable, non-toxic nanocarrier for topical delivery. Inclusion of the existing orally administered drug moiety into nanocarriers for topical delivery is proposed in order to enhance therapeutics payload with reduced side effects which serves as a better treatment approach for relief of the psoriasis condition.

**Keywords:** Skin, psoriasis, cytokines, nanocarriers, topical, route of administration.

## 1. INTRODUCTION

Psoriasis is a serious, chronic, noncontagious disease of the skin that affects a patient's full lifespan. However, to date, there is no safe, effective, patient compliant and affordable treatment that is available for psoriatic patients. It is an autoimmune disease affecting people mostly at the age of 20 to 30 years [1]. In 2016, the World Health Organization (WHO) reported that in most developed countries, the prevalence rate of psoriasis was found between 1.5 to 5 % [2]. The countries which are closer to the equator were lesser prone to the condition than the countries which are distant from it [3].

International Federation of Psoriasis Association (IFPA) organizes annually "World Psoriasis Day" on October 29

and the consortium has recognized 125 million psoriasis and psoriatic arthritis people worldwide and contemplated that there is a dire need to make multilateral endeavors to help the patients fight against stigmatism of the disease [4].

## 2. IMMUNOPATHOGENESIS

Various factors, such as genetic, environmental, psychological, nutritional, lifestyle, infection, *etc.*, act as triggers to activate the innate as well as the acquired immune system. These systems play an interdependent role in the immunopathogenesis of psoriasis. This recurrent inflammatory skin condition involves a large number of cell types, genes, mediators, *etc.* Either internal or external stimulus enhances cytokine production from keratinocytes [5] and further, the recruitment and adhesion of immune cells into the skin cells result in psoriatic lesions [6].

Characteristic features of psoriatic lesions are described as below [3, 7]

\*Address correspondence to this author at the School of Pharmaceutical Sciences, Lovely Professional University, Phagwara, Punjab 144411, India; Tel: 91-182-4444042; Fax: 7087732988; E-mails: sheetupharma@gmail.com, sheetu.21001@lpu.co.in



Full length article

## Nanocarriers for treatment of dermatological diseases: Principle, perspective and practices

Arya Kadukkattil Ramanunny<sup>a</sup>, Sheetu Wadhwa<sup>a</sup>, Monica Gulati<sup>a</sup>, Sachin Kumar Singh<sup>a,\*</sup>, Bhupinder Kapoor<sup>a</sup>, Harish Dureja<sup>b</sup>, Dinesh Kumar Chellappan<sup>c</sup>, Krishnan Anand<sup>d</sup>, Kamal Dua<sup>e</sup>, Rubiya Khursheed<sup>a</sup>, Ankit Awasthi<sup>a</sup>, Rajan Kumar<sup>a</sup>, Jaskiran Kaur<sup>a</sup>, Leander Corrie<sup>a</sup>, Narendra Kumar Pandey<sup>a</sup>

<sup>a</sup> School of Pharmaceutical Sciences, Lovely Professional University, Phagwara, 144411, Punjab, India

<sup>b</sup> Department of Pharmaceutical Sciences, Maharshi Dayanand University, Rohtak, Haryana, India

<sup>c</sup> School of Pharmacy, International Medical University, Bukit Jalil, 57000, Kuala Lumpur, Malaysia

<sup>d</sup> Department of Chemical Pathology, School of Pathology, Faculty of Health Sciences and National Health Laboratory Service, University of the Free State, Bloemfontein, South Africa

<sup>e</sup> Discipline of Pharmacy, Graduate School of Health, University of Technology Sydney, Ultimo, NSW, 2007, Australia

### ARTICLE INFO

#### Keywords:

Nanocarriers  
Skin diseases  
Conventional formulations  
Stratum corneum

### ABSTRACT

Skin diseases are the fourth leading non-fatal skin conditions that act as a burden and affect the world economy globally. This condition affects the quality of a patient's life and has a pronounced impact on both their physical and mental state. Treatment of these skin conditions with conventional approaches shows a lack of efficacy, long treatment duration, recurrence of conditions, systemic side effects, etc., due to improper drug delivery. However, these pitfalls can be overcome with the applications of nanomedicine-based approaches that provide efficient site-specific drug delivery at the target site. These nanomedicine-based strategies are evolved as potential treatment opportunities in the form of nanocarriers such as polymeric and lipidic nanocarriers, nanoemulsions along with emerging others viz. carbon nanotubes for dermatological treatment. The current review focuses on challenges faced by the existing conventional treatments along with the topical therapeutic perspective of nanocarriers in treating various skin diseases. A total of 213 articles have been reviewed and the application of different nanocarriers in treating various skin diseases has been explained in detail through case studies of previously published research works. The toxicity related aspects of nanocarriers are also discussed.

### 1. Introduction

One of the most common non-fatal diseases that occur globally is that of the skin and are associated with a considerable burden that encompasses psychological, social, and financial consequences on the patients, their kith and kin, and on society (Basra and Shahrukh, 2009). The degree of severity of the condition is well explained based on the extent of loss of skin barrier function which might involve the activation of the immune system. As a consequence of this activation, some of the skin diseases are reported with co-morbidities such as asthma, cardiovascular diseases, metabolic syndrome, and depression, etc., (Wakkee and Nijsten, 2009).

Skin diseases are the fourth leading non-fatal conditions subsequent to iron deficiency anemia, tuberculosis, and sense organ diseases (Gulati

and Bhogal, 2020; Seth et al., 2017). Even though the condition is non-fatal, the visibility of the skin problem to the population as well as its severity causes extreme distress, pain, and stigmatization. Mostly, the severity of dermatological diseases are analyzed on the basis of several criteria that include age, gender, ethnicity, skin color, genetic composition, environmental, geographical, and climatic variations, socioeconomic status, occupational risks, and hygiene.

However, the reports on skin diseases from each community show unique pattern that accounts to wide variation in reported conditions from different communities in the same country (El-Khateeb et al., 2011). The variation in geographical boundaries causes differences in the type and severity of skin disease affecting that population. As an example, in developed countries such as North America and Australia the prevalence of melanoma has been reported to be highest among

\* Corresponding author. School of Pharmaceutical Sciences, Lovely Professional University, Phagwara, 144411, Punjab, India.

E-mail addresses: [singsachin23@gmail.com](mailto:singsachin23@gmail.com), [sachin\\_pharma06@yahoo.co.in](mailto:sachin_pharma06@yahoo.co.in) (S.K. Singh).

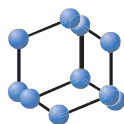
<https://doi.org/10.1016/j.ejphar.2020.173691>

Received 24 August 2020; Received in revised form 15 October 2020; Accepted 26 October 2020

Available online 28 October 2020

0014-2999/© 2020 Elsevier B.V. All rights reserved.

## REVIEW ARTICLE

BENTHAM  
SCIENCE

## Treatment Strategies Against Psoriasis: Principle, Perspectives and Practices



Arya Kadukkattil Ramanunny<sup>1</sup>, Sheetu Wadhwa<sup>1</sup>, Sachin Kumar Singh<sup>1,\*</sup>, Deep Shikha Sharma<sup>1</sup>, Rubiya Khursheed<sup>1</sup> and Ankit Awasthi<sup>1</sup>

<sup>1</sup>School of Pharmaceutical Sciences, Lovely Professional University, Phagwara - 144411, Punjab, India

**Abstract: Background:** Psoriasis is a genetically predisposed autoimmune disease mediated by cytokines released by the activated immune cells. It manifests inflammatory, scaly red or white silvery flaky skin which may be a fluid-filled lesion with soreness and itchiness. The prevalence rate of psoriasis is increasing day by day. Despite having such a high prevalence rate, the treatment of psoriasis is still limited. Hence, there is a need to rethink the various treatment strategies available in the allopathic as well as in the alternative systems of medicine.

**Methods:** Various bibliographic databases of previously published peer-reviewed research papers were explored and systematic data culminated in terms of various treatment strategies used for the management of psoriasis. The prime focus is given towards modern as well as alternative systems of medicine such as phototherapy, a combination of phototherapy with pharmacotherapy such as Ayurveda, Yoga and naturopathy, Unani, Siddha, and Homeopathy to treat psoriasis.

**Results:** A comprehensive review of 161 papers, including both research and review articles, was carried out to make the article readily understandable. The pathogenesis including inflammatory mediators and type of psoriasis is discussed before the treatment strategies to understand the pathophysiology of the disease. The uniqueness, procedure, advantages, and limitations of conventional, advanced, and traditional systems of medicine to treat psoriasis are discussed in detail. Emphasis has also been given towards marine sources such as fish oil, marine sponges, and algae.

**Conclusion:** Although there are many modern and alternative treatment strategies available to treat psoriasis, none of them have been proven to provide complete relief to patients. Moreover, they are associated with certain side effects. In order to overcome them, novel drug delivery systems have been utilized and found effective; however, their stability and safety become the major impediments towards their successful positioning. Traditional and alternative treatment strategies have found to be safe and effective but their use is localized to certain areas. In a nutshell, to achieve successful treatment of psoriasis, there is a need to focus on the development of stable and non-toxic novel drug delivery systems or the promotion of traditional systems to treat psoriasis.

**Keywords:** Psoriasis, novel drug delivery systems, phototherapy, alternative systems, marine sources, homeopathy.

## 1. INTRODUCTION

Psoriasis is an autoimmune disease with marked hyperproliferation and abnormal epidermal differentiation at typical body sites, mostly the extensor surfaces of the elbows, knees, natal cleft, umbilicus, scalp, and nails. It is a chronic inflammatory skin disorder characterized by red or white itchy scales or plaques which might be painful [1]. The condition is triggered by many genetic and environmental

factors. It is not only a skin disease as it has a great impact on the physical and psychological quality of life of the person. Some of the comorbidities associated are cardiovascular diseases, obesity, vascular diseases, diabetic mellitus, hypertension, gastrointestinal diseases including inflammatory bowel disease (Crohn's disease), hepatic disease, infection, and mood disorders such as depression, anxiety, suicidal mentation, and stigmatization [2]. It mostly occurs during the early age of 20 to 30 years and in the late age of 50 to 60 years [3]. The condition at this peak age period (teenage) makes the person lose confidence in approaching people due to stigmatization and thereby mentally debilitated and struggle for a secure life.

\*Address correspondence to this author at the School of Pharmaceutical Sciences, Lovely Professional University, Phagwara - 144411, Punjab, India; Tel: +919888720835; Fax: +91 1824501900; E-mails: singhsachin23@gmail.com; sachin\_pharma06@yahoo.co.in

## ARTICLE HISTORY

Received: May 18, 2019  
Revised: August 19, 2019  
Accepted: October 15, 2019

DOI:  
10.2174/1567201816666191120120551





## Self-nanoemulsifying composition containing curcumin, quercetin, *Ganoderma lucidum* extract powder and probiotics for effective treatment of type 2 diabetes mellitus in streptozotocin induced rats

Rubiya Khursheed<sup>a</sup>, Sachin Kumar Singh<sup>a,\*</sup>, Bimlesh Kumar<sup>a</sup>, Sheetu Wadhwa<sup>a</sup>, Monica Gulati<sup>a</sup>, Anupriya A<sup>a</sup>, Ankit Awasthi<sup>a</sup>, Sukriti Vishwas<sup>a</sup>, Jaskiran Kaur<sup>a</sup>, Leander Corrie<sup>a</sup>, AryaK.R.<sup>a</sup>, Rajan Kumar<sup>a</sup>, Niraj Kumar Jha<sup>b</sup>, Piyush Kumar Gupta<sup>c</sup>, Flavia Zacconi<sup>d</sup>, Kamal Dua<sup>e,f</sup>, Nitin Chitranshi<sup>g</sup>, Gulam Mustafa<sup>h</sup>, Ankit Kumar<sup>i</sup>

<sup>a</sup> School of Pharmaceutical Sciences, Lovely Professional University, Phagwara, Punjab 144411, India

<sup>b</sup> Department of Biotechnology, School of Engineering & Technology (SET), Sharda University, Plot No.32-34 Knowledge Park III, Greater Noida, Uttar Pradesh 201310, India

<sup>c</sup> Department of Life Sciences, School of Basic Sciences and Research, Sharda University, Plot no. 32-34, Knowledge Park III, Greater Noida 201310, Uttar Pradesh, India

<sup>d</sup> Departamento de Química Orgánica, Facultad de Química y de Farmacia, Pontificia Universidad Católica de Chile, Santiago, Chile

<sup>e</sup> Discipline of Pharmacy, Graduate School of Health, University of Technology Sydney, Australia

<sup>f</sup> Faculty of Health, Australian Research Centre in Complementary and Integrative Medicine, University of Technology Sydney, Ultimo, NSW 2007, Australia

<sup>g</sup> Faculty of Medicine, Health and Human Sciences, Macquarie University, F10A, 2 Technology Place, North Ryde, NSW 2109, Australia

<sup>h</sup> Department of Pharmaceutical Sciences, College of Pharmacy, Aldawadmi, Shaqra University, King Saud University

<sup>i</sup> Amity Institute of Pharmacy, Amity University Madhya Pradesh, Maharajpura, Gwalior, Madhya Pradesh 474005, India

### ARTICLE INFO

#### Keywords:

Curcumin  
Quercetin  
Mushroom polysaccharide  
Probiotics  
SNEDDS

### ABSTRACT

Liquid self-nanoemulsifying drug delivery system (L-SNEDDS) of curcumin and quercetin were prepared by dissolving them in isotropic mixture of Labrafil M1944CS®, Capmul MCM®, Tween-80® and Transcutol P®. The prepared L-SNEDDS were solidified using *Ganoderma lucidum* extract, probiotics and Aerosil-200® using spray drying. These were further converted into pellets using extrusion-spheronization. The mean droplet size and zeta potential of L-SNEDDS were found to be  $63.46 \pm 2.12$  nm and  $-14.8 \pm 3.11$  mV while for solid SNEDDS pellets, these were  $72.46 \pm 2.16$  nm and  $-38.7 \pm 1.34$  mV, respectively. The dissolution rate for curcumin and quercetin each was enhanced by 4.5 folds while permeability was enhanced by 5.28 folds (curcumin) and 3.35 folds (quercetin) when loaded into SNEDDS pellets. The C<sub>max</sub> for curcumin and quercetin containing SNEDDS pellets was found  $532.34 \pm 5.64$  ng/mL and  $4280 \pm 65.67$  ng/mL, respectively. This was 17.55 and 3.48 folds higher as compared to their naïve forms. About 50.23– and 5.57-folds increase in bioavailability was observed for curcumin and quercetin respectively, upon loading into SNEDDS pellets. SNEDDS pellets were found stable at accelerated storage conditions. The developed formulation were able to normalize the levels of blood glucose, lipids, antioxidant biomarkers, and tissue architecture of pancreas and liver in streptozotocin induced diabetic rats as compared to their naïve forms.

### 1. Introduction

Type 2 diabetes mellitus (T2DM) is a chronic metabolic disorder of elevated blood glucose level (BGL) that is attributed to non-utilization of insulin, because of insulin resistance (IR) (Khursheed et al., 2019). The oral antihyperglycemic drugs used to manage T2DM are divided into various classes such as sulfonylureas (SUs), biguanides, dipeptidyl peptidase 4 (DPP-4) inhibitors, meglitinides, sodium glucose cotrans-

porter inhibitors (SGLT2), alpha glucosidase inhibitors, thiazolidinedione (TZD) and peptide analogues (Waring, 2016; Zheng et al., 2019). However, the long term use of these drugs suffer is limited by the associated side effects (Garber et al., 2016). Phytomedicines are generally considered as safer as compared to synthetic drugs. A number of drugs from plant origin have been extensively reported in literature to manage T2DM, either alone or in combination with synthetic drugs (Singh et al., 2018). However, formulation development of the synthetic as

\* Corresponding author at: School of Pharmaceutical Sciences, Lovely Professional University, Phagwara 144411, Punjab, India.

E-mail address: [singhsachin23@gmail.com](mailto:singhsachin23@gmail.com) (S.K. Singh).

REVIEW



## Opening eyes to therapeutic perspectives of bioactive polyphenols and their nanoformulations against diabetic neuropathy and related complications

Rubiya Khursheed<sup>a</sup>, Sachin Kumar Singh<sup>a</sup>, Sheetu Wadhwa<sup>a</sup>, Monica Gulati<sup>a</sup>, Bhupinder Kapoor<sup>a</sup>, Ankit Awasthi<sup>a</sup>, Arya Kr<sup>a</sup>, Rajan Kumar<sup>a</sup>, Faheem Hyder Pottoo<sup>b</sup>, Vijay Kumar<sup>c</sup>, Harish Dureja<sup>d</sup>, Krishnan Anand<sup>e</sup>, Dinesh Kumar Chellappan<sup>f</sup>, Kamal Dua<sup>g</sup> and K. Gowthamarajan<sup>h,i</sup>

<sup>a</sup>School of Pharmaceutical Sciences, Lovely Professional University, Phagwara, Punjab, India; <sup>b</sup>Department of Pharmacology, College of Clinical Pharmacy, Imam Abdulrahman Bin Faisal University, Dammam, Saudi Arabia; <sup>c</sup>Department of Biotechnology, School of Bioengineering and Biosciences, Faculty of Technology and Sciences, Lovely Professional University, Phagwara, Punjab, India; <sup>d</sup>Department of Pharmaceutical Sciences, Maharshi Dayanand University, Rohtak, Haryana, India; <sup>e</sup>Department of Chemical Pathology, School of Pathology, Faculty of Health Sciences and National Health Laboratory Service, University of the Free State, Bloemfontein, South Africa; <sup>f</sup>Department of Life Sciences, School of Pharmacy, International Medical University, Bukit Jalil, Kuala Lumpur, Malaysia; <sup>g</sup>Discipline of Pharmacy, Graduate School of Health, University of Technology Sydney, Australia; <sup>h</sup>Department of Pharmaceutics, JSS College of Pharmacy, JSS Academy of Higher Education & Research, Ooty, Nilgiris, Tamil Nadu, India; <sup>i</sup>Centre of Excellence in Nanoscience & Technology, JSS College of Pharmacy, JSS Academy of Higher Education & Research, Ooty, Nilgiris, Tamil Nadu, India

### ABSTRACT

**Introduction:** Diabetic neuropathy (DN) is one of the major complications arising from hyperglycaemia in diabetic patients. In recent years polyphenols present in plants have gained attention to treat DN. The main advantages associated with them are their action via different molecular pathways to manage DN and their safety. However, they failed to gain clinical attention due to challenges associated with their formulation development such as lipophilicity, poor bioavailability, rapid systemic elimination, and enzymatic degradation.

**Area covered:** This article includes different polyphenols that have shown their potential against DN in preclinical studies and the research carried out towards development of their nanoformulations in order to overcome aforementioned issues.

**Expert opinion:** In this review various polyphenol based nanoformulations such as nanospheres, self-nanoemulsifying drug delivery systems, niosomes, electrospun nanofibers, metallic nanoparticles explored exclusively to treat DN are discussed. However, the literature available related to polyphenol based nanoformulations to treat DN is limited. Moreover, these experiments are limited to preclinical studies. Hence, more focus is required towards development of nanoformulations using simple and single step process as well as inexpensive and non-toxic excipients so that a stable, scalable, reproducible and non-toxic formulation could be achieved and clinical trials could be initiated.

### ARTICLE HISTORY

Received 3 August 2020  
Accepted 2 November 2020

### KEYWORDS

Diabetic Neuropathy;  
nanomedicines;  
polyphenols; drug Delivery

## 1. Introduction

Diabetic neuropathy (DN) is the most prevalent microvascular complication associated with diabetes mellitus (DM) [1]. DN involves extensive array of structural and neurochemical alterations which influence autonomic and peripheral nervous system and leads to morbidity and fatality [2]. DN causes impairment in nerves due to high glucose deposition in the body. Apart from increased blood glucose level (BGL) which occurs in DM [3], some other factors such as hypercholesterolemia, dyslipidemia, mechanical injury, injury to fragile nerve fibers, and smoking are also contributing to the progression of DN [4,5]. The most prevalent type of neuropathy is diabetic polyneuropathy and is seen mostly in 30% of diabetic patients. It is assumed that 50% of patients with DM will develop DN over time. The incidence of DN in DM ranges broadly from 9.6% to 88.7% worldwide [6].

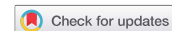
DN is the main root cause of diabetic foot ulcer (DFU) which further leads to 50–75% of non-traumatic amputations.

DN can lead to many other complications such as neurodegeneration in brain leading to memory deficits and Alzheimer's, dementia, and cognitive decline [6].

Various drugs used to treat DN are tricyclic agents (imipramine, amitriptyline), serotonin-nor epinephrine reuptake inhibitors (SNRI) (duloxetine, venlafaxine), carboxamides (carbamazepine, oxcarbazepine), GABA analogs (gabapentin, pregabalin), and opioid analgesics (tramadol, tapentadol). The tricyclic agents have been limited for their use because of side effects such as arrhythmia, orthostatic hypotension and drowsiness, etc. [7]. The treatment with SNRI requires administration of higher dose which leads to side effects such as constipation and somnolence [8]. The popularity of carboxamides against DN is also decreasing due to its alarming unwanted side effects like osteoporosis and bone marrow suppression [9]. Furthermore, the side effects of GABA analogs include ankle edema, sedation, and cerebral edema [10]. The side effects associated with opioid analgesics are constipation, and headache [11].



REVIEW



## Recent advances in intraocular and novel drug delivery systems for the treatment of diabetic retinopathy

Deep Shikha Sharma<sup>a</sup>, Sheetu Wadhwa<sup>a</sup>, Monica Gulati<sup>a</sup>, Arya Kadukkattil Ramanunna<sup>a</sup>, Ankit Awasthi<sup>a</sup>, Sachin Kumar Singh<sup>a</sup>, Rubiya Khursheed<sup>a</sup>, Leander Corrie<sup>a</sup>, Nitin Chitranshi<sup>b</sup>, Vivek Kumar Gupta<sup>b</sup> and Sukriti Vishwas<sup>a</sup>

<sup>a</sup>School of Pharmaceutical Sciences, Lovely Professional University, Phagwara, India; <sup>b</sup>Faculty of Medicine, Health and Human Sciences, Macquarie University, North Ryde, Australia

### ABSTRACT

**Introduction:** Diabetic retinopathy (DR) is associated with damage to the retinal blood vessels that lead eventually to vision loss. The existing treatments of DR are invasive, expensive, and cumbersome. To overcome challenges associated with existing therapies, various intraocular sustained release and novel drug delivery systems (NDDS) have been explored.

**Areas covered:** The review discusses recently developed intraocular devices for sustained release of drugs as well as novel noninvasive drug delivery systems that have met a varying degree of success in local delivery of drugs to retinal circulation.

**Expert opinion:** The intraocular devices have got very good success in providing sustained release of drugs in patients. The development of NDDS and their application through the ocular route has certainly provided an edge to treat DR over existing therapies such as anti-VEGF administration but their success rate is quite low. Moreover, most of them have proved to be effective only in animal models. In addition, the extent of targeting the drug to the retina still remains variable and unpredictable. The toxicity aspect of the NDDS has generally been neglected. In order to have successful commercialization of nanotechnology-based innovations well-designed clinical research studies need to be conducted to evaluate their clinical superiority over that of the existing formulations.

### ARTICLE HISTORY

Received 4 April 2020  
Accepted 2 November 2020

### KEYWORDS

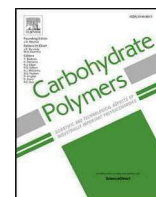
Diabetic retinopathy; intraocular devices; novel drug delivery system; vascular endothelial growth factor

## 1. Introduction

Diabetes Mellitus (DM) is a metabolic disorder that occurs due to the elevated blood glucose level. DM is broadly categorized into two types- Type-1 (T1DM) and Type-2 (T2DM). Over 422 million people worldwide have diabetes and almost 1.6 million deaths are directly related to diabetes each year. The global prevalence of diabetes is more than 8.5% in the population over 18 years. The number of diabetic people is expected to increase to 700 million by 2045 [1]. Diabetic retinopathy (DR) is a common comorbidity among patients having a prolonged history of DM. It damages retinal blood vessels and retinal nerves and is considered as a leading cause of vision loss or complete blindness in the diabetic population worldwide. DR is classified into two types: proliferative diabetic retinopathy (PDR) and non-proliferative diabetic retinopathy (NPDR). In PDR, neovascularization (abnormal growth of the blood vessels) of ocular blood vessels takes place, which leads to sudden vision loss. NPDR is further divided into three categories, i.e. mild, moderate, and severe NPDR. In mild NPDR, microaneurysms (balloon-like swelling) occur that damage the small retinal blood vessels. In moderate NPDR, blood vessels of the retina get blocked causing a deficiency in the supply of oxygen and nutrients required for normal retinal functioning. In severe NPDR, many blood vessels of the retina get blocked and severe oxygen and nutrient depletion

happens at the level of the retina. Prevalence of anatomical and physiological retinal eye barriers poses a challenge to treatment of DR. Success of any treatment of DR depends on the targeting of the drug to the posterior segment of the eye, i.e. by crossing ocular barriers and reaching the retina for the management of DR [2].

In particular, ocular diseases have been treated by two primary modalities, i.e. topical drops and intravitreal injections. Since decades topical drops have been a mainstay, however, the compliance has become a major challenge to efficacious therapy about 33% of the patients undergoing therapy have been reported to discontinue their therapeutic schedule after one year [3,4]. The introduction of intraocular injections has provided the first effective back-of-the-eye therapy. The approval of ranibizumab and aflibercept for the treatment of wet age-related macular degeneration (wAMD) has provided a breakthrough in intraocular drug delivery. However, in recent studies, it has been reported that use and injection frequency did not replicate the trial outcomes in most cases due to insufficient administration frequency [3,5]. The discovery of implantable intraocular devices such as Vitrasert<sup>®</sup>, Retisert<sup>®</sup>, Ozurdex<sup>®</sup>, and Iluvein<sup>®</sup> has been able to provide long-term residence within the eye [6,7]. Till date, these intraocular devices have been explored to deliver small molecules therapeutics. Hence, they offer significant scope to deliver highly efficacious protein-based drugs through the novel and smart drug delivery



## Exploring role of probiotics and *Ganoderma lucidum* extract powder as solid carriers to solidify liquid self-nanoemulsifying delivery systems loaded with curcumin

Rubiya Khursheed<sup>a</sup>, Sachin Kumar Singh<sup>a,\*</sup>, Sheetu Wadhwa<sup>a</sup>, Monica Gulati<sup>a</sup>, Ankit Awasthi<sup>a</sup>, Rajan Kumar<sup>a</sup>, Arya Kadukkattil Ramanunni<sup>a</sup>, Bhupinder Kapoor<sup>a</sup>, Pushpendra Kumar<sup>b</sup>, Leander Corrie<sup>a</sup>

<sup>a</sup> School of Pharmaceutical Sciences, Lovely Professional University, Phagwara, 144411, Punjab, India

<sup>b</sup> School of Chemical Engineering and Physical Sciences, Department of Chemistry, Lovely Professional University, Phagwara, 144411, Punjab, India

### ARTICLE INFO

#### Keywords:

Curcumin  
*Ganoderma lucidum* extract powder  
 Probiotics  
 Solid-SNEDDS  
 Spheroids

### ABSTRACT

Solid self-nanoemulsifying drug delivery system (S-SNEDDS) containing Curcumin (CRM) were prepared using combination of *Ganoderma lucidum* extract powder (GLEP) and probiotics (PB) as carriers. Liquid SNEDDS containing CRM were prepared by mixing Capmul MCM, Labrafil M1944CS, Tween 80 and Transcutol P. These were further spray dried and finally converted into spheroids. The droplet size of reconstituted S-SNEDDS powder and spheroids was found in the range of 35 to 37 nm, zeta potential in the range of -21.48 to -23.22 mV and drug loading in the range of 95-96%. The release of drug from formulations was found to be more than 90%. Similarly, significant improvement ( $p < 0.05$ ) in permeability of CRM was observed through SNEDDS using Caco2 cell lines. The non-significant difference ( $p > 0.05$ ) in drug loading, droplet size, dissolution rate and angle of repose between L-SNEDDS and S-SNEDDS indicated the potential of GLEP-PB to produce stable SNEDDS.

### 1. Introduction

Development of an oral formulation containing lipophilic drugs has been a consistent challenge for formulation scientists because these drugs possess dissolution rate limited oral absorption and bioavailability (Brown et al., 2004; Gowthamarajan & Singh, 2010; Sachin Kumar Singh et al., 2011). The issue becomes even more cumbersome when the drug gets degraded in the gastrointestinal tract (GIT) (B. Kumar et al., 2018). A large number of formulation strategies have been explored to improve the dissolution rate and gastrointestinal (GI) stability of such drugs. These include formulation of nanosuspension (Mahesh, Singh, & Gulati, 2014), complexes (Danki & Thube, 2010; Singh, Pathak, & Bali, 2012; Singh, Srinivasan, Gowthamarajan et al., 2012; Singh, Srinivasan, Singare, Gowthamarajan, & Prakash, 2012; Zoeller, Dressman, & Klein, 2012), solid lipid nanoparticles (V. V. Kumar et al., 2007), solid dispersions (Kaur, Singh, Garg, Gulati, & Vaidya, 2015), liquisolid compacts (Jyoti et al., 2019; Singh, Srinivasan, Gowthamarajan et al., 2012), metastable polymorphs (Renuka, Kumar, Gulati, & Kaur, 2014), co-crystals (Pandey et al., 2017), metallic nanoparticles (Kumari et al.,

2020) etc. However, these techniques have certain limitations such as toxicity and low stability etc. In recent years, liquid self-nanoemulsifying drug delivery systems (L-SNEDDS) have been reported as potential nanocarriers for delivering lipophilic and gastrointestinal labile drugs through oral route with improved bioavailability (Beg et al., 2016; Garg et al., 2017, 2019; Ghosh et al., 2020; Inugala et al., 2015; J. H. Kang, Oh, Oh, Yong, & Choi, 2012; Kazi et al., 2019; Khan, Kotta, Ansari, Sharma, & Ali, 2015; R. Kumar et al., 2019; Mohsin et al., 2016; Sharma et al., 2018). These L-SNEDDS, upon getting mixed with GI fluids get self-emulsified and form oil and water emulsion. The drug gets encapsulated in the emulsion droplets, gets solubilized at molecular level and gets absorbed through lymphatic route (Shakeel, Haq, Alanazi, & Alsarra, 2014). Thereby, it gets protected from GI fluids as well as hepatic first pass metabolism (Ghai & Sinha, 2012). Despite having such a great potential in overcoming poor aqueous solubility and oral bioavailability of drugs, L-SNEDDS suffer from some challenges such as difficulty in handling, transportation issues, palatability, dose variation as a unit dosage form as well as stability issues due to their liquid nature (Kamel & Mahmoud, 2013; J. H. Kang et al., 2012; Singh,

\* Corresponding author.

E-mail address: [sachin.16030@lpu.co.in](mailto:sachin.16030@lpu.co.in) (S.K. Singh).

<https://doi.org/10.1016/j.carbpol.2020.116996>

Received 29 April 2020; Received in revised form 22 August 2020; Accepted 23 August 2020

Available online 29 August 2020

0144-8617/© 2020 Elsevier Ltd. All rights reserved.



Full length article

## OUTBREAK of novel corona virus disease (COVID-19): Antecedence and aftermath

Ankit Awasthi, Sukriti Vishwas, Leander Corrie, Rajesh Kumar, Rubiya Khursheed, Jaskiran Kaur, Rajan Kumar, K.R. Arya, Monica Gulati, Bimlesh Kumar, Sachin Kumar Singh<sup>\*</sup>, Narendra Kumar Pandey, Sheetu Wadhwa, Pardeep Kumar, Bhupinder Kapoor, Rajneesh Kumar Gupta, Ankit Kumar

School of Pharmaceutical Sciences, Lovely Professional University, Phagwara, Punjab, 144411, India

### ARTICLE INFO

**Keywords:**  
 COVID-19  
 Diagnostic kits  
 Plasma therapy  
 Hydroxychloroquine  
 Antiviral drugs

### ABSTRACT

Outbreak of Coronavirus disease 2019 (COVID-19) started in mid of December 2019 and spread very rapidly across the globe within a month of its outbreak. Researchers all across the globe started working to find out its possible treatments. However, most of initiatives taken were based on various hypotheses and till date no successful treatments have been achieved. Some strategies adopted by China where existing antiviral therapy was initially used to treat COVID-19 have not given very successful results. Researchers from Thailand explored the use of combination of anti-influenza drugs such as Oseltamivir, Lopinavir and Ritonavir to treat it. In some cases, combination therapy of antiviral drugs with chloroquine showed better action against COVID-19. Some of the clinical studies showed very good effect of chloroquine and hydroxychloroquine against COVID-19, however, they were not recommended due to serious clinical toxicity. In some cases, use of rho kinase inhibitor, fasudil was found very effective. In some of the countries, antibody-based therapies have proved fairly successful. The use of BCG vaccines came in light; however, they were not found successful due to lack of full-proof mechanistic studies. In Israel as well as in other developed countries, pluristems allogeneic placental expanded cell therapy has been found successful. Some phytochemicals and nutraceuticals have also been explored to treat it. In a recent report, the use of dexamethasone was found very effective in patients suffering from COVID-19. Its effect was most striking among patients on ventilator. The research for vaccines that can prevent the disease is still going on. In light of the dynamic trends, present review focuses on etiopathogenesis, factors associated with spreading of the virus, and possible strategies to treat this deadly infection. In addition, it attempts to compile the recent updates on development of drugs and vaccines for the dreaded disease.

### 1. Introduction

Though research on coronavirus disease 2019 (COVID-19) was going on at global level since last two decades, highly virulent transmission of COVID-19 came into existence as highly fatal human pathogen during June 2012 in Arabian Peninsula ([https://www.business-standard.com/article/international/china-suspends-public-trans-port-in-wuhan-confirms-571-cases-of-coronavirus-120012300122\\_1.html](https://www.business-standard.com/article/international/china-suspends-public-trans-port-in-wuhan-confirms-571-cases-of-coronavirus-120012300122_1.html)). At that time, it was christened as Middle East Respiratory Syndrome Coronavirus (MERS-CoVs). Corona virus is an enveloped, positive sense ribonucleic acid (RNA) virus found in various species mainly in

mammals and birds (Lee, 2015). The World Health Organization (WHO) named the coronavirus (CoVs) as severe acute respiratory syndrome coronavirus-2(SARS-CoV-2) recently.

The components of SARS-CoV-2 are spike glycoprotein (S), membrane protein (M), nucleocapsid protein (N) and envelope protein (E). The spikes present on the virus consist of a single-pass trans membrane anchor, a large ectodomain and short intracellular tail. The ecto domain contains two subunits S1 and S2 (Li, 2016). The homo trimers of S-protein help in building of spikes on the viral surface which play a key role in its attachment with host receptors (Beniac et al., 2006; Delmas and Laude, 1990). The M glycoprotein performs three major functions i. e. it provides shape to the virions, aids in promoting curvature of membrane, and facilitates binding to the nucleocapsid (Nal et al., 2005;

<sup>\*</sup> Corresponding author.;

E-mail addresses: [singsachin23@gmail.com](mailto:singsachin23@gmail.com), [sachin\\_pharma06@yahoo.co.in](mailto:sachin_pharma06@yahoo.co.in) (S.K. Singh).

<https://doi.org/10.1016/j.ejphar.2020.173381>

Received 27 April 2020; Received in revised form 4 July 2020; Accepted 13 July 2020

Available online 25 July 2020

0014-2999/© 2020 Elsevier B.V. All rights reserved.

# Validated Reverse Phase-High-Performance Liquid Chromatography Method for Estimation of Fisetin in Self-Nanoemulsifying Drug Delivery System

Rajan Kumar,<sup>1</sup> Rakesh Kumar,<sup>1</sup> Rubiya Khursheed,<sup>1</sup>  
Ankit Awasthi,<sup>1</sup> Arya Kadukkattil Ramanunni,<sup>1</sup> Jaskiran Kaur,<sup>1</sup>  
Navneet Khurana,<sup>1</sup> Sachin Kumar Singh,<sup>1</sup> Shelly Khurana,<sup>2</sup>  
Narendra Kumar Pandey,<sup>1</sup> Bhupinder Kapoor,<sup>1</sup> and Neha Sharma<sup>1</sup>

<sup>1</sup>School of Pharmaceutical Sciences, Lovely Professional University, Phagwara, Punjab, India.

<sup>2</sup>Department of Pharmacy, Government Polytechnic College, Amritsar, Punjab, India.

## ABSTRACT

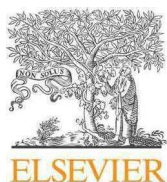
Fisetin (FS) is a polyphenolic phytoconstituent reported to have various pharmacological activities such as antioxidant, anti-parkinsonian, and antidepressant. An analytical method was developed and validated for the estimation of FS by ultrafast liquid chromatography using C-18 reverse phase column. Acetonitrile and orthophosphoric acid (0.2% v/v) in the ratio of 30:70 v/v was used as mobile phase. Flow rate was set at 1 mL/min. Chromatogram of FS was detected at wavelength of 362 nm. Retention time for FS was found to be 7.06 min. The developed method was found to be linear in the range of 2–10 µg/mL with regression coefficient of 0.9985. The method was validated as per the International Conference on Harmonization (ICH) Q2 (R1) guidelines. The percentage recovery was in the range of 95%–105%, which indicated the accuracy of the method. The percentage relative standard deviation (RSD) was found to be <2%, which indicates the precision of the method. Limit of detection (LOD) and limit of quantification (LOQ) were found to be 0.46 and 1.41 µg/mL, respectively. The developed method was found to be robust as there was no significant change in response with change in flow rate, ratio of mobile phase, and pH. The method was successfully applied for estimation of drug loading and drug release from self-nanoemulsifying drug delivery system (SNEDDS). The % drug loading of FS in prepared liquid SNEDDS formulation was found to be 101.95%. The results of dissolution studies indicated 67.78% FS release in water at the end of 60 min.

**Keywords:** fisetin, SNEDDS, HPLC, validation

## INTRODUCTION

Flavonoids are the naturally occurring plant molecules. Fisetin (FS; 2-(3,4-dihydroxyphenyl)-3,7-dihydroxy-4H-chromen-4-one) is one of the polyphenolic flavonol (Fig. 1). It is a pale-yellow compound having molecular weight 286.24 g/mol. The melting point of FS is 330°C. It is naturally synthesized in various fruits (apples, mangoes, strawberries, kiwis, grapes, and persimmons) and vegetables (onions, tomatoes, and cucumbers). The reported pharmacological activities of FS are anti-inflammatory,<sup>1,2</sup> antiepileptic,<sup>3</sup> nephroprotective,<sup>4</sup> antiulcer,<sup>5</sup> antineuropathic,<sup>6</sup> hepatoprotective,<sup>7</sup> neurotrophic,<sup>8</sup> and antidepressant.<sup>9</sup> Besides having various pharmacological activities, FS also have some of the pharmaceutical challenges. FS have very low solubility and oral bioavailability.<sup>10</sup> Therefore, researchers try to improve the solubility and bioavailability of FS by formulating nanoformulations such as liposomes,<sup>11,12</sup> polymeric nanoparticles,<sup>13</sup> and self-nanoemulsifying drug delivery system (SNEDDS).<sup>14</sup> To evaluate these nanoformulations on various parameters such as drug loading, drug dissolution, and permeability, there is a need to develop a simple, sensitive, and reproducible method for its quantification.

There are some of the methods that have been reported for the quantification of FS. Bouzid *et al.* reported the presence of FS along with some other flavonoids in the extract of *Arbutus unedo* L. by analyzing the extract over high-performance liquid chromatography (HPLC) using methanol:water (50:50, v/v, pH 2.8) as mobile phase. But the information regarding method development and validation for FS was not available.<sup>15</sup> Mignet *et al.* developed the liposomal formulation of FS and used HPLC technique to measure the percentage encapsulation of FS. To perform HPLC analysis they used methanol:2% glacial acetic acid (52:48, v/v) as mobile phase. But, in this study also details about method development and validation of FS were not reported.<sup>12</sup> Some bioanalytical methods are also reported for the evaluation of FS in the biological samples,<sup>16,17</sup> but detailed information is not available in the literature regarding validation of these methods. Kadari *et al.* demonstrated application of LC-MS/MS for estimation of



## Treatment strategies against diabetes: Success so far and challenges ahead

Rubiya Khursheed<sup>a</sup>, Sachin Kumar Singh<sup>a,\*</sup>, Sheetu Wadhwa<sup>a</sup>, Bhupinder Kapoor<sup>a</sup>,  
Monica Gulati<sup>a</sup>, Rajan Kumar<sup>a</sup>, Arya Kadukkattil Ramanunni<sup>a</sup>, Ankit Awasthi<sup>a</sup>, Kamal Dua<sup>b</sup>

<sup>a</sup> School of Pharmaceutical Sciences, Lovely Professional University, Phagwara, 144411, Punjab, India

<sup>b</sup> Discipline of Pharmacy, Graduate School of Health, University of Technology Sydney, Australia

### ARTICLE INFO

#### Keywords:

Diabetes  
Insulin  
Herbal drugs  
Synbiotics  
Formulations  
Mushrooms

### ABSTRACT

The growing disease burden of diabetes mellitus is an important public health concern, affecting over 400 million people globally. This epidemic, if not controlled in time, leads to life threatening complications, compromise in quality of life, and eventually mortality. Over time, many attempts have been made for the effective treatment of diabetes but true success has never been achieved. Pharmacological and non-pharmacological approaches for the treatment of hyperglycaemia have been ever-evolving due to limitations of current therapies. Non pharmacological management which includes diet management and exercise, has been the primary focus for self-management of diabetes. The pharmacological management includes oral antihyperglycaemics, phyto-constituents, and combination products. Advancements such as nanocarrier delivery systems have been made in drug delivery to overcome the challenges such as poor bioavailability associated with conventional dosage forms currently employed in diabetes treatment. In recent years, much emphasis has been given to synbiotics that act on gut microbiota, as an emerging therapy for diabetes. The current review discusses different treatment strategies for diabetes management starting from insulin therapy to synbiotics. The combination of herbal phyto-constituents with synthetic drugs, synthetic drug combinations, novel drug delivery systems for insulin are highlighted. Moreover, the role of gut dysbiosis in diabetes and its treatment by administration of synbiotics in various clinical as well as non clinical studies has been discussed in detail.

### 1. Introduction

Diabetes mellitus (DM) is a chronic metabolic disorder of elevated blood glucose level (BGL) either because of deficiency of secretion of a hormone known as insulin or due to damage of pancreatic  $\beta$  cells. It may also be attributed to non-utilization of insulin because of insulin resistance (IR) (Matzinger et al., 2018). In many cases, both the conditions i.e. diminished insulin secretion as well as IR play a role in the development of DM (Ren et al., 2018). Glucose, which is the major fuel for the body, enters the cells from the bloodstream with the help of insulin which is secreted by the  $\beta$  cells of pancreas and hence the BGL drops down. DM is a major killer worldwide and its unprecedented rise poses a serious threat to mankind. The pervasiveness of this ailment and its complications is increasing in a unmanageable manner (Egan and Dinneen, 2019; Guillausseau et al., 2008). As a consequence of this prevailing ailment, the quality of life and the life span get extensively declined (Holland-Carter et al., 2017). As the blood flows in every organ of the body, an increased BGL may cause many long term microvascular and macrovascular complications with the progress of the

disease with time. The microvascular complications include retinopathy, cataract, nephropathy, neuropathy while the macrovascular complications include stroke, cardiovascular disease, coronary artery disease, cerebrovascular disease and diabetic foot, eventually leading to amputation (Forouhi and Wareham, 2019; Thomas et al., 2018).

The aim of present study is to have an extensive review on current pharmacotherapies, phytotherapies as well as nutraceutical based therapies for effective management of diabetes along with their merits and limitations.

### 2. Types of DM

The major classification of DM includes type 1 DM, type 2 DM, and type 3 DM (T1DM, T2DM and T3DM) which differ in their pathophysiology. The T-helper cells, cytotoxic lymphocytes and autoantibodies lead to autoimmune loss of pancreatic  $\beta$  cells of the endocrine pancreas which diminishes insulin secretion and leads to T1DM (Acharjee et al., 2013; Vitak et al., 2017) whereas T2DM occurs due to a combined effect of diminished insulin secretion and IR (Acharjee et al., 2013).

\* Corresponding author.

E-mail address: [sachin.16030@lpu.co.in](mailto:sachin.16030@lpu.co.in) (S.K. Singh).

<https://doi.org/10.1016/j.ejphar.2019.172625>

Received 19 May 2019; Received in revised form 11 August 2019; Accepted 20 August 2019

Available online 23 August 2019

0014-2999/ © 2019 Elsevier B.V. All rights reserved.



## Certificate of Participation

This is to certify that Prof./Dr./Mr./Ms. Abhya K.R.

has Presented E-poster/Oral presentation on Phytochemical Aspects and Therapeutic

Perspective of Alpinia galanga

presentation in International Conference of Pharmacy (ICP-2019) on the theme of " Pharmacy: Realigning the focus on health" held on 13 -14th September 2019 organized by School of Pharmaceutical Sciences, Lovely Professional University, Punjab in a collaboration with Indian Pharmacy Graduates' Association (IPGA) Phagwara chapter.

Date of Issue: 14.09.2019  
Place of Issue: Phagwara (India)

Prepared by  
(Administrative Officer-Records)

Dr. Himanshu Kumar  
Organizing Secretary

Dr. Monica Gulati  
Chairperson, Local Organizing Committee



## National Conference

on  
Recent Advancements in the Field of Pharmaceutical Sciences  
(RAPSCON-2019)

Sponsored by  
Association of Pharmaceutical Teachers of India

on  
27<sup>th</sup> March 2019

### ORGANIZED BY

Sri Sai College of Pharmacy, Manawala, Amritsar, Punjab, India

### Certificate

This is to certify that Prof./Dr./Ms./Mr. Arya K.R. has participated as Speaker/Chairperson/

Co-chairperson/Poster evaluator/member of LOC/Delegate/Poster presentation entitled Possible Traditional and

Alternative Therapies for the treatment of Psoriasis.

Dr. Dinesh Kumar  
Organizing Secretary

Dr. Rajesh Kumar Goel  
APTI President (Punjab)

Mrs. Pooja Sharma  
Organizing Chair

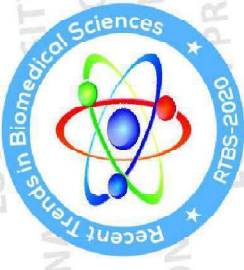
Er. S.K. Puri  
Chairman SSGI

Certificate No. 2255665



**National Conference on  
Recent Trends in Biomedical Sciences  
(RTBS-2020)**

**2<sup>nd</sup> and 3<sup>rd</sup> July, 2021**



**Certificate of Participation**

This is to certify that **Dr. / Mr. / Ms.**

**Arya K R**

**Lovely Professional University Punjab**

**presented Oral / Poster**

**on title Preliminary studies to identify suitable extraction method of 1? Acetoxychavicol acetate from Alpina galanga rhizome**

**in the National Conference on "Recent Trends in Biomedical Sciences - 2020" organized by Department of Medical Laboratory Sciences, Lovely Professional University, Punjab.**

Date of Issue : 19-07-2021

Place of Issue: Phagwara (India)

Prepared by  
(Administrative Officer-Records)

Organizing Secretary

Chairman



# LOVELY FACULTY OF TECHNOLOGY AND SCIENCES

[Under the Aegis of Lovely Professional University, Jalandhar-Delhi G.T. Road, Phagwara (Punjab)]

Certificate No.235107

## *Certificate of Participation*

*This is to certify that Prof./Dr./Mr./Ms. Arya K R of School of Pharmaceutical sciences, Lovely Professional University, Punjab has participated in Poster Prestation/Oral Presentation on the topic entitled Development and validation of RP-HPLC method for 1'acetooxychavicol acetate and its application in application in optimizing the yield of ACA during its isolation from Alpinia galanga extract as well as its quantification in nanoemulsion. in International Conference on Plant Physiology and Biotechnology (ICPPB) held from 10-12 September 2021 organized by Department of Molecular Biology and Genetic Engineering, School of Bio-engineering and Biosciences, under the aegis of Lovely Professional University, Punjab.*

Date of Issue : 22-10-2021  
Place : Phagwara (Punjab), India



Prepared by  
(Administrative Officer-Records)



Dr. Vijay Kumar  
Organizing Secretary, ICPPB-2021



Dr. Umesh Gautam  
Co-Convenor, ICPPB-2021



Dr. Neeta Raj Sharma  
Convener, ICPPB-2021

9<sup>th</sup>

SFEC 2022  
22<sup>nd</sup> to 24<sup>th</sup> April 2022

## International Congress of SOCIETY FOR ETHNOPHARMACOLOGY, INDIA

(Globalizing Local Knowledge and Localizing Global Technologies)

Theme : Redefining Ethnopharmacology for the Global Health and Wellbeing

# Certificate of Participation

**Arya K R**

This is to certify that Prof./Dr./Mr./Ms. ....

has Presented a PAPER in ORAL / POSTER SESSION in the 9<sup>th</sup> International Congress of the Society for Ethnopharmacology, India (SFEC-2022) held at JSS College of Pharmacy, JSS Academy of Higher Education & Research, Mysuru, Karnataka, India from 22<sup>nd</sup> to 24<sup>th</sup>, April 2022.

Title of presentation: .....  
Evaluation of topical non-aqueous nano-emulsion of *Alpinia galanga* extract for effective treatment in psoriasis

  
Dr. T.M. Pramod Kumar  
Organizing Chairman, SFEC - 2022

  
Dr. K. Mruthunjaya  
Organizing Secretary, SFEC - 2022

  
Mr. Birendra K. Sarkar  
President - SFE - India

# DIVISION OF RESEARCH AND DEVELOPMENT

[Under the Aegis of Lovely Professional University, Jalandhar-Delhi G.T. Road, Phagwara (Punjab)]

Certificate No. 167386

## Certificate of Participation

This is to certify that Mr./Ms.

Arya KR

S/O,D/O,W/O

Mr. K R Ramanunny

student of

Lovely Faculty of Applied Medical Sciences

Registration No. 11815948 pursuing

Ph.D Pharmaceuticals

participated in the

National Workshop on Advanced Instrumentation

held on 20-04-2019 organized by

Central Instrumentation Facility, Division of Research and Development

Lovely Professional University (Punjab).

Date of Issue : 13-06-2019

Place of Issue: Phagwara (India)



Prepared by  
(Administrative Officer-Records)



Organizing Secretary

Head,  
Division of Research and Development





# CERTIFICATE

## OF Participation

This Certificate is awarded to

**Arya K R**

---

In recognition of your participation in the “2nd National Pharmacy Workshop - Online” entitled “Nanotechnology: An Effective Way to Improve Bioavailability and Bioactivity” organized by the faculty of pharmacy, Tishk International University, held on

March 27, 2021, Erbil, Kurdistan Region, Iraq.

We would like to express our appreciation.

**Dr. Esra Bayrakdar**  
Head of Department

**Dr. Duran Kala**  
Dean

SERIAL NO. :12/2020 -2021



International Journal of Advance Study  
and Research Work (ISSN: 2581-5997)

Certificate of Completion

This is to Certify that

Arya K R

has successfully completed online course on **"Hands-On-Training for Managing the References using Endnote X9 Software"** organized by International Journal of Advance Study and Research Work on 23 April 2020.

  
Managing Editor

Date: 24 April 2020

[www.ijasrw.com](http://www.ijasrw.com)



Certificate No. 229207

## Certificate of Participation

This is to certify that **Ms. Arya K R D/o Sh. K R Ramanunny** participated in **Short Term Course on Innovative Practices in Scientific Writing and Communication 2.0** organized by Lovely Professional University w.e.f. **July 26, 2021 to August 02, 2021** (7 days) and obtained "O" Grade.

Date of Issue : 02-08-2021

Place : Phagwara (Punjab), India



Prepared by  
(Administrative Officer-Records)

Dr. Bimlesh Kumar  
Associate Professor  
Department of Pharmaceutical Sciences  
Lovely Professional University

Dr. Sunaina Ahuja  
Head-Human Resource  
Development Center  
Lovely Professional University

Dr. Monica Gulati  
Senior Dean  
Faculty of Applied Medical Science  
Lovely Professional University

**Note:** The Grades reflected are based on the performance of the participant at the time of training and performance is subject to change subsequently.

**Grade Description:**

O : 90% and above

A : 75 % to less than 90%

B : 60% to less than 75 %

C : 50% to less than 60%

D : Below 50%